

NASA/TM—2000-209916



# The Alternative Low Noise Fan

James H. Dittmar, David M. Elliott, Robert J. Jeracki, and Royce D. Moore  
Glenn Research Center, Cleveland, Ohio

Tony L. Parrott  
Langley Research Center, Hampton, Virginia

## The NASA STI Program Office . . . in Profile

Since its founding, NASA has been dedicated to the advancement of aeronautics and space science. The NASA Scientific and Technical Information (STI) Program Office plays a key part in helping NASA maintain this important role.

The NASA STI Program Office is operated by Langley Research Center, the Lead Center for NASA's scientific and technical information. The NASA STI Program Office provides access to the NASA STI Database, the largest collection of aeronautical and space science STI in the world. The Program Office is also NASA's institutional mechanism for disseminating the results of its research and development activities. These results are published by NASA in the NASA STI Report Series, which includes the following report types:

- **TECHNICAL PUBLICATION.** Reports of completed research or a major significant phase of research that present the results of NASA programs and include extensive data or theoretical analysis. Includes compilations of significant scientific and technical data and information deemed to be of continuing reference value. NASA's counterpart of peer-reviewed formal professional papers but has less stringent limitations on manuscript length and extent of graphic presentations.
- **TECHNICAL MEMORANDUM.** Scientific and technical findings that are preliminary or of specialized interest, e.g., quick release reports, working papers, and bibliographies that contain minimal annotation. Does not contain extensive analysis.
- **CONTRACTOR REPORT.** Scientific and technical findings by NASA-sponsored contractors and grantees.

- **CONFERENCE PUBLICATION.** Collected papers from scientific and technical conferences, symposia, seminars, or other meetings sponsored or cosponsored by NASA.
- **SPECIAL PUBLICATION.** Scientific, technical, or historical information from NASA programs, projects, and missions, often concerned with subjects having substantial public interest.
- **TECHNICAL TRANSLATION.** English-language translations of foreign scientific and technical material pertinent to NASA's mission.

Specialized services that complement the STI Program Office's diverse offerings include creating custom thesauri, building customized data bases, organizing and publishing research results . . . even providing videos.

For more information about the NASA STI Program Office, see the following:

- Access the NASA STI Program Home Page at <http://www.sti.nasa.gov>
- E-mail your question via the Internet to [help@sti.nasa.gov](mailto:help@sti.nasa.gov)
- Fax your question to the NASA Access Help Desk at (301) 621-0134
- Telephone the NASA Access Help Desk at (301) 621-0390
- Write to:  
NASA Access Help Desk  
NASA Center for AeroSpace Information  
7121 Standard Drive  
Hanover, MD 21076

NASA/TM—2000-209916



# The Alternative Low Noise Fan

James H. Dittmar, David M. Elliott, Robert J. Jeracki, and Royce D. Moore  
Glenn Research Center, Cleveland, Ohio

Tony L. Parrott  
Langley Research Center, Hampton, Virginia

National Aeronautics and  
Space Administration

Glenn Research Center

Trade names or manufacturers' names are used in this report for identification only. This usage does not constitute an official endorsement, either expressed or implied, by the National Aeronautics and Space Administration.

Available from

NASA Center for Aerospace Information  
7121 Standard Drive  
Hanover, MD 21076  
Price Code: A99

National Technical Information Service  
5285 Port Royal Road  
Springfield, VA 22100  
Price Code: A99

# THE ALTERNATIVE LOW NOISE FAN

James H. Dittmar, David M. Elliott, Robert J. Jeracki, and Royce D. Moore  
National Aeronautics and Space Administration  
Glenn Research Center  
Cleveland, Ohio 44135

Tony L. Parrott  
National Aeronautics and Space Administration  
Langley Research Center  
Hampton, Virginia 23681

## SUMMARY

A 106 bladed fan with a design takeoff tip speed of 1100 ft/sec was hypothesized as reducing perceived noise because of the shift of the blade passing harmonics to frequencies beyond the perceived noise rating range. A 22 in. model of this Alternative Low Noise Fan, ALNF, was tested in the NASA Glenn 9×15 Wind Tunnel. The fan was tested with a 7 vane long chord stator assembly and a 70 vane conventional stator assembly in both hard and acoustically treated configurations. In addition a partially treated 7 vane configuration was tested wherein the acoustic material between the 7 long chord stators was made inactive.

The noise data from the 106 bladed fan with 7 long chord stators in a hard configuration was shown to be around 4 EPNdB quieter than a low tip speed Allison fan at takeoff and around 5 EPNdB quieter at approach. Although the tone noise behaved as hypothesized, the majority of this noise reduction was from reduced broadband noise related to the large number of rotor blades. This 106 bladed ALNF is a research fan designed to push the technology limits and as such is probably not a practical device with present materials technology. However, a low tip speed fan with around 50 blades would be a practical device and calculations indicate that it could be 2 to 3 EPNdB quieter at takeoff and 3 to 4 EPNdB quieter at approach than the Allison fan.

7 vane data compared with 70 vane data indicated that the tone noise was controlled by rotor wake—stator interaction but that the broadband noise is probably controlled by the interaction of the rotor with incoming flows.

A possible multiple pure tone noise reduction technique for a fan/acoustic treatment system was identified.

The data from the fully treated configuration showed significant noise reductions over a large frequency range thereby providing a real tribute to this bulk absorber treatment design. The tone noise data with the partially treated 7 vane configuration indicated that acoustic material in the source noise generation region may be more effective than similar material outside of the generation region.

## INTRODUCTION

The conventional method for reducing fan noise has been to go to a low tip speed, high bypass ratio fan. This type of fan would typically have a low number of rotor blades with the number of stator vanes selected to provide for cutoff of the blade passing tone. In references 1 and 2 an alternative method was proposed to reduce the perceived noise of the fan tones. A paper study was conducted in these references on a 6 ft diameter fan. The baseline fan had 53 rotor blades and 90 stator vanes. This fan had an 1100 ft/sec tip speed. A conventional low speed design approach to the fan was undertaken. This resulted in a 20 bladed fan at 800 ft/sec tip speed with 44 stator vanes. An alternative design approach which maintained the 1100 ft/sec tip speed was also investigated. This alternative method used a high number of rotor blades to shift the harmonic tones to frequencies above the perceived noise rating range leaving only the blade passing tone to be rated. A set of low number, long chord stator vanes was then used to reduce the level of the blade passing tone. In reference 1 the noise reduction possibilities of the two design approaches, conventional and alternative, were evaluated using hypothetical spectra. The noise reduction possibilities were calculated as reductions from the baseline fan noise level.

Figure 1(a) shows a hypothetical noise spectra for the baseline fan. This is for a 6 ft fan with 53 rotor blades turning at 1100 ft/sec tip speed. The fan has 90 stator vanes resulting in a cuton fan such that the blade passing tone

propagates out the fan ducting to the far field. In this figure the blade passing tone is arbitrarily set at 100 dB and each harmonic is reduced 3 dB from the previous one. As can be seen there are three harmonics in the perceived noise rating range.

The conventional approach to noise reduction is represented in figure 1(b). Here the fan has 20 rotor blades turning at 800 ft/sec tip speed. The fan has 44 stator vanes which results in a cutoff fan so no blade passing tone is shown in the spectrum. The lower tip speed results in all of the tones being reduced by 6 dB from those of the baseline fan. The harmonics again are each reduced 3 dB from the previous one. As seen in figure 1(b) there are 13 tones in the rated range. The large number of tones is the result of the lower tip speed and the lower number of rotor blades combining to provide a lower blade passing frequency. Each of these tones is much lower in magnitude than the baseline fan tones. The net result is that the conventional low noise fan is 9.1 PNdB quieter than the baseline fan.

The spectrum for the alternative low noise fan is seen in figure 1(c). This fan has 106 rotor blades turning at 1100 ft/sec which shifts all but the blade passing tone to frequencies above the perceived noise rating ranges. The fan has 14 long chord stator vanes which should result in a 6 dB reduction in the blade passing tone. The perceived noise reduction of this alternative approach is 10.4 PNdB, slightly more reduction than the conventional fan's noise reduction.

To verify the predicted noise reduction potential of the alternative low noise fan, a 22 in. diameter model was constructed and tested in the Glenn 9×15 Foot Low Speed Wind Tunnel. This paper presents the design of this Alternative Low Noise Fan (ALNF) and the results from the acoustic testing in the wind tunnel.

## APPARATUS AND PROCEDURE

A 0.305 scale model of the Alternative Low Noise Fan, 22 in. in diameter, was built and tested in the Glenn 9×15 Foot Low Speed Wind Tunnel. This fan was designed with 106 rotor blades and 14 long chord stator vanes to be an alternative approach to a conventional low tip speed, low rotor blade number, cutoff fan such as the Allison Engine Company model fan also tested in the 9×15 wind tunnel (ref. 3). The Alternative Low Noise Fan was also tested using a more conventional 70 vane stator to separately examine the noise reduction achieved by the low number of long chord stators.

### Aerodynamic Design

The aerodynamic design point of the Alternative Low Noise Fan was taken to be the takeoff condition. Here the fan was designed to produce a stage pressure ratio of 1.3 at 1100 ft/sec tip speed. An existing flow path from a 20 in. fan tested previously in a test cell at Glenn Research Center (ref. 4) was scaled by a factor of 1.1 and used for this fan. Cross section drawings of the ALNF with 14 and 70 stators are found in figures 2(a) and (b) respectively. Both the 14 and 70 vane sets have the same solidity. Table I shows some of the key parameters for the ALNF fan design. A complete aerodynamic design for the fan stage is found in appendix A and the blade coordinates are shown in appendix B. The design in appendix A is for the 106 bladed rotor with the 14 vane stator. The 70 vane design has the leading edge of the 70 vane stator at the same location as the 14 vane stator and has the same stator inlet and exhaust conditions. The fan was designed to be tested with both hard wall and acoustically treated flow paths.

### Acoustic Treatment Design

The acoustic treatment design goal was to reduce the noise at the blade passing frequency, ~18 000 Hz at take-off for the scale model fan, and to reduce multiple pure tones that might be roughly centered at 9 000 Hz for the 22 in. model fan. To accomplish the reduction at blade passing frequency the design concentrated on reducing the 92, 78 and 64 spinning mode orders. A single degree of freedom liner was designed with a target design impedance of  $(2.67+1.90i)$  pc. A perforated sheet over bulk absorber design was chosen to achieve this impedance. The perforated plate had 30 percent open area and was designed to be 0.037 in. thick with 0.048 in. diameter holes. The bulk absorber was Kevlar packed to a  $4.5 \text{ lb/ft}^3$  density in a 0.325 backing depth. A sketch of this acoustic absorber

design is shown in figure 3(a). Because of strength requirements it was not possible to fabricate the flow path pieces with perforated sheet as thin as the desired thickness. The actual liner as fabricated is sketched in figure 3(b). The sheet thickness is 0.062 in. with the side facing the bulk absorber having been countersunk so that the straight portion of the hole is 0.037 in. long before the countersunk portion begins. It was hypothesized that this perforated plate would act acoustically the same as the designed plate of 0.037 in.

The acoustic treatment was installed in the fan nacelle as shown in figure 2. The material was on the outer flow path wall of the inlet and on the inner and outer flow path surfaces between the rotor and stator and downstream of the stator. In the long chord stator version of figure 2(a), acoustic treatment was also placed on the inner and outer flow path walls in the space between the stator vanes.

#### Fan Noise Testing

The Acoustic testing was done in the NASA Glenn 9×15 Anechoic Wind Tunnel. A photograph of the Alternative Low Noise Fan in this facility is shown in figure 4. The acoustic treatment on the tunnel walls is shown in the photograph along with a traversing microphone used to acquire noise data. The acoustic data were obtained by both the traversing microphone and fixed microphones installed in the wind tunnel. A top view sketch of the tunnel showing the traversing and fixed microphones is shown in figure 5.

A photograph of the 106 bladed fan is shown in figure 6(a). Here the complexity of fitting 106 blades into the hub can be seen with two different types of blades, short and long stem, being needed to fit into the hub, figure 6(b). A photograph of the 14 vane stator assembly is shown in figure 7 and the 70 vane stator is shown in figure 8. Acoustic data were taken both with a hard wall nacelle and with the acoustically treated nacelle. The acoustically treated configurations were tested first. In going from the acoustically treated to the hard configurations most of the nacelle acoustic surfaces were replaced with hard wall pieces. However for economy of manufacture, the pieces between the stators in the long chord configuration and the pieces directly behind the stators in the short chord configuration were made hard by filling the holes in the acoustic material with an epoxy material. This process then dictated that the acoustically treated configurations be tested first before the holes were filled.

During the initial part of the testing schedule with the acoustically treated nacelle, aerodynamic data were obtained before acoustic data were taken. This aerodynamic data showed that the fan flow was limited by internal flow problems. This occurred with both the short and long chord stator versions. A plot of pressure ratio versus weight flow is shown in figure 9. More complete aerodynamic information is found in reference 5. The first configuration, 14 vanes with acoustic treatment, showed higher pressure ratios and lower weight flows than design. Changes in the fan nozzle area did not bring about the flow increases expected and high losses in the duct were suspected. An attempt was made to improve the flow rate by removing every other one of the 14 long chord stators, resulting in a 7 vane configuration. These vanes were permanently cut out of the stator assembly. A photograph of this 7 vane configuration is found in figure 10. The removal of every other vane increased the flow but did not bring the weight flow to the desired level. Configurations with 70 stator vanes and with only partial treatment showed additional improvements. However, the proper flows were only obtained for both the 7 and 70 vane configurations when the fan was in the hard wall configuration. This indicates that in some way the acoustic treatment was the cause of the flow problem. Some possible causes might include extra frictional losses from flow over the perforated plate or cross flows inside the bulk material in the treatment.

Acoustic data were obtained for the 7 and 70 vane configurations with both hard wall and acoustically treated nacelles. In addition a 7 vane configuration was tested where the nacelle was acoustically treated but the region between the long chord stators was hard. This configuration was an attempt to determine if the acoustic treatment between the stators was more effective because of its proximity to the source than other treatment in the nacelle. Table II shows a list of the tested configurations.

The Alternative Low Noise Fan was designed to achieve a 1.3 pressure ratio at 1100 ft/sec tip speed which was the takeoff condition. However, during the testing of the ALNF, the rotor blades encountered a high stress region at speeds greater than 1000 ft/sec tip speed. This appeared to be a flutter instability and the stress level increased with increasing tip speed. The coating material on the mid span dampers also showed wear after operating at tip speeds above 1000 ft/sec. Some aerodynamic data were obtained at tip speeds above 1000 ft/sec because of the short time needed to obtain the data but the acoustic data was limited to 1000 ft/sec because it was not deemed prudent to remain at these high stress levels for the time needed to make an acoustic survey, ~20 min. Table III shows the tip speeds, from 600 to 1000 ft/sec where the acoustic data were obtained for the 5 configurations listed in table II.

The acoustic data were obtained by the traverse at 48 steps yielding emission angles from 24.6° to 135° at a tunnel Mach number of 0.1 and by three fixed location microphones in the aft yielding emission angles of 136.4°, 147.2° and 158.1°. Two narrow band spectra were taken of the data at 5.9 and 59 Hz bandwidth. From these a 1/3rd Octave spectra was also constructed. Sound power and PNdB values were calculated from the 1/3rd octave data. All of the noise data presented in the report are in 1 ft loss less form at the emitted angles unless otherwise specifically noted. Appendix C contains noise data taken at roughly 10° intervals for the 59 Hz bandwidth narrow band spectra and the 1/3rd octave spectra.

## RESULTS AND DISCUSSION

### Hard Wall Configurations

**Comparison of 7 Vane Data With Allison Fan.**—In a previous report, reference 6, some comparisons were made between the hard wall data for the ALNF and the Allison fan at the takeoff condition. This comparison was to be at 1100 ft/sec tip speed for the ALNF and 840 ft/sec for the Allison fan. At these conditions they were both to yield a pressure ratio of 1.3. As mentioned previously, the ALNF data were limited to 1000 ft/sec which yielded a pressure ratio of 1.24. At the 840 ft/sec tip speed the Allison fan had a 1.26 pressure ratio. (This is a slight correction from the 1.27 pressure ratio stated in reference 6.) Using a noise variation of 10 log thrust the pressure rise ratio of 0.26/0.24 would result in approximately a 0.4 dB correction that should be added to the 1000 ft/sec ALNF data for comparison with the Allison data. For most of the direct spectrum to spectrum comparisons of the two fans, this 0.4 dB is not significant and is not included on the plots. It is however, included in the effective perceived noise comparisons that will follow.

Some of the information from reference 6 is repeated herein for completeness. A comparison between the 7 vane stator ALNF at 1,000 ft/sec tip speed and the Allison fan at 840 ft/sec is shown in figure 11. Here narrow band spectra from 0 to 50 000 Hz with a bandwidth of 59 Hz is shown in part A at 92.5°. This spectrum was presented in Reference 6 as being at 90° but an error was made in the indexing process and the spectra are actually at 92.5°. For consistency with the previous report, the 92.5° position will be used throughout this report. These data are shown as taken on the 22 in. diameter model which has frequencies higher than they would be for the 6 ft diameter full scale fan. For example, the ALNF blade passing tone is apparent around 18 000 Hz and the tone at twice blade passing frequency is just visible near 36 000 Hz. On the 6 ft diameter fan these would be about 5 000 and 10 000 Hz. On this figure the blade passing tone for the Allison fan would be around 2 750 Hz but since it is cut-off it is not visible in the spectra. Tones at twice blade passing frequency, 5 500 Hz and four times blade passing frequency 11 000 Hz are clearly visible and the tone at 3 times blade passing frequency, around 8 250, can be seen above the background. These would be lower on the full scale fan with blade passing frequency being around 840 Hz, 2 bpf at 1680 Hz, 3bpf at 2520 and 4bpf at 336 0Hz.

As can be seen by looking at figure 11(a), not only has the ALNF achieved its goal of being as quiet as the Allison fan but it appears even quieter. The tone levels of the ALNF would have a lower perceived noise rating than the tones of the Allison fan not only because of the frequency shift to the lower rated regions of the spectra as indicated by reference 3 but also because the levels themselves are lower. As can be seen again in figure 11(a), the blade passing tone sound pressure level of the ALNF is lower than that of the 2 times blade passing frequency tone of the Allison fan and is about the same level as the 3 times blade passing frequency tone. Therefore the perceived noise of the tones for the ALNF will be lower than the perceived noise of the tones for the Allison fan.

Possibly more interesting, however, is the broadband noise reduction apparent in the spectra. The ALNF appears to have lower broadband noise over a frequency range from about 2 000 to 16 000 Hz. The broadband noise reduction would be from about 600 to 5 000 Hz for the full scale 6 ft diameter fan. This broadband reduction would have an even larger noise reduction effect on the perceived noise than would the lower tones.

The magnitude of the effect of the broadband noise reduction can be better observed in 1/3rd octave spectra as used by the perceived noise rating method. Figure 11(b) shows the 1/3rd octave spectra for the 92.5° angle. When viewed on the 1/3rd octave basis, the broadband noise reduction becomes even more evident. This broadband noise reduction would result in perceived noise reductions at most reasonable fan sizes.

A 1/3rd octave power level plot is shown in figure 12. This power level result, integrated over the entire data survey shows the significance of the broadband reduction.

An indication of this perceived noise reduction can be seen in figure 13. Here the Effective Perceived Noise for a single fan flyover at 1000 ft altitude on a standard day has been calculated for the Allison fan and the ALNF at scale factors ranging from 2 to 6. Here the EPNdB of the ALNF has been increased by 0.4 dB to account for the lower pressure ratio. The scale factor is the ratio of the full scale fan diameter to the 22 in. fan diameter. For example, the 6 ft diameter fan would be at a scale factor of ~3.27.

As can be seen the ALNF is significantly quieter at all of the scale factors shown. As the scale factor increases the two fans start to come closer together in level. This is because the frequency shift of the larger scale has brought the higher frequencies of the model data, where the two fans have the same levels (20 000 Hz and above, figure 11(b)), down into the most highly rated range of the EPNdB calculation.

The previously reported results from reference 6, and summarized above, were for comparisons at the takeoff condition. A further comparison was made at the approach condition and also showed the ALNF to be quieter. Figure 14 shows spectral comparisons at the 92.5° angle for the ALNF and the Allison fan at the approach condition. Here the Allison fan approach condition is taken as 50 percent speed, 500 ft/sec tip speed, with a pressure ratio of 1.083. The ALNF data were taken from the condition closest to the Allison fan conditions. Here the ALNF data were taken at 6402 rpmc and a pressure ratio of 1.075. Using the same 10 log of thrust correction, the pressure rise ratio of 0.083/0.075 yields a correction of 0.35 dB that should be added to the ALNF data. Again this correction is not applied to the spectrum but it is applied to the perceived noise calculations.

Figure 14(a) shows the narrow band data, 0 to 50 000 Hz with a bandwidth of 59 Hz for the 22 in. model fan. Again, as for the takeoff case, the blade passing tone of the ALNF (around 12,000 Hz) is lower in level than the Allison 2 BPF tone (around 5,000 Hz). As with the takeoff data the ALNF tones at approach will have a lower perceived noise contribution than the Allison tones. Figure 14(a) also shows broadband reduction as did the takeoff data in the 0 to 10 000 Hz range but some broadband noise increase is also shown at higher frequencies that was not observed in the takeoff data.

Figure 14B shows the 1/3rd octave spectra at this 92.5° angle. The large region where the ALNF is quieter, 1 000 to 10 000 Hz, appears to more than overcome the areas where the ALNF is noisier. Figure 15 shows the overall power level comparison for the two fans at approach power. Again the large area of noise reduction for ALNF overshadows the area of noise increase.

The approach flyover noise at 1000 ft, standard day conditions is shown in figure 16. Calculations are shown for Allison fan and the ALNF at scale factors ranging from 2 to 6. (A 6 ft diameter fan would have a scale factor of 3.27.) In figure 16, 0.35 dB has been added to the ALNF data to correct for its slightly lower pressure ratio. At the lower scale factors where the low frequency for the scaled ALNF reduction dominated (fig. 14), significant EPNdB reductions are seen for the ALNF. At a scale factor of 2 the advantage is over 10 EPNdB. As the scale factor is increased, the higher frequencies where the noise increases for ALNF are seen (fig. 14) become part of the EPNdB calculation and the noise increases start to offset some of the noise reduction. At a scale factor of 3, the ALNF is about 5 dB quieter and at a scale factor of 6 the reduction is only a little over 1 EPNdB. Thus a noise improvement is seen for all of the represented scale factors with more reduction visible at the lower scale factors.

Comparisons of the ALNF and Allison data, shown here at takeoff and approach, show a significant EPNdB noise advantage for the high blade number ALNF. Some of this noise reduction is the result of the larger blade number shifting the tones to higher frequencies where they would be weighted lower or not weighted at all by the perceived noise calculation. This was the original design intent of the fan. However, most of the EPNdB noise reduction results from the lower broadband levels of the ALNF.

In reference 6, two possible explanations were advanced for the broadband noise reduction: (1) A reduced turbulence strength impacting the stator brought about by a reduction in the initially generated turbulence and an increased decay of this turbulence and (2) A shift in the turbulence to smaller length scales which results in reduced levels of low frequency noise. Both of these explanations can be related to the increased number of rotor blades.

The reduced turbulence strength explanation centers on the fact that the pressure rise of the ALNF is spread over 106 short chord rotor blades while the Allison fan has the pressure rise provided by 18 larger chord blades. This provides lower loading per blade for the ALNF with less losses per blade. The result would then be smaller initial wake defects and lower initial turbulence for the ALNF. In addition, since the wake/turbulence decays with the distance downstream measured in rotor chords, the ALNF with its smaller rotor chord would have more decay resulting in even lower turbulence levels striking the stator.

The reduced length scale mechanism comes from the increased number of rotor blades giving a smaller gap between blades. These smaller gaps do not permit as many of the large scale turbulence eddies to be generated. This can result in the reduction in the low frequency noise that these large scale eddies generate. Looking at this in

another manner for a Liepmann type of turbulence spectra, the integral length scale for the ALNF would be much lower than that for the Allison fan. Hanson and Horan, reference 7, have indicated that at low frequencies these small length scales generate less noise. In figure 10 of reference 7, done for a 12 ft diameter fan (scale factor of 6.5), significant noise reductions were observed at the low frequencies with smaller length scales. At higher frequencies, the smaller length scales generate extra noise. This behavior is similar to the ALNF-Allison data comparison at approach (fig. 14). The similarity of the data and theory may indicate that the length scale mechanism is the explanation for the ALNF noise reduction at approach. In summary, the ALNF shows significant EPNdB noise advantages primarily from the broadband noise reduction brought about by the increased number of rotor blades.

The 106 bladed ALNF is a research fan designed to push the technology level and as such it would probably not be a practical device with present materials technology. However, a fan with about 50 blades could be a practical device. In reference 6, estimates of the noise of a low tip speed fan with 50 blades, done both with the reduced turbulence level method and the reduced length scale method, were compared with that of an 18 bladed low tip speed fan. A noise reduction of the order of 2 to 3 EPNdB was estimated at the takeoff condition.

Using the same noise ratios for the 50 bladed fan versus an 18 bladed fan as was done in reference 6, the approach noise would be 3 to 4 PNdB quieter for the 50 bladed fan for a fan with a scale factor of 3.0. (More reduction would occur at lower scale factors and less at higher ones.) These results reinforce the conclusion of reference 6 that a significant noise reduction would be possible for a high blade number low tip speed fan.

#### Variation With Speed

The noise variation with speed of the ALNF in the hard wall configuration with 7 stators is shown in figures 17 to 21. Figure 17 shows a series of narrow band spectra taken at the 92.5° angle. The narrow band spectra for the different speed are shown two at a time so they can be more easily compared. Figure 17(a) shows the 6402 rpmc (600ft/sec tip speed) and the 7736 rpmc (725 ft/sec) data points. Increases in both the tone and broadband noise are seen here as the speed is increased. Figure 17(b) repeats the 7736 rpm (725 ft/sec) spectrum and adds the 8537 rpmc (800 ft/sec) spectra. In this figure the presence of some multiple pure tones (MPTs) is observed. This is very low in tip speed for shock induced multiple pure tones to be appearing and these MPTs may be the result of blade to blade spacing differences. Mismatch between blade spacing is entirely possible and indeed likely with this many rotor blades in this scale model fan. In figure 17(b), the broadband noise is seen to increase with speed but the blade passing tone and its harmonics are lower at the 8537 rpm point than at the 7736 point. This may be do in part to the transfer of energy from these tones to the MPTs. Figure 17(c), 9604 rpmc and 8537 rpmc follows the same trend

On figure 17(d) a large increase in multiple pure tone noise is seen in going from 9604 rpmc (900 ft/sec) to 10137 rpmc (950 ft/sec). This is most likely the result of the shock induced multiple pure tone mechanism being seen in the 10137 rpmc data. At the highest speed tested, 10671 rpmc (100ft/sec), figure 17(e), the blade passing tone is seen to increase again.

Figure 18 shows the 1/3rd octave data for the 92.5° angle. Here the trends are the same as seen in the narrow band data. In particular, the increase in MPT activity from 9604 to 10147 rpmc is shown most clearly in figure 18(d).

Figure 19 shows the 1/3rd octave variation of the sound power at the different speeds. Here again in figure 19(d) the significant increase in multiple pure tone noise is observed in going from 9604 to 10137 rpmc. As mentioned previously, this is probably the region where the shock induced multiple pure tones are being observed.

Effective perceived noise levels were calculated for the various speed conditions and are plotted in figure 20. These EPNdB values are for the 1000 ft flyover of one fan on a standard day. As can be seen the EPNdB level increases as the tip speed is increased for all of the scale factors.

A typical variation of the EPNdB with speed is seen in figure 21 for the scale factor of 3.0. Here the EPNdB is plotted versus the corrected fan rpm (rpmc). The noise is seen to increase slowly as the speed is increased from 6402 to 7736 rpmc and then to 8537 rpmc. As the speed is increased further to 9604, 10137, and 10671 rpmc, the noise increase with speed becomes larger, thus creating a parabolic shaped curve. This corresponds to the increase in the multiple pure tone noise which is in the rated frequency range.

## 7 Vane Data Comparison With 70 Vane Data

As mentioned previously, a 70 vane stator was also tested to determine the noise reduction effect of the low number of long chord stator vanes (7 vane case). Figure 22 shows the data comparison between the 7 and 70 vane data at two angles for two fan speeds.

Figures 22(a) and (b) show the data comparisons at a subsonic tip speed, 8537 rpmc (800 ft/sec tip speed) where no shock induced MPTs should be present and the rotor alone blade passing tone should not propagate. Part A is for the 24.5° angle and part B is for the 130.5° angle. These are the same two data plots shown in reference 6. In reference 6, the 130.5° angle data was, because of an indexing error mentioned previously, mislabeled as 128°. Significant reductions in the blade passing tone are observed in going from 70 to 7 vanes.

Previous work has been done on the effect of stator vane number on the broadband noise generated by rotor wake turbulence—stator interaction noise (ref. 8). This work indicated that the noise was reduced with lower stator vane numbers, varying approximately as 10 times the log of the ratio of the stator number. Therefore it would be expected that in going from 70 to 7 vanes that the broadband noise would be reduced about 10 dB. In the front, 24.5°, there is no effect of the vane number on the broadband noise and there is only a small 3 dB or so effect seen in the rear, 130.5°. In both cases much less than the expected 10 dB. A probable explanation for this lack of broadband noise reduction is that the rotor wake turbulence-stator noise mechanism is no longer dominant for the broadband noise of the ALNF as a result of the large number of rotor blades. As indicated previously the rotor wake of the 106 bladed fan is lower in initial magnitude, decays more rapidly in a fixed axial distance and has a smaller turbulence length scale. As a result the strength of the rotor wake turbulence-stator noise mechanism is reduced and another noise mechanism becomes dominant.

In the 70 blade data at the 130.5° angle some MPT noise is seen with a significant spike at one half blade passing frequency. This is probably the result of the rotor blades having more blade to blade variations in the 70 vane data because of mid span damper wear. This situation will be discussed more fully in the following high speed data discussion.

Figures 22(c) and (d) show the data at 10671 rpmc, 1000 ft/sec tip speed, for the 24.5 and 130.5° angles respectively. As can be seen here again there is little broadband noise reduction indicating that some source other than rotor wake turbulence—stator interaction is the dominant broadband mechanism. Of particular interest in this data is the strong tone at one half blade passing frequency for the 70 vane data. At the 130.5° position this tone is significantly louder than the blade passing tone. In figure 22(d), 130.5°, the 7 vane data exhibits multiple pure tone activity mostly in the 3000 to 4000 Hz range. The 70 vane data has most of its MPT activity at one half blade passing frequency. An explanation for this difference may be found in the construction of the rotor. Figure 6(b) shows the construction of the rotor hub. In order to fit the 106 blades into the hub, every other blade has a longer stem. In other works, two types of blades were installed in the hub, ones with short stems and ones with long stems. As can be seen in figure 6(a), the blades are “locked” together with mid span dampers (part span shroud). At the beginning of the program, during the 7 vane testing, these mid span dampers fit very tightly and effectively locked the blades together even with the fan at rest. As the testing program continued some wear was observed on these part span dampers, particularly after the high speed, high stress points taken at speeds above 1000 ft/sec tip speed. During the 70 vane testing the wheel was much looser with the ability for more blade to blade movement because of the worn dampers. A probable explanation for the tone at one half blade passing frequency is that the long and short stem blades are twisting differently resulting in blade to blade angle changes. This would result in a wheel with a 53 cell pattern. This then could explain the 70 vane data having its MPT activity centered around one half blade passing frequency.

This change in the structure of the MPT noise may point to a possible noise reduction technique. It may be possible to design a fan to generate its multiple pure tone noise at one specific frequency, like one half blade passing frequency, which could then be more effectively removed by acoustic treatment. The acoustic treatment could be tuned to be most effective in removing the tone at this frequency and the net result would be a quieter fan/ acoustic treatment system.

The 1/3rd octave data for two speeds, 800 and 1000 ft/sec, at two angles 24.5° and 130.5° are shown in figure 23. Parts A and B are 24.5° and 130.5° for 800 ft/sec tip speed and parts C and D are 24.5° and 130.5° for 1000 ft/sec tip speed. These figures support the same general conclusions as drawn from the narrow band data, specifically that little change in broadband noise was observed in going from 70 to 7 vanes. This further indicates that some source other than rotor wake turbulence—stator interaction is the primary broadband noise source for the ALNF.

The sound power level for the 7 and 70 vane configurations at 800 ft/sec tip speed and 1000 ft/sec are shown in figure 24. Figure 24(a) shows the low speed 800 ft/sec case and on an overall power basis does show a few decibel broadband noise reduction when going from 70 to 7 vanes at 1 000 Hz and above but much less than the expected 10 dB. At the higher speed, 1000 ft/sec for figure 24(b), some broadband reduction is observed but again much less than expected. The difference in multiple pure tone activity is very evident in figure 24(b). The 7 vane case has its MPTs in a broad range from 3 000 to 4 000 Hz while the 70 vane configuration has a strong spike at one half blade passing frequency, in the 10 000 Hz band.

Sound power levels were obtained for the front and aft quadrants to further investigate the small amount of broadband reductions observed. Ninety degrees was arbitrarily chosen for the split between front and aft power. Figures 25(a) and (b) are for the front and aft powers at 800 ft/sec and figures 25(c) and (d) are for the front and aft powers for the 1000 ft/sec tip speed case. For both of the front power comparisons figures 25(a) and (c), very little broadband noise difference exists between the 7 and 70 vane cases. This indicates that in the front some source other than the rotor wake turbulence-stator mechanism is controlling the broadband noise for both the 70 and 7 vane cases. In the aft, figures 25(b) and (d), some broadband noise reduction is seen but much less than the 10 dB expected. This indicates that although some reduction in rotor wake turbulence-stator noise is observed, a noise floor is reached such that the 7 vane data broadband noise is not controlled by rotor wake turbulence-stator interaction. This floor level is then caused by some other source. The fact that almost no reduction occurs in the front indicates that the controlling broadband noise source is probably related to an interaction involving the rotor. The interaction of the wall boundary layer with the rotor or the interaction of incoming turbulence with the rotor are two possibilities for the controlling broadband noise mechanism for the ALNF.

### Acoustic Treatment Results

**7 Vane-Hard Versus Fully Treated.**—The ALNF was tested in both a hard configuration and an acoustically treated configuration. As shown in figure 2, acoustic treatment was present on the outer flow path surface for the fan inlet and on both inner and outer flow path surfaces for areas downstream of the rotor. This section compares the noise data for the 7 vane hard configuration and the 7 vane fully treated configuration.

As indicated in figure 9, the fully treated configuration had lower flow rates and higher pressure ratio than the hard configuration at the same tip speed. The higher losses, which give the higher pressure ratios and lower flows of the treated case, would tend to result in the fan generating more noise. So, while the acoustic treatment would be removing noise, the fan could be generating more noise to begin with. Therefore comparisons between hard and treated cases are subject to question because the fan source noise has changed between the two configurations. The exact amount of treatment attenuation is then not available from these comparisons but the comparisons are performed because they give qualitative results for the treatment performance.

Spectra comparing the hard and fully treated 7 vane configurations are found in figures 26 to 31. Figures 26 and 27 are for the 6402 rpmc, 600 ft/sec tip speed data point, figures 28 and 29 for the 8537 rpmc, 800 ft/sec, and figures 30 and 31 for the 10671 rpmc, 1000 ft/sec, data point. Each of the figures has part A for the 24.5° angle, B for the 92.5° angle and C for the 130.5° angle. Narrow band spectra are found if figures 26, 28 and 30 with the corresponding 1/3rd octave data in figures 27, 29 and 31.

In general, the spectral data show little attenuation at the 24.5° angle. In fact, at the lower speeds 6402 rpmc (fig. 26(a)) and 8537 rpmc (fig. 28(a)), small noise increases are seen with the treated configurations. It should be noted that not much attenuation would be expected at this far forward an inlet angle and therefore the noise increase may be indicative of the additional fan noise present at the treated configuration operating conditions. As more aft angles are investigated, 92.5 and 130.5°, the treatment does show attenuation at all speeds. As the speed is increased, more attenuation is observed until sizable attenuations are observed at the aft angles of the 10671 rpmc, 1000 ft/sec tip speed case (figs. 30(c) and 31(c)). Of particular note is the large frequency range over which attenuation is observed. Again looking at the 1/3rd octave data of figure 31(c), noise attenuations are observed all the way from 1 000 to 100 000 Hz. This range of attenuation is a real tribute to the broadband nature of this bulk absorber design.

Sound power levels for the six speeds tested are found in figure 32 starting with the lowest speed, 6402 rpmc (600 ft/sec tip speed) in part A and going up to 10671 rpmc (1000 ft/sec) in part F. As can be seen in this figure, only small amounts of attenuation are seen at low speed with ever increasing attenuations as the speed is increased. The most attenuation occurs at 10137 rpmc (950 ft/sec tip speed) and at 10671 rpmc (1000 ft/sec) where large attenuations of the multiple pure tones are observed. As has been noted in the past, multiple pure tone noise is particularly attenuable by treatment and this data continues to show that trend. (see, for example, ref. 9)

Front and aft PWLs are shown in figures 33 and 34 respectively. For the front power ( $90^\circ$  and forward) at the lower speeds, 6402 and 7736 rpmc, the noise increases with the fully treated configuration. Again this is possibly the result of a change in the fan noise generation since the fan had a different operating point. As the speed is increased, the treatment starts to show attenuation particularly in the MPT frequency range below blade passing tone until sizable attenuations are observed at 10671 rpmc. The aft PWLs, figure 34, show attenuations at all speeds with the amount of the attenuation increasing as the speed is increased.

The difference between the hard and fully treated power levels is shown in figure 35 with the lowest speed, 6402 rpmc, being part A and proceeding till part F which is the highest speed, 10671 rpmc. The level of attenuation is of the order of 3 dB at the lower speeds and increases with increasing speed until as much as 17 dB is seen around 4000 Hz at the 10671 rpmc (1000 ft/sec tip speed) condition. Again, looking at figure 35(f), the large frequency range of attenuation, from 2 000 to 100 000 Hz is a real tribute to the bulk absorber design.

Figures 36 and 37 show the delta PWLs for the front and rear power levels respectively. In the front, figure 36, at low speeds, the extra noise from the fully treated configuration is seen as negative attenuations. As the speed is increased, the inlet attenuations become larger so that at the higher speeds the front power deltas show a positive noise reduction for the treated configuration. In the aft, figure 37, attenuations are seen for all of the speeds with more attenuation at the higher speeds than at the lower speeds. By comparing the inlet and aft power level deltas it is seen that more noise is removed from the aft quadrant than from the front quadrant. This is particularly true at the higher frequencies, 10 000 Hz and above. The additional attenuation in the aft is as expected because of the additional treatment in the exhaust duct as compared with that in the inlet.

#### Effect Of Treatment Between Stators

A partially treated configuration was tested with the long chord stators. Here the acoustic treatment between the long chord stators was made acoustically hard by filling with an epoxy resin. This experiment was done to determine if acoustic material within the noise source region would be more effective at removing noise.

Figures 38 to 43 show spectral comparisons between the fully treated and partially treated configurations at the three speeds of 6402 rpmc (600 ft/sec tip speed), 8537 rpmc (800 ft/sec) and 10671 rpmc (1000 ft/sec). These comparisons suffer from the same problem as did the hard versus fully treated comparisons in that the fan operating line is not the same for the two cases. Figure 9 shows the operating line for the fully treated and partially treated cases. These two operating lines are closer together than the hard and fully treated line but some differences still exist that can obscure the acoustic results.

The spectral comparisons of figures 38 to 43 show that the acoustic material between the stators is removing a significant amount of noise toward the aft angles. Noise reductions are seen at the tones and over a broad bandwidth. More attenuation is seen in the aft and more attenuation is present at the higher speeds as was observed for the fully treated cases.

Figure 44 shows the power level comparisons at the six speeds of 6402, 7736, 8537, 9604, 10137 and 10671 rpmc. Again the power level comparisons show increased differences between the fully treated and the partially treated configurations as the speed is increased.

Figures 45 and 46 show the front and aft powers. In the front only small differences are seen between the fully treated and partially treated cases while in the aft significant amounts of attenuation are observed for the treatment between the stators.

The delta PWL values are seen in figure 47. Positive differences in PWL correspond to increased attenuation with full acoustic treatment. As mentioned before the total attenuation and the difference between the fully and partially treated cases increases with speed. The front and aft delta PWLs are shown in figures 48 and 49. Differences of less than 2 dB exist in the front PWL between the fully treated and partially treated configurations. In the aft, however, the differences are larger with the treatment between the stators showing 4 to 5 dB of increased attenuation around the blade passing tone.

When this experiment was conducted, it was believed that rotor wake turbulence-stator interaction would be the primary source of broadband noise. In that case, the material between the stators might be more effective at broadband noise suppression because it was within the noise source region. However, as mentioned earlier in the report as a result of reduced rotor wake strength and smaller turbulence length scale, there is strong indication that the rotor wake turbulence-stator interaction mechanism is not the primary broadband noise source for the 7 vane stator configuration and that a rotor related source is probably dominant. In this case, the material between the stators would

be expected to be no more effective than any other treatment downstream of the rotor in reducing the aft broadband noise.

Table IV shows the approximate surface areas of the treatment in the 7 vane configuration. In the aft, the treatment between the stators, is ~37 percent of the total treatment downstream of the rotor. Since the passage height is approximately the same for all of the treatment downstream of the rotor, the attenuation of each section should be roughly proportional to the treated area. Then 37 percent of the downstream attenuation should come from the treatment between the stators. To check this a number of aft PWL points were checked at a frequency that should be controlled by broadband noise. The total aft PWL attenuations were taken from figure 37 and the attenuations from the treatment between the stators from figure 49. Table V contains attenuation comparisons, one at each speed for the 25 000 Hz 1/3rd octave band. The percentage attenuation from the treatment between the stators varies from 40 percent at 6402 rpmc to 56 percent at 10671 rpmc with an average around 50 percent. This is only slightly more than the 37 percent that this material should be removing. This indicates for the broadband noise that the material between the stators is behaving a little better but not much different than the other lining material downstream of the rotor.

As mentioned previously in the report, that although the broadband noise was not controlled by rotor wake-stator interaction, the blade passing tone did appear to be controlled by rotor wake-stator interaction. Therefore the material between the stators, being within the noise generation region, may have a proportionally greater effect on the blade passing tone. If the leading edge of the stator is taken as the reference point, the acoustic treatment between the stators represents 44 percent of the material downstream of this point. Table VI compares the 1/3rd octave band aft powers for the bands that contain the blade passing tone at the various speeds tested. Here it is seen that the percentage of the total noise that is removed by the material between the stators is much higher for the blade passing frequency than for the broadband noise. The percentage goes as high as 75 percent at the 10671 rpmc case with the average being 65 percent. These high values indicate that the material between the stators may be more effective than the other treatment material. This material may be more effective because its proximity to the source may allow more noise to be incident onto the acoustic treatment than would occur for downstream treatment sections.

Although the data does not prove the point conclusively, it does indicate that acoustic treatment within the noise source region, the BPF case, does act more effectively than treatment away from the source. It is also seen that this same treatment material between the stators acts approximately the same as the other materials in the duct when it is not within the noise source region, the broadband case.

#### 70 Vane-Hard Versus Fully Treated

The ALNF was tested with the 70 vane stator set in both a hard and acoustically treated configuration. As shown in figure 2, acoustic treatment was present on the outer flow path surface for the fan inlet and on both the inner and outer flow path surfaces for areas downstream of the rotor. This section compares the noise data for the 70 vane hard configuration and the 70 vane fully treated configuration.

As indicated in figure 9, the fully treated 70 vane configuration had lower flow rates and higher pressure ratios than the hard configuration at the same tip speed. The difference between the hard and treated operating lines is not as great as that which existed for the 7 vane configurations but the difference is still significant. The higher losses which give the higher pressure ratios and lower weight flows of the treated case would tend to result in the fan generating more noise. So, while the acoustic treatment would be removing noise, the fan could be generating more noise to begin with. Therefore comparisons between hard and treated cases are subject to question because the fan source has changed between the two configurations. The exact amount of treatment attenuation is then not available from these comparisons but the comparisons are performed here because they give qualitative results for the treatment performance.

Spectra comparing the hard and fully treated 70 vane configurations are found in figures 50 to 55. Figures 50 and 51 are for the 6402 rpmc, 600ft/sec tip speed data point, figures 52 and 53 for the 8537 rpmc, 800 ft/sec, and figures 54 and 55 for the 10671 rpmc, 1000 ft/sec, data point. Each of the figures has part A for the 24.5° angle, B for the 92.5° angle and part C for the 130.5° angle. Narrow band spectra are found in figures 50, 52 and 54 with the corresponding 1/3rd octave data in figures 51, 53 and 55.

In general, the spectral data show little attenuation at the 24.5° angle. In fact some regions of noise increase are seen at this far forward angle (figs. 50(a), 52(a) and 54(a)). It should be noted that not much attenuation would be

expected at this far forward an inlet angle but the noise increase may be indicative of the additional fan noise present at the treated operating condition. As the more aft angles are investigated, 92.5 and 130.5°, the treatment does show attenuation at all speeds. Significant attenuation is observed at the high speed, 10671 rpmc, condition and the MPT tone at 1/2 blade passing frequency is particularly attenuated (figs. 54(c) and 55(c)). As mentioned previously, tailoring the MPTs to occur at one particular frequency, here at one half blade passing frequency, could be used as a noise reduction technique. The high attenuation possible at for a specific frequency could be combined with the MPTs at one frequency to provide a very effective fan/acoustic treatment system.

Again as with the 7 vane data, the large frequency range over which attenuation is observed is of particular note. Looking at the 1/3rd octave data of figure 55(c), noise attenuations are observed all the way from 1 000 to 100 000 Hz. This large frequency range of attenuation is a real tribute to the broadband nature of this bulk absorber design.

Sound power levels for the six speeds are found in figure 56 starting with the lowest speed, 6402 rpmc (600 ft/sec tip speed) in part A and going up to 10671 rpmc (1000 ft/sec tip speed) in part F. Significant attenuations are seen at all speeds with the most attenuations being seen at the 10137 and 10671 rpmc data points. These large attenuations at these higher speeds seem centered around the removal of the multiple pure tone noise. As has been noted in the past, multiple pure tone noise is particularly attenuable by treatment and this data continues the trend.

Front and aft PWLs are shown in figures 57 and 58 respectively. At the lower speeds, 6402, 7736, and 8537 rpmc, the attenuations in the front power are small. At the higher speeds some significant attenuation is seen particularly in the MPT region of the spectra. The aft PWLs, figure 58, show attenuations at all speeds. Large attenuations are seen at the higher speeds in the MPT regions of the spectra.

The difference between the hard and fully treated power levels is seen in figure 59 with the lowest speed, 6402 rpmc, being part A and the highest speed, 10671 rpmc, being part F. Significant attenuations are seen at all speeds with as much as 16 dB being seen at the blade passing frequency at 10137 rpmc (fig. 59(e)). Again the frequency range of the attenuation is of particular note.

Figures 60 and 61 show the delta PWLs for the front and rear power levels respectively. At the lower speeds in the front, 6402 to 8537 rpmc, figures 60(a) to (c), the peak attenuation is of the order of 5 dB at the lower frequencies with some regions of noise increase at the higher frequencies. At the higher speeds, 10137 and 10671 rpmc, figures 60(e) and (f), the peak attenuation is over 10 dB in the region of the blade passing tone with little or no regions of noise addition. In the aft, figure 61, the noise attenuations are greater than in the front with peak attenuations at all angles being over 10 dB and with no regions of noise addition. This additional attenuation in the aft is as expected because of the additional treatment in the aft as opposed to the inlet.

## CONCLUDING REMARKS

A 106 bladed fan with a design takeoff tip speed of 1100 ft/sec was hypothesized as reducing perceived noise because of the shift of the blade passing tone harmonics to frequencies beyond the perceived noise rating range. A 22 in. model of this alternative low noise fan, ALNF, was tested in the NASA Glenn acoustically treated 9×15 tunnel to confirm this hypothesis. The ALNF was tested with both a 7 vane long chord stator assembly to reduce interaction noise and a 70 vane conventional stator assembly. Both the 7 and 70 vane configurations were tested in hard and acoustically treated configurations. The 7 vane configuration was also tested in a partially treated configuration where the acoustic treatment between the 7 stator vanes was made hard to evaluate the relative effectiveness of this treatment that was presumably in the noise source generation region.

The noise data from the 106 bladed fan with the 7 vane long stator in an acoustically hard version, no acoustic treatment, was compared with the noise of a low tip speed fan previously designed by Allison and tested in the same 9×15 wind tunnel. The 106 bladed fan at 1000 ft/sec tip speed was shown to be around 4 EPNdB quieter than the Allison fan at 840 ft/sec for the takeoff condition and 5 EPNdB quieter at approach (600 ft/sec ALNF, 500 ft/sec Allison) for a 1000 ft flyover of an ~6 ft diameter fan on a standard day. EPNdB reductions were obtained from the tone noise reduction and frequency shift as expected from the design but the majority of the noise reduction came from reduced broadband noise of the ALNF. This broadband reduction was related to the large number of ALNF rotor blades. The large number of rotor blades resulted in smaller initial wakes which decayed more rapidly in a fixed distance and had smaller turbulence length scales.

The 106 bladed ALNF is a research fan designed to push the technology and as such it probably is not a practical device with present materials technology. However, a low tip speed fan with 50 blades could be a practical

device. Estimates of the noise of a low tip speed fan indicate that it would have a 2 to 3 EPNdB advantage at takeoff and 3 to 4 EPNdB advantage at approach speed over the Allison fan in a low tip speed device about 6 ft in diameter.

Tone noise reductions were observed in the hard wall data when the 70 vane stator was changed to the 7 vane stator. These reductions were expected with the lower number of long chord stators reducing the rotor wake stator interaction noise. However, the expected level of reduction in broadband noise was not observed, indicating that some source other than rotor wake turbulence–stator interaction is the primary broadband noise source. The low level of rotor wake turbulence–stator interaction noise is attributed to the large number of rotor blades reducing both the magnitude and scale of the wake turbulence.

The structure of the MPTs at higher speeds changed considerably as the fan dampers started to wear. The MPTs became strongly centered at one half blade passing frequency because the design of the blade stems allowed every other blade to find a different operating position when the dampers were no longer keeping the blades in fixed positions. With every other blade looking differently, the MPTs came out primarily at one half blade passing frequency. This occurrence points to a possible noise reduction technique. A net noise reduction could be achieved for a high tip speed fan by designing blade to blade differences so that the MPTs would be generated at a specific frequency, like the one half blade passing frequency observed herein, and designing acoustic treatment to remove that frequency. Acoustic treatment is specifically effective when it can be designed for a small frequency range. Therefore a design combining the MPTs at one frequency and acoustic treatment tailored specifically to remove that frequency could result in higher noise reductions from the fan/acoustic treatment system.

The Alternative Low Noise Fan results with acoustic treatment were somewhat obscured because the fan performed on a different operating line with the acoustic treatment. This different line was expected to give more fan noise with the treatment operating line than without the treatment possibly yielding less measured attenuation than the treatment actually provided. Even with these different operating lines, the fully treated cases, 7 and 70 vane comparisons, showed significant noise reduction over a very large frequency range. These large amounts of attenuation over such a large frequency range are a real tribute to this bulk absorber treatment design.

Data from the partially treated configuration, acoustic treatment material between the stator vanes made hard, was compared with the full treatment data and the effect of the material between the stators was measured. The intent here was to see if acoustic material within the region where noise was generated would be more effective than material outside this region. The broadband data showed the lining material between the stators to be about as effective as the other acoustic material downstream of the rotor. Since the previous 7 versus 70 vane data indicated that the broadband noise was probably controlled by an interaction on the rotor, all of the treatment material, including that between the stators was outside of the broadband noise generation region and would be expected to behave similarly. The blade passing tone noise, however, was believed to be controlled by rotor wake–stator interaction noise and the treatment material between the stators would be in the tone source generation region. The blade passing tone data appeared to show the acoustic material between the stators as being more effective than material outside of the noise generation area. This is possibly because more of the noise is incident on the acoustic material close to the source than on material downstream. This result would indicate that acoustic treatment is more effective if placed within the source generation region.

## REFERENCES

1. Dittmar, James H., and Woodward, Richard P., An Evaluation of Some Alternative Approaches for Reducing Fan Tone Noise, NASA TM-105356, 1992.
2. Dittmar, James H., A concept for a Counterrotating Fan with Reduced Tone Noise. NASA TM-105736, 1992.
3. Woodward Richard P., et.al., Benefits of Swept and Leaned Stators for Fan Noise Reduction, NASA TM TBD, AST Paper AST018, 1997.
4. Gelder, T.F., and Soltis, R.F., Inlet Noise of 0.5 Meter-Diameter NASA QF-1 Fan as Measured in an Unmodified Compressor Aerodynamic Test Facility and in an Anechoic Chamber, NASA TN D-8121, 1975.
5. Jeracki, Robert J., The Aerodynamic Performance of the Alternative Low Noise Fan, to be published.
6. Dittmar, James H., A Method to Further Reduce the Perceived Noise of Low Tip Speed Fans, NASA AST Report, AST 027, 1998.

7. Hanson, Donald B., and Horan, Kelly, Turbulence/Cascade Interaction: Spectra of Inflow, Cascade Response, and Noise. AIAA Paper 98-2319. Presented at the 4th AIAA/CEAS Aeroacoustics Conference, 1998.
8. Ganz, Ulrich W., et. al., Boeing 18-Inch Fan Rig Broadband Noise Test, NASA CR-1998-208704, 1998.
9. Sofrin, T.G., and Pickett, G.F., Multiple Pure tone Noise Generated by Fans at Supersonic Tip Speeds, in NASA SP 304, 1970.

TABLE I.—ALTERNATIVE LOW NOISE FAN MODEL

Fan diameter .....	22 in.
Takeoff pressure ratio .....	1.3
Takeoff tip speed .....	1100 ft/sec
Rotor blade number .....	106
Stator vane number .....	14 long chord 70 short chord
Nacelle configurations .....	hardwall acoustic treatment

TABLE II.—TEST CONFIGURATIONS

7 long chord stator vanes, acoustically treated nacelle
7 long chord stator vanes, acoustically treated nacelle except the treatment between the stators has been made hard
7 long chord stator vanes, hard wall nacelle
70 short chord stator vanes, acoustically treated nacelle
70 short chord stator vanes, hard wall nacelle

TABLE III.—TEST CONDITIONS

Corrected, rpm	Tip speed, ft/sec
6402	600
7736	725
8537	800
9604	900
10137	950
10671	1000

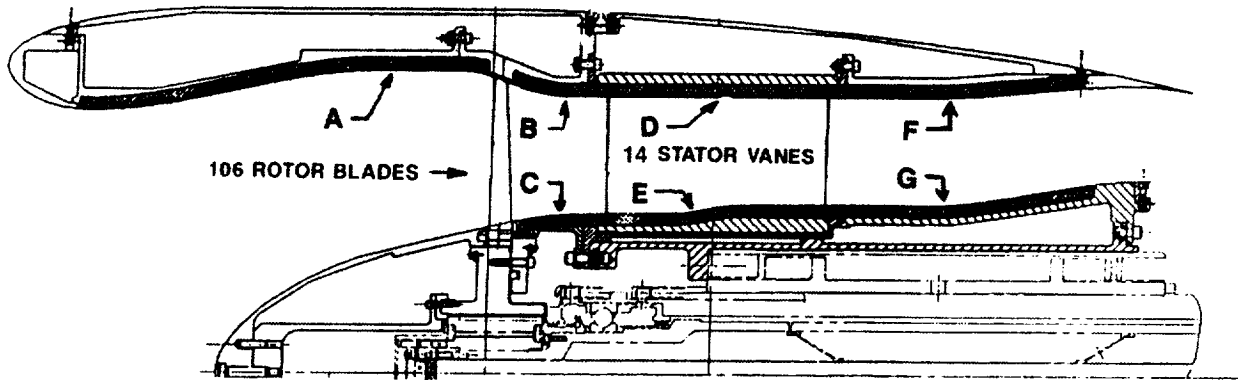


TABLE IVa.—TREATED AREAS LONG CORD STATOR

Treatment section	Approximate surface area in. <sup>2</sup>
A	924
B	188
C	113
D	446
E	268
F	565
G	399
Total between stators	714
Total downstream of rotor	1919
Total downstream of stator L.E.	1618

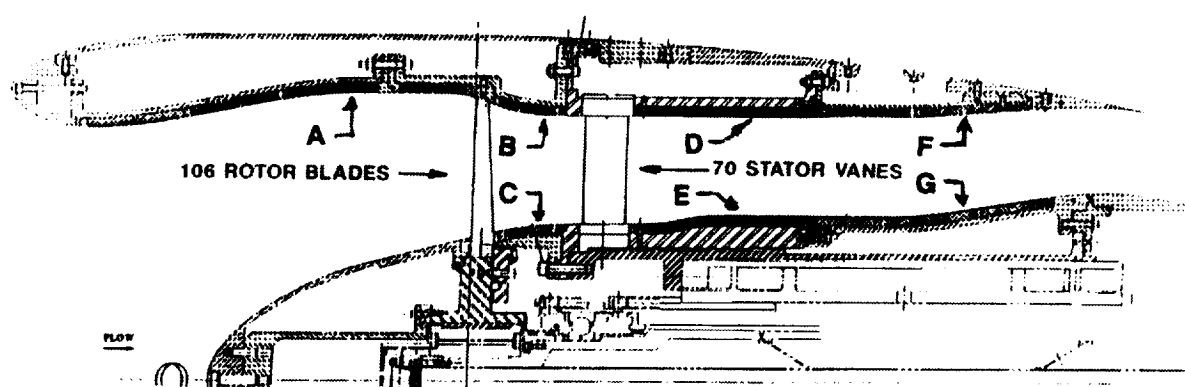


TABLE IVb.—TREATED AREAS SHORT CORD STATOR

Treatment section	Approximate surface area in. <sup>2</sup>
A	924
B	188
C	113
D	440
E	264
F	565
G	399

TABLE V.—BROADBAND TREATMENT ATTENUATIONS

Corrected revolutions/minute	Frequency band containing broadband noise	Full treatment attenuation	Treatment between stators attenuation	Percentage of attenuation from treatment between stators
10671	25 000	8.0	4.5	56
10137	25 000	7.0	3.75	54
9604	25 000	9.0	4.75	53
8537	25 000	7.5	3.75	50
7736	25 000	7.5	3.5	47
6402	25 000	7.5	3.0	40

TABLE VI.—BLADE PASSING TONE ATTENUATIONS

Corrected revolutions/minute	Frequency band containing broadband noise	Full treatment attenuation	Treatment between stators attenuation	Percentage of attenuation from treatment between stators
10671	20 000	7.0	5.25	75
10137	20 000	6.0	4.25	71
9604	16 000	6.5	4.75	73
8537	16 000	7.0	4.75	68
7736	12 500	5.25	3.0	57
6402	12 500	7.0	3.0	43

REDUCTION OF 3 dB PER HARMONIC

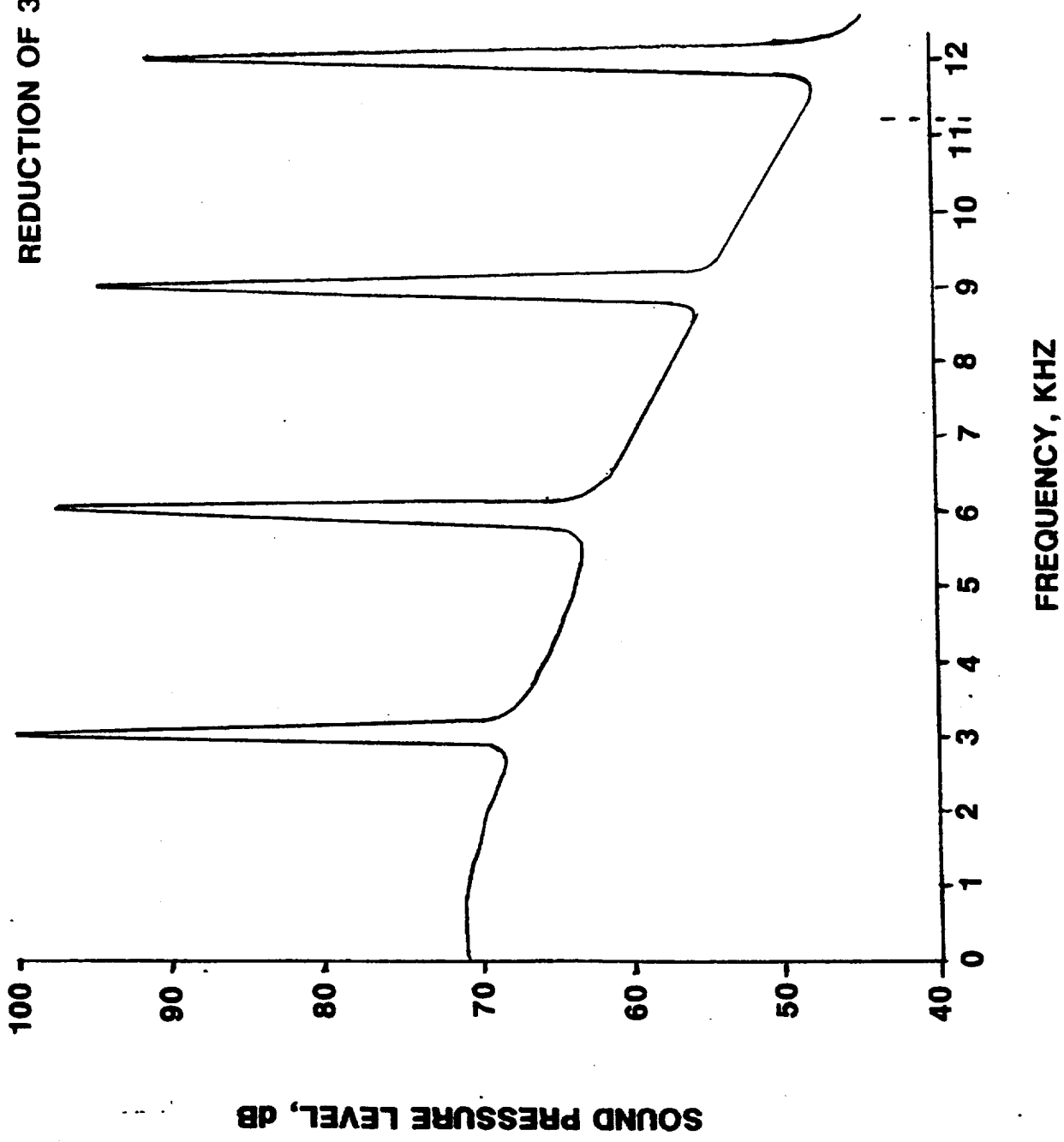


FIGURE 1 FAN SPECTRA  
A. BASELINE FAN

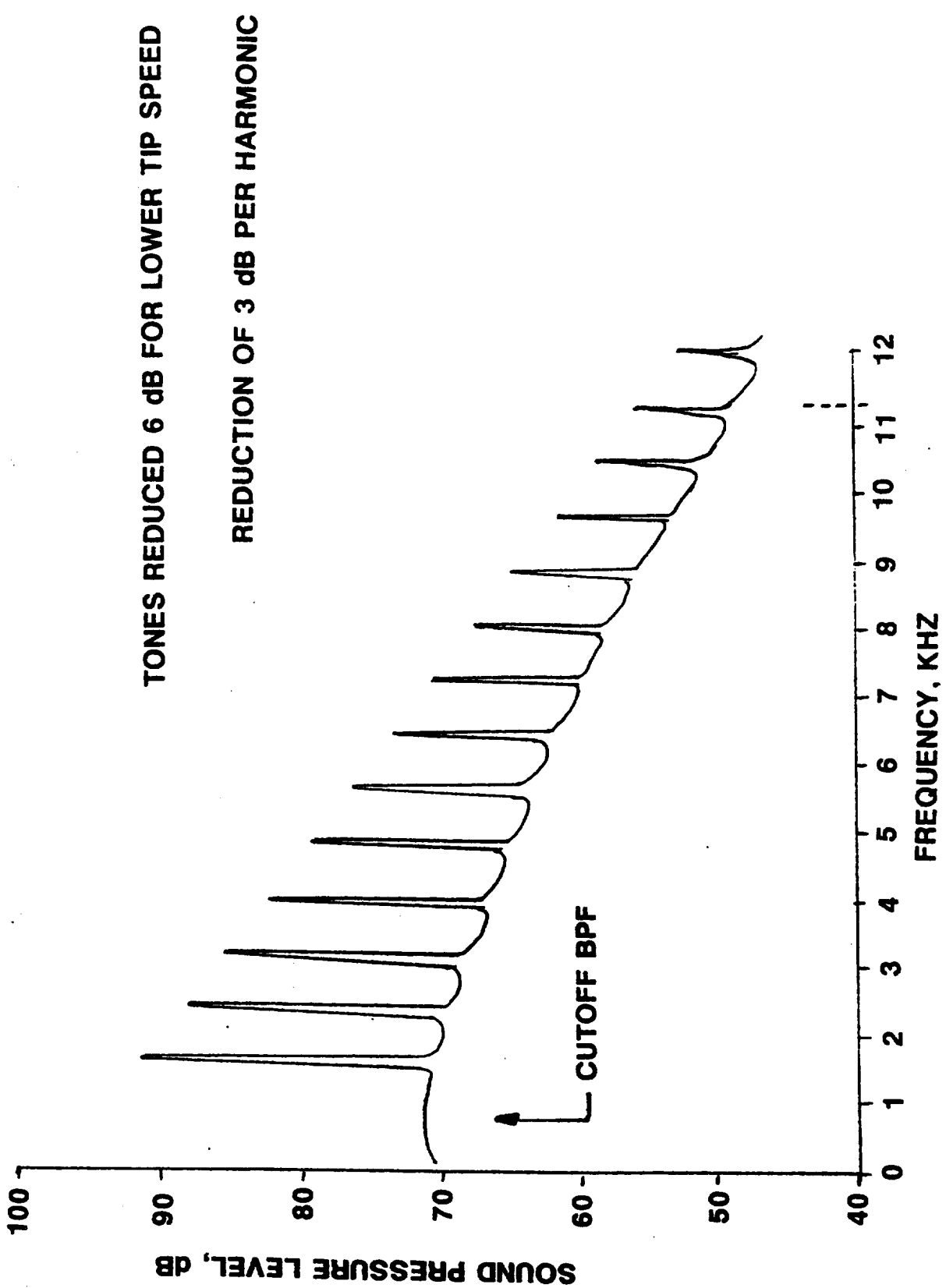


FIGURE 1 CONTINUED  
B. CONVENTIONAL FAN

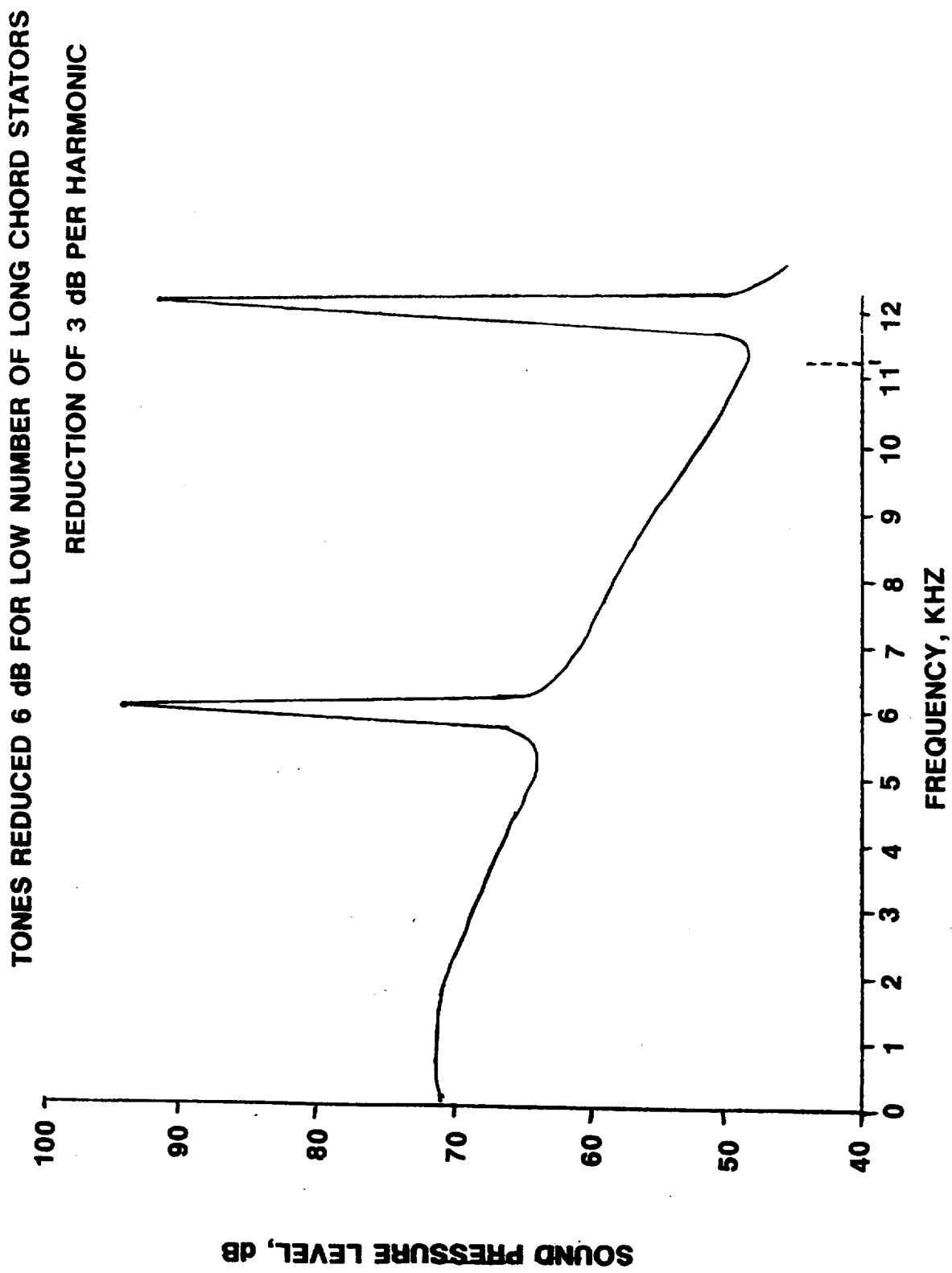


FIGURE 1 CONCLUDED

C. ALTERNATIVE LOW NOISE FAN

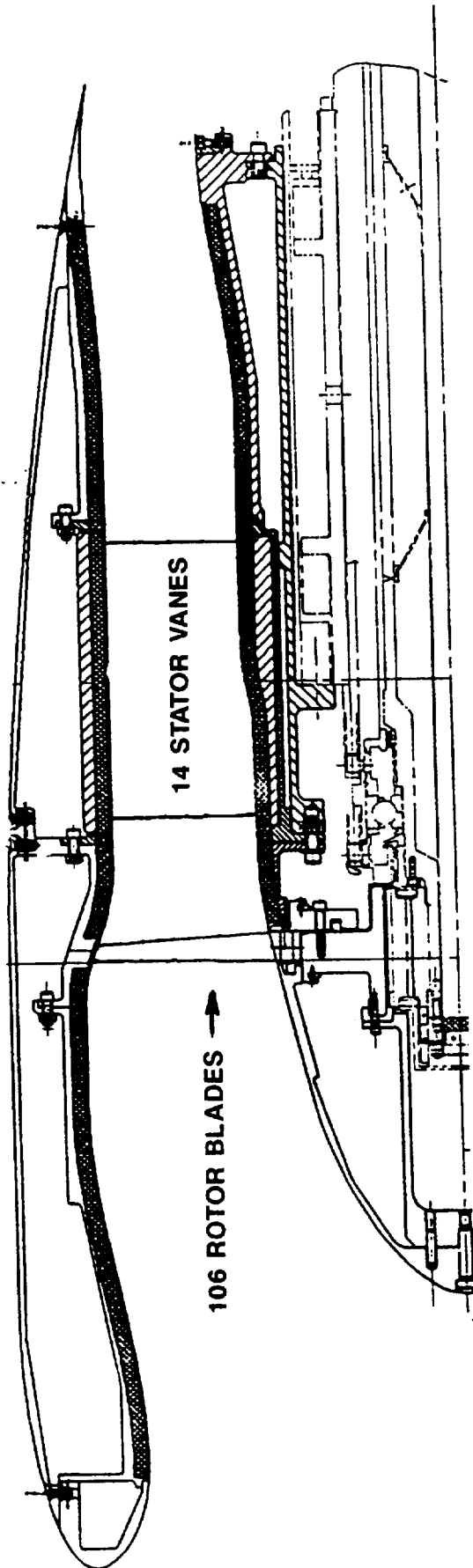
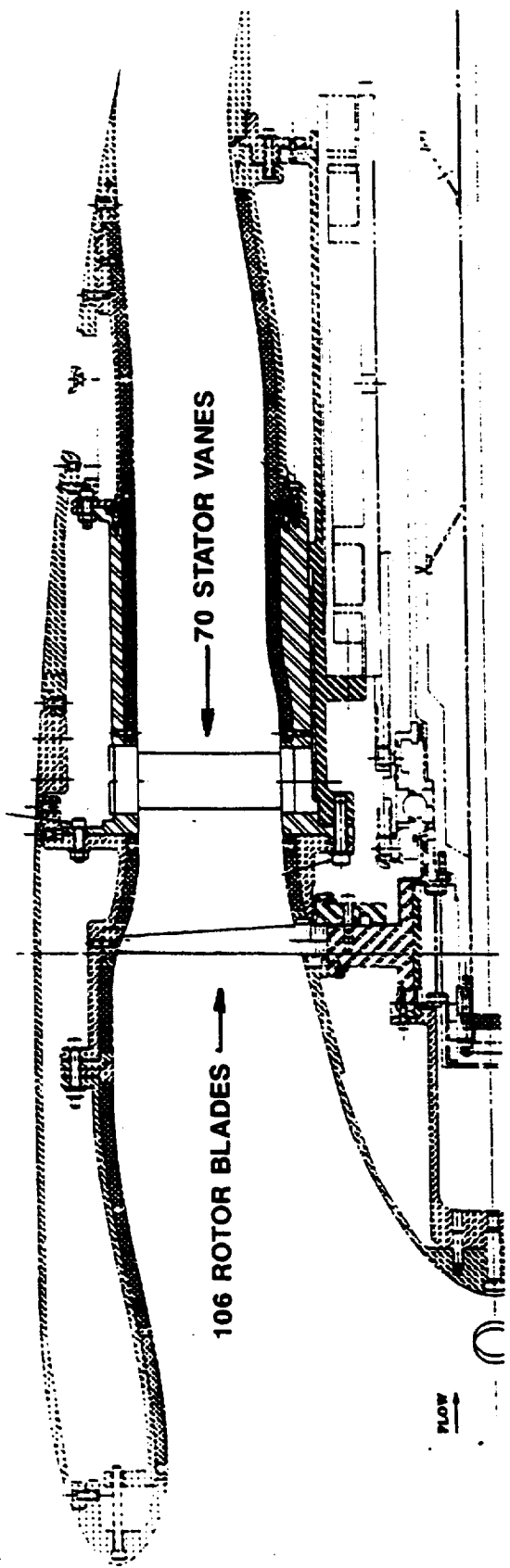


FIGURE 2 ALTERNATIVE LOW NOISE FAN

A. 14 VANE STATOR



**FIGURE 2 CONCLUDED**

**B. 70 VANE STATOR**

**FIGURE 3. ACOUSTIC TREATMENT**

**A. DESIGN**

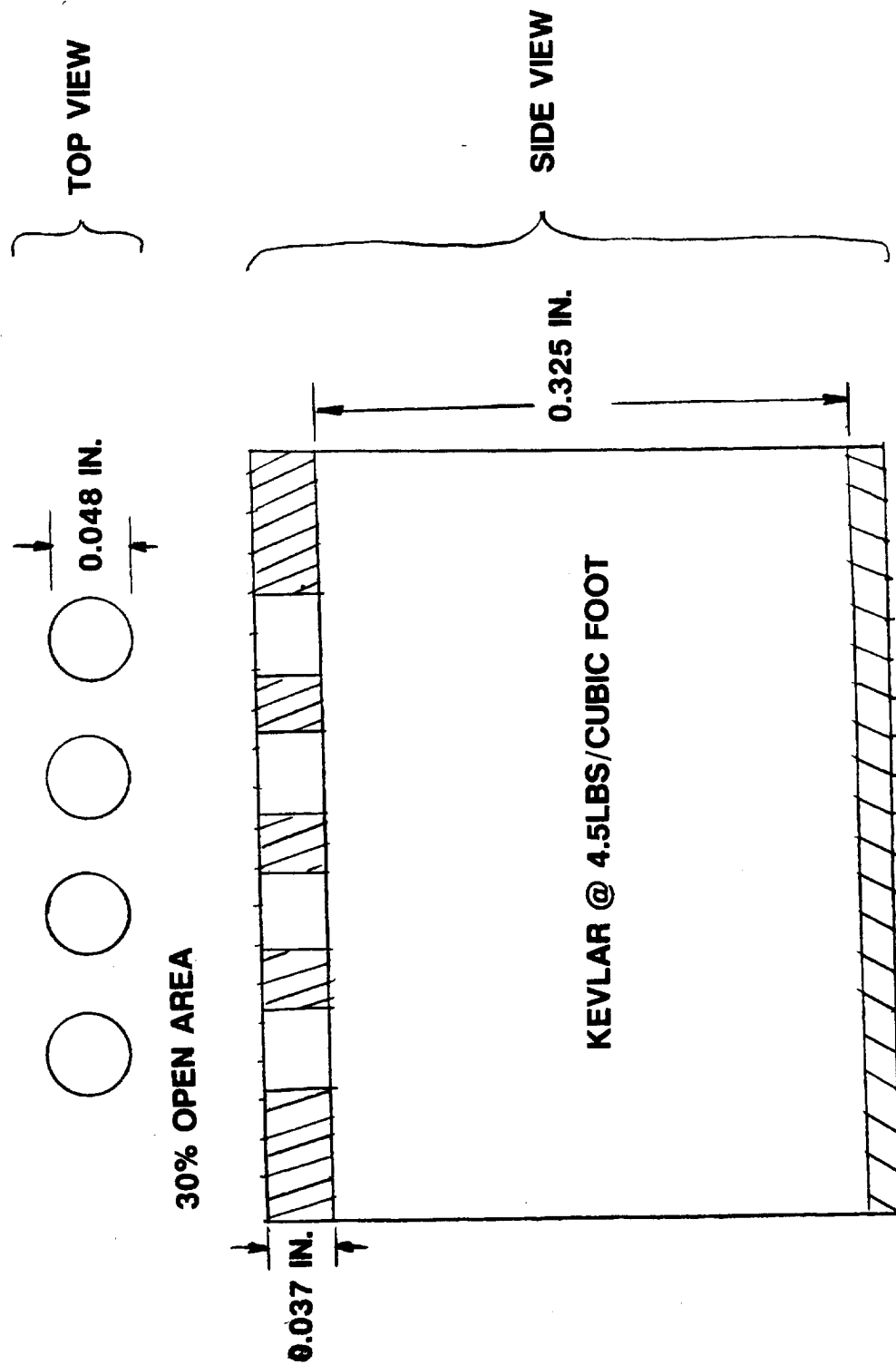


**FIGURE 3. CONCLUDED**

**B. MANUFACTURED**

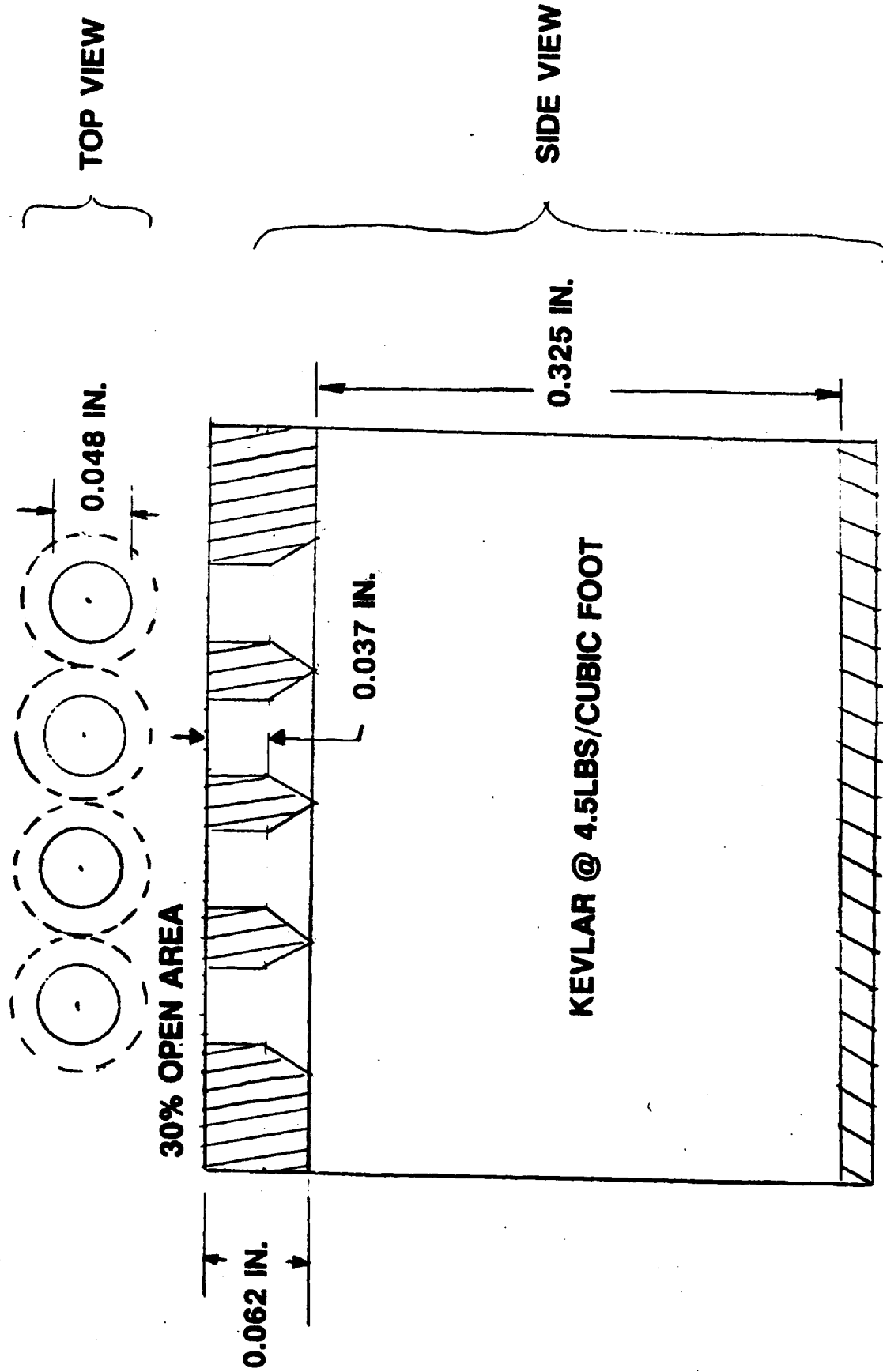


FIGURE 4 ALTERNATIVE LOW NOISE FAN IN WIND TUNNEL

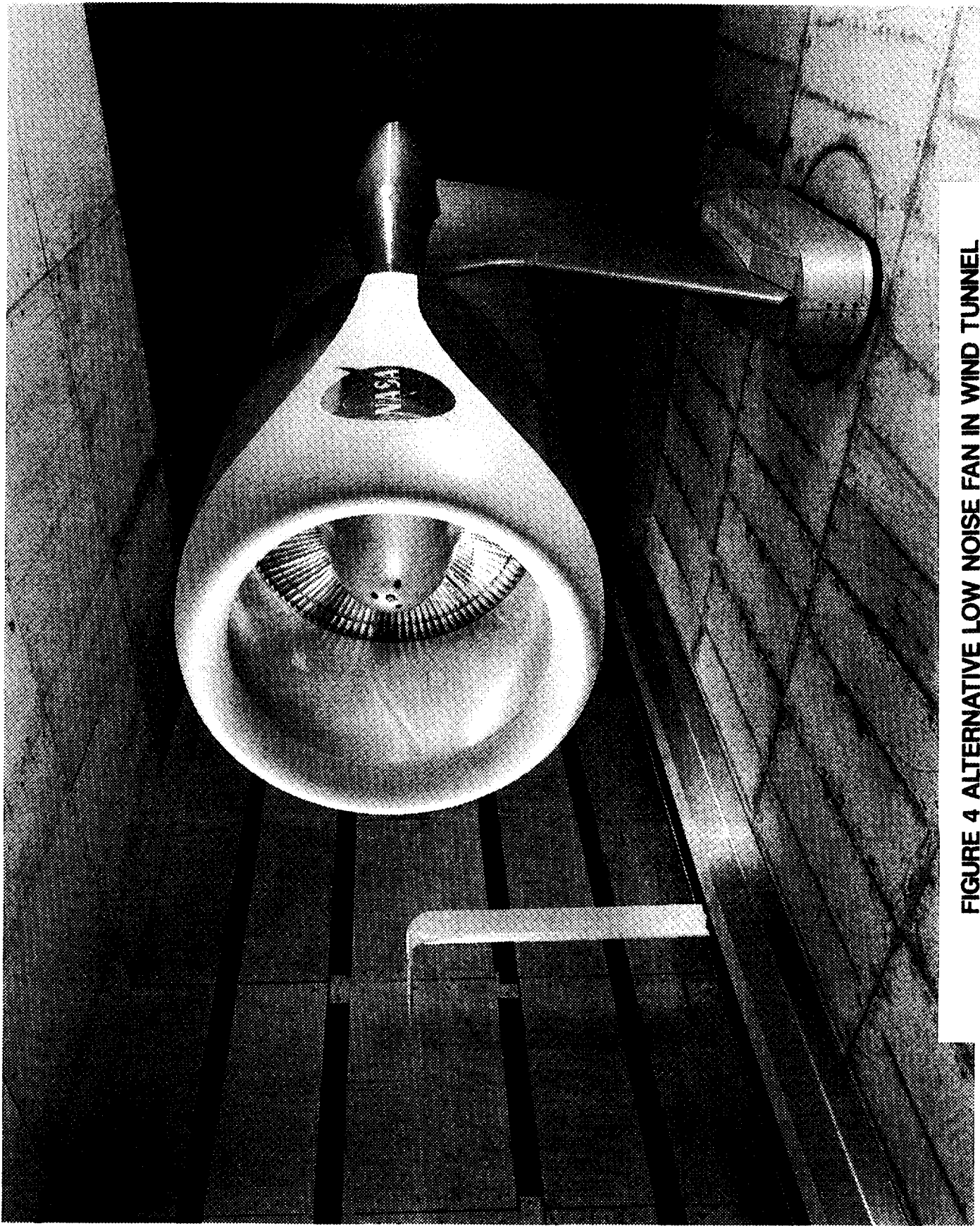
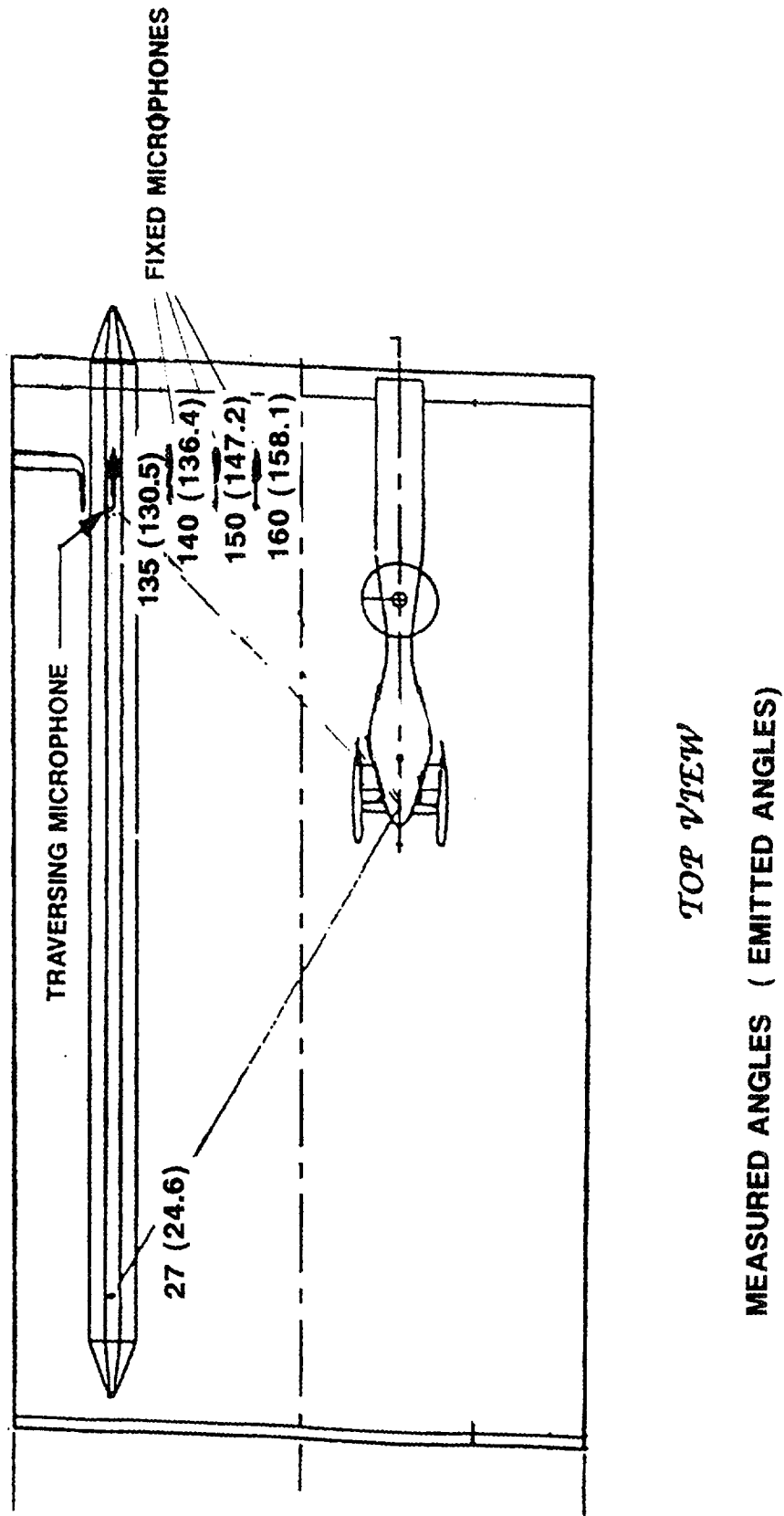
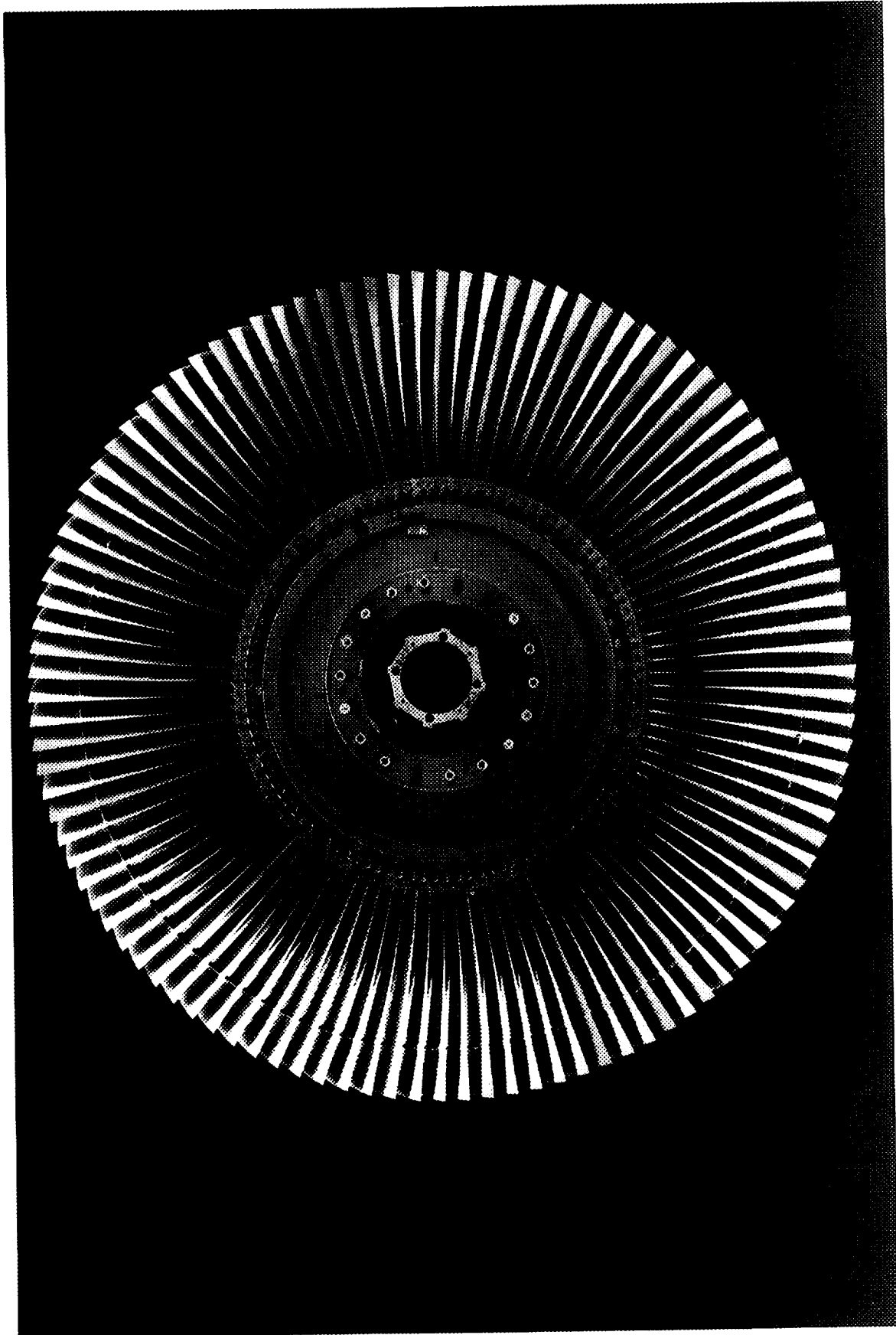
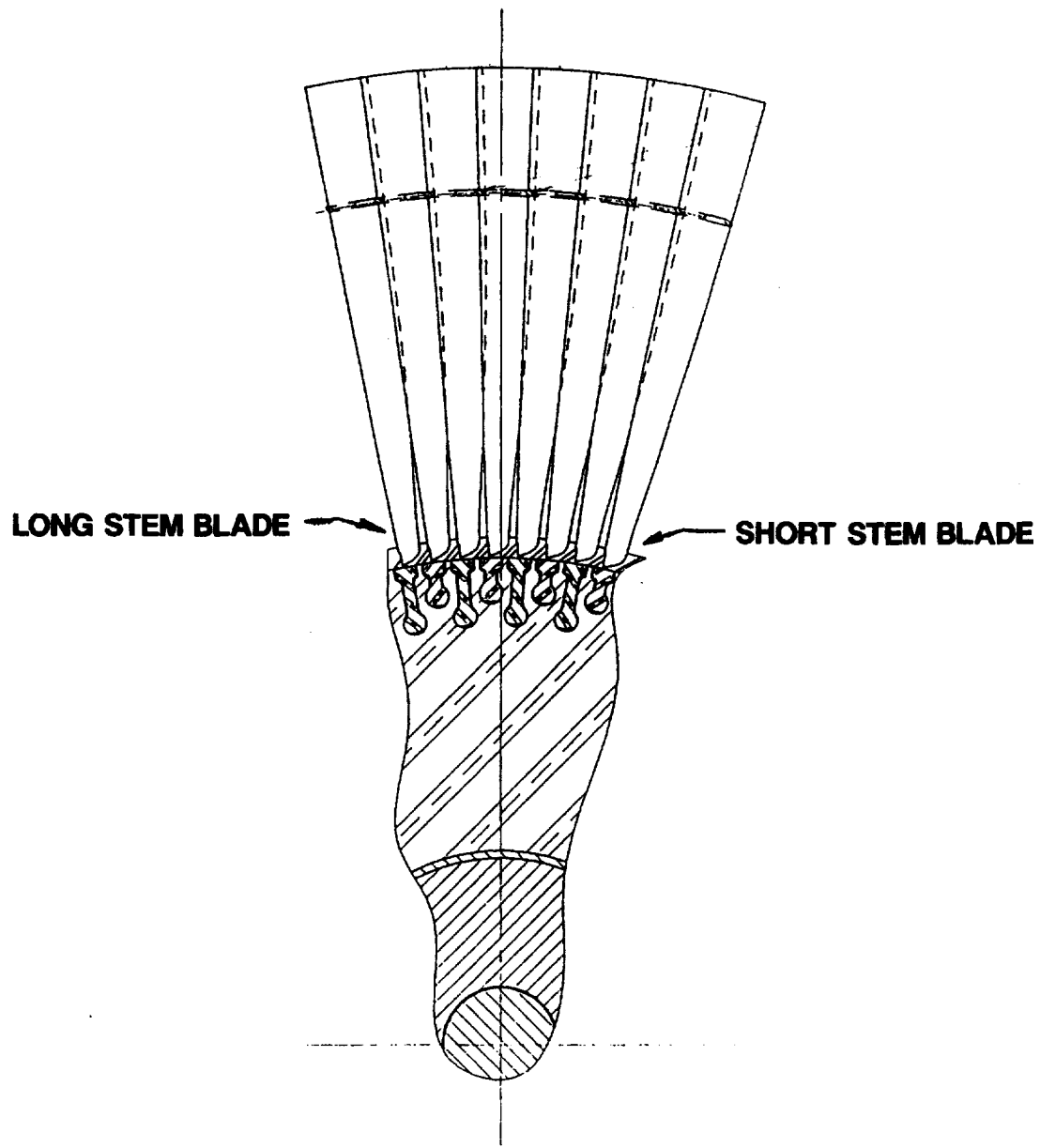


FIGURE 5 MODEL IN 9X15 TEST SECTION





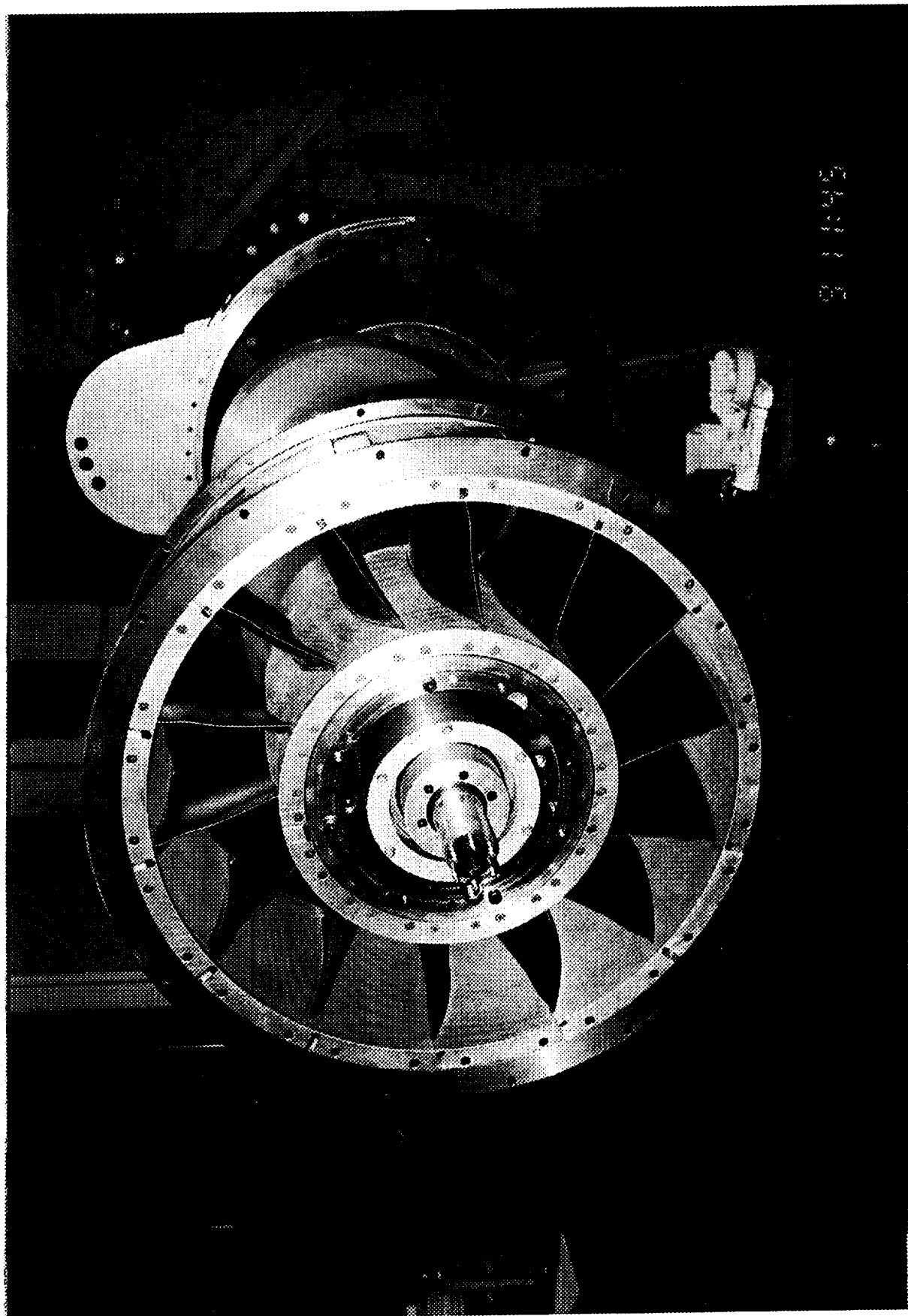
**FIGURE 6. 106 BLADED FAN ROTOR**  
**A. FULL WHEEL**



**FIGURE 6 CONTINUED**

**B. SECTOR OF WHEEL**

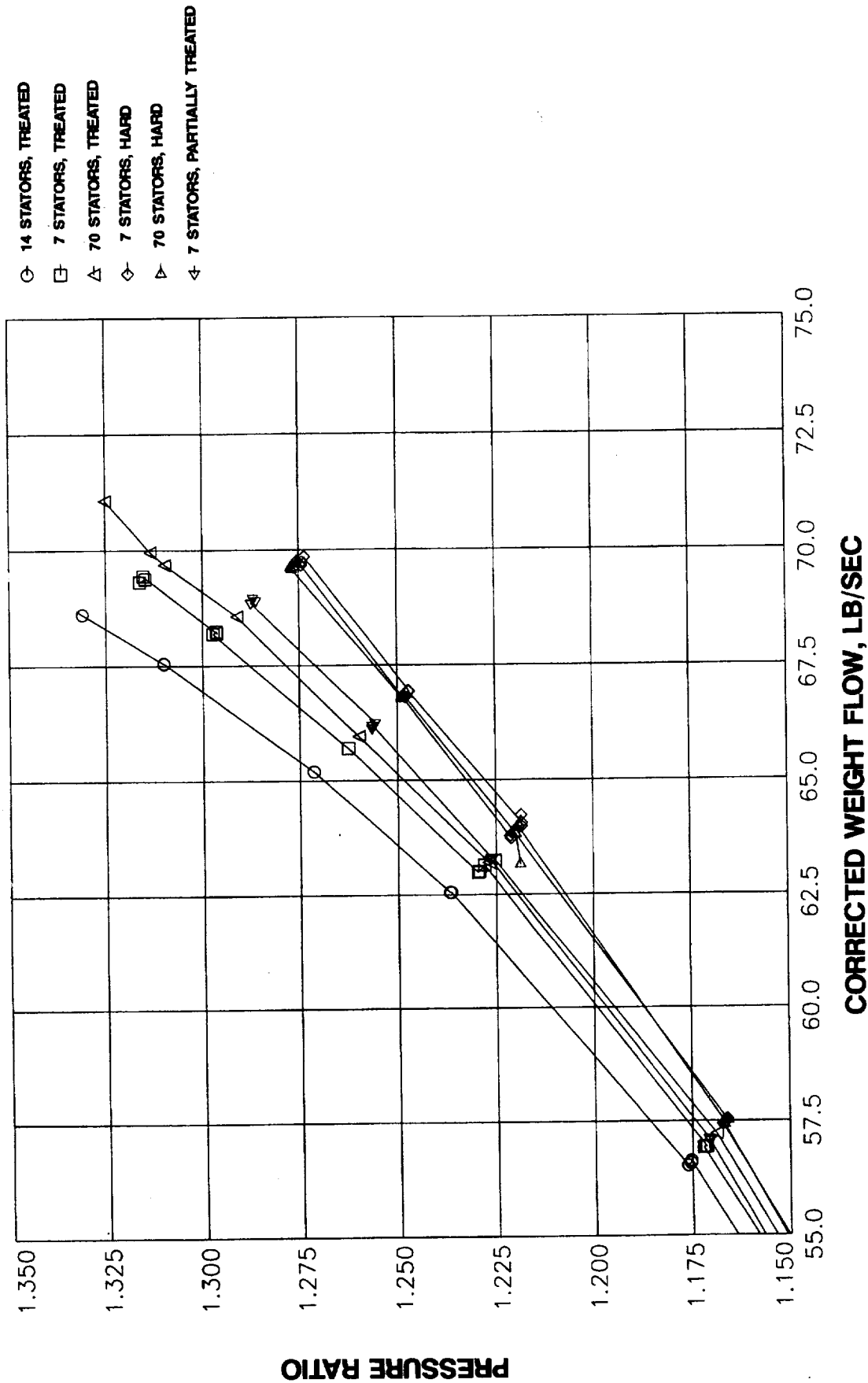
**FIGURE 7. 14 VANE STATOR ASSEMBLY**





**FIGURE 8. 70 VANE STATOR ASSEMBLY**

**FIGURE 9 FAN OPERATING LINES**



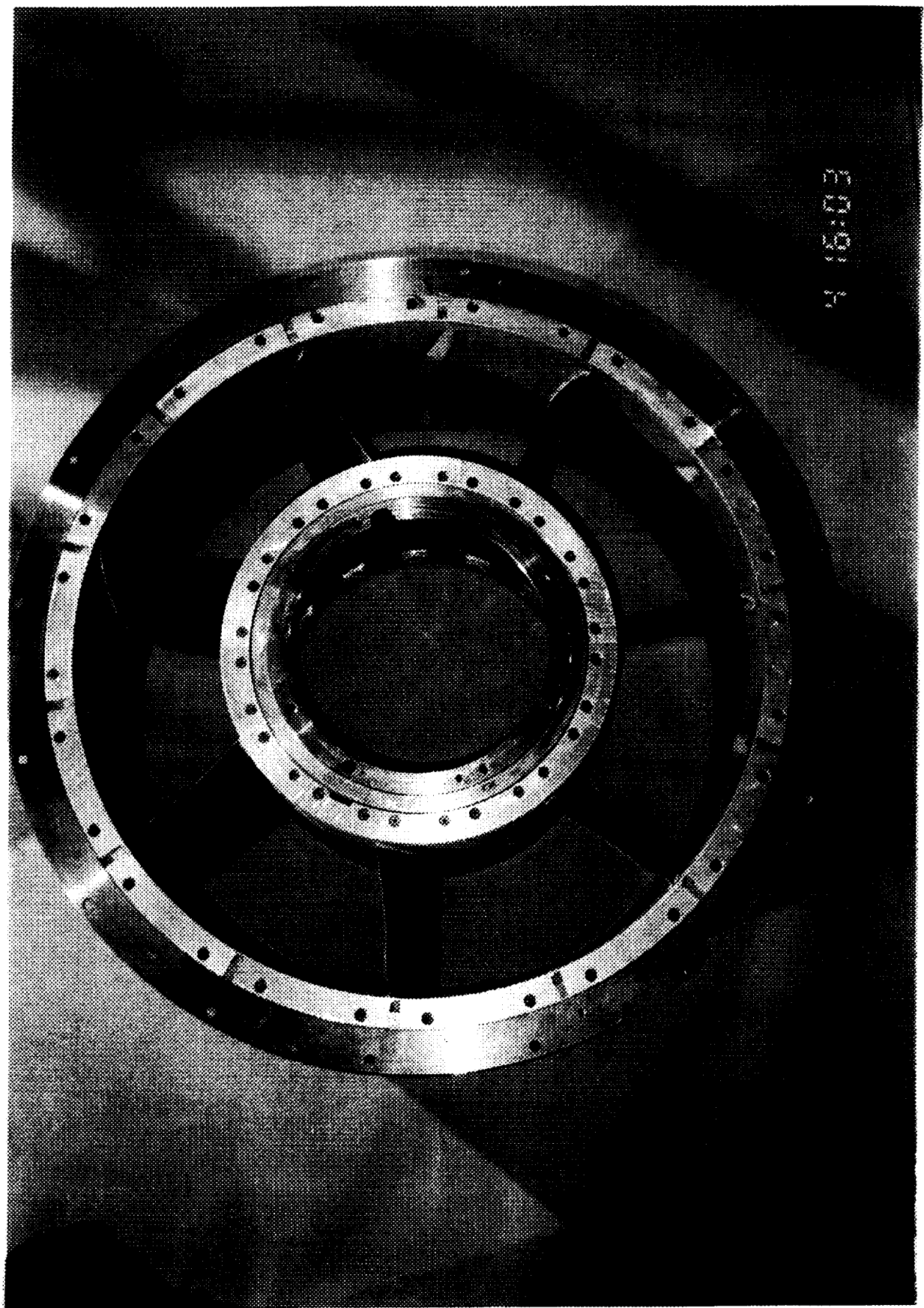
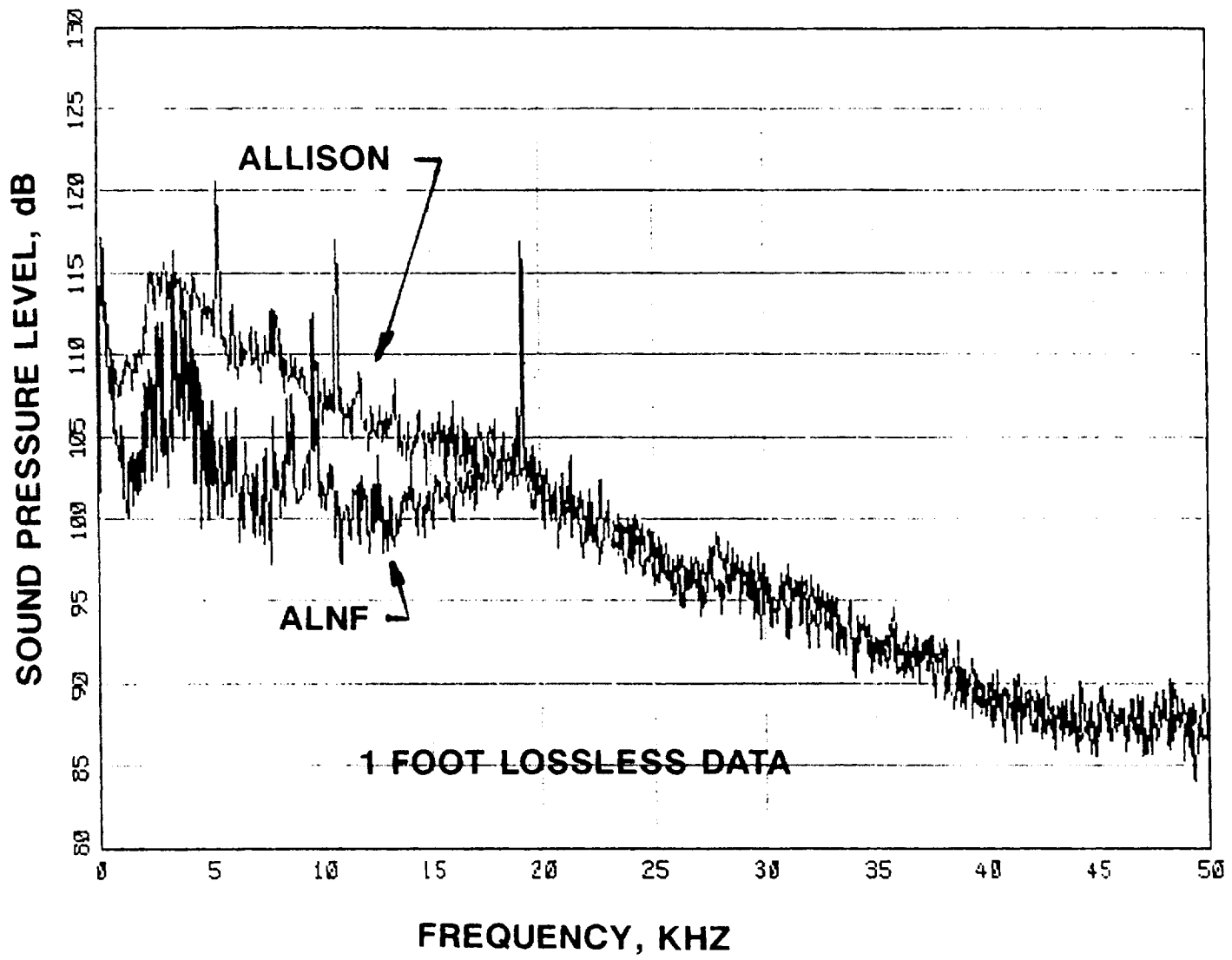


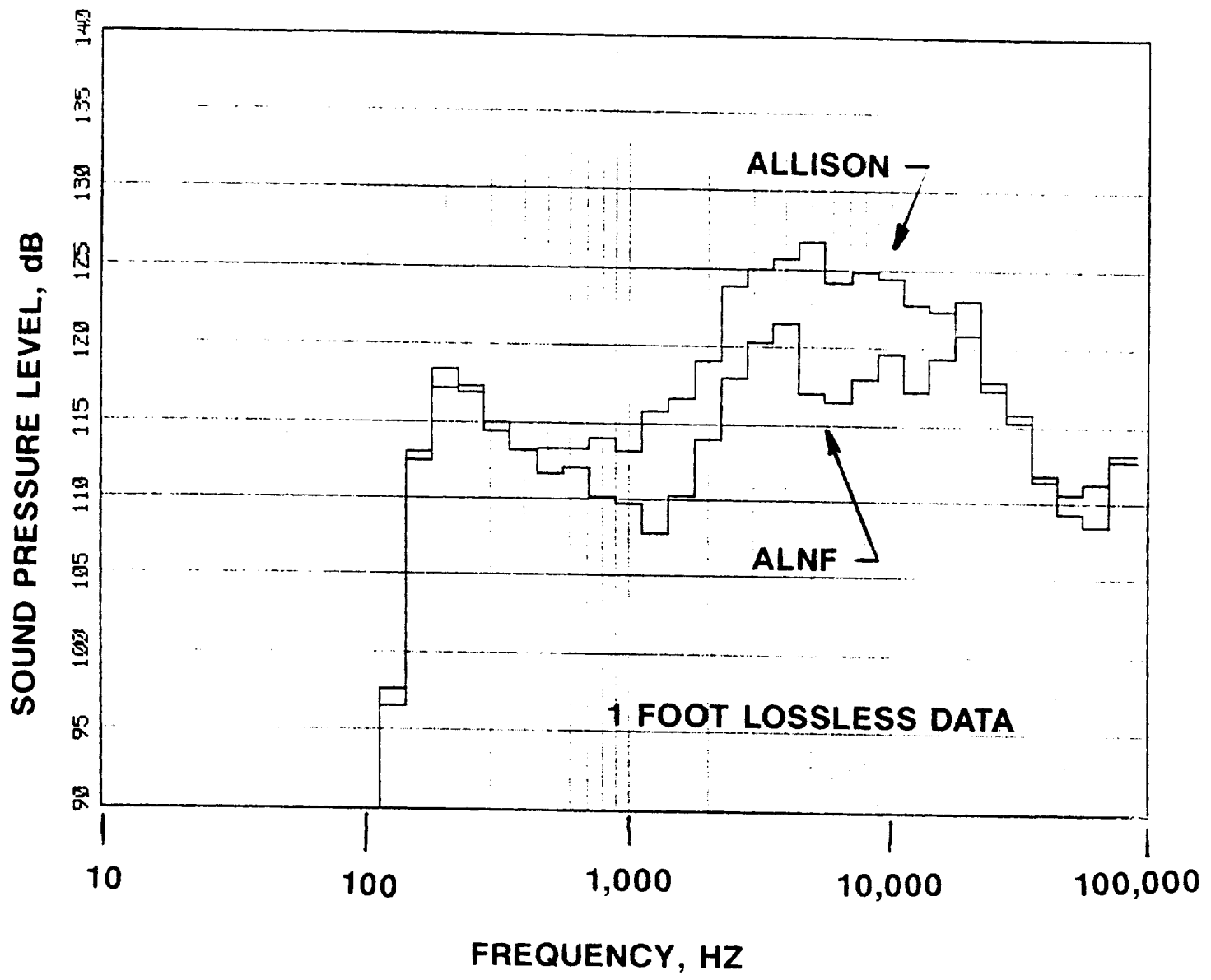
FIGURE 10. 7 VANE STATOR ASSEMBLY



**FIGURE 11 COMPARISON WITH ALLISON FAN**

NOMINAL TAKEOFF, ALLISON 840 FT/SEC, ALNF 1000 FT/SEC

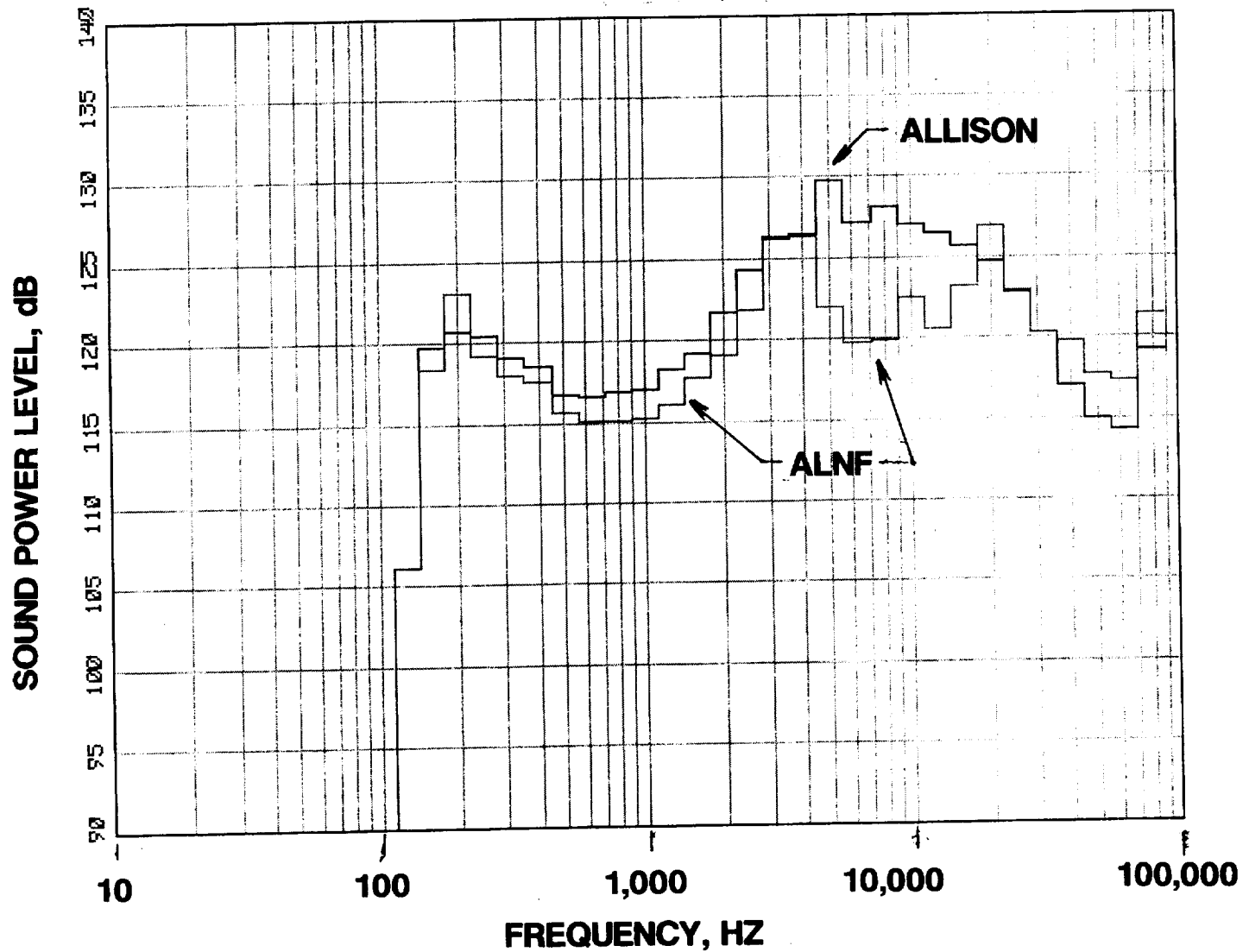
A NARROWBAND DATA AT 92.5 DEGREES EMITTED ANGLE



**FIGURE 11 COMPARISON WITH ALLISON FAN**

NOMINAL TAKEOFF, ALLISON 840 FT/SEC, ALNF 1000 FT/SEC

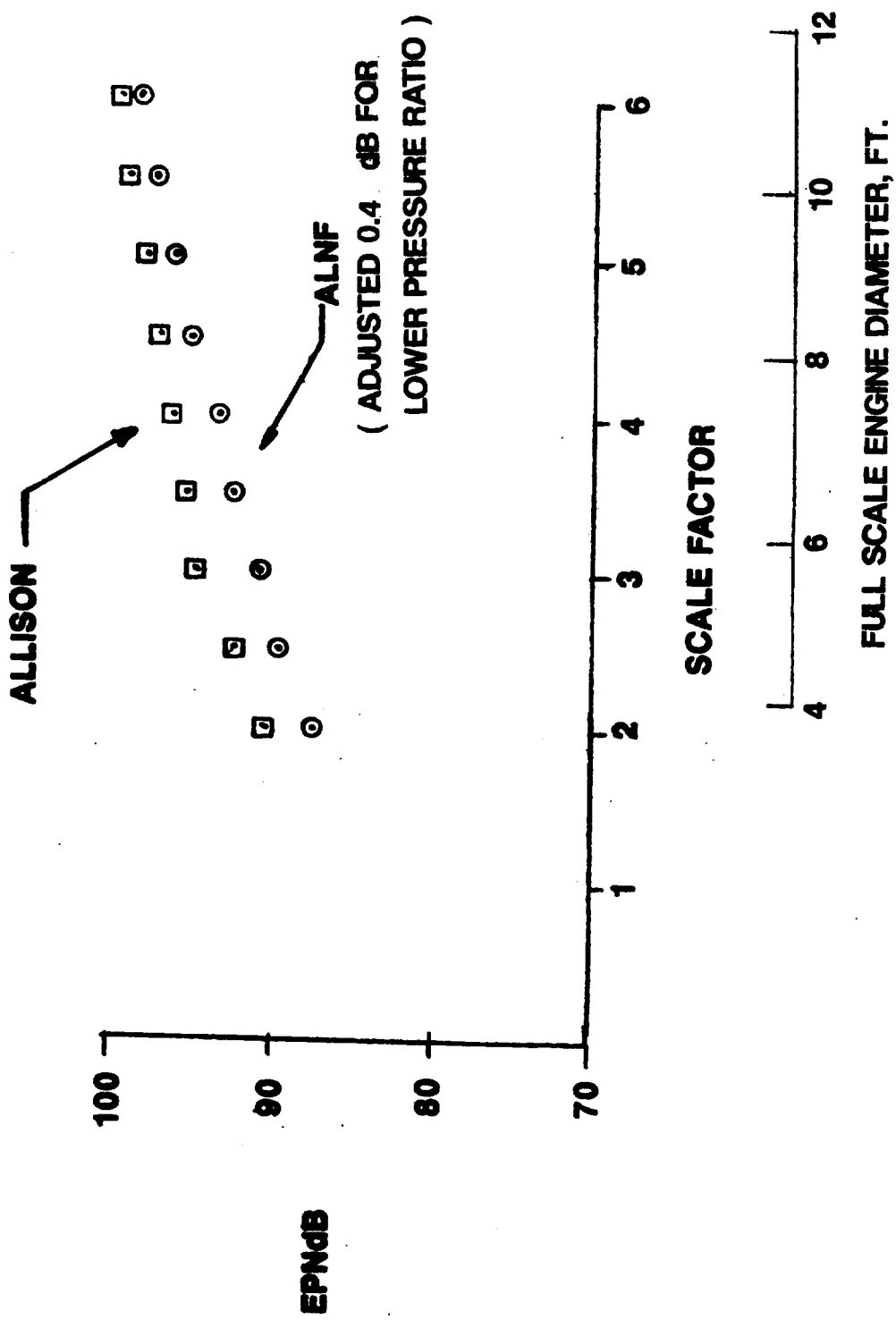
B 1/3RD OCTAVE DATA AT 92.5 DEGREES EMITTED ANGLE

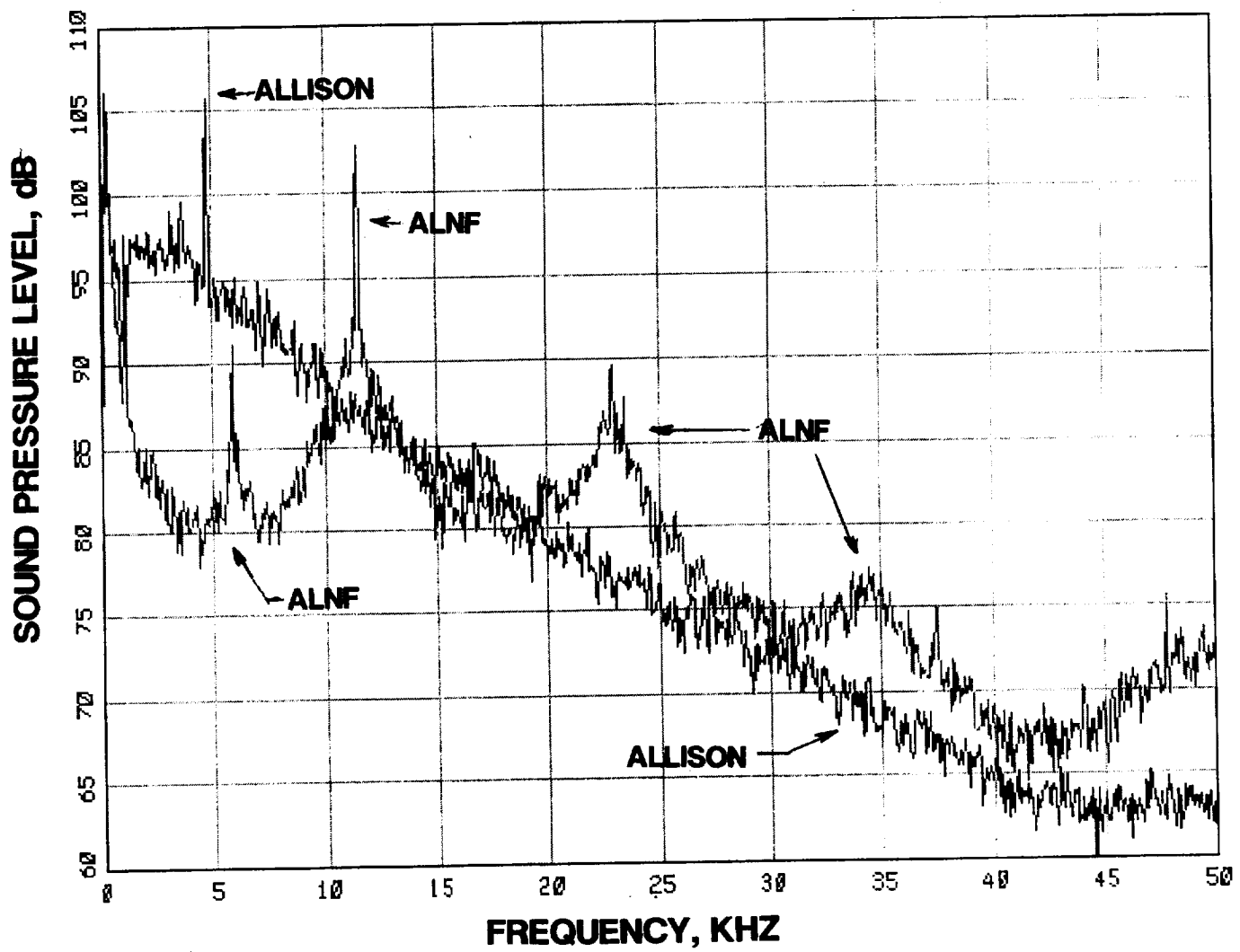


**FIGURE 12 SOUND POWER LEVEL COMPARISON  
WITH ALLISON FAN**

**NOMINAL TAKEOFF, ALLISON 840FT/SEC, ALNF 1000FT/SEC**

**FIGURE 13 FLYOVER NOISE AT 1000 FT, STANDARD DAY  
TAKEOFF CONDITION**

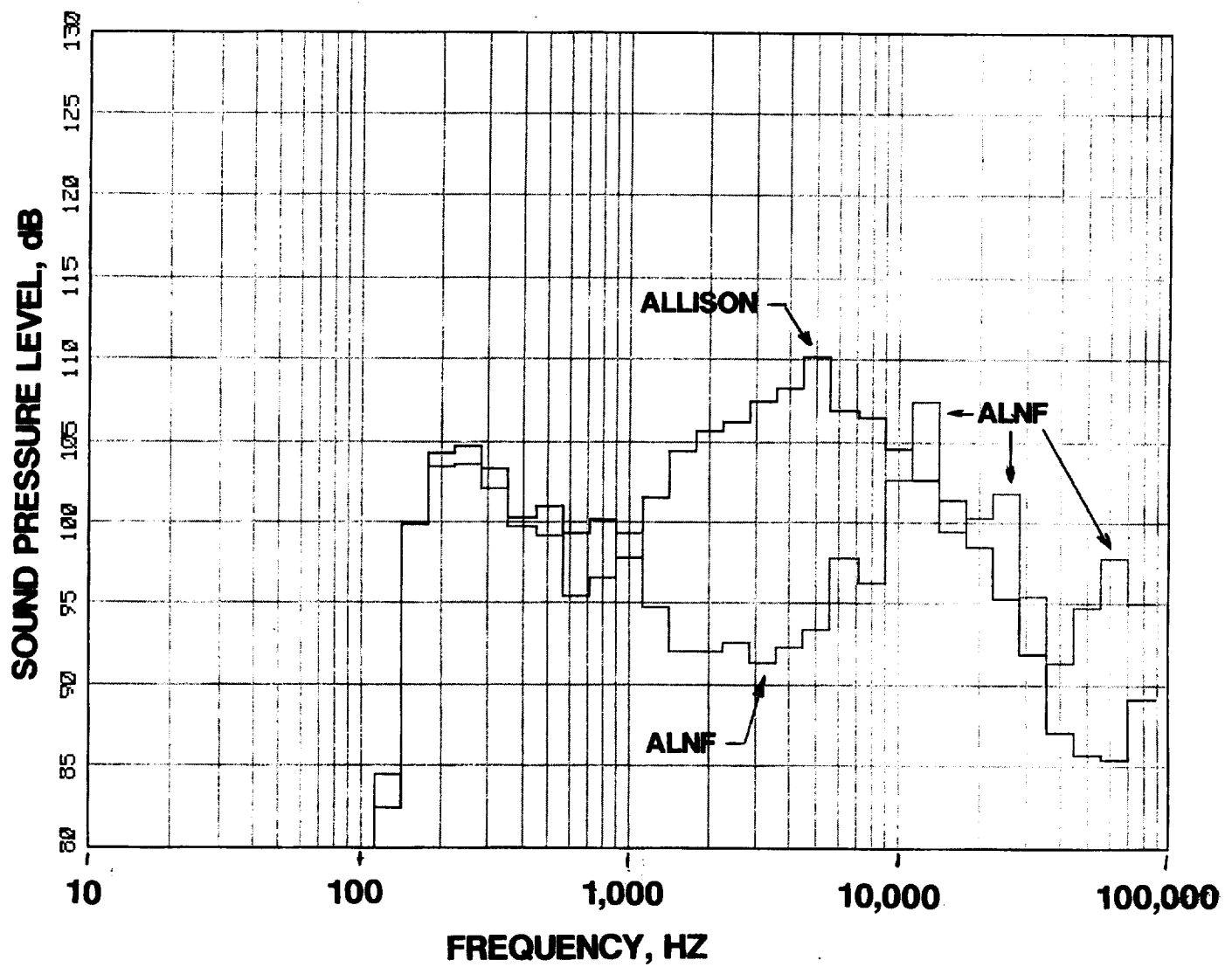




**FIGURE 14 COMPARISON WITH ALLISON FAN**

**NOMINAL APPROACH, ALLISON 500 FT/SEC, ALNF 600FT/SEC**

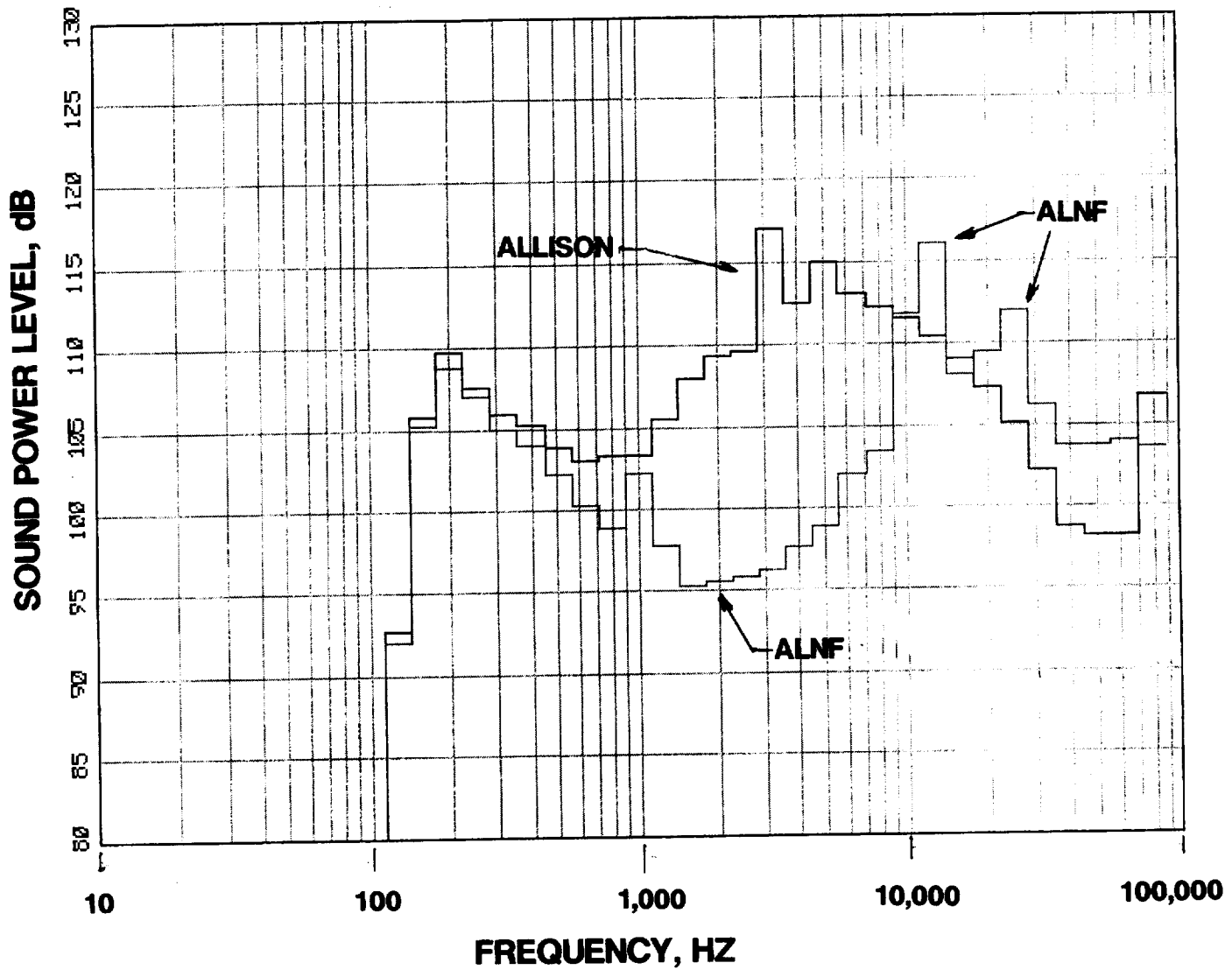
**A. NARROWBAND DATA AT 92.5 DEGREES EMITTED ANGLE**



**FIGURE 14 COMPARISON WITH ALLISON FAN**

NOMINAL APPROACH, ALLISON 500 FT/SEC, ALNF 600 FT/SEC

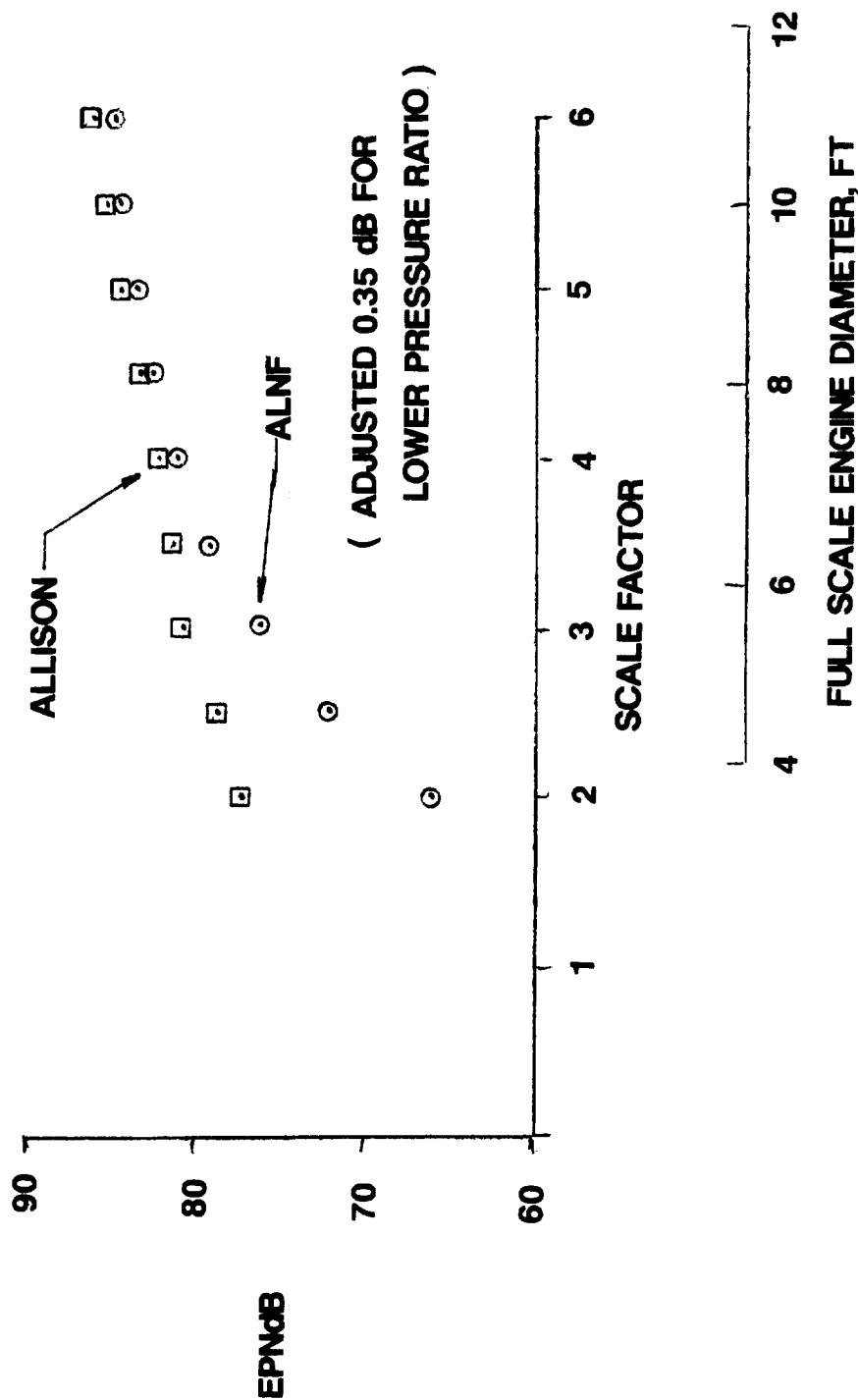
## B. 1/3RD OCTAVE DATA AT 92.5 DEGREES EMITTED ANGLE



**FIGURE 15 SOUND POWER LEVEL COMPARISON  
WITH ALLISON FAN**

**NOMINAL APPROACH, ALLISON 500 FT/SEC, ALNF 600 FT/SEC**

**FIGURE 16 FLYOVER NOISE AT 1000 FT, STANDARD DAY  
APPROACH CONDITION**



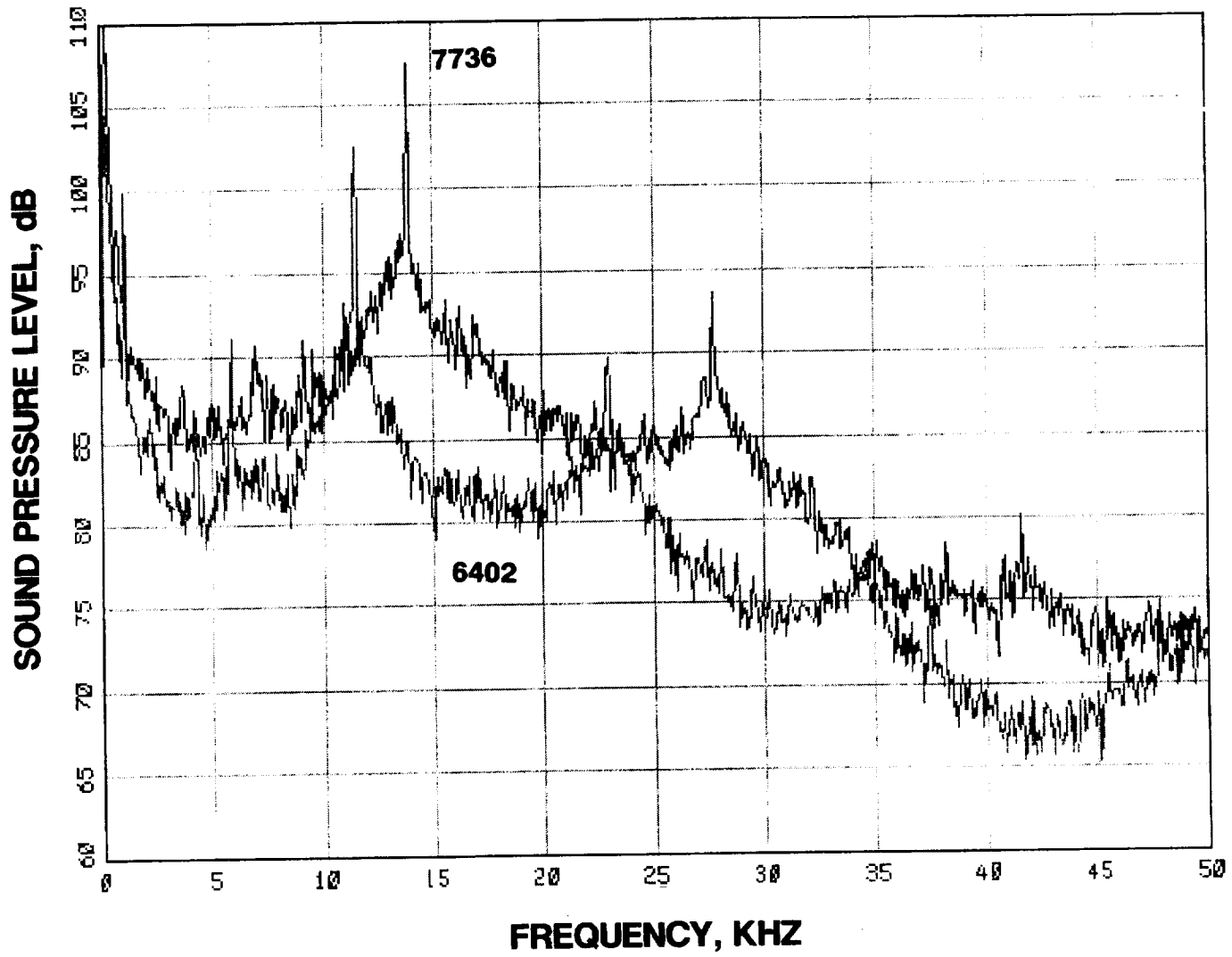
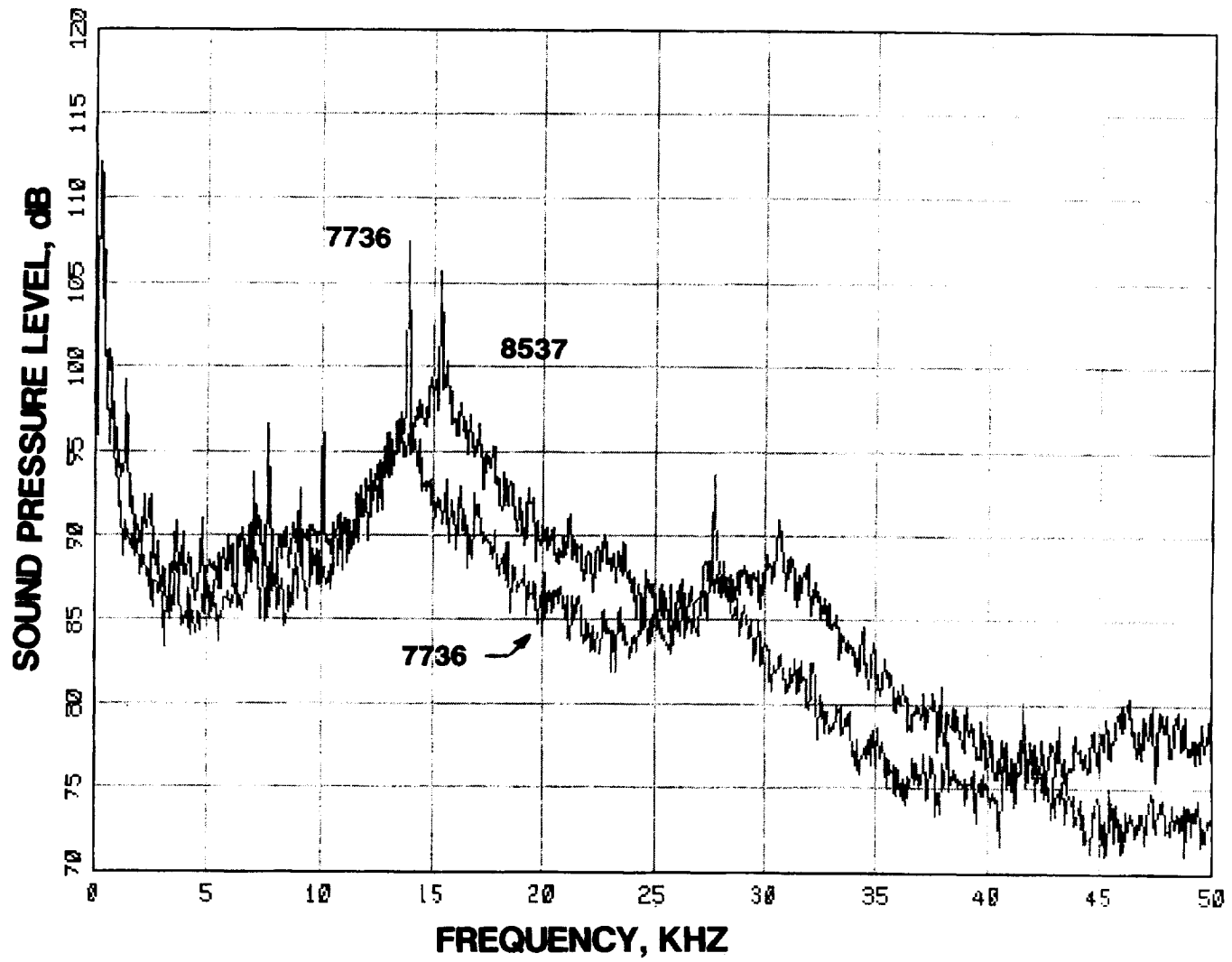


**FIGURE 17 COMPARISON OF SOUND PRESSURE LEVEL**

**AT DIFFERENT SPEEDS**

**A. 7736 RPMC, 6402 RPMC**

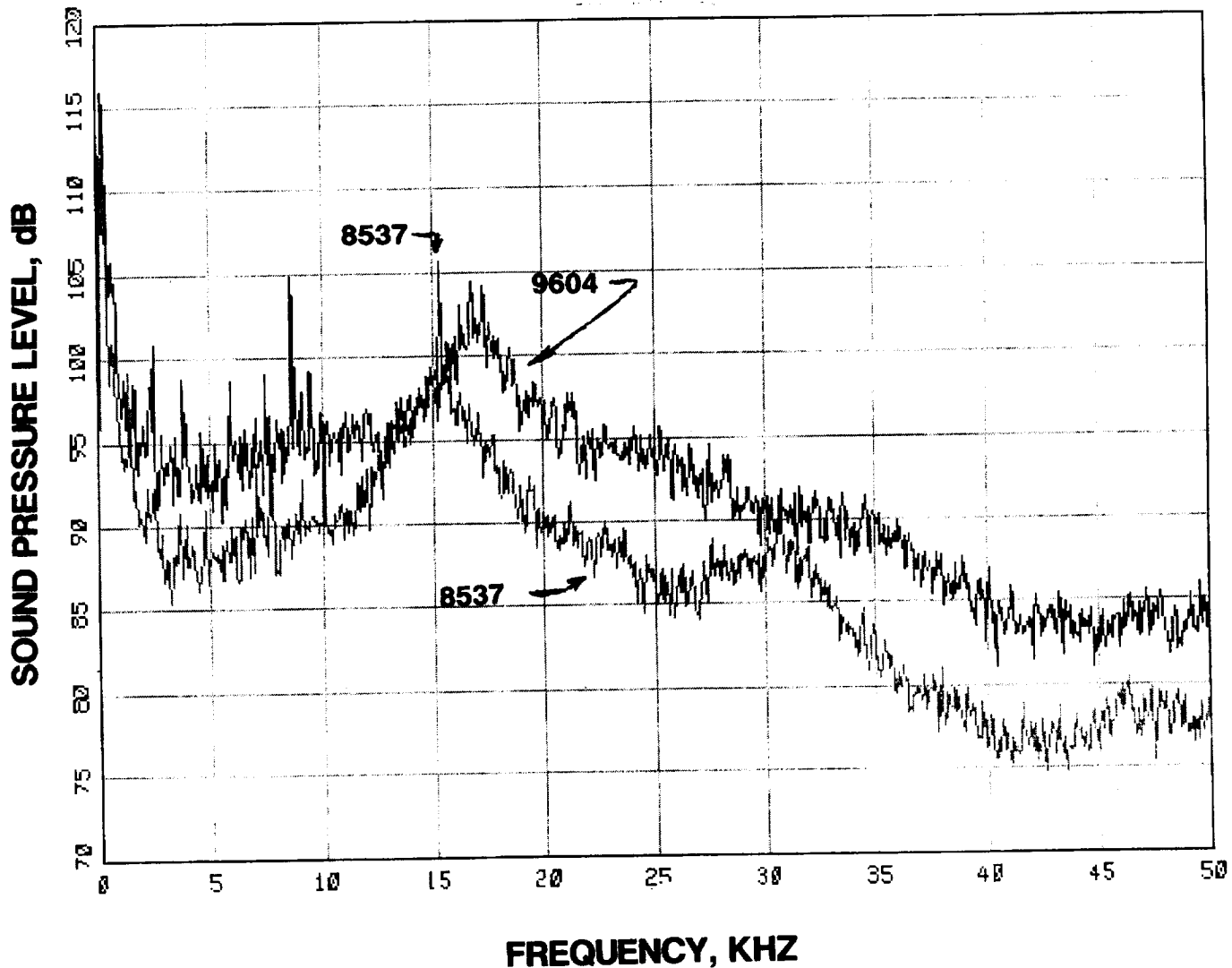
**92.5 DEGREES EMITTED ANGLE**



**FIGURE 17 CONTINUED**

**B. 8537 RPMC, 7736 RPMC**

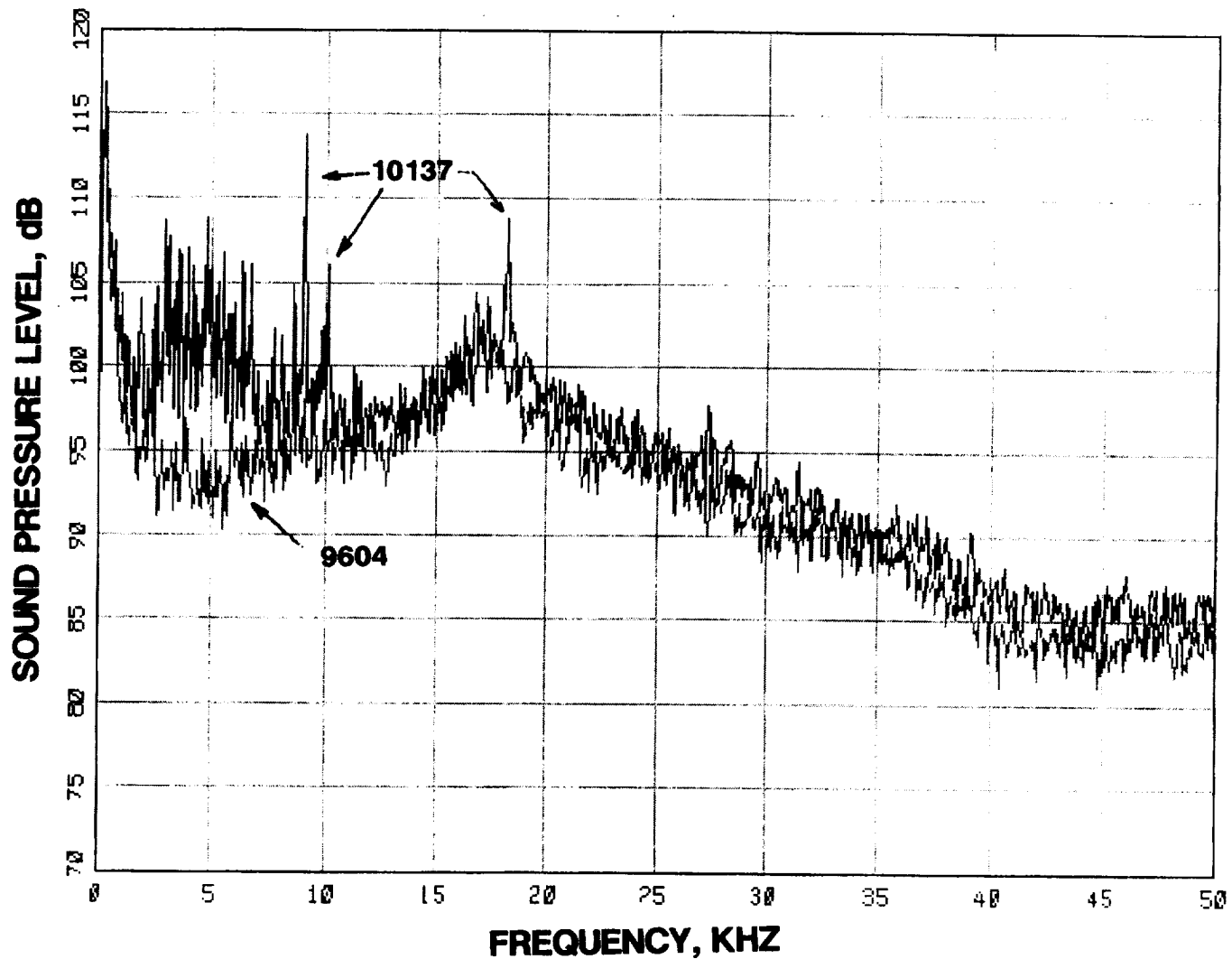
**92.5 DEGREES EMITTED ANGLE**



**FIGURE 17 CONTINUED**

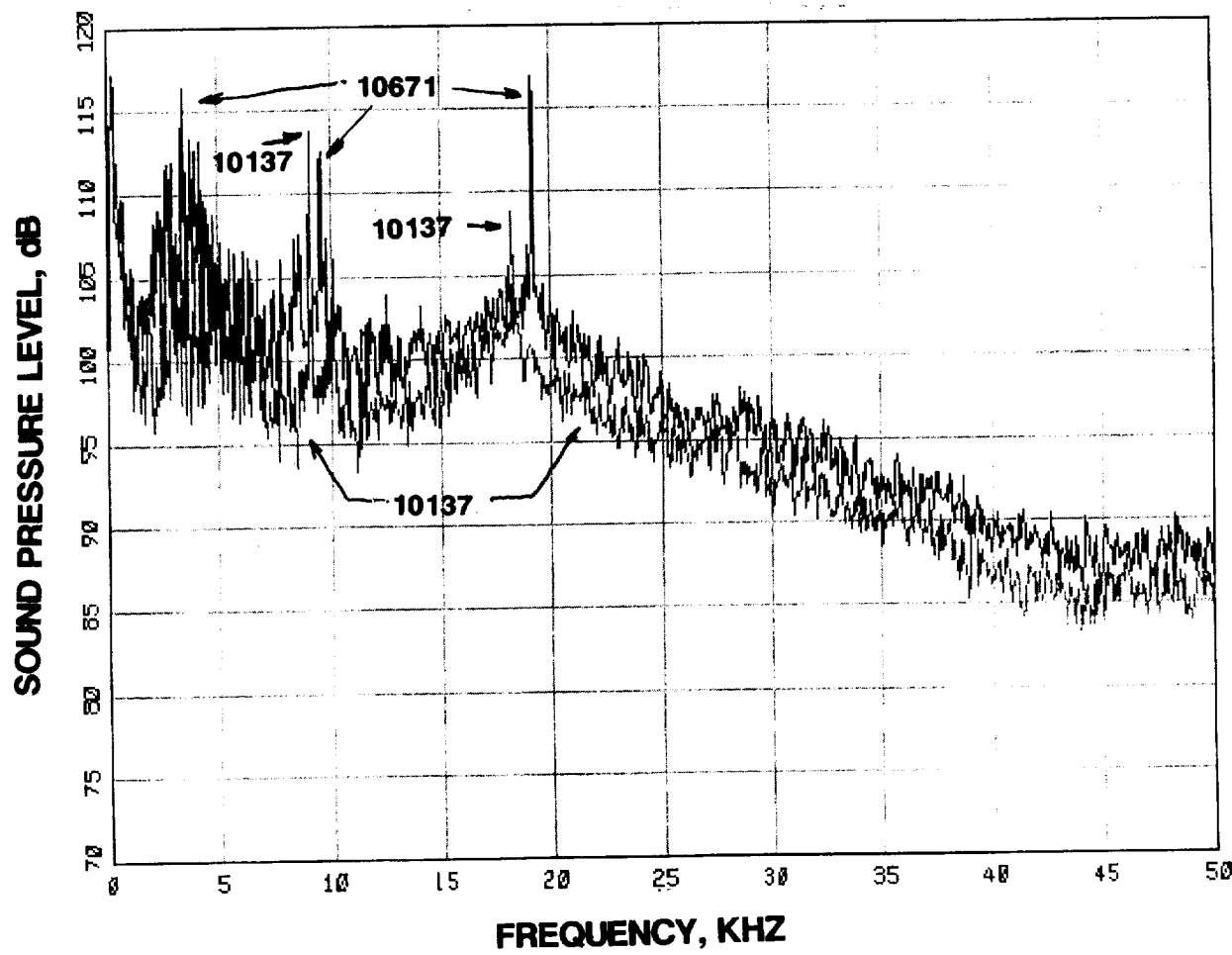
**C. 9604 RPMC, 8537 RPMC**

**92.5 DEGREES EMITTED ANGLE**



**FIGURE 17 CONTINUED**

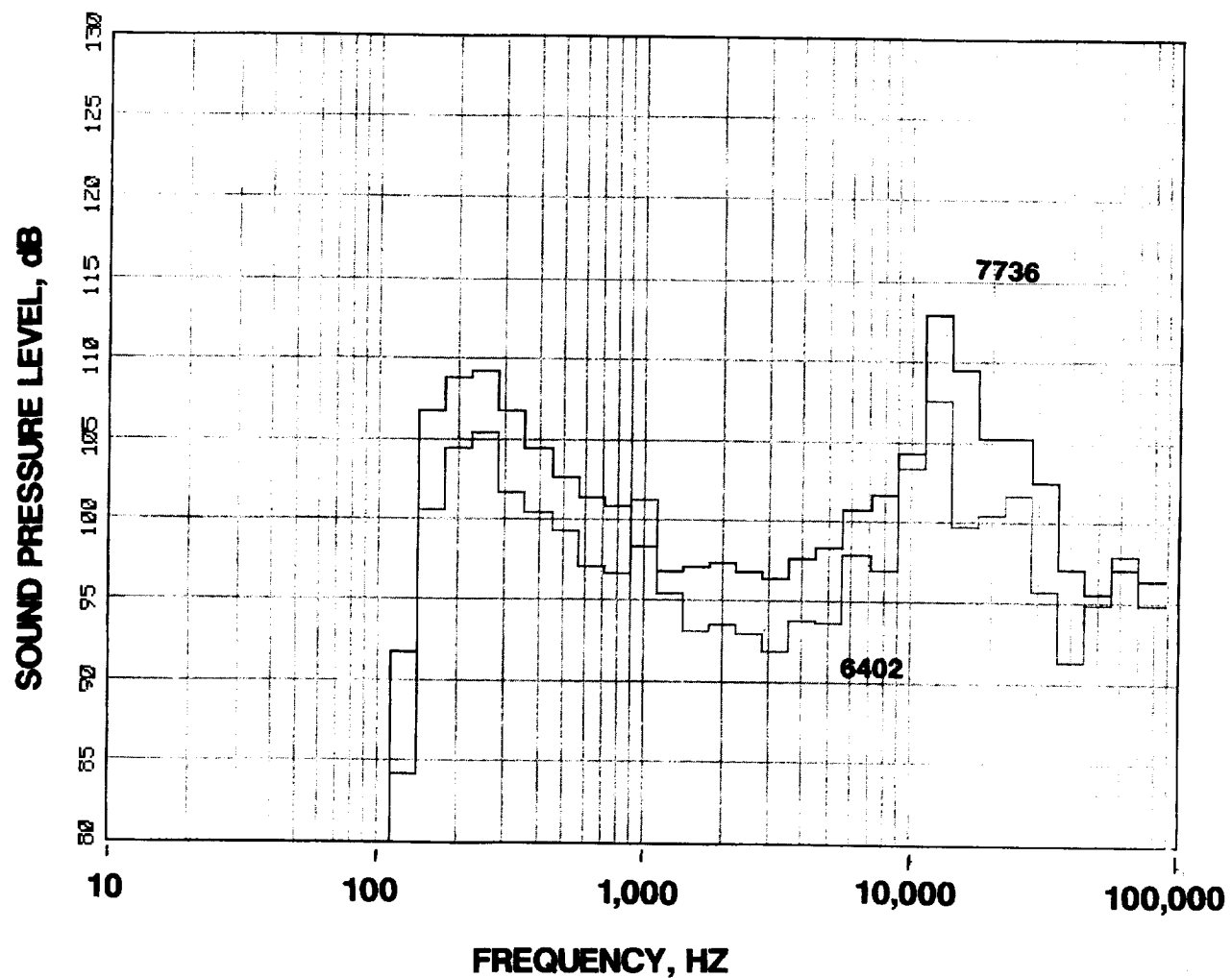
**D. 10137 RPMC, 9604 RPMC  
92.5 DEGREES EMITTED ANGLE**



**FIGURE 17 CONCLUDED**

**E. 10671 RPMC, 10137 RPMC**

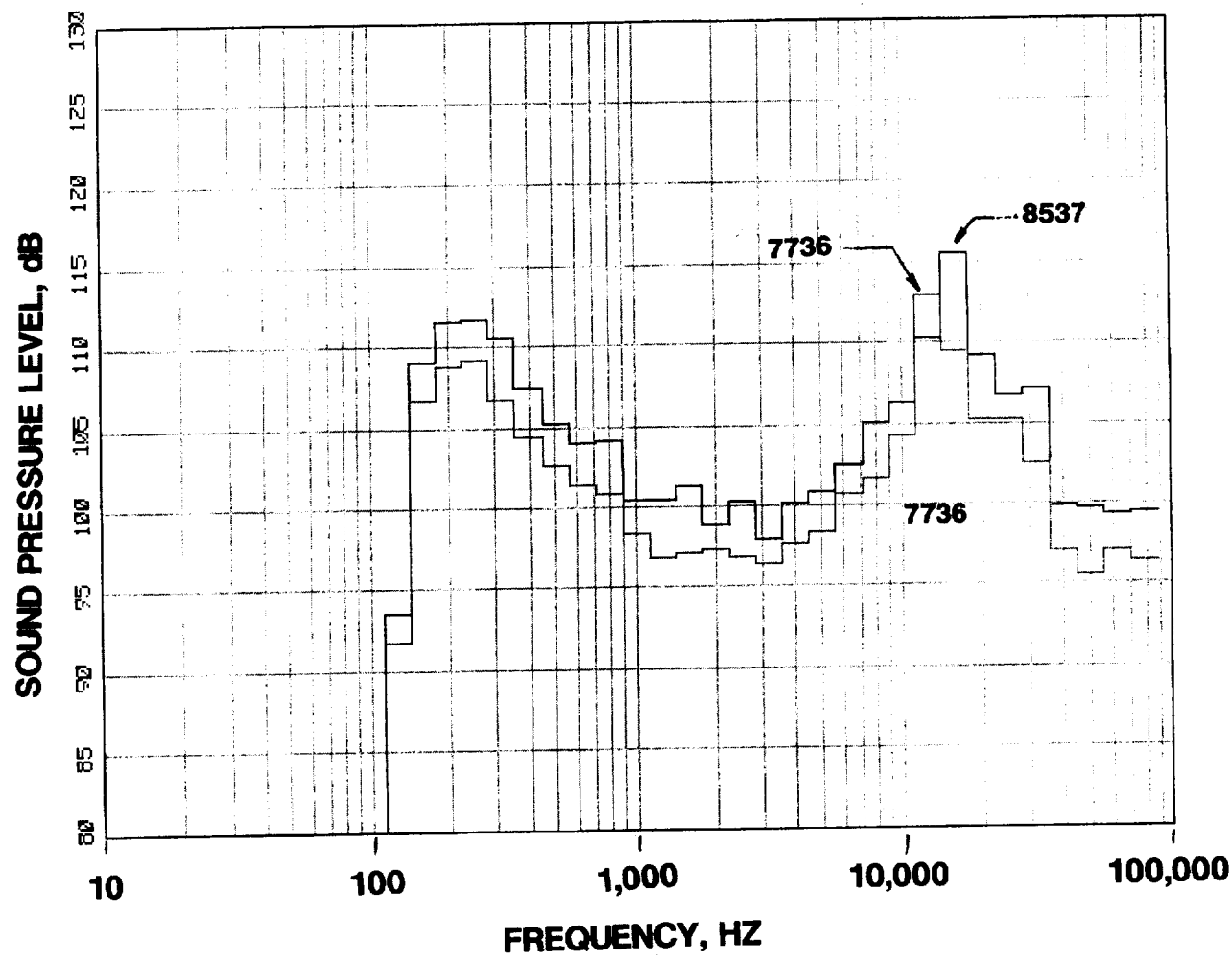
**92.5 DEGREES EMITTED ANGLE**



**FIGURE 18 COMPARISON OF SOUND PRESSURE LEVEL  
AT DIFFERENT SPEEDS**

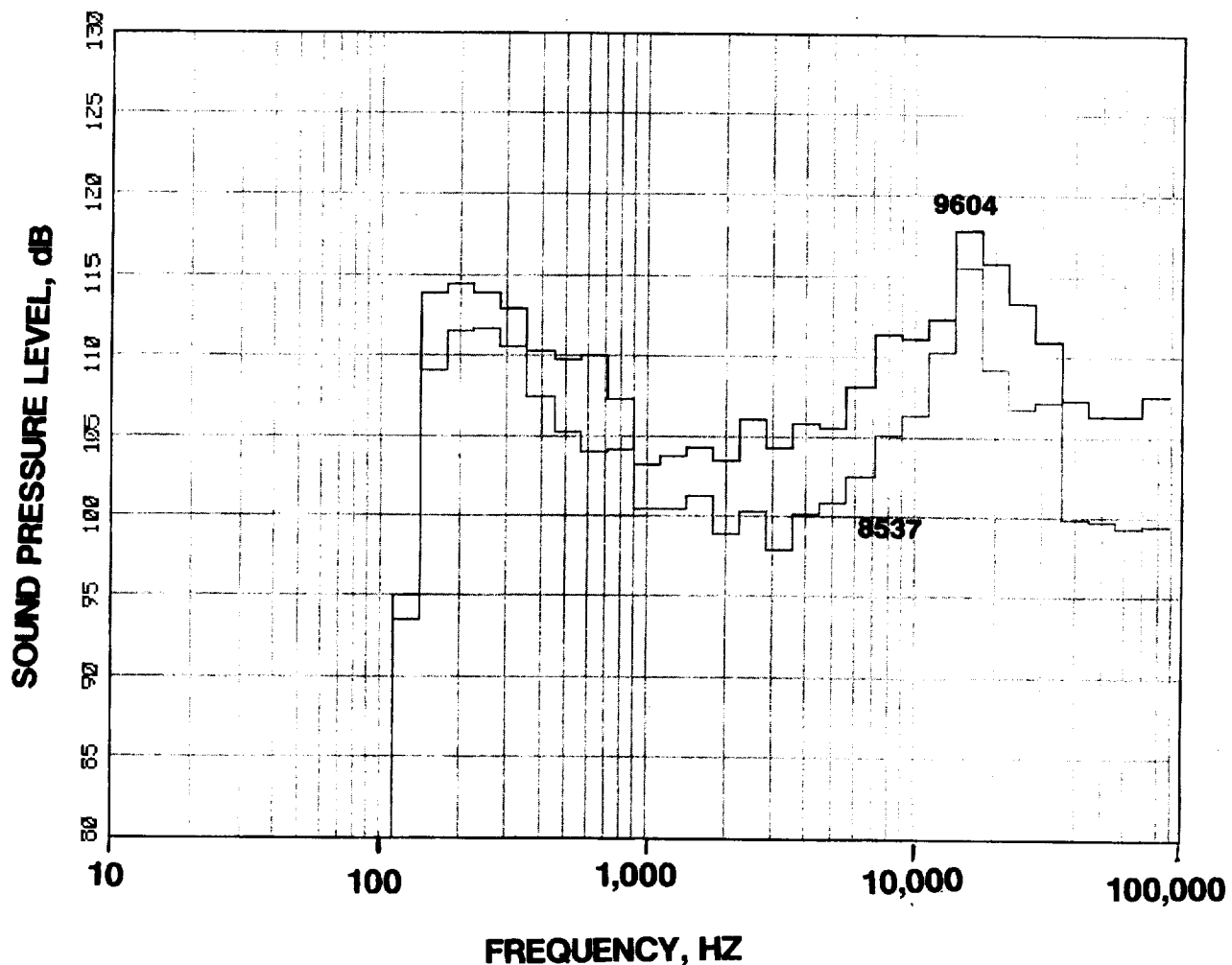
A. 7736 RPMC, 6402 RPMC

92.5 DEGREES EMITTED ANGLE



**FIGURE 18 CONTINUED**

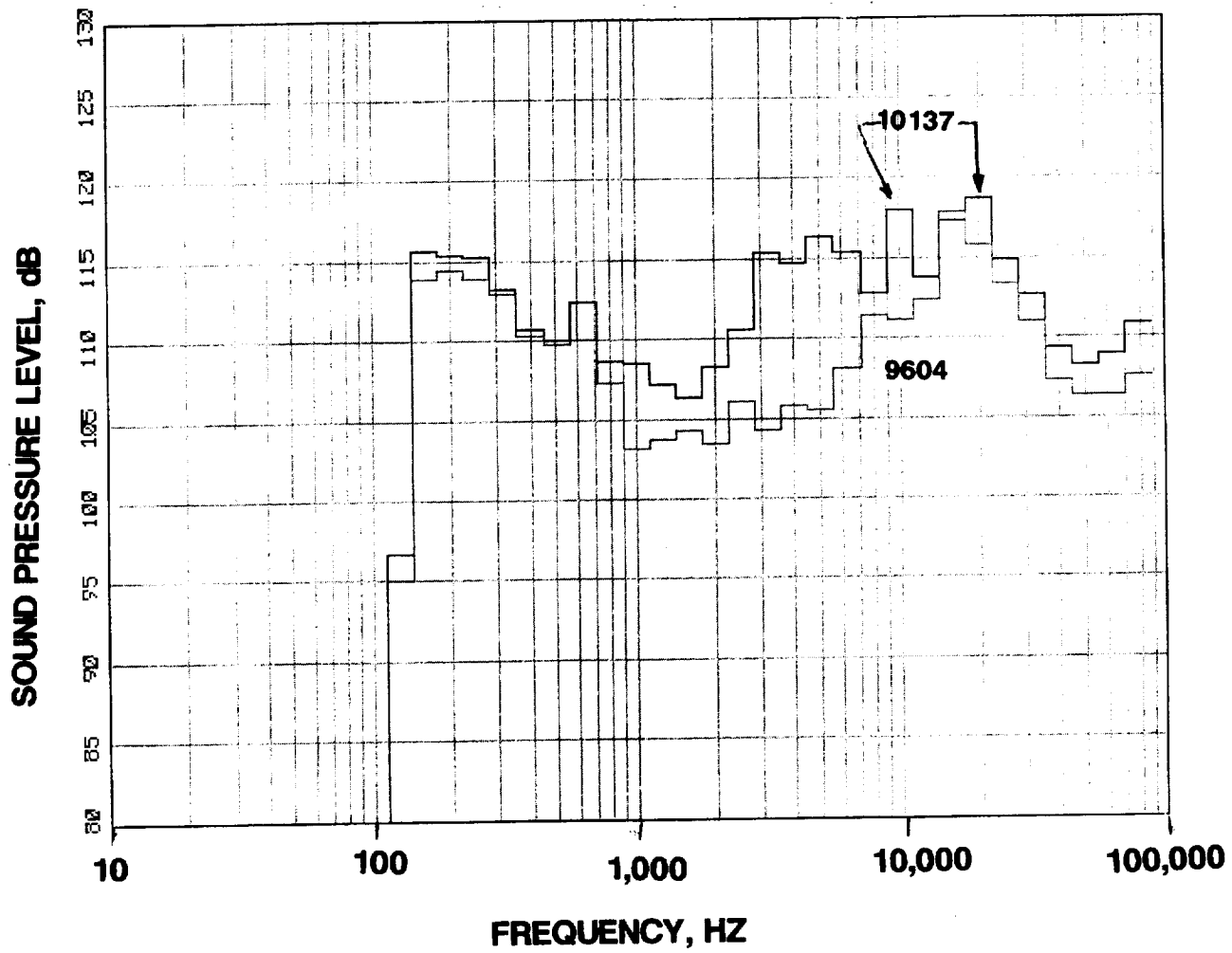
**B. 8537 RPMC, 7736 RPMC  
92.5 DEGREES EMITTED ANGLE**



**FIGURE 18 CONTINUED**

**C. 9604 RPMC, 8537 RPMC**

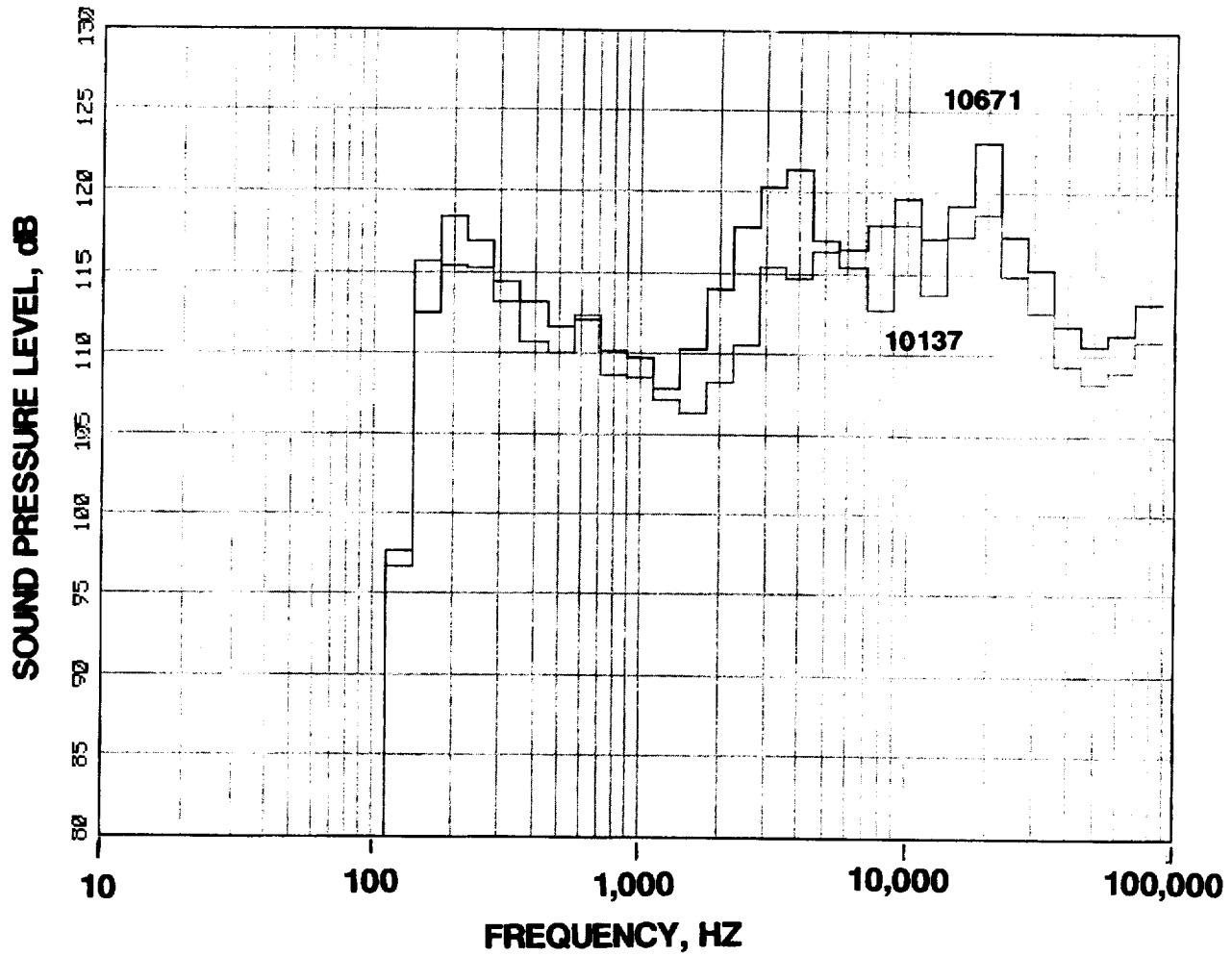
**92.5 DEGREES EMITTED ANGLE**



**FIGURE 18 CONTINUED**

**D. 10137 RPMC, 9604 RPMC**

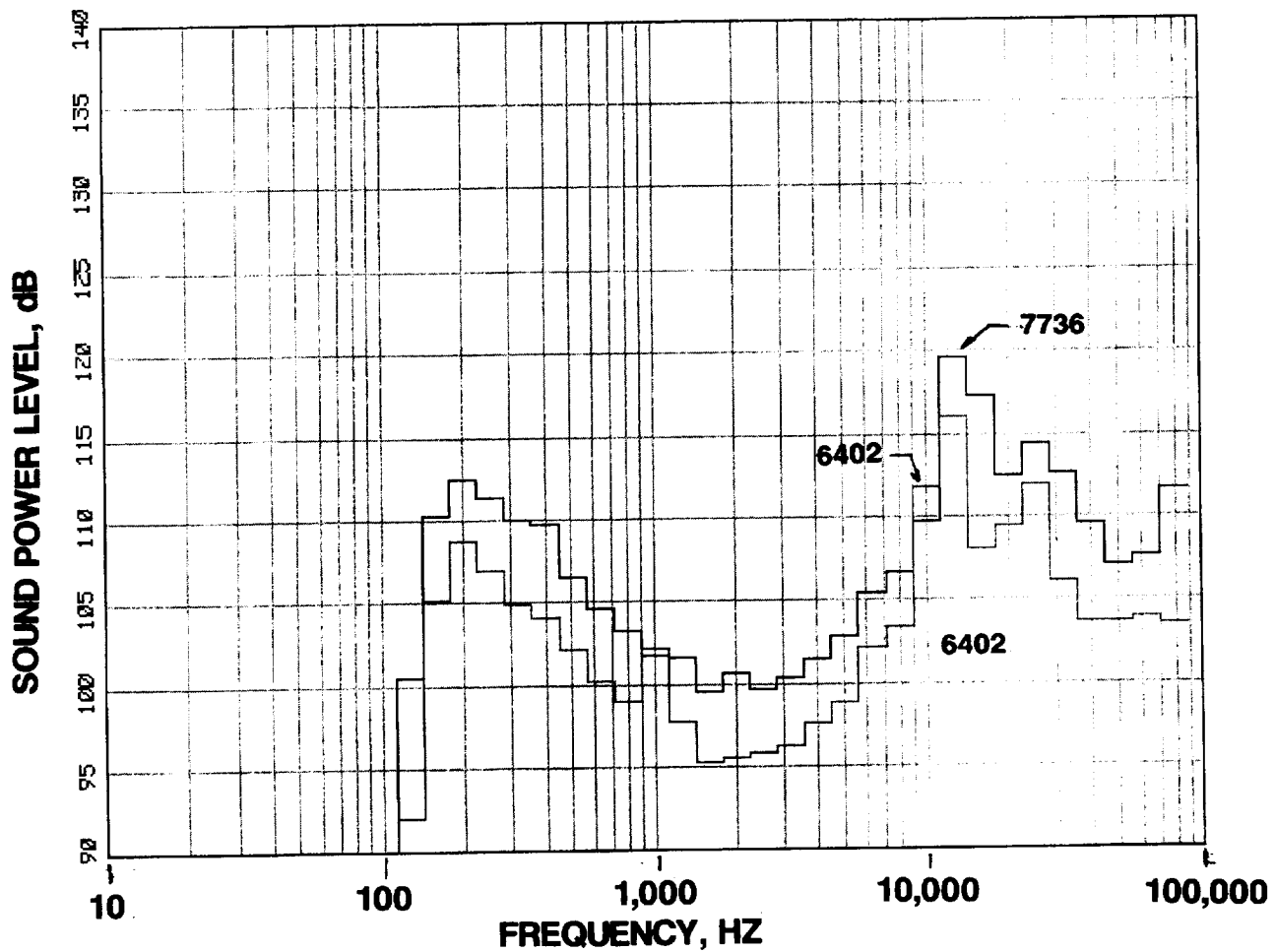
**92.5 DEGREES EMITTED ANGLE**



**FIGURE 18 CONCLUDED**

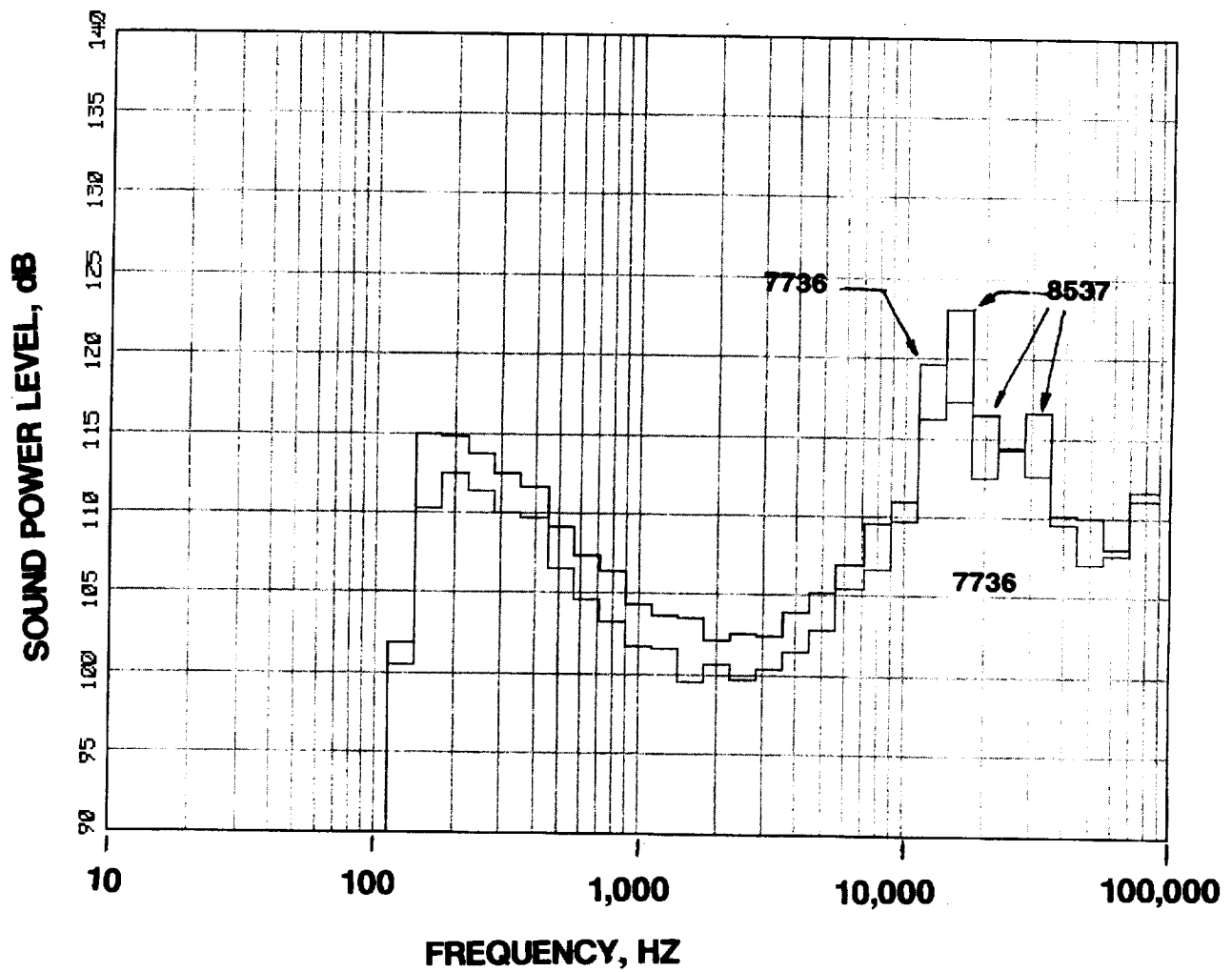
**E. 10671 RPMC, 10137 RPMC**

**92.5 DEGREES EMITTED ANGLE**



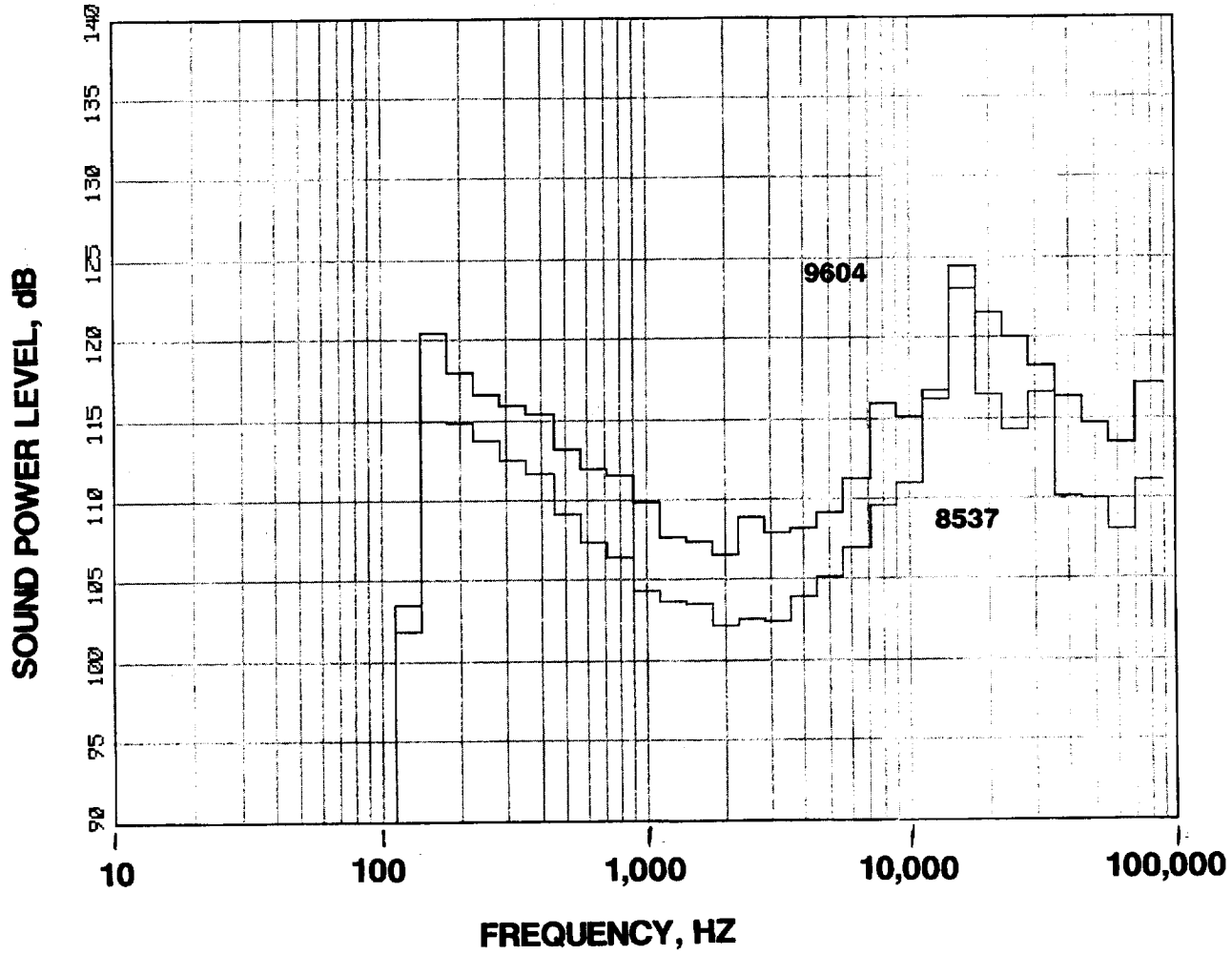
**FIGURE 19 COMPARISON OF SOUND POWER LEVEL  
AT DIFFERENT SPEEDS**

A. 7736 RPMC, 6402 RPMC



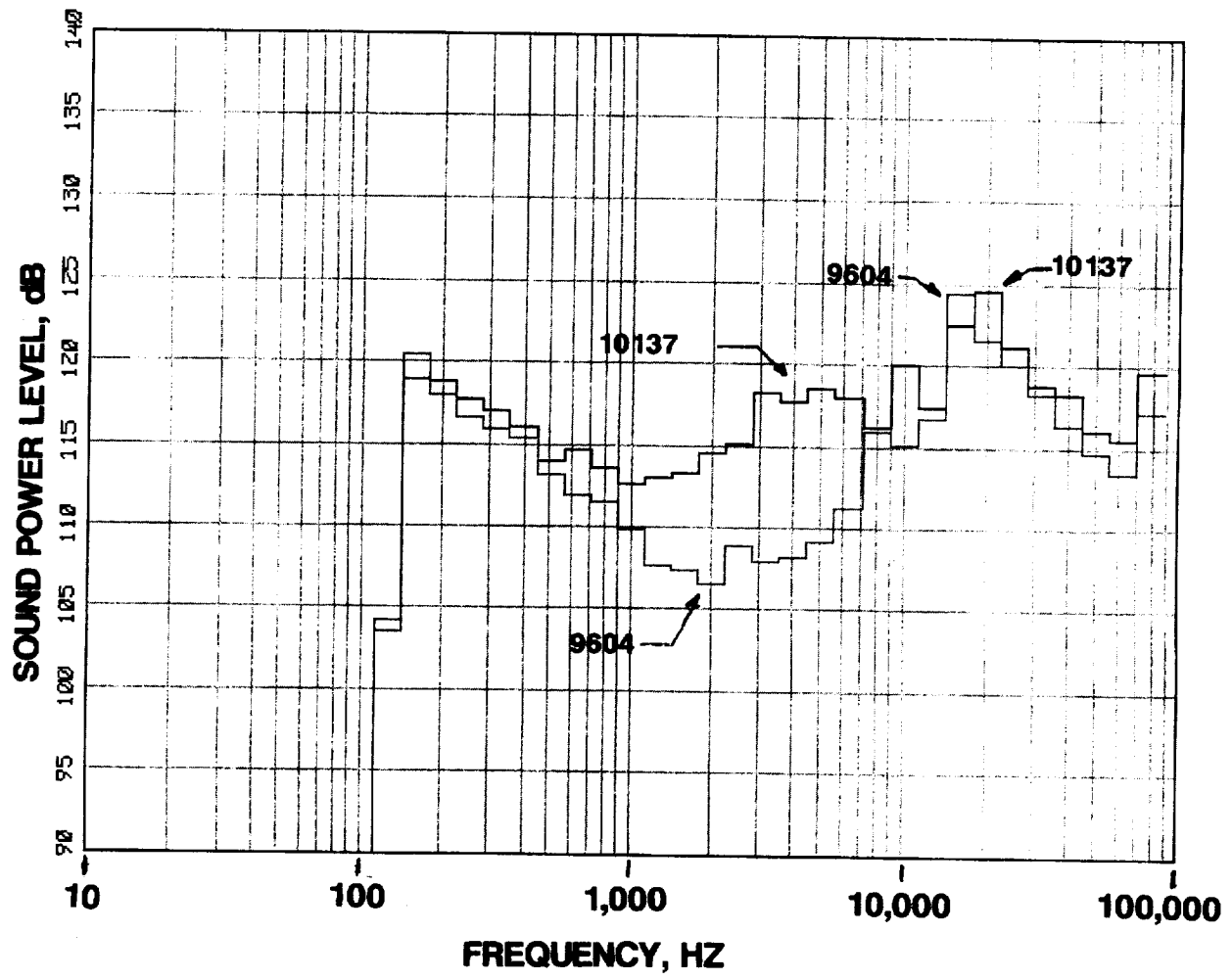
**FIGURE 19 CONTINUED**

**B. 8537 RPMC, 7736 RPMC**



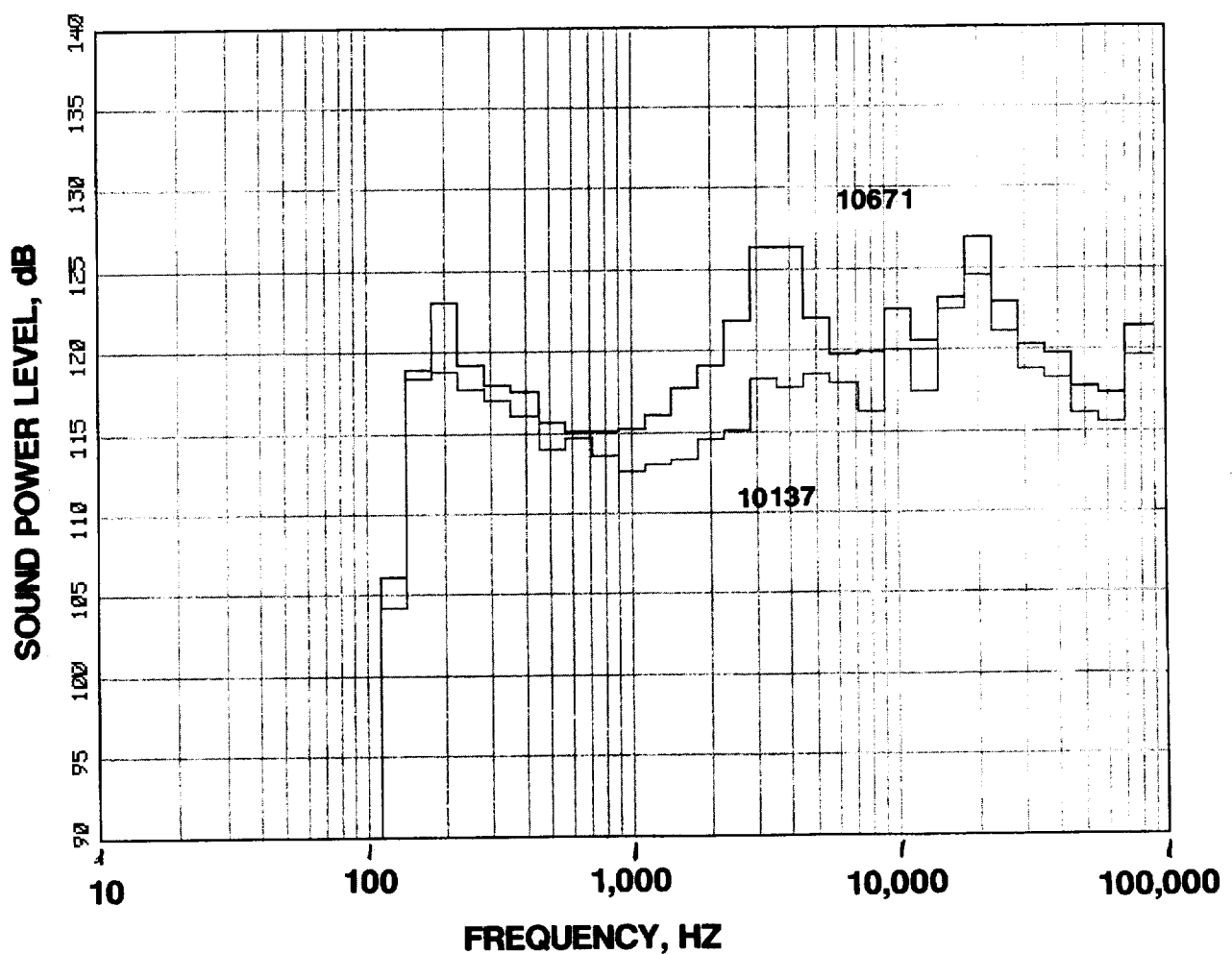
**FIGURE 19 CONTINUED**

**C. 9604 RPMC, 8537 RPMC**



**FIGURE 19 CONTINUED**

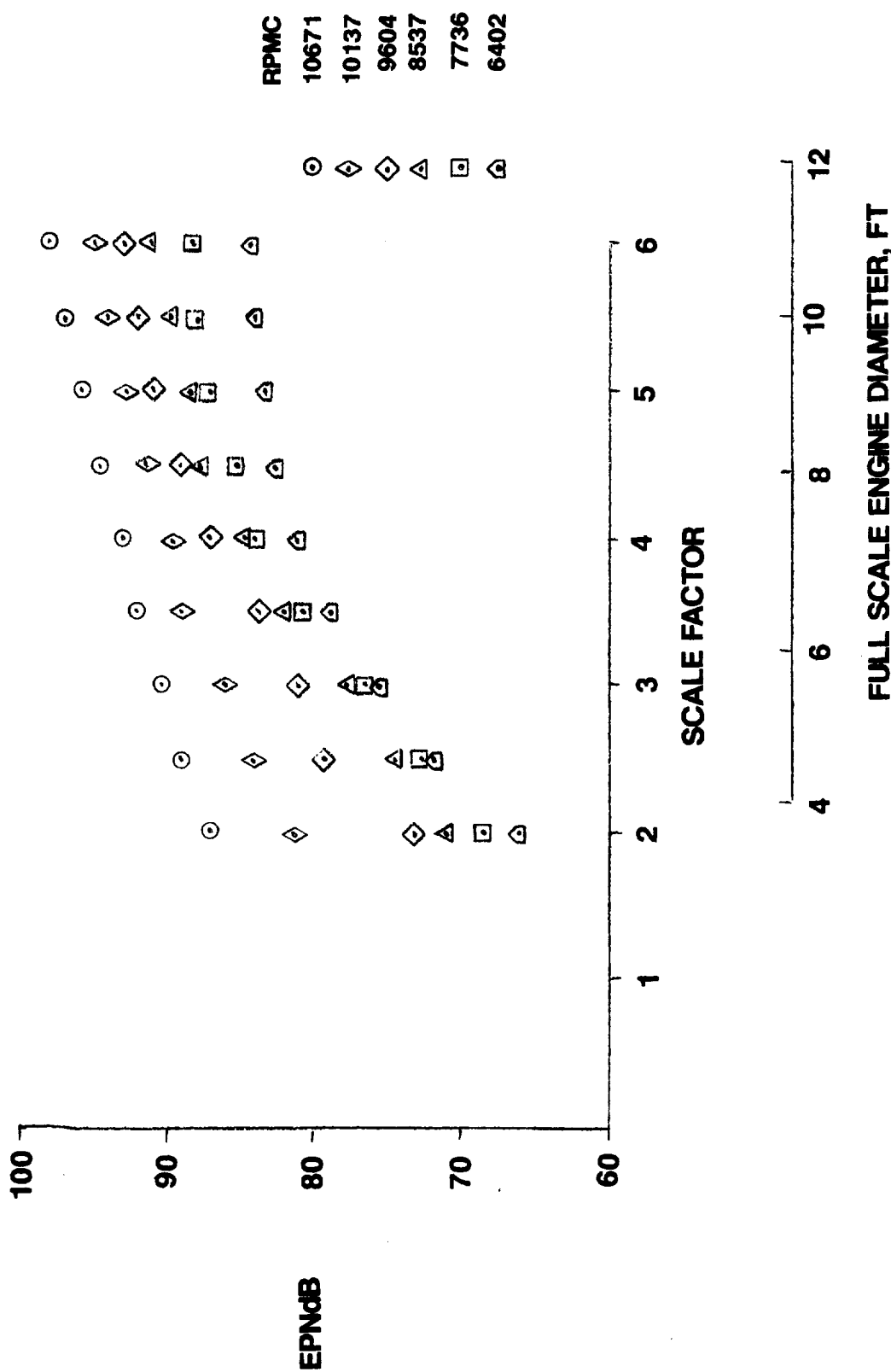
**D. 10137 RPMC, 9604 RPMC**



**FIGURE 19 CONCLUDED**

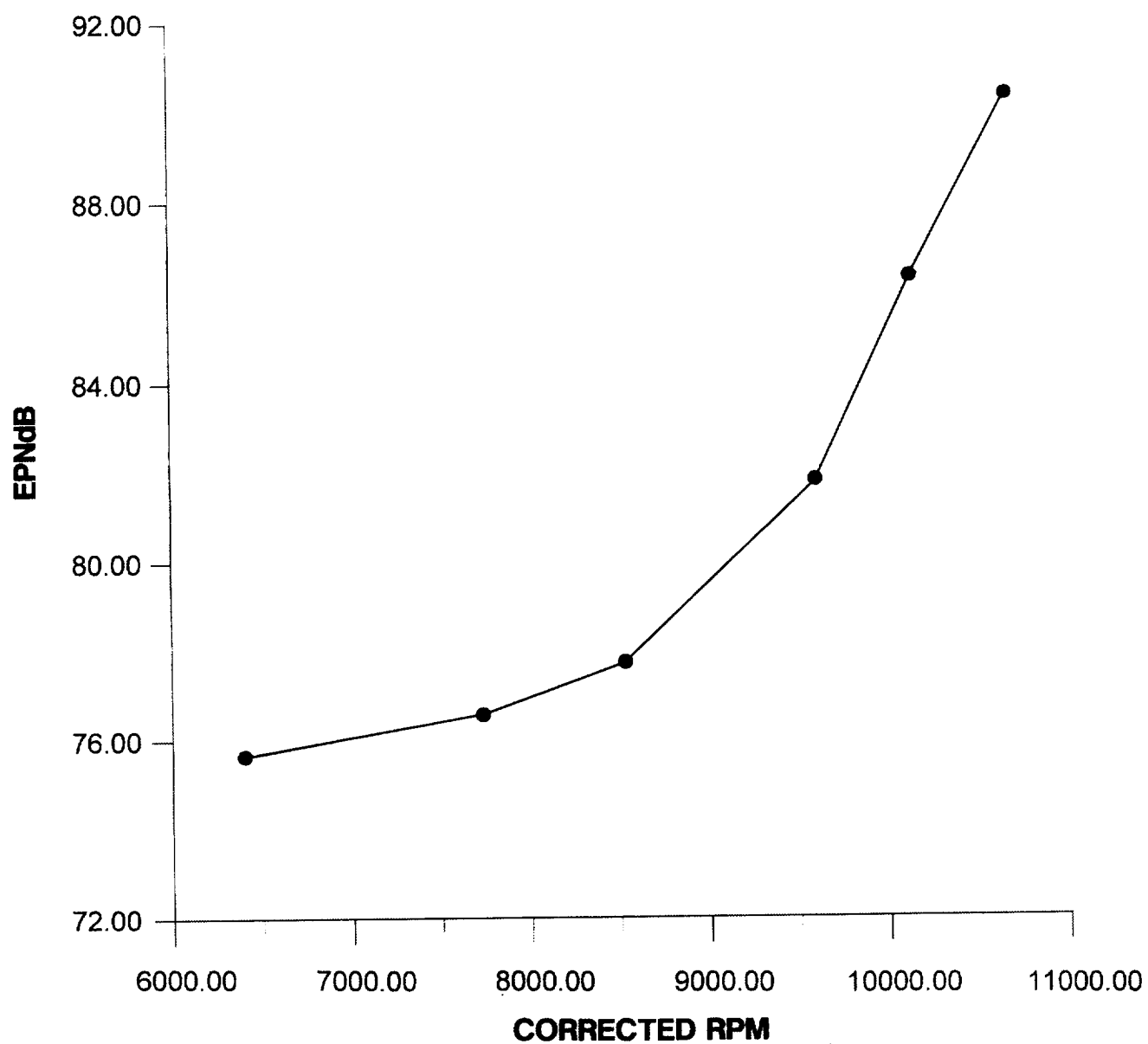
**E. 10671 RPMC, 10137 RPMC**

**FIGURE 20 FLYOVER NOISE AT 1000 FT, STANDARD DAY**



**FIGURE 21 EPNdB VERSUS SPEED**

**SCALE FACTOR EQUAL 3.0**



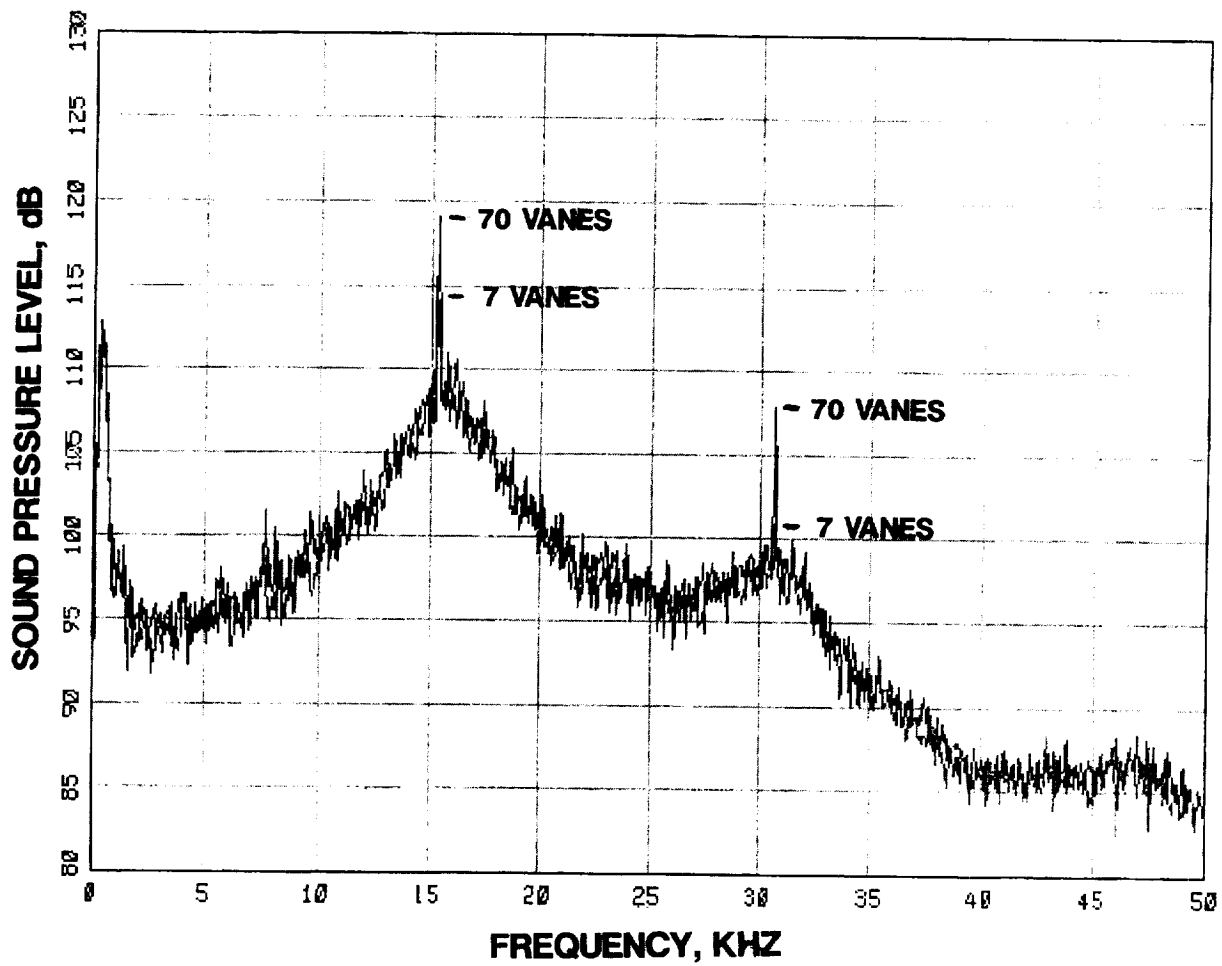


**FIGURE 22 COMPARISON OF 7 VANE AND 70 VANE DATA**

**A 8537 RPMC, 24.5 DEGREES**

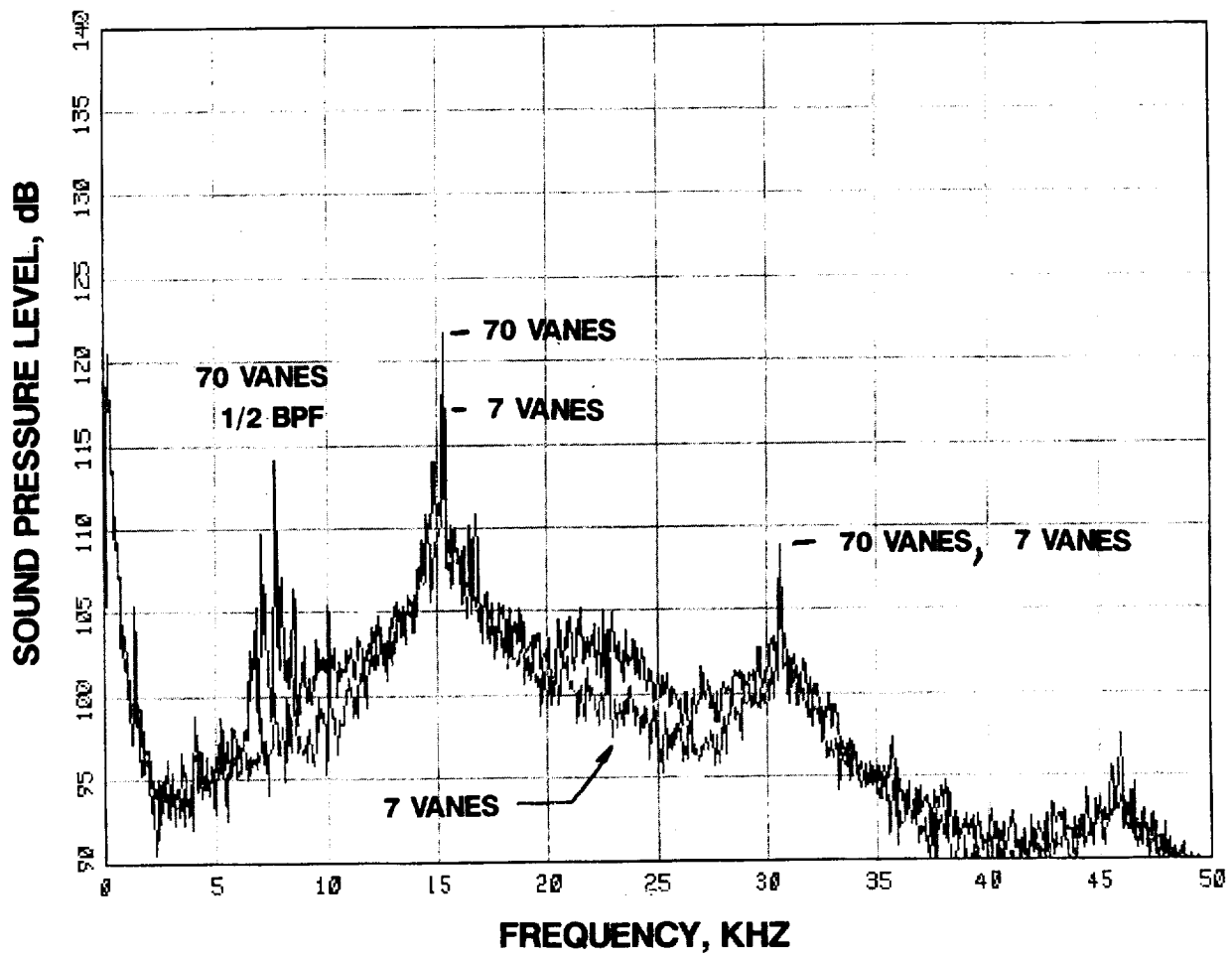


**FIGURE 22 CONTINUED**

**B 8537 RPMC, 130.5 DEGREES**

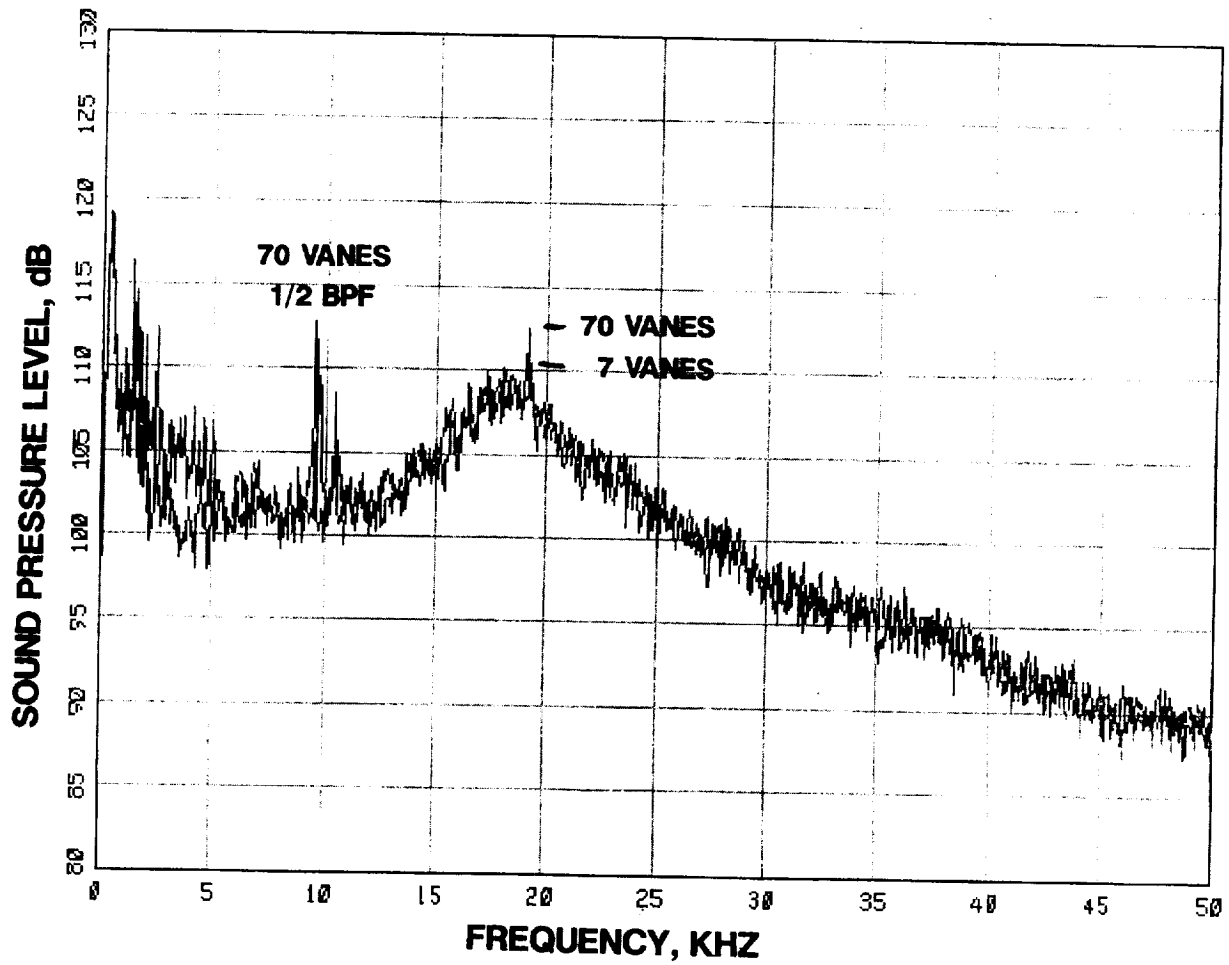


**FIGURE 22 CONTINUED**

**C 10671 RPMC, 24.5 DEGREES**

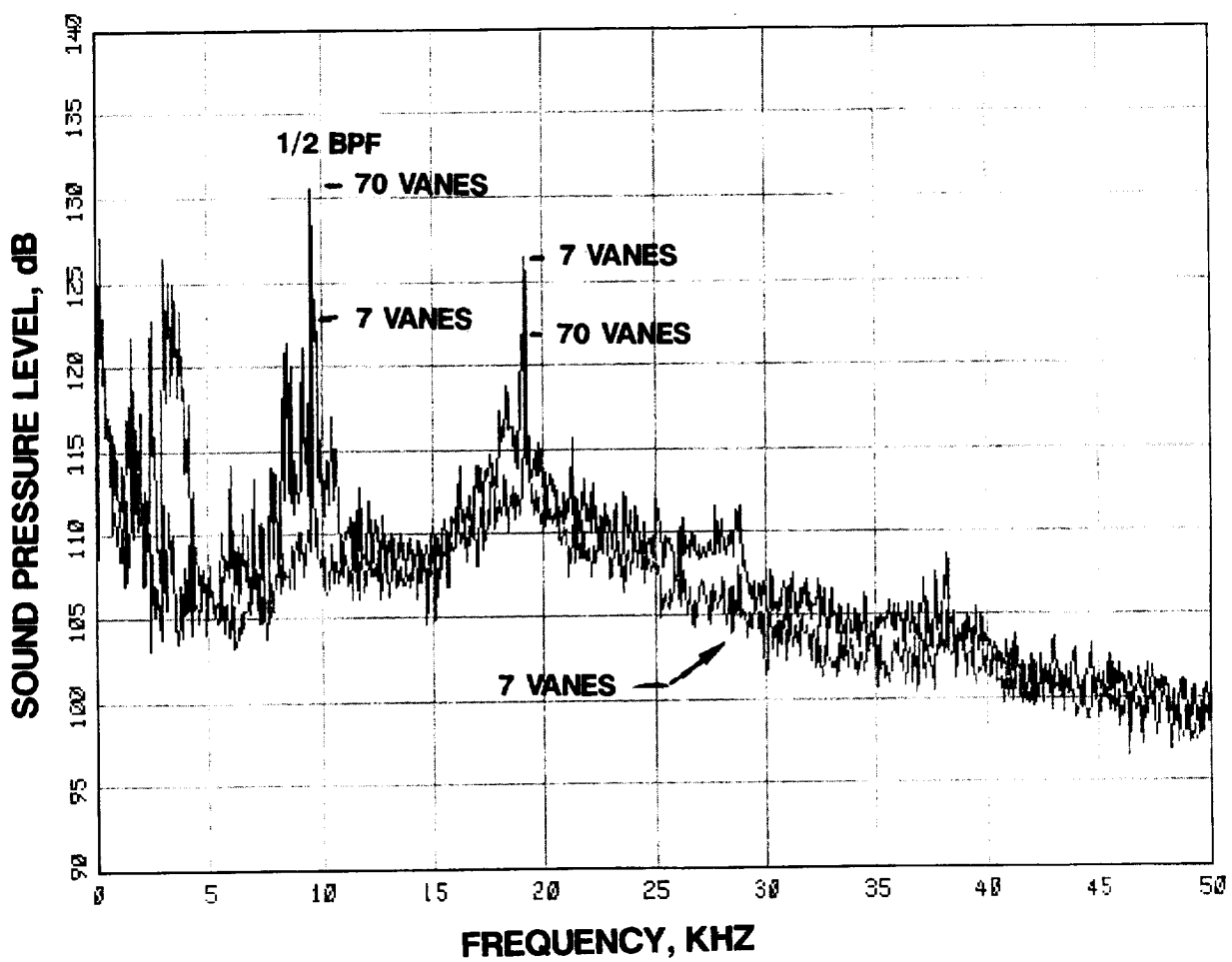


**FIGURE 22 CONCLUDED**

**D 10671 RPMC, 130.5 DEGREES**

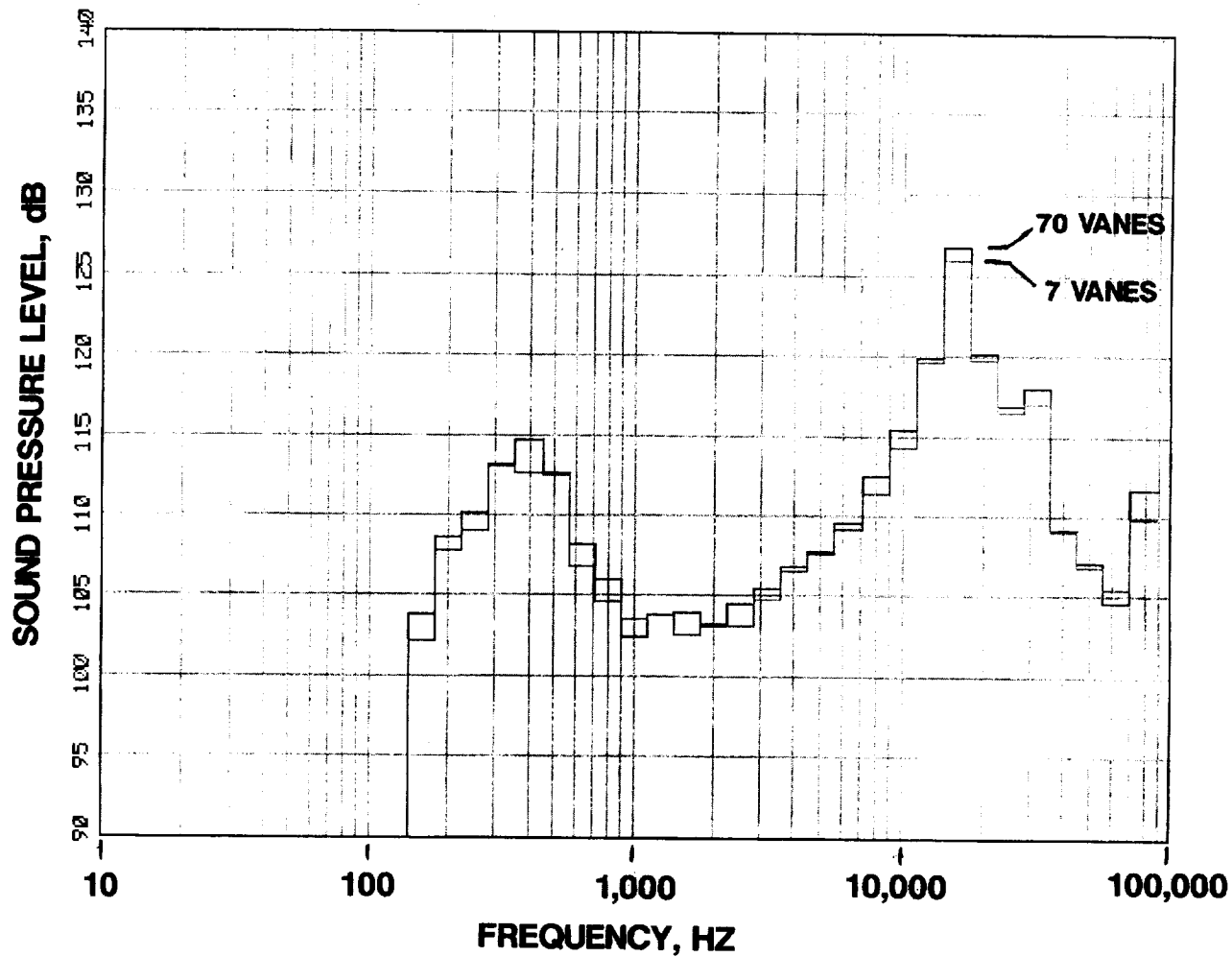


**FIGURE 23 1/3RD OCTAVE COMPARISON OF**

**7 VANE AND 70 VANE DATA**

**A 8537 RPMC, 24.5 DEGREES**

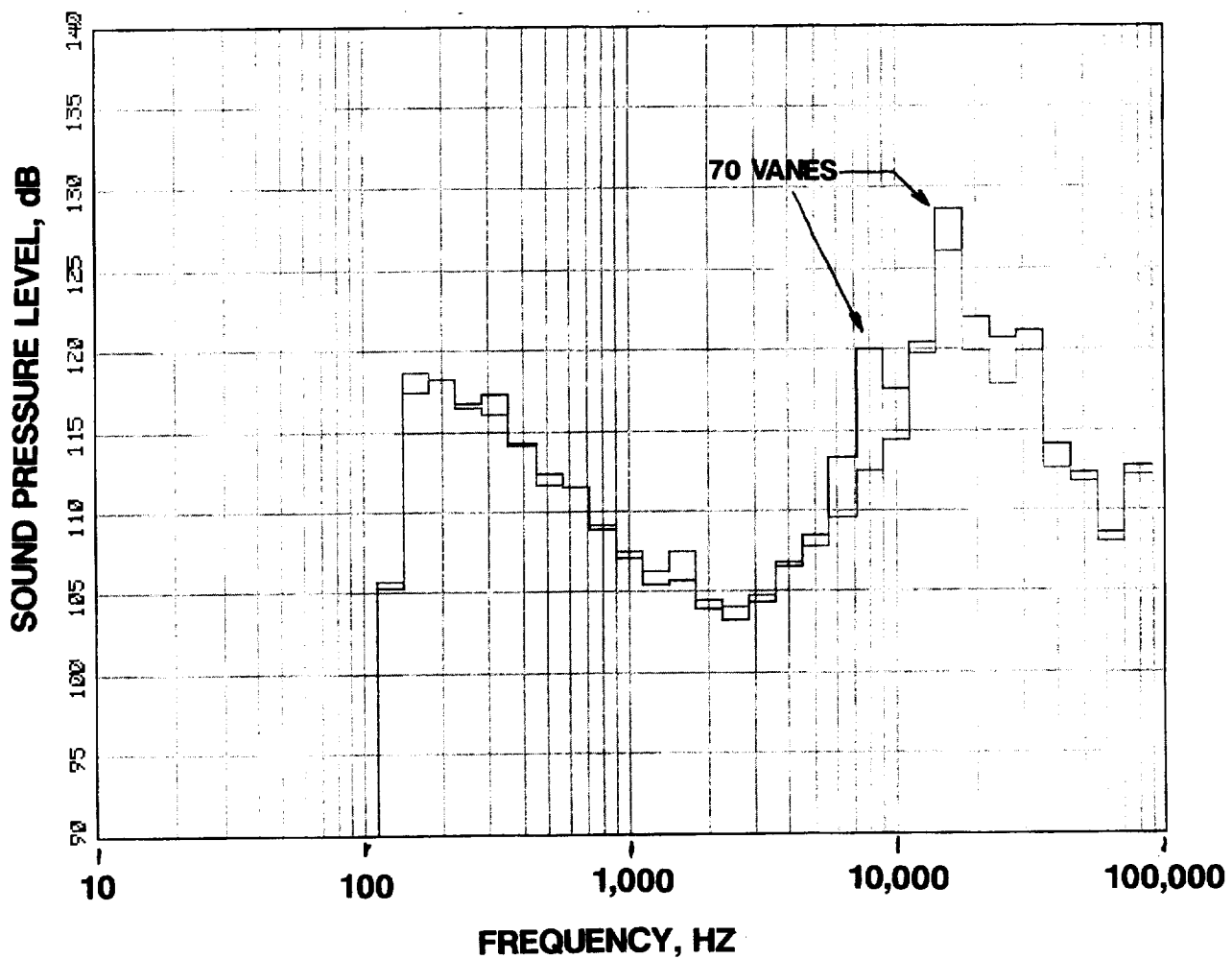


**FIGURE 23 CONTINUED**

**B 8537 RPMC, 130.5 DEGREES**

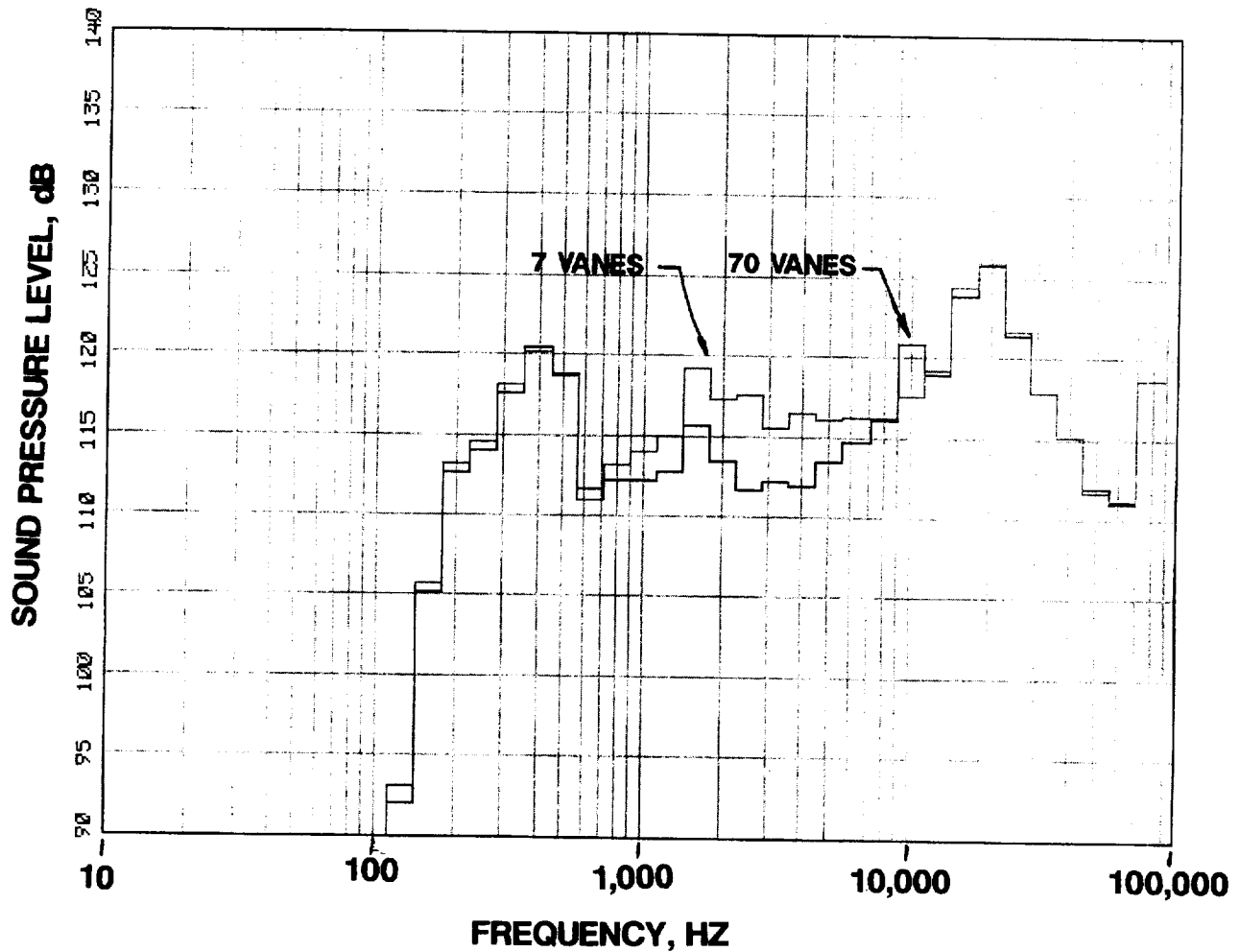


**FIGURE 23 CONTINUED**

**C 10671 RPMC, 24.5 DEGREES**

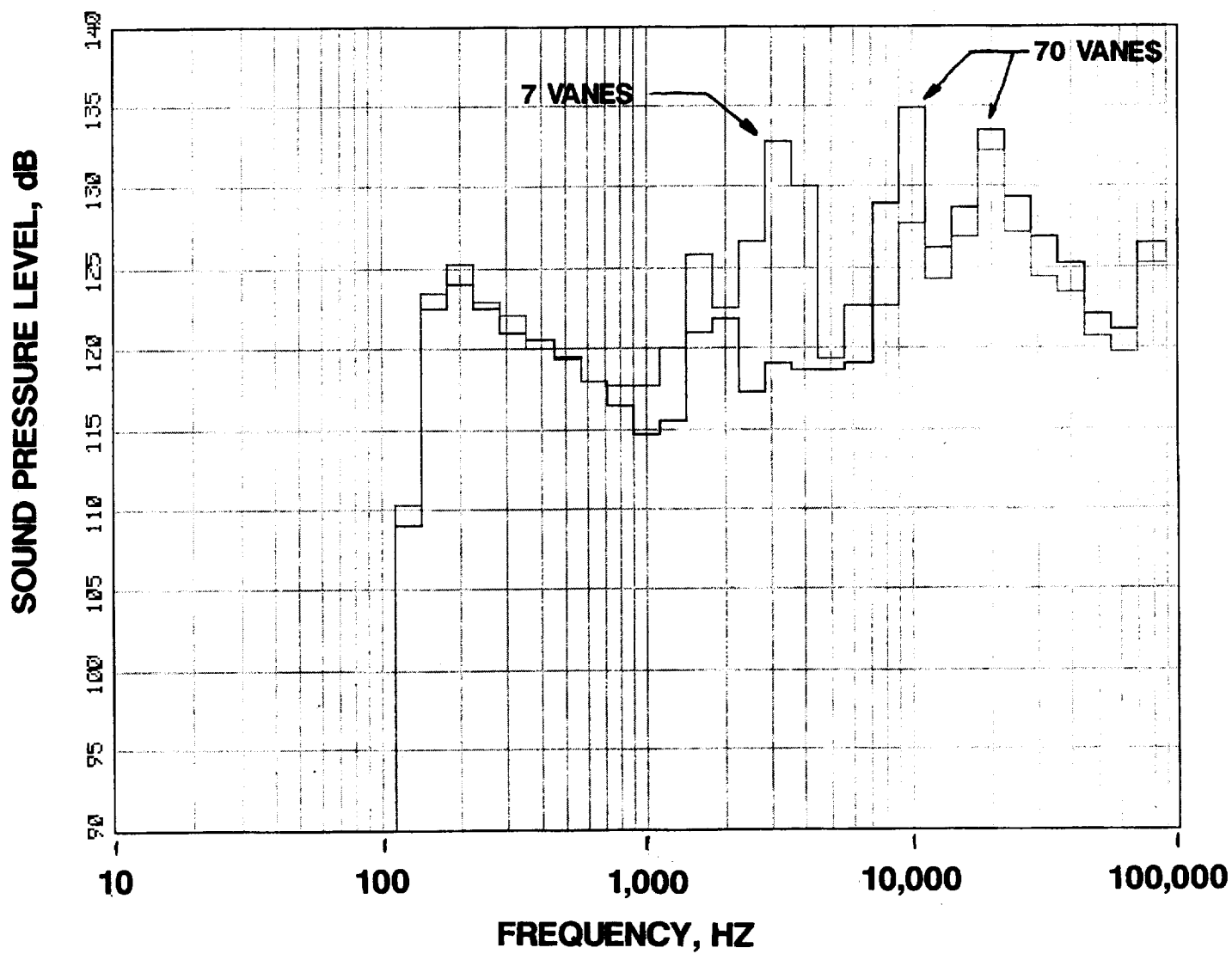


**FIGURE 23 CONCLUDED**

**D 10671 RPMC, 130.5 DEGREES**

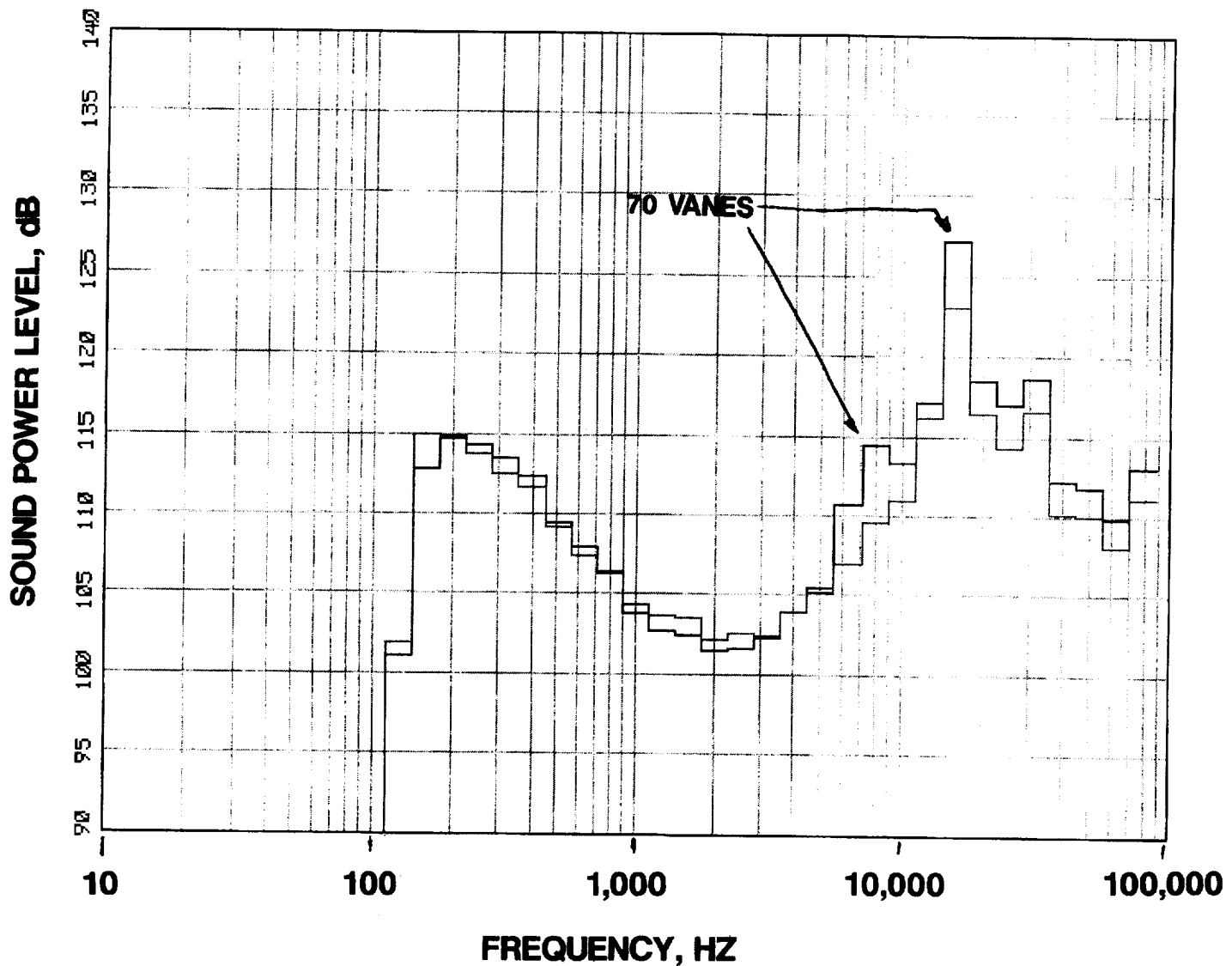


**FIGURE 24 SOUND POWER LEVEL COMPARISON OF  
7 VANE AND 70 VANE DATA  
A 8537 RPMC**

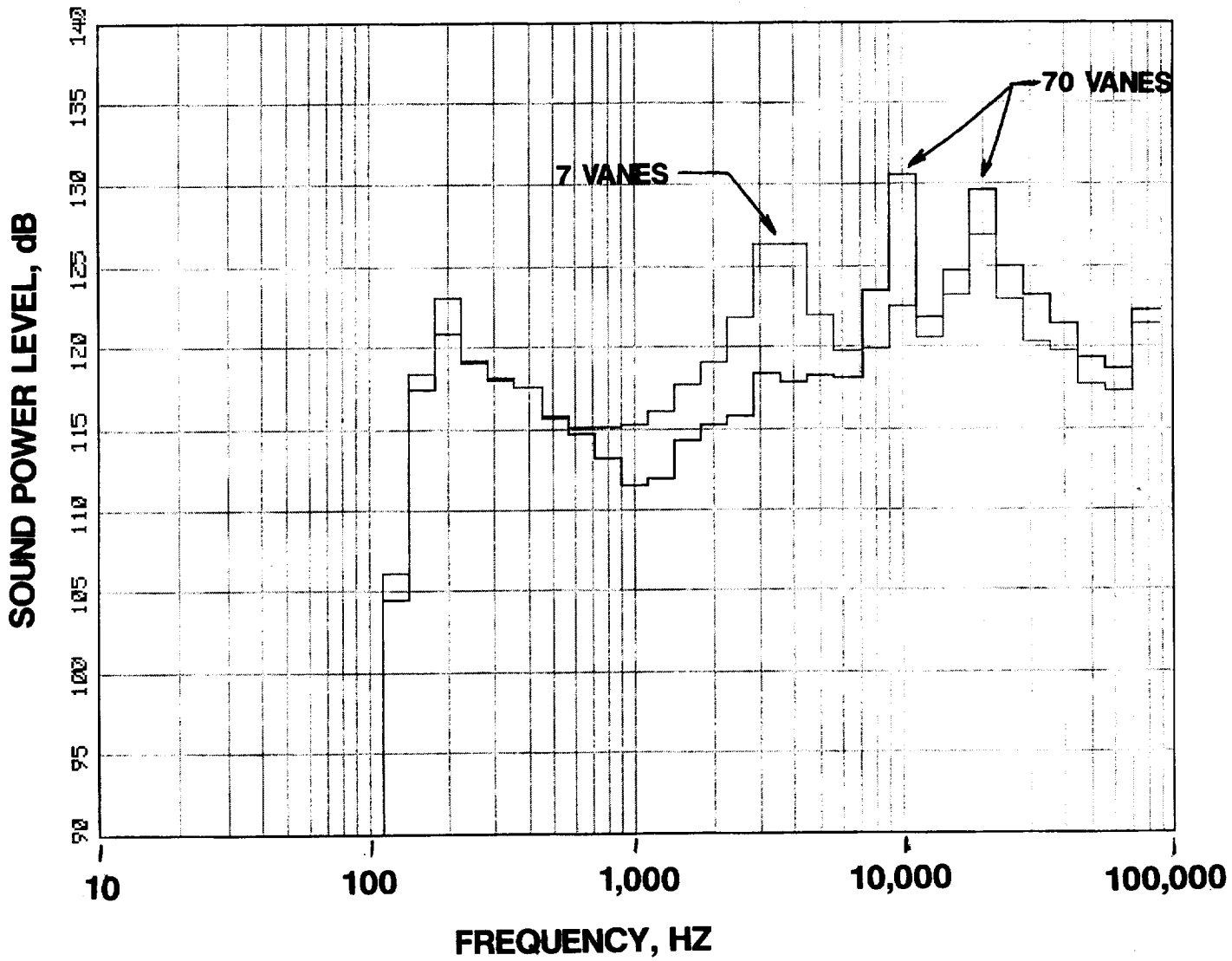


**FIGURE 24 CONCLUDED**

**B 10671 RPMC**

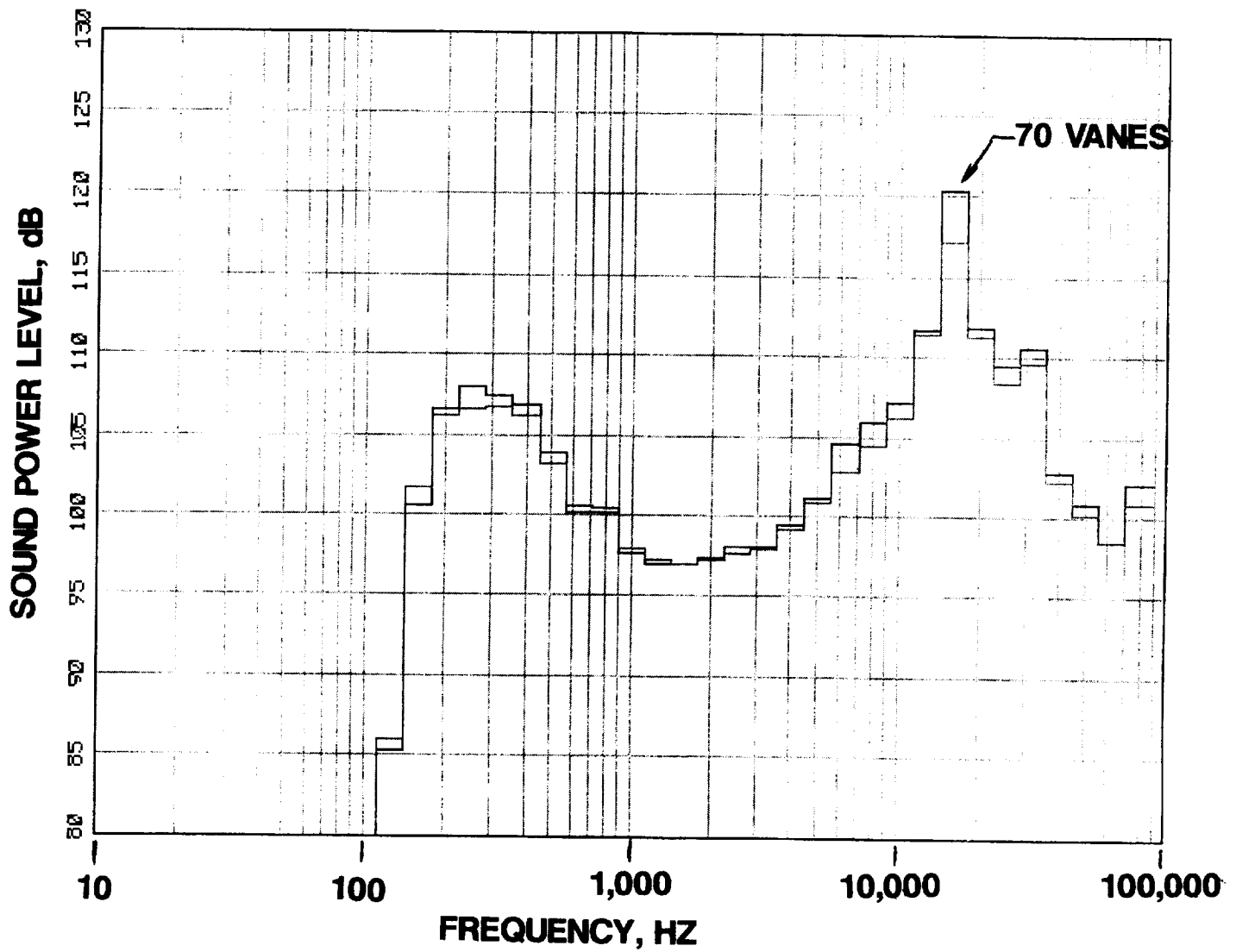


**FIGURE 25 FRONT AND AFT POWER LEVEL COMPARISONS OF**

**7 VANE AND 70 VANE DATA**

**A FRONT POWER AT 8537 RPMC**

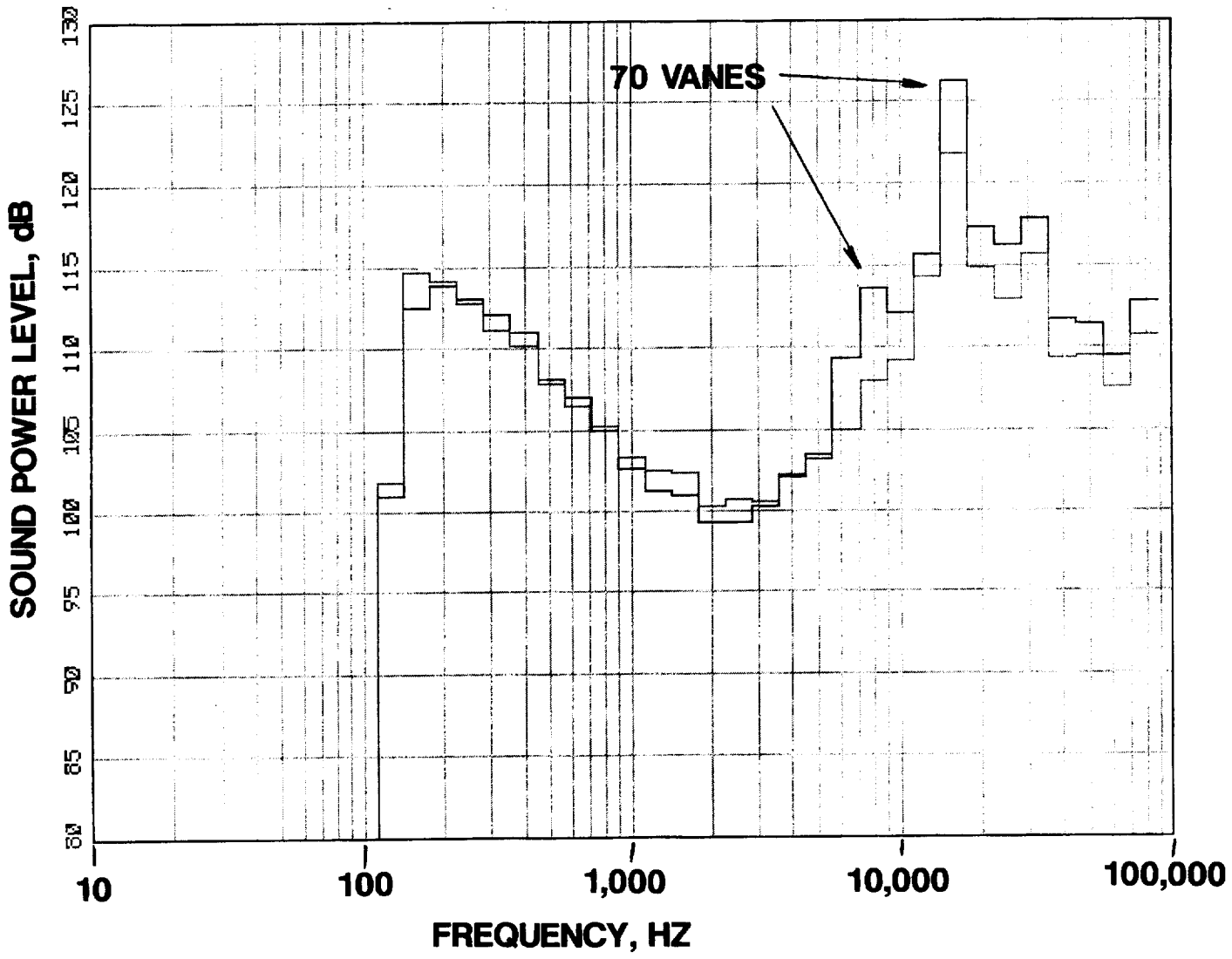


**FIGURE 25 CONTINUED**

**B AFT POWER AT 8537 RPMC**

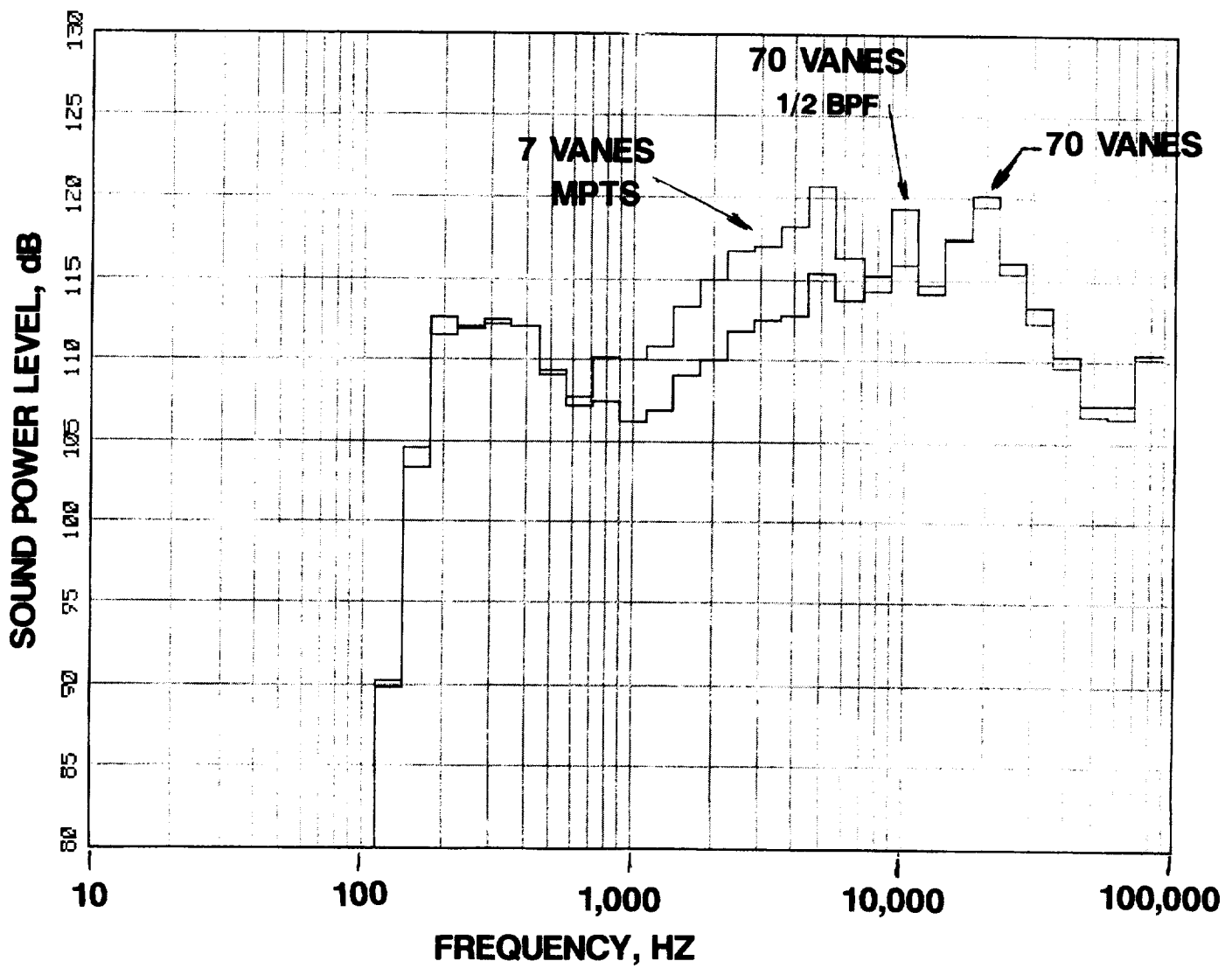


**FIGURE 25 CONTINUED**

**C FRONT POWER AT 10671 RPMC**

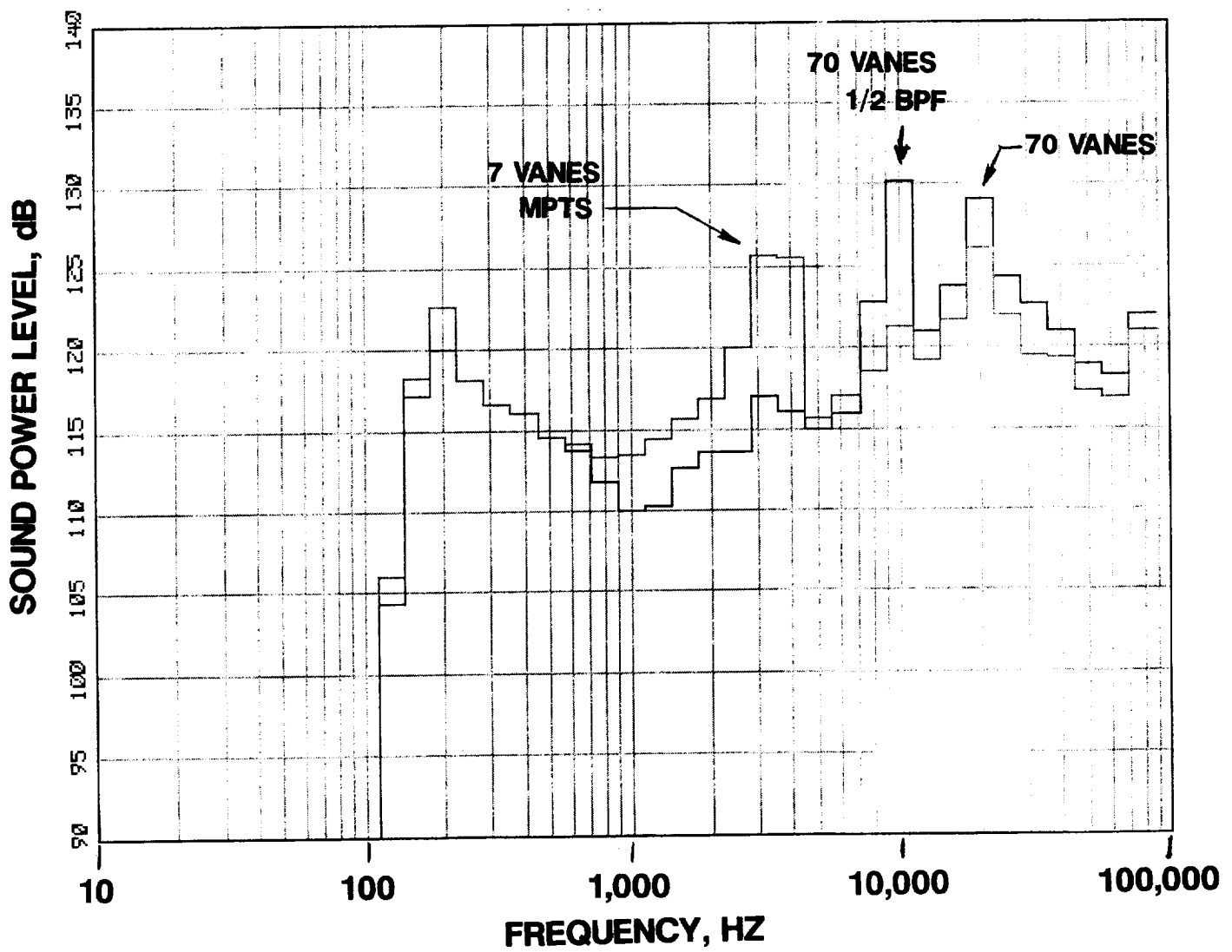


**FIGURE 25 CONCLUDED**

**D AFT POWER AT 10671 RPMC**

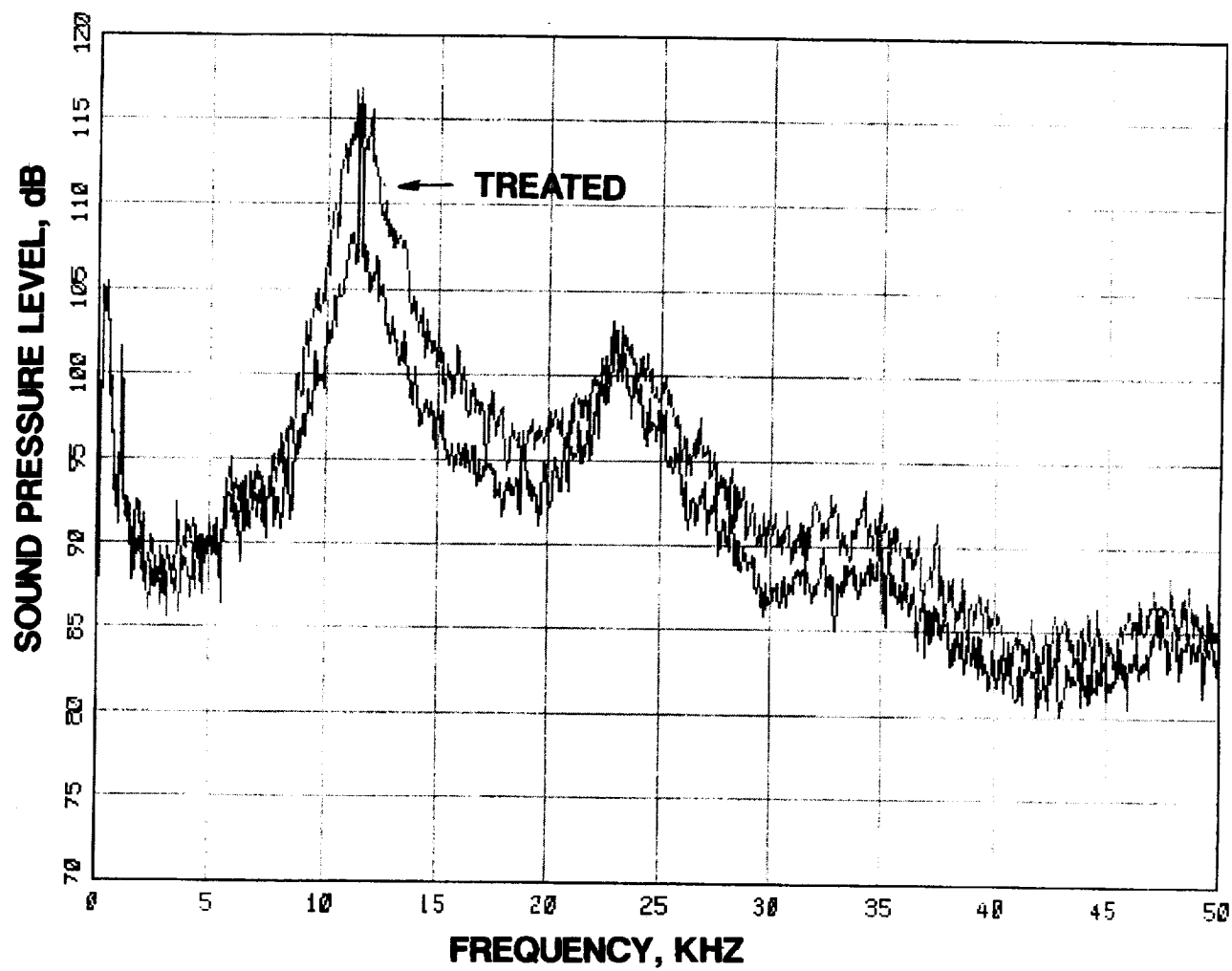


**FIGURE 26 SPECTRAL COMPARISON OF HARD AND FULLY TREATED DATA FOR THE 7 VANE CONFIGURATION AT 6402 RPMC**  
**A 24.5 DEGREES**

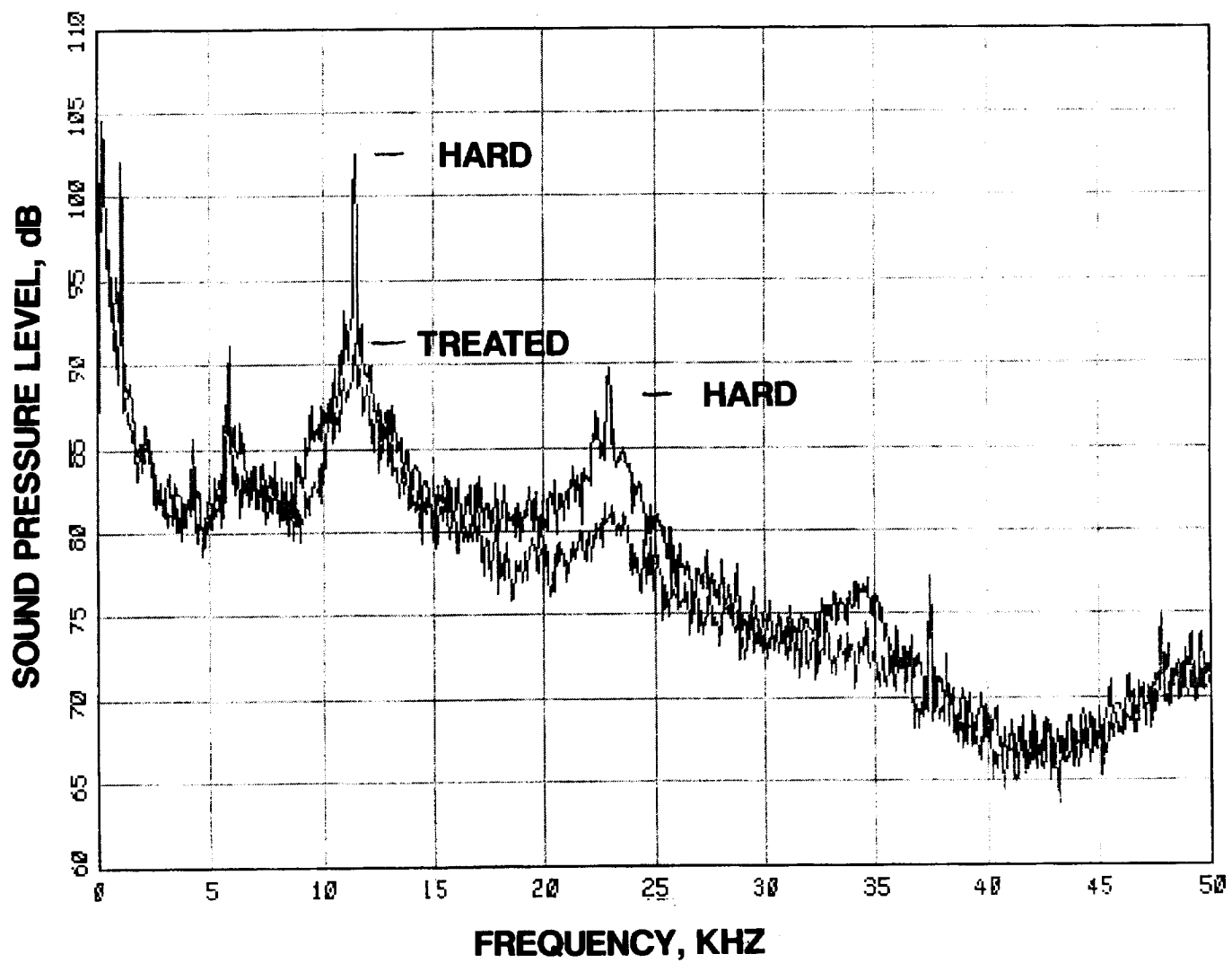


**FIGURE 26 CONTINUED**

**B 92.5 DEGREES**

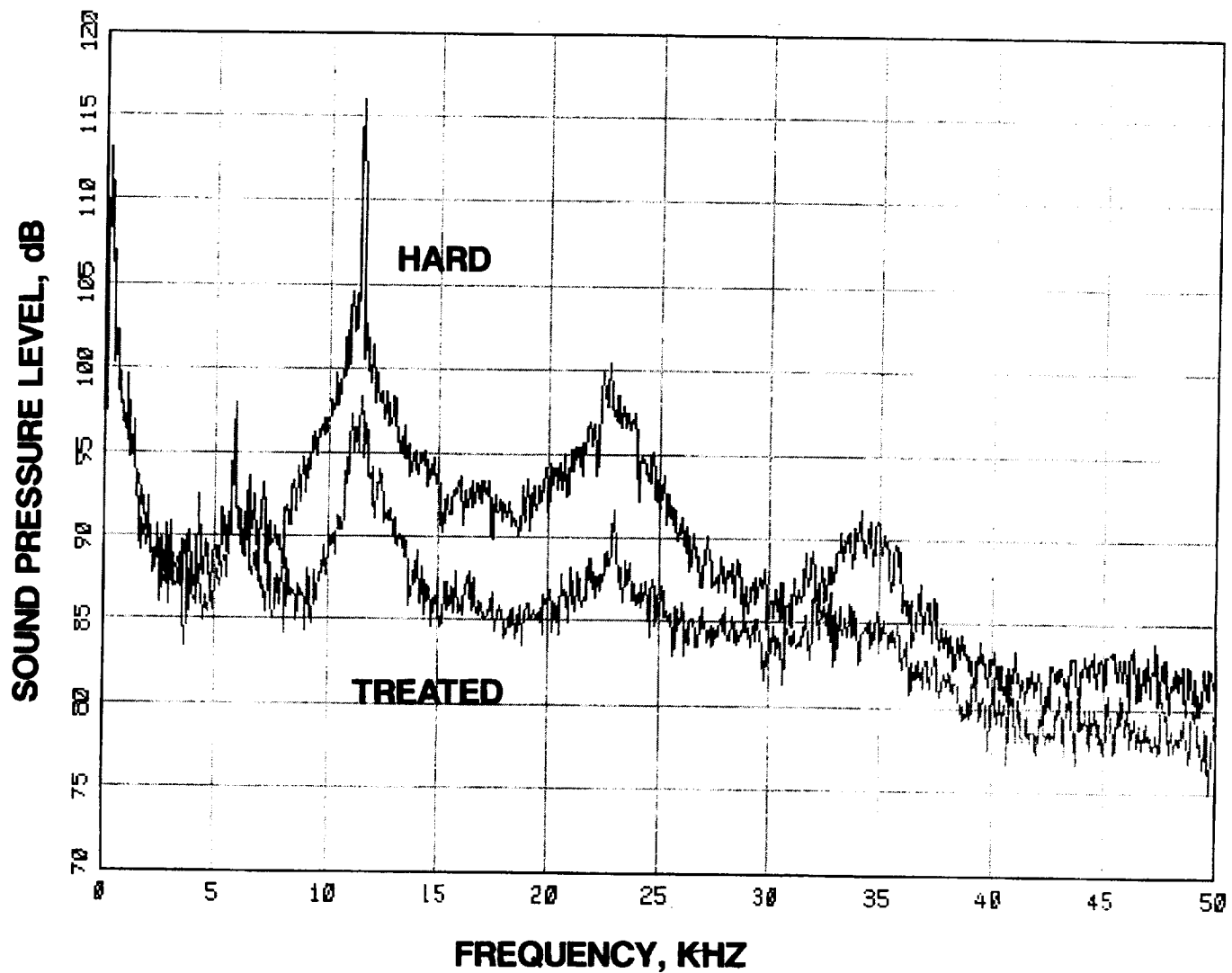


**FIGURE 26 CONCLUDED**

**C 130.5 DEGREES**

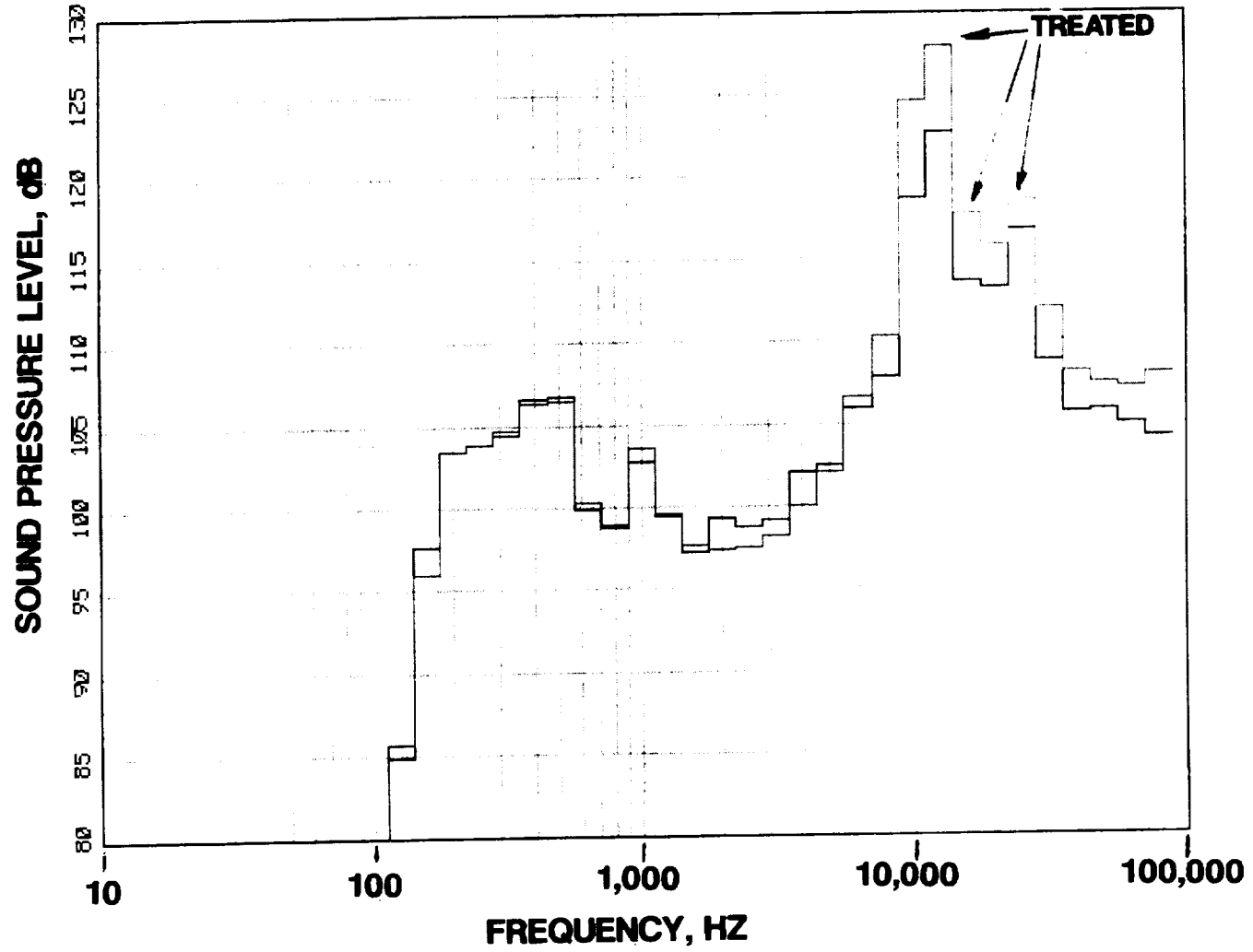


**FIGURE 27 1/3RD OCTAVE COMPARISON OF HARD AND  
FULLY TREATED DATA FOR THE 7 VANE CONFIGURATION AT 6402 RPMC**  
**A 24.5 DEGREES**

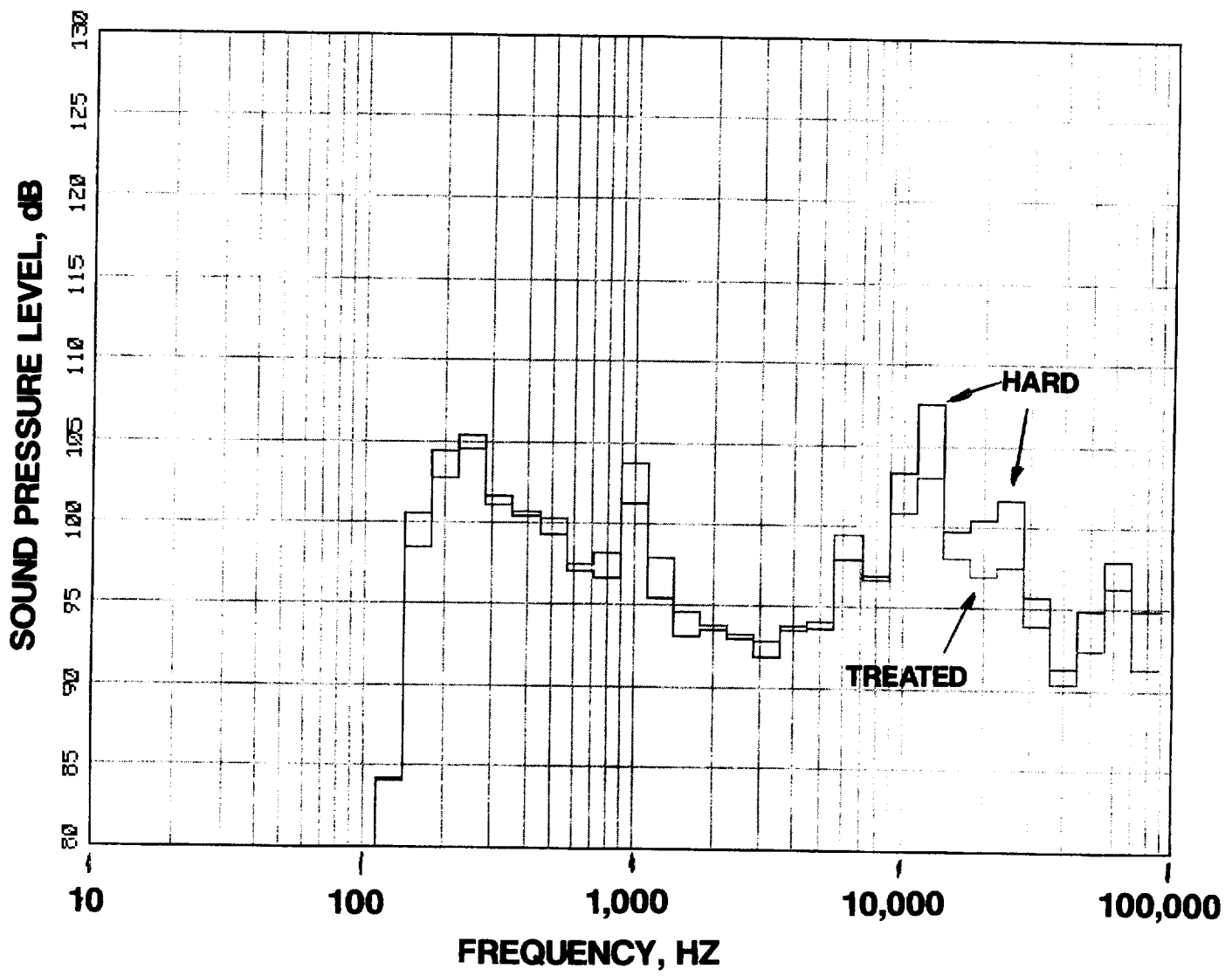


**FIGURE 27 CONTINUED**

**B 92.5 DEGREES**

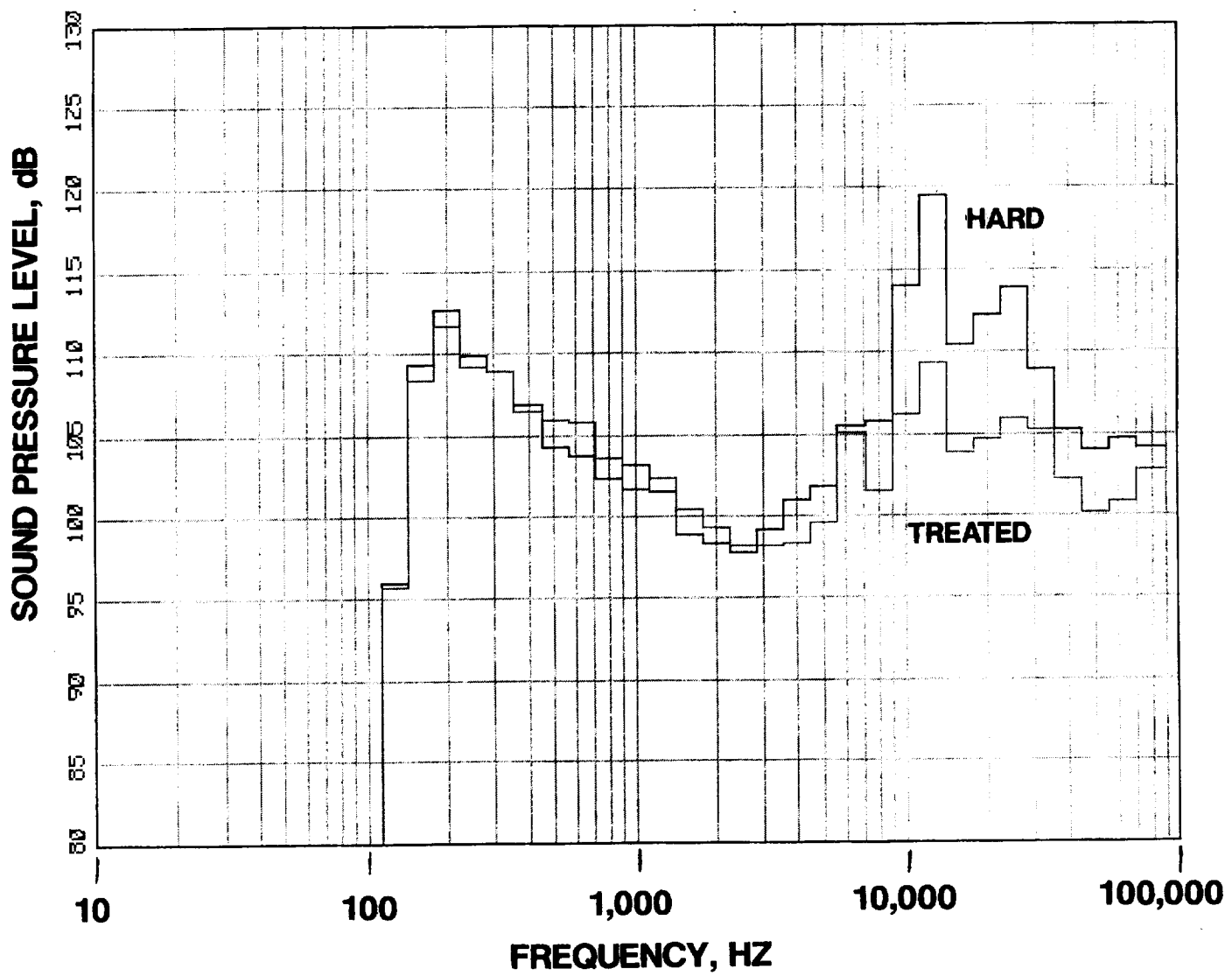


**FIGURE 27 CONCLUDED**

**C 130.5 DEGREES**

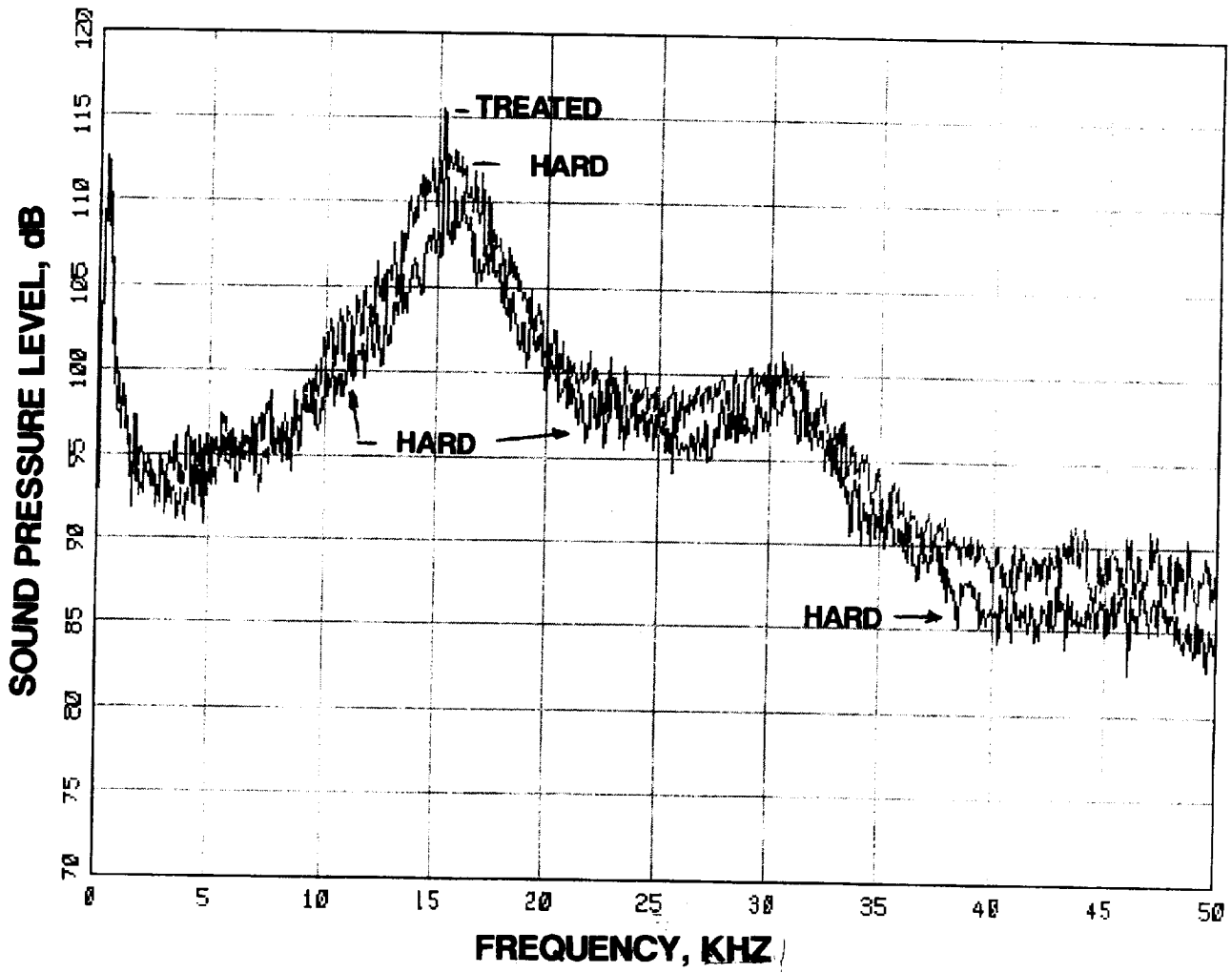


**FIGURE 28 SPECTRAL COMPARISON OF HARD AND FULLY TREATED  
DATA FOR THE 7 VANE CONFIGURATION AT 8537 RPMC  
A 24.5 DEGREES**

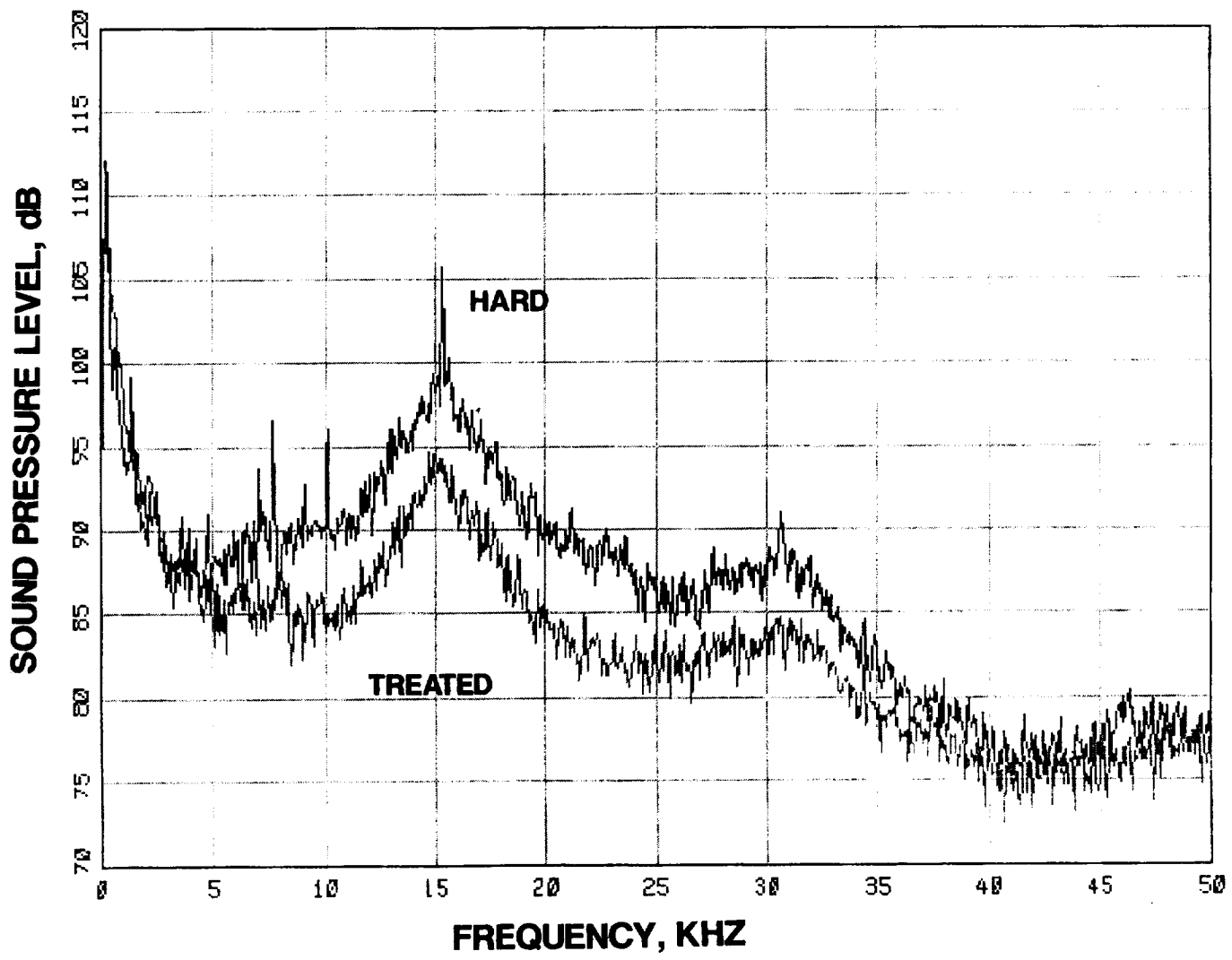


**FIGURE 28 CONTINUED**

**B 92.5 DEGREES**

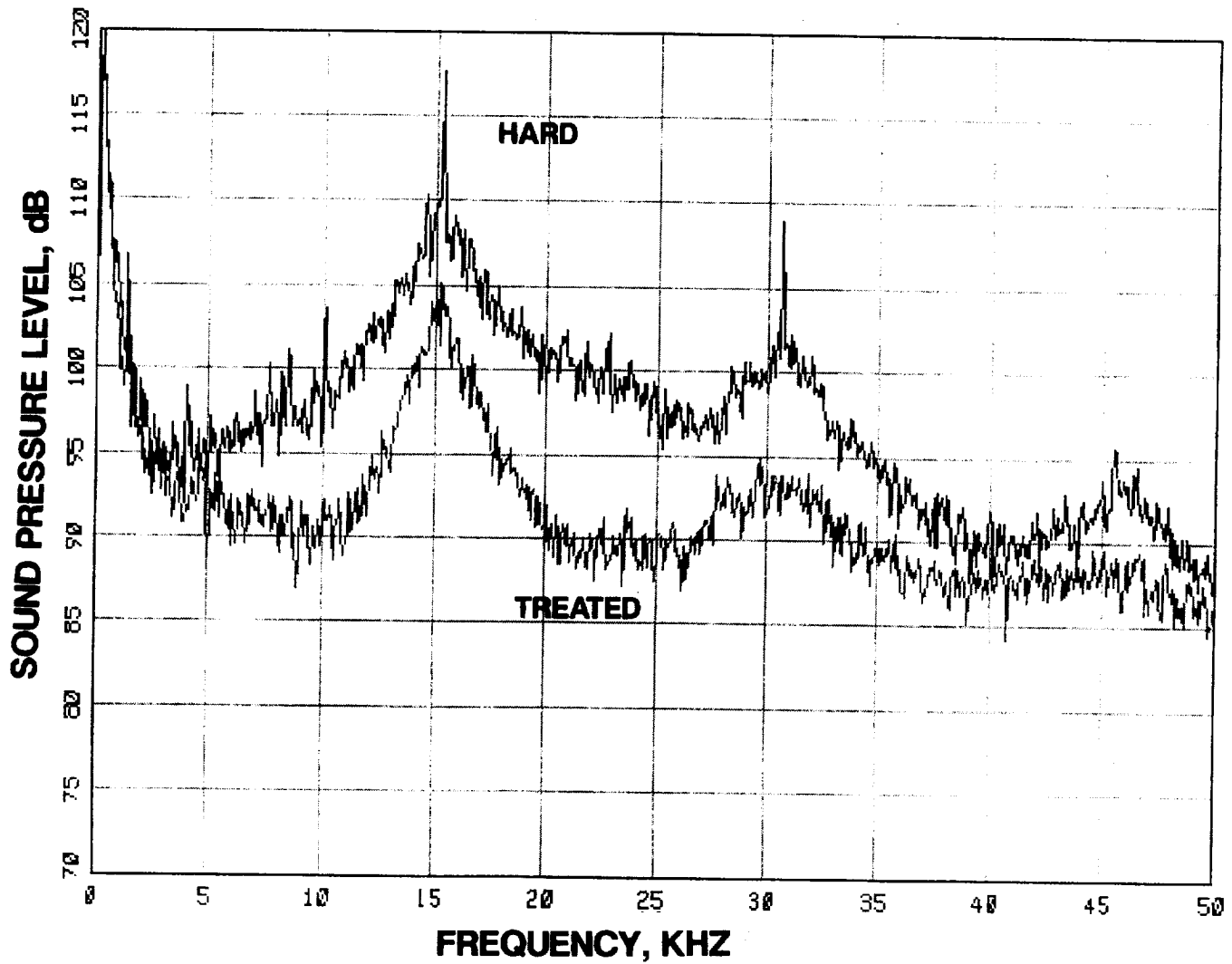


**FIGURE 28 CONCLUDED**

**C 130.5 DEGREES**

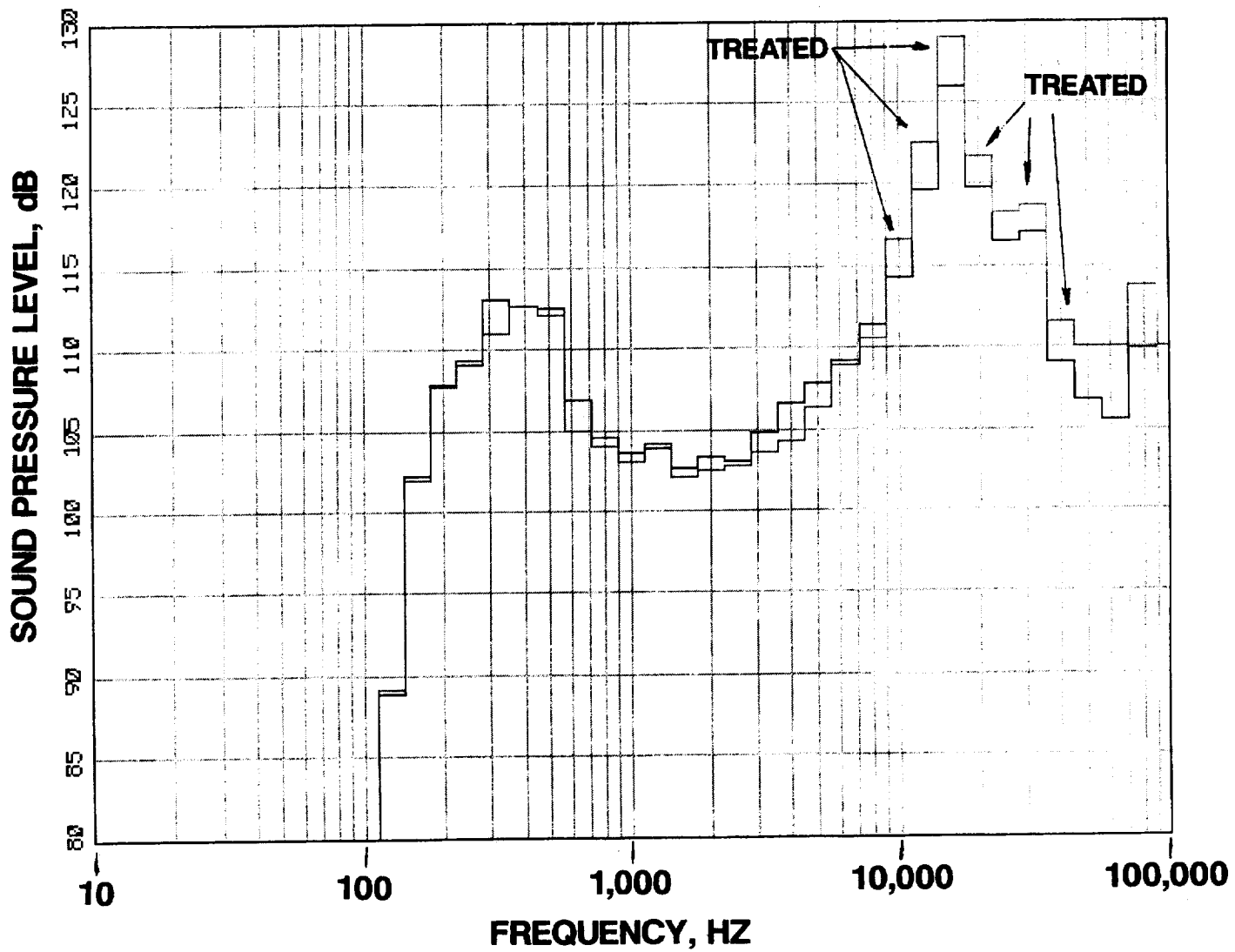


**FIGURE 29 1/3RD OCTAVE COMPARISON OF HARD AND FULLY  
TREATED DATA FOR THE 7 VANE CONFIGURATION AT 8537 RPMC**

**A 24.5 DEGREES**

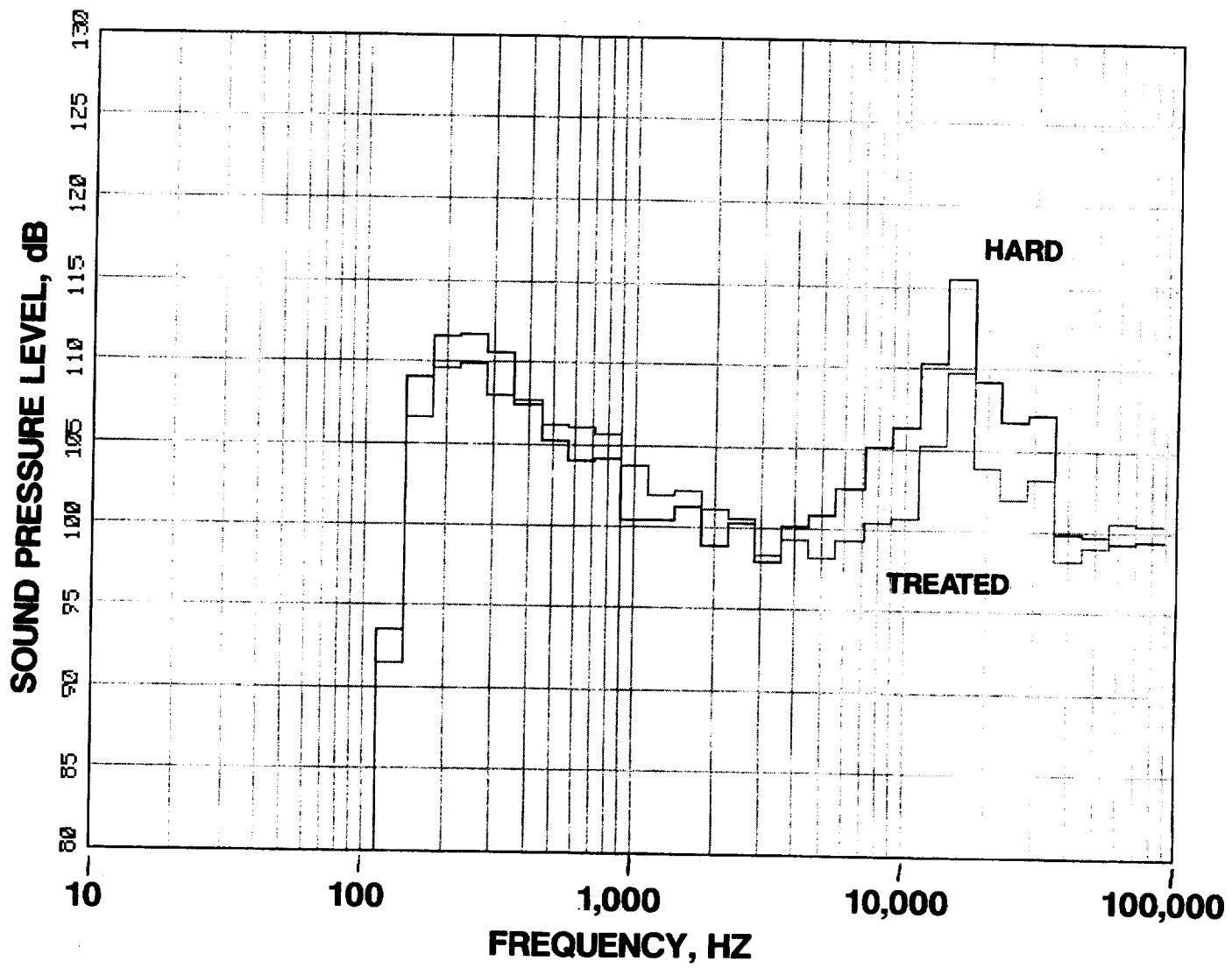


**FIGURE 29 CONTINUED**

**B 92.5 DEGREES**

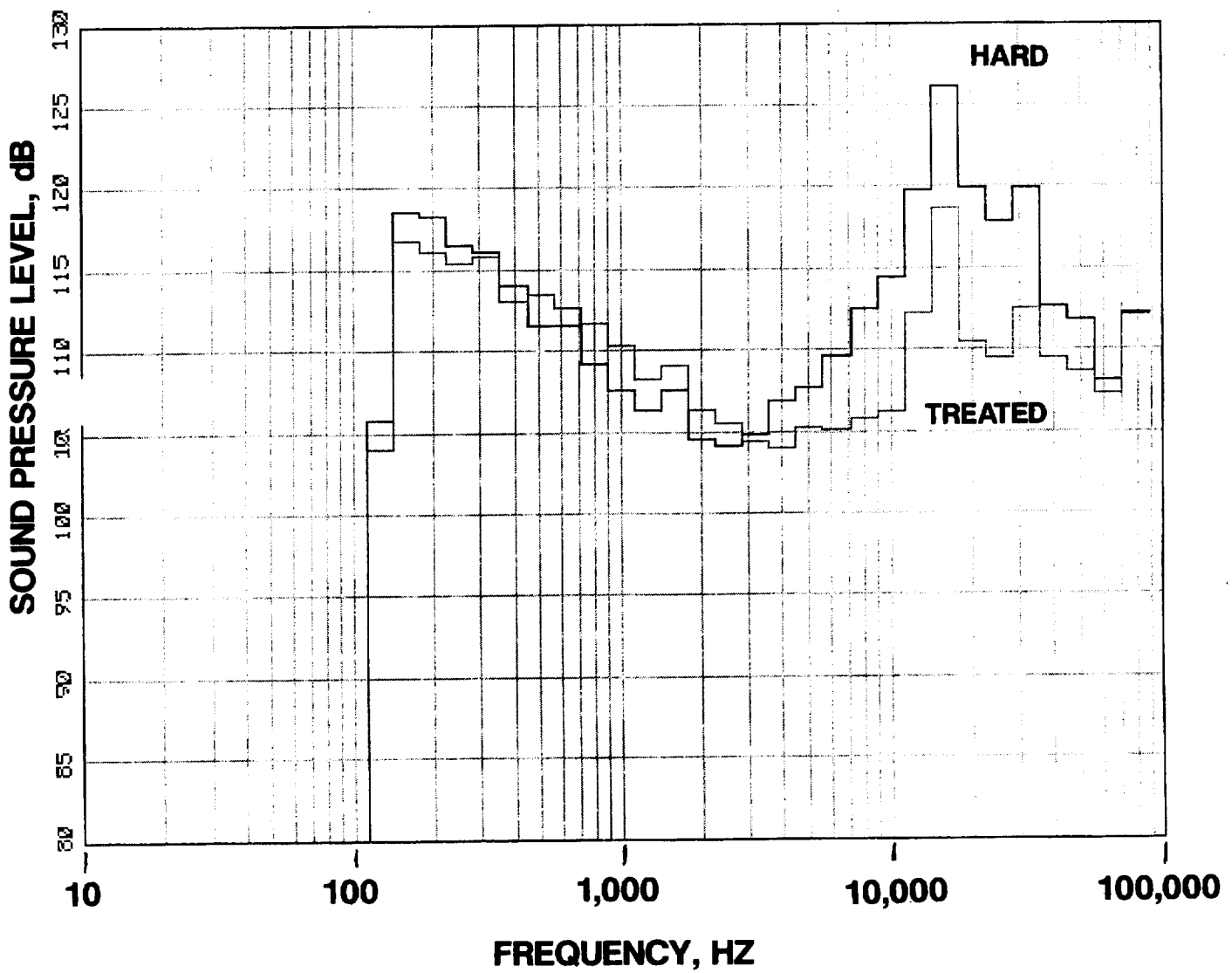


**FIGURE 29 CONCLUDED**

**C 130.5 DEGREES**

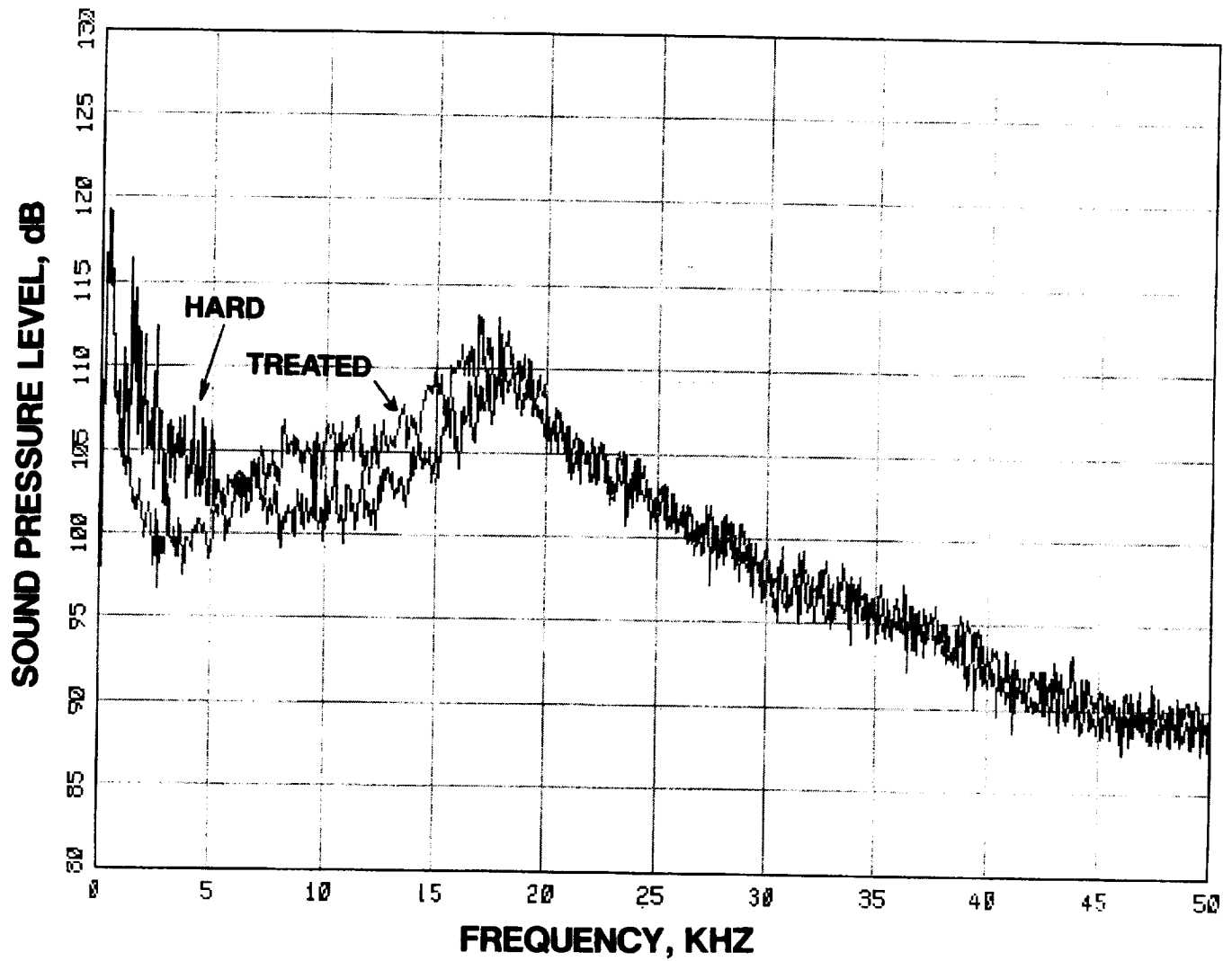


**FIGURE 30 SPECTRAL COMPARISON OF HARD AND FULLY  
TREATED DATA FOR THE 7 VANE CONFIGURATION AT 10671 RPMC**

**A 24.5 DEGREES**

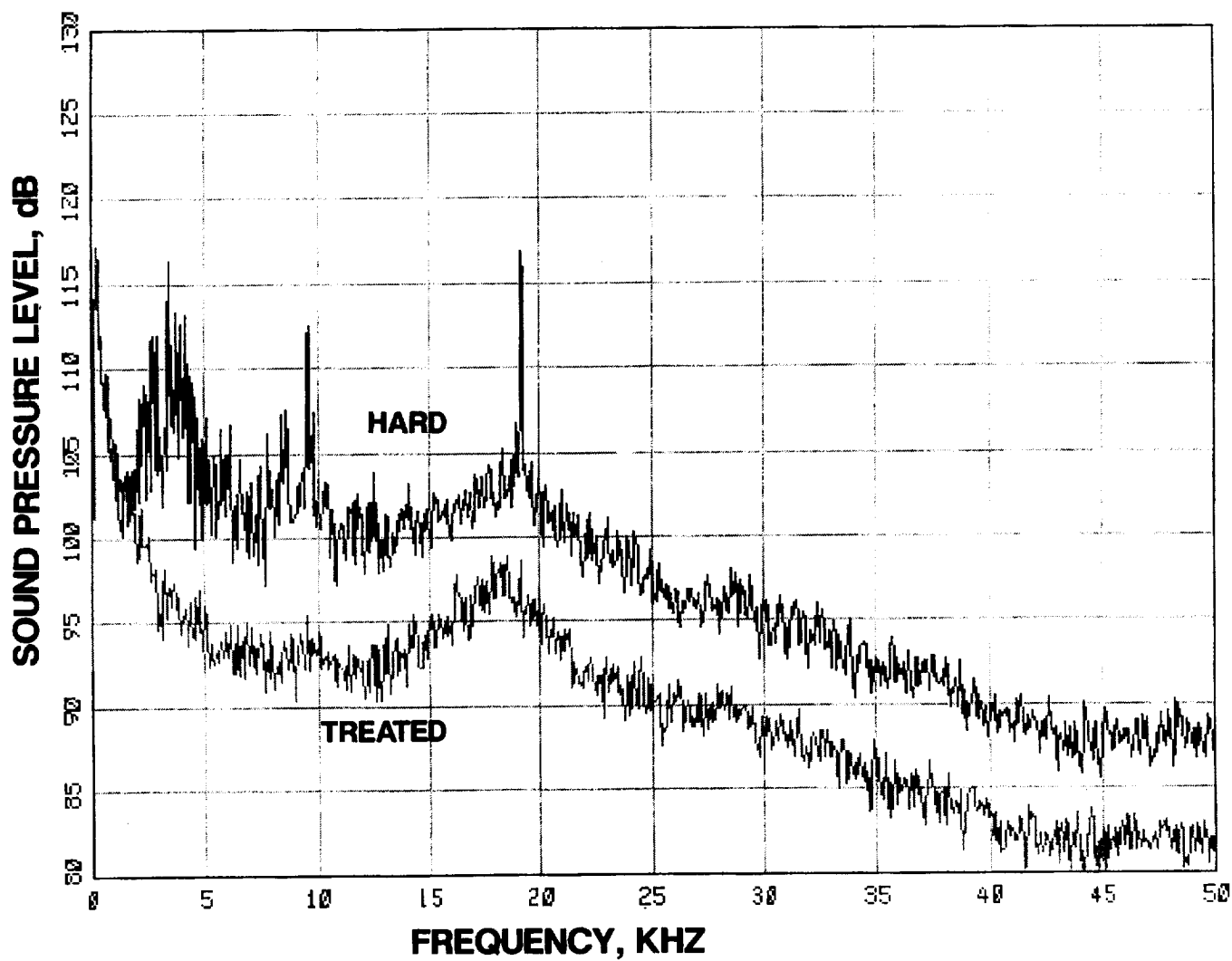


**FIGURE 30 CONTINUED**

**B 92.5 DEGREES**

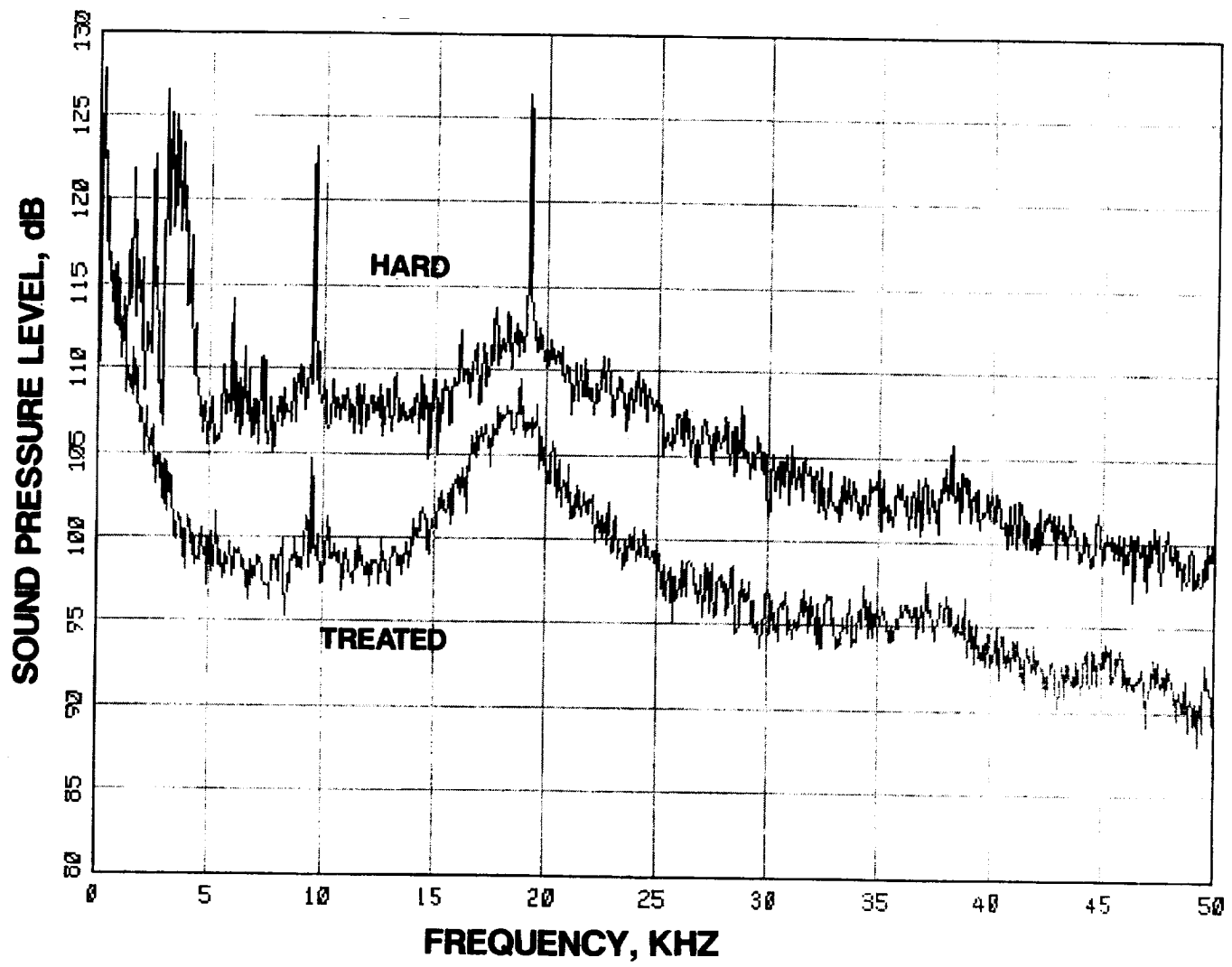


**FIGURE 30 CONCLUDED**

**C 130.5 DEGREES**

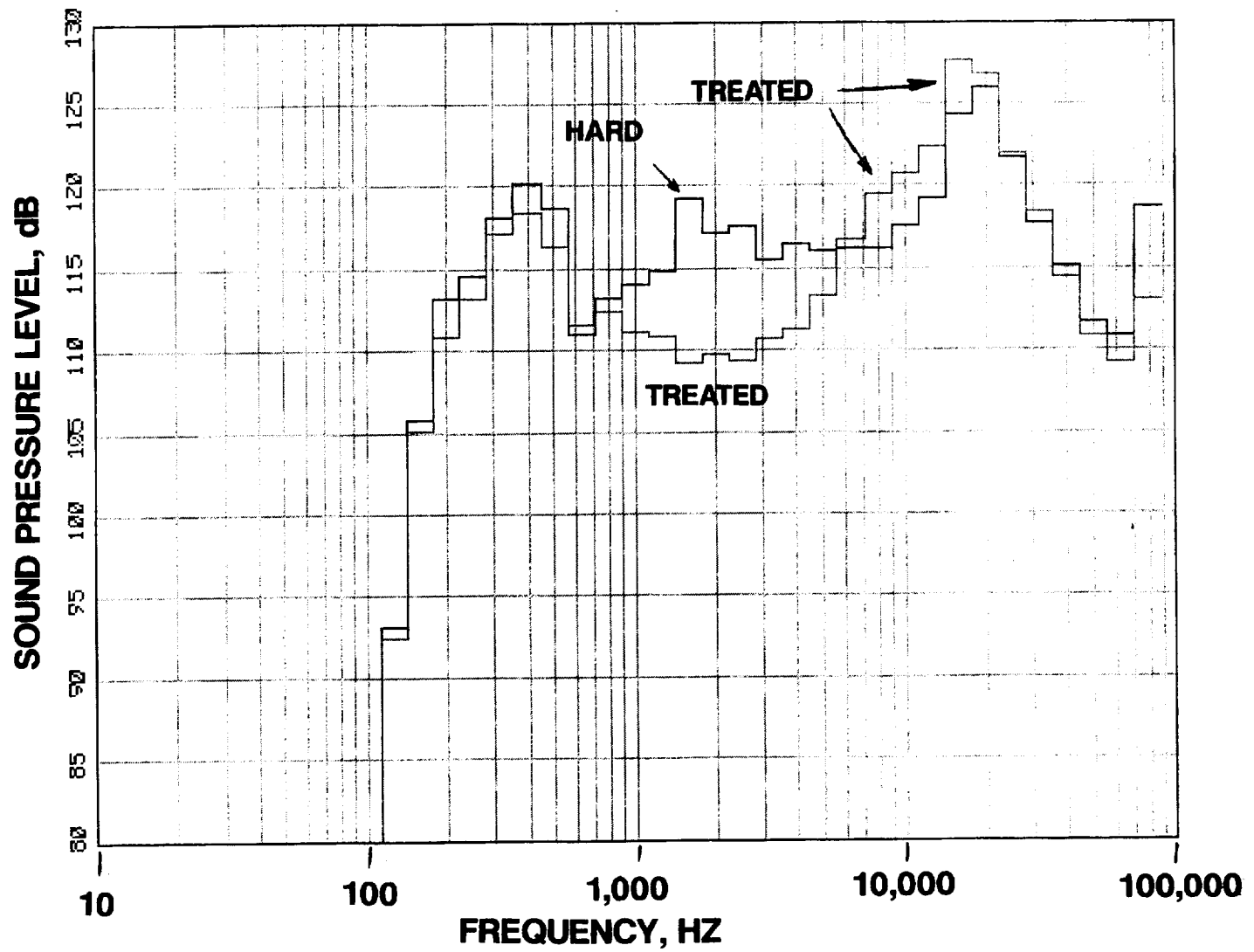


**FIGURE 31 1/3RD OCTAVE COMPARISON OF HARD AND FULLY  
TREATED DATA FOR THE 7 VANE CONFIGURATION AT 10671 RPMC  
A 24.5 DEGREES**

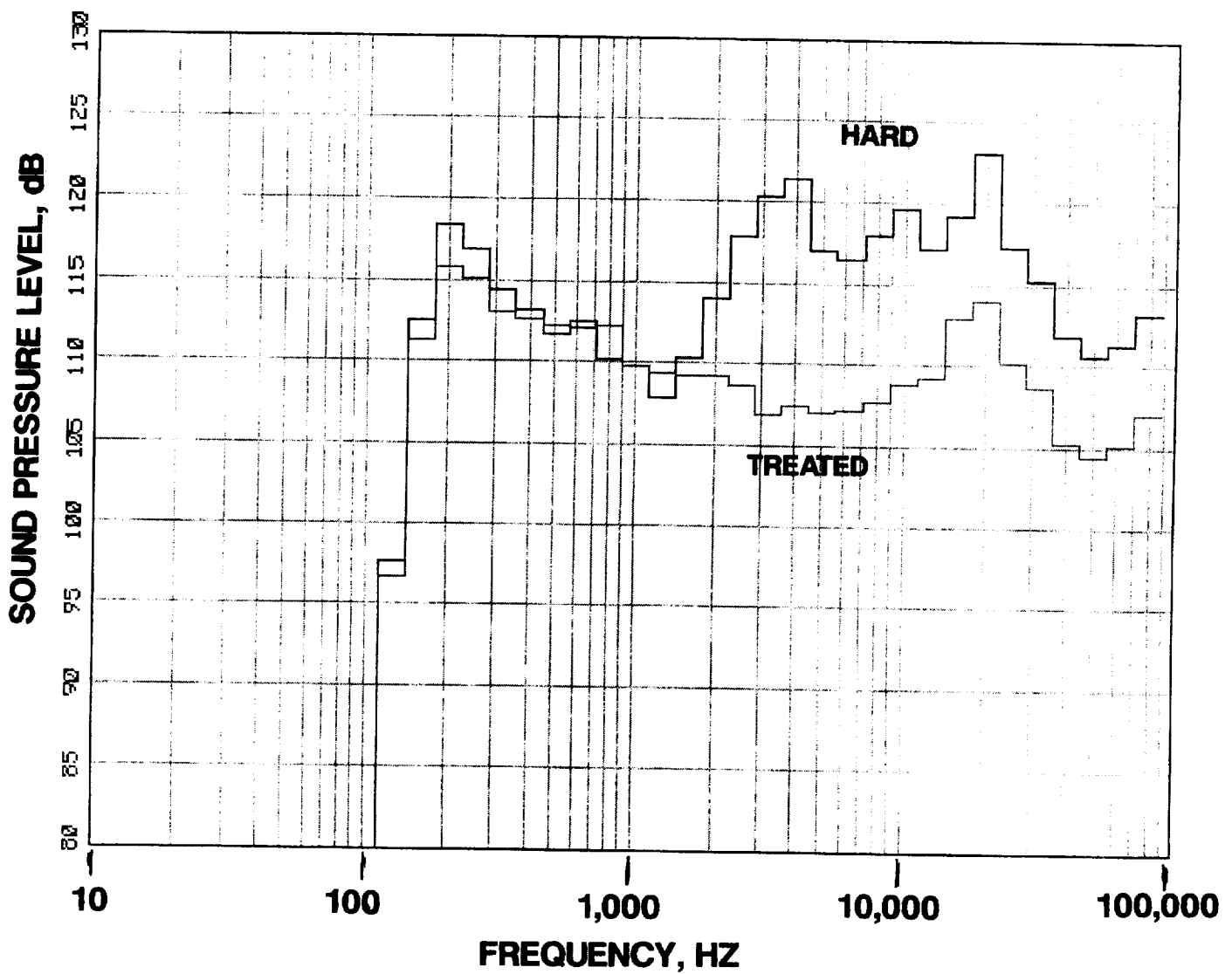


**FIGURE 31 CONTINUED**

**B 92.5 DEGREES**

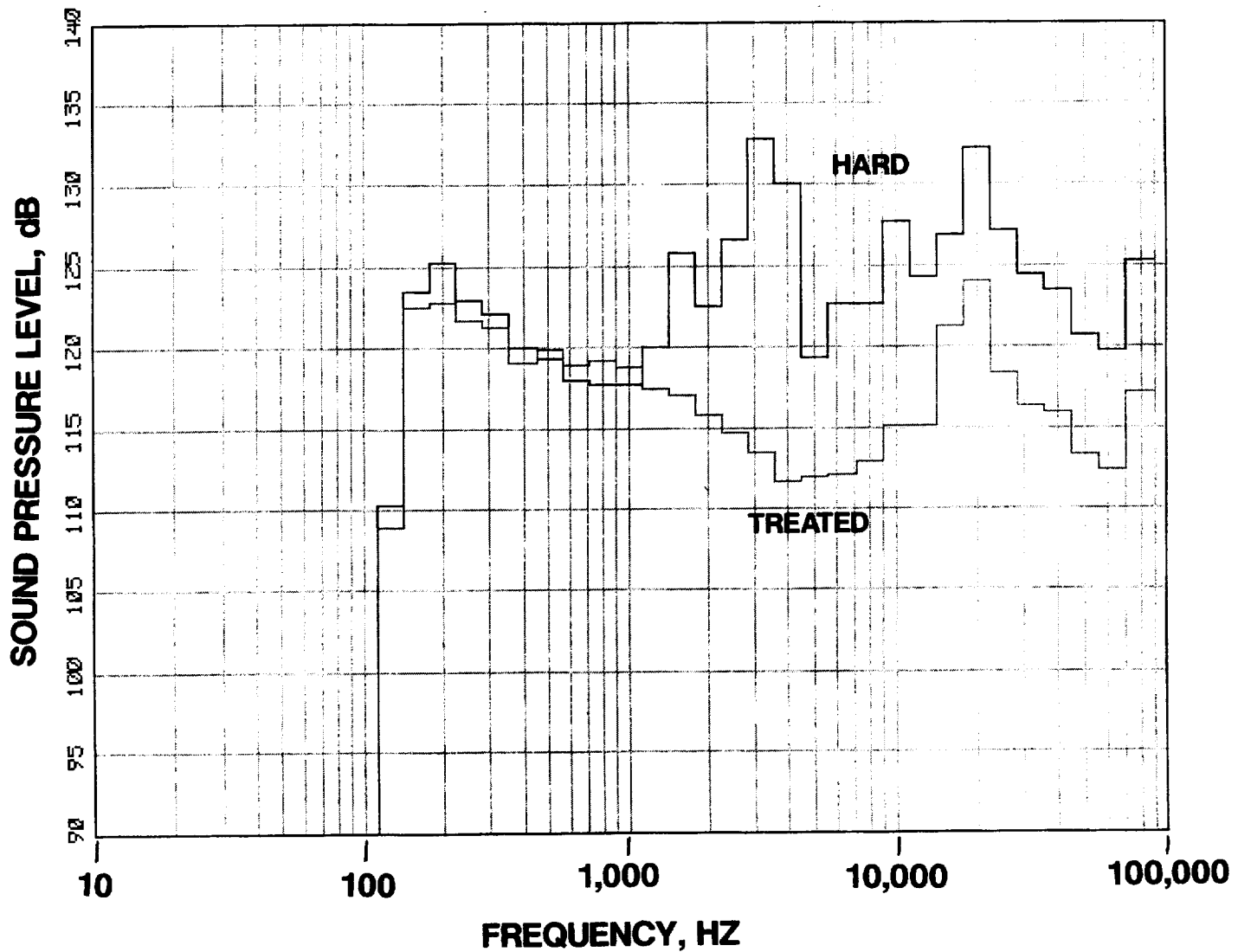


**FIGURE 31 CONCLUDED**

**C 130.5 DEGREES**

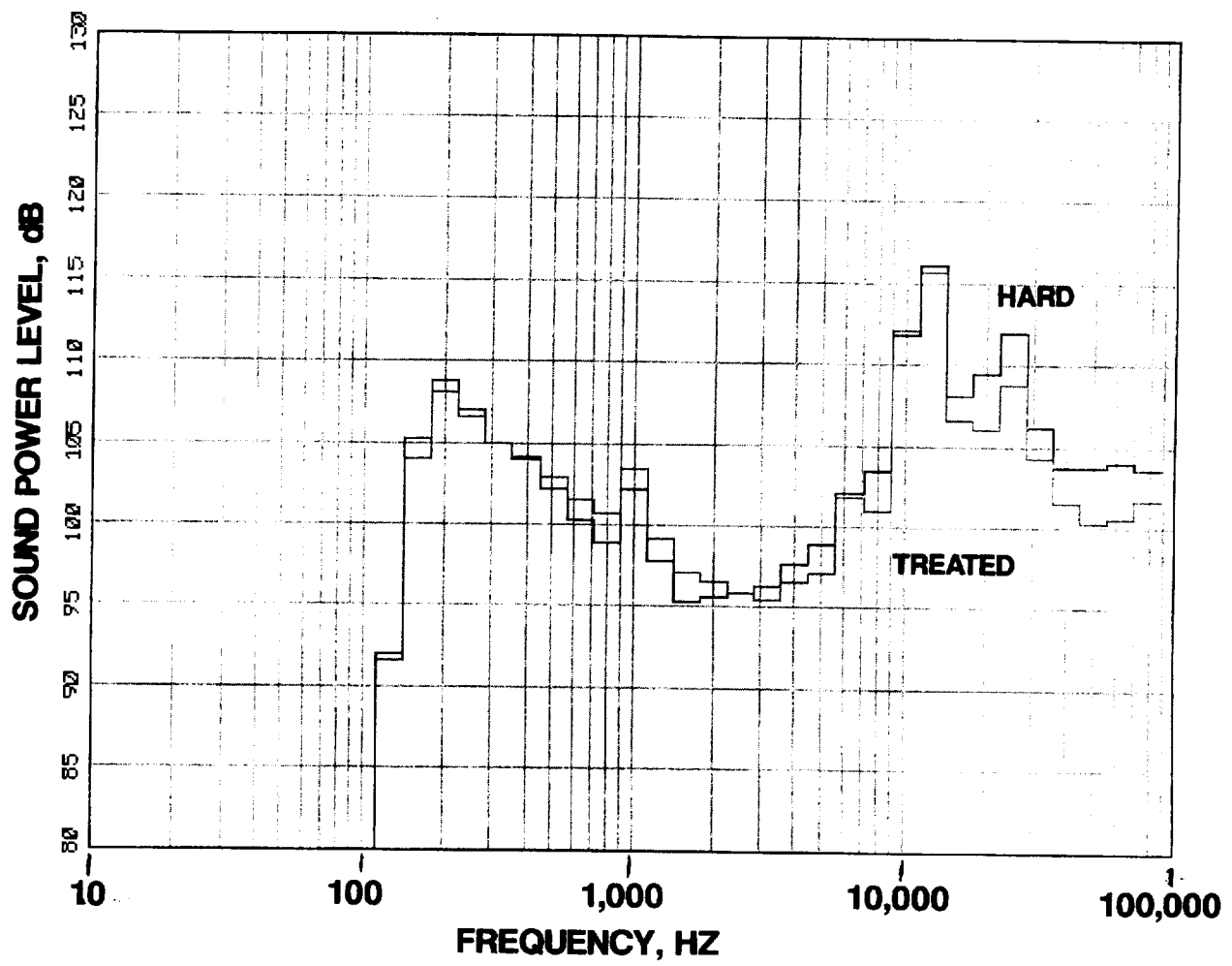


**FIGURE 32 SOUND POWER LEVEL COMPARISON OF HARD AND FULLY  
TREATED DATA FOR THE 7 VANE CONFIGURATION**

**A 6402 RPMC**

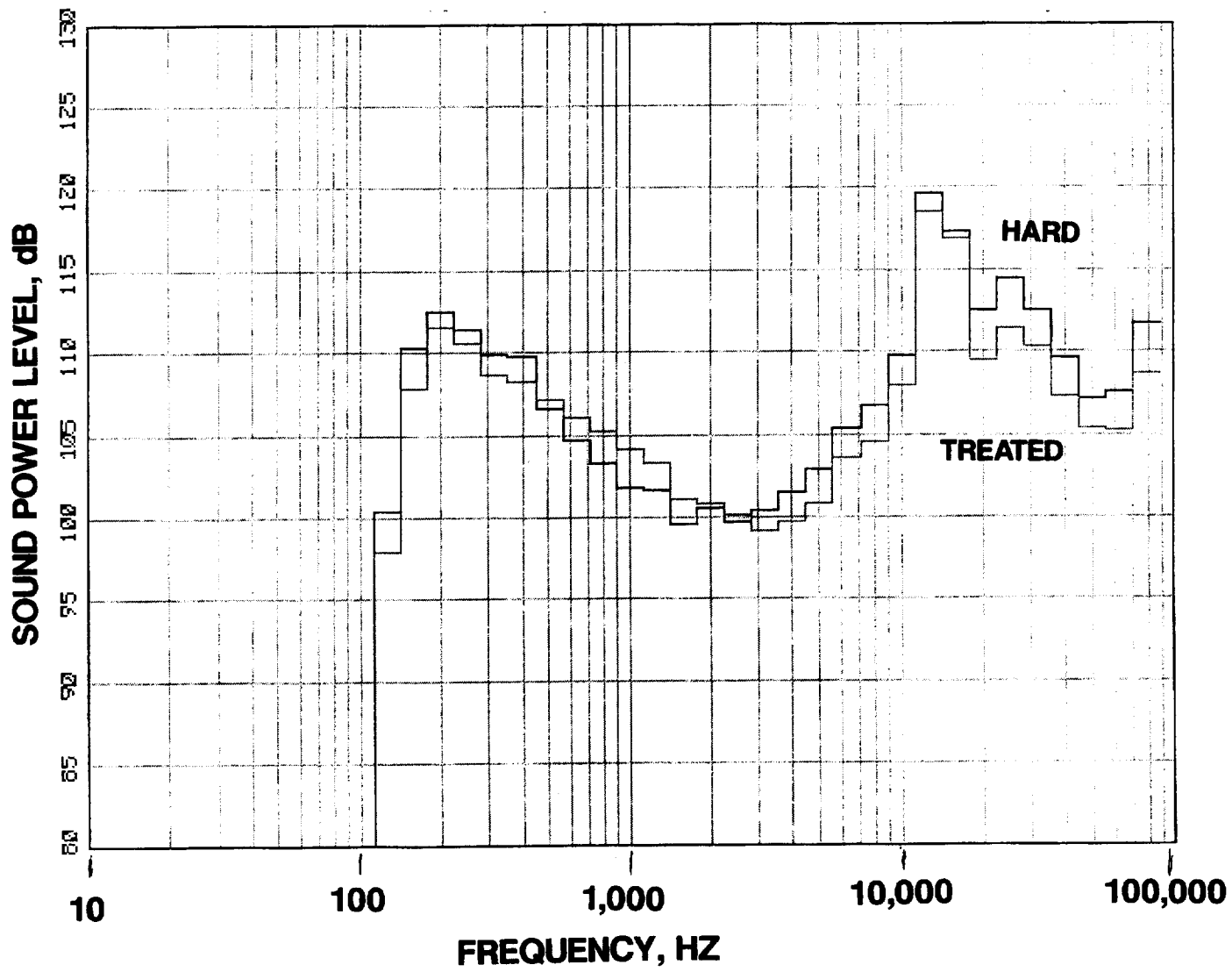


**FIGURE 32 CONTINUED**

**B 7736 RPMC**

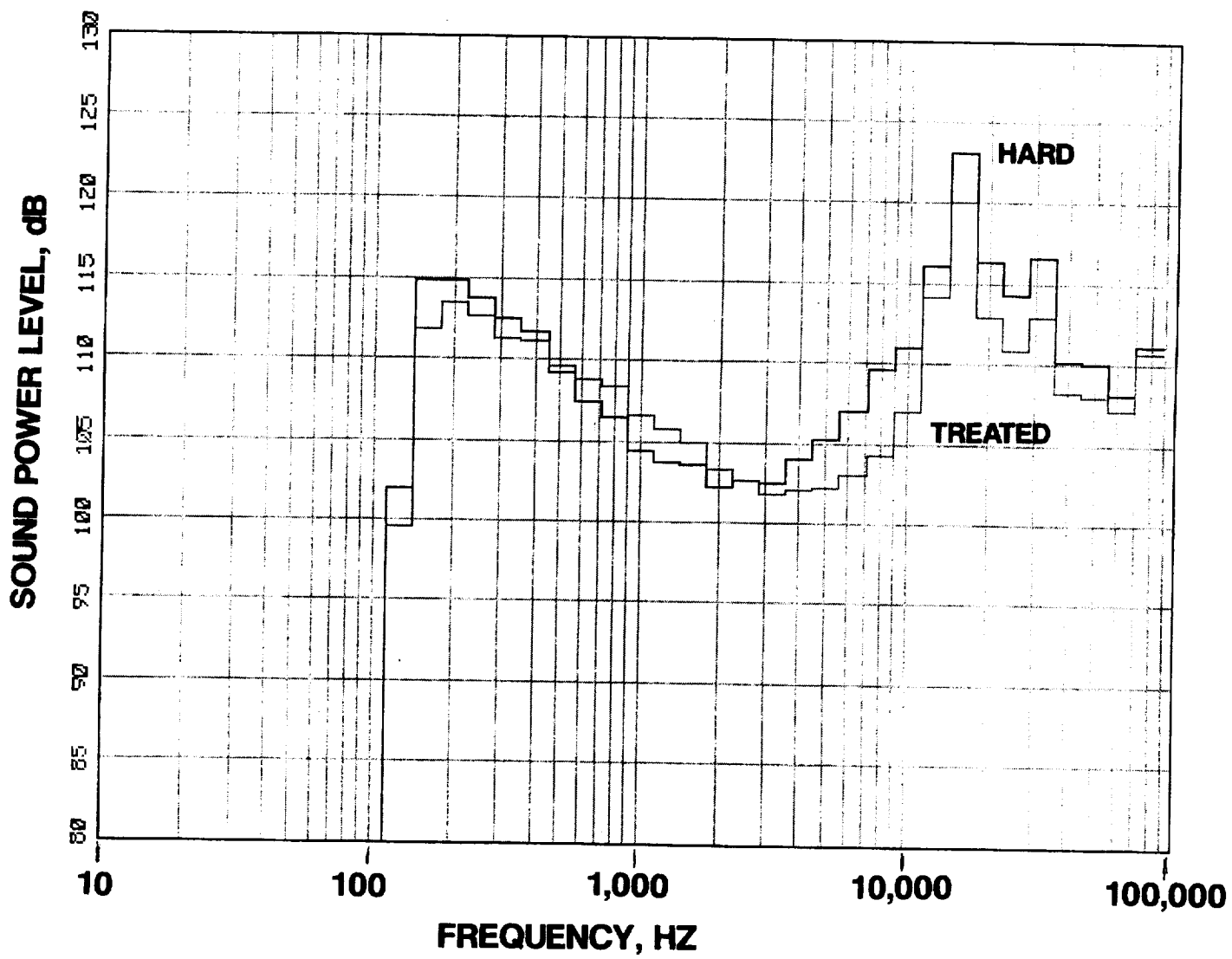


**FIGURE 32 CONTINUED**

**C 8537 RPMC**

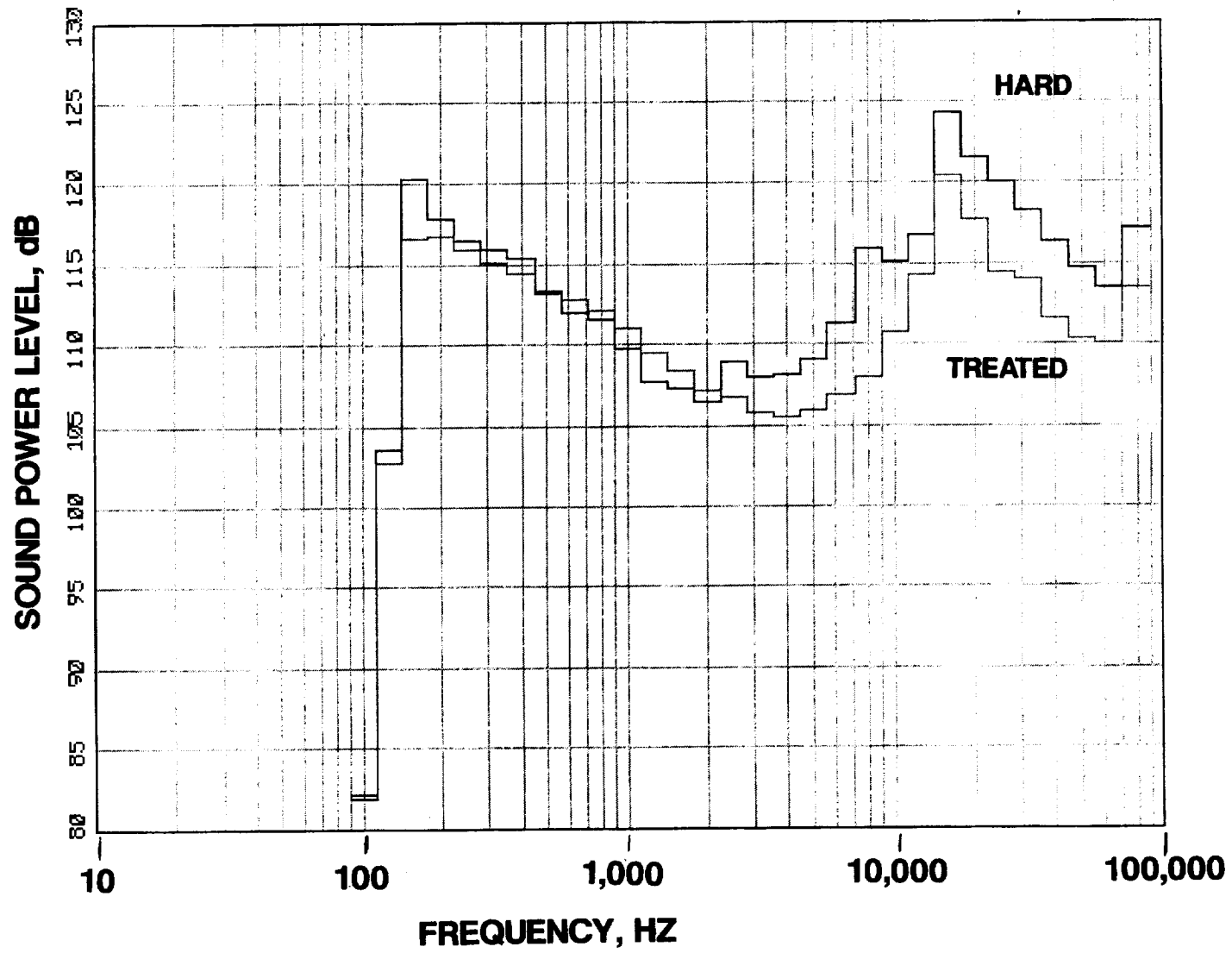


**FIGURE 32 CONTINUED**

**D 9604 RPMC**

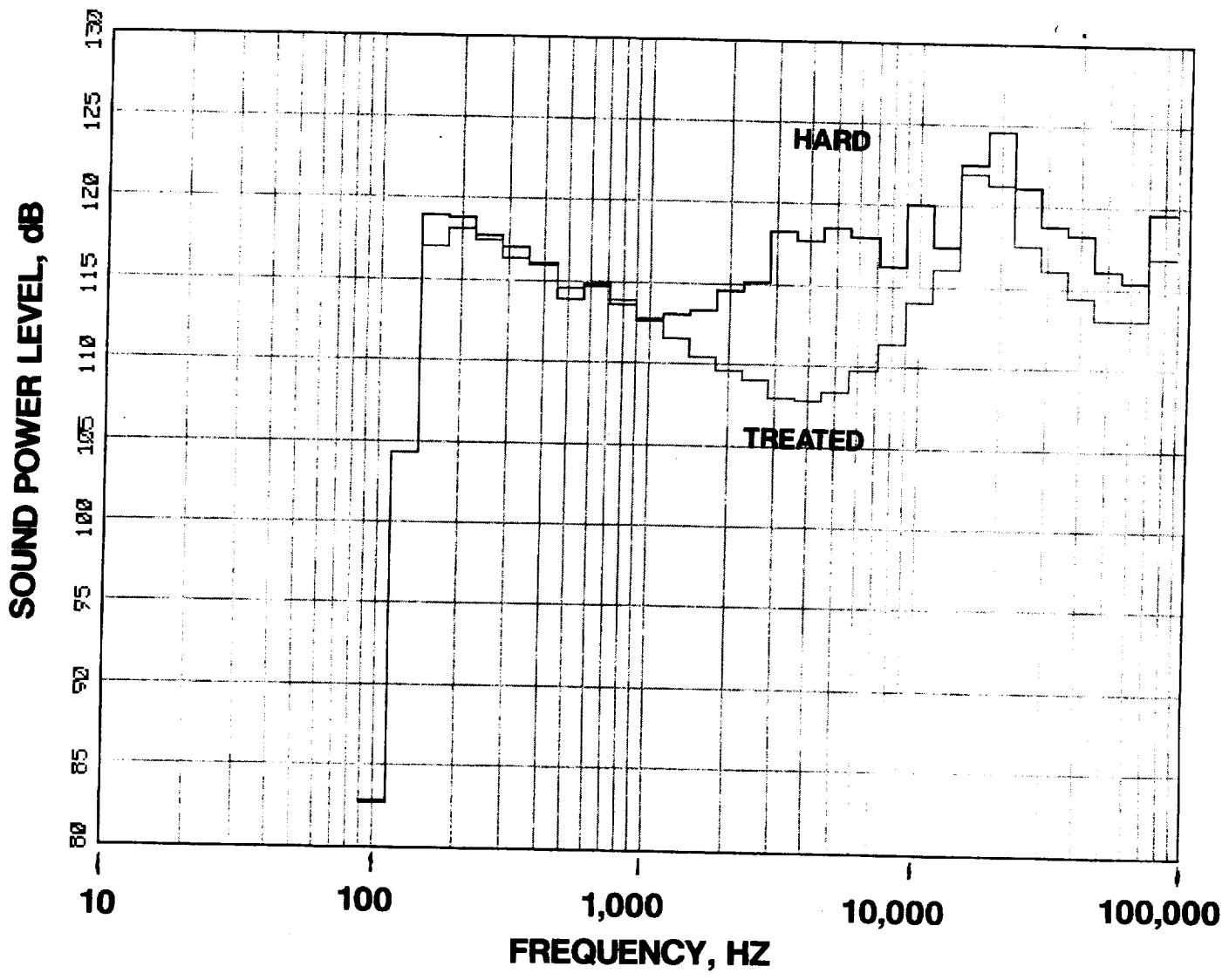


**FIGURE 32 CONTINUED**

**E 10137 RPMC**

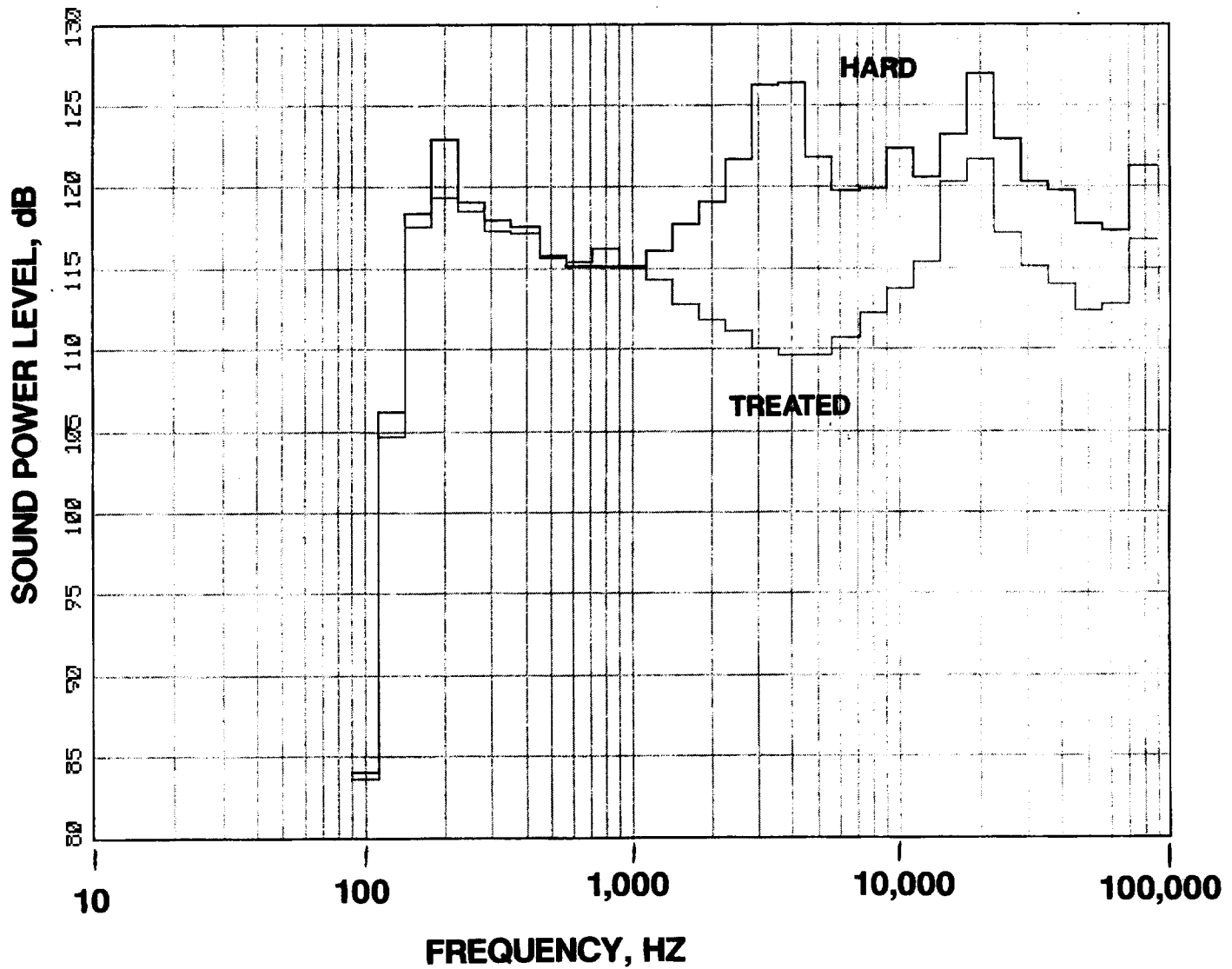


**FIGURE 32 CONCLUDED**

**F 10671 RPMC**

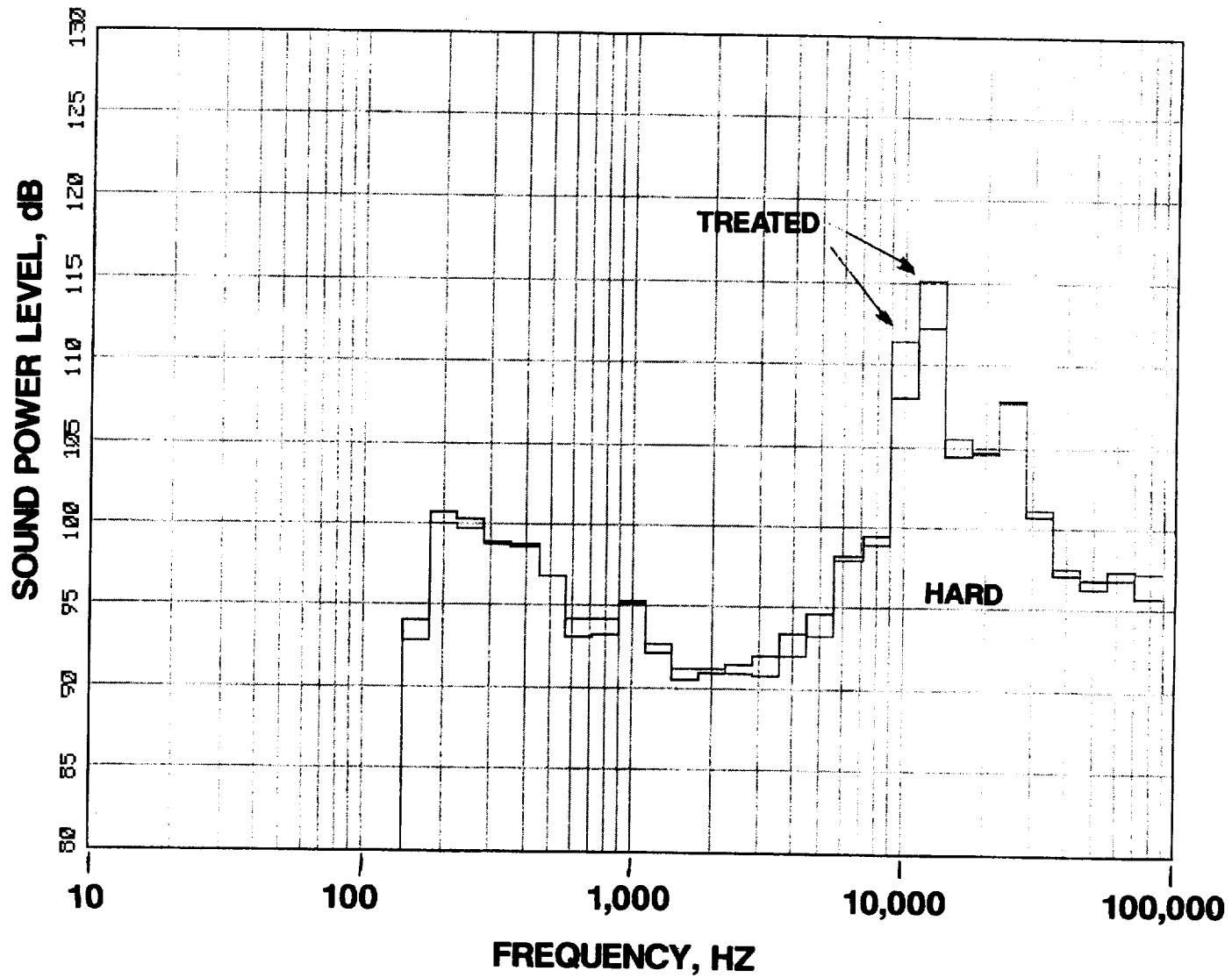


**FIGURE 33 FRONT SOUND POWER LEVEL COMPARISON OF HARD AND FULLY TREATED DATA FOR THE 7 VANE CONFIGURATION**

A 6402 RPMC

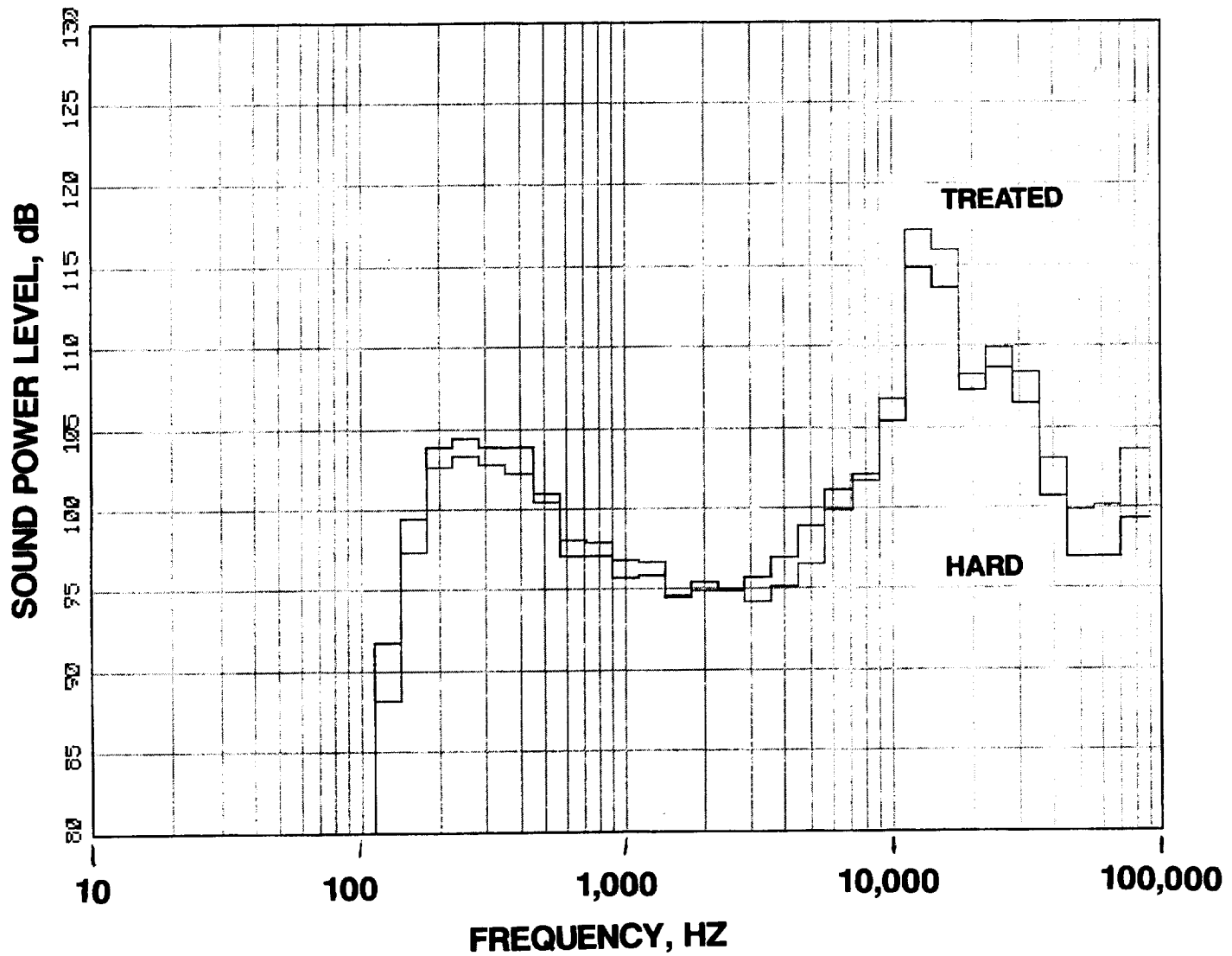


**FIGURE 33 CONTINUED**

**B 7736 RPMC**

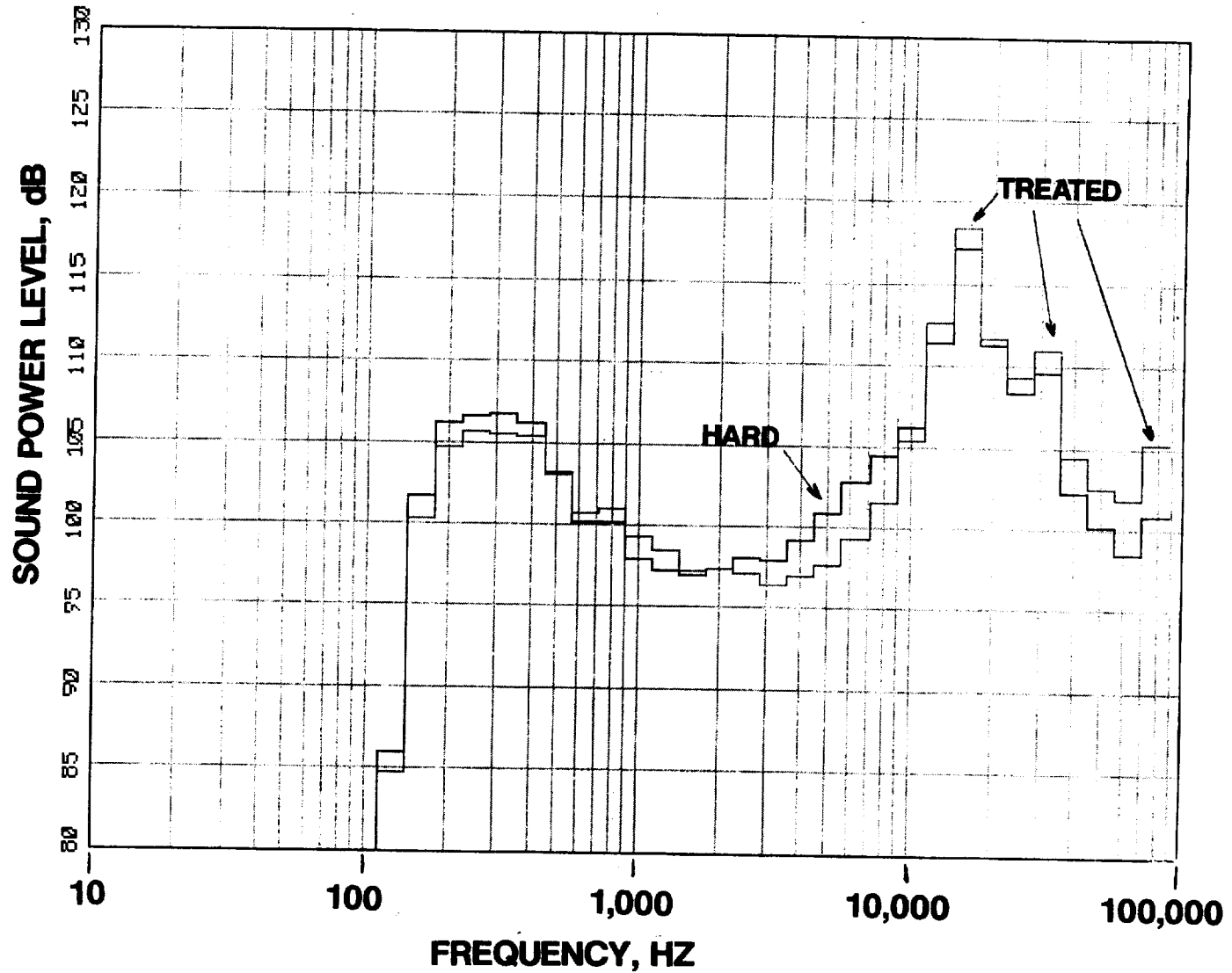


**FIGURE 33 CONTINUED**

**C 8537 RPMC**

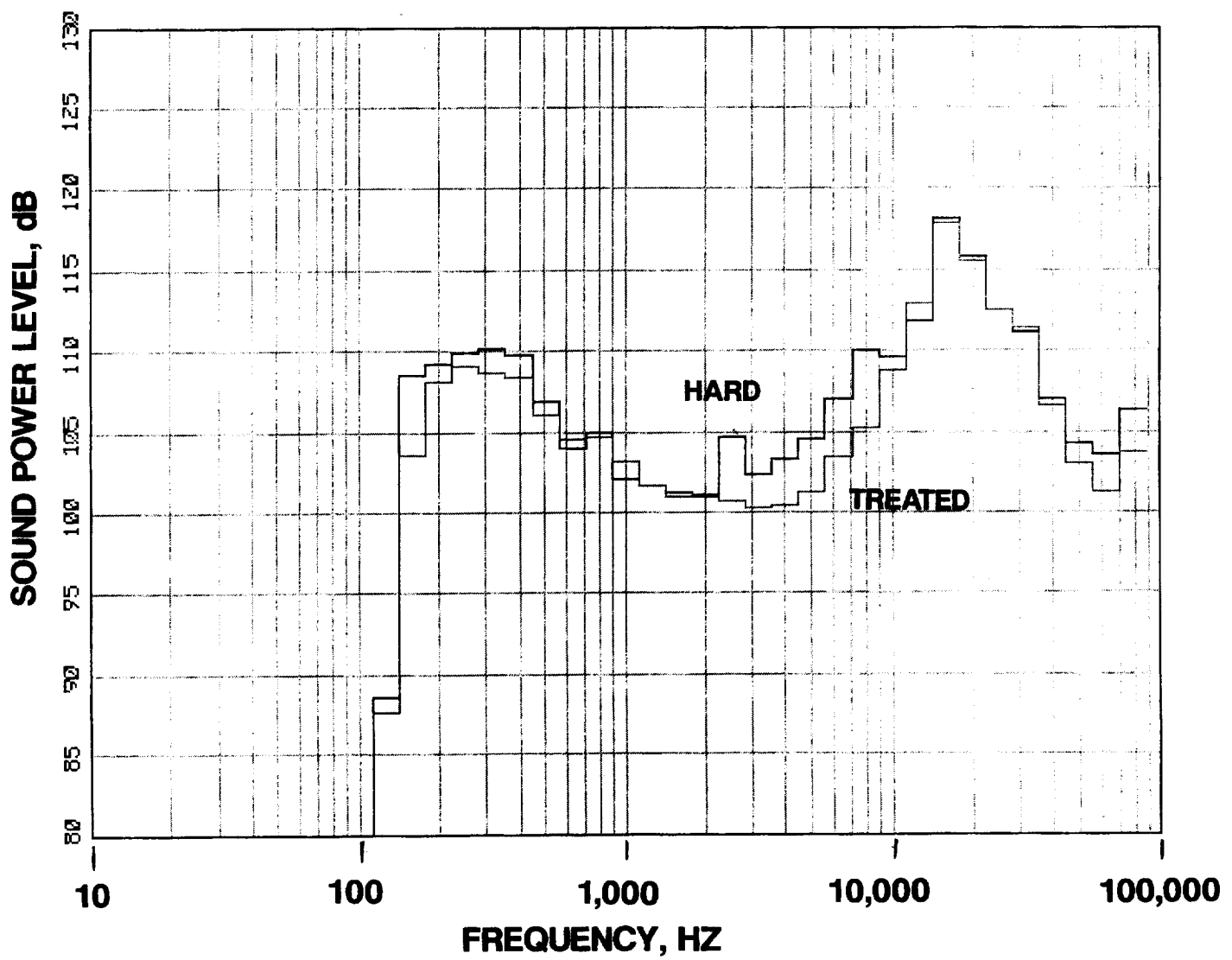


**FIGURE 33 CONTINUED**

**D 9604 RPMC**

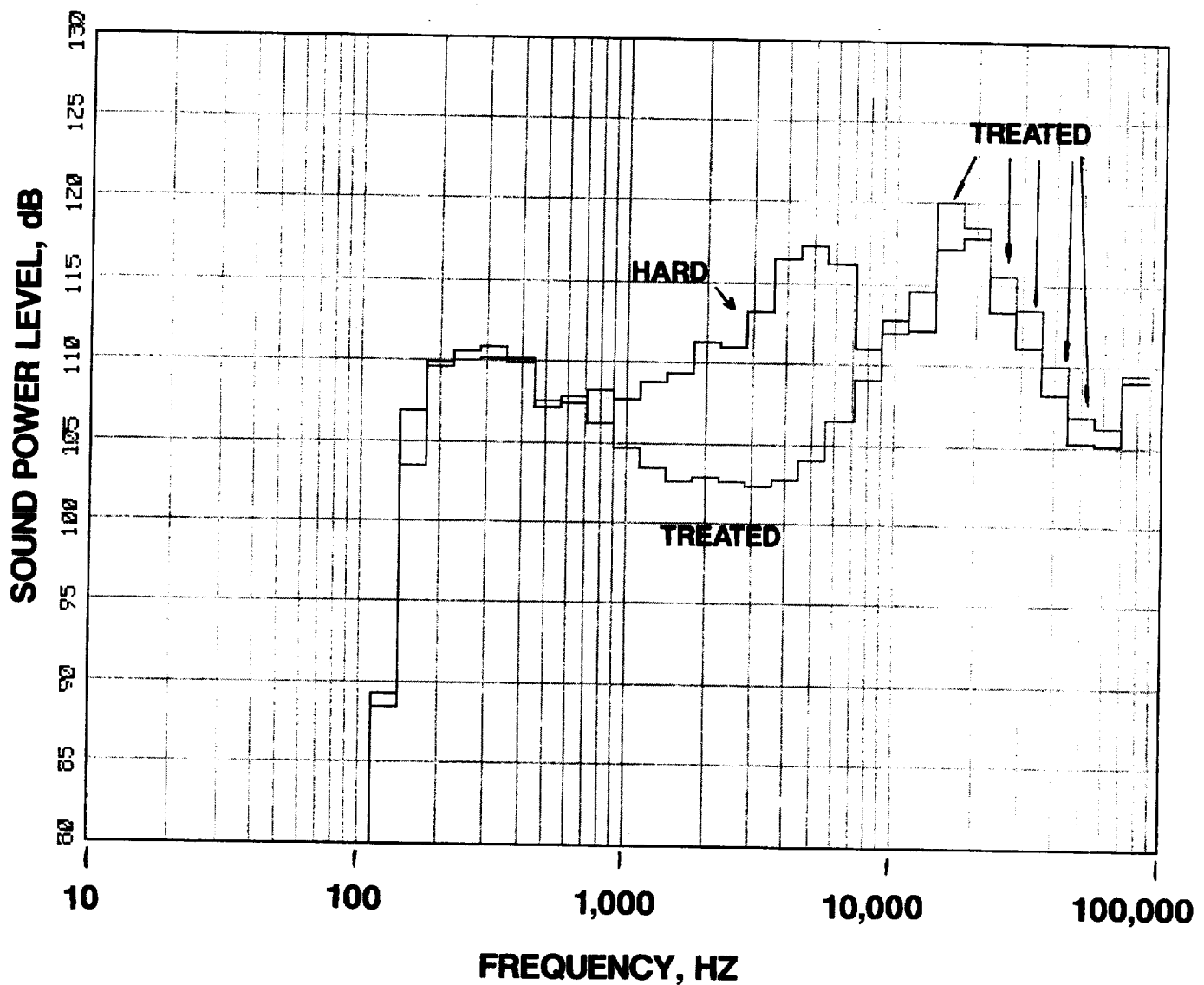


**FIGURE 33 CONTINUED**

**E 10137 RPCMC**

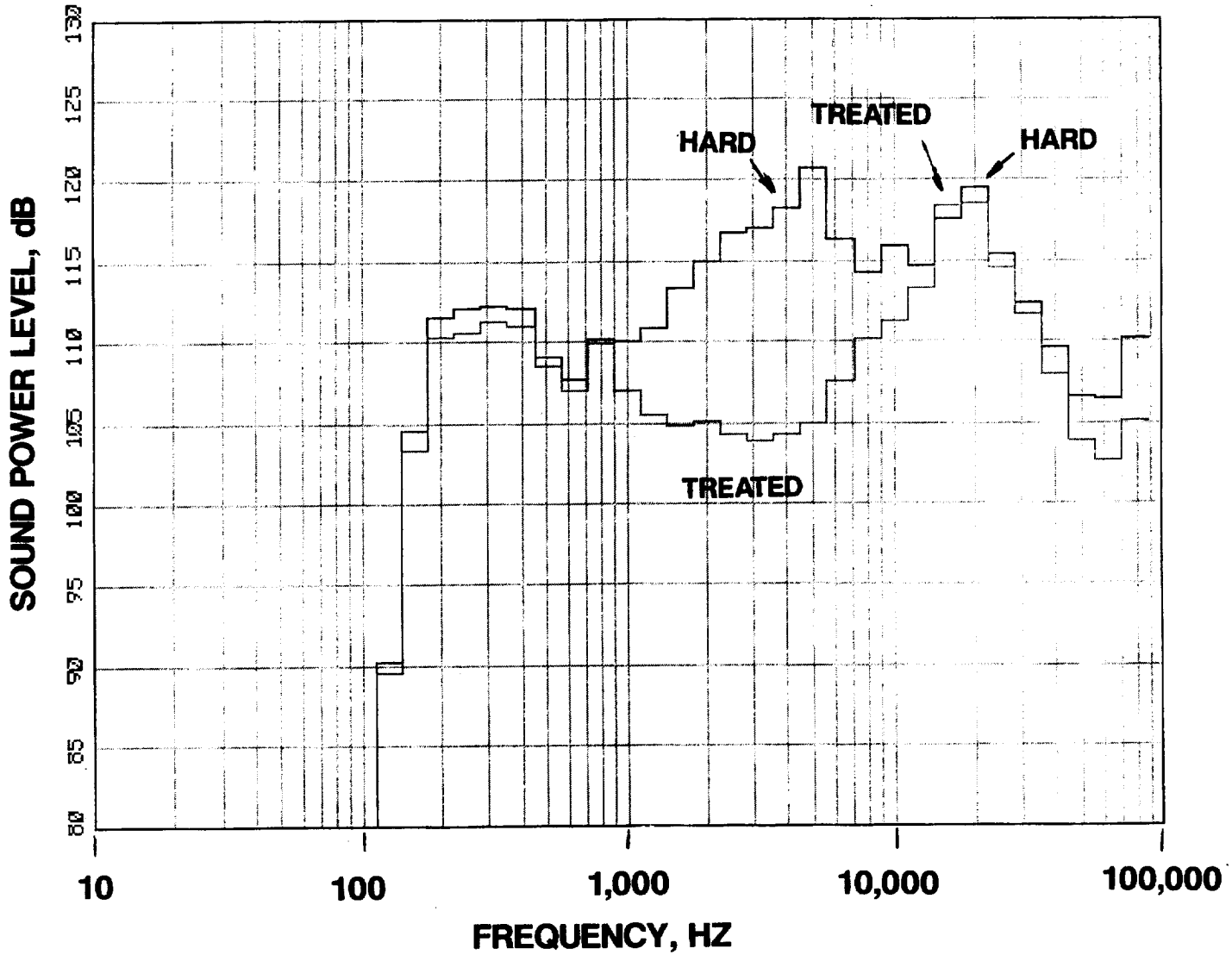


**FIGURE 33 CONCLUDED**

**F 10671 RPMC**

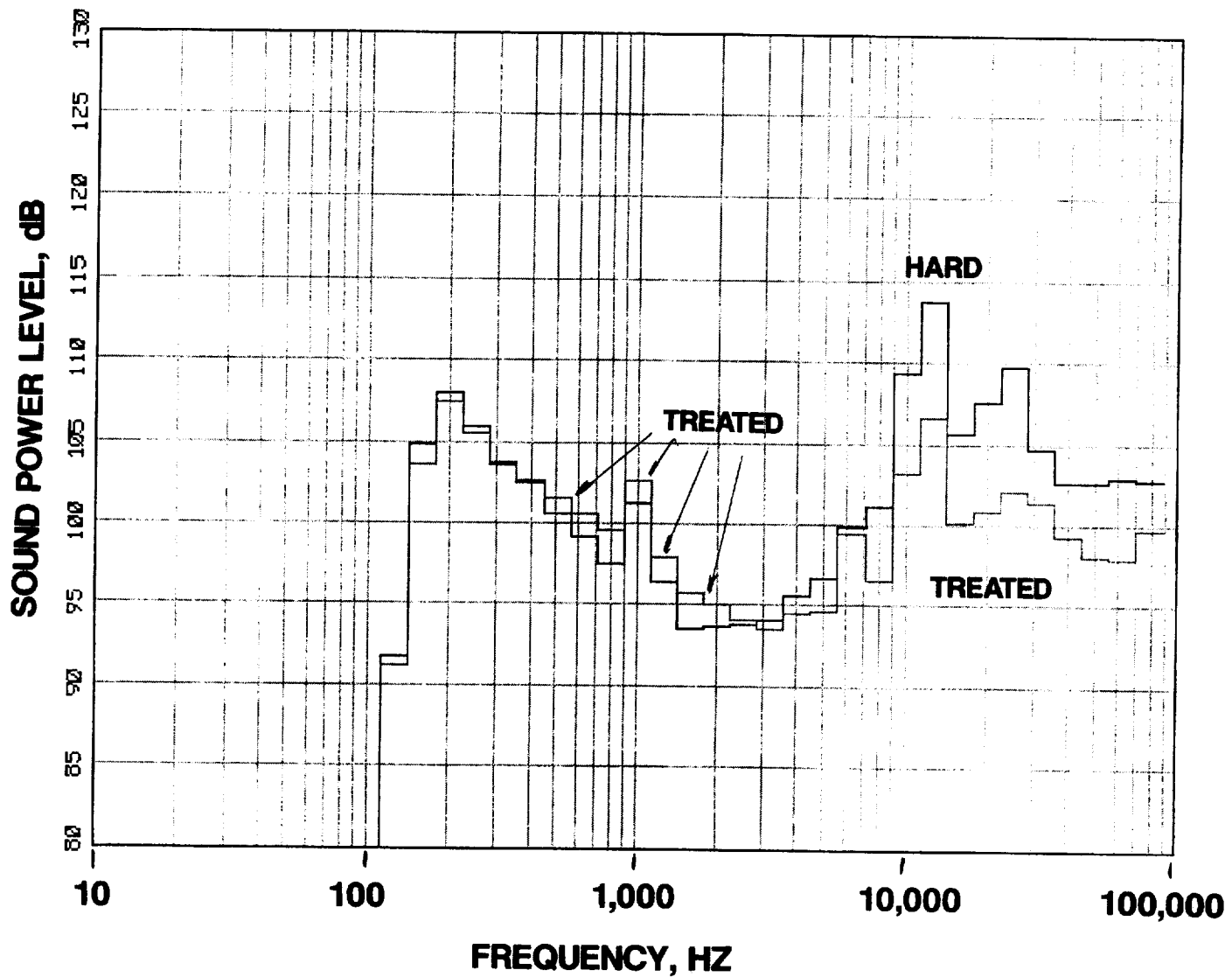


**FIGURE 34 AFT SOUND POWER LEVEL COMPARISON OF HARD AND FULLY TREATED DATA FOR THE 7 VANE CONFIGURATION**

**A 6402 RPMC**

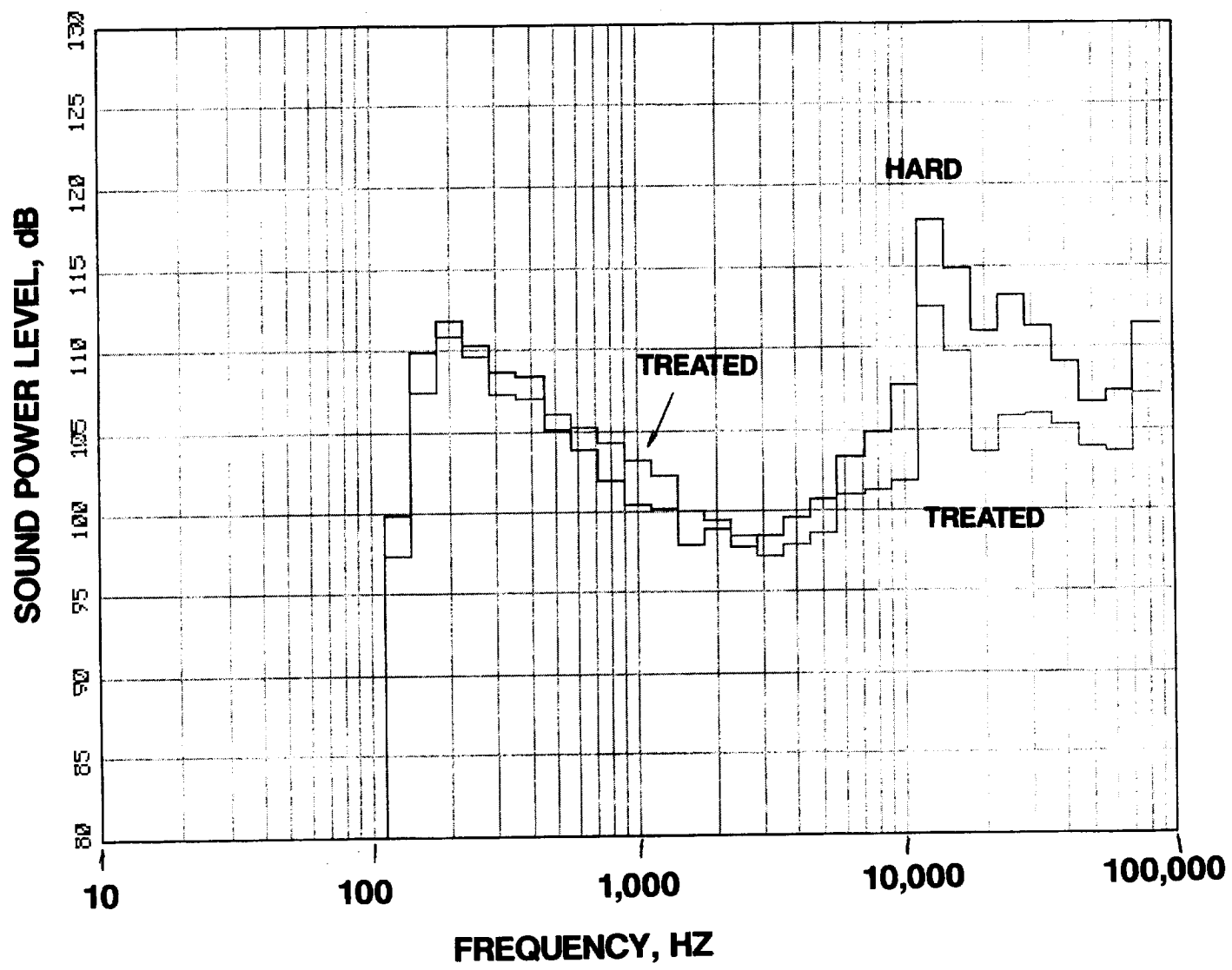


**FIGURE 34 CONTINUED**

**B 7736 RPMC**

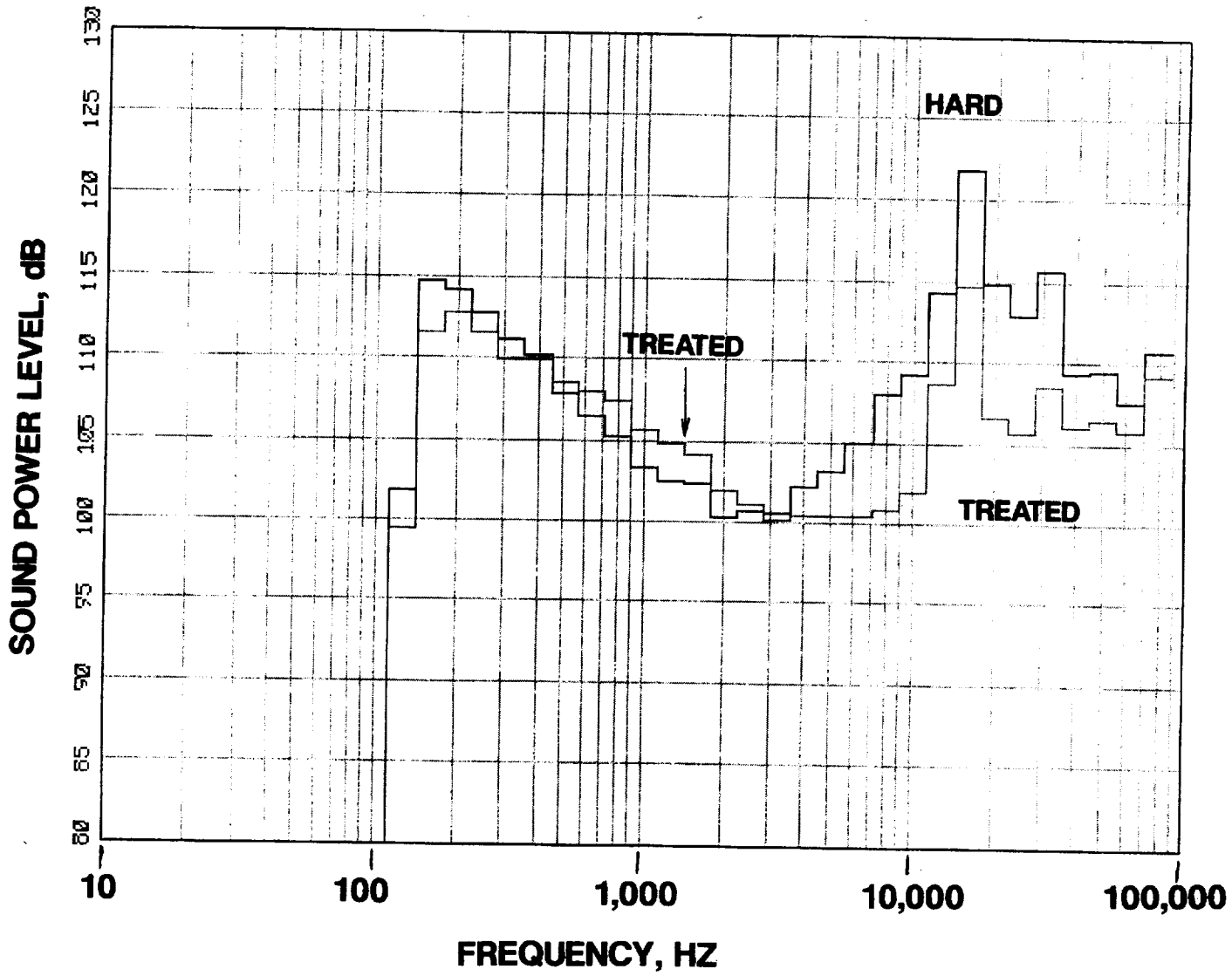


**FIGURE 34 CONTINUED**

**C 8537 RPMC**

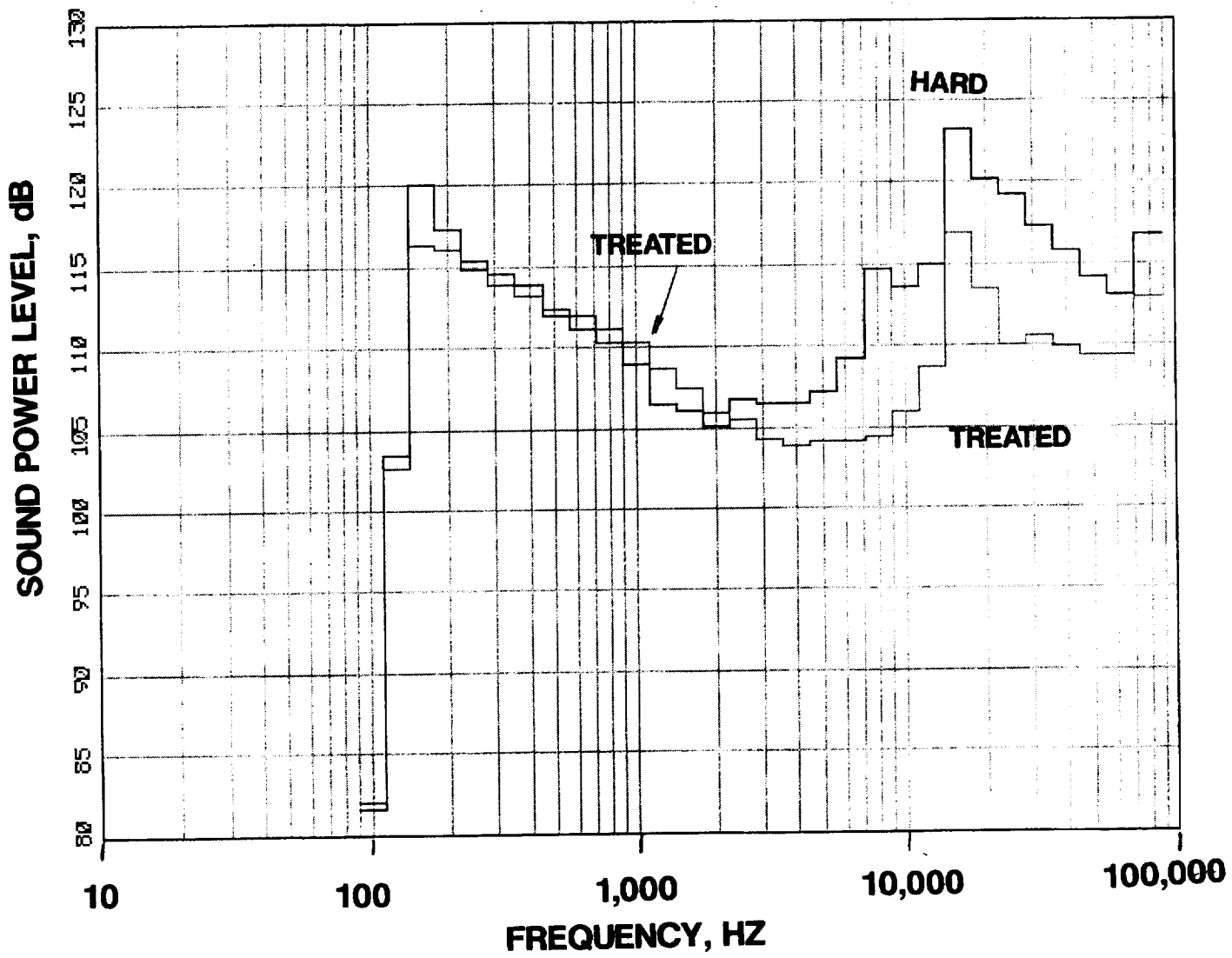


**FIGURE 34 CONTINUED**

**D 9604 RPMC**

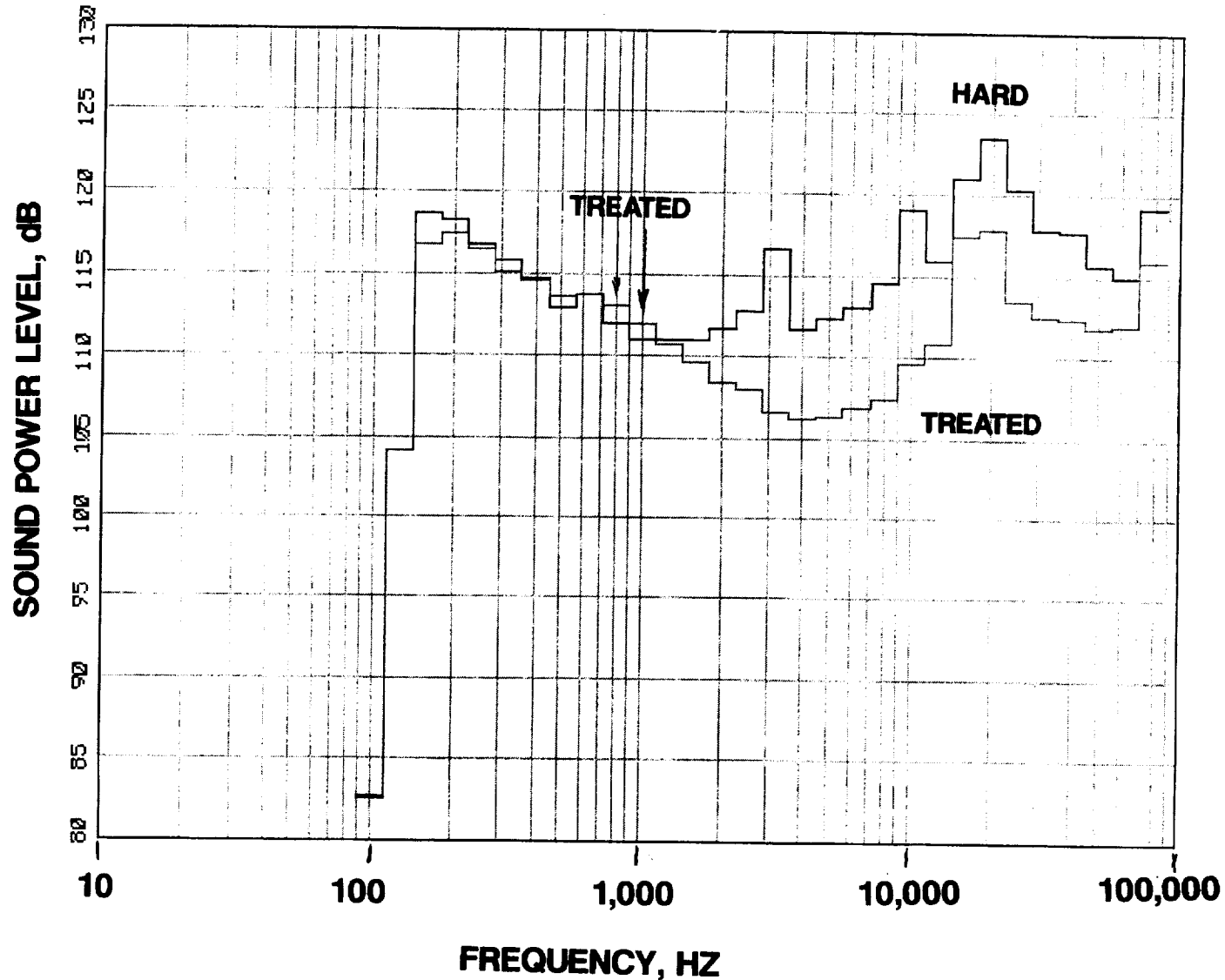


**FIGURE 34 CONTINUED**

**E 10137 RPMC**

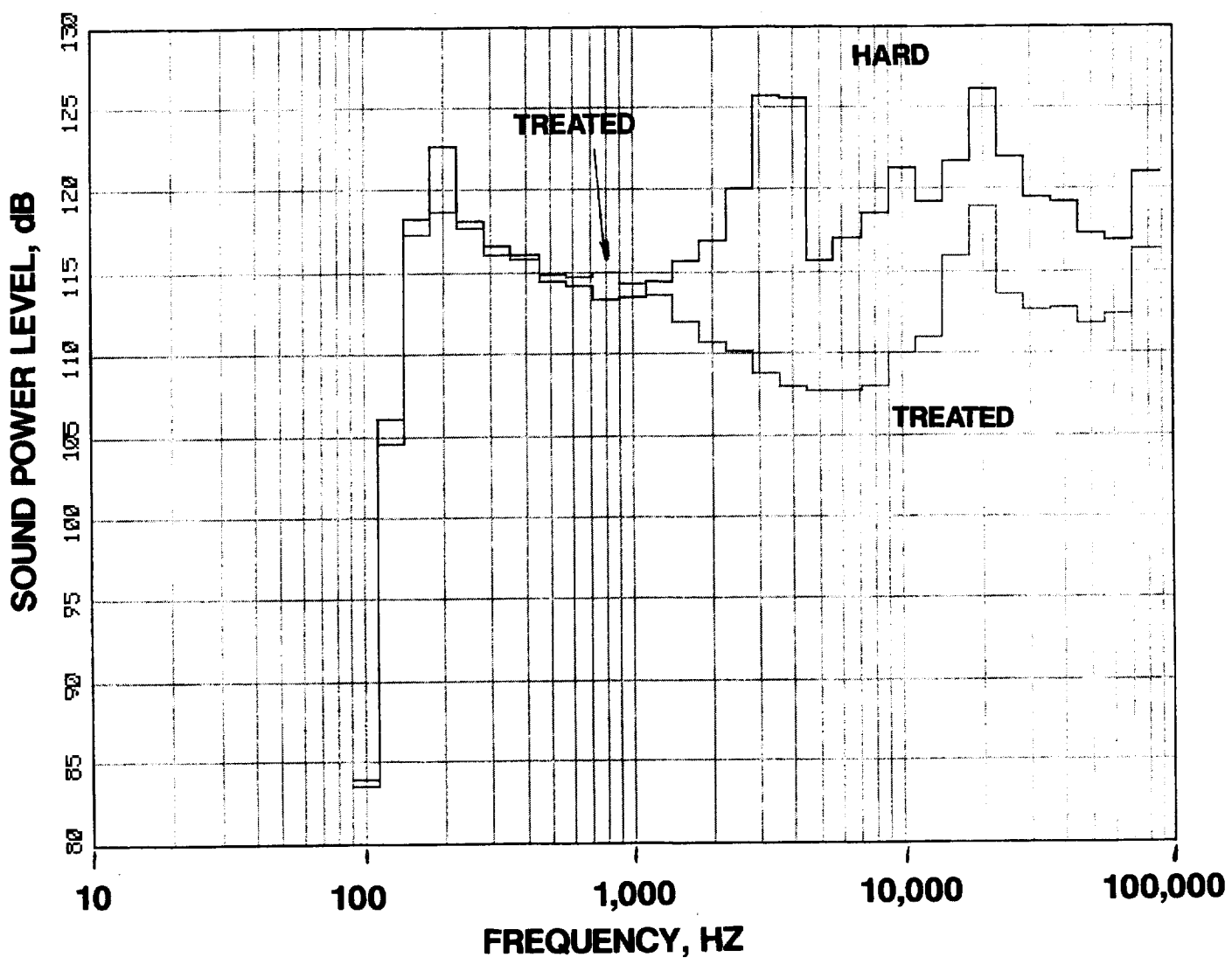


**FIGURE 34 CONCLUDED**

**F 10671 RPMC**

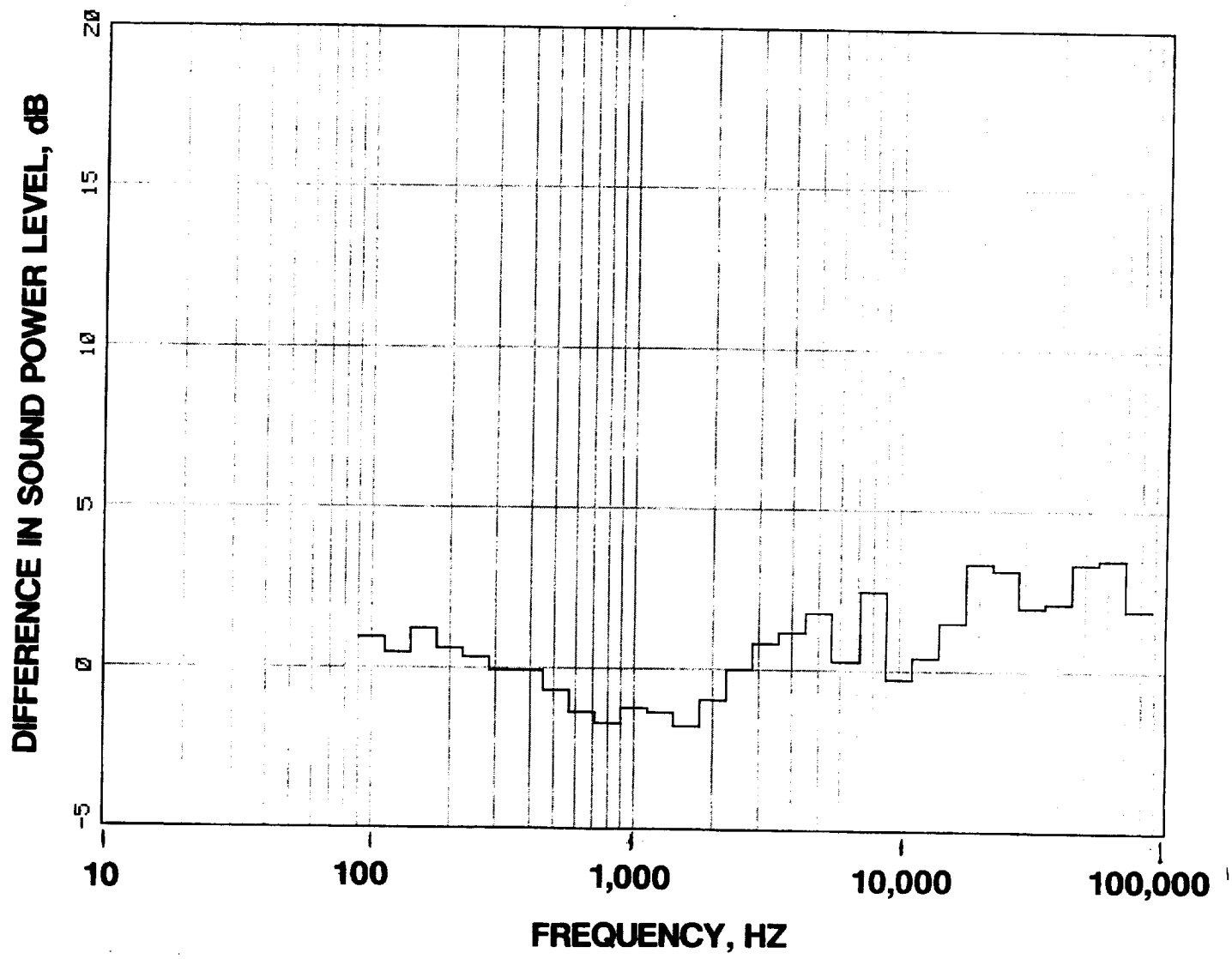


**FIGURE 35 DIFFERENCE IN SOUND POWER LEVEL, HARD MINUS  
TREATED, FOR THE 7 VANE CONFIGURATION**

**A 6402 RPMC**

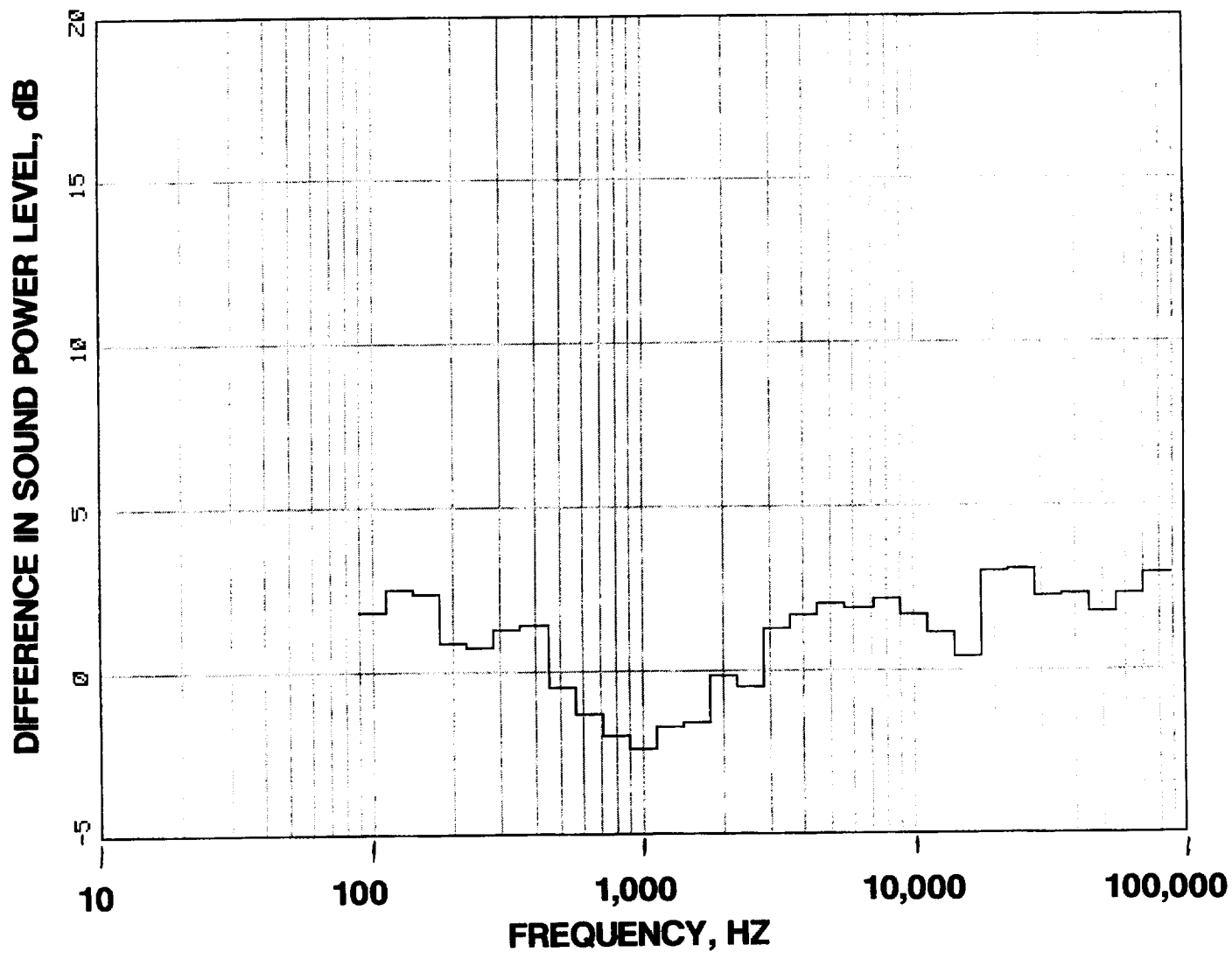


**FIGURE 35 CONTINUED**

**B 7736 RPMC**

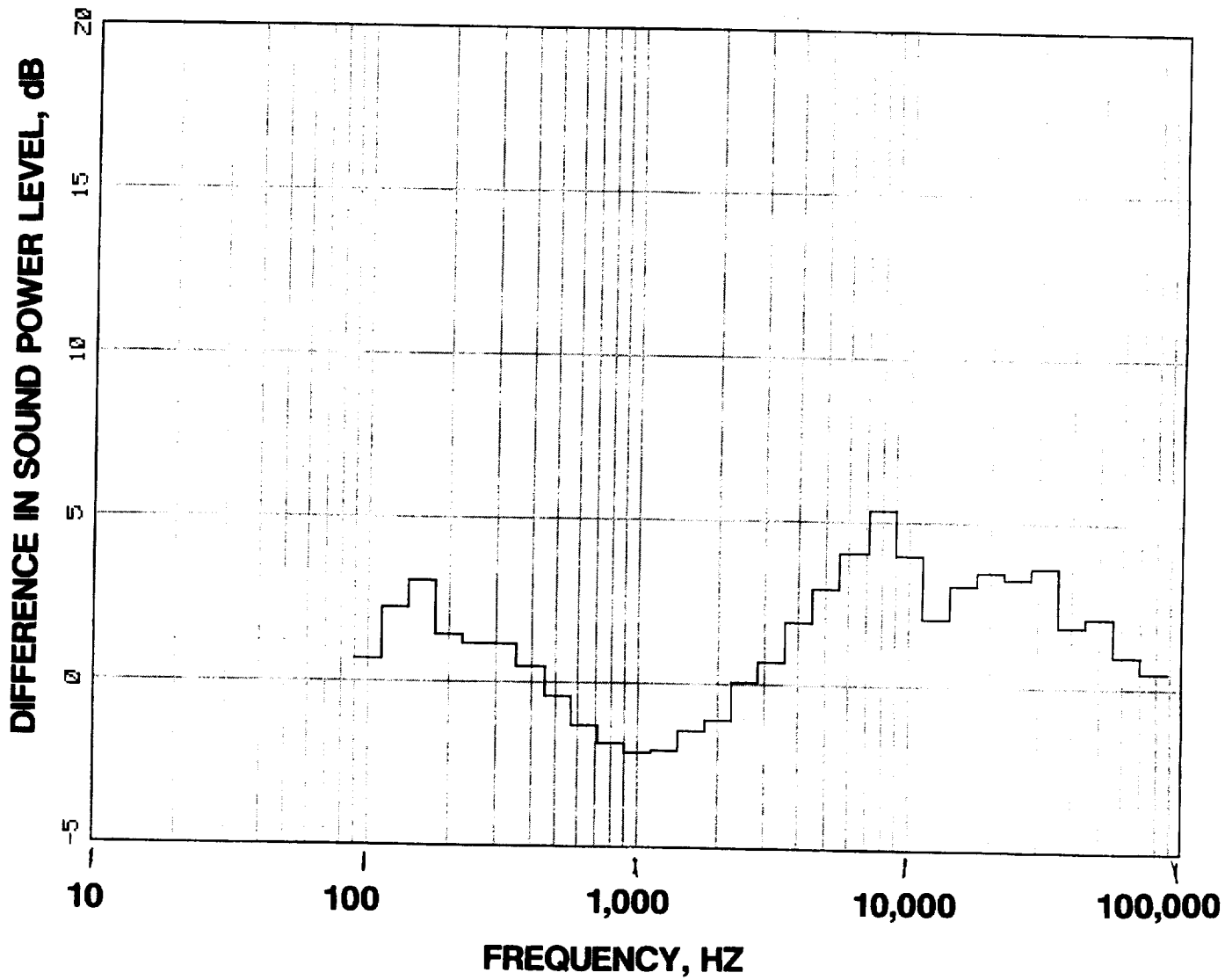


**FIGURE 35 CONTINUED**

**C 8537 RPMC**

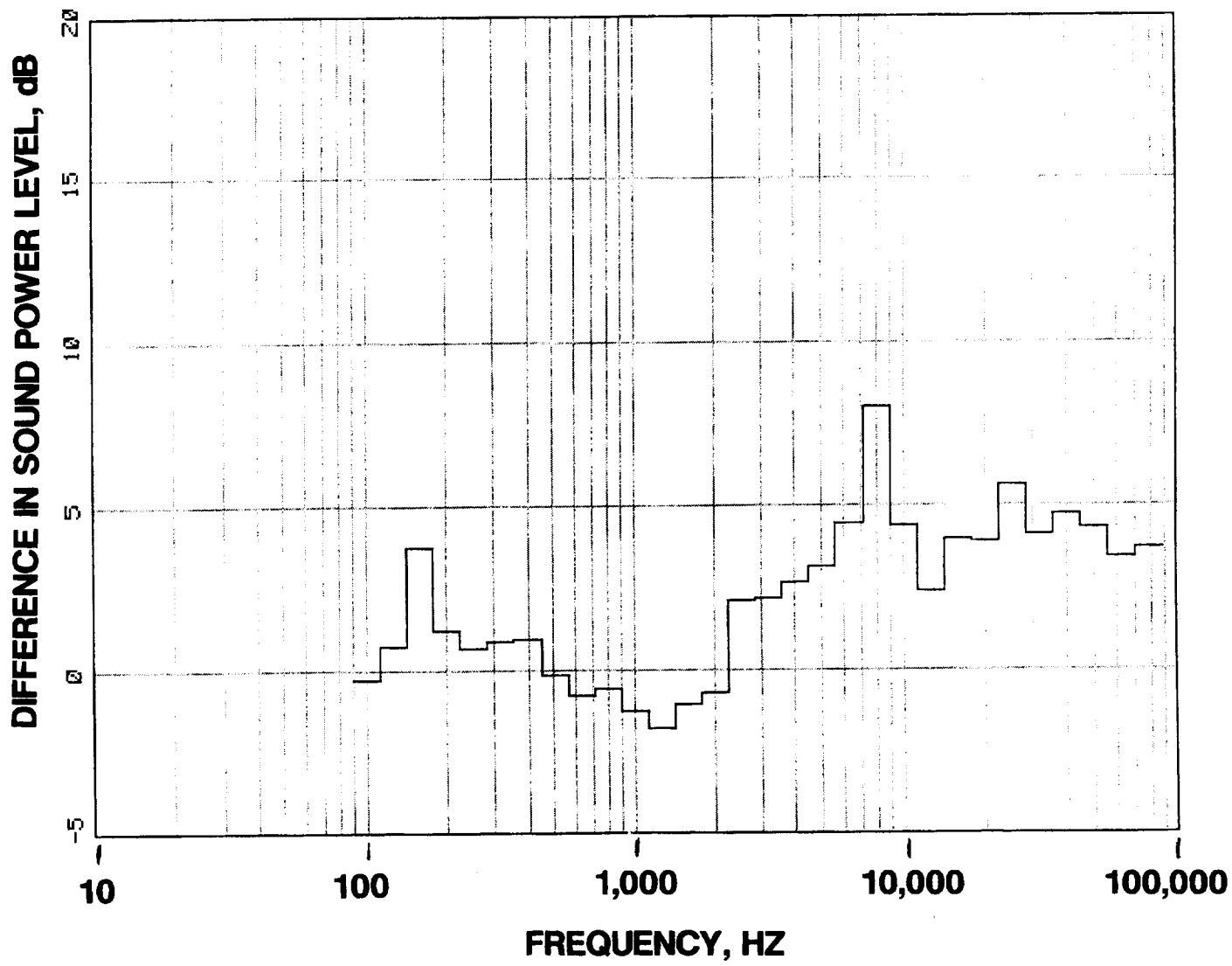


**FIGURE 35 CONTINUED**

**D 9604 RPMC**

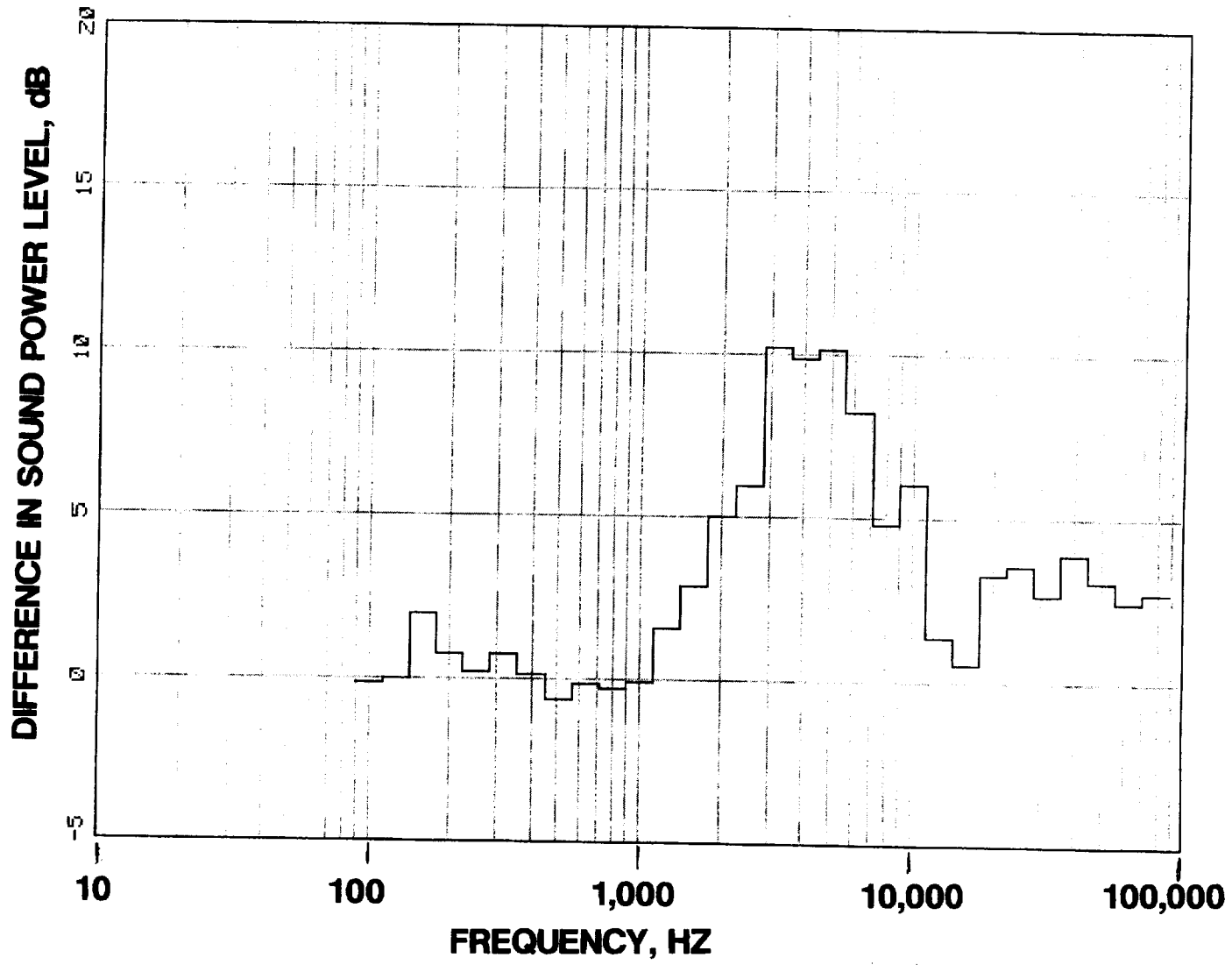


**FIGURE 35 CONTINUED**

**E 10137 RPMC**

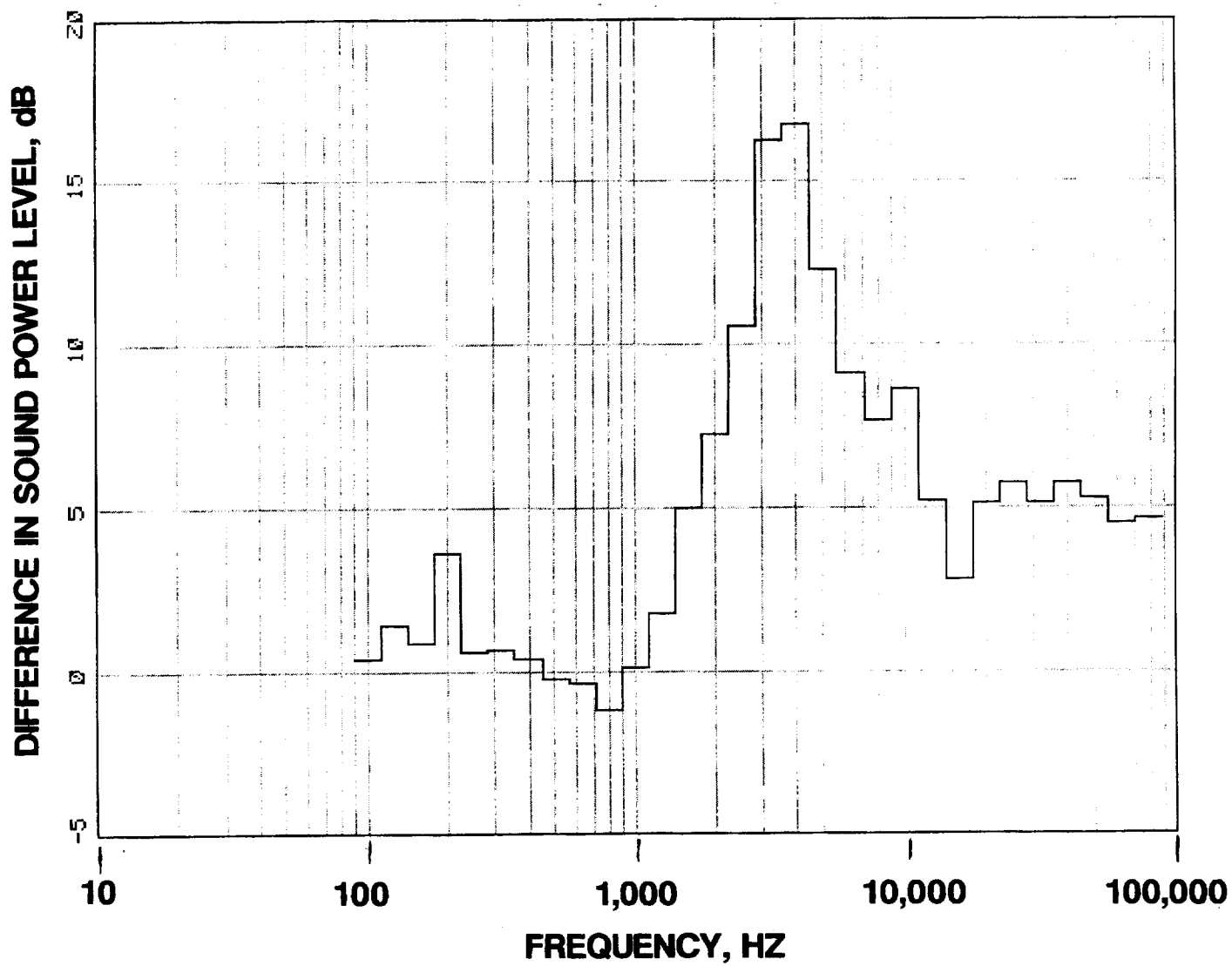


**FIGURE 35 CONCLUDED**

**F 10671 RPMC**

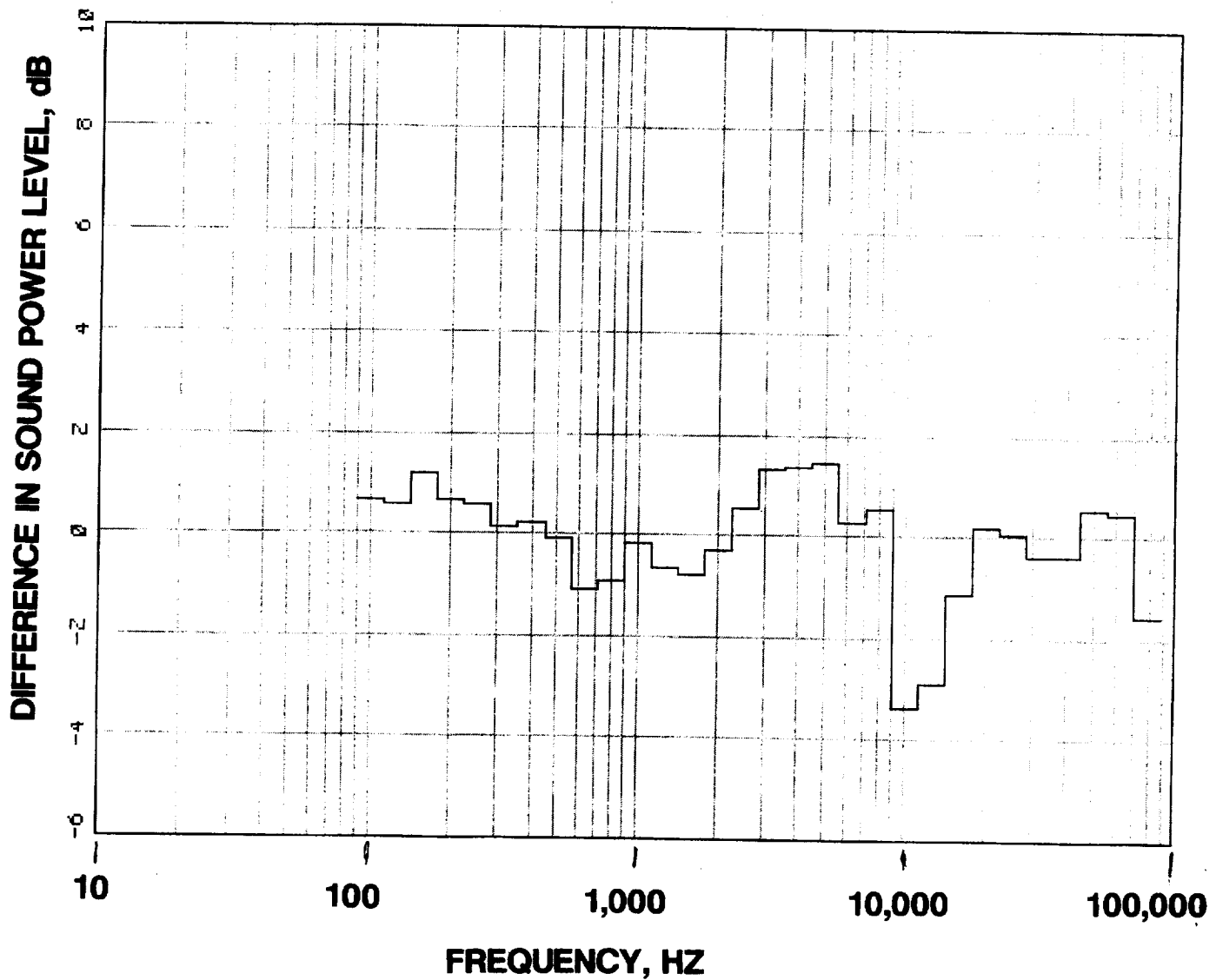


**FIGURE 36 DIFFERENCE IN FRONT SOUND POWER LEVEL, HARD  
MINUS TREATED, FOR THE 7 VANE CONFIGURATION**

**A 6402 RPMC**

DIFFERENCE IN SOUND POWER LEVEL, dB

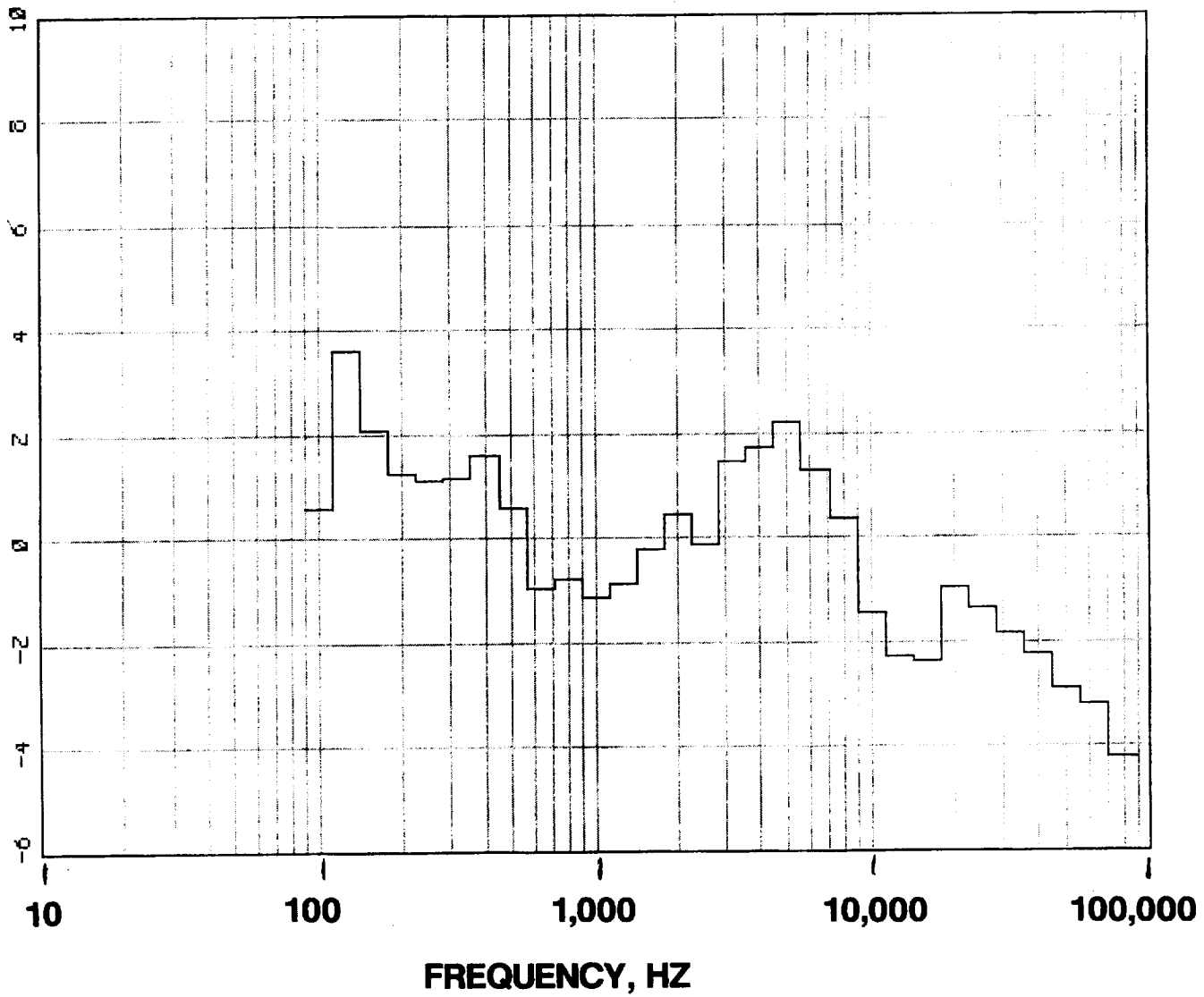


**FIGURE 36 CONTINUED**

**B 7736 RPMC**

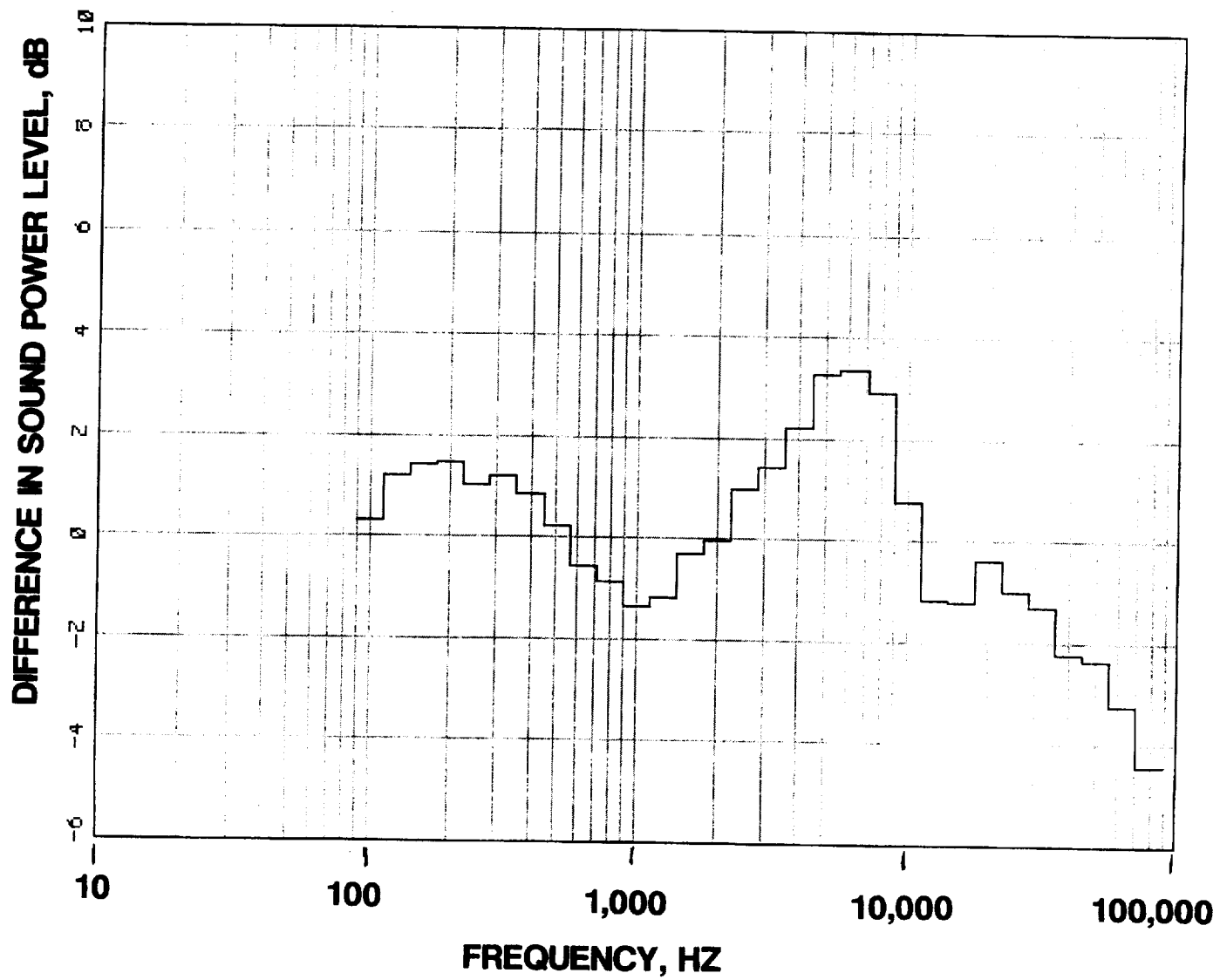


**FIGURE 36 CONTINUED**

**C 8537 RPMC**

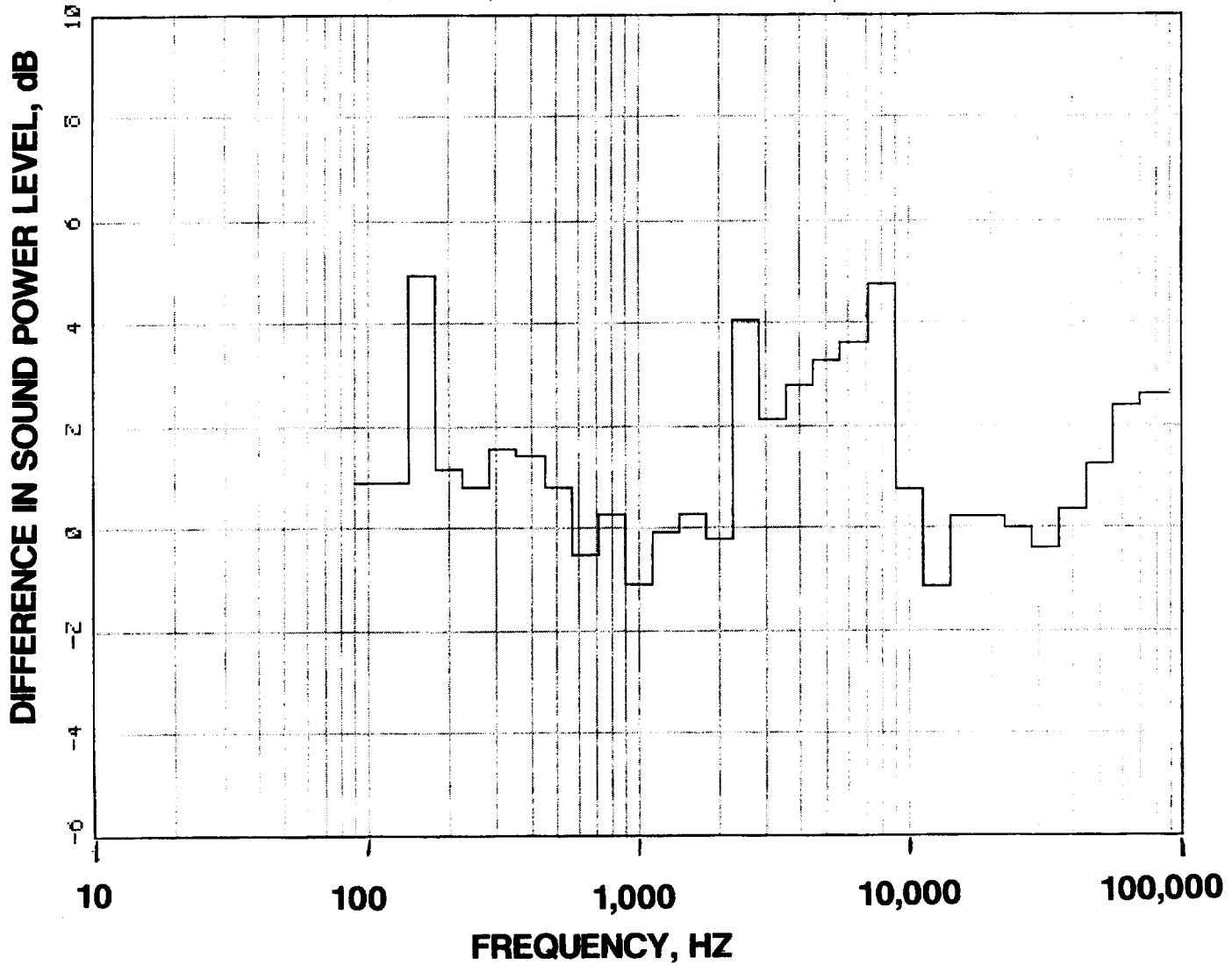


**FIGURE 36 CONTINUED**

**D 9604 RPMC**

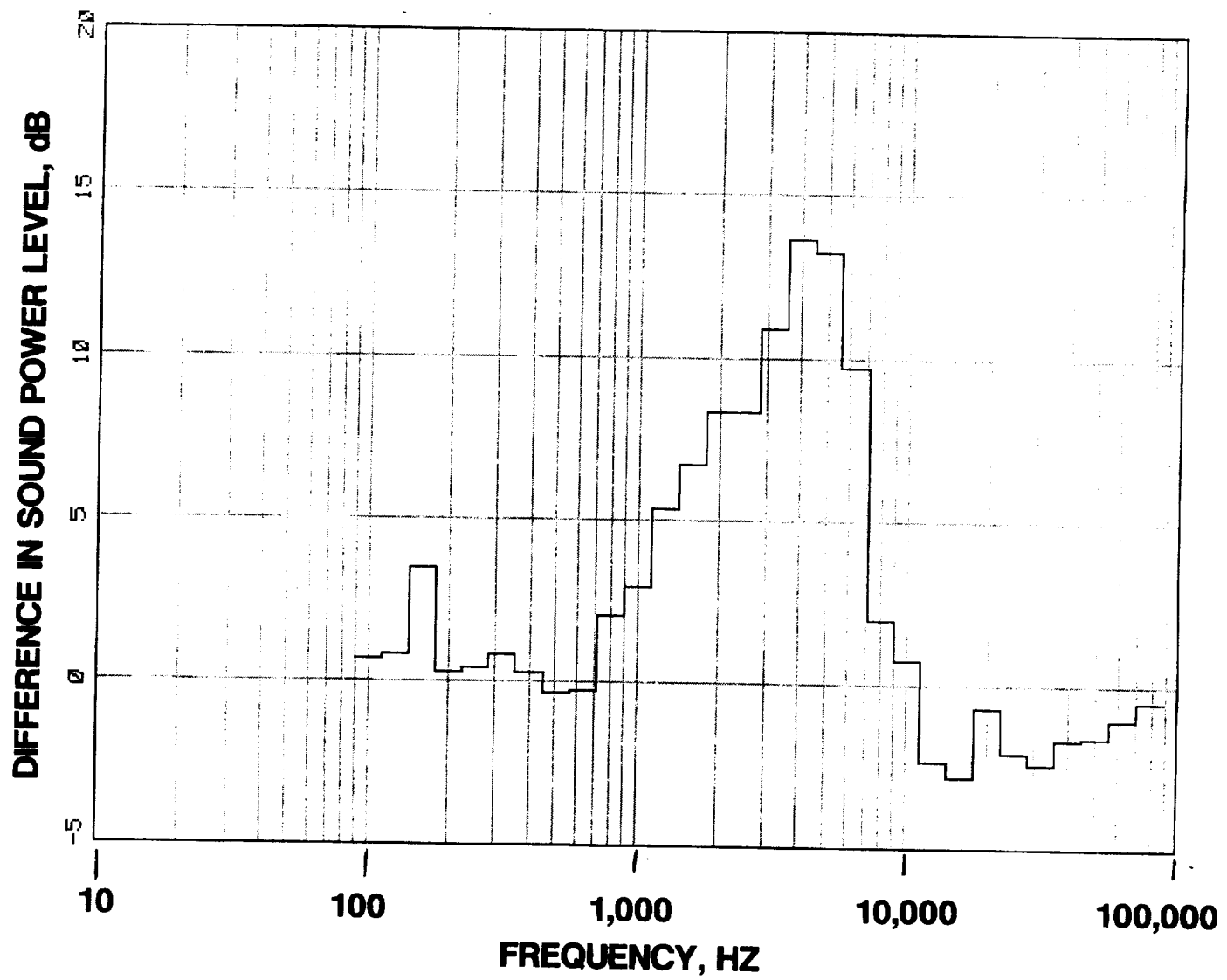


**FIGURE 36 CONTINUED**

**E 10137 RPMC**

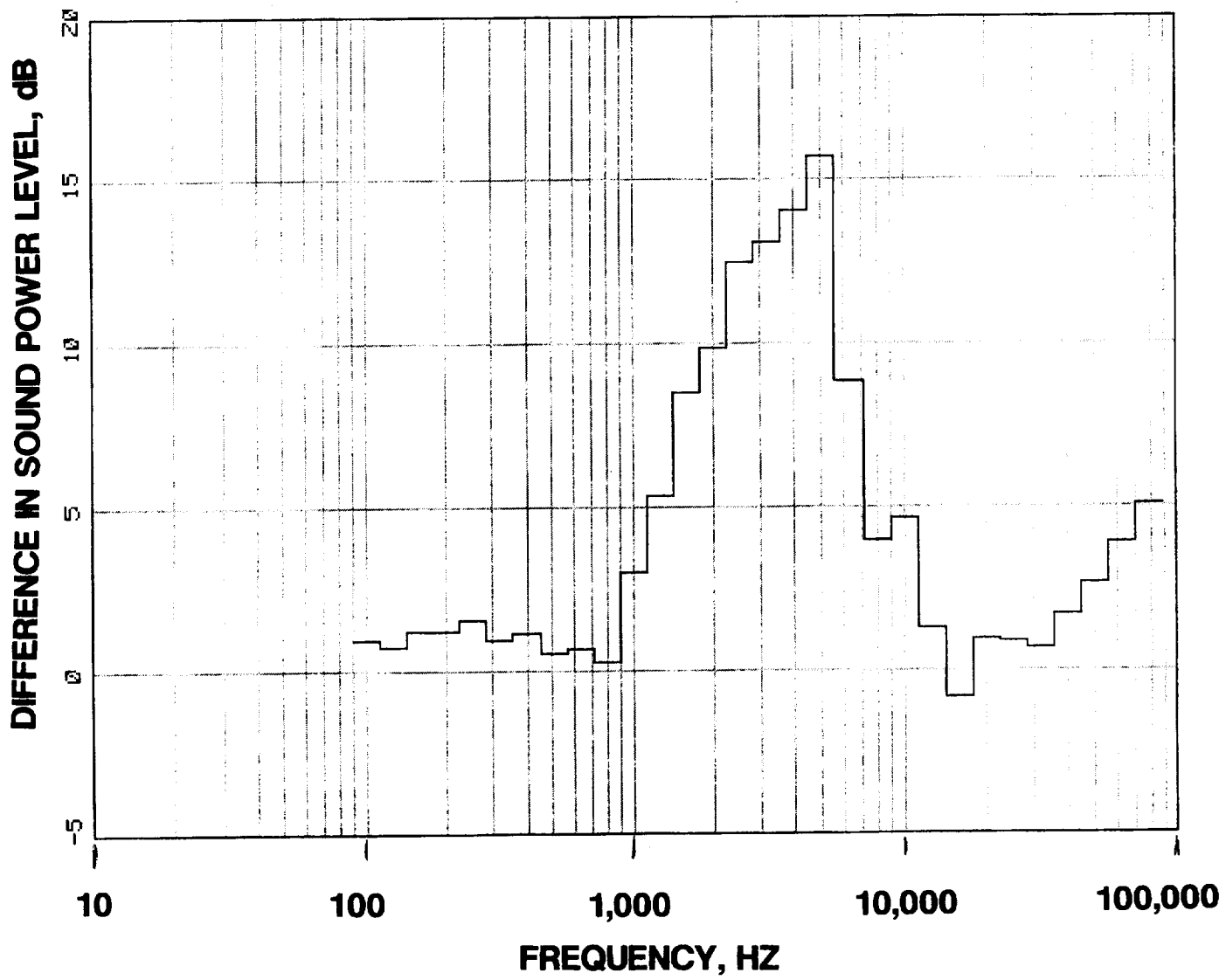


**FIGURE 36 CONCLUDED**

**F 10671 RPMC**

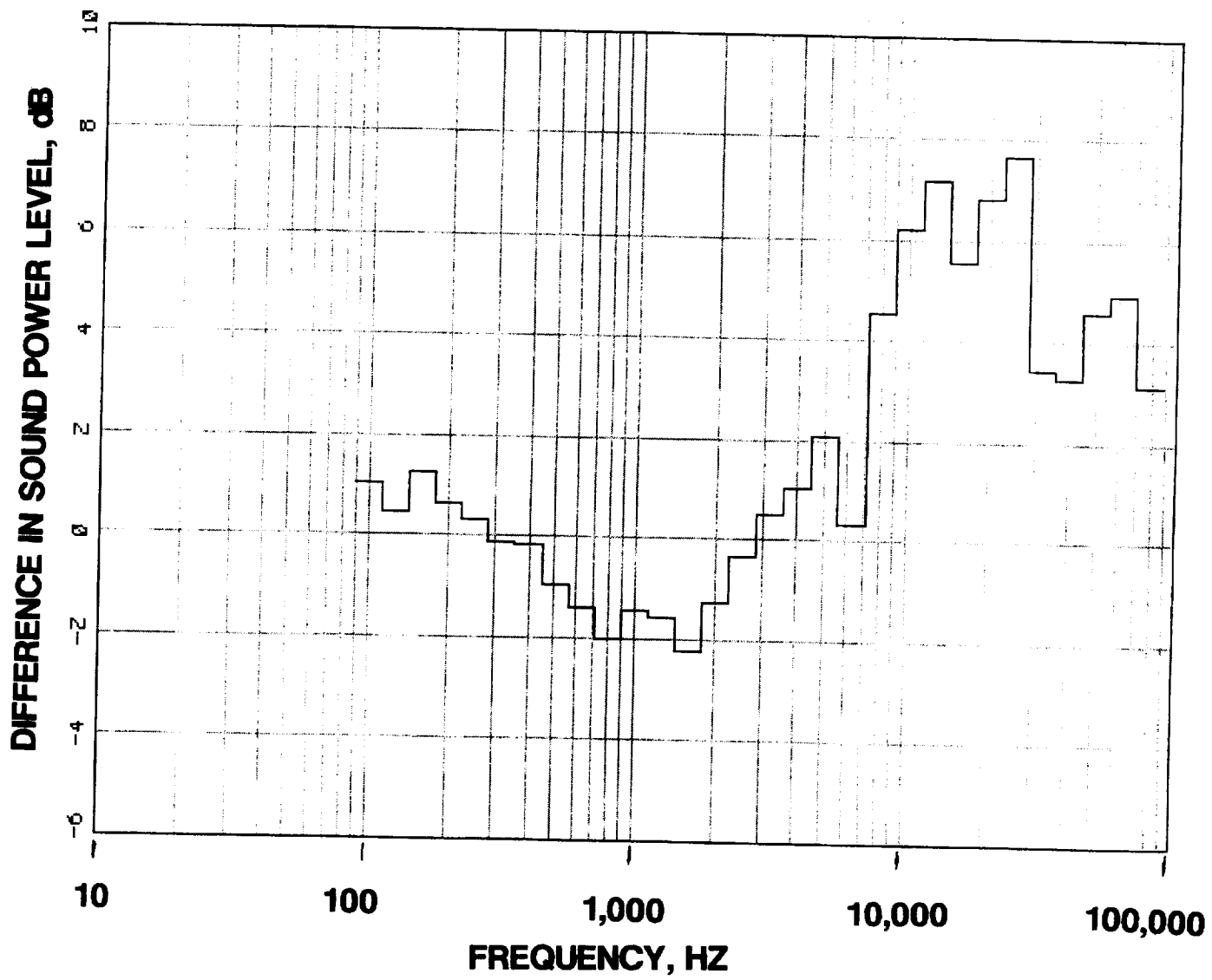


**FIGURE 37 DIFFERENCE IN AFT SOUND POWER LEVEL,  
HARD MINUS TREATED, FOR THE 7 VANE CONFIGURATION**

**A 6402 RPMC**

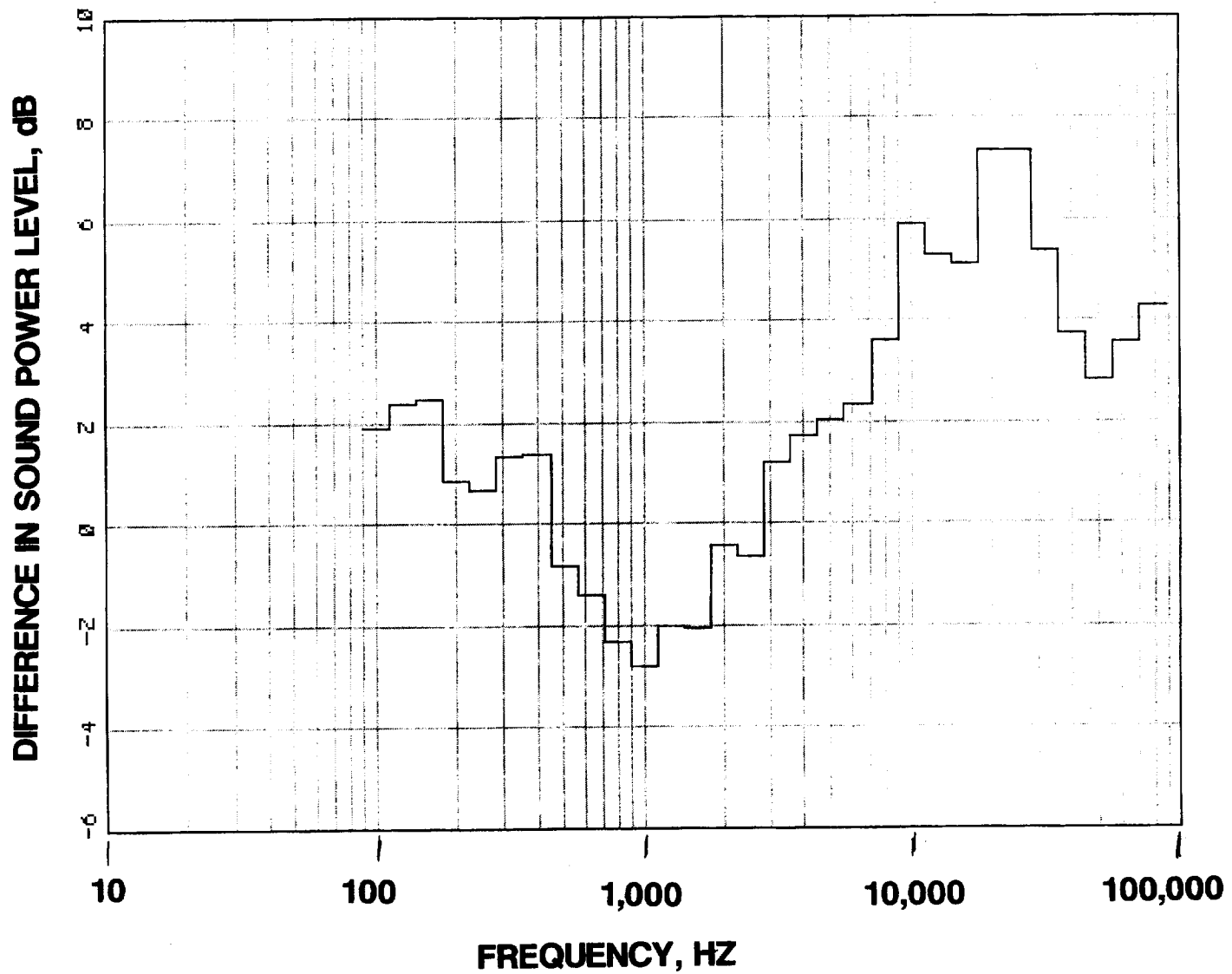


**FIGURE 37 CONTINUED**

**B 7736 RPMC**

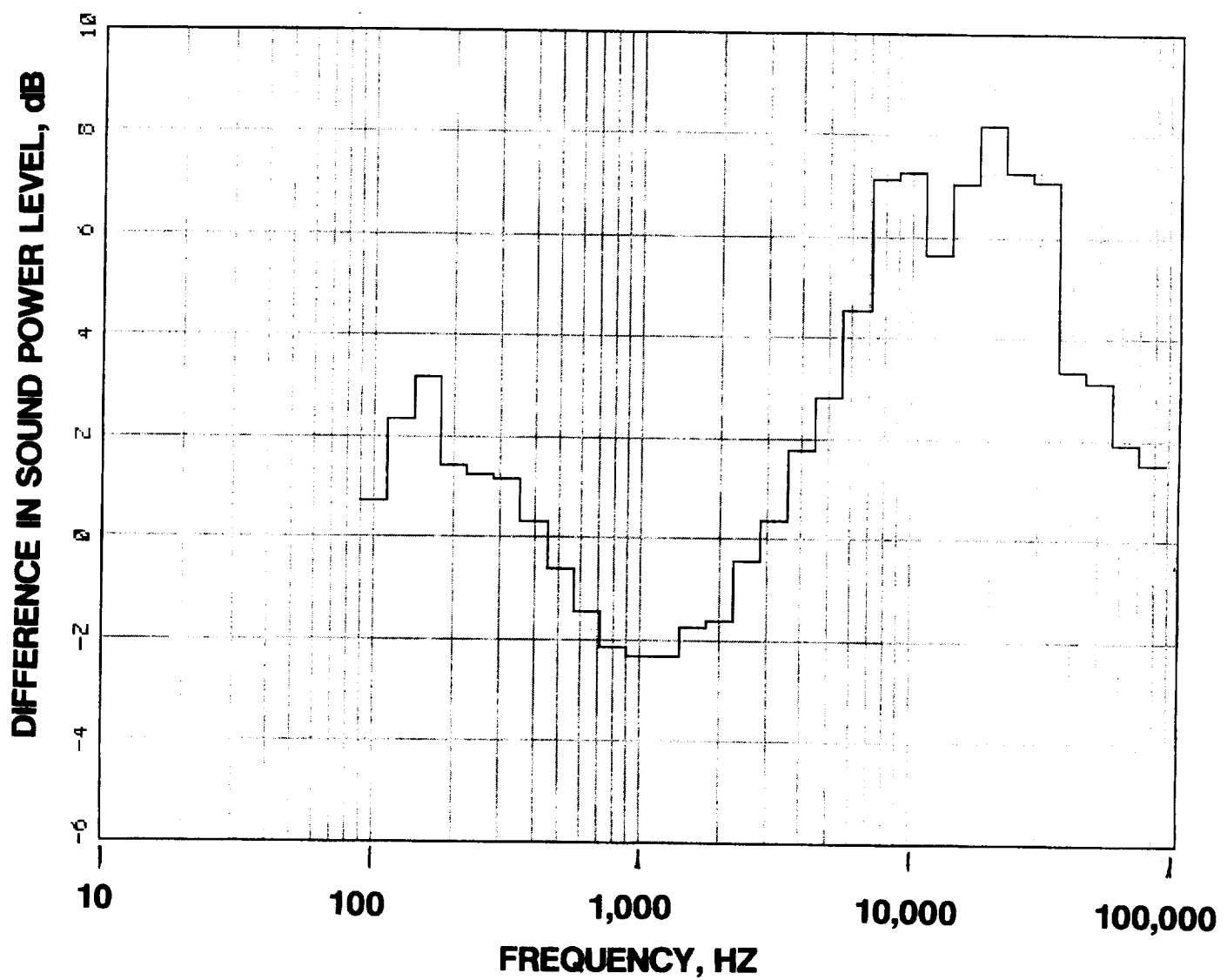


**FIGURE 37 CONTINUED**

**C 8537 RPMC**

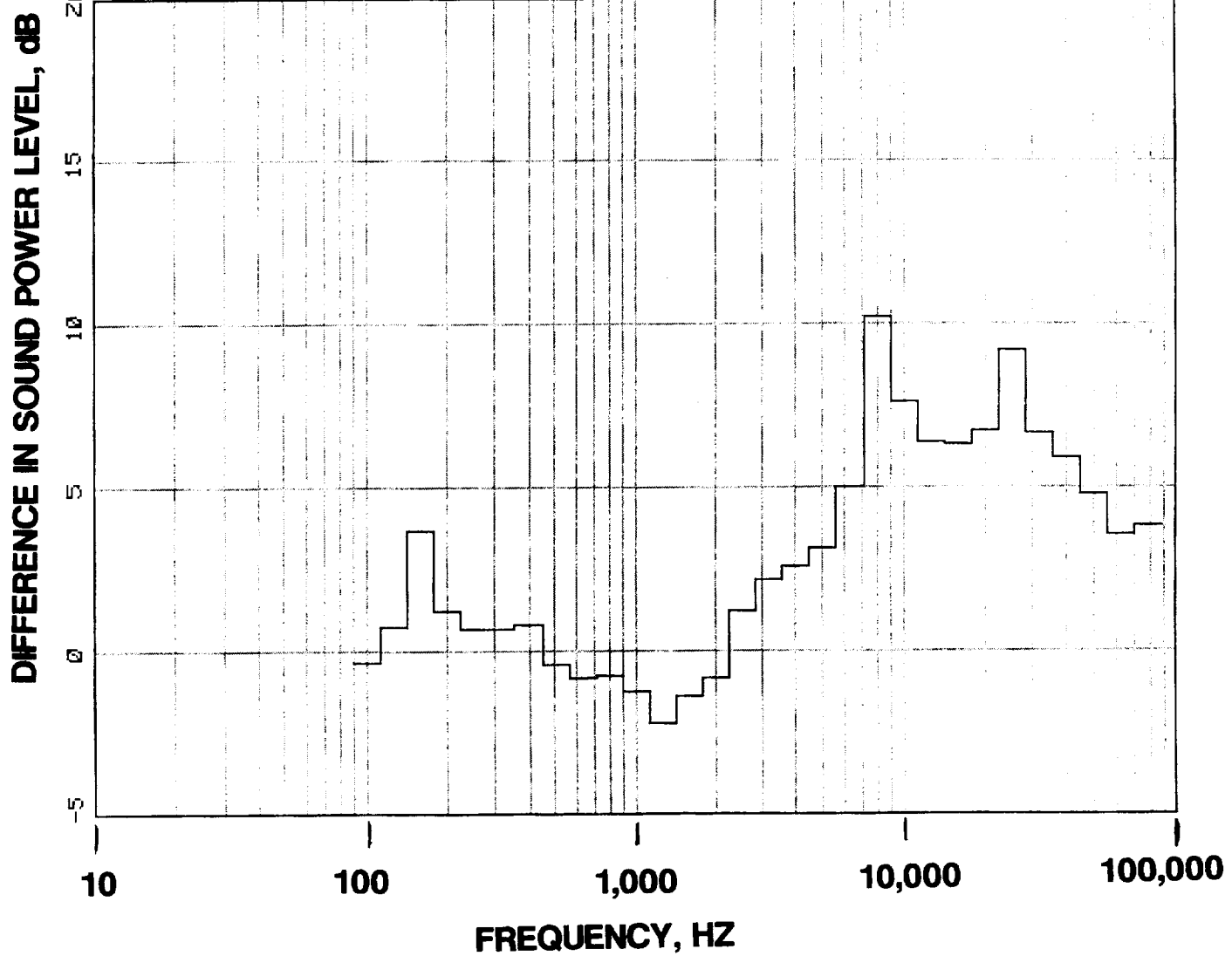


**FIGURE 37 CONTINUED**

**D 9604 RPMC**

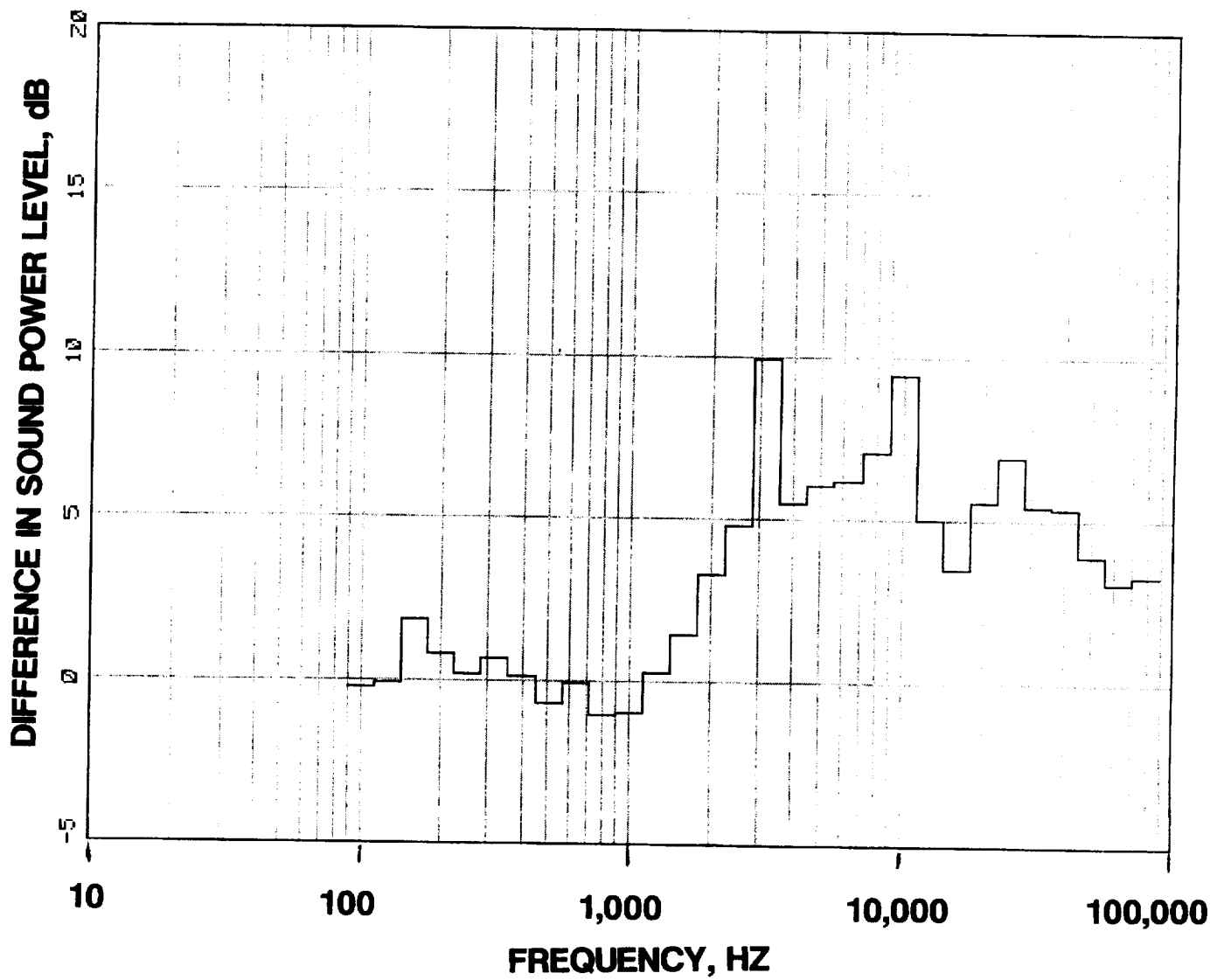


**FIGURE 37 CONTINUED**

**E 10137 RPMC**

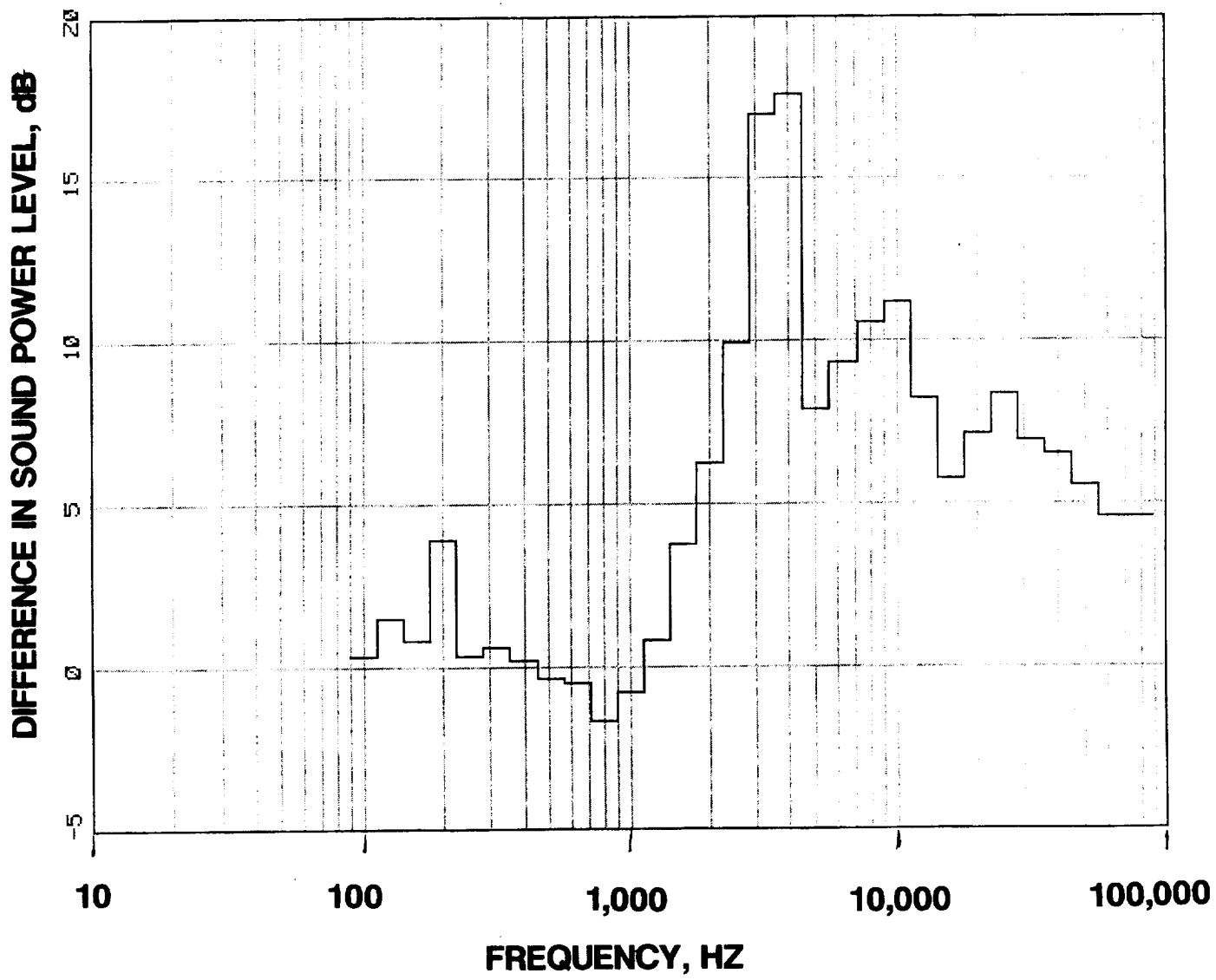


**FIGURE 37 CONCLUDED**

**F 10671 RPMC**

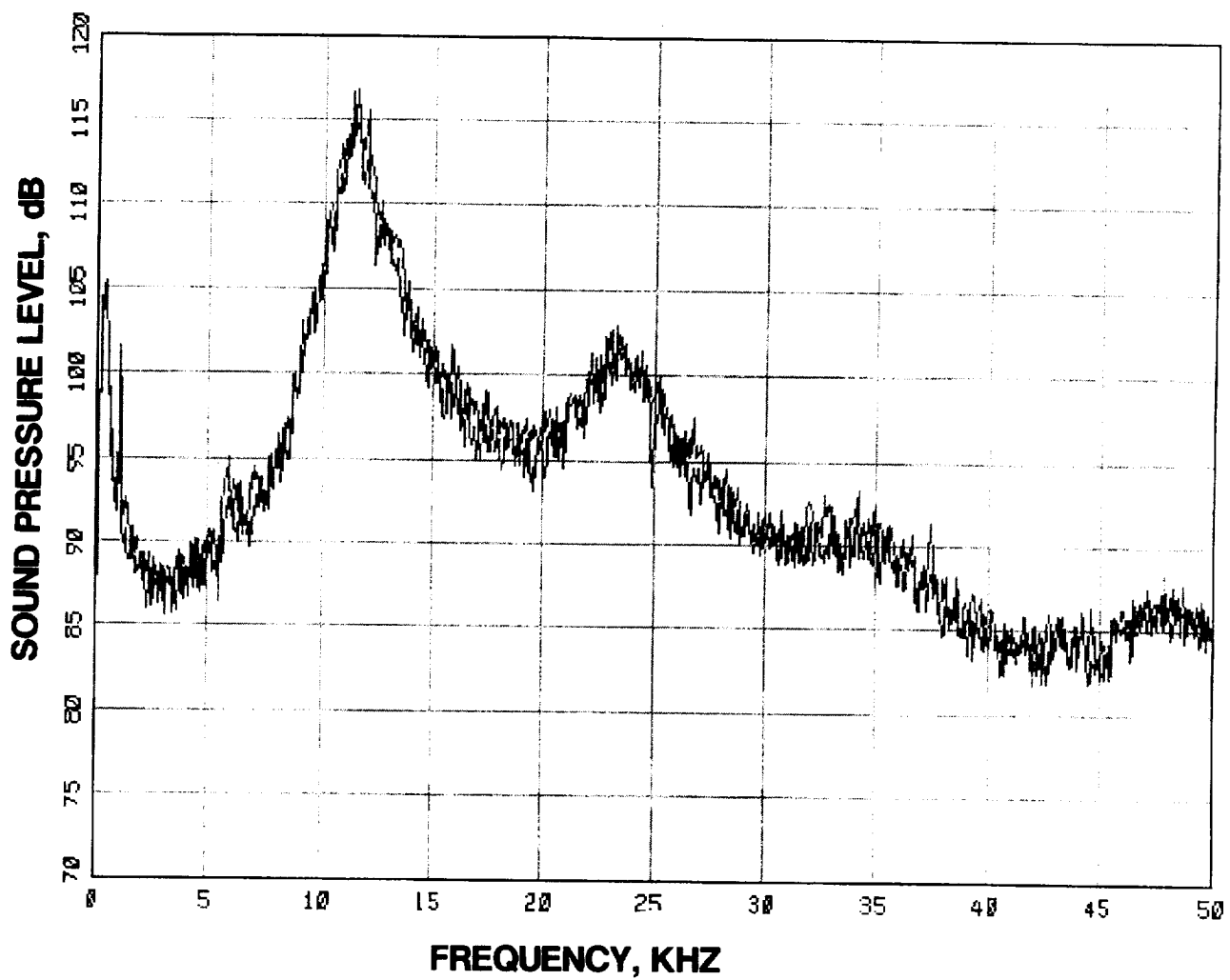


**FIGURE 38 SPECTRAL COMPARISON OF PARTIALLY TREATED AND FULLY TREATED DATA FOR THE 7 VANE CONFIGURATION AT 6402 RPMc**

**A 24.5 DEGREES**

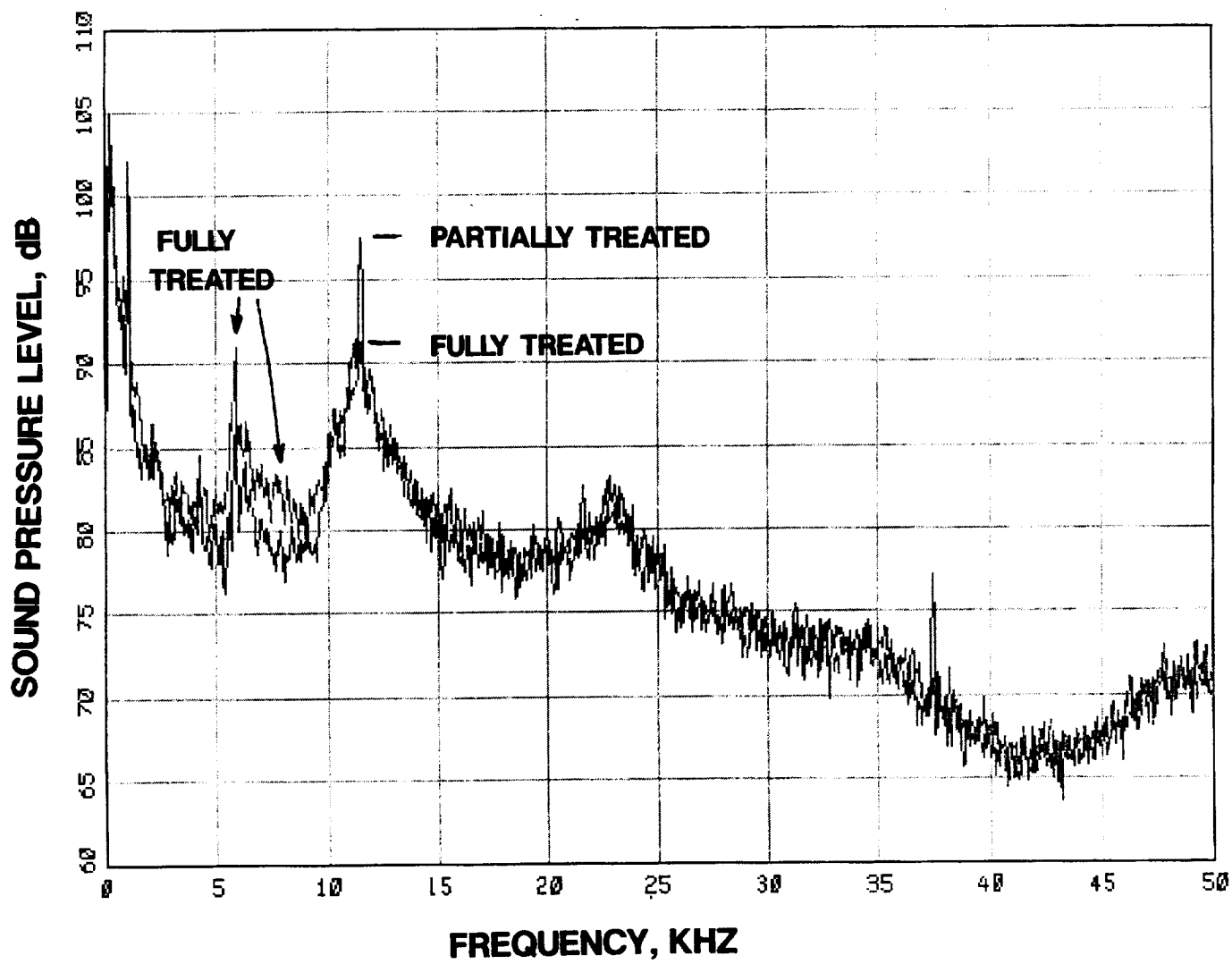


**FIGURE 38 CONTINUED**

**B 92.5 DEGREES**

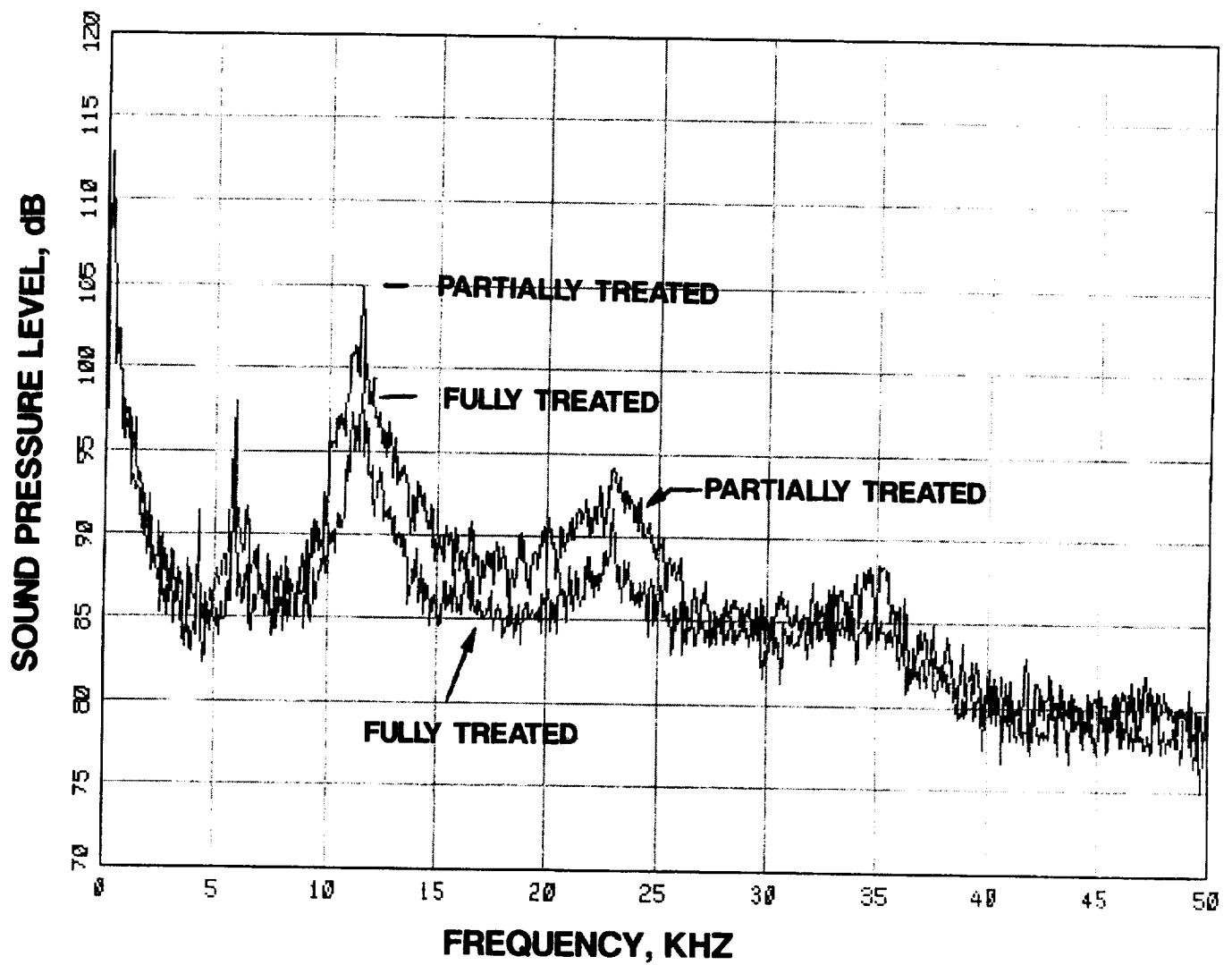


**FIGURE 38 CONCLUDED**

**C 130.5 DEGREES**

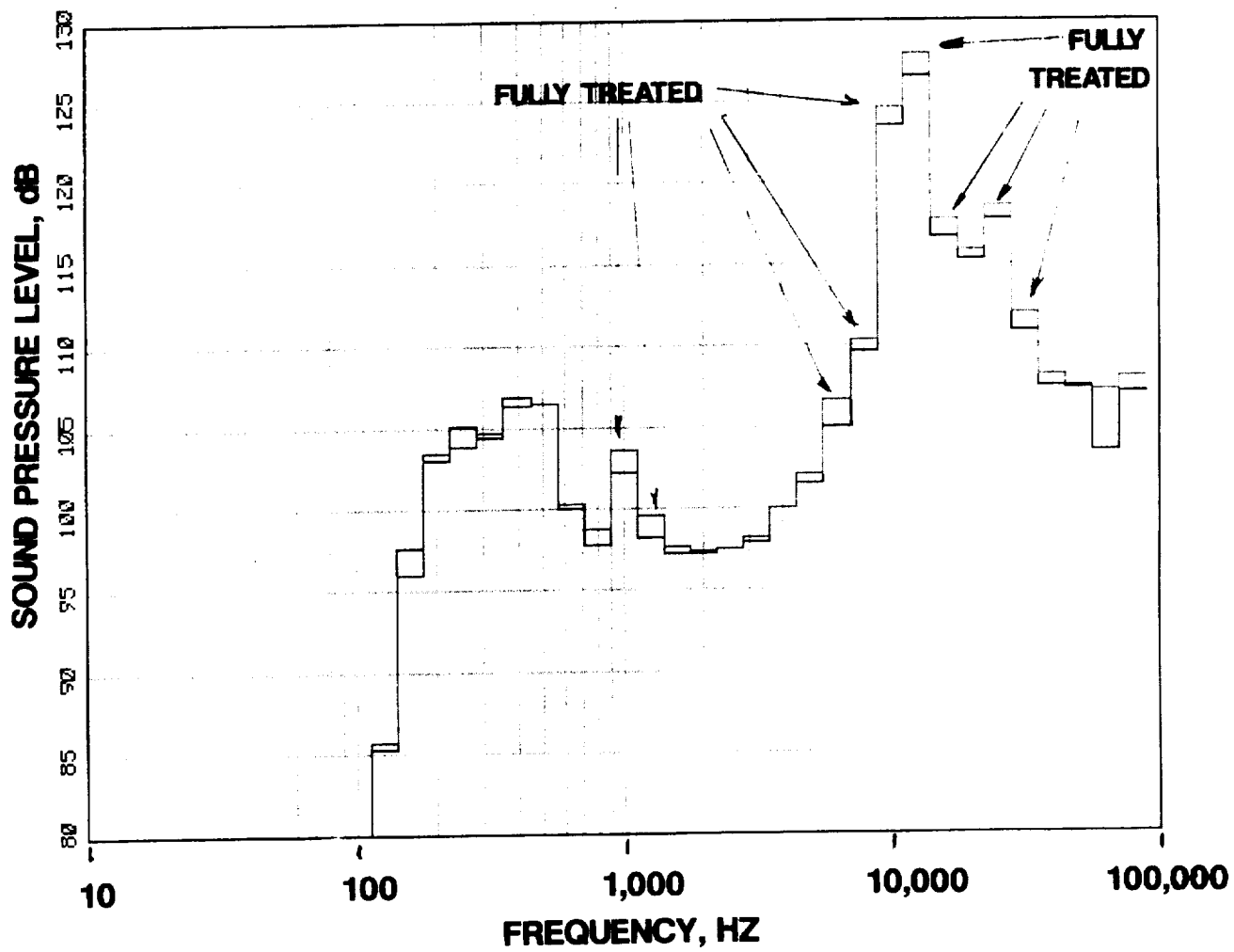


**FIGURE 39 1/3RD OCTAVE COMPARISON OF PARTIALLY TREATED AND FULLY TREATED DATA FOR THE 7 VANE CONFIGURATION AT 6402 RPMC**

**A 24.5 DEGREES**

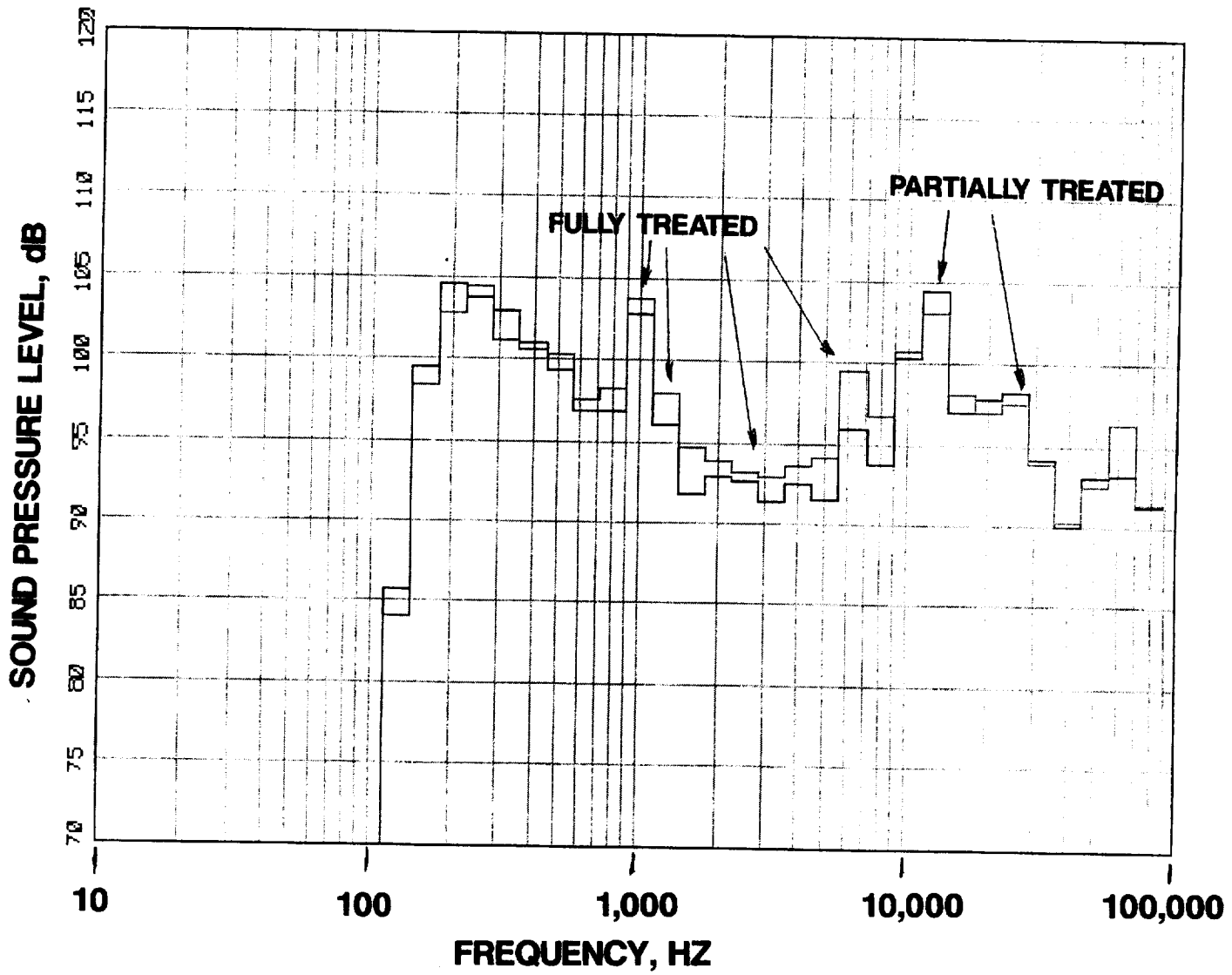


**FIGURE 39 CONTINUED**

**B 92.5 DEGREES**

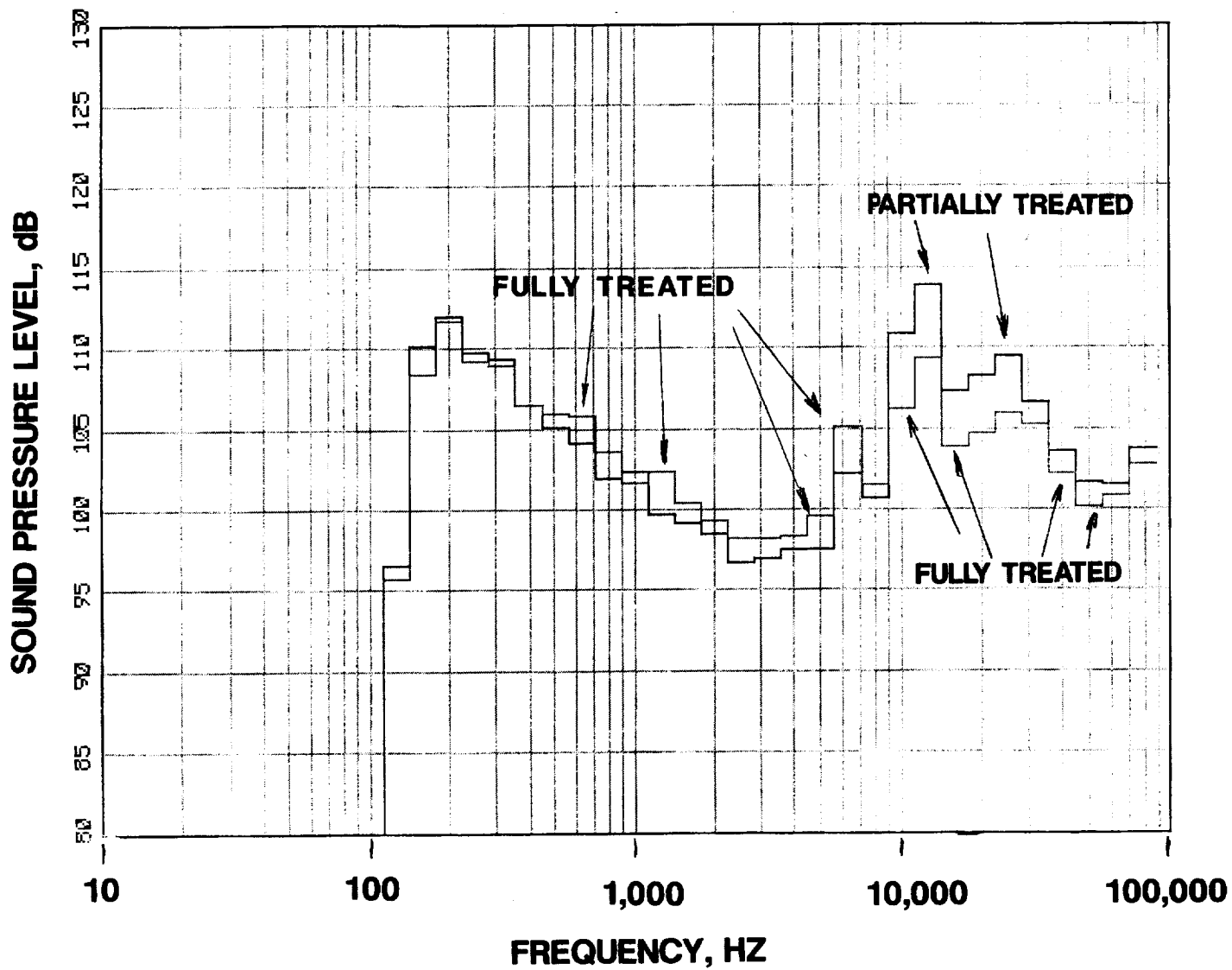


**FIGURE 39 CONCLUDED**

**C 130.5 DEGREES**

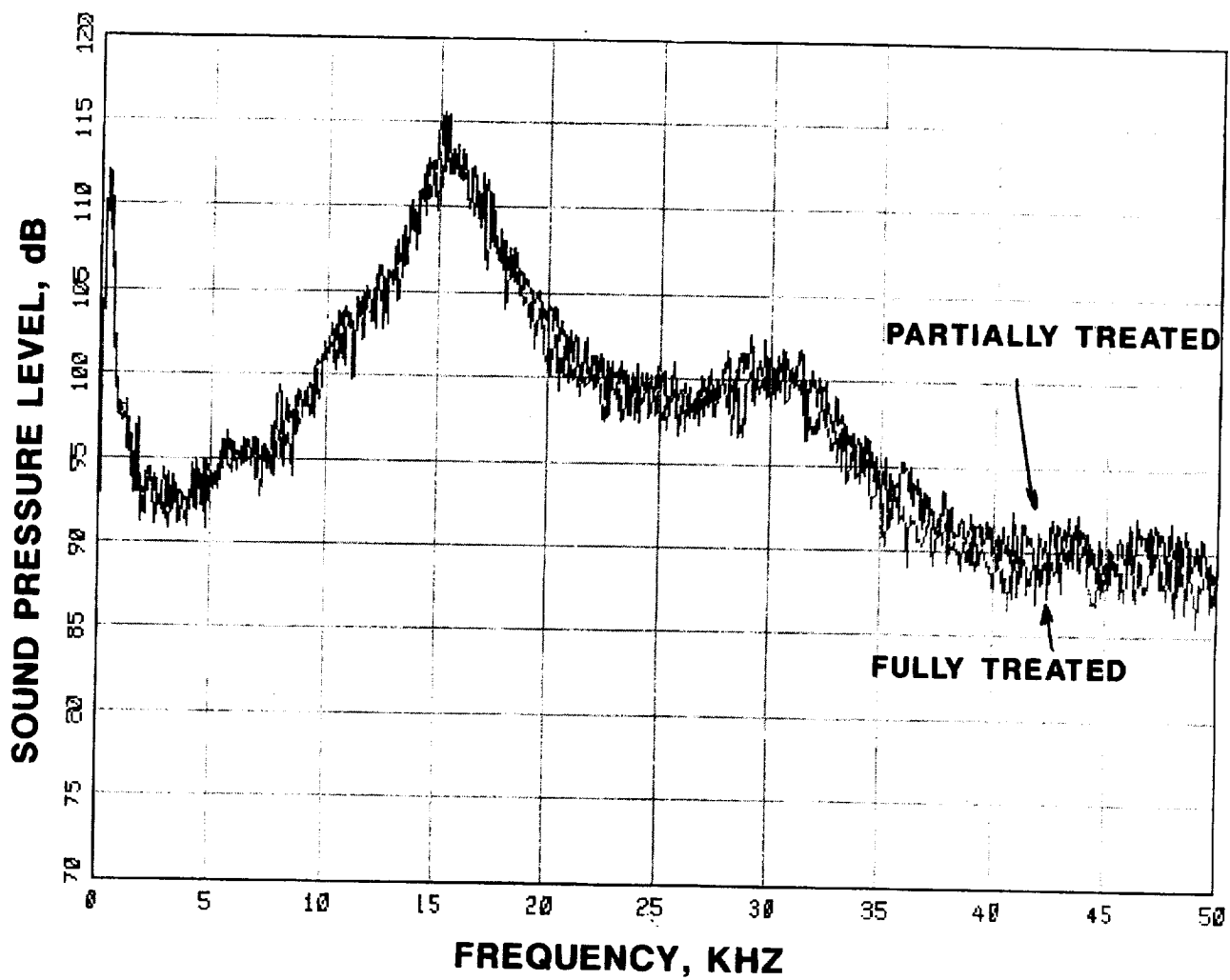


**FIGURE 40 SPECTRAL COMPARISON OF PARTIALLY TREATED  
AND FULLY TREATED DATA FOR THE 7 VANE CONFIGURATION  
AT 8537 RPMC**

**A 24.5 DEGREES**

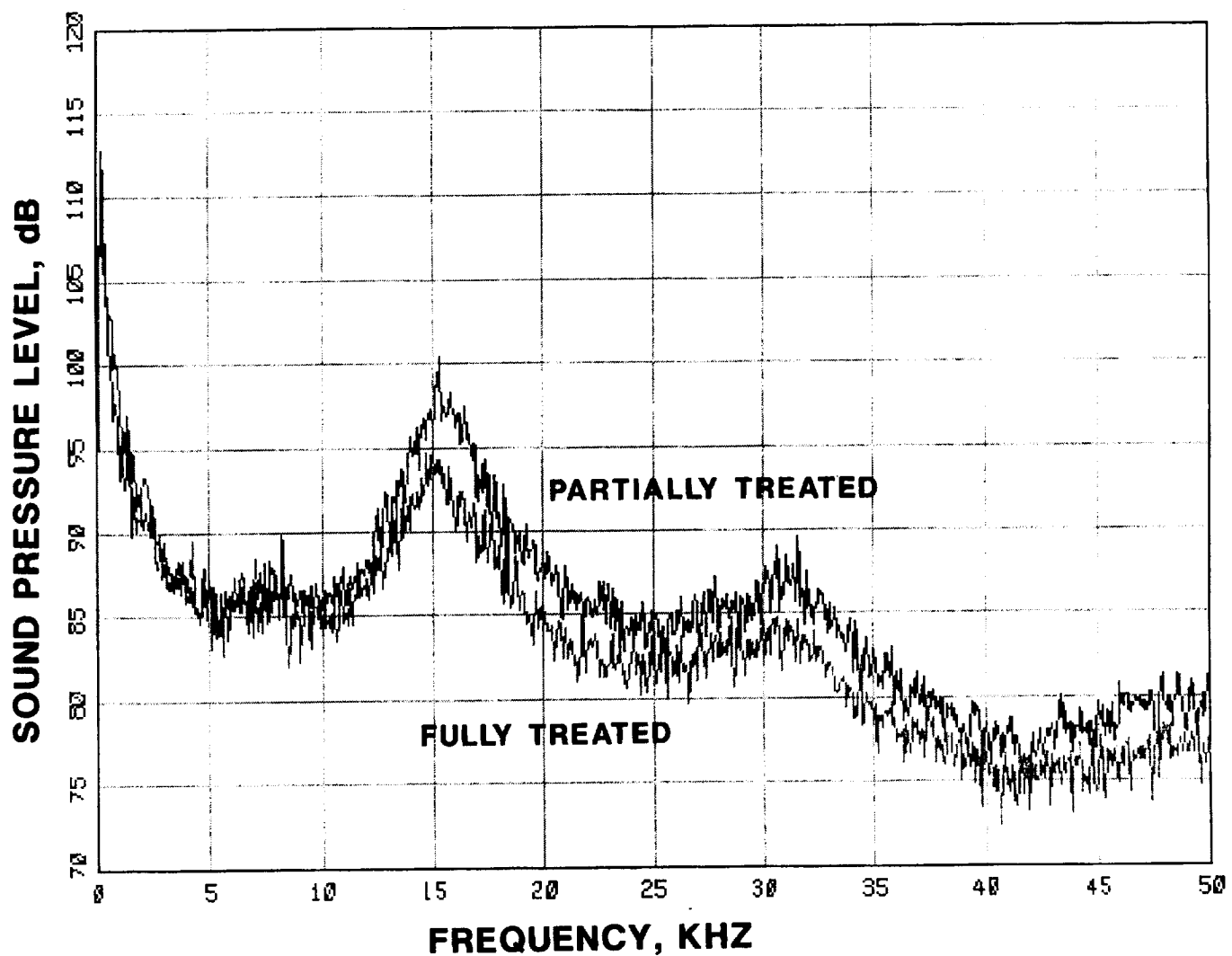


**FIGURE 40 CONTINUED**

**B 92.5 DEGREES**

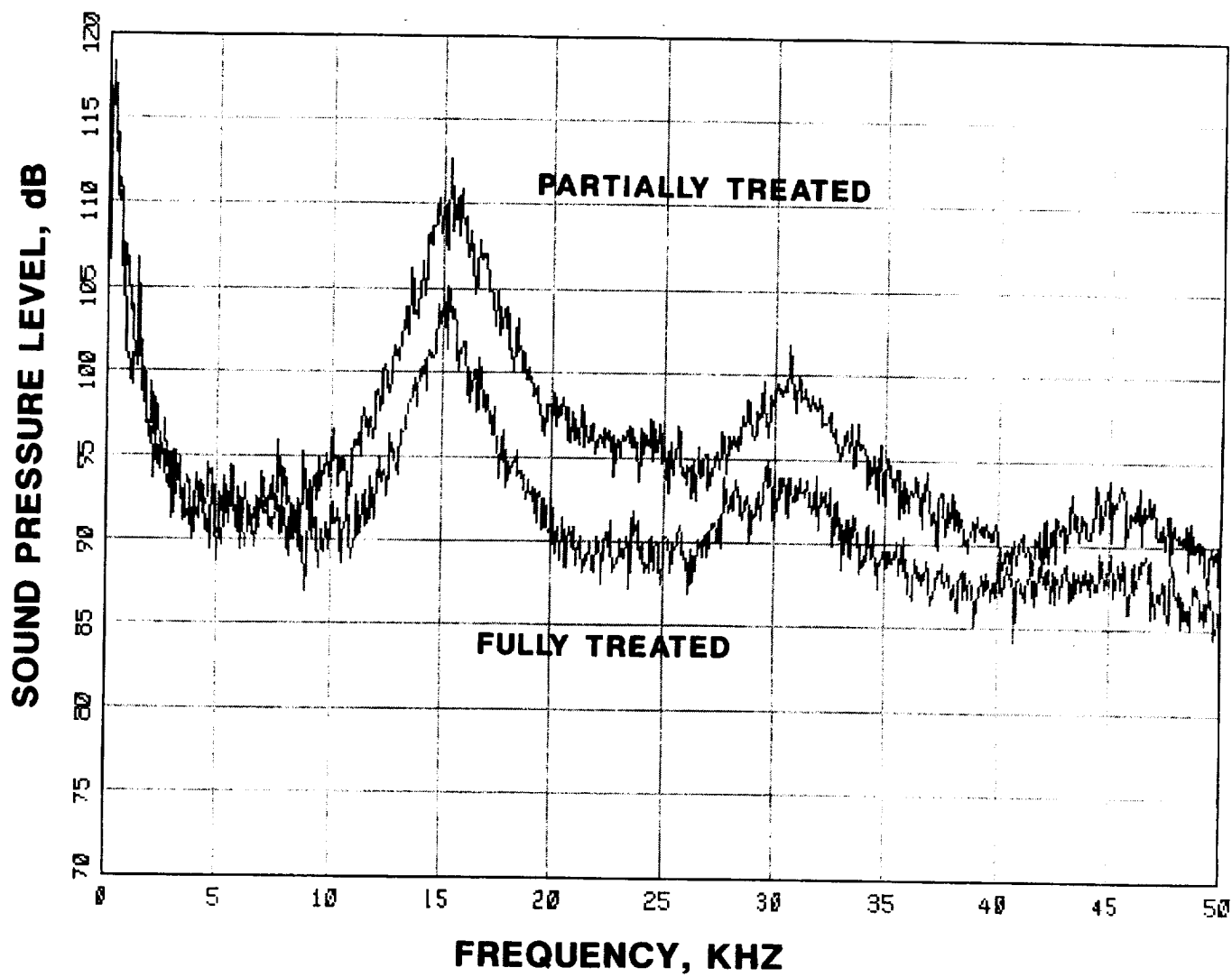


**FIGURE 40 CONCLUDED**

**C 130.5 DEGREES**

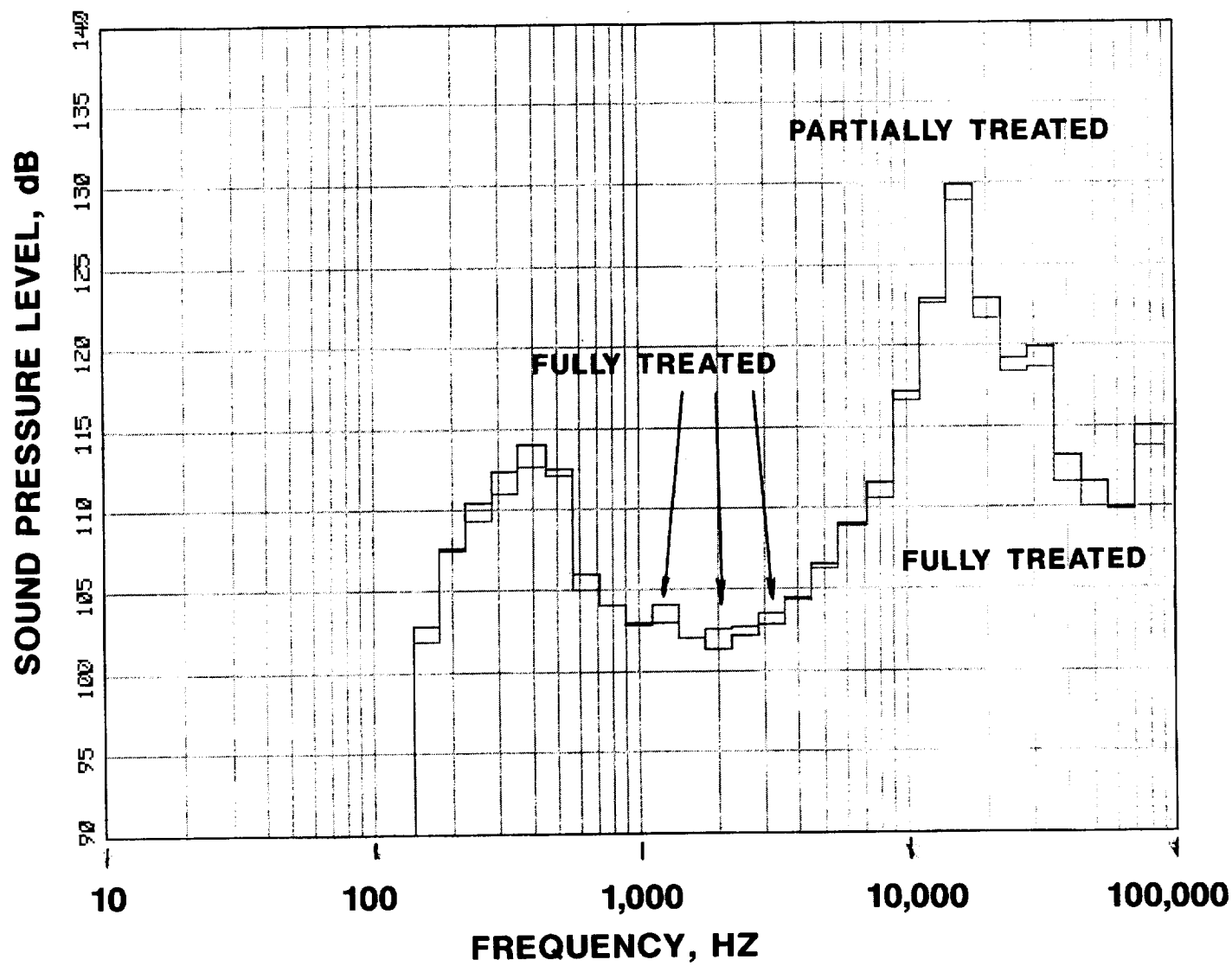


**FIGURE 41 1/3RD OCTAVE COMPARISON OF PARTIALLY  
TREATED AND FULLY TREATED DATA FOR THE 7 VANE  
CONFIGURATION AT 8537 RPMC  
A 24.5 DEGREES**

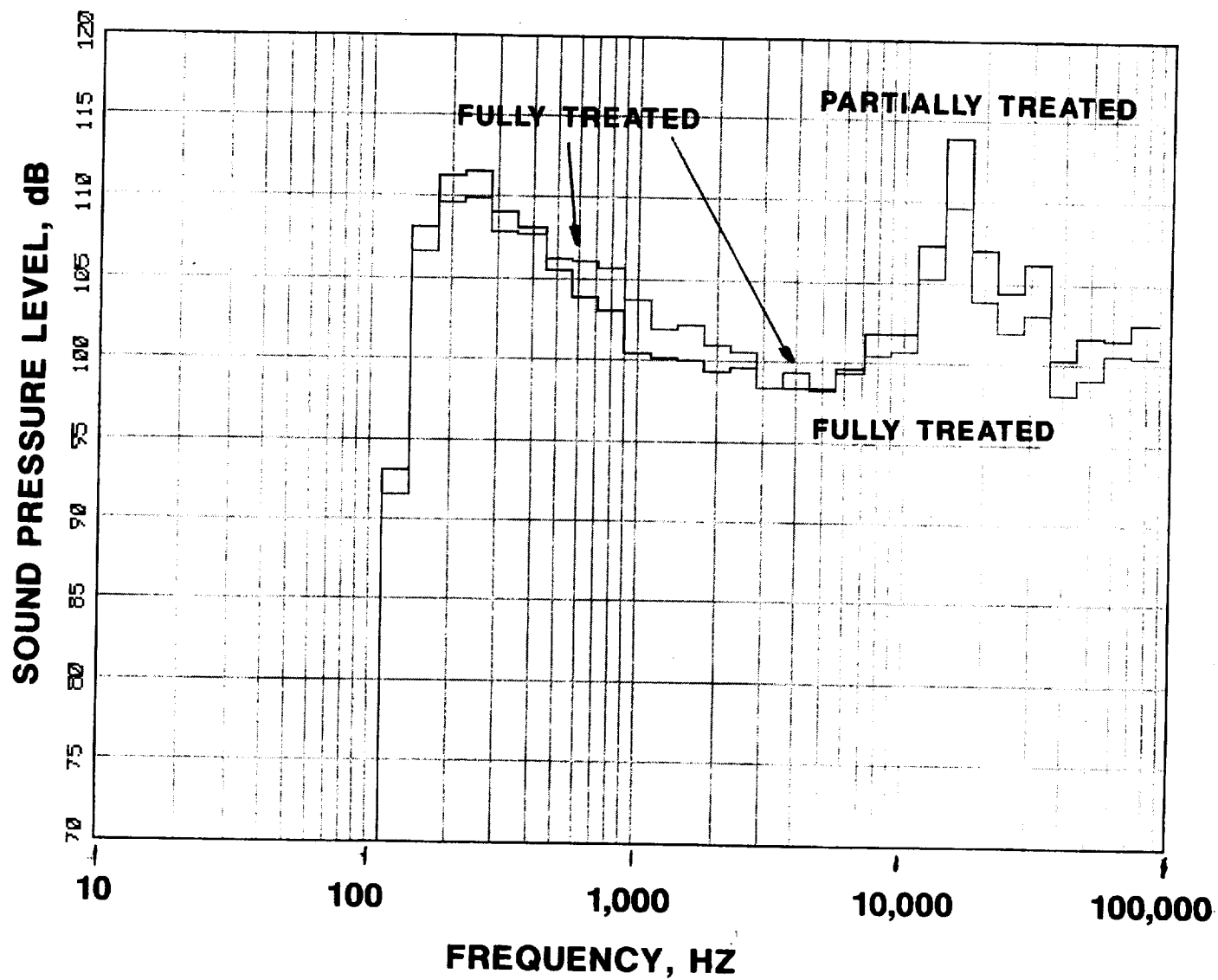


**FIGURE 41 CONTINUED**

**B 92.5 DEGREES**

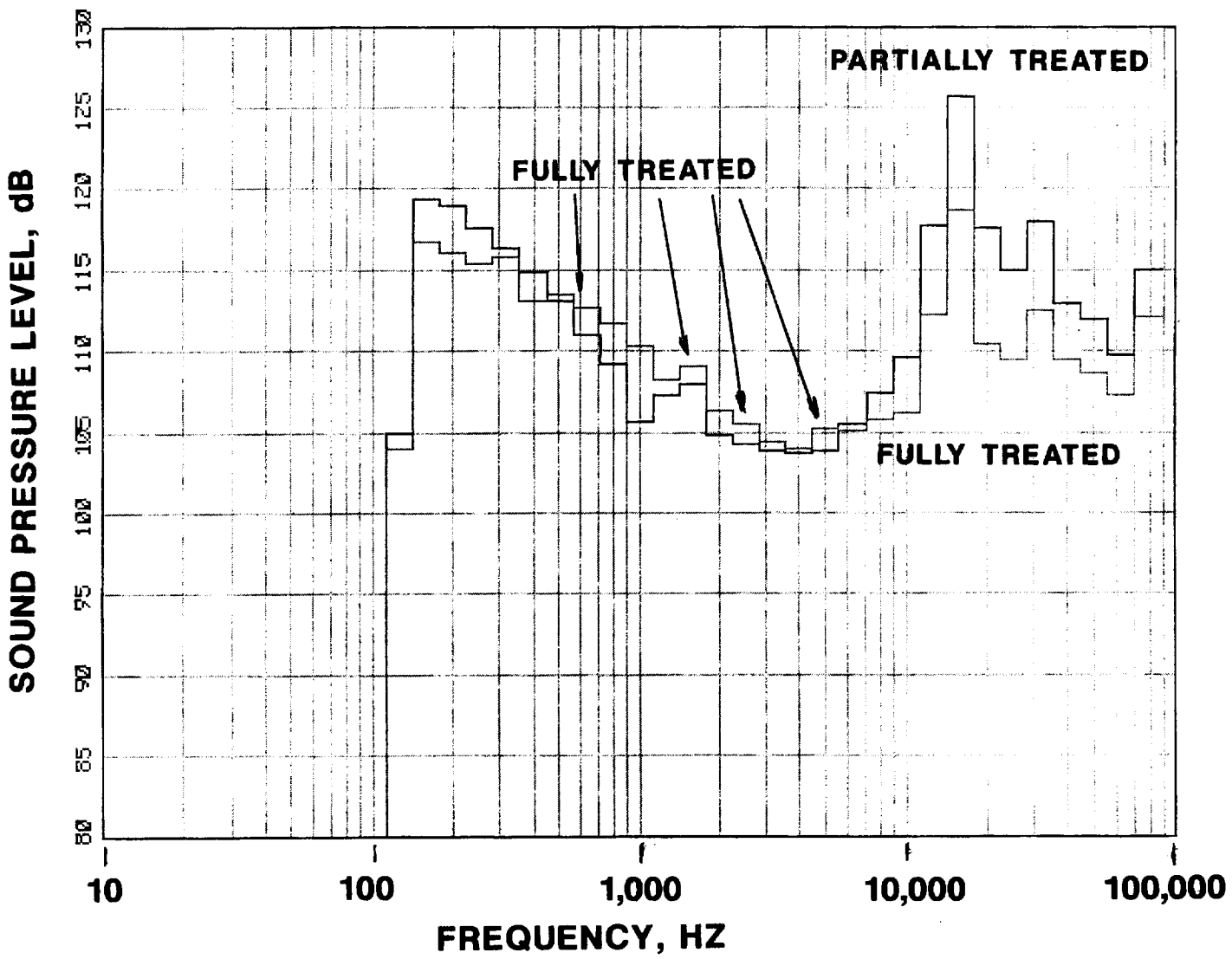


**FIGURE 41 CONCLUDED**

**C 130.5 DEGREES**

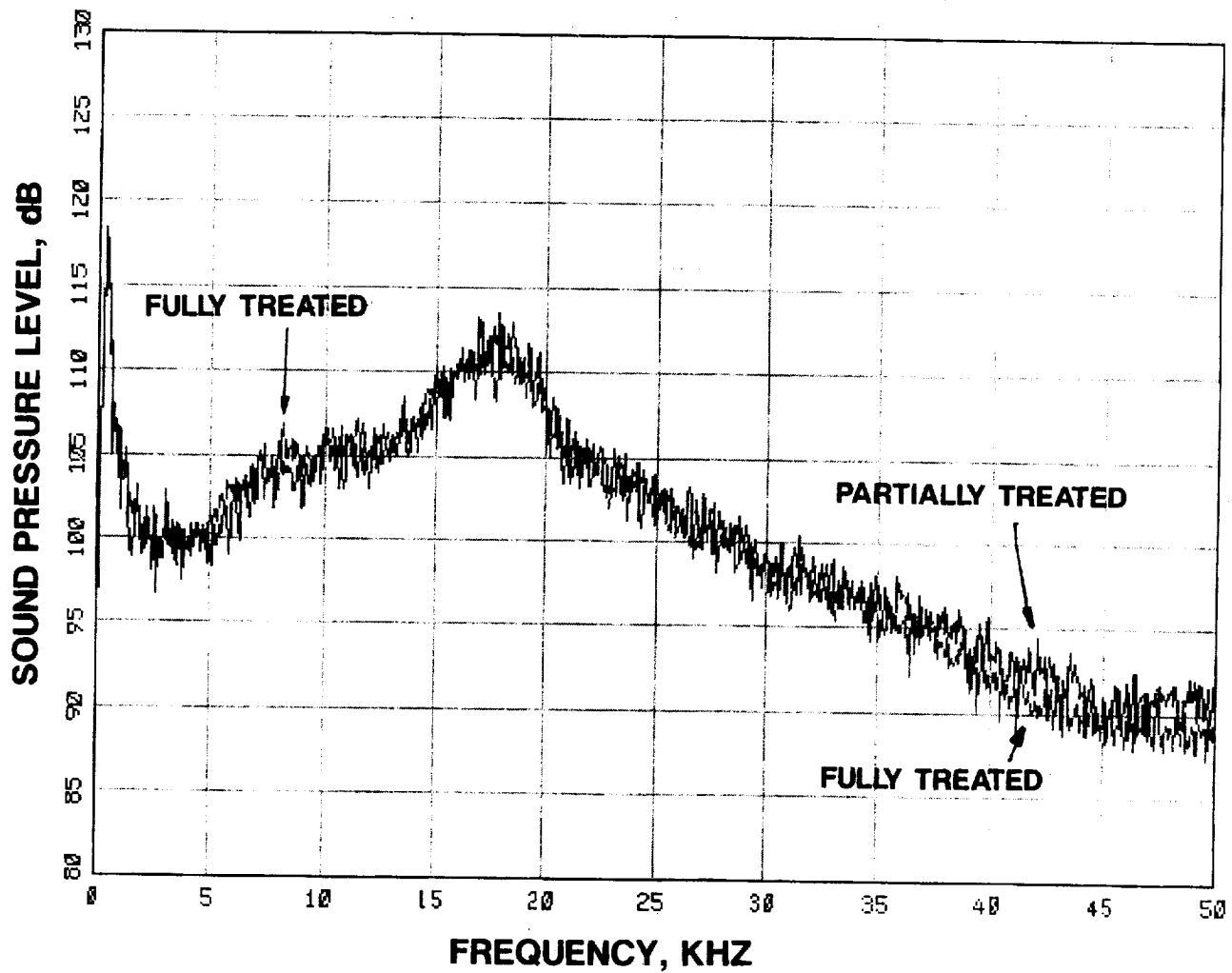


**FIGURE 42 SPECTRAL COMPARISON OF PARTIALLY TREATED AND  
FULLY TREATED DATA FOR THE 7 VANE CONFIGURATION  
AT 10671 RPMC  
A 24.5 DEGREES**

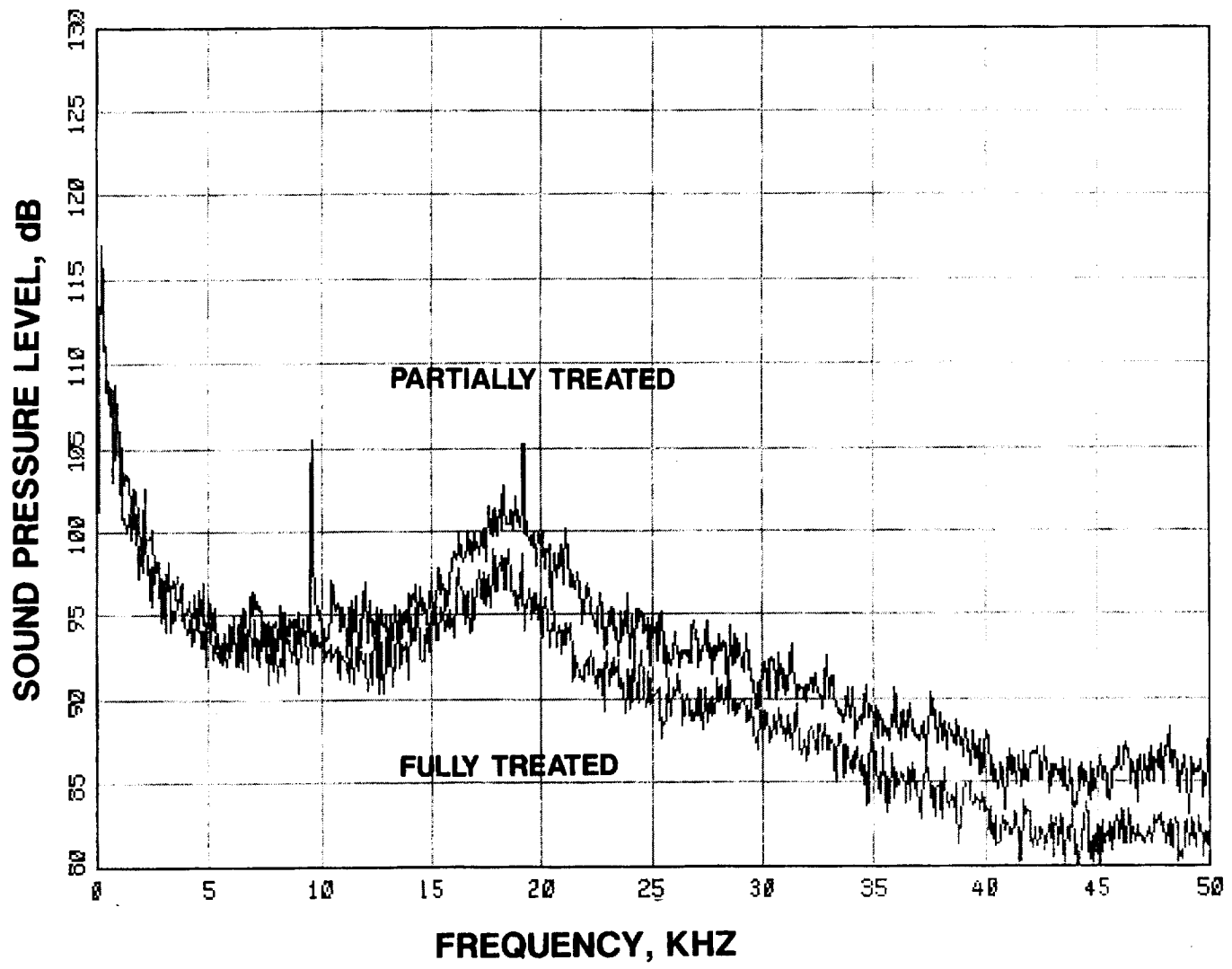


**FIGURE 42 CONTINUED**

**B 92.5 DEGREES**

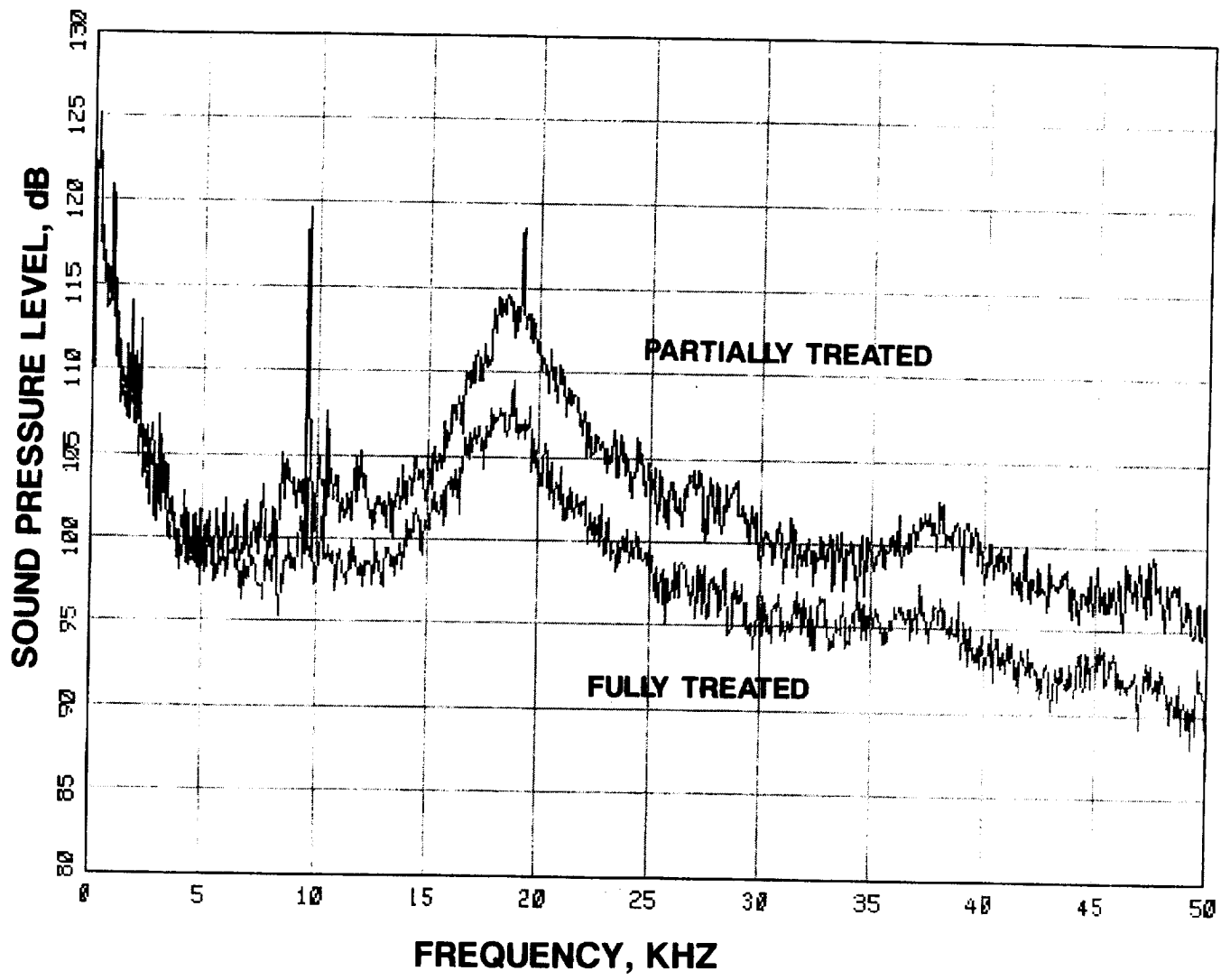


**FIGURE 42 CONCLUDED**

**C 130.5 DEGREES**

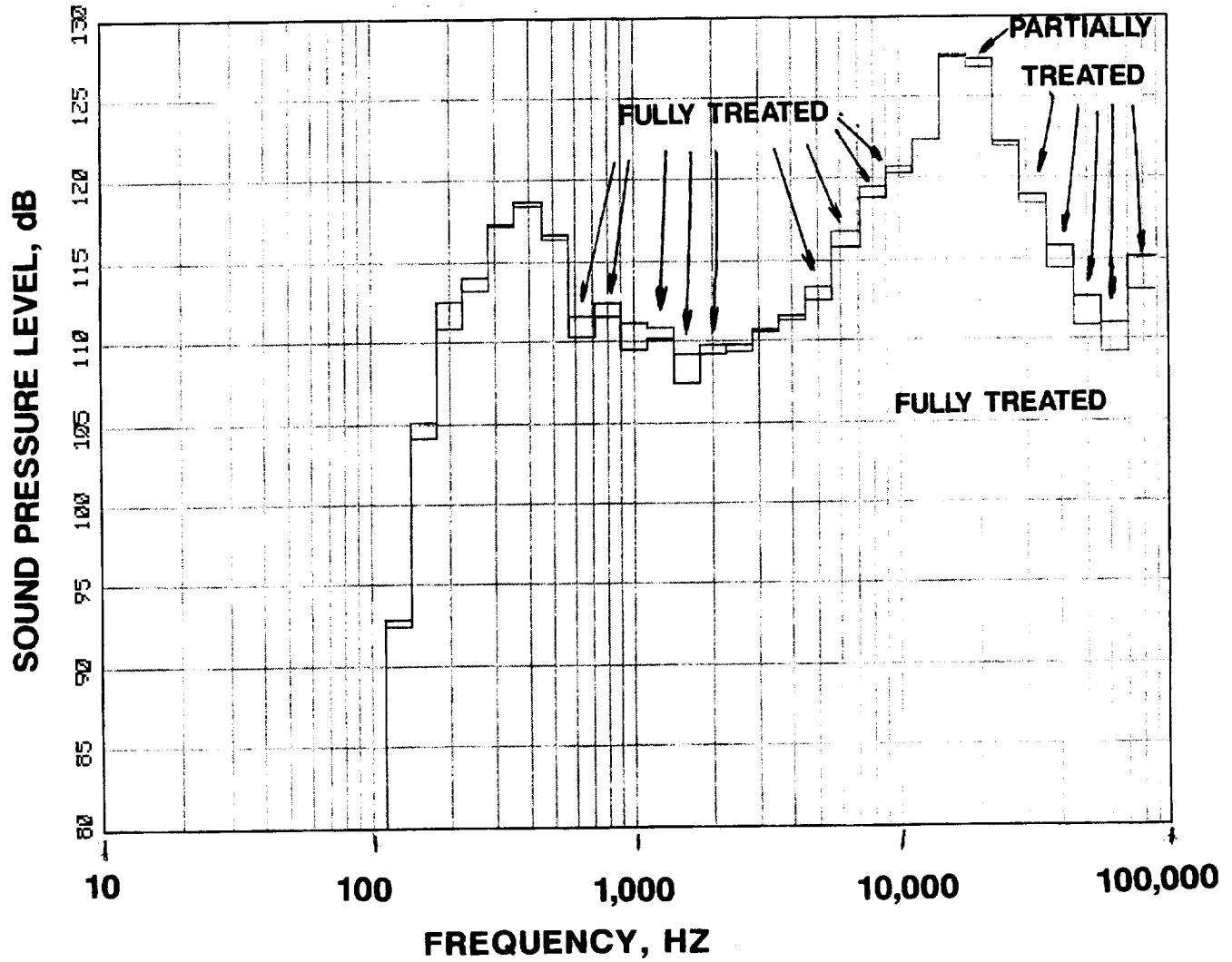


**FIGURE 43. 1/3RD OCTAVE COMPARISON OF PARTIALLY TREATED AND FULLY TREATED DATA FOR THE 7 VANE CONFIGURATION AT 10671 RPMC A 24.5 DEGREES**

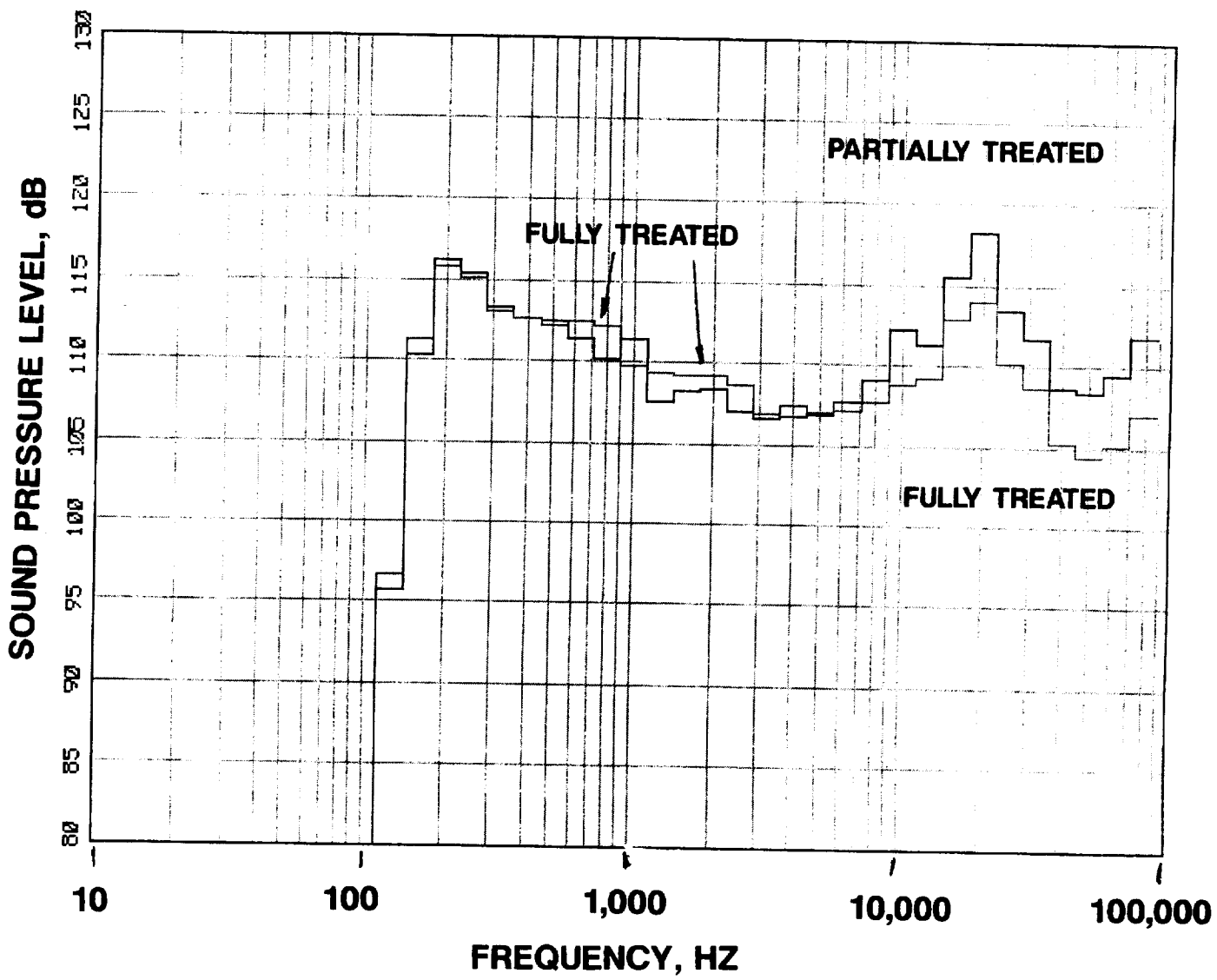


**FIGURE 43 CONTINUED**

**B 92.5 DEGREES**

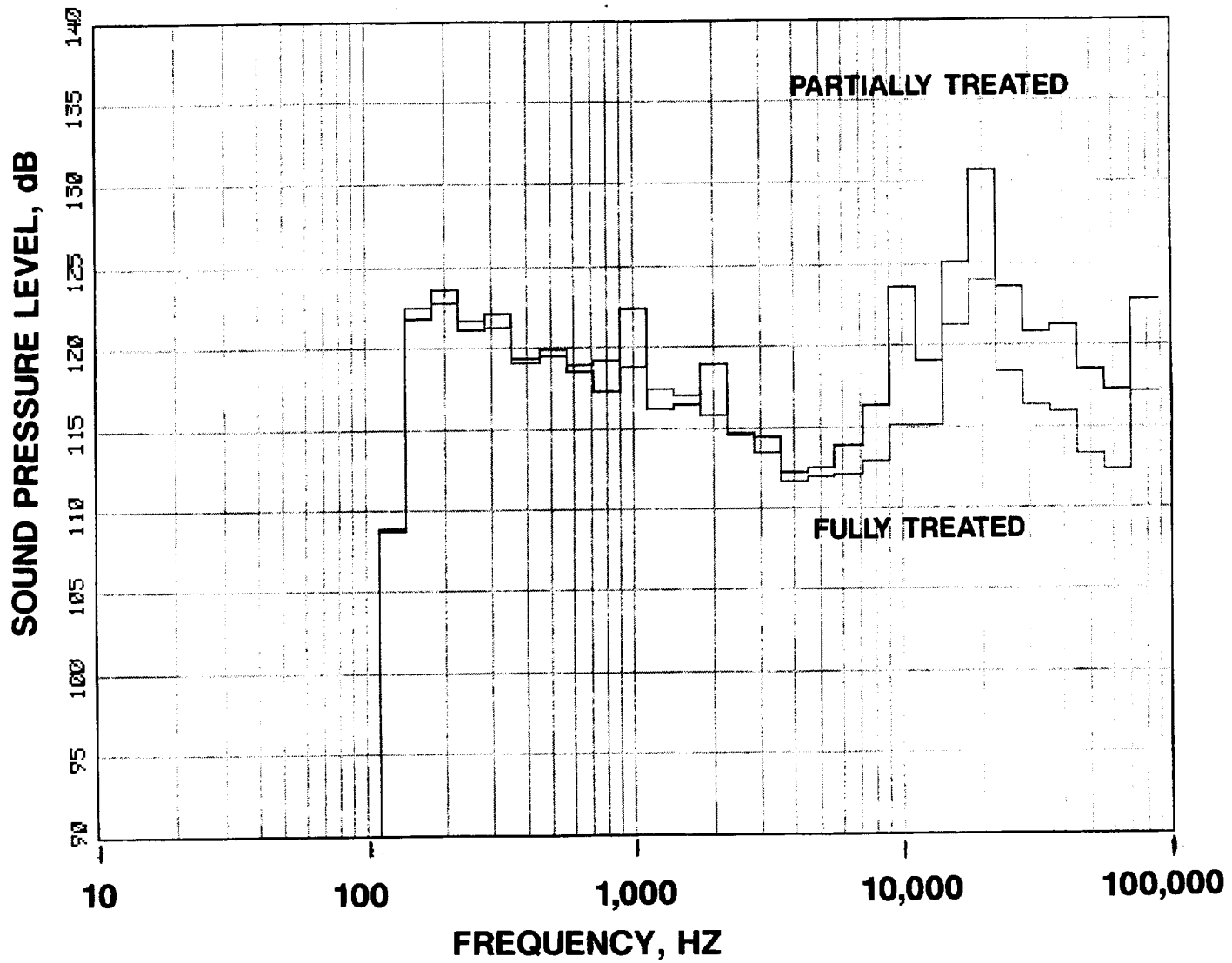


**FIGURE 43 CONCLUDED**

**C 130.5 DEGREES**

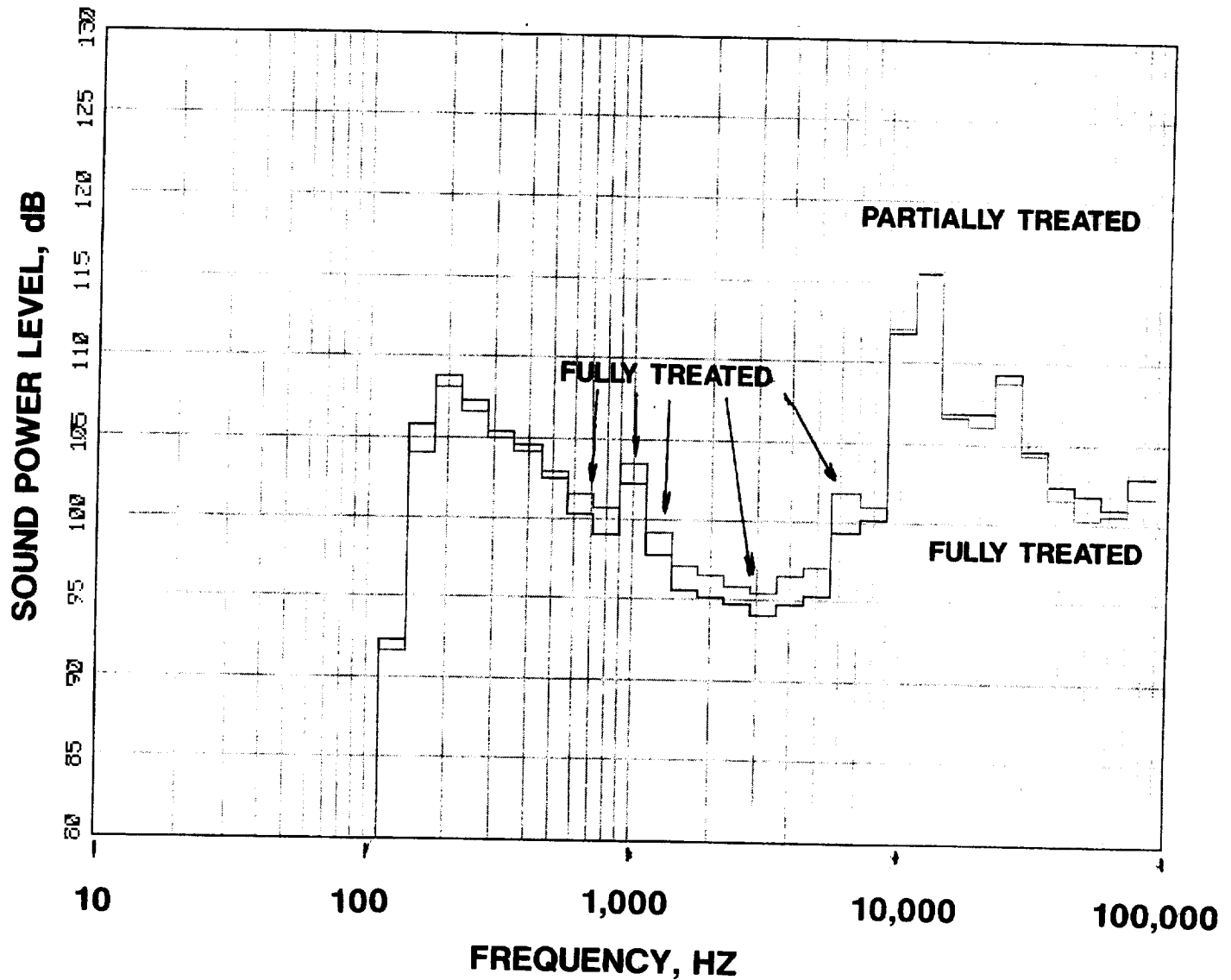


**FIGURE 44 SOUND POWER LEVEL COMPARISON OF PARTIALLY  
TREATED AND FULLY TREATED DATA FOR THE 7 VANE  
CONFIGURATION**

**A 6402 RPMC**

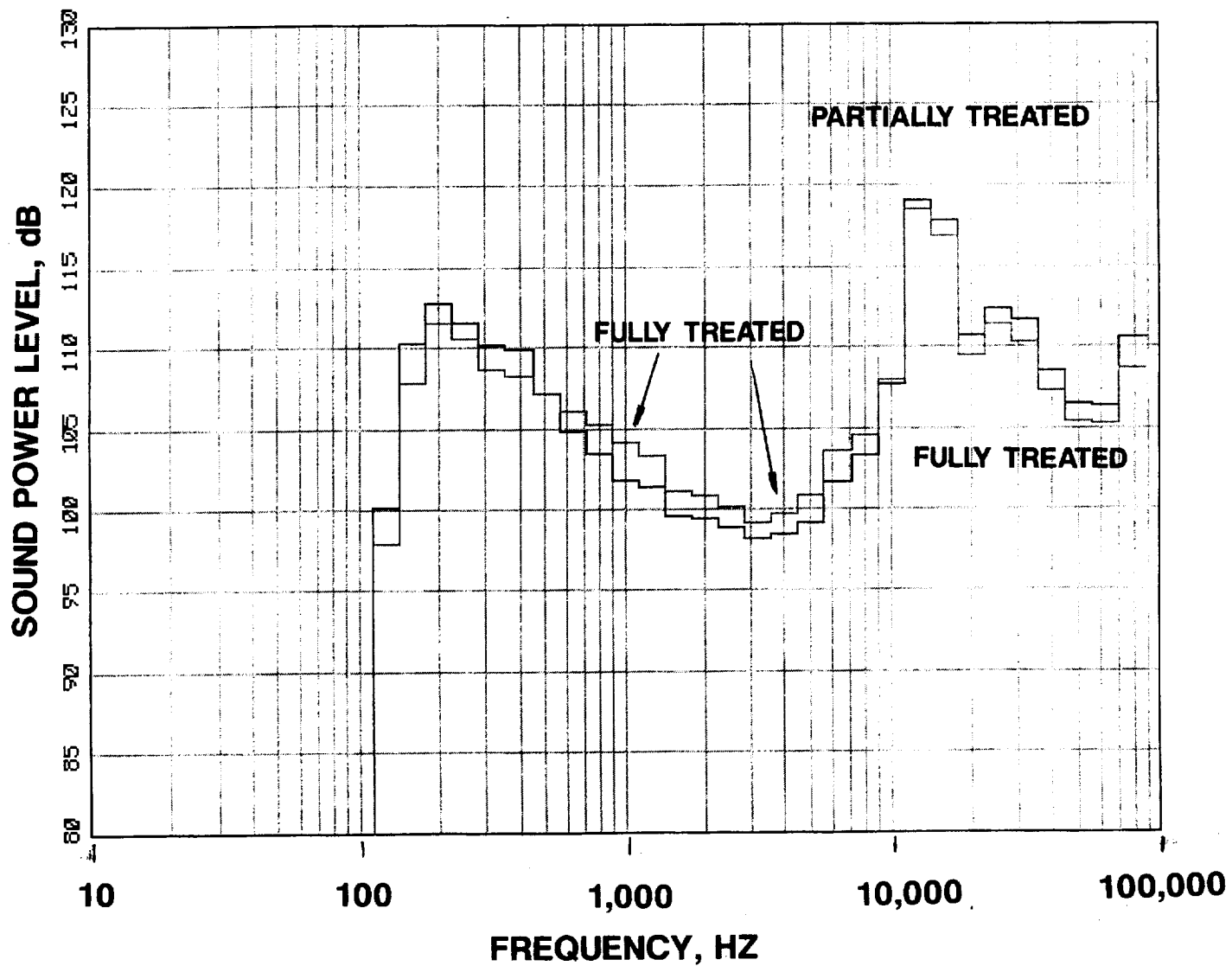


**FIGURE 44 CONTINUED**

**B 7736 RPMC**

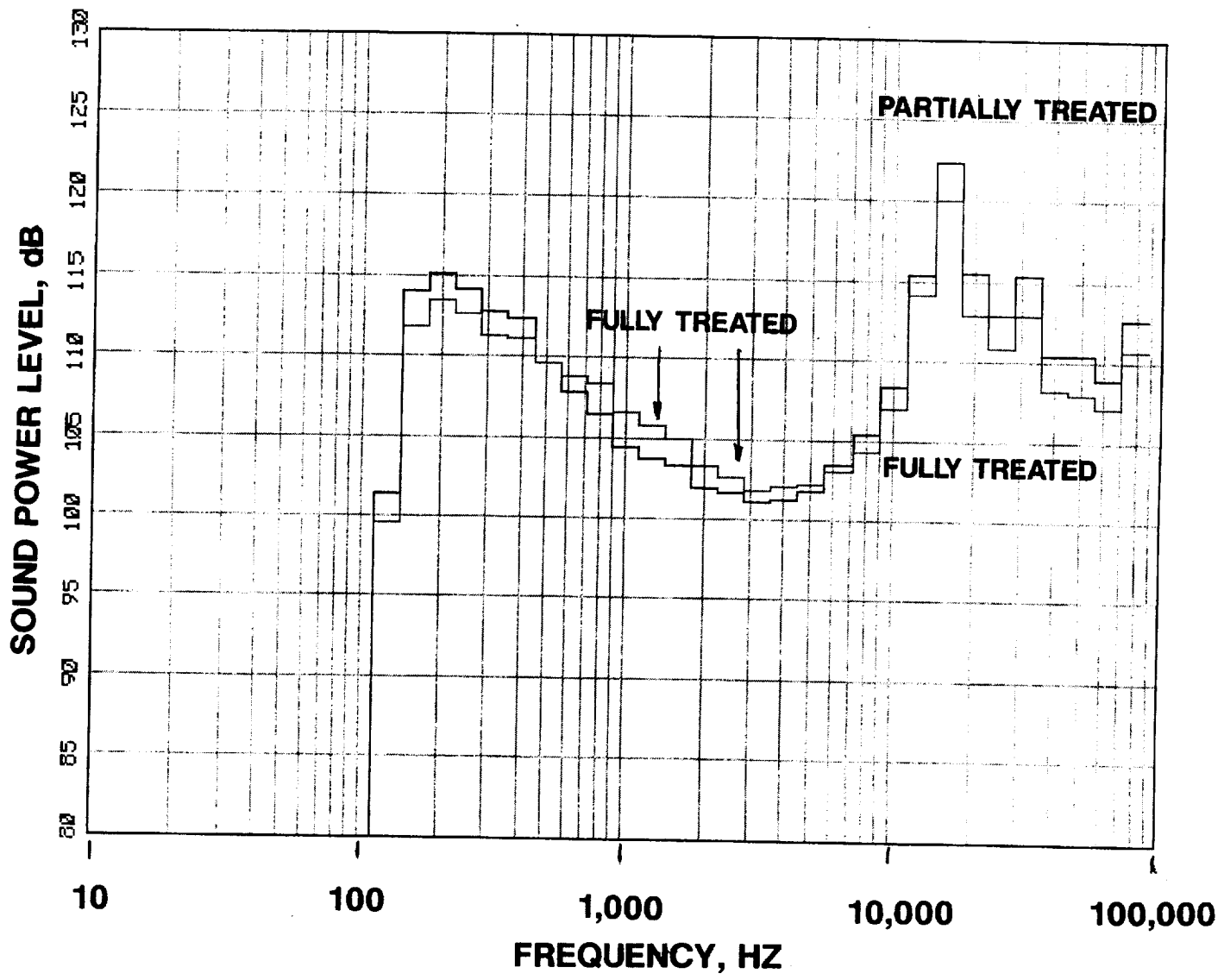


**FIGURE 44 CONTINUED**

**C 8537 RPMC**

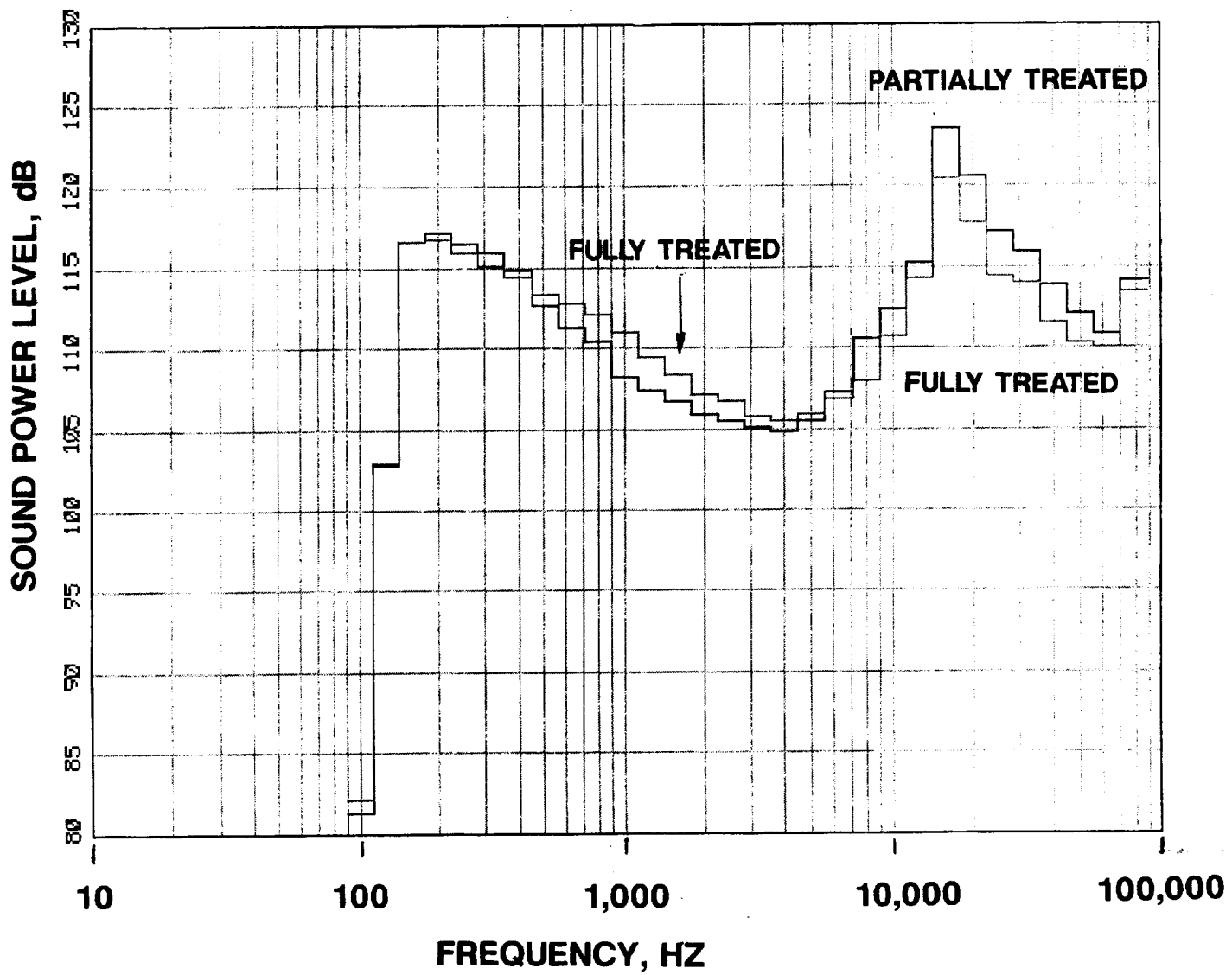


**FIGURE 44 CONTINUED**

**D 9604 RPMC**

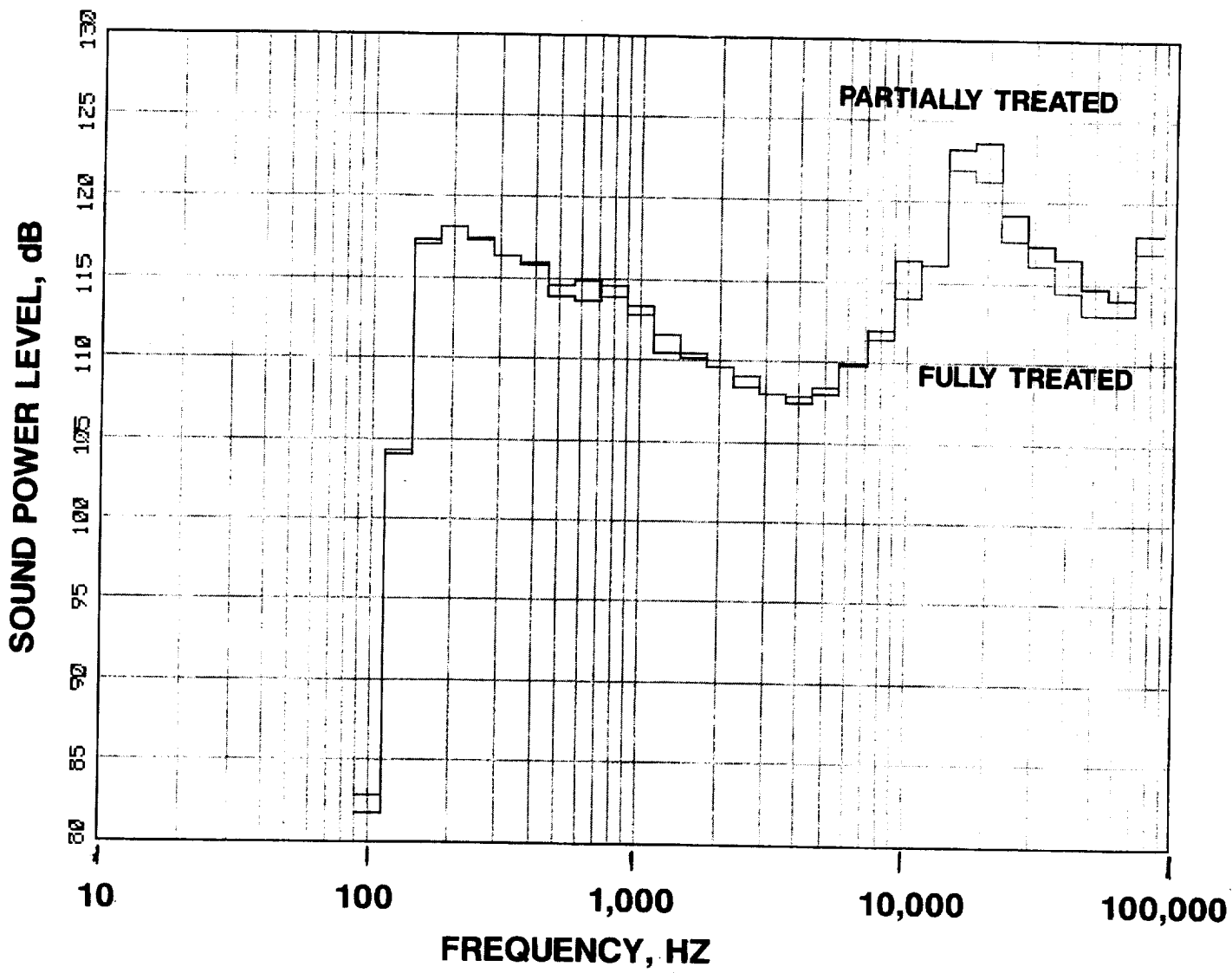


**FIGURE 44 CONTINUED**

**E 10137 RPMC**

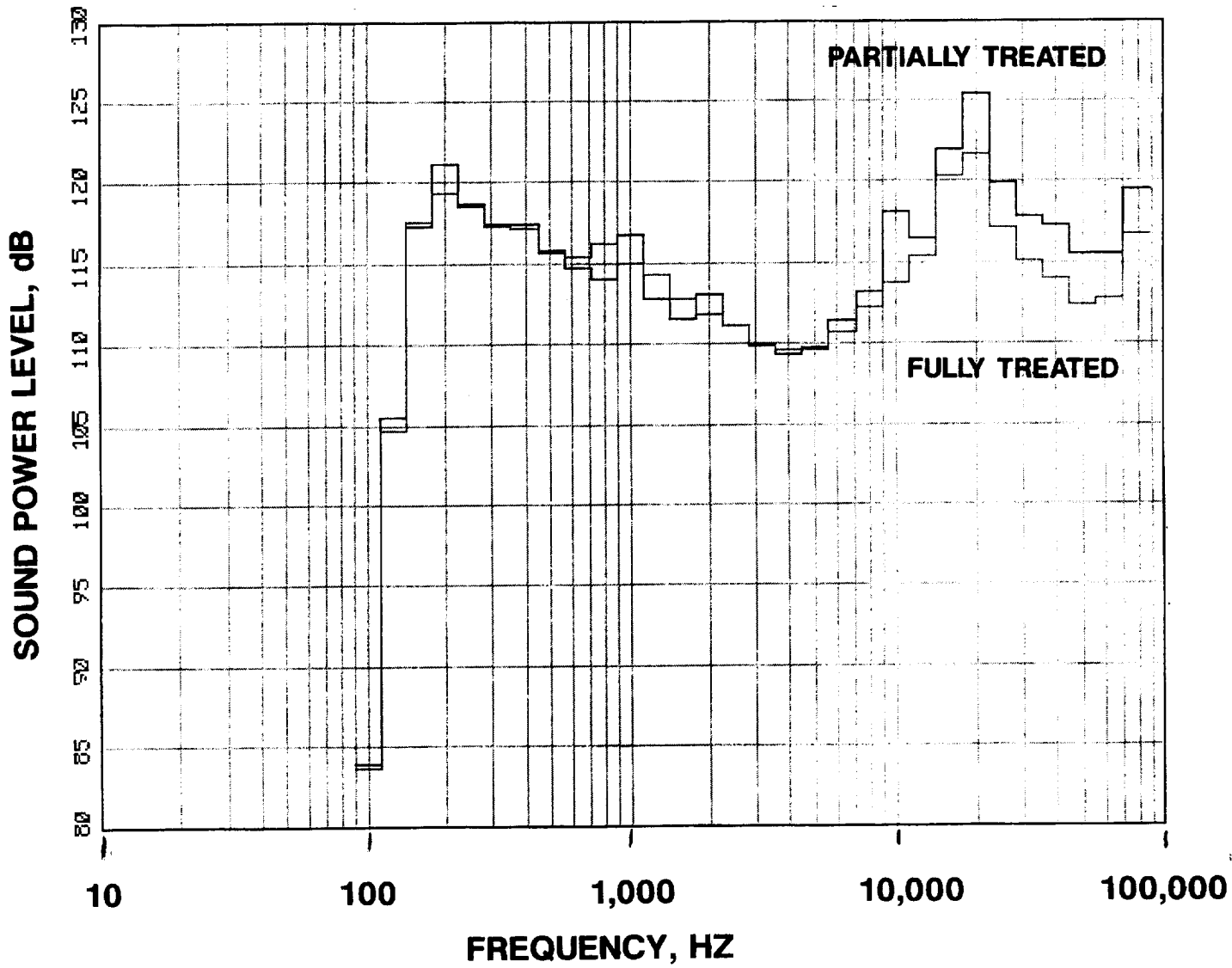


**FIGURE 44 CONCLUDED**

**F 10671 RPMC**

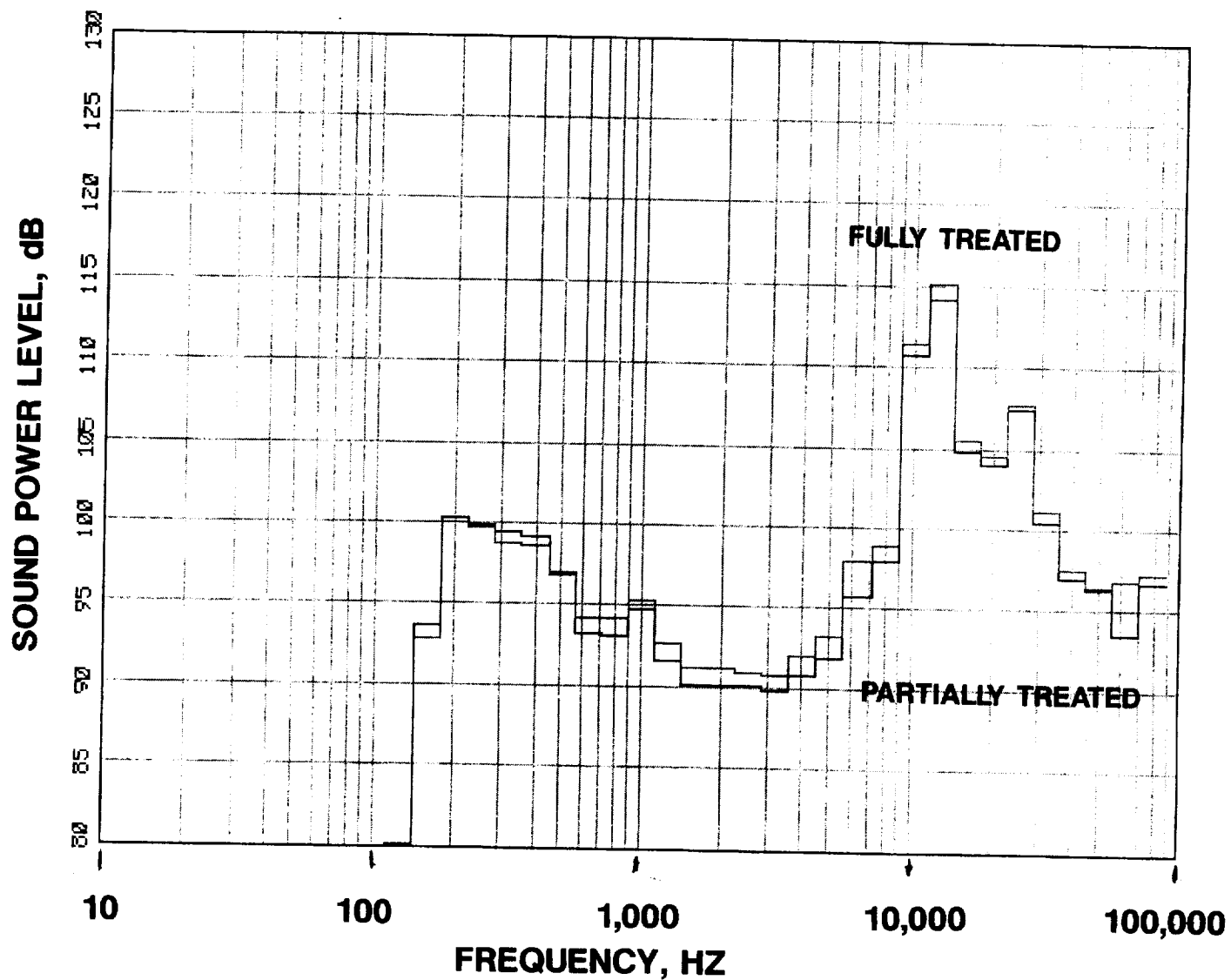


**FIGURE 45 FRONT SOUND POWER LEVEL COMPARISON OF  
PARTIALLY TREATED AND FULLY TREATED DATA FOR THE  
7 VANE CONFIGURATION  
A 6402 RPMC**

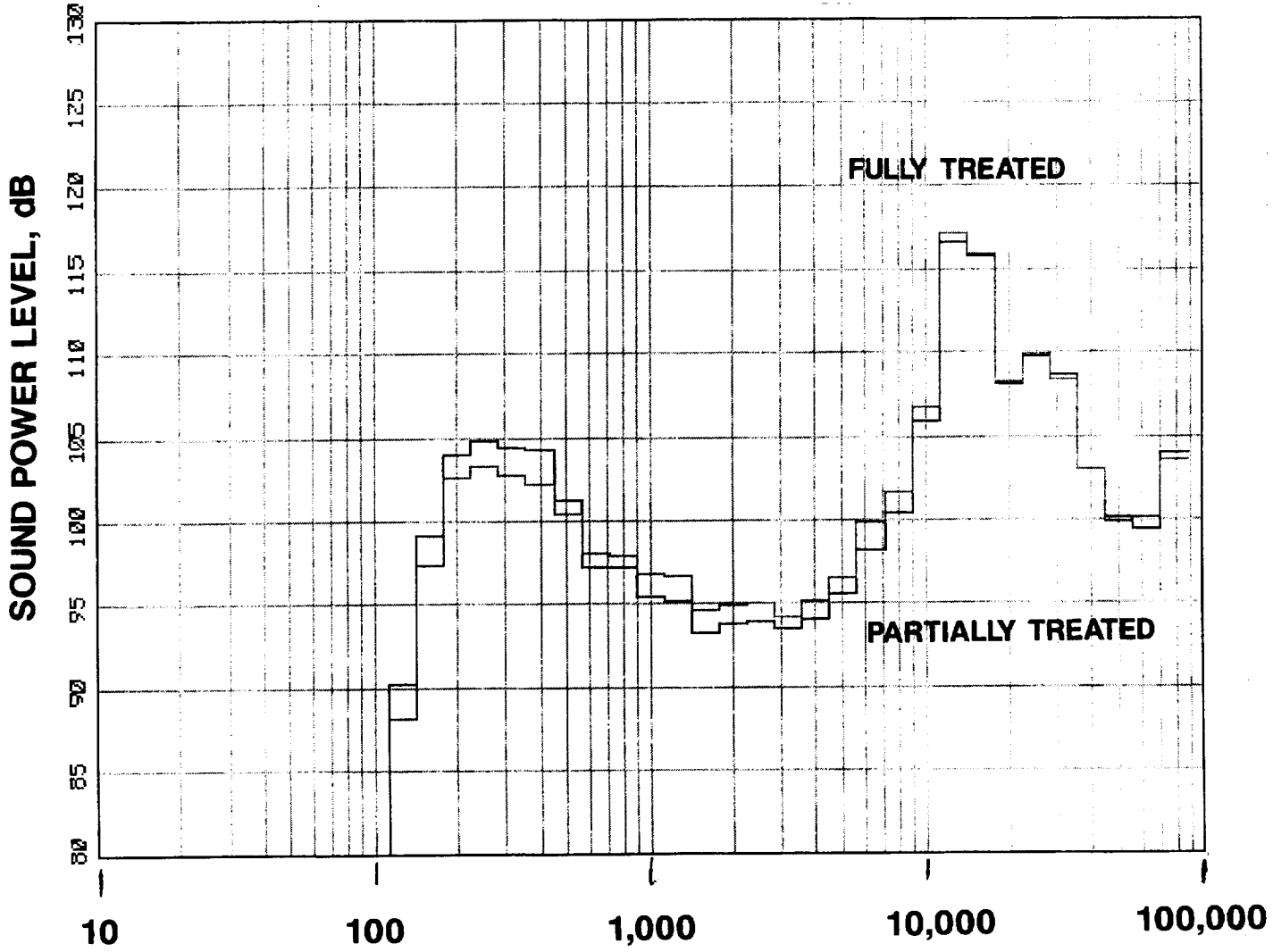


**FIGURE 45 CONTINUED**

**B 7736 RPMC**

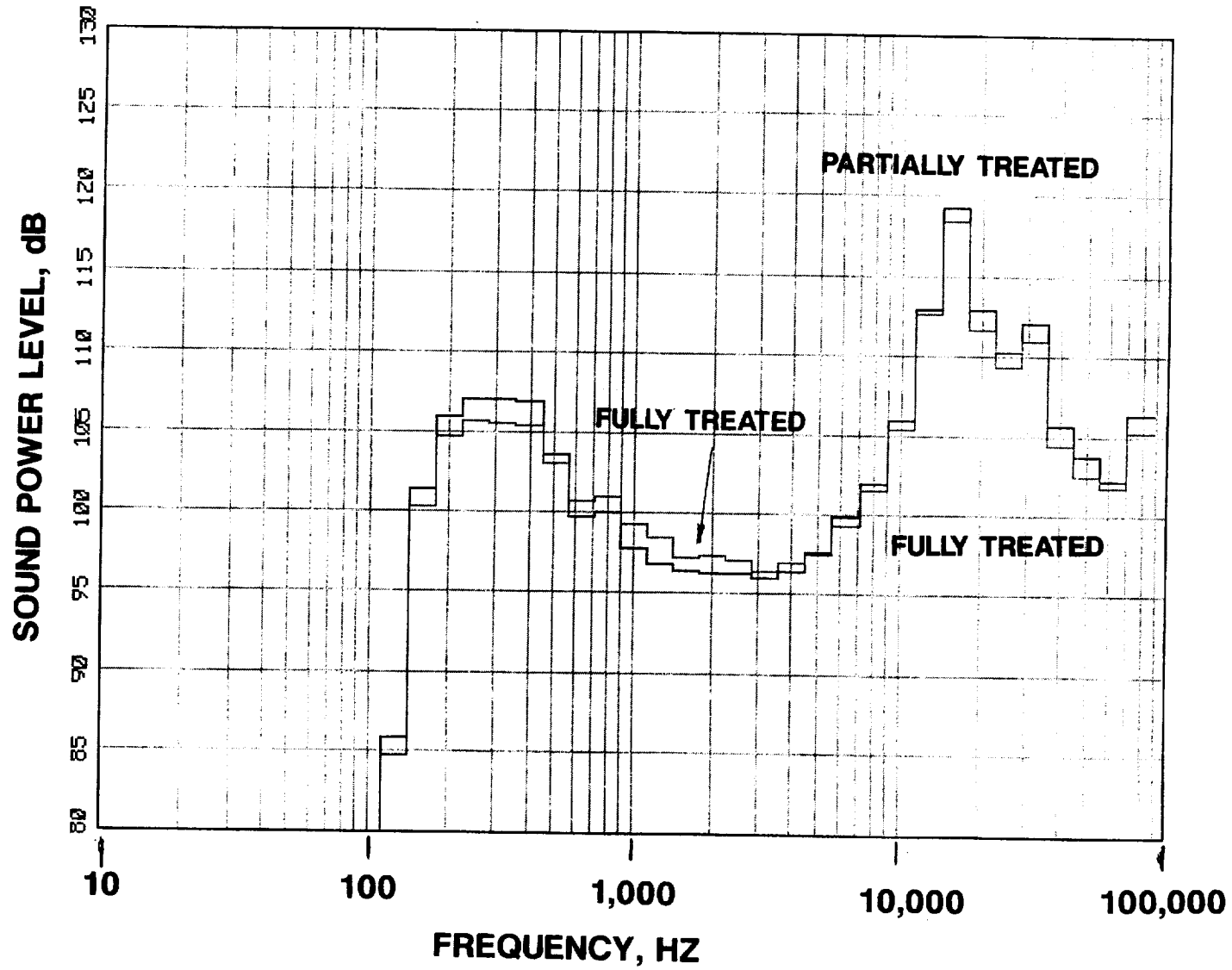


**FIGURE 45 CONTINUED**

**C 8537 RPMC**

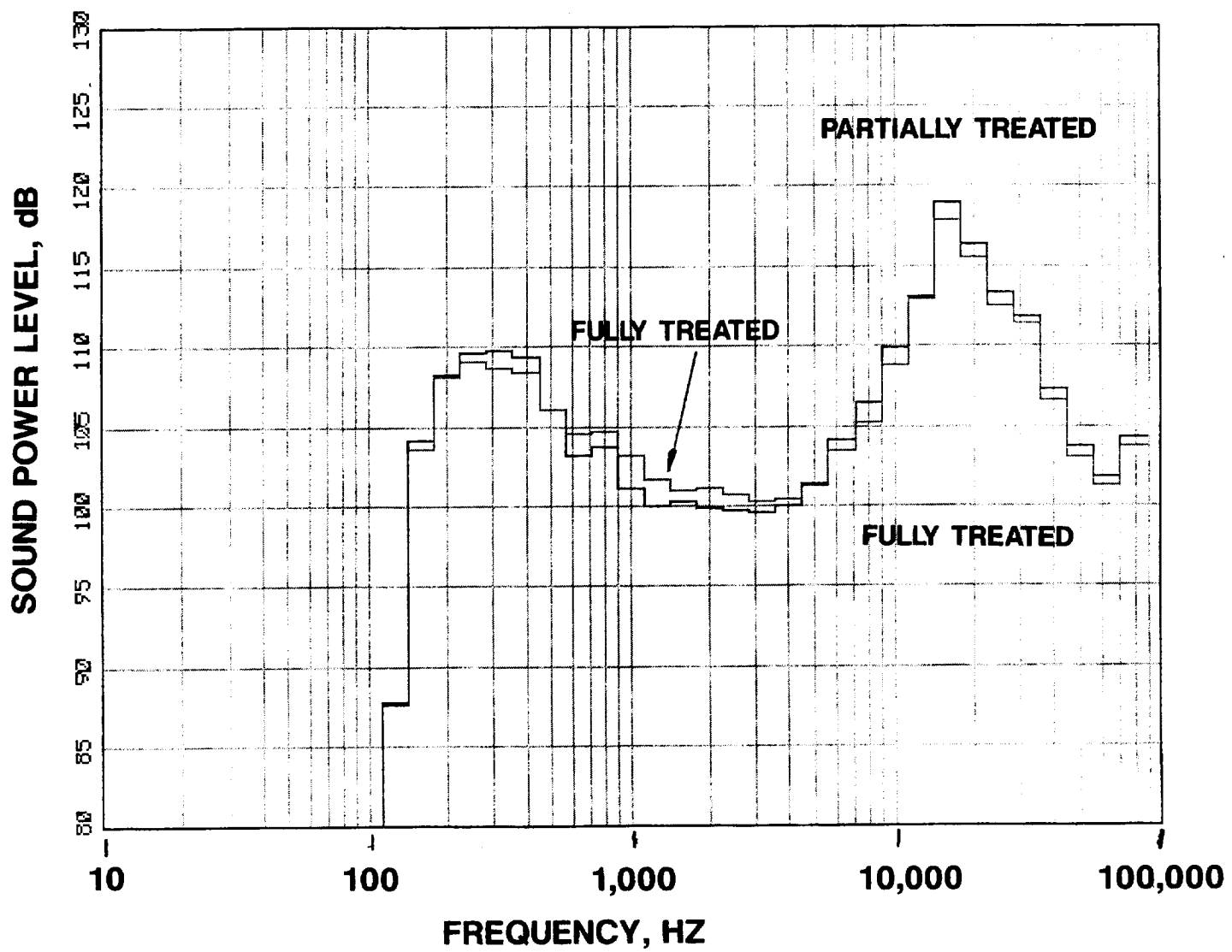


**FIGURE 45 CONTINUED**

**D 9604 RPMC**

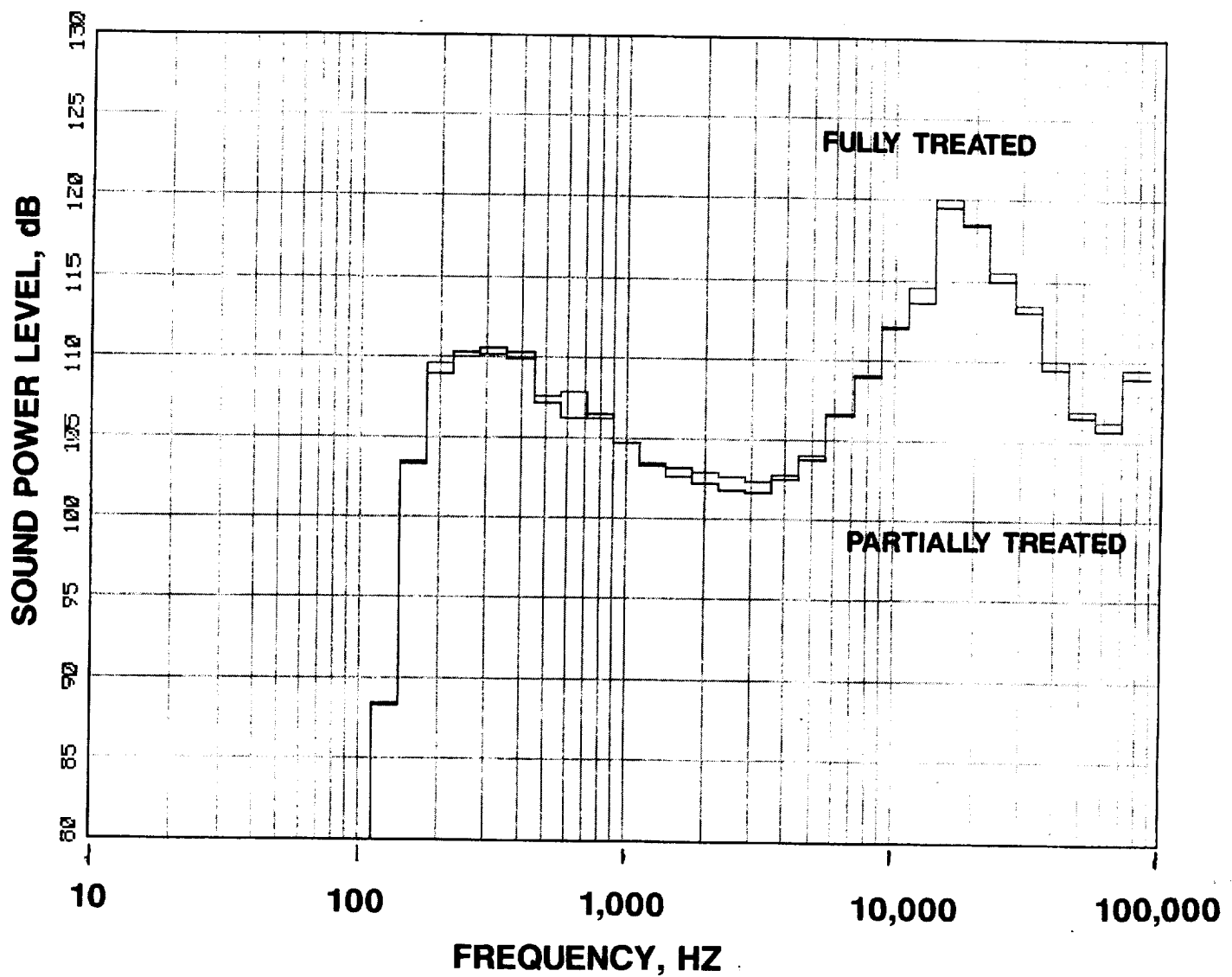


**FIGURE 45 CONTINUED**

**E 10137 RPMC**

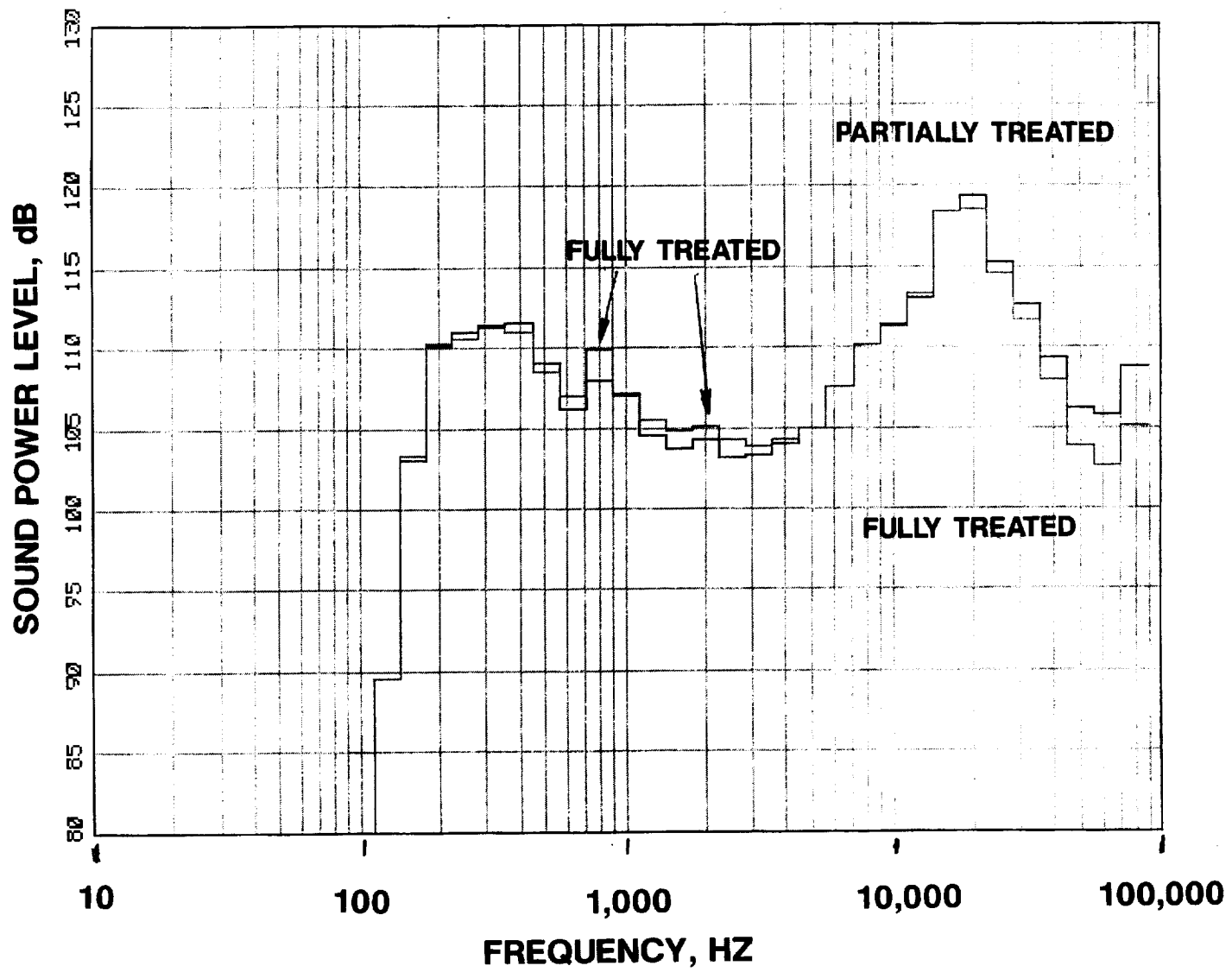


**FIGURE 45 CONCLUDED**

**F 10671 RPMC**

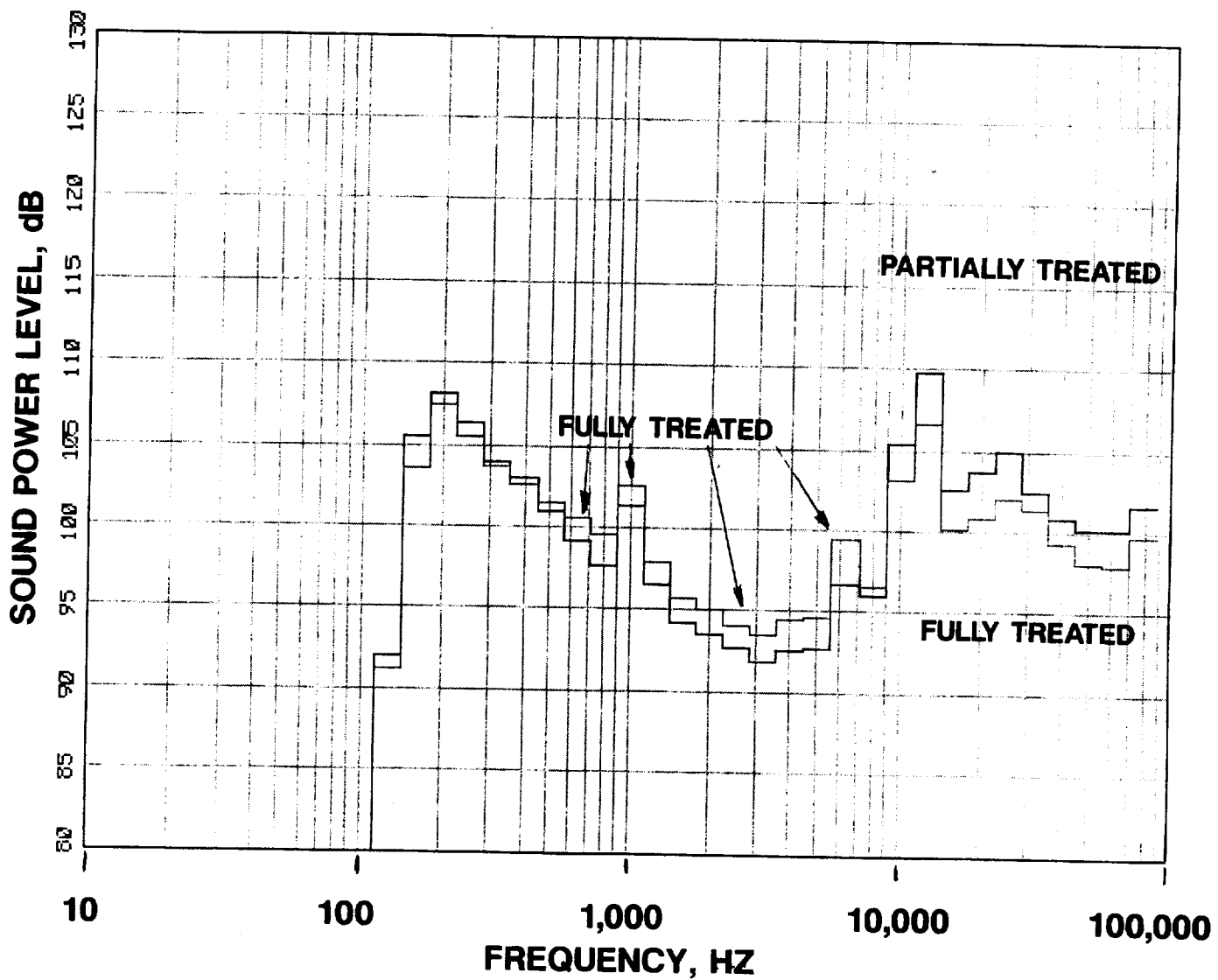


**FIGURE 46 AFT SOUND POWER LEVEL COMPARISON OF  
PARTIALLY TREATED AND FULLY TREATED DATA FOR  
THE 7 VANE CONFIGURATION**

**A 6402 RPMC**

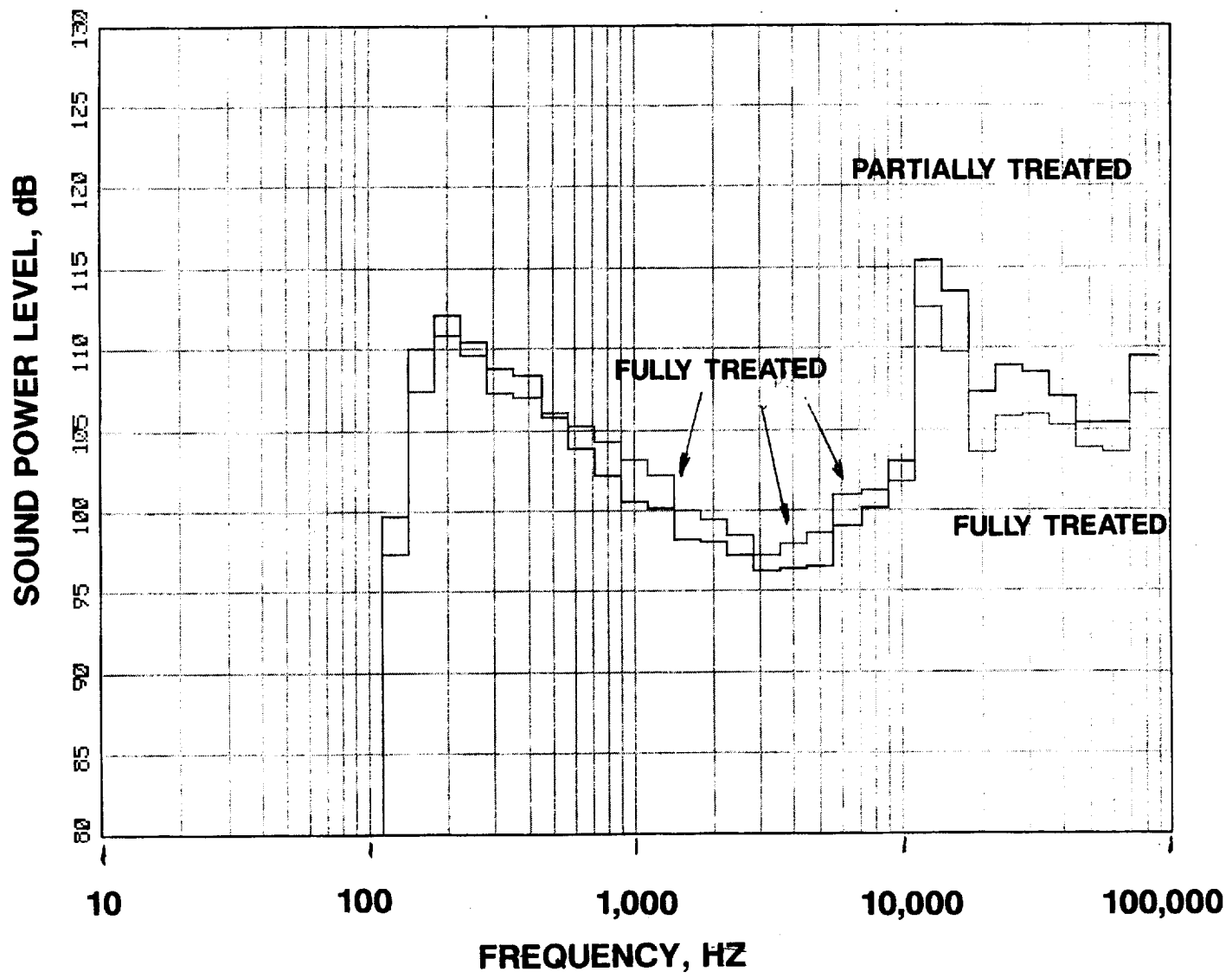


**FIGURE 46 CONTINUED**

**B 7736 RPMC**

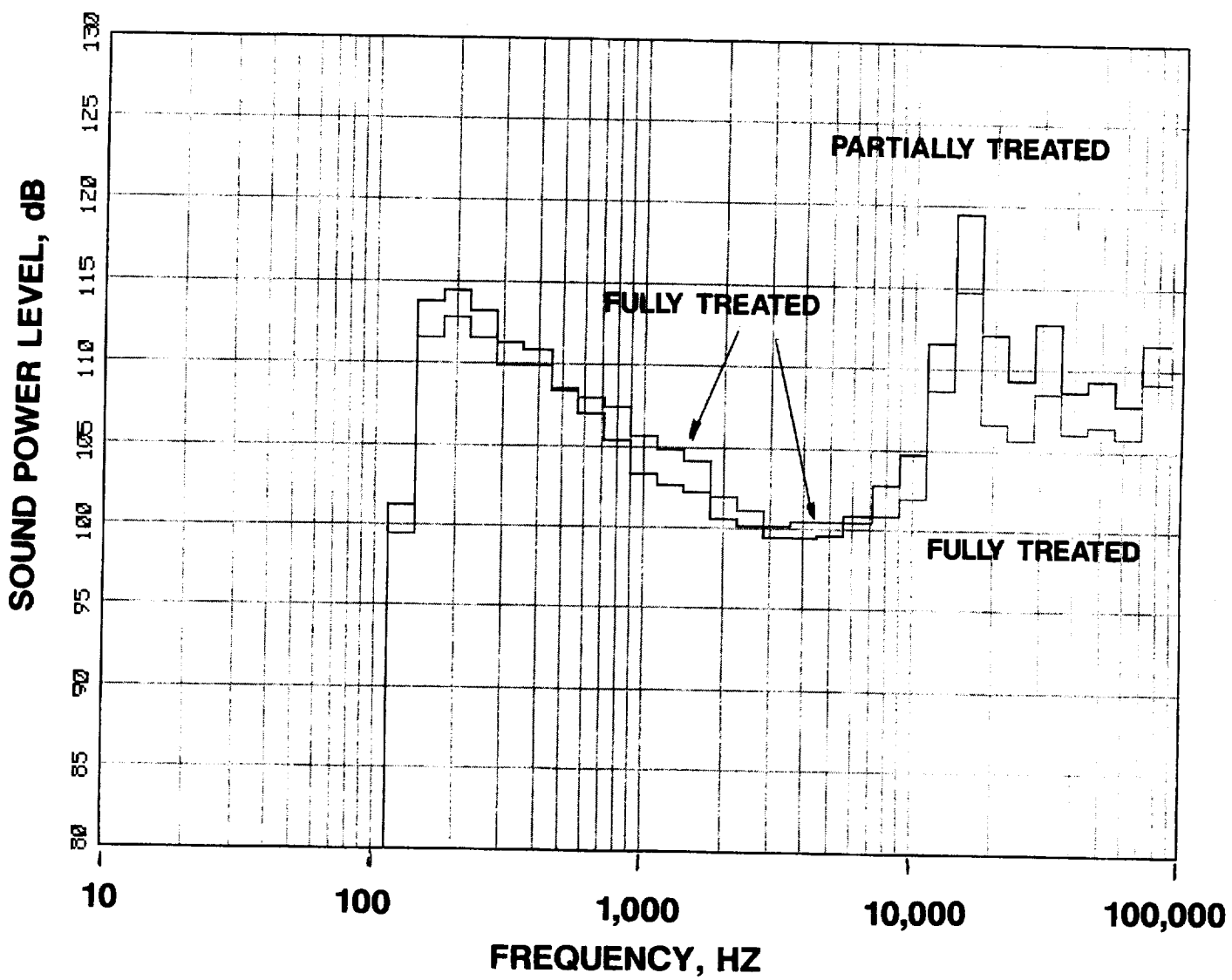


**FIGURE 46 CONTINUED**

**C 8537 RPMC**

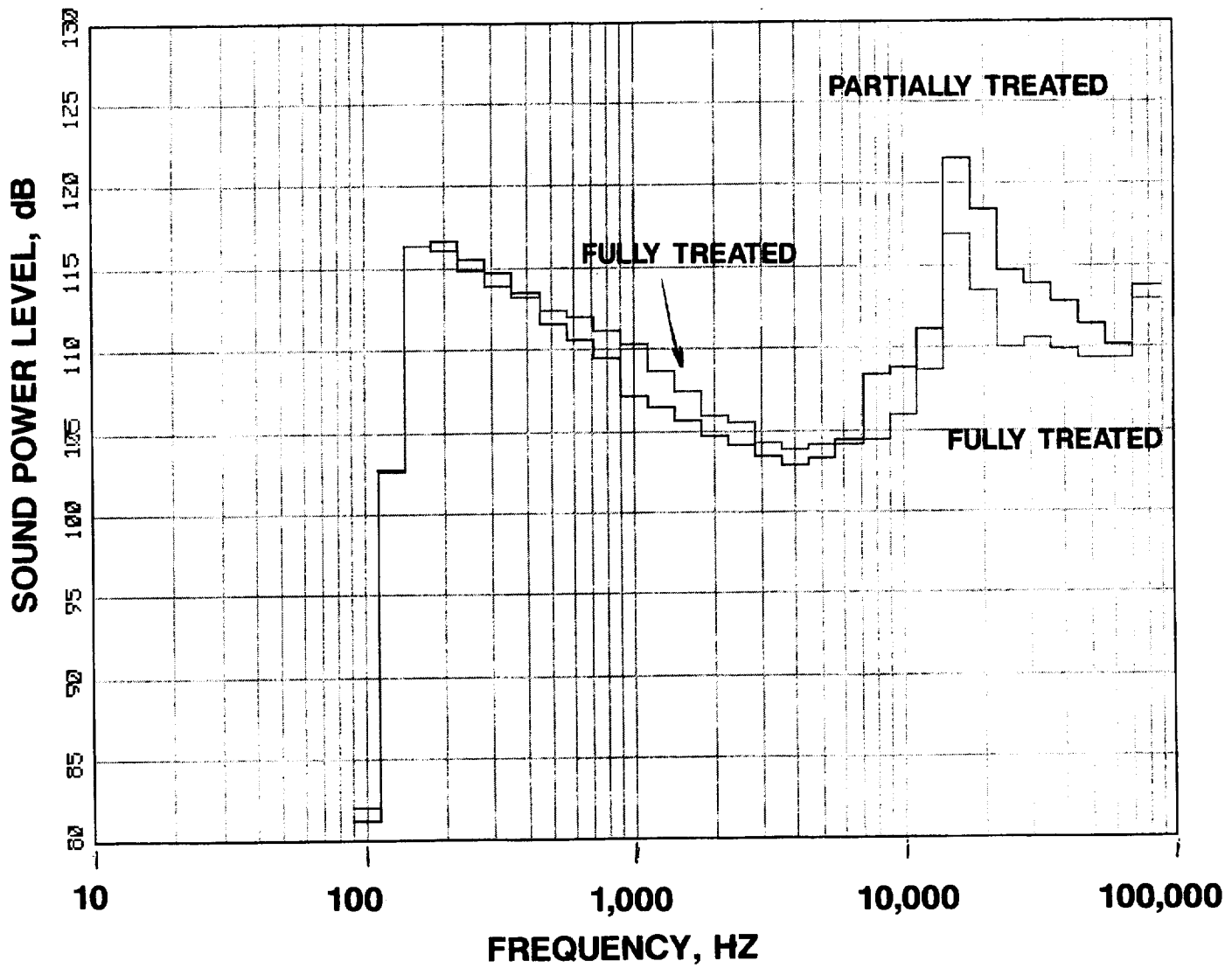


**FIGURE 46 CONTINUED**

**D 9604 RPMC**

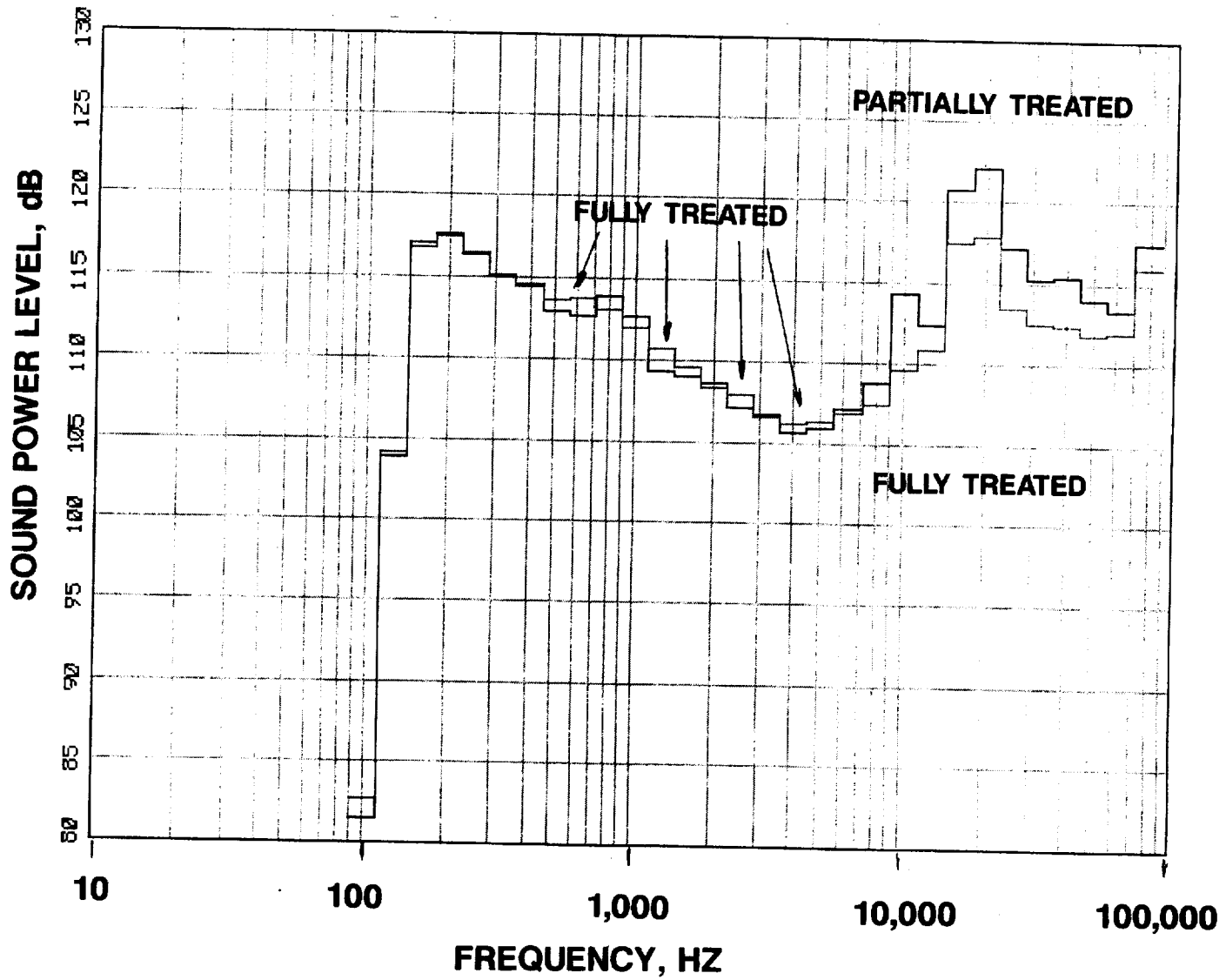


**FIGURE 46 CONTINUED**

**E 10137 RPMC**

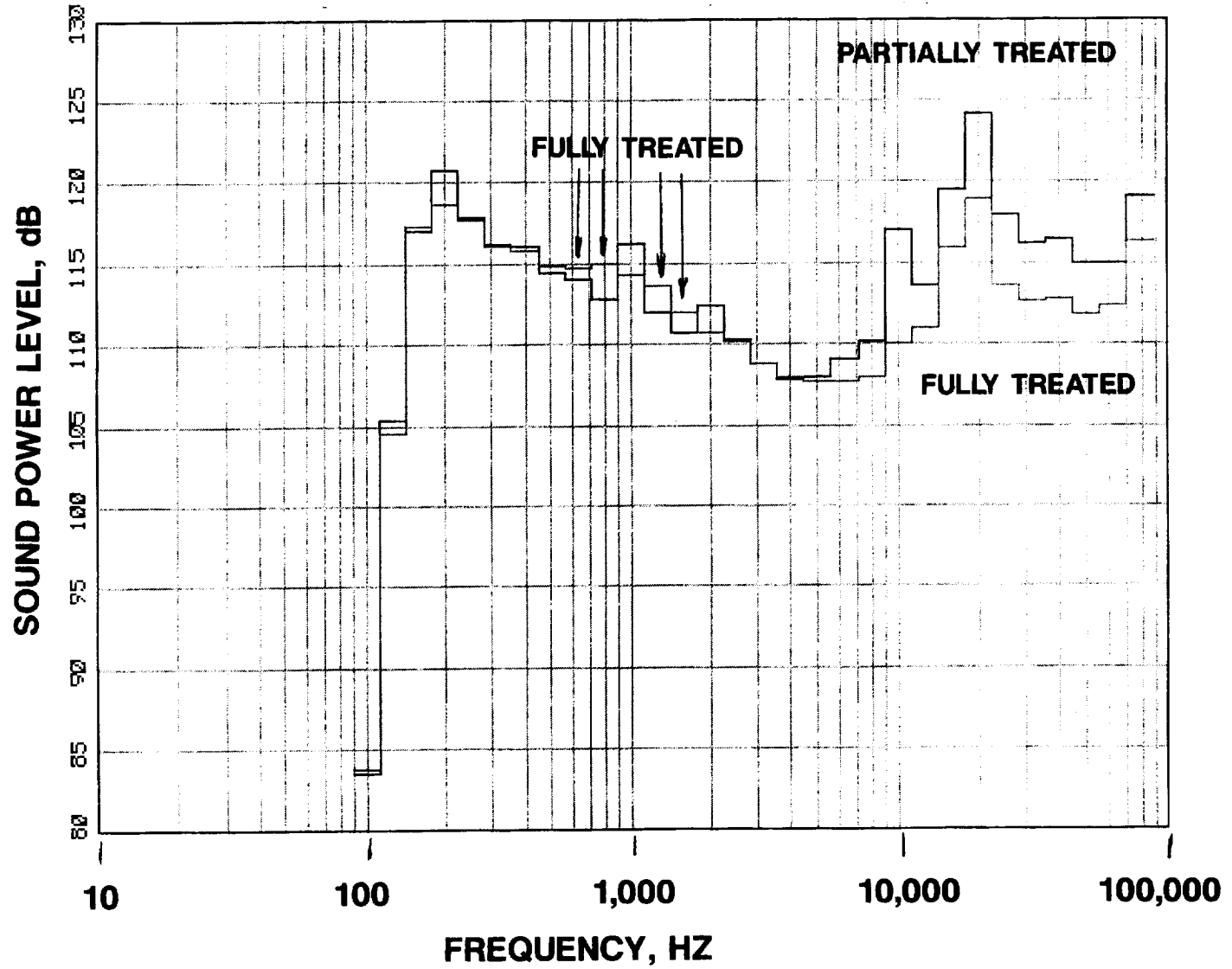


**FIGURE 46 CONCLUDED**

**F 10671 RPMC**

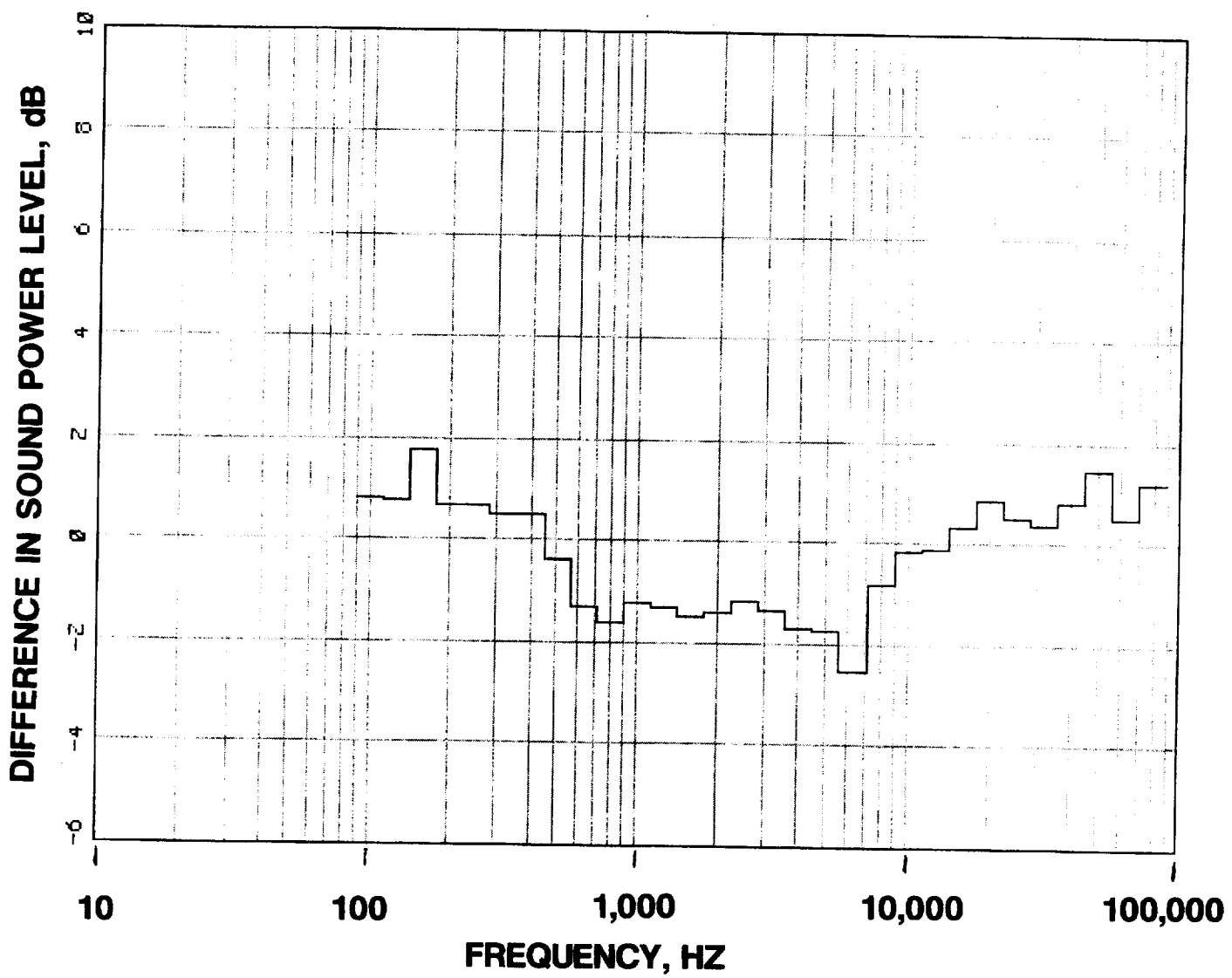


**FIGURE 47 DIFFERENCE IN SOUND POWER LEVEL, PARTIALLY  
TREATED MINUS FULLY TREATED, FOR THE  
7 VANE CONFIGURATION**

**A 6402 RPMC**

**DIFFERENCE IN SOUND POWER LEVEL, dB**

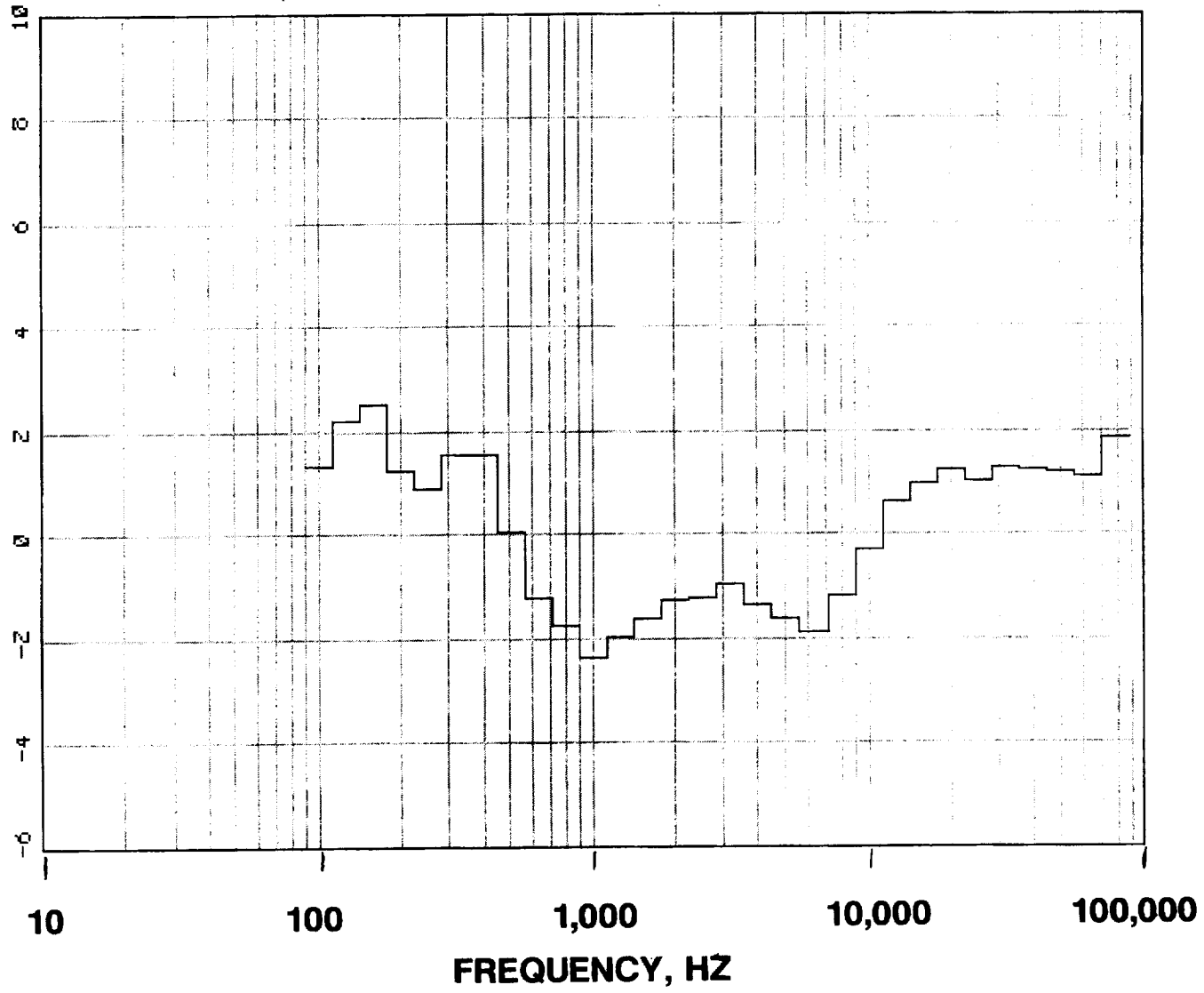


**FIGURE 47 CONTINUED**

**B 7736 RPMC**

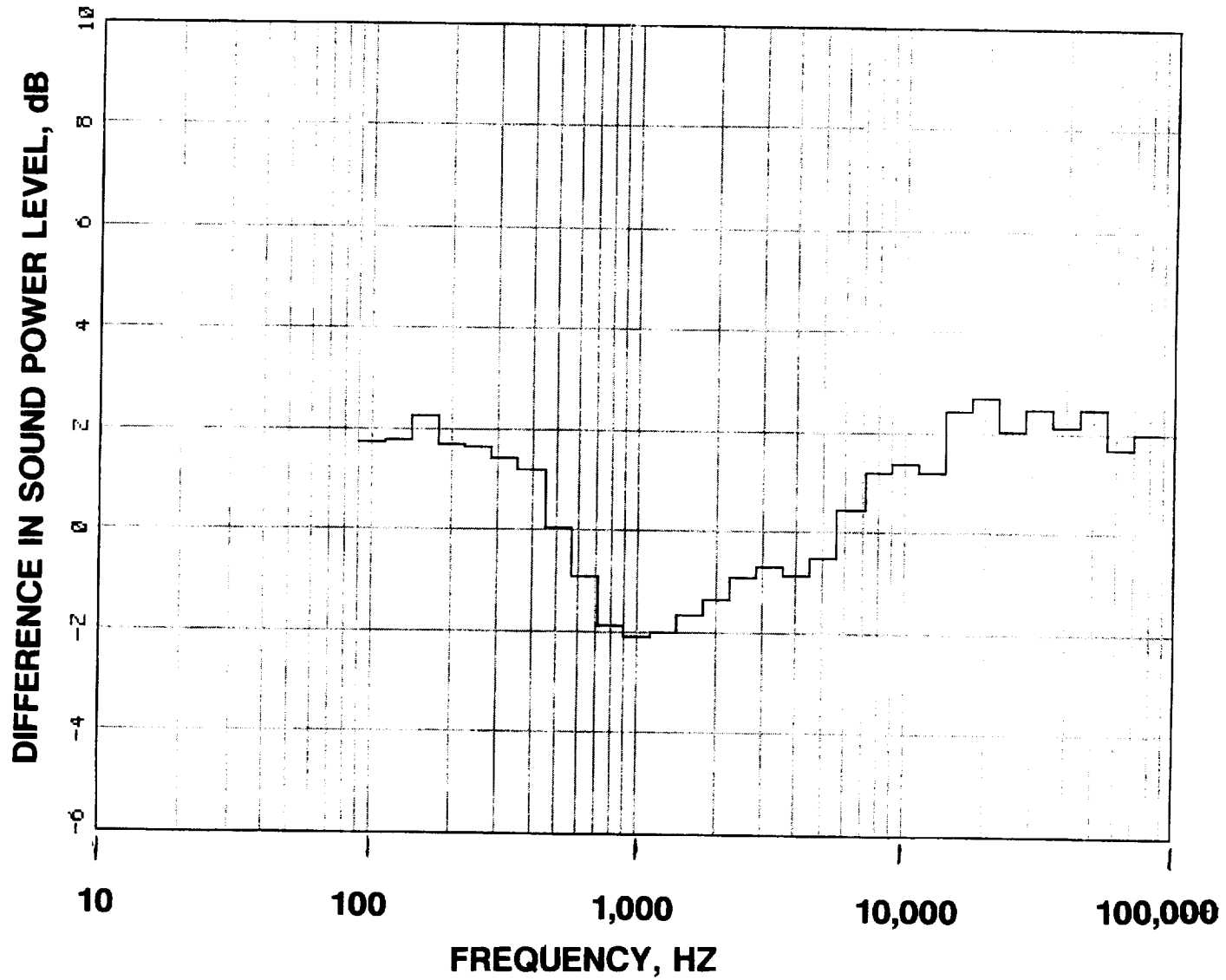


**FIGURE 47 CONTINUED**

**C 8537 RPMC**

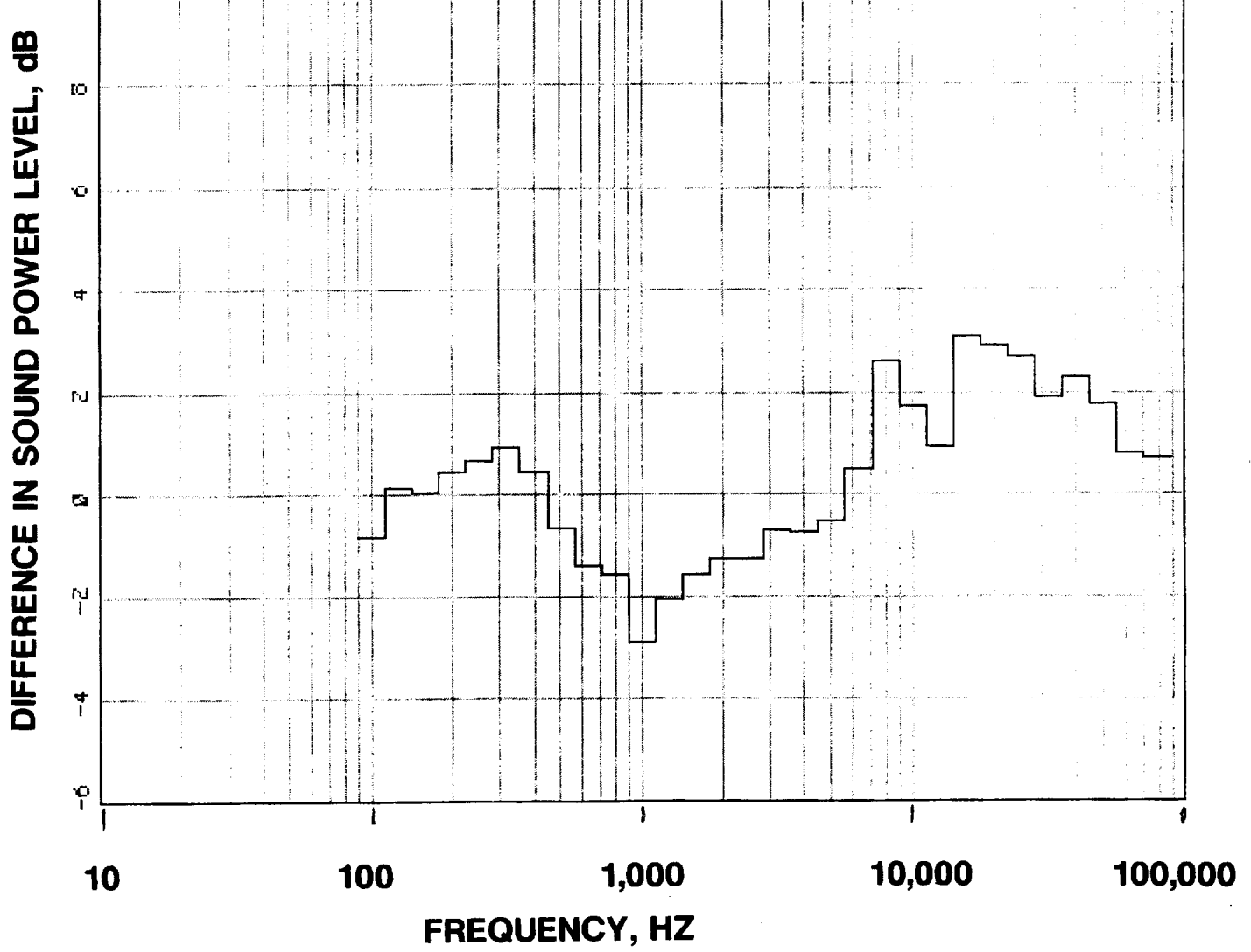


**FIGURE 47 CONTINUED**

**D 9604 RPMC**

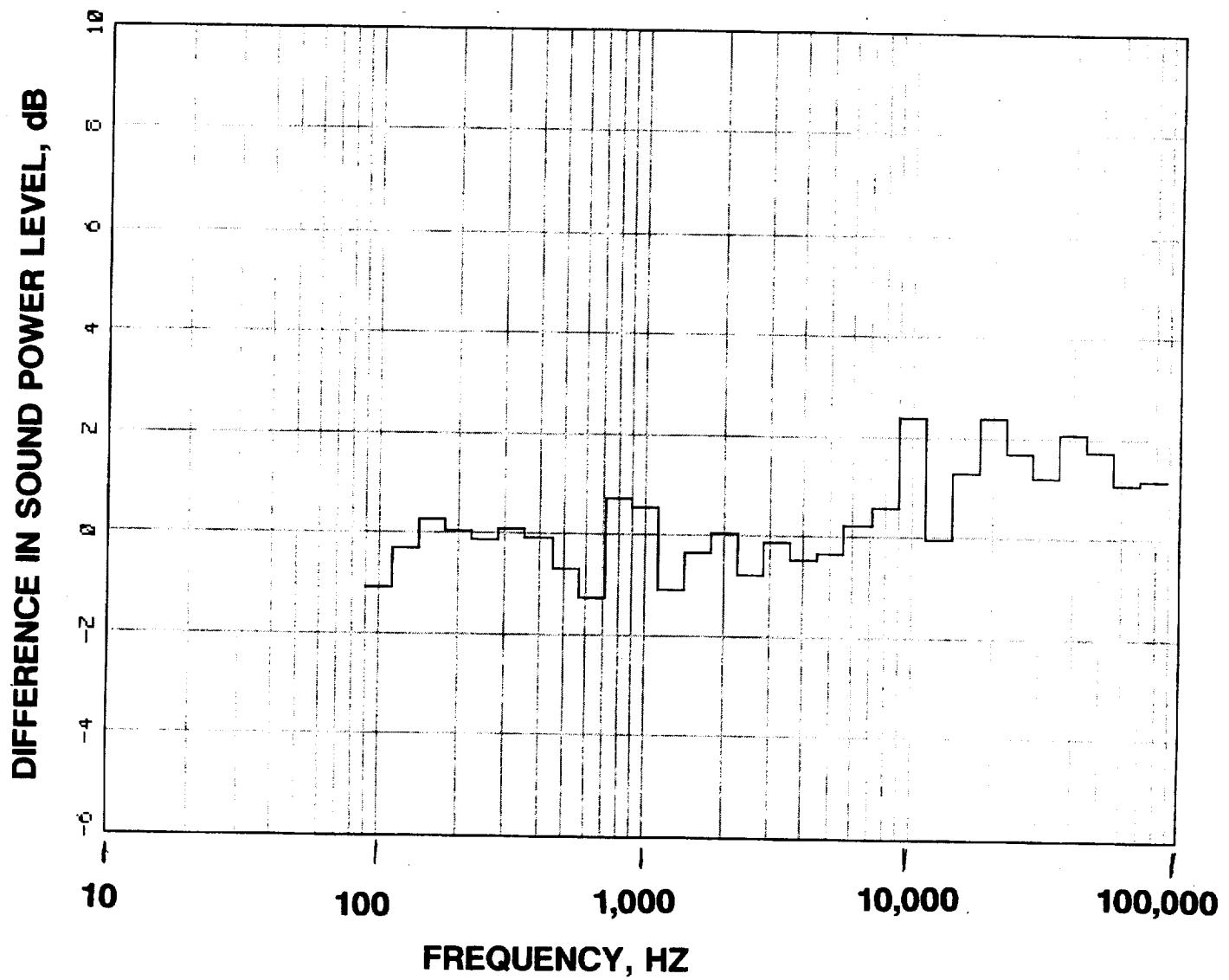


**FIGURE 47 CONTINUED**

**E 10137 RPMC**

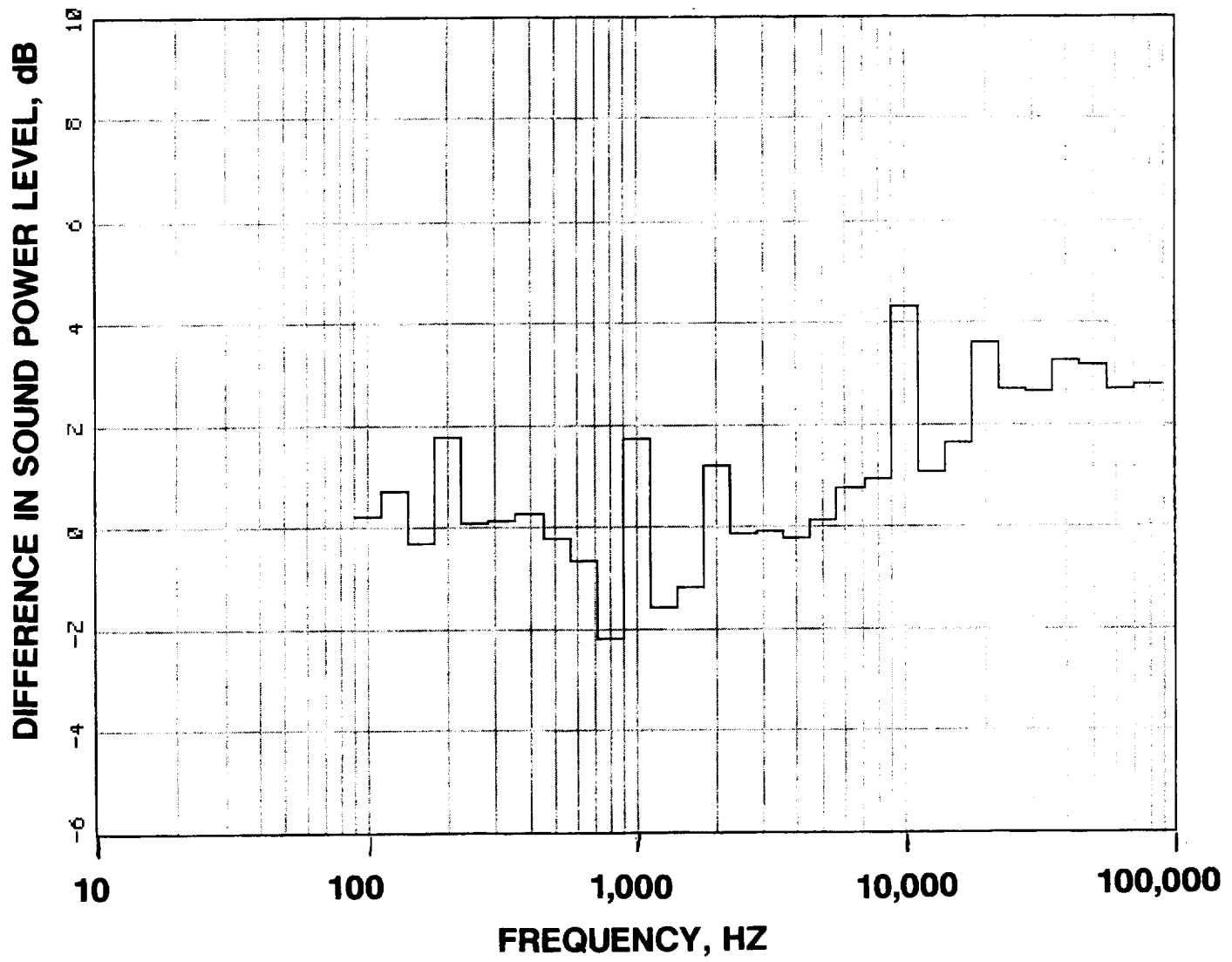


**FIGURE 47 CONCLUDED**

**F 10671 RPMC**

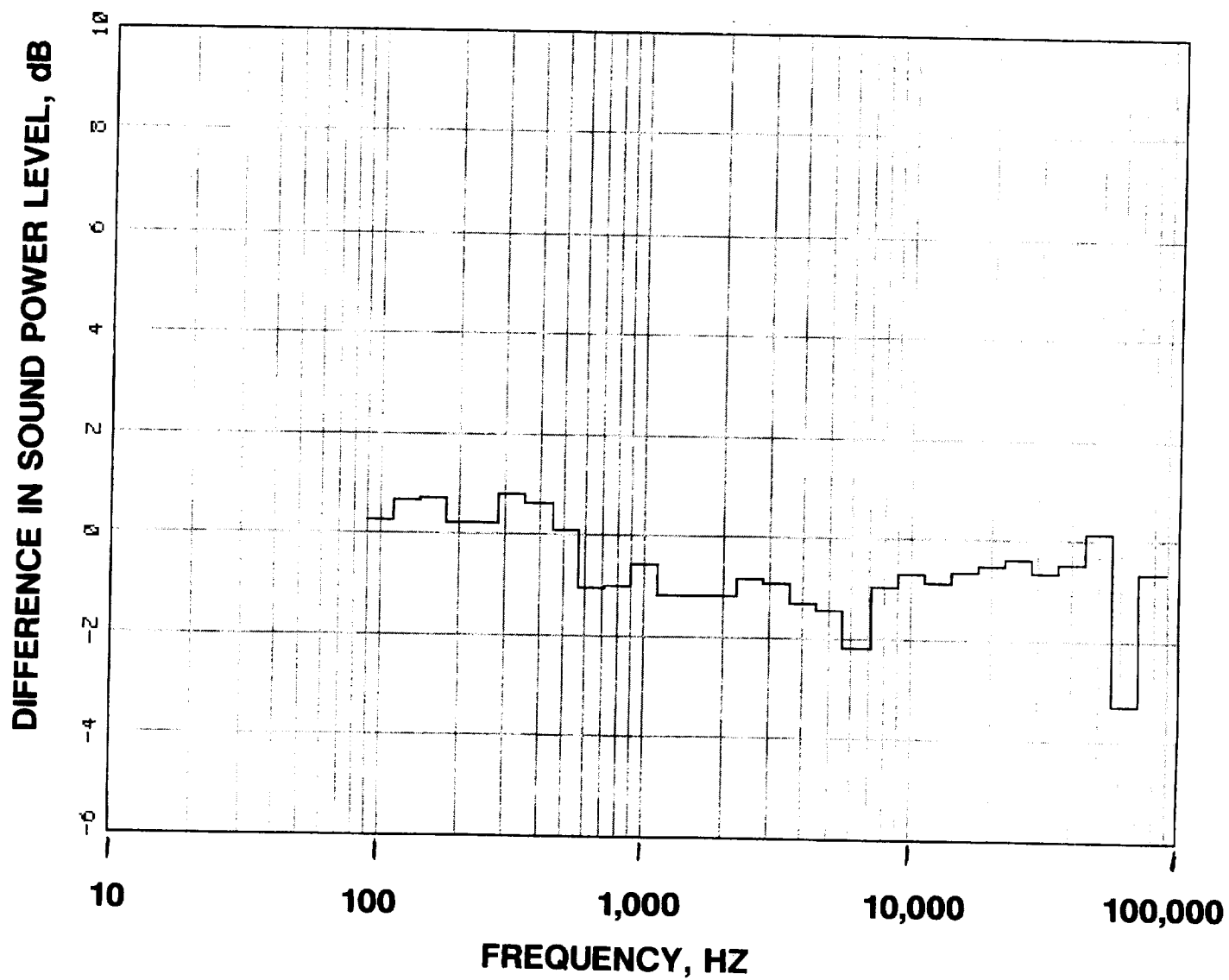


**FIGURE 48 DIFFERENCE IN FRONT SOUND POWER LEVEL,  
PARTIALLY TREATED MINUS FULLY TREATED, FOR THE 7 VANE  
CONFIGURATION**

A 6402 RPMC

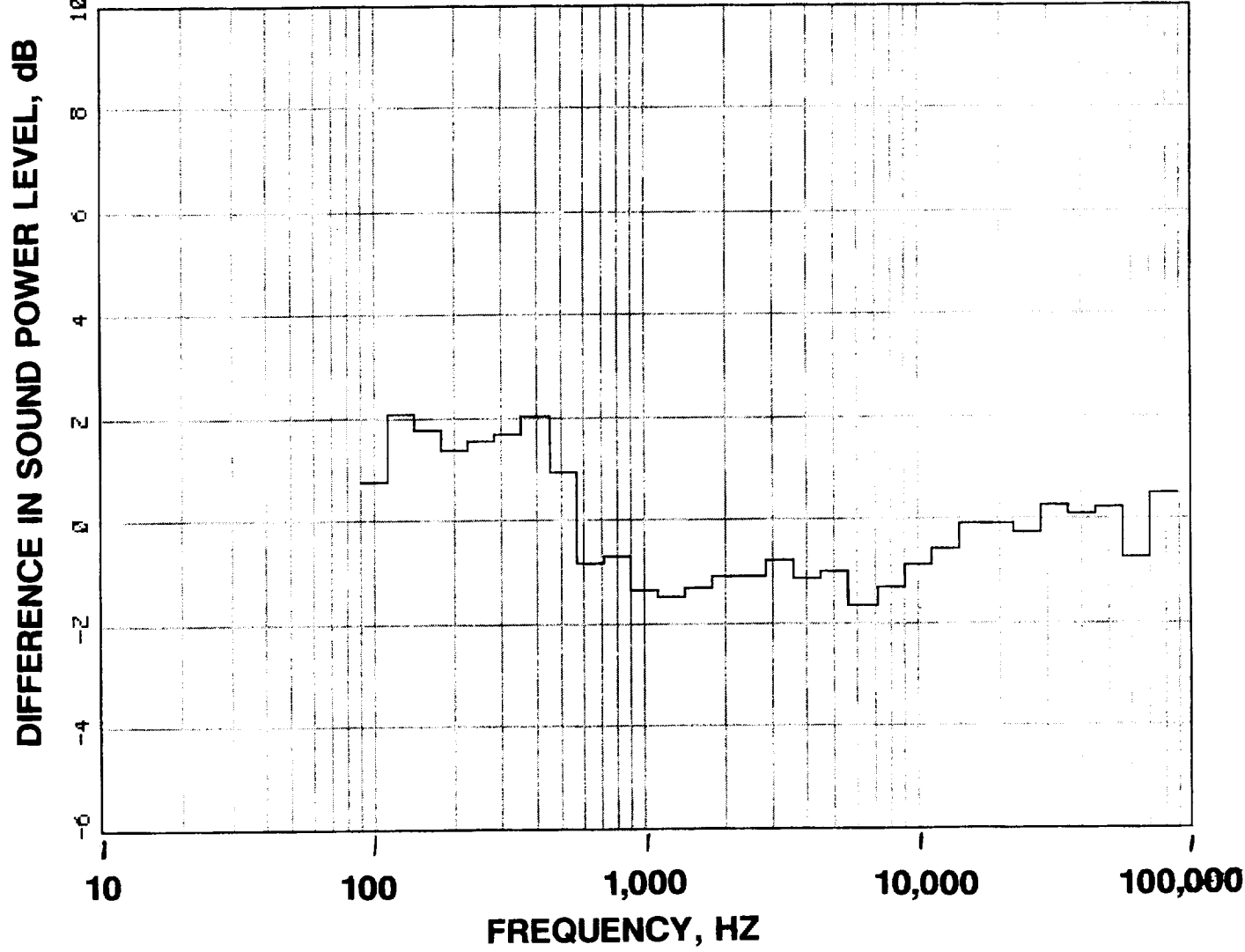


**FIGURE 48 CONTINUED**

**B 7736 RPMC**

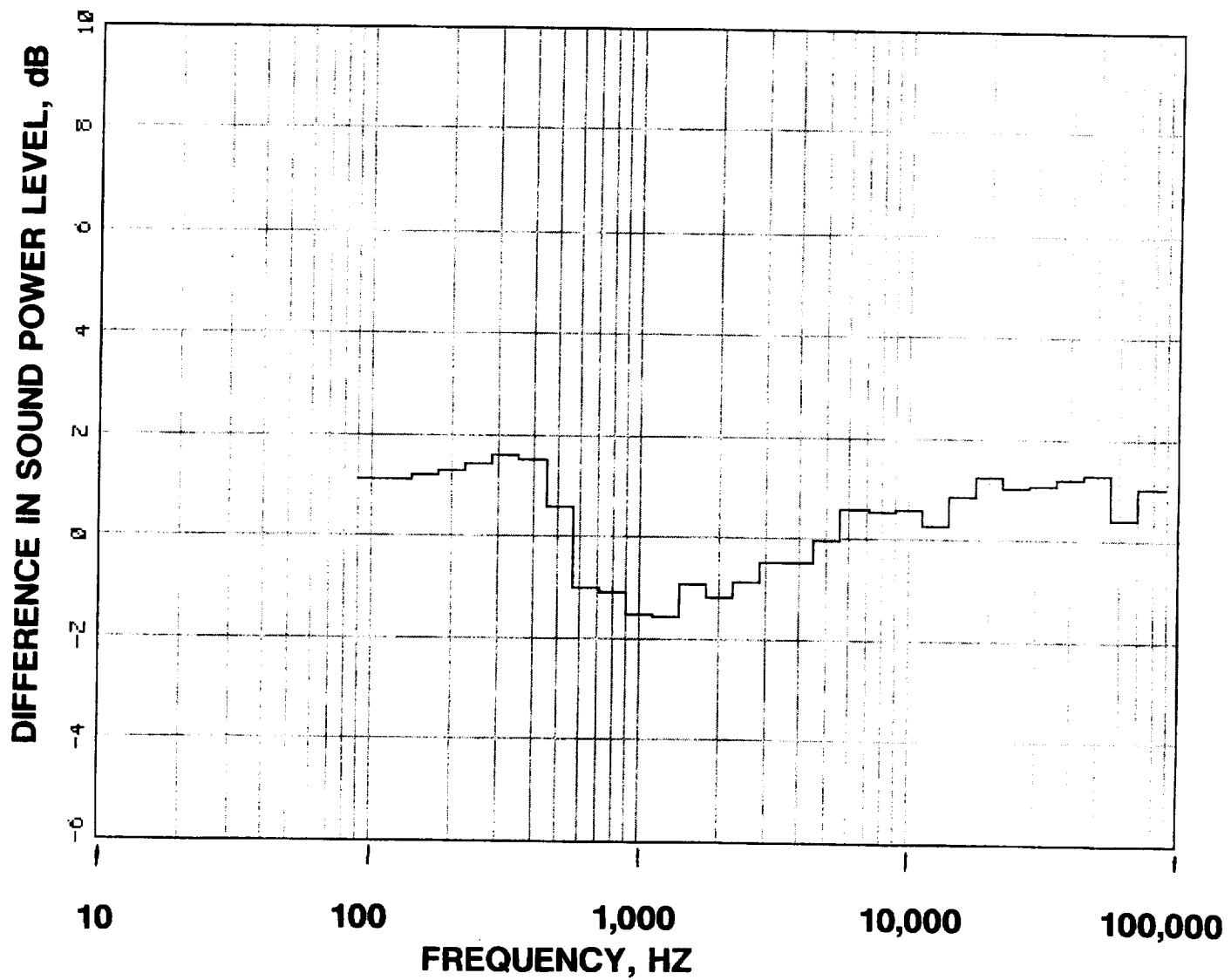


**FIGURE 48 CONTINUED**

**C 8537 RPMC**

DIFFERENCE IN SOUND POWER LEVEL, dB

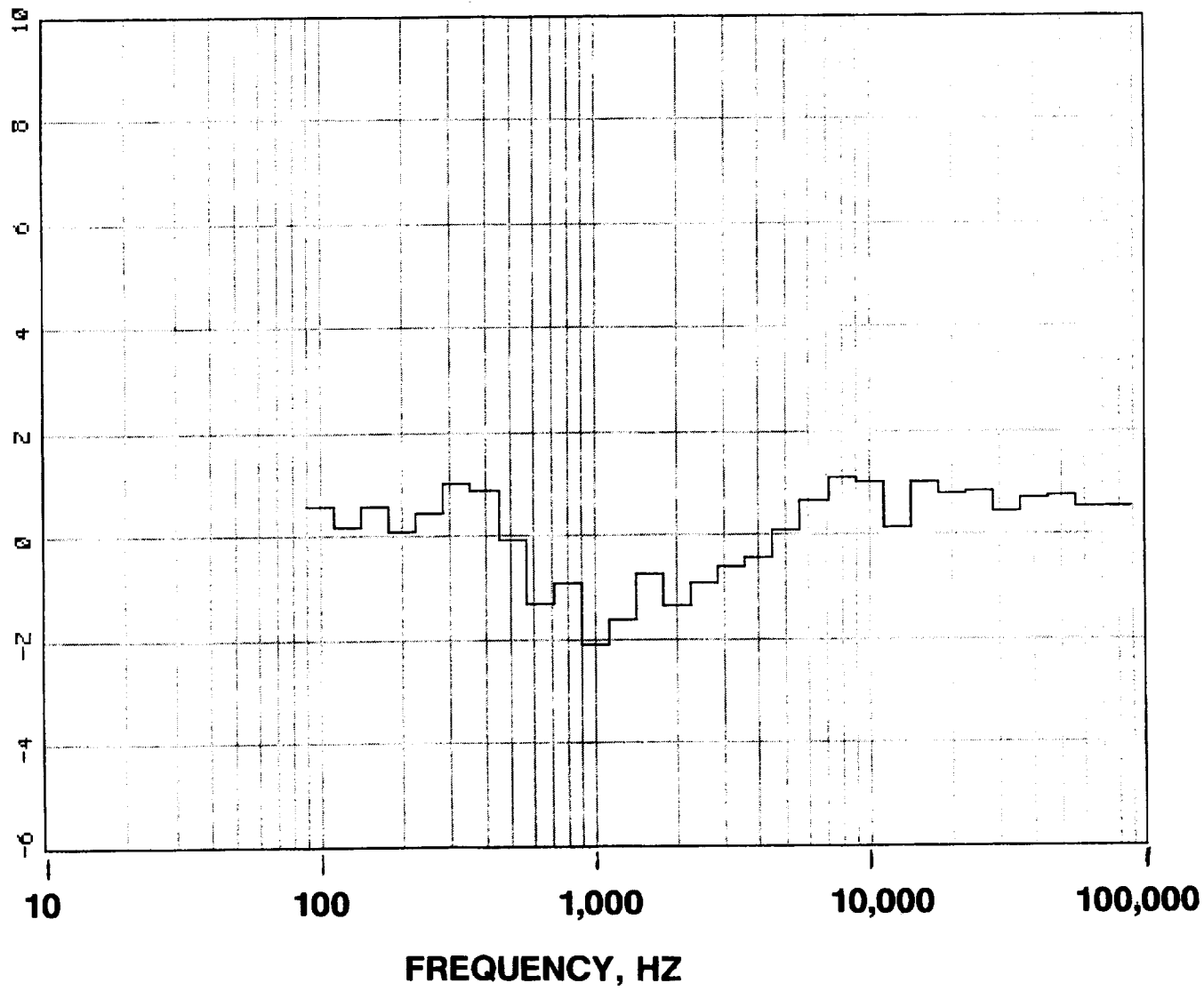


**FIGURE 48 CONTINUED**

**D 9604 RPMC**

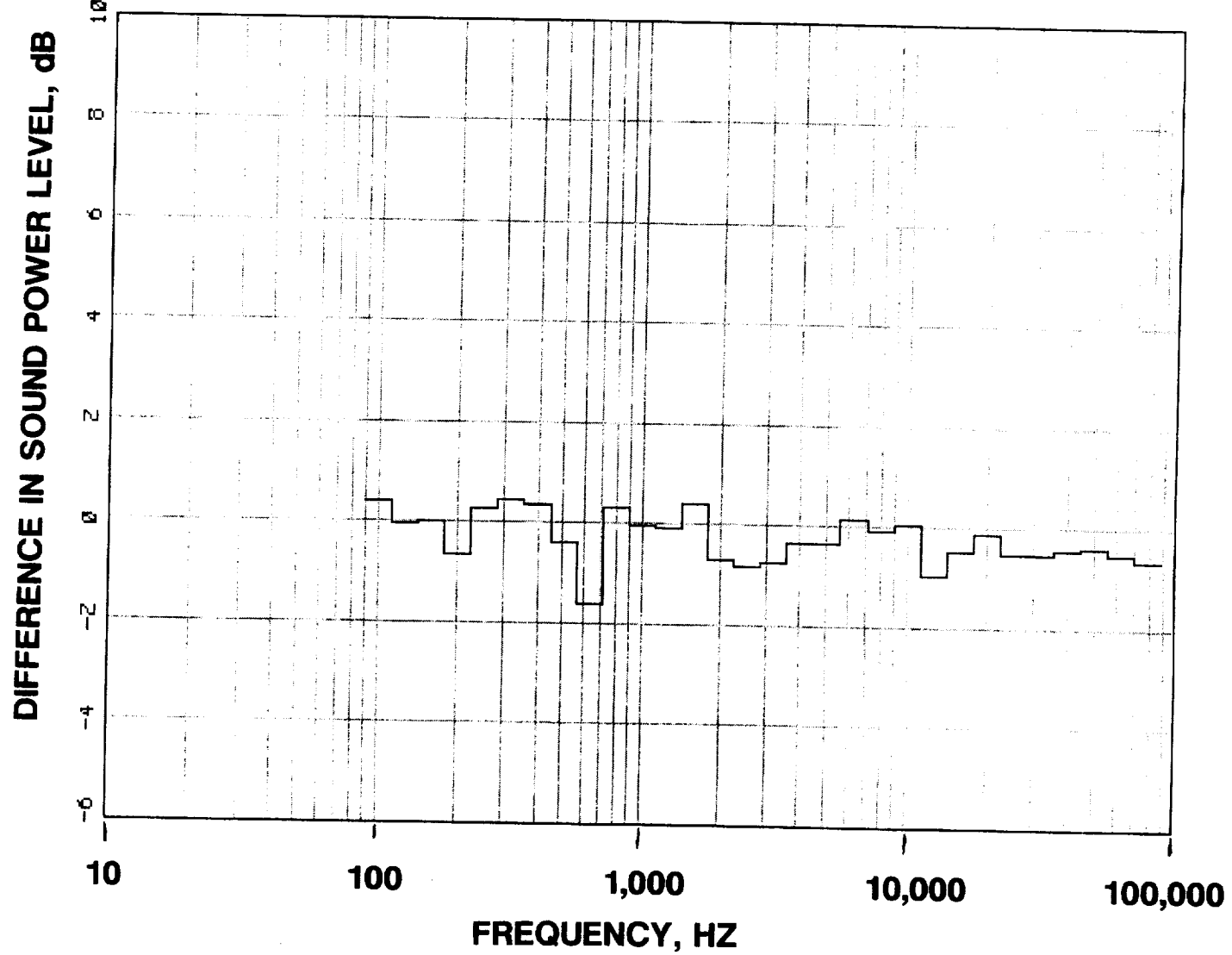


**FIGURE 48 CONTINUED**

**E 10137 RPMC**

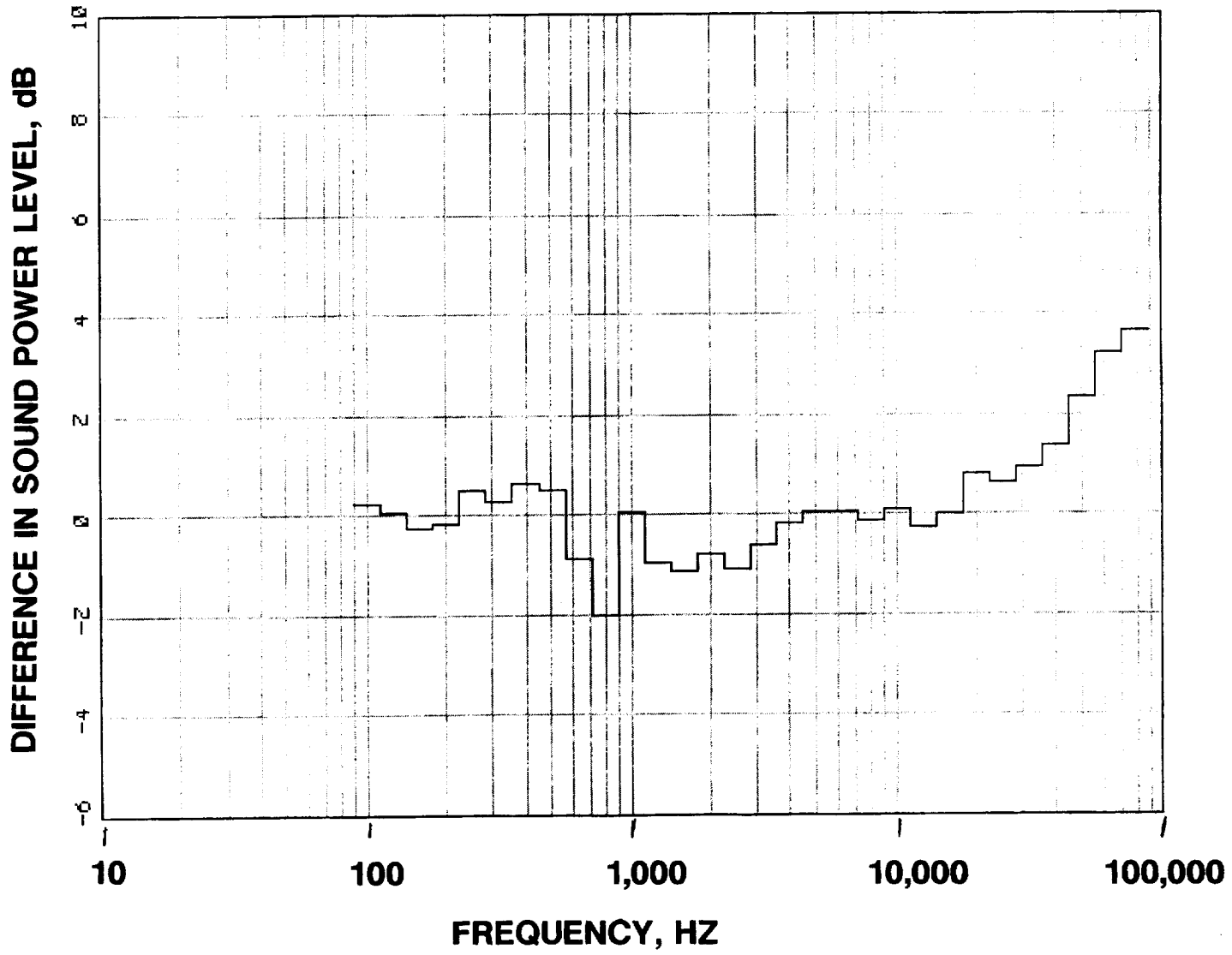


**FIGURE 48 CONCLUDED**

**F 10671 RPMC**

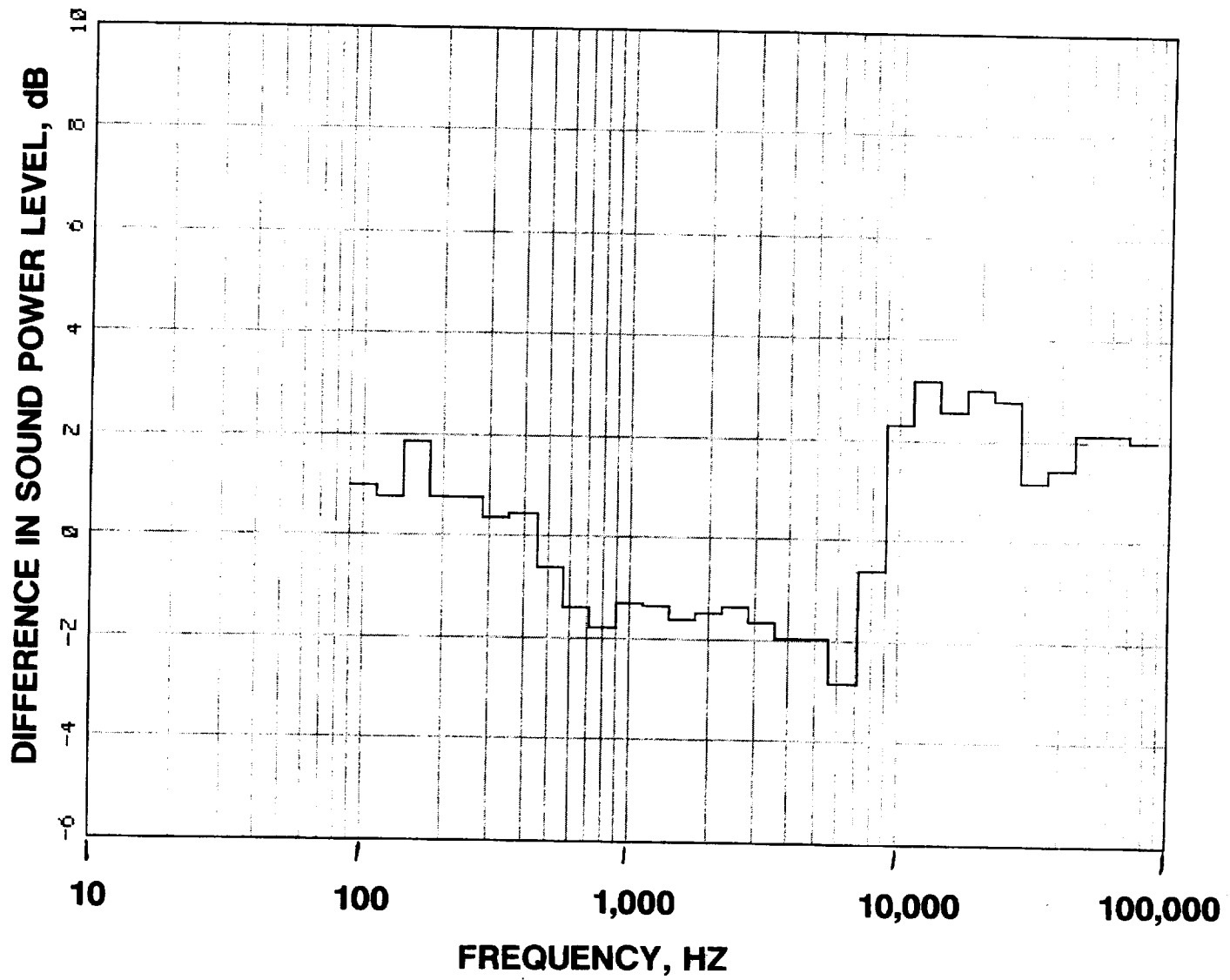


**FIGURE 49 DIFFERENCE IN AFT SOUND POWER LEVEL,  
PARTIALLY TREATED MINUS FULLY TREATED, FOR THE 7 VANE  
CONFIGURATION**

**A 6402 RPMC**

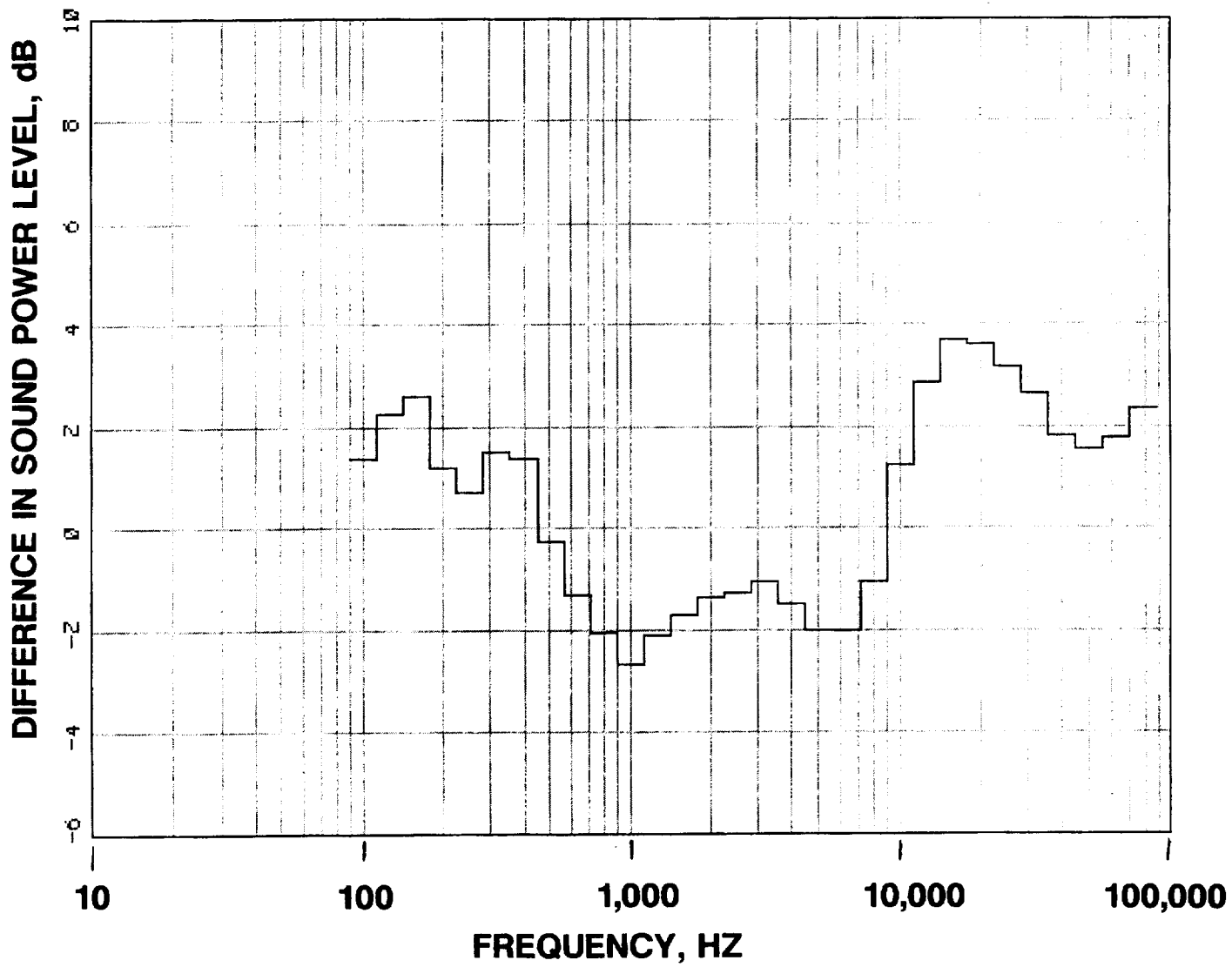


**FIGURE 49 CONTINUED**

**B 7736 RPMC**

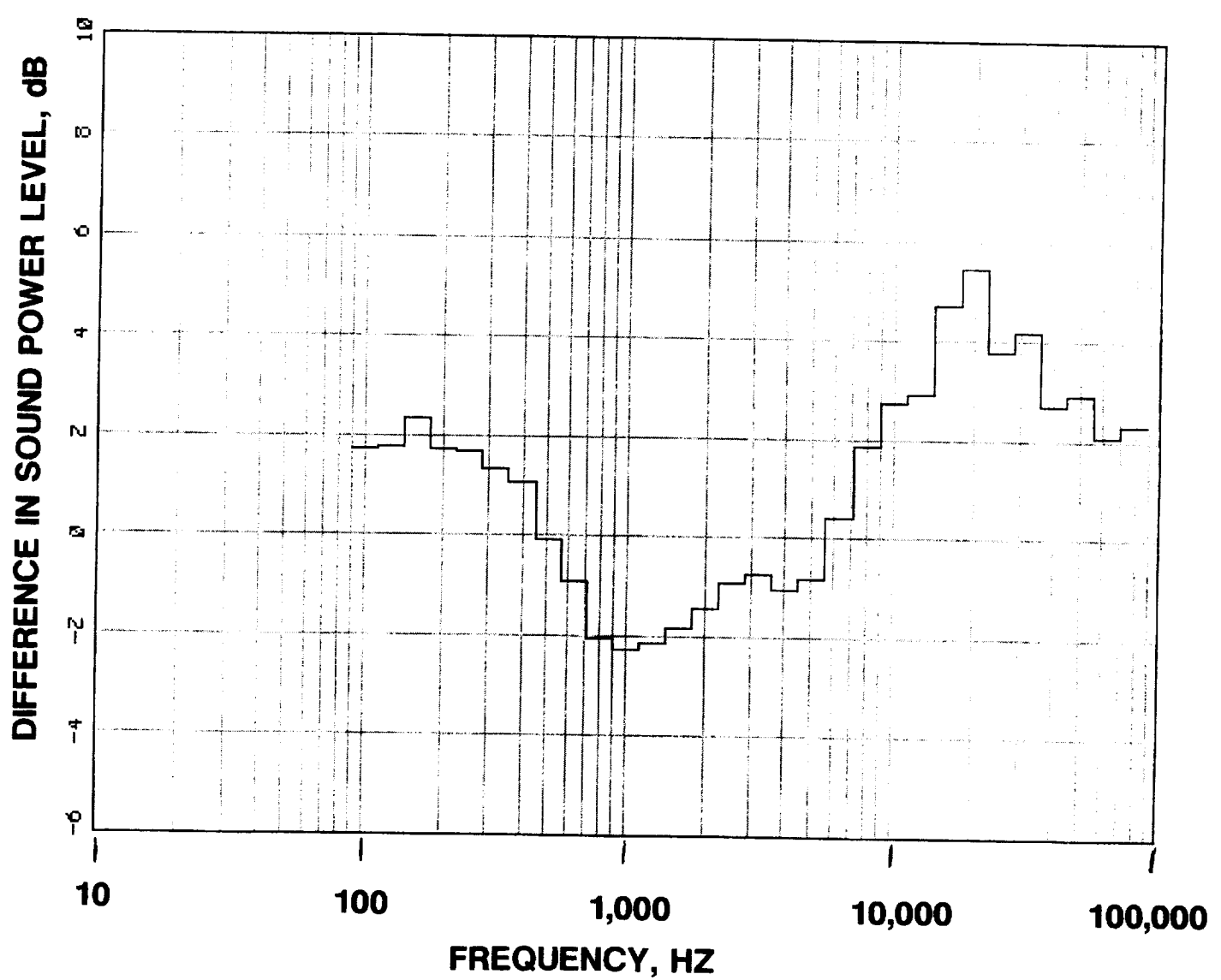


**FIGURE 49 CONTINUED**

**C 8537 RPMC**

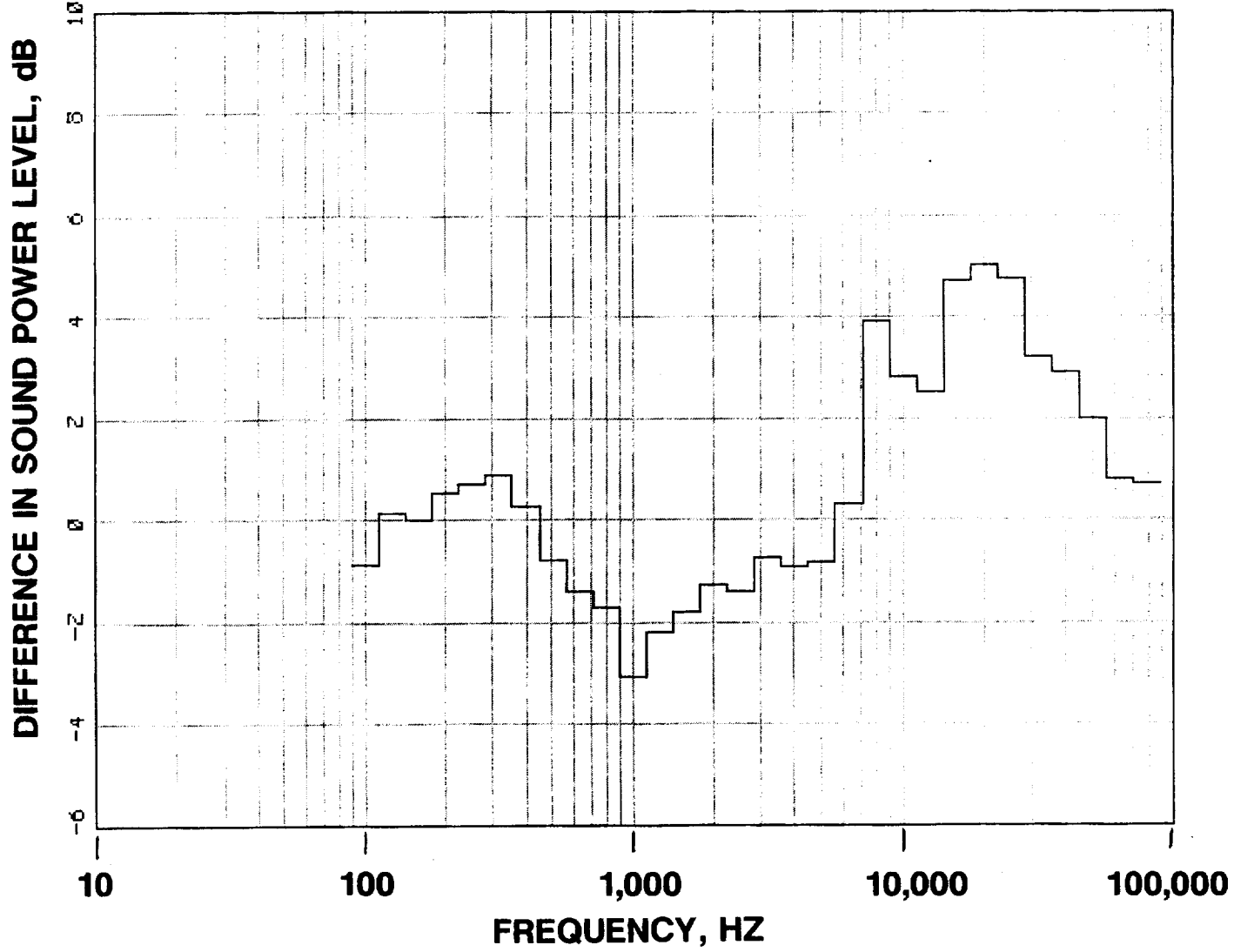


**FIGURE 49 CONTINUED**

**D 9604 RPMC**

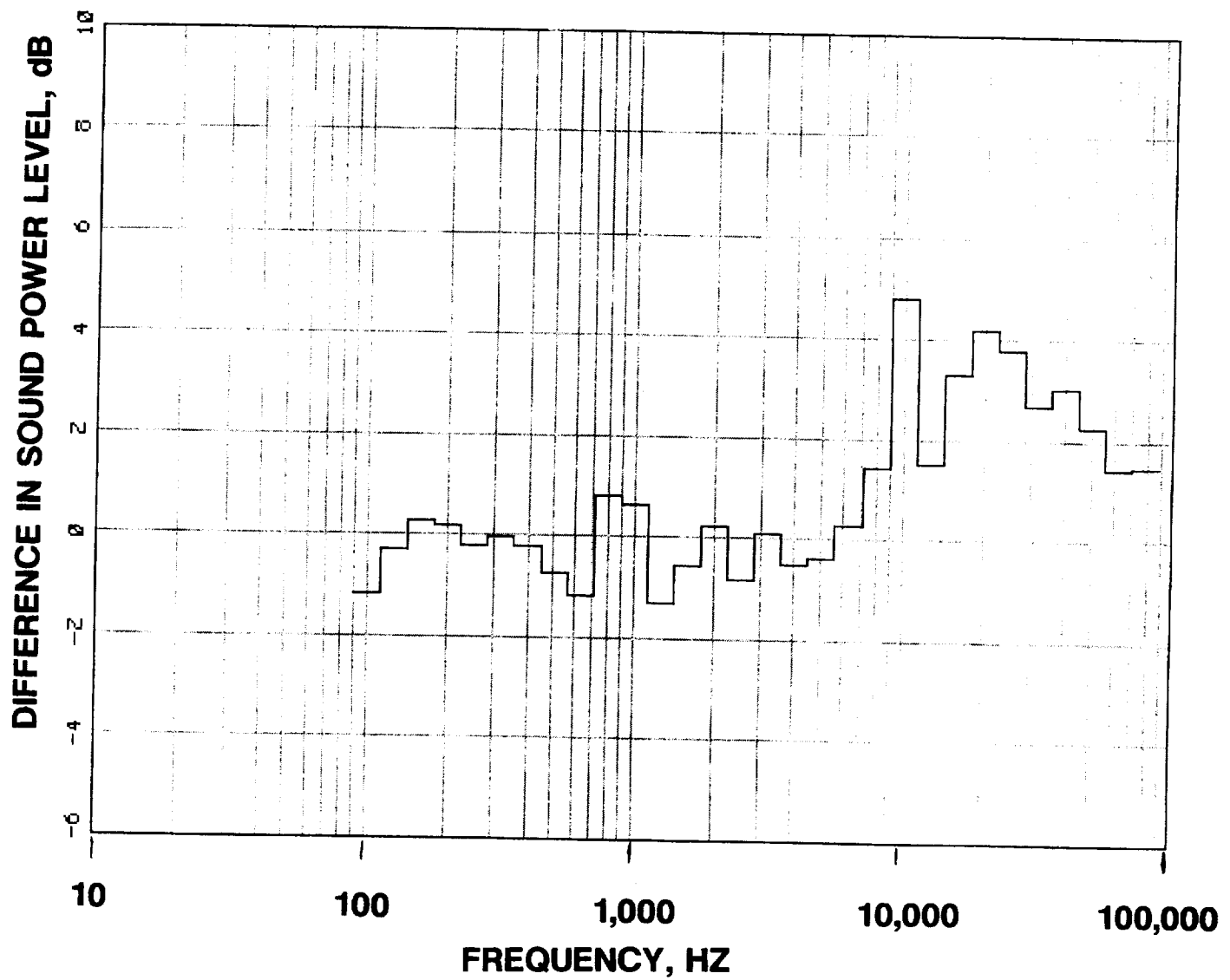


**FIGURE 49 CONTINUED**

**E 10137 RPMC**

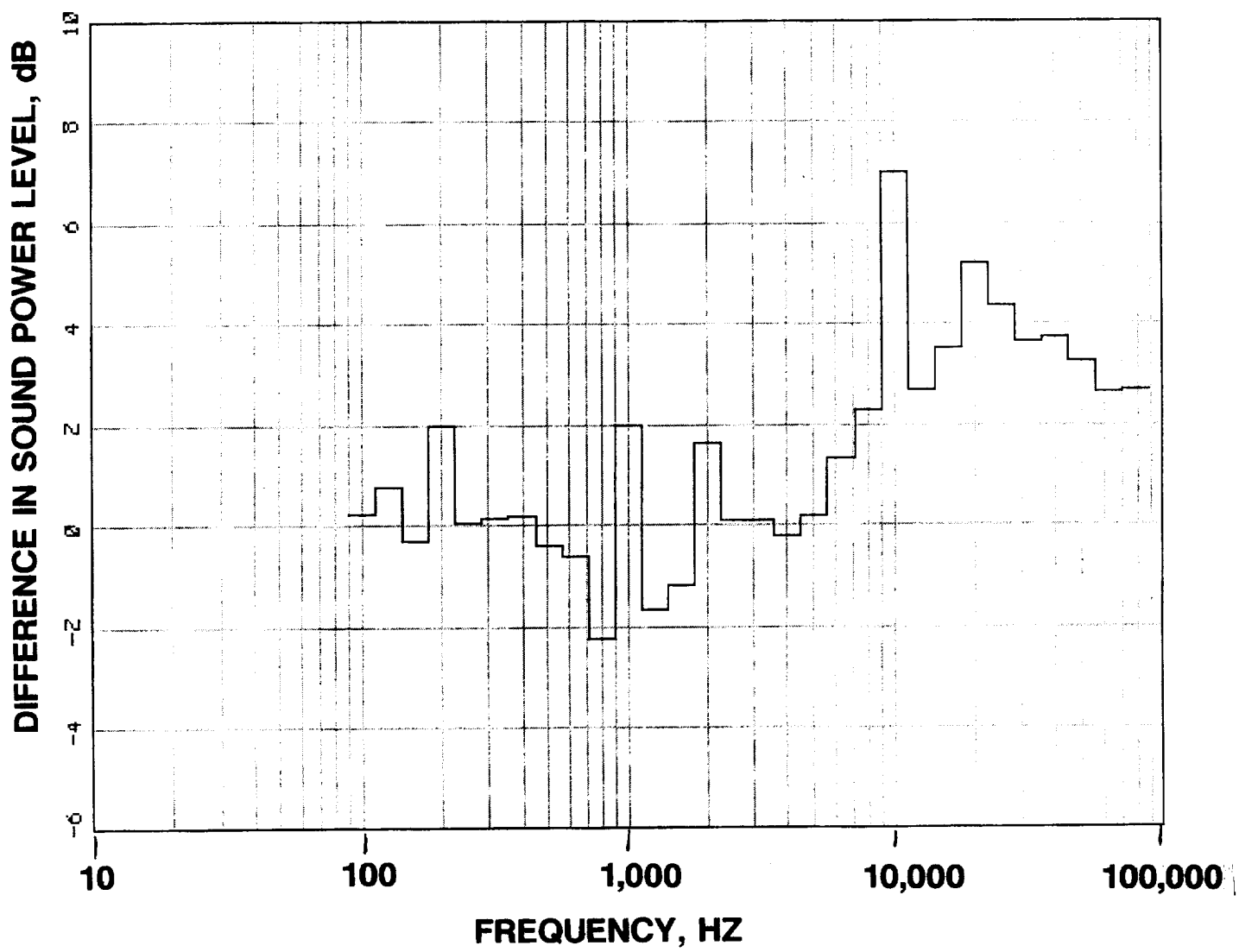


**FIGURE 49 CONCLUDED**

**F 10671 RPC**

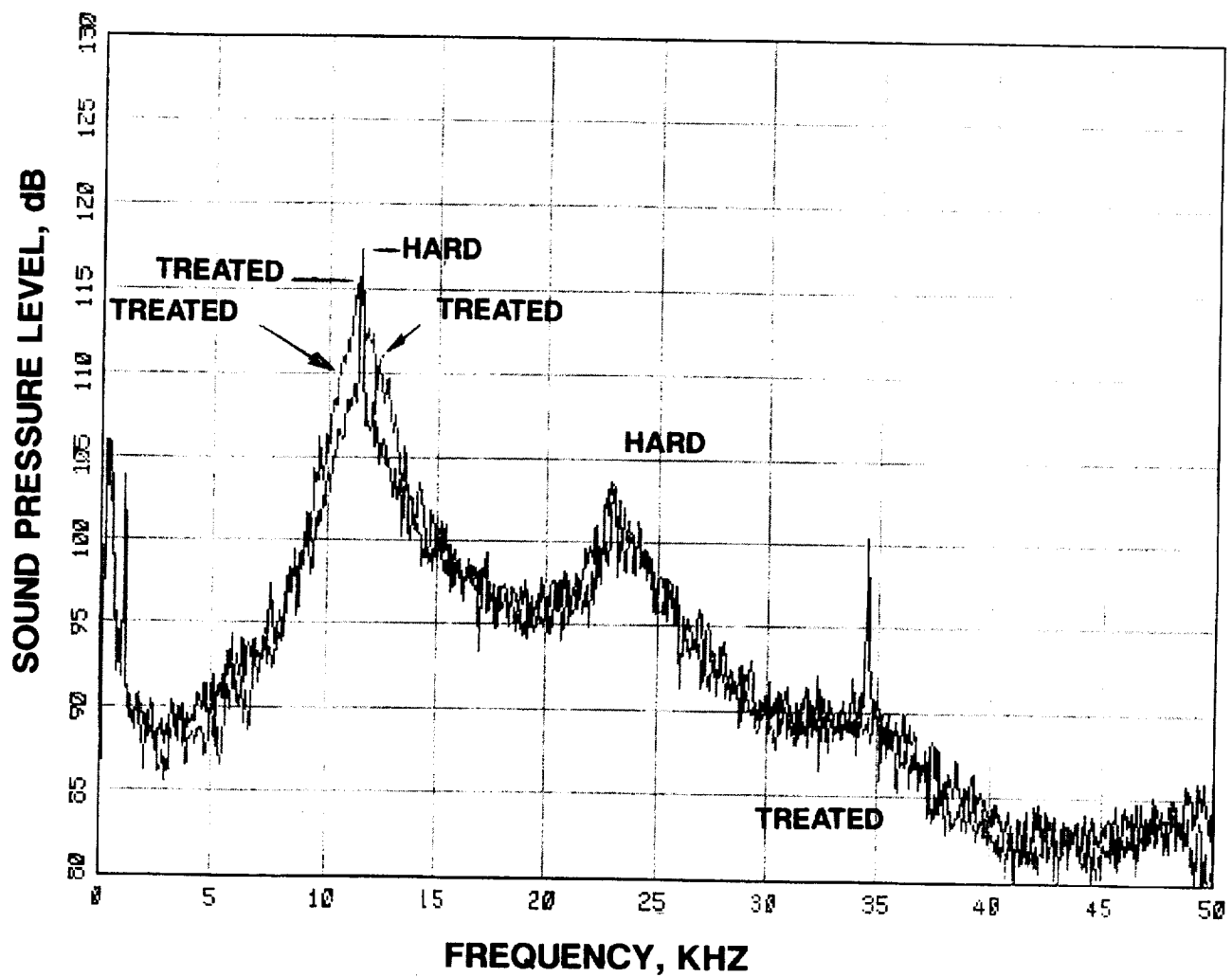


**FIGURE 50 SPECTRAL COMPARISON OF HARD AND FULLY  
TREATED DATA FOR THE 70 VANE CONFIGURATION AT 6402 RPMC**

**A 24.5 DEGREES**

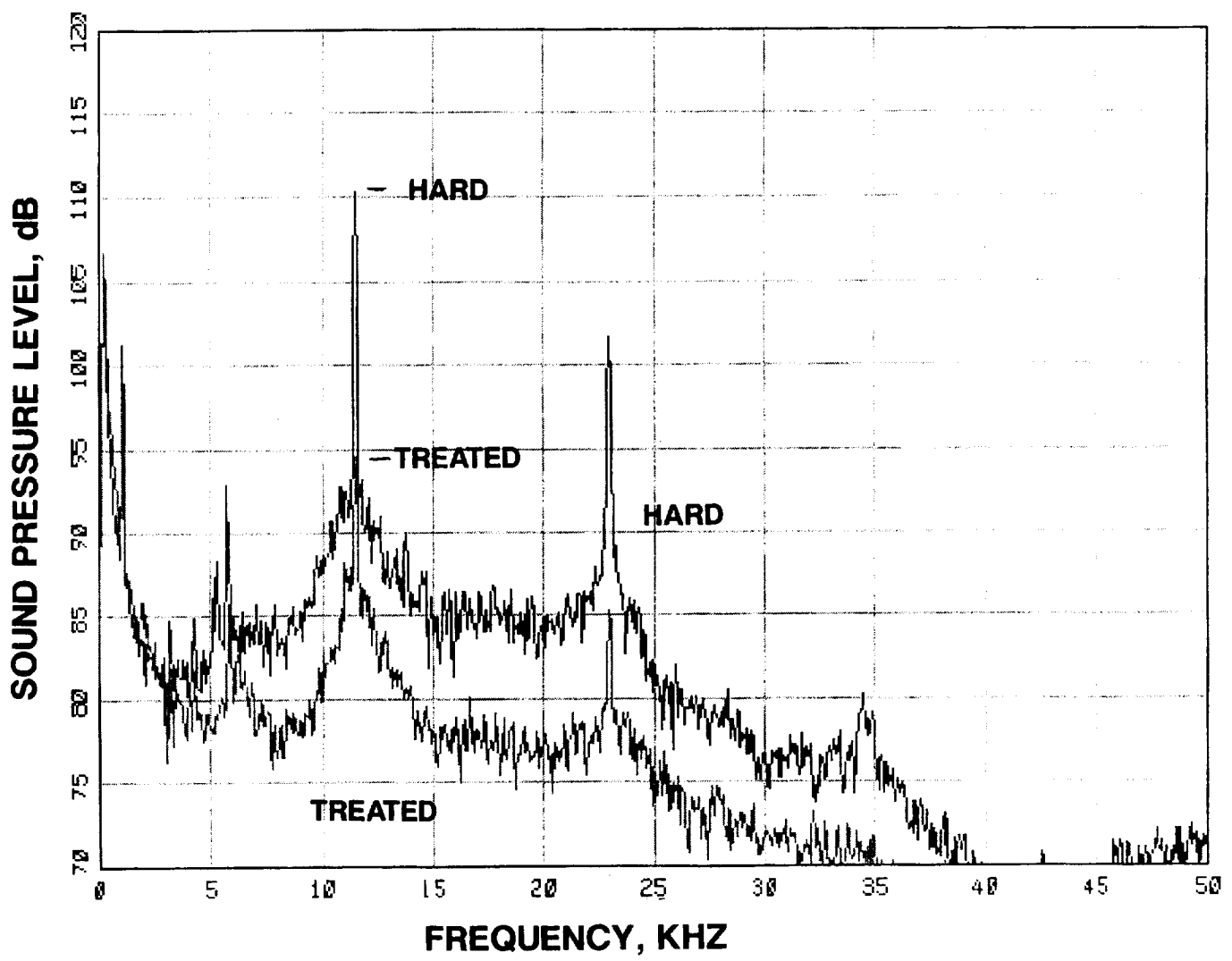


**FIGURE 50 CONTINUED**

**B 92.5 DEGREES**

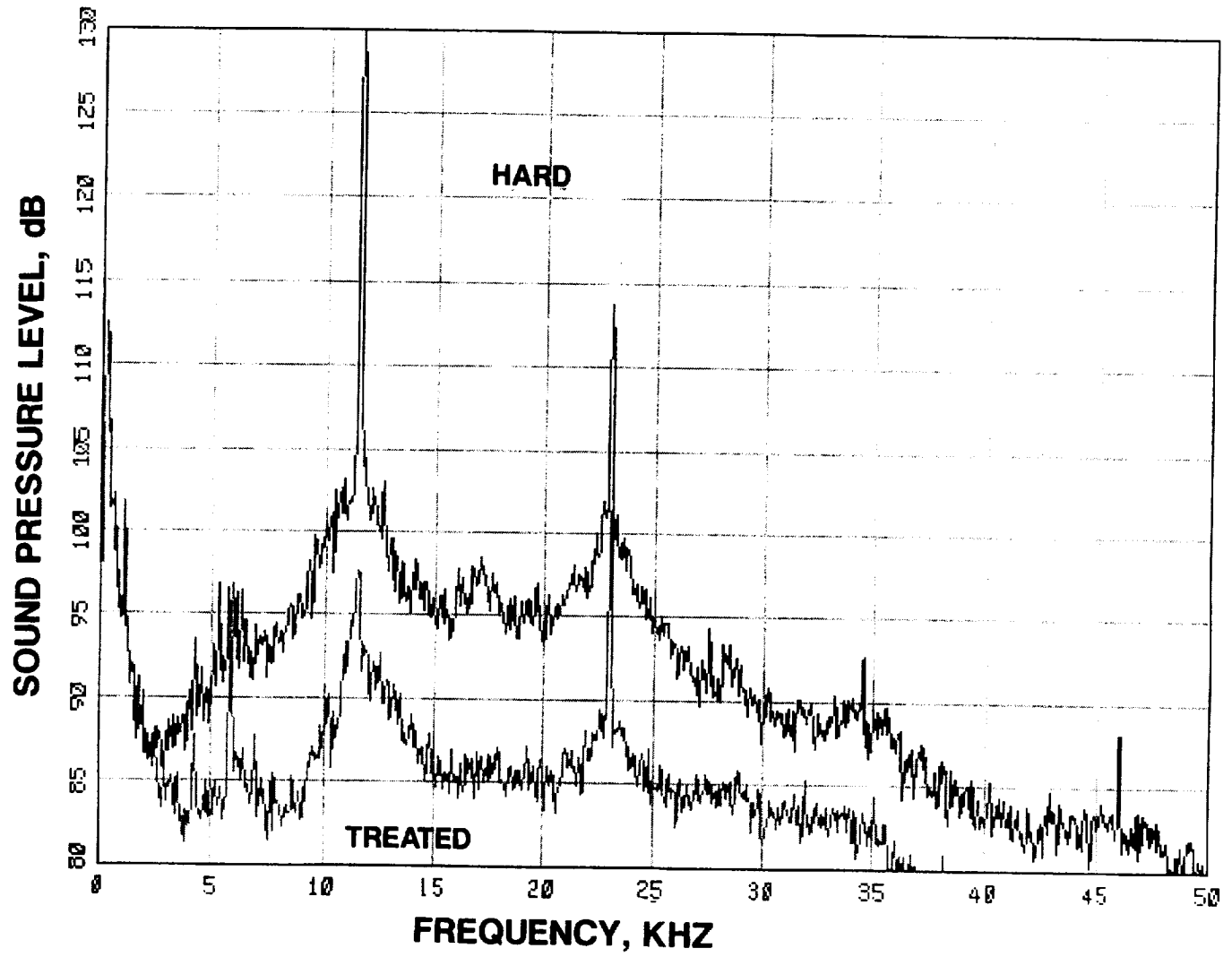


**FIGURE 50 CONCLUDED**

**C 130.5 DEGREES**

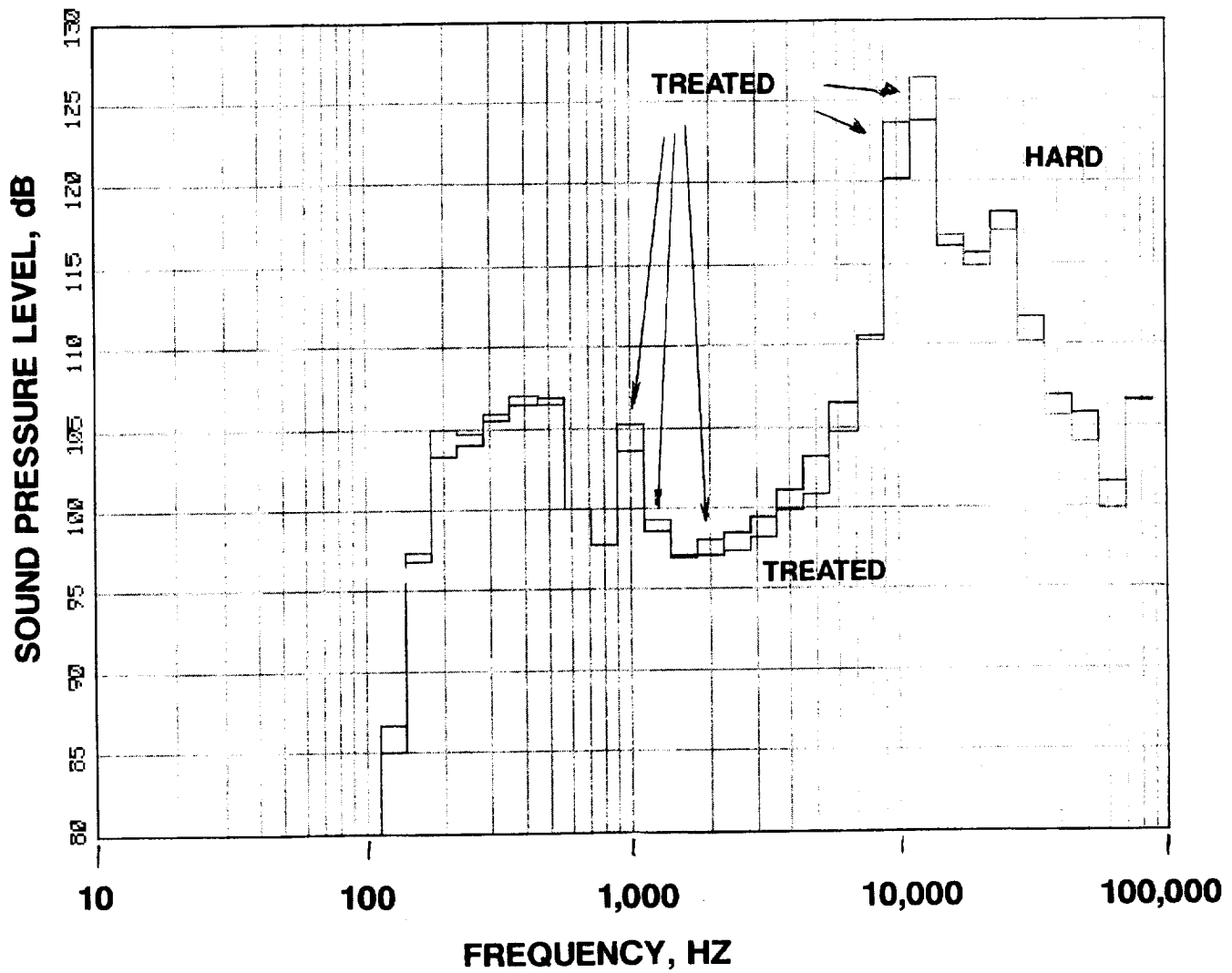


**FIGURE 51 1/3RD OCTAVE COMPARISON OF HARD AND FULLY  
TREATED DATA FOR THE 70 VANE CONFIGURATION AT 6402 RPMC  
A 24.5 DEGREES**

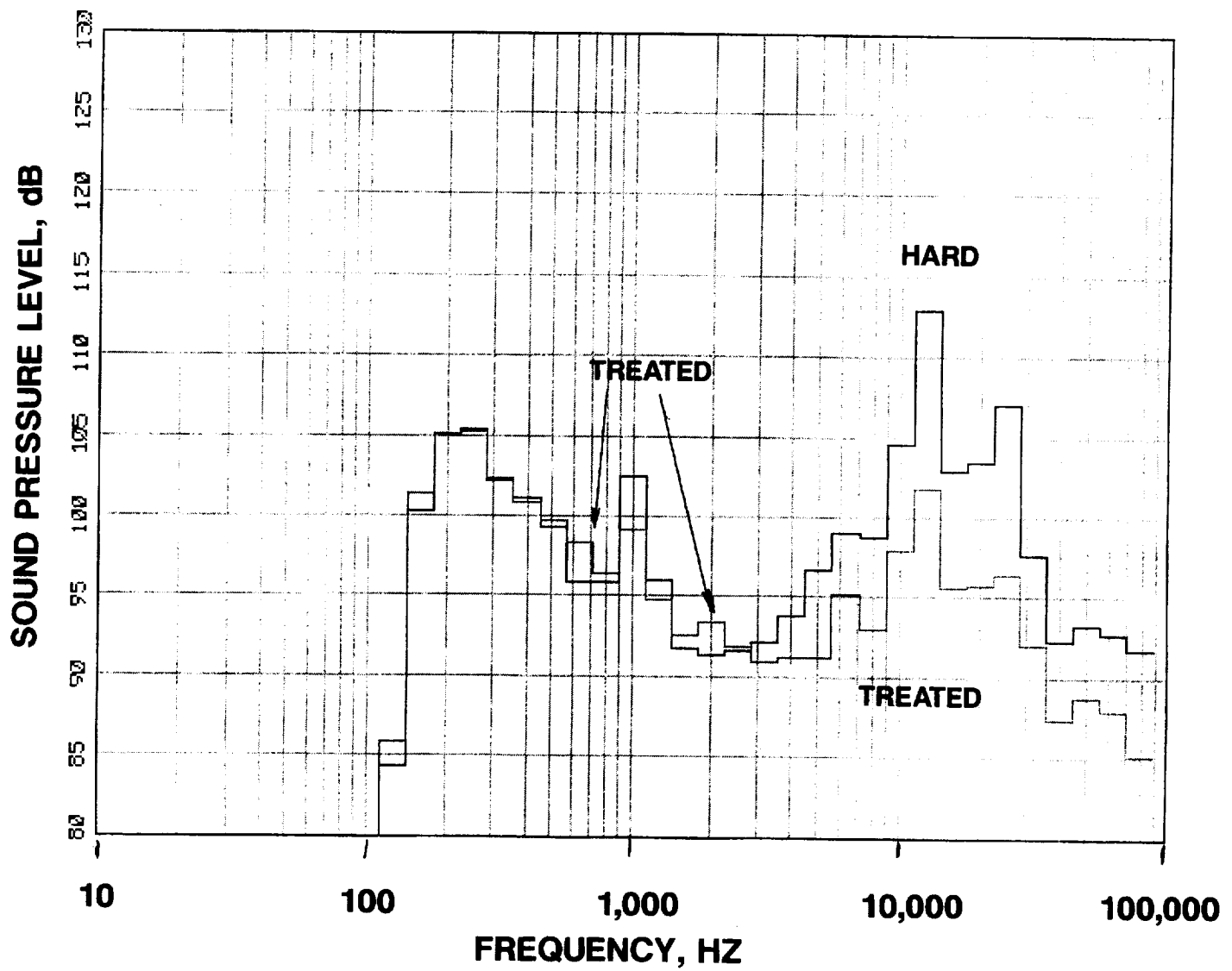


**FIGURE 51 CONTINUED**

**B 92.5 DEGREES**

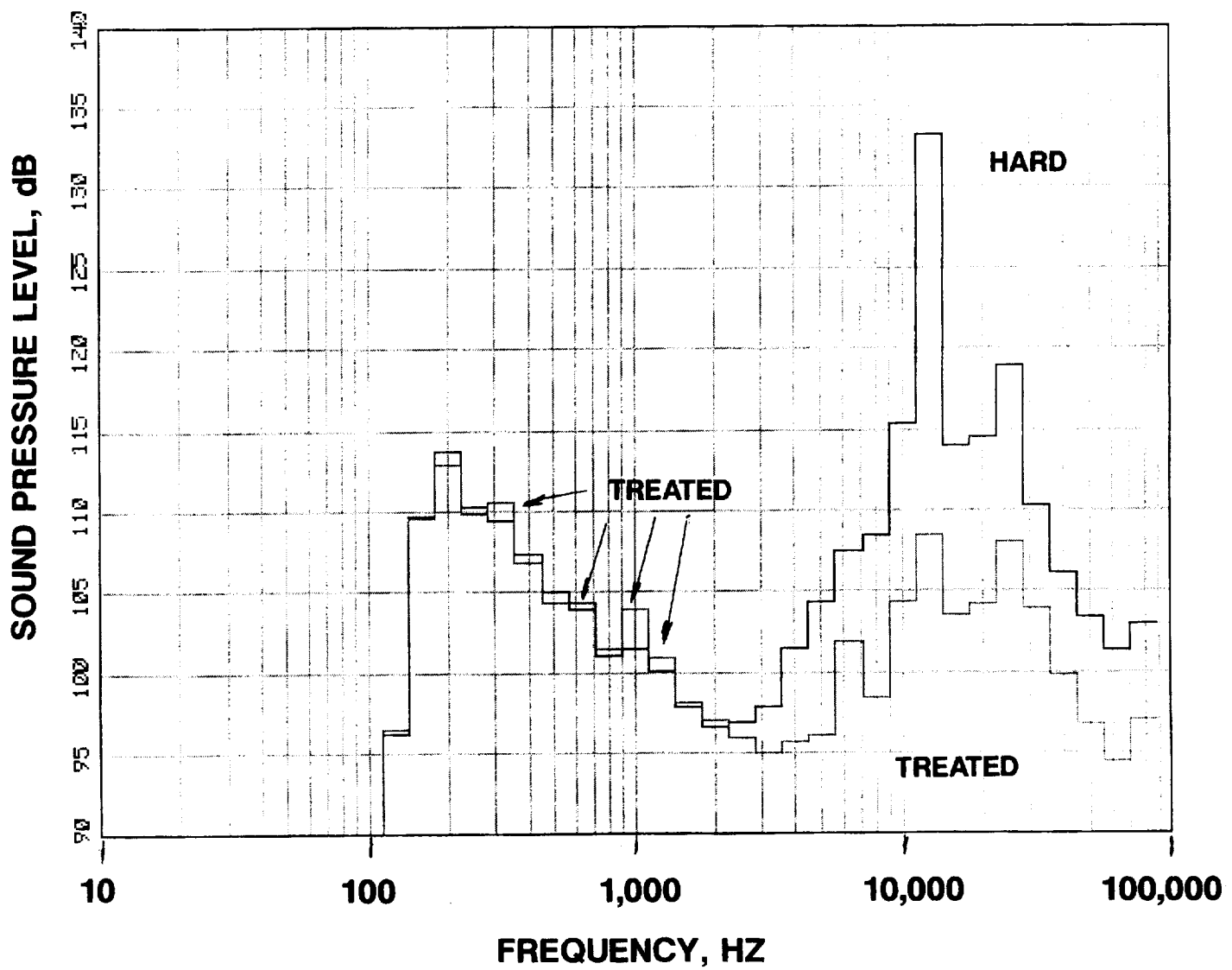


**FIGURE 51 CONCLUDED**

**C 130.5 DEGREES**

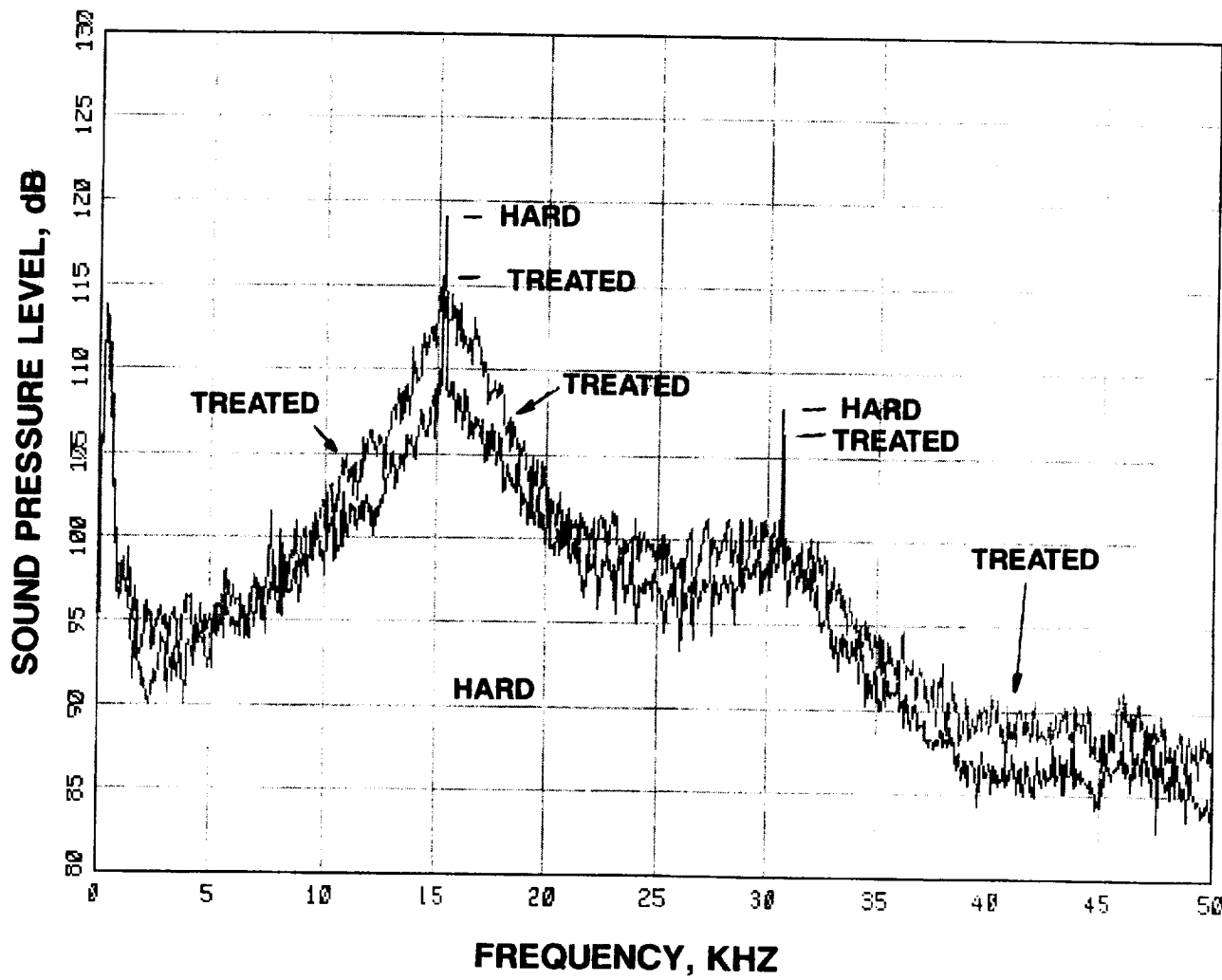


**FIGURE 52 SPECTRAL COMPARISON OF HARD AND FULLY  
TREATED DATA FOR THE 70 VANE CONFIGURATION AT 8537 RPMC**

**A 24.5 DEGREES**

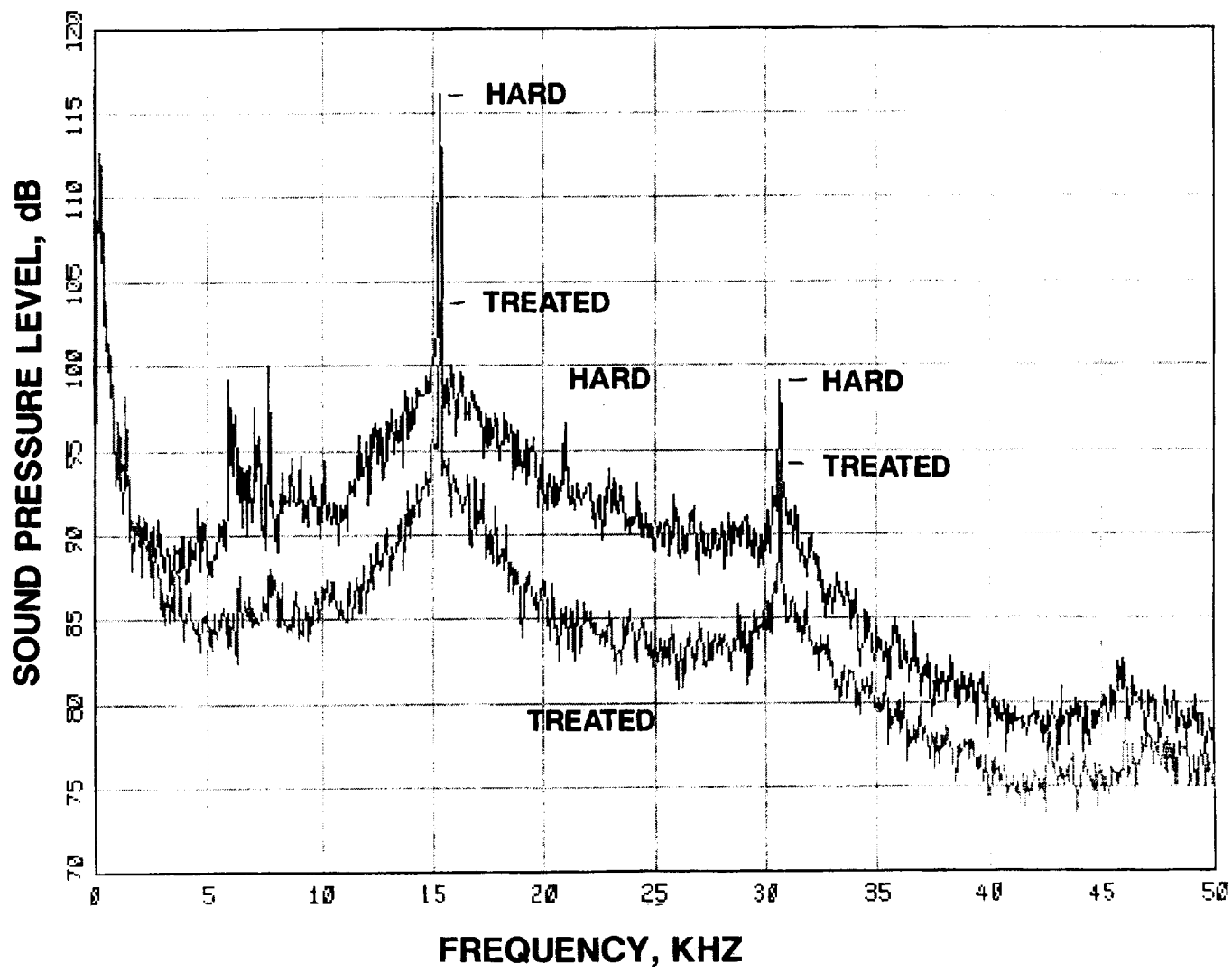


**FIGURE 52 CONTINUED**

**B 92.5 DEGREES**

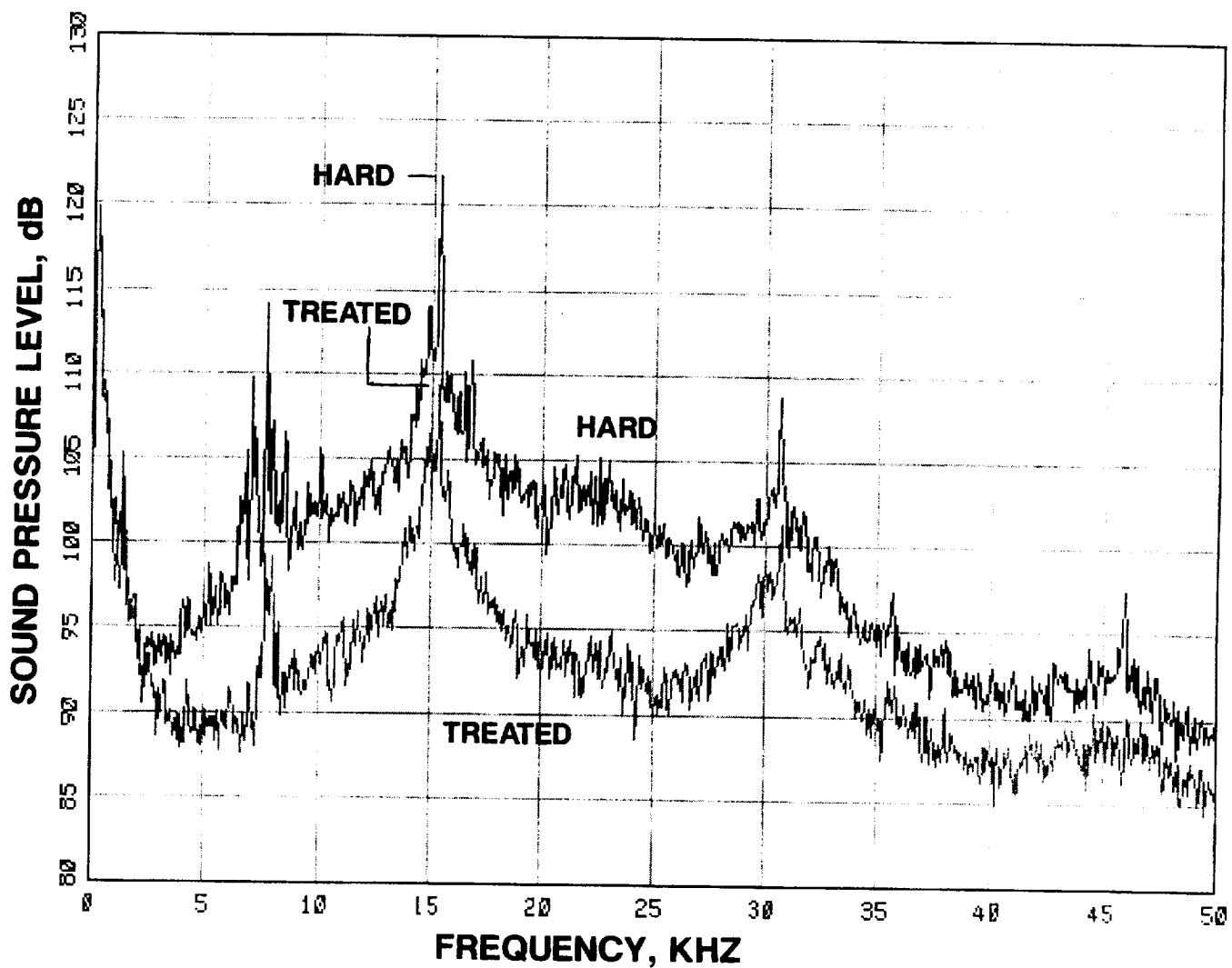


**FIGURE 52 CONCLUDED**

**C 130.5 DEGREES**

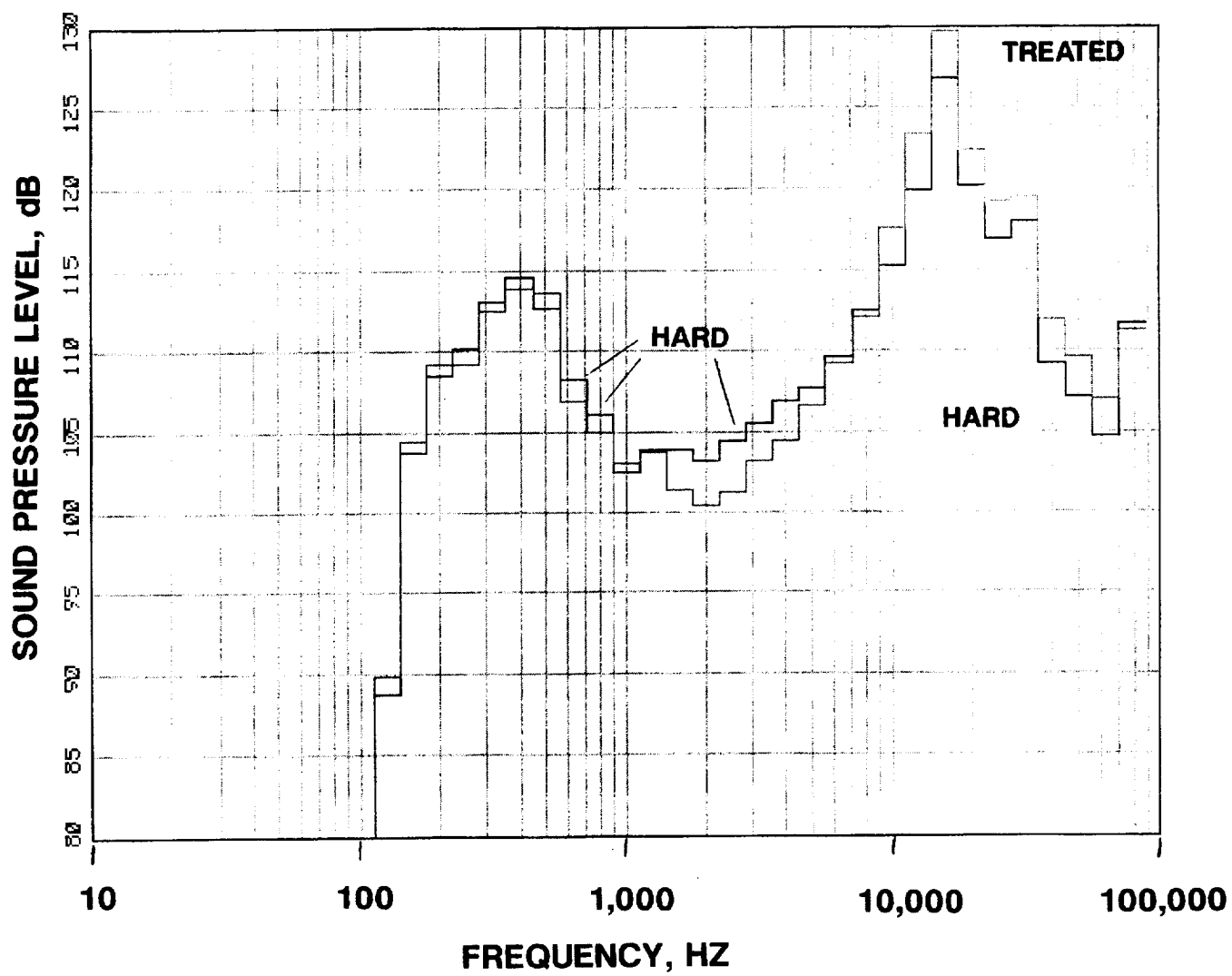


**FIGURE 53 1/3RD OCTAVE COMPARISON OF HARD AND FULLY  
TREATED DATA FOR THE 70 VANE CONFIGURATION AT 8537 RPMC  
A 24.5 DEGREES**

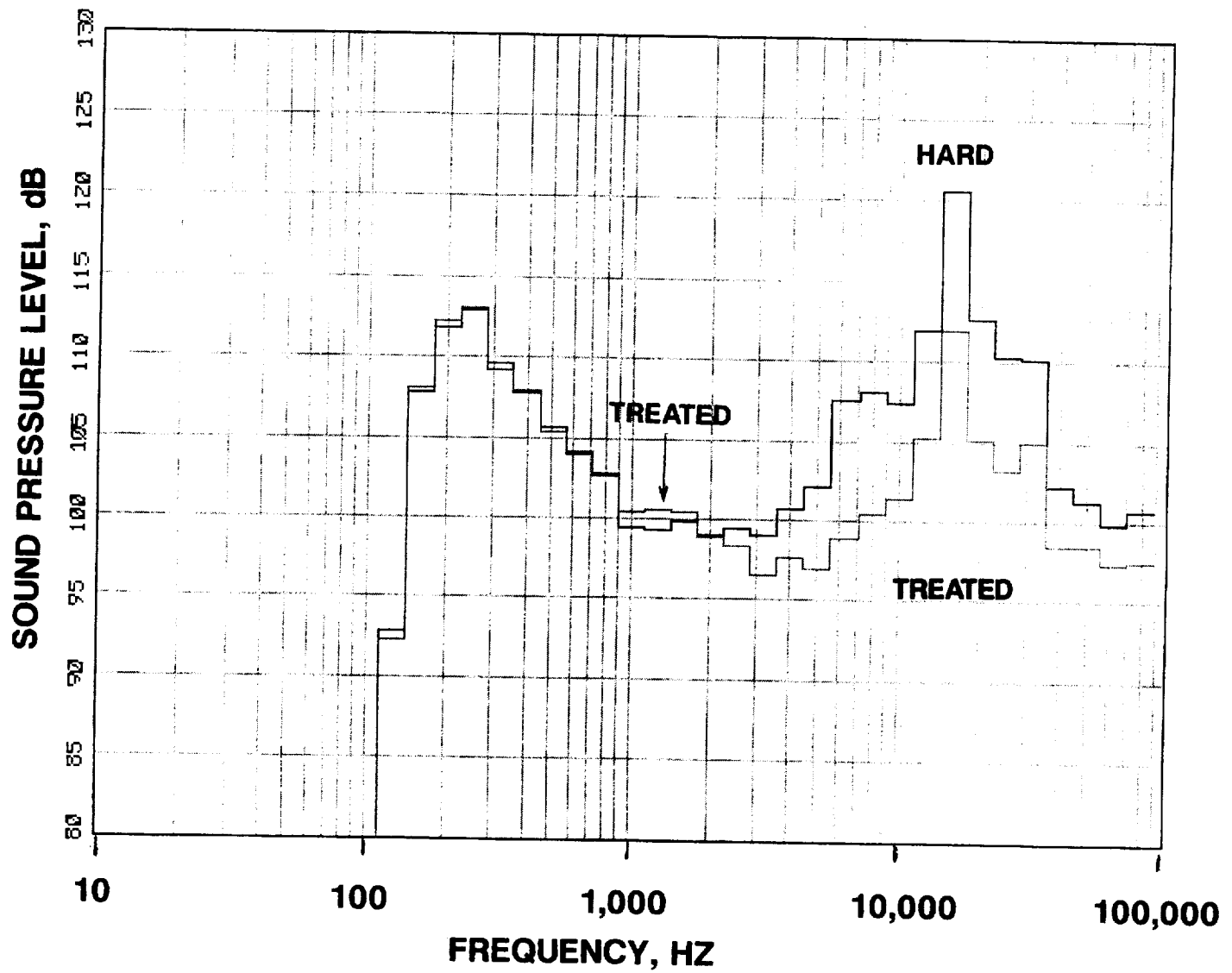


**FIGURE 53 CONTINUED**

**B 92.5 DEGREES**

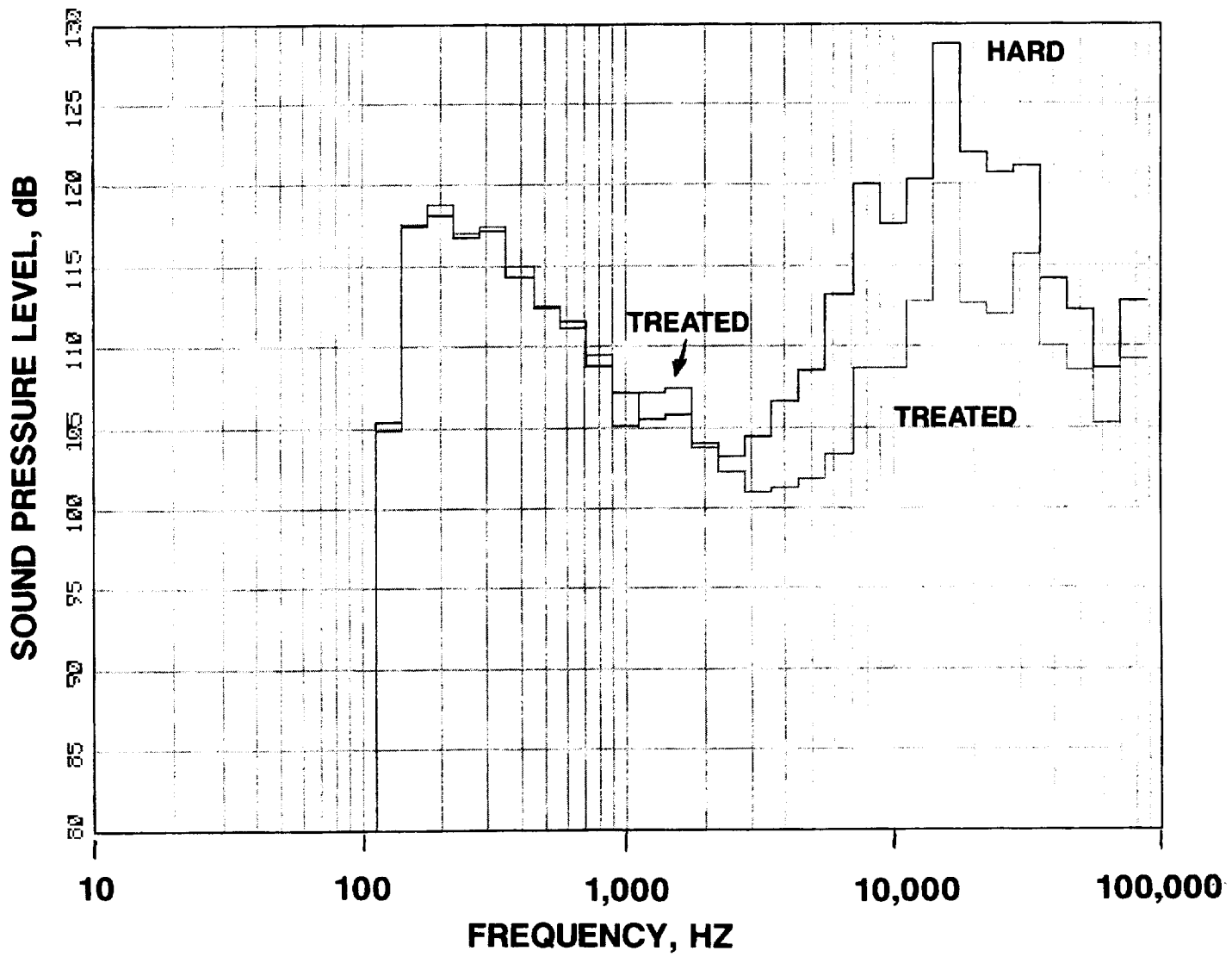


**FIGURE 53 CONCLUDED**

**C 130.5 DEGREES**

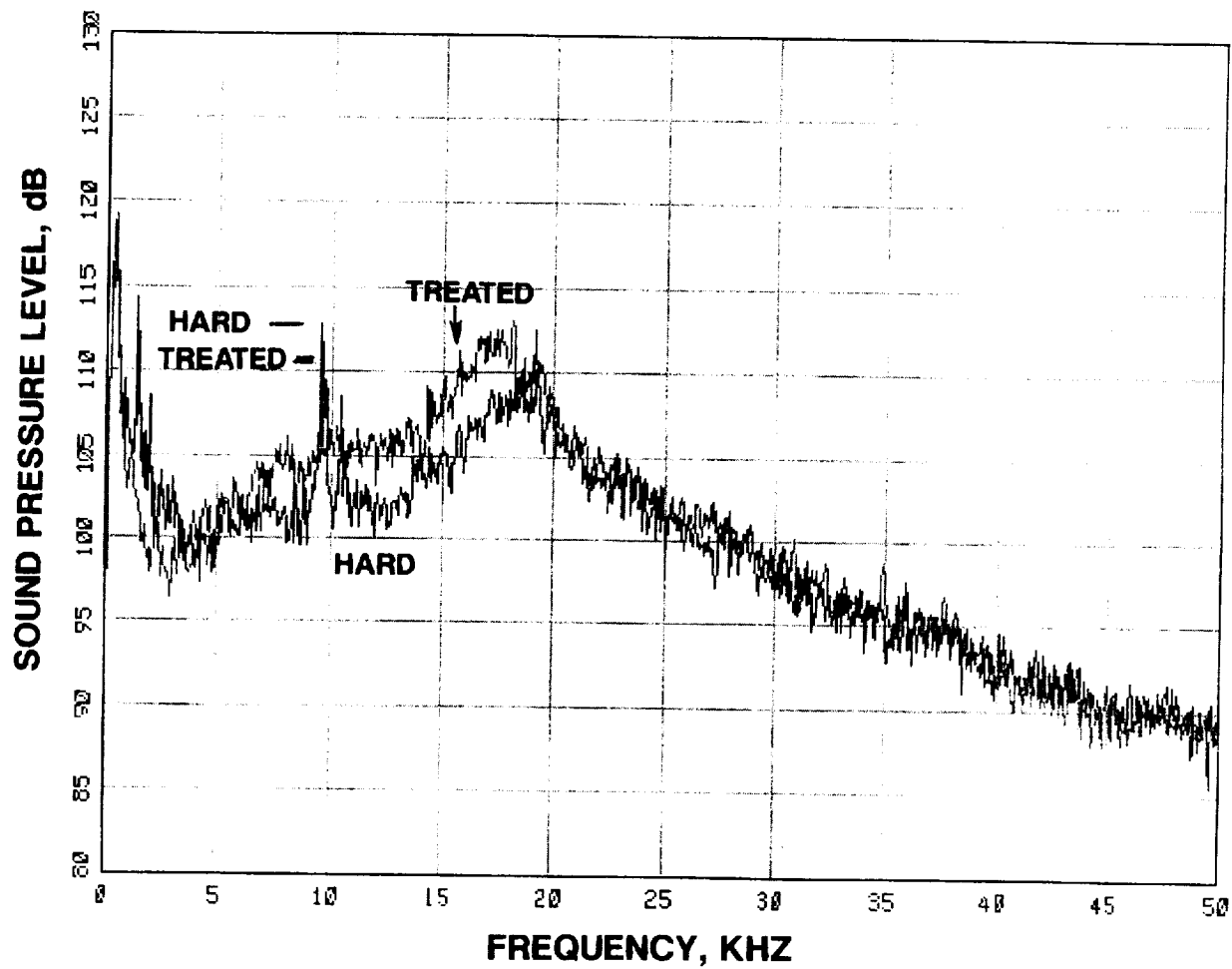


**FIGURE 54 SPECTRAL COMPARISON OF HARD AND FULLY  
TREATED DATA FOR THE 70 VANE CONFIGURATION AT 10671 RPMC  
A 24.5 DEGREES**

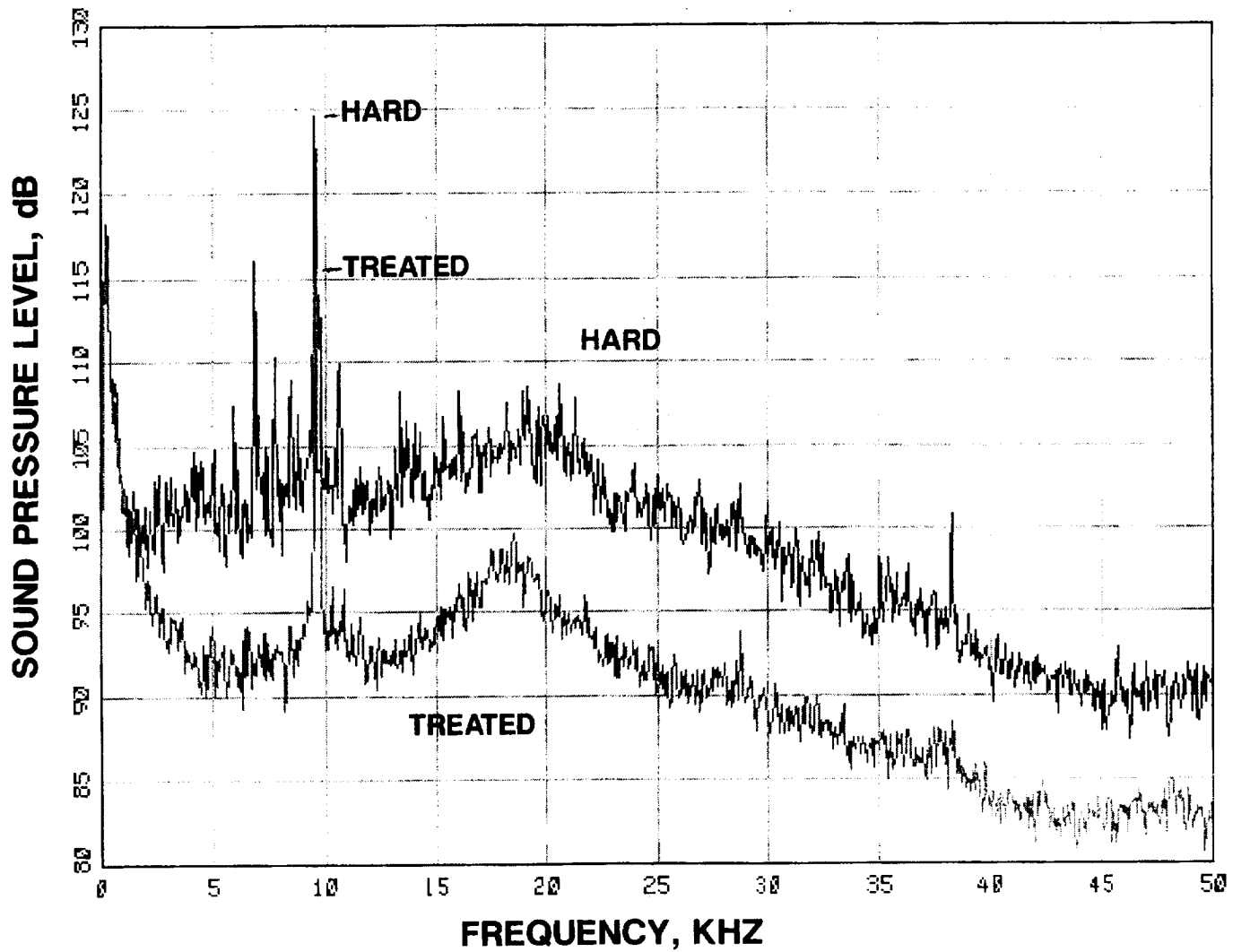


**FIGURE 54 CONTINUED**

**B 92.5 DEGREES**

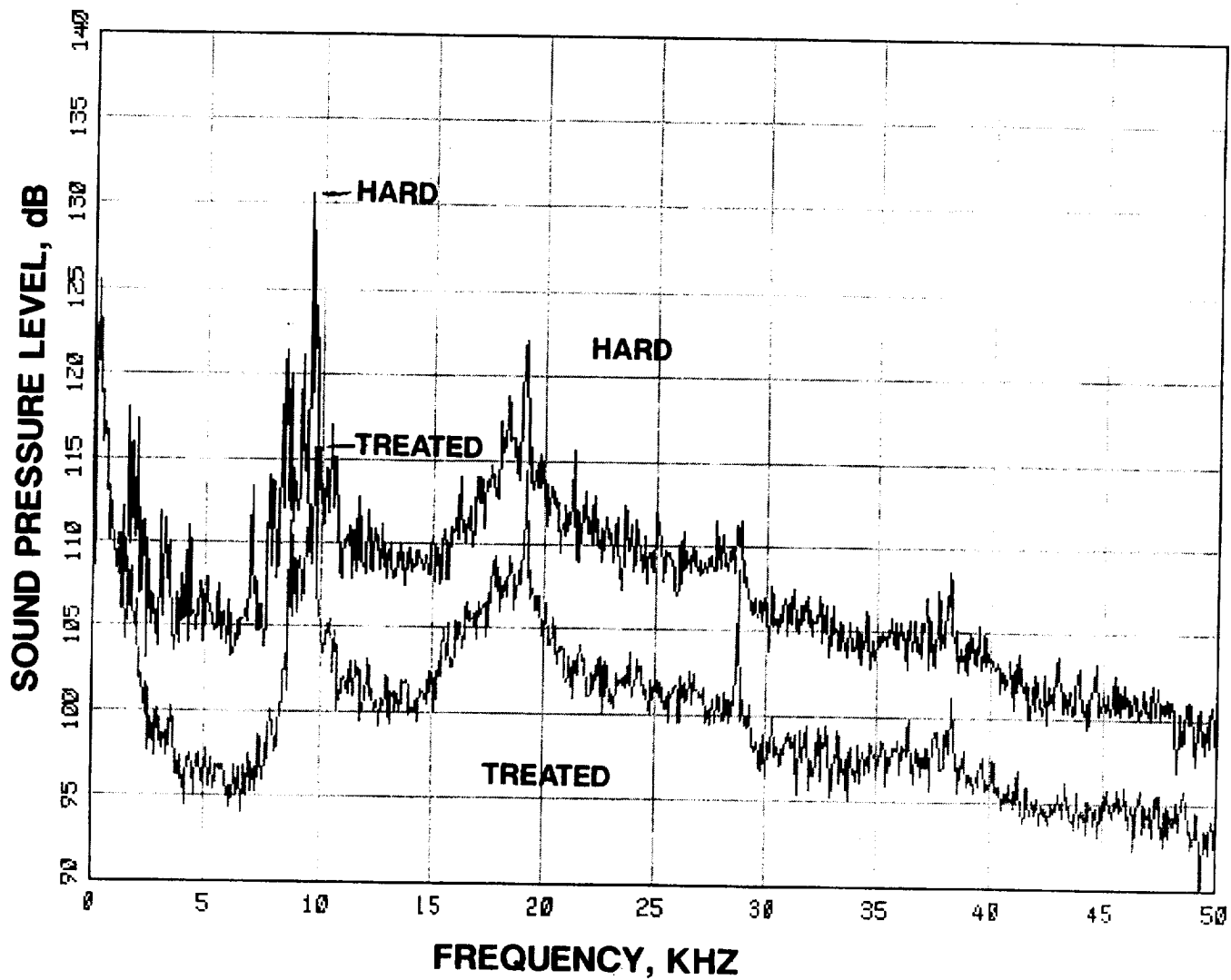


**FIGURE 54 CONCLUDED**

**C 130.5 DEGREES**

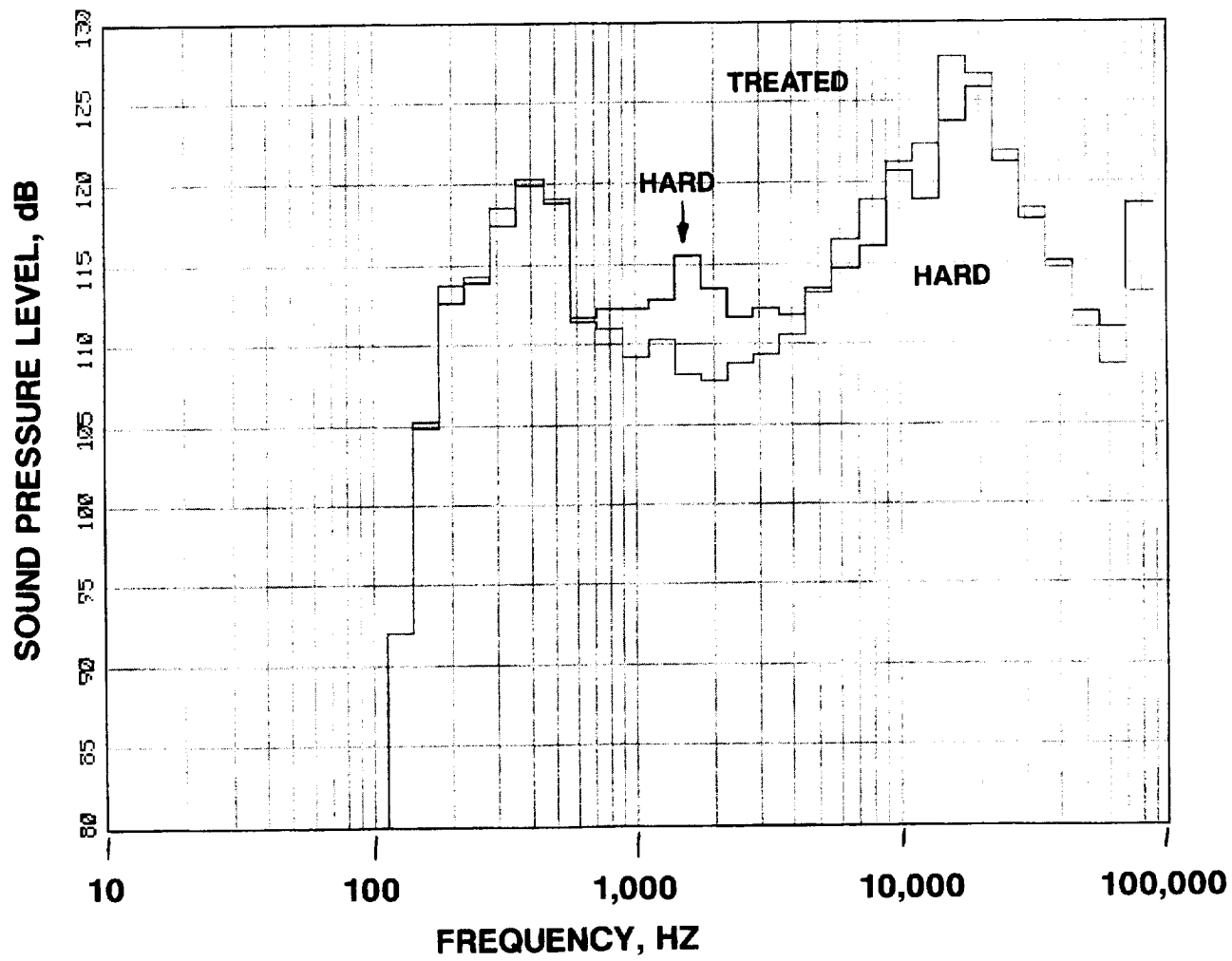


**FIGURE 55 1/3RD OCTAVE COMPARISON OF HARD AND FULLY  
TREATED DATA FOR THE 70 VANE CONFIGURATION AT 10671 RPMC  
A 24.5 DEGREES**

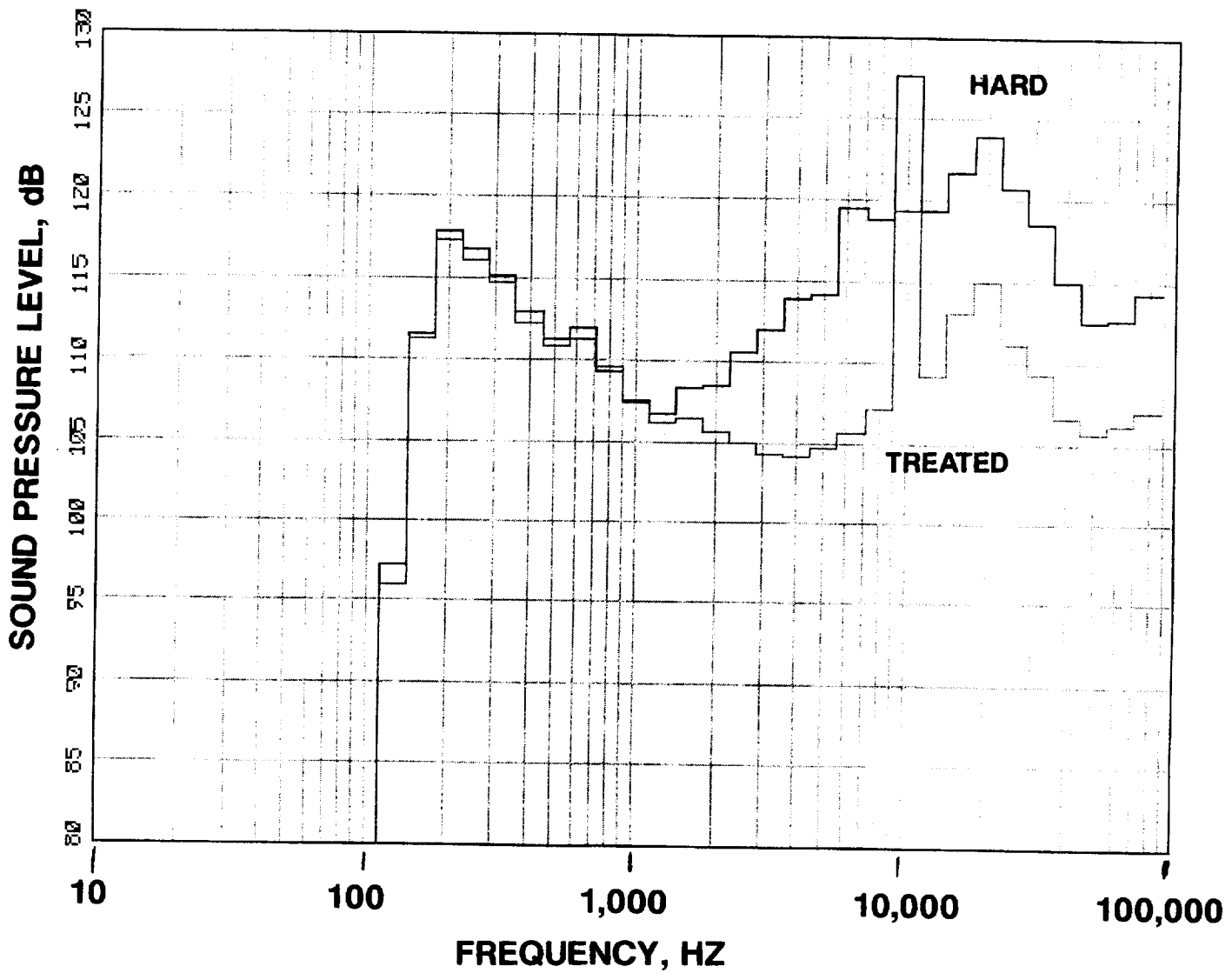


**FIGURE 55 CONTINUED**

**B 92.5 DEGREES**

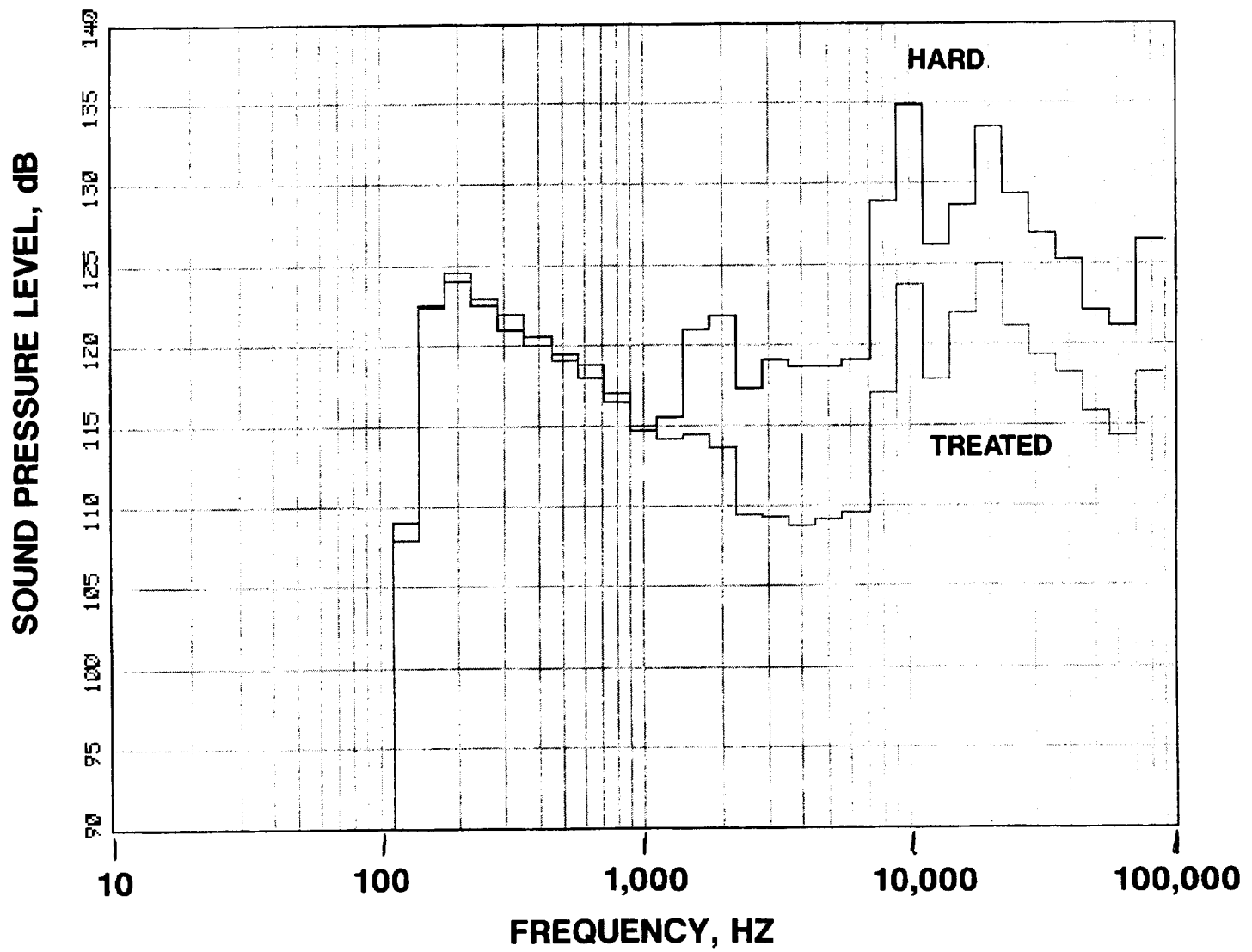


**FIGURE 55 CONCLUDED**

**C 130.5 DEGREES**

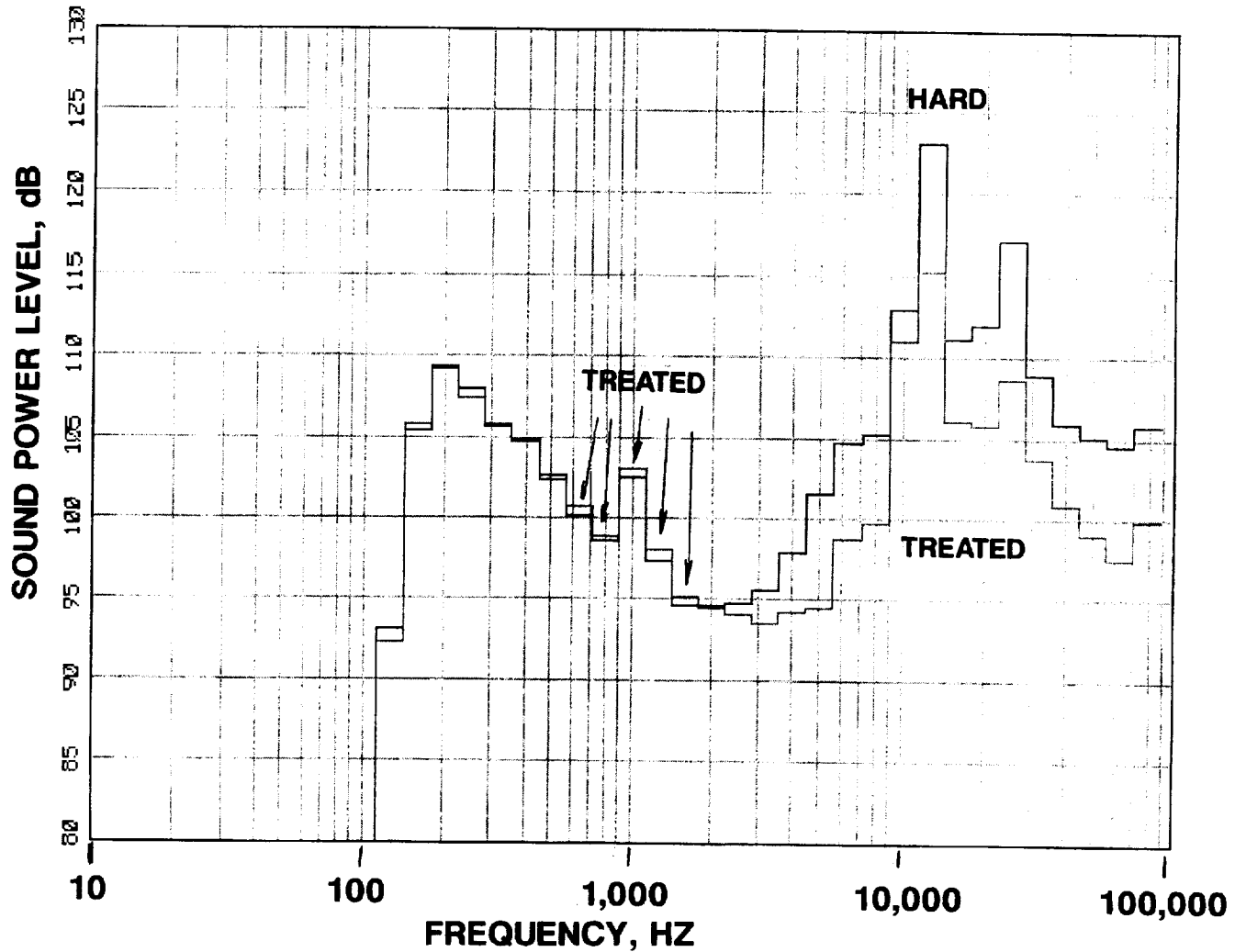


**FIGURE 56 SOUND POWER LEVEL COMPARISON OF HARD AND FULLY TREATED DATA FOR THE 70 VANE CONFIGURATION**

**A 6402 RPMc**

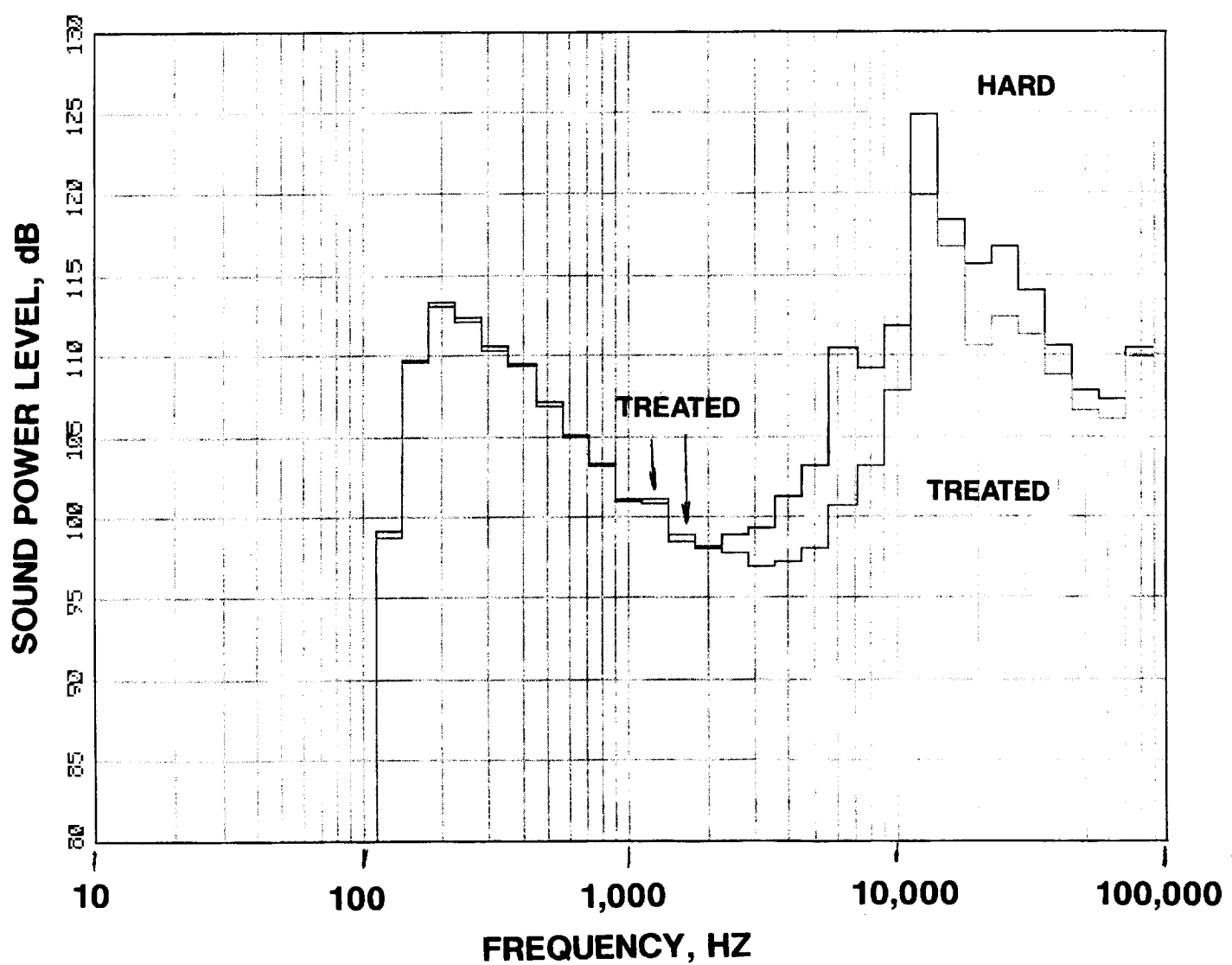


**FIGURE 56 CONTINUED**

**B 7736 RPMC**

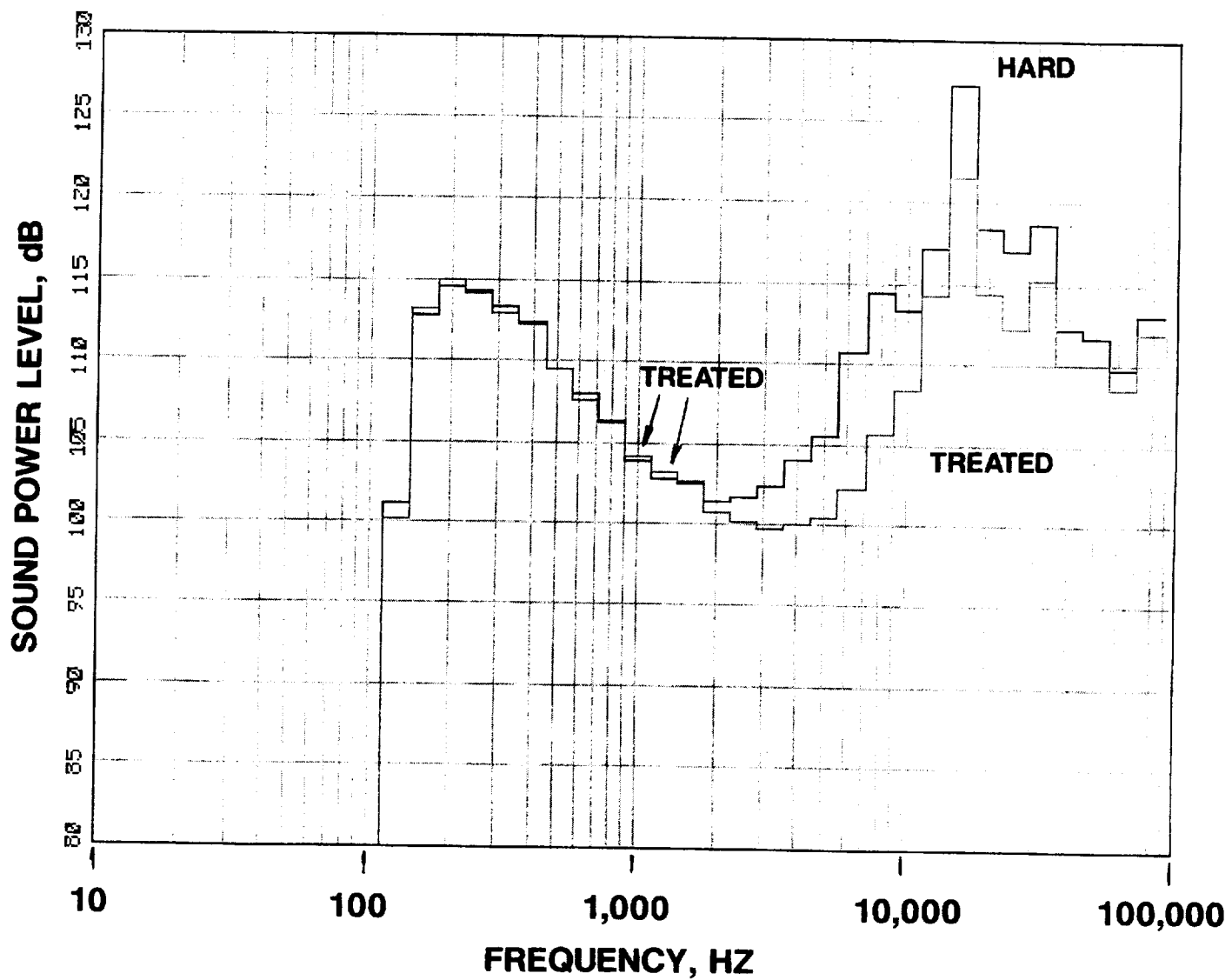


**FIGURE 56 CONTINUED**

**C 8537 RPMC**

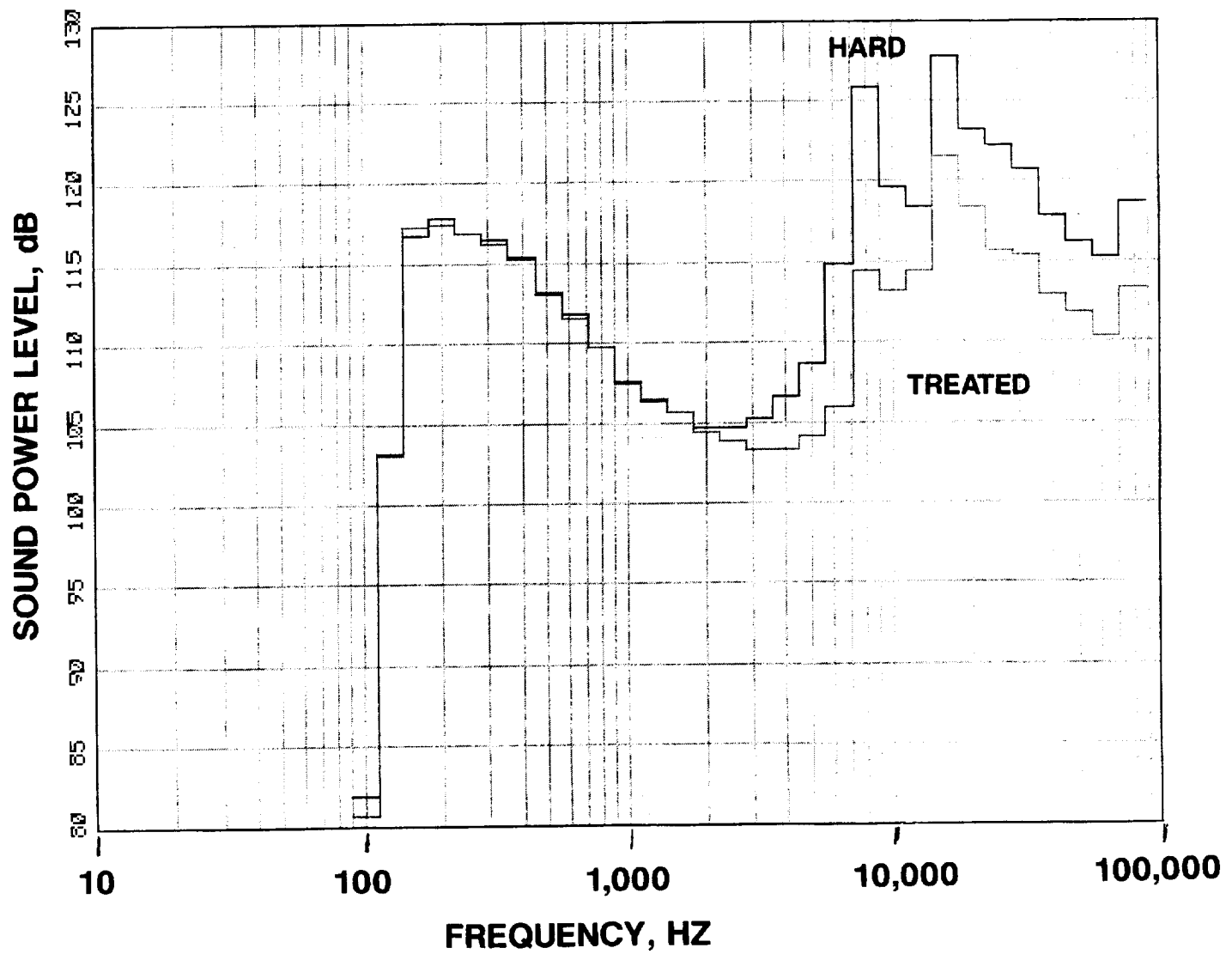


**FIGURE 56 CONTINUED**

**D 9604 RPMC**

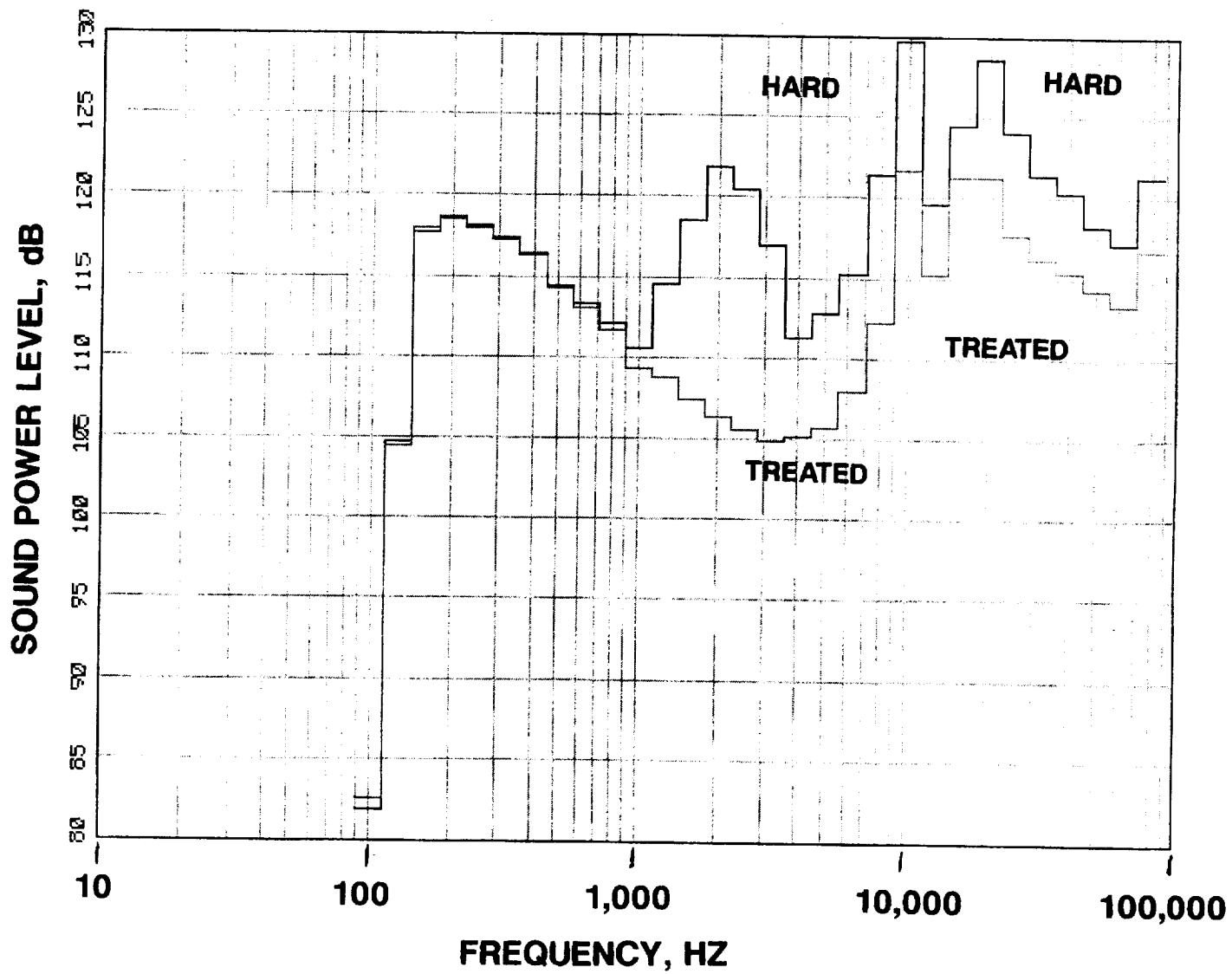


**FIGURE 56 CONTINUED**

**E 10137 RPMC**

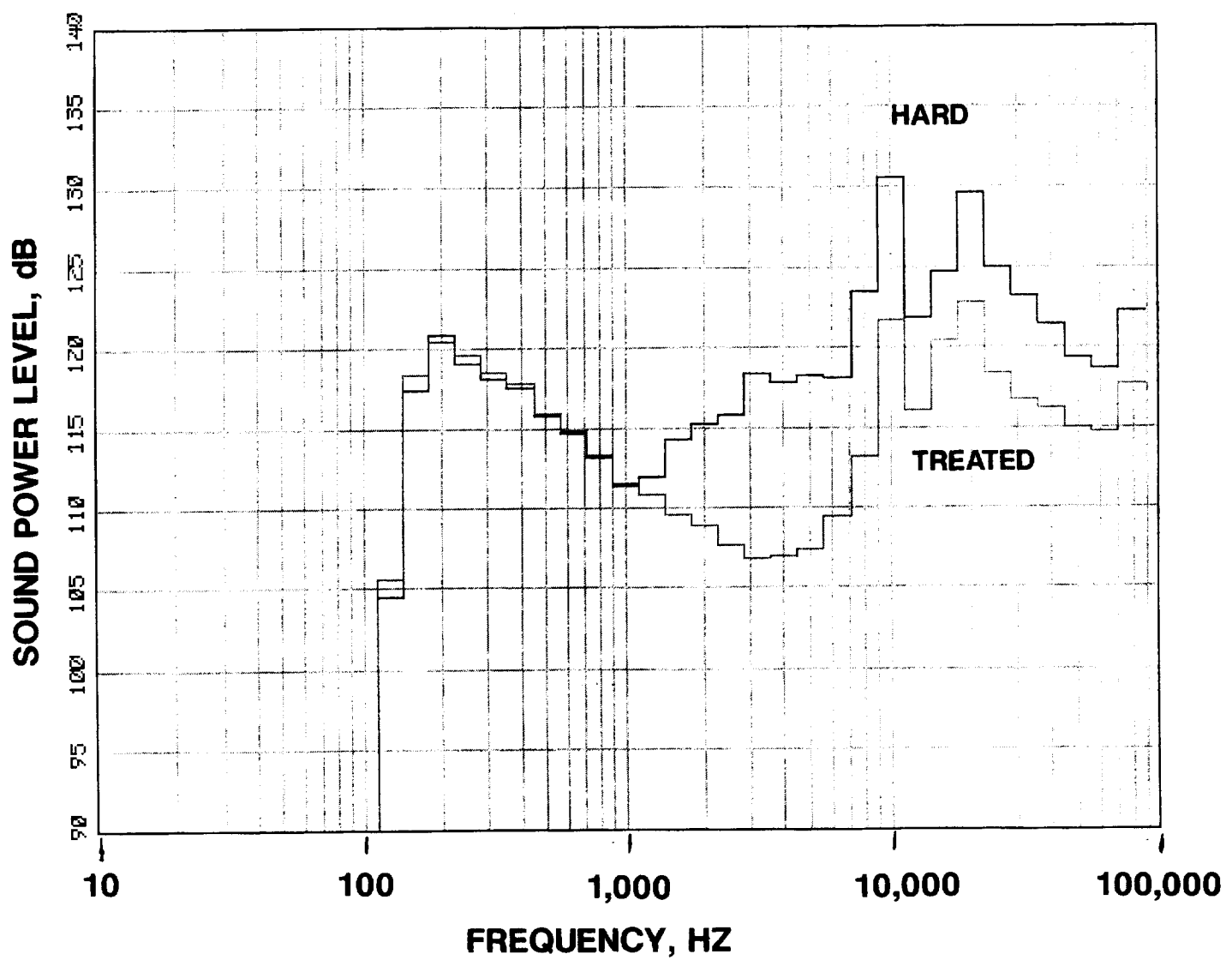


**FIGURE 56 CONCLUDED**

**F 10671 RPMC**

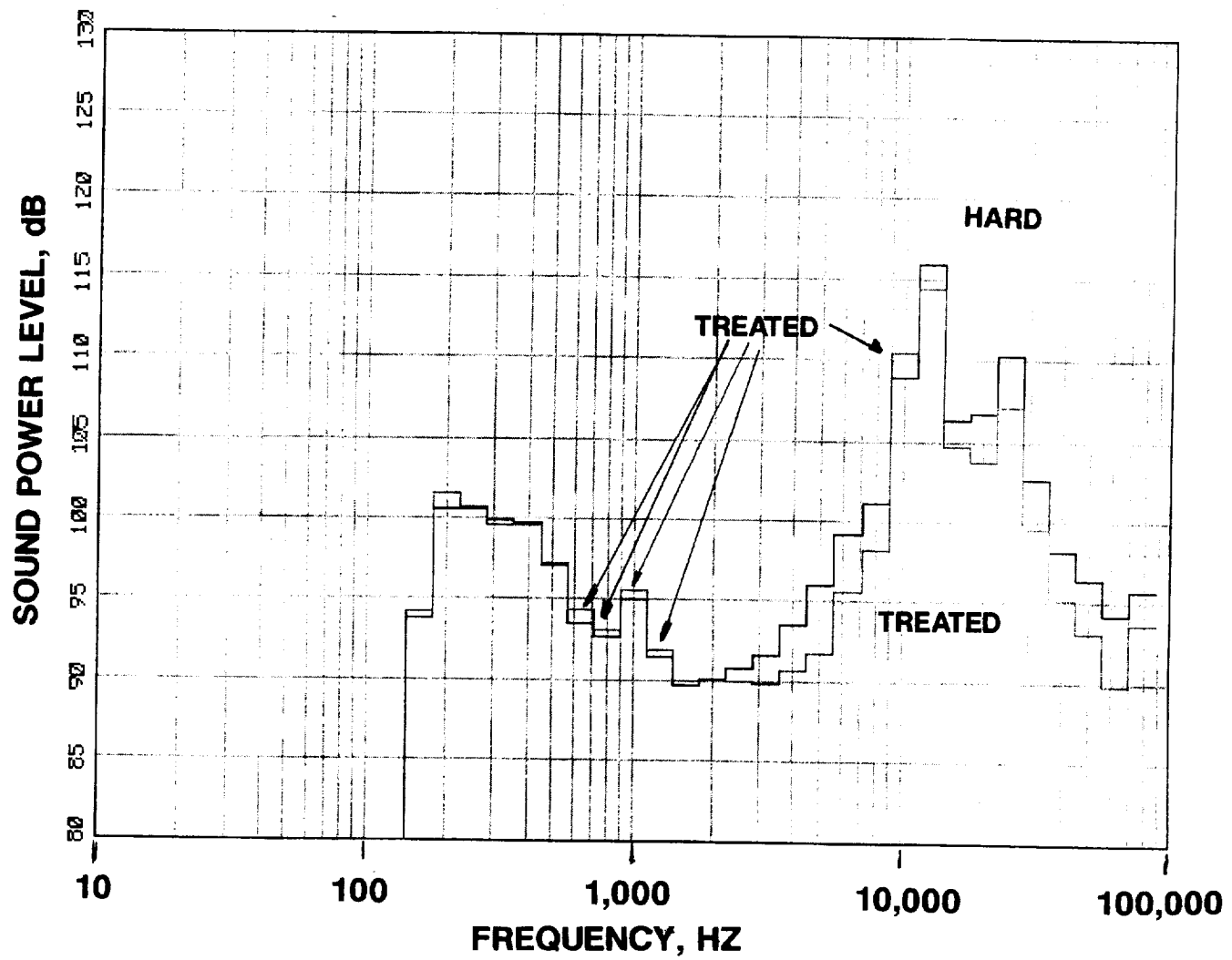


**FIGURE 57 FRONT SOUND POWER LEVEL COMPARISON OF HARD  
AND FULLY TREATED DATA FOR THE 70 VANE CONFIGURATION**

**A 6402 RPMC**

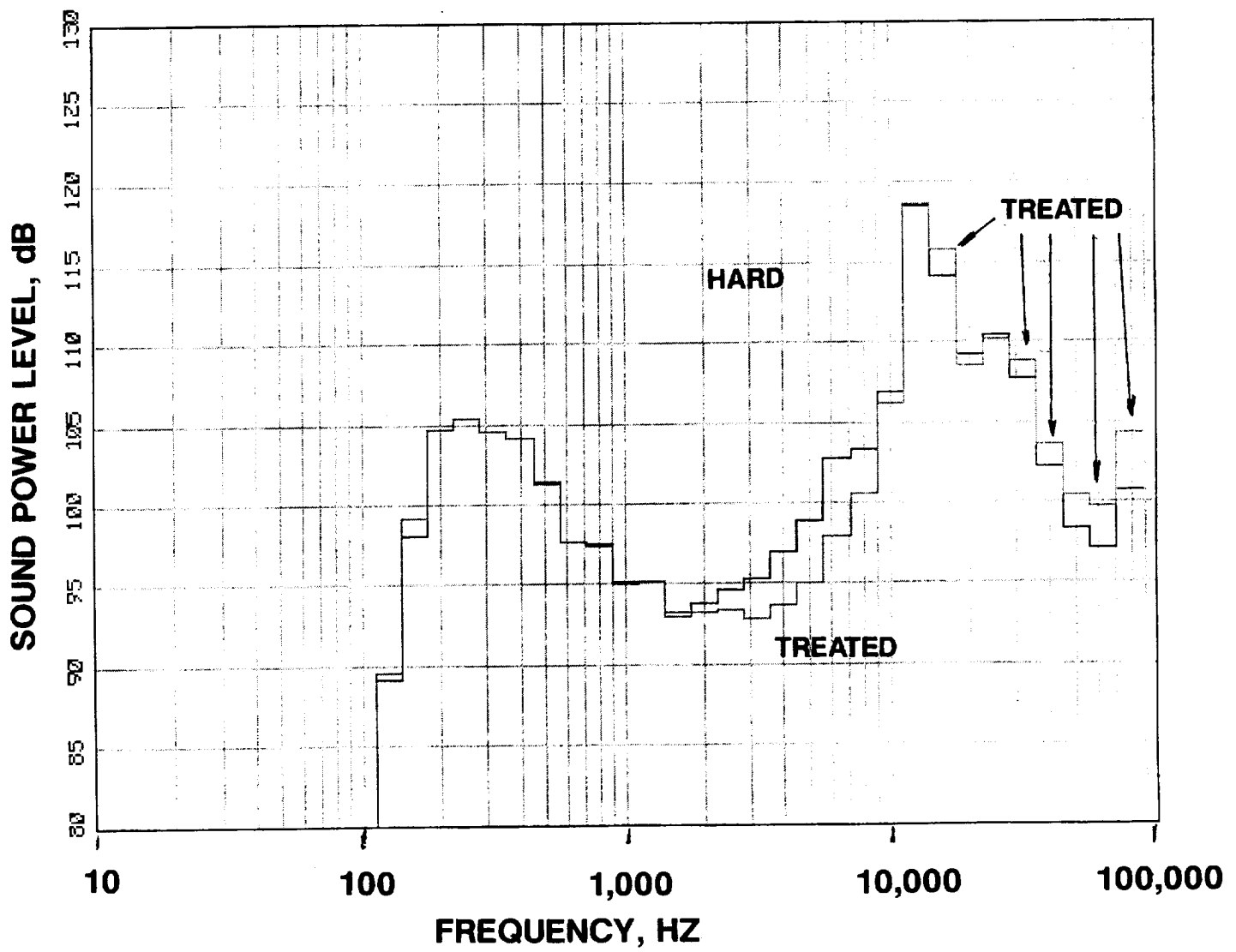


**FIGURE 57 CONTINUED**

**B 7736 RPMC**

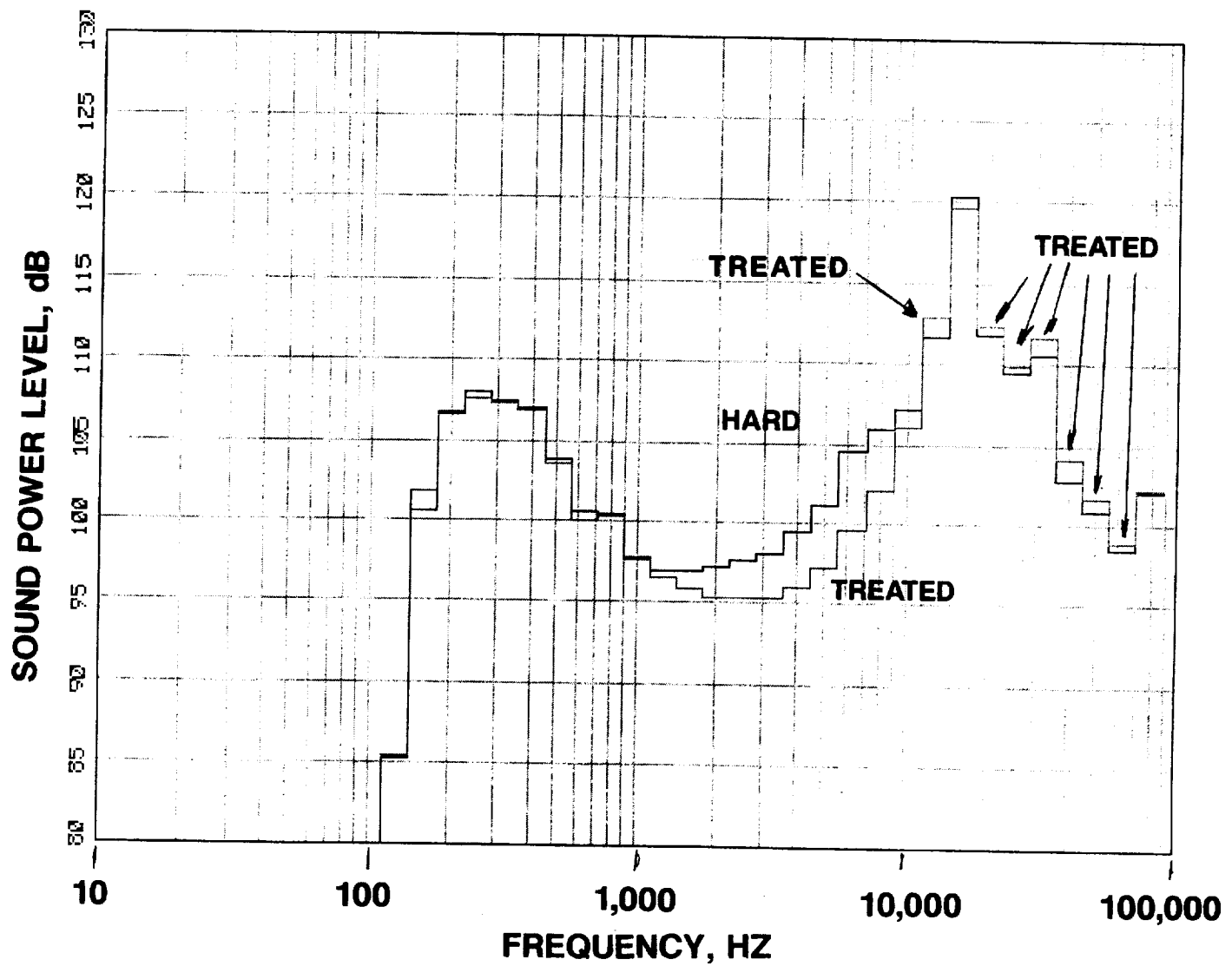


**FIGURE 57 CONTINUED**

**C 8537 RPMC**

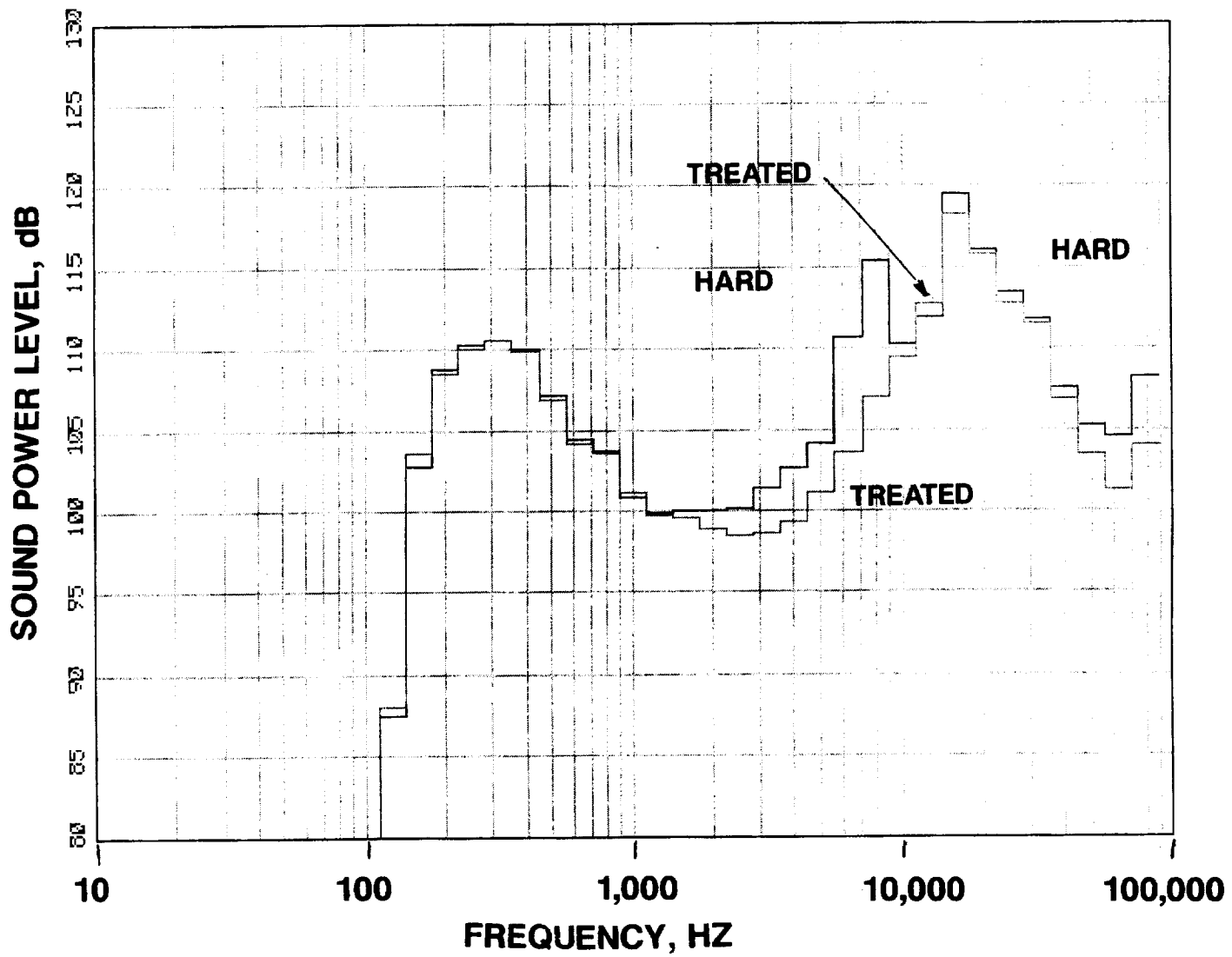


**FIGURE 57 CONTINUED**

**D 9604 RPMC**

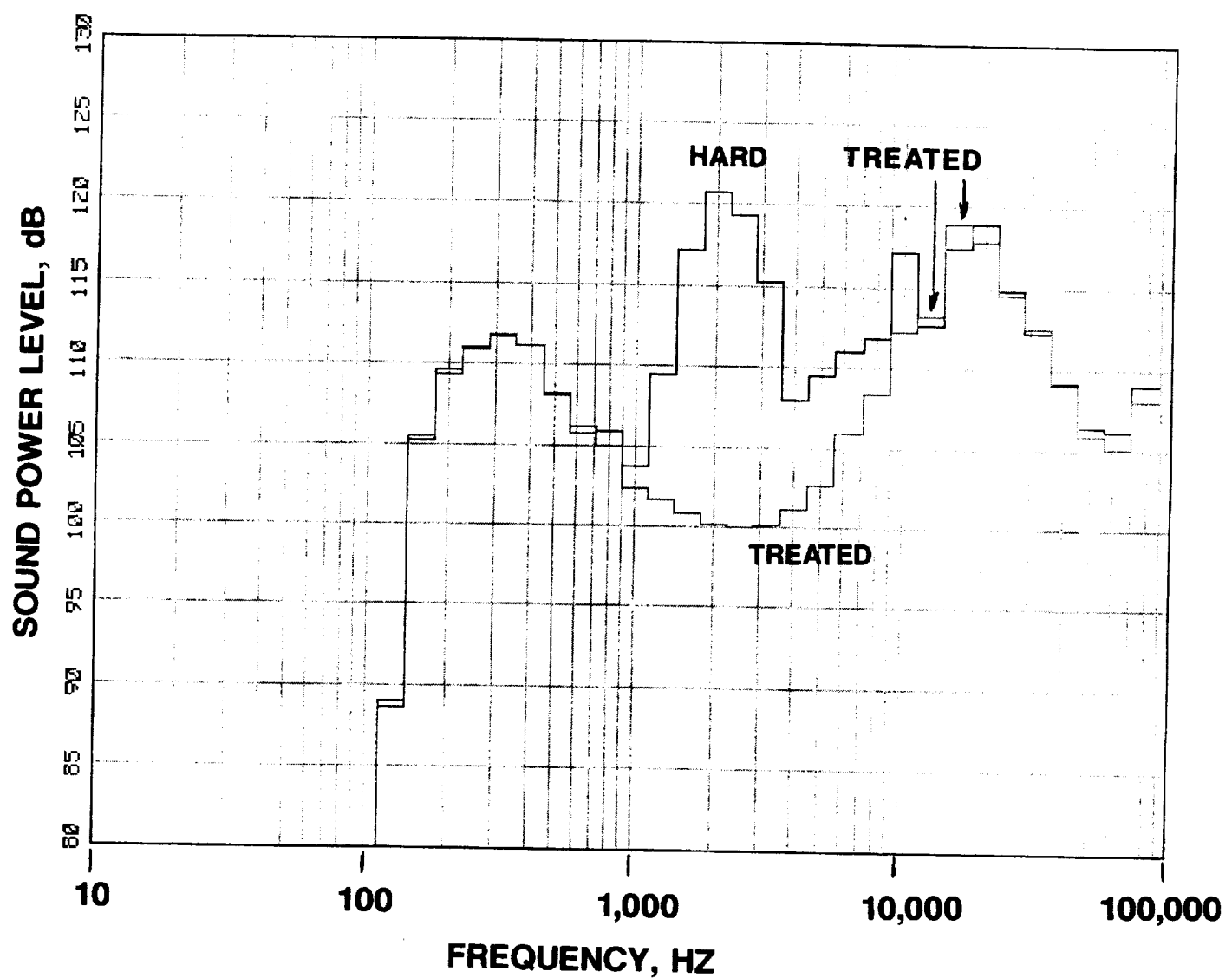


**FIGURE 57 CONTINUED**

**E 10137 RPMC**

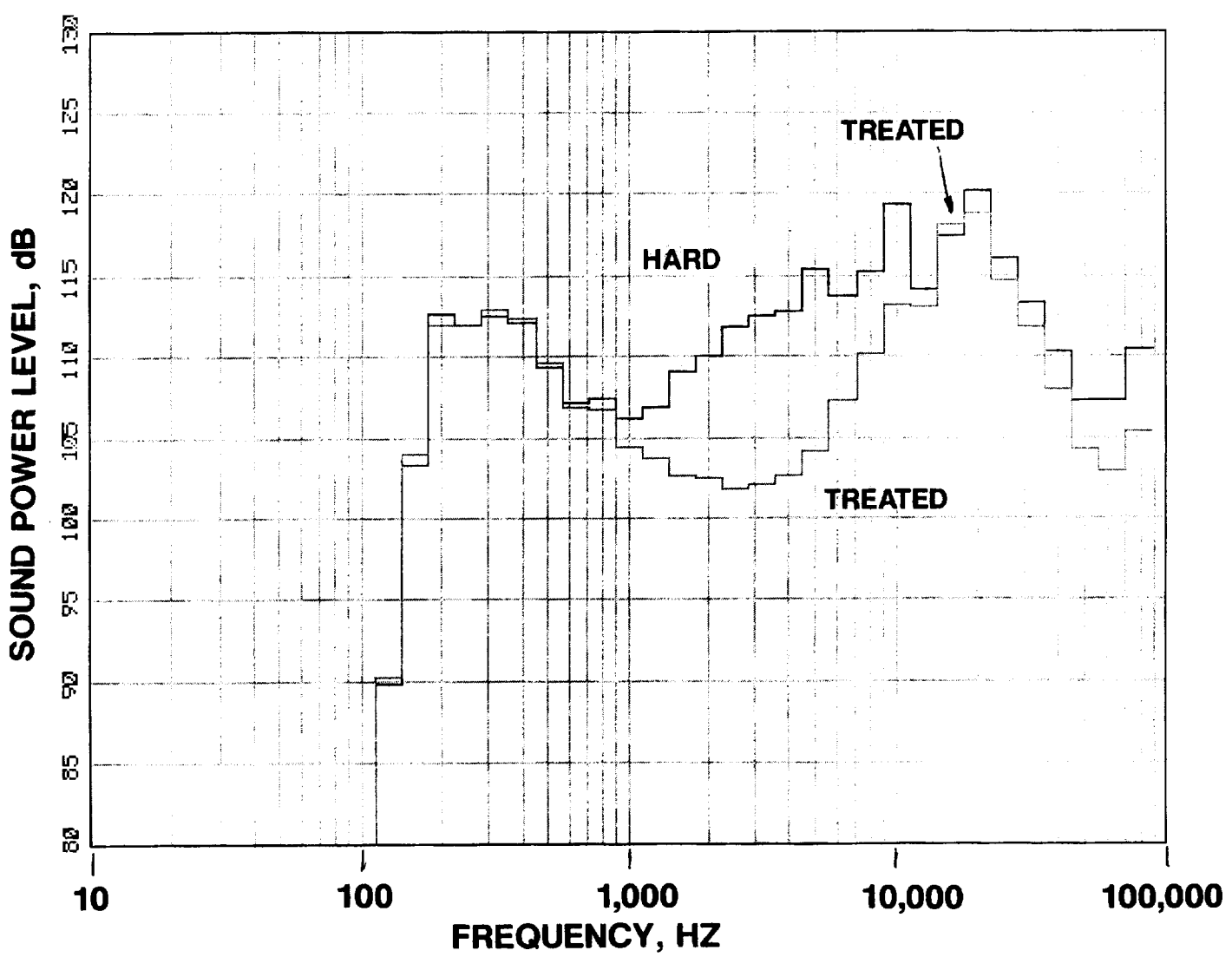


**FIGURE 57 CONCLUDED**

**F 10671 RPMC**

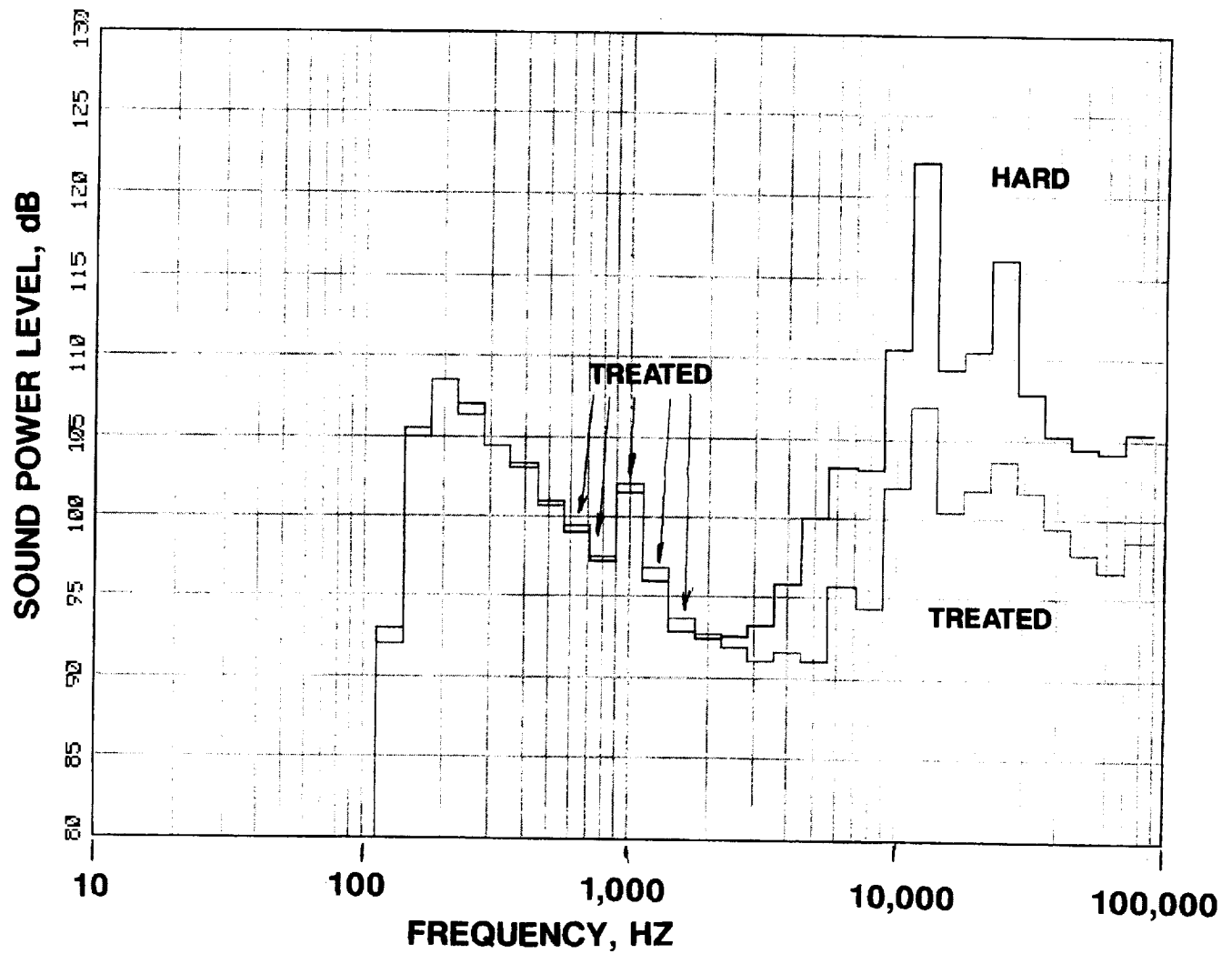


**FIGURE 58 AFT SOUND POWER LEVEL COMPARISON OF HARD AND FULLY TREATED DATA FOR THE 70 VANE CONFIGURATION**

**A 6402 RPMC**

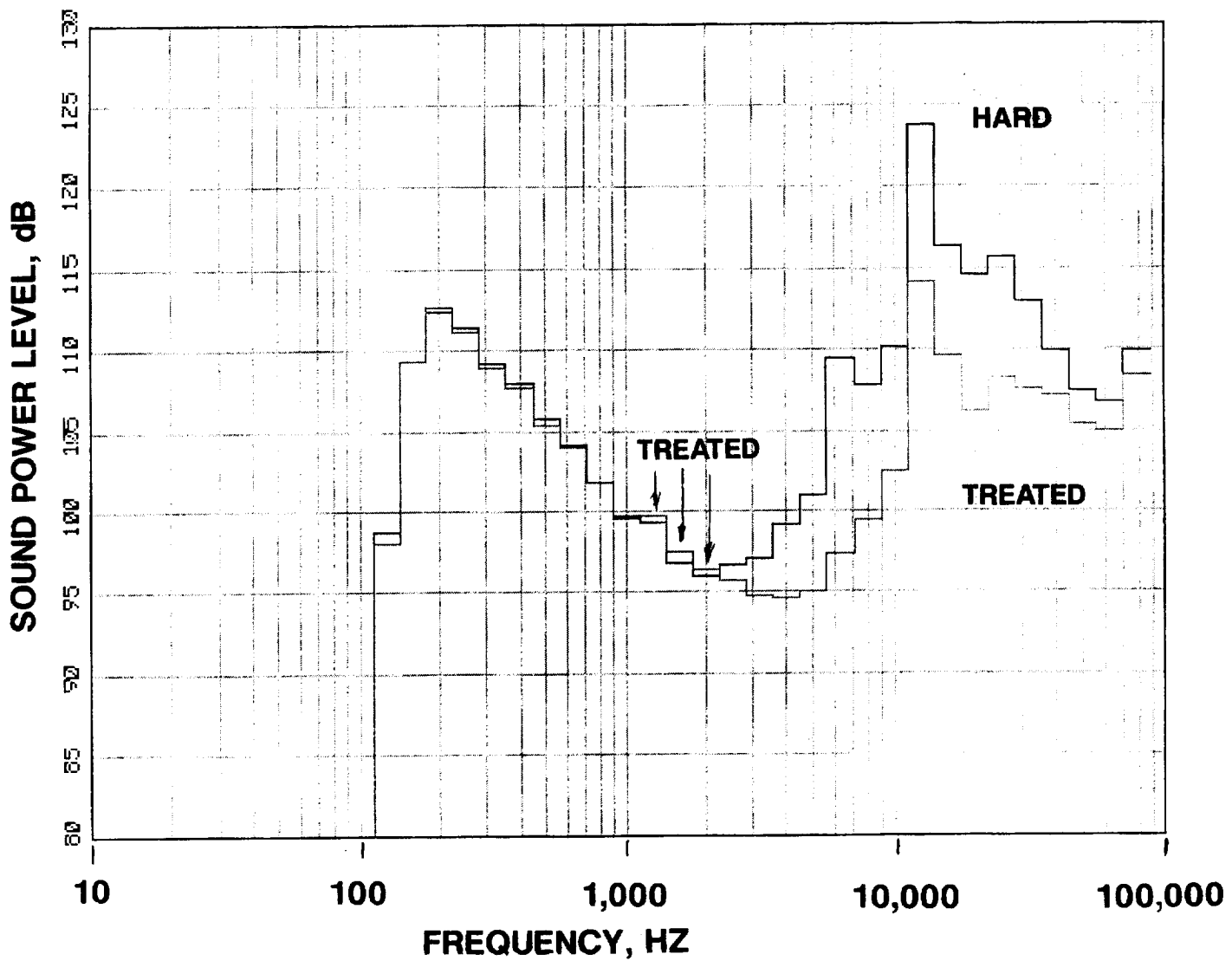


**FIGURE 58 CONTINUED**

**B 7736 RPMC**

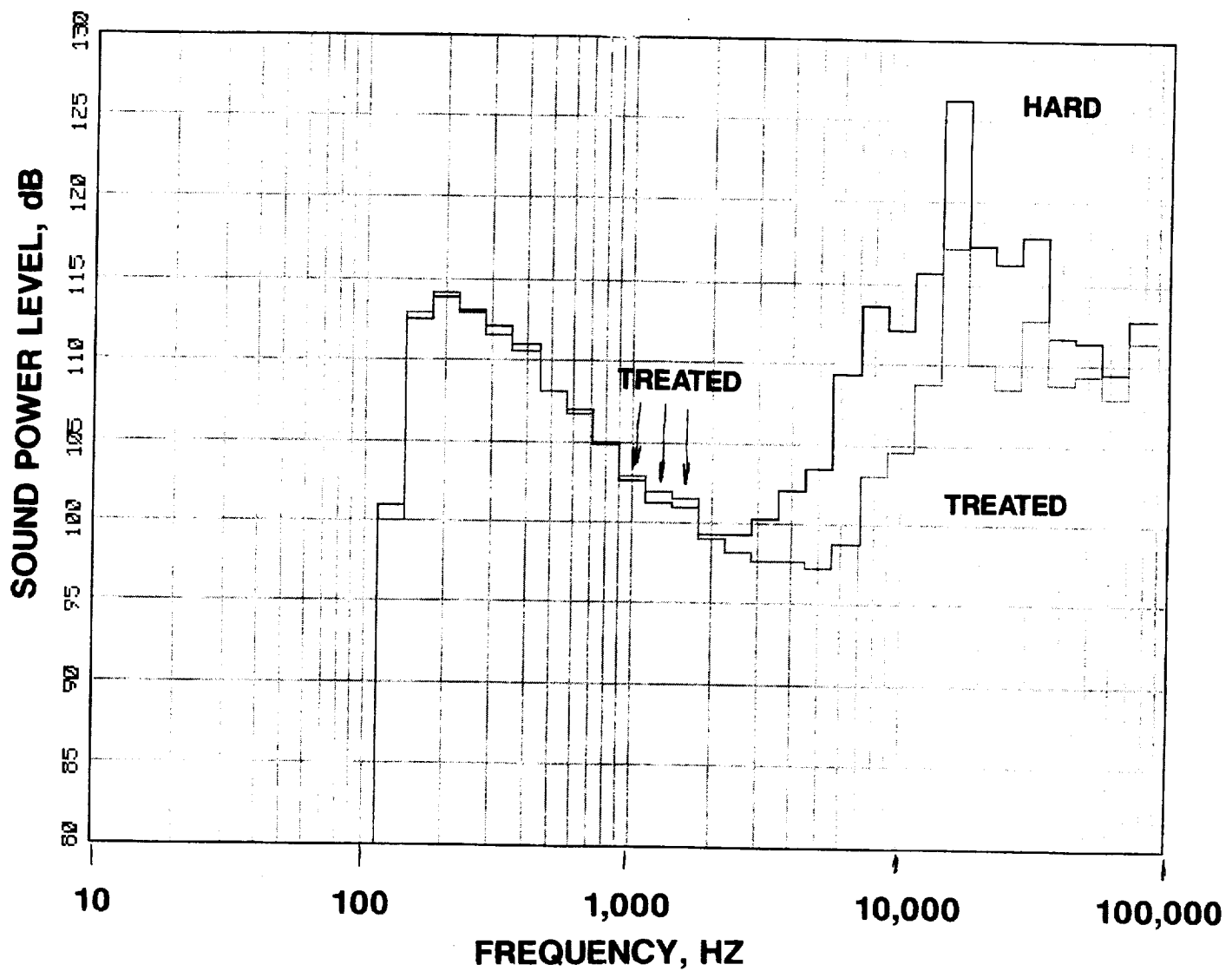


**FIGURE 58 CONTINUED**

**C 8537 RPMC**

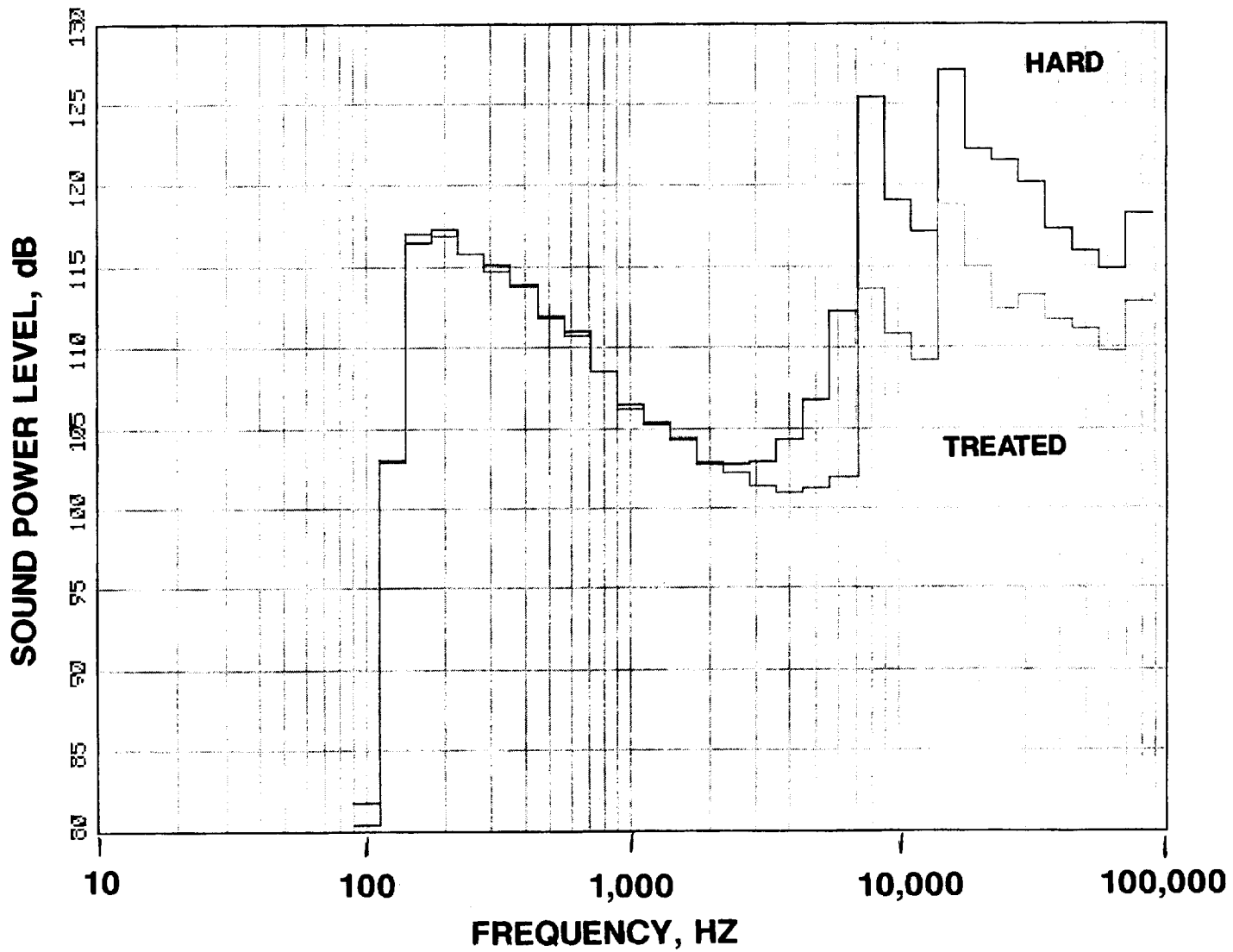


**FIGURE 58 CONTINUED**

**D 9604 RPMC**

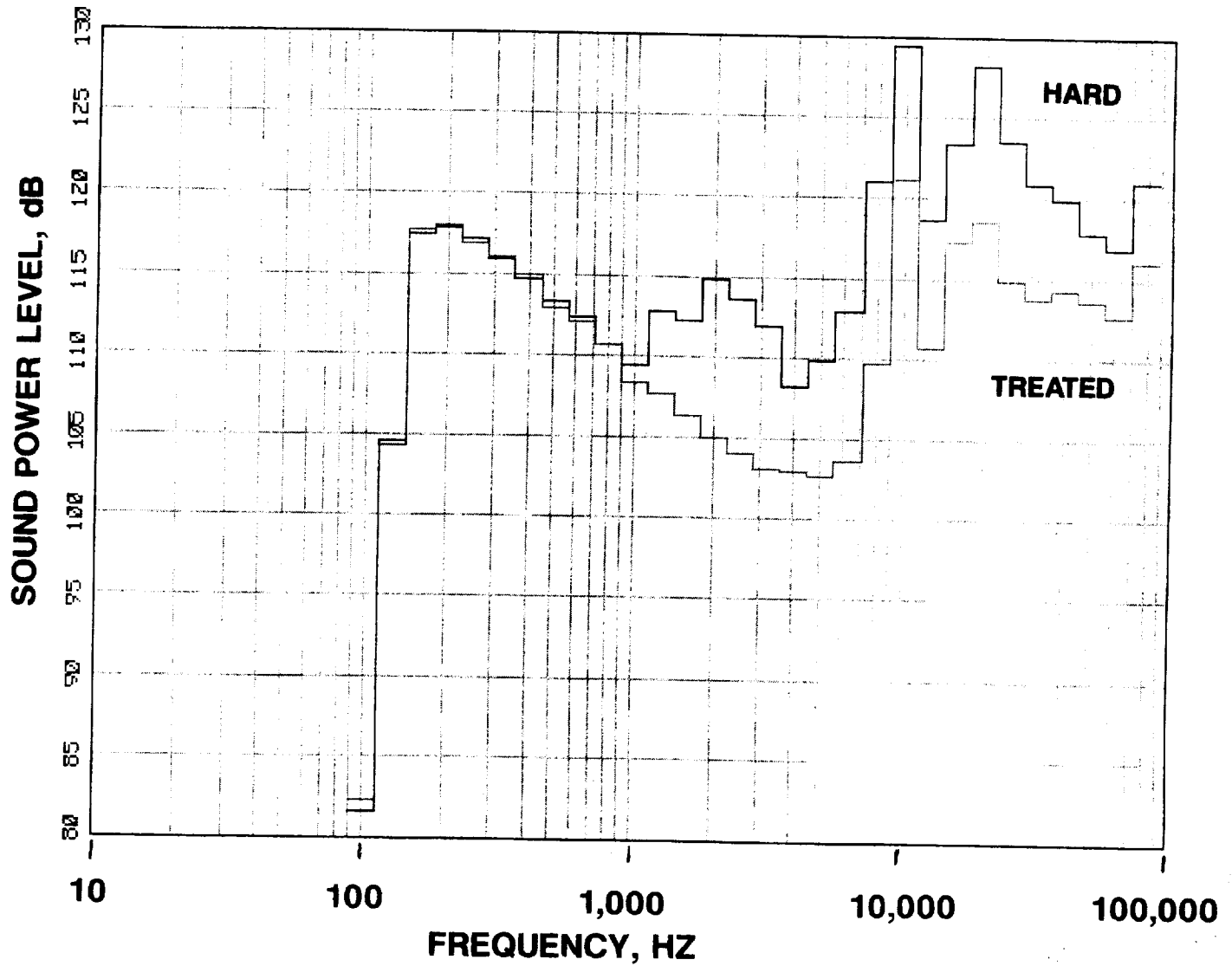


**FIGURE 58 CONTINUED**

**E 10137 RPMC**

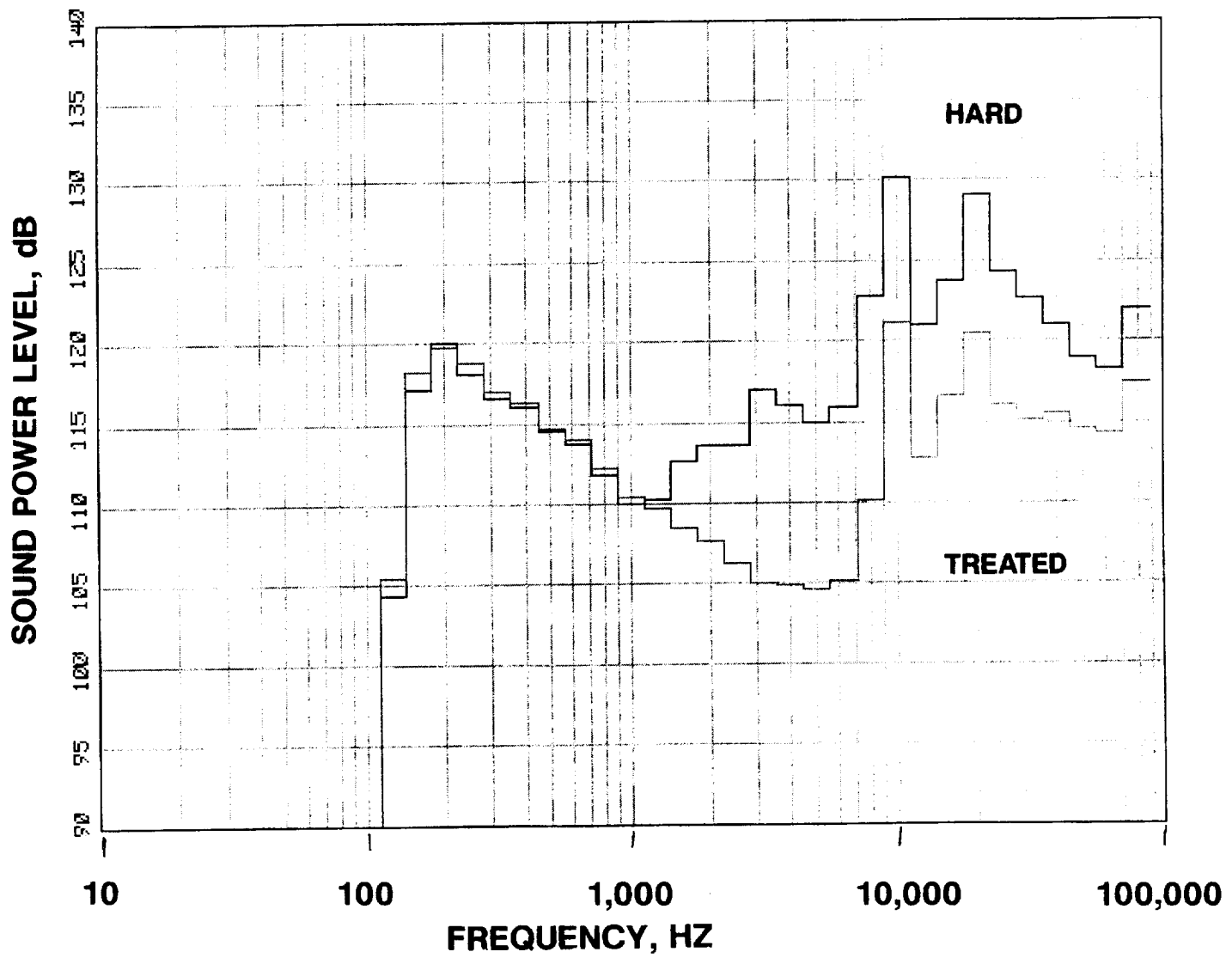


**FIGURE 58 CONCLUDED**

**F 10671 RPMC**

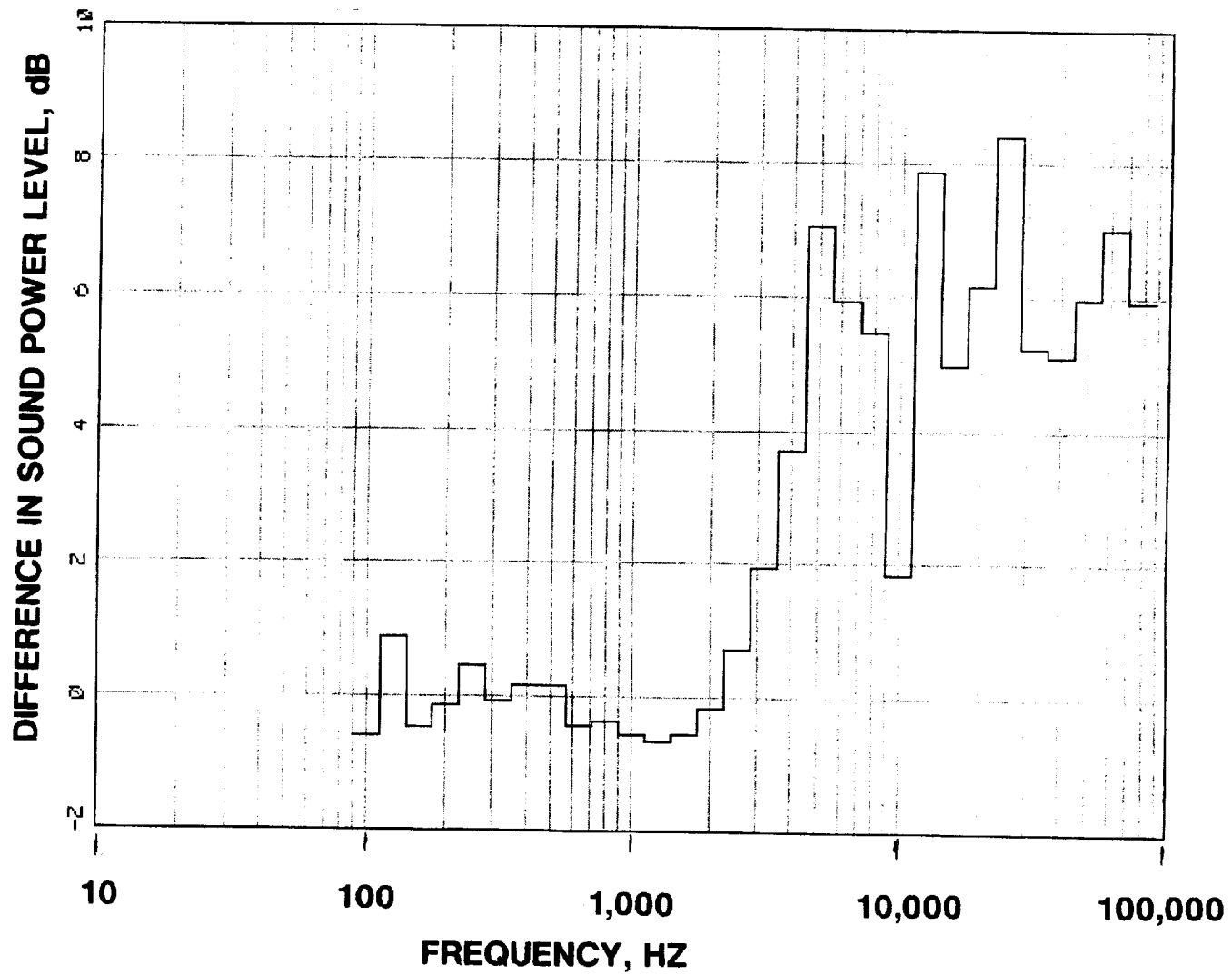


**FIGURE 59 DIFFERENCE IN SOUND POWER LEVEL, HARD MINUS  
TREATED, FOR THE 70 VANE CONFIGURATION**

**A 6402 RPMC**

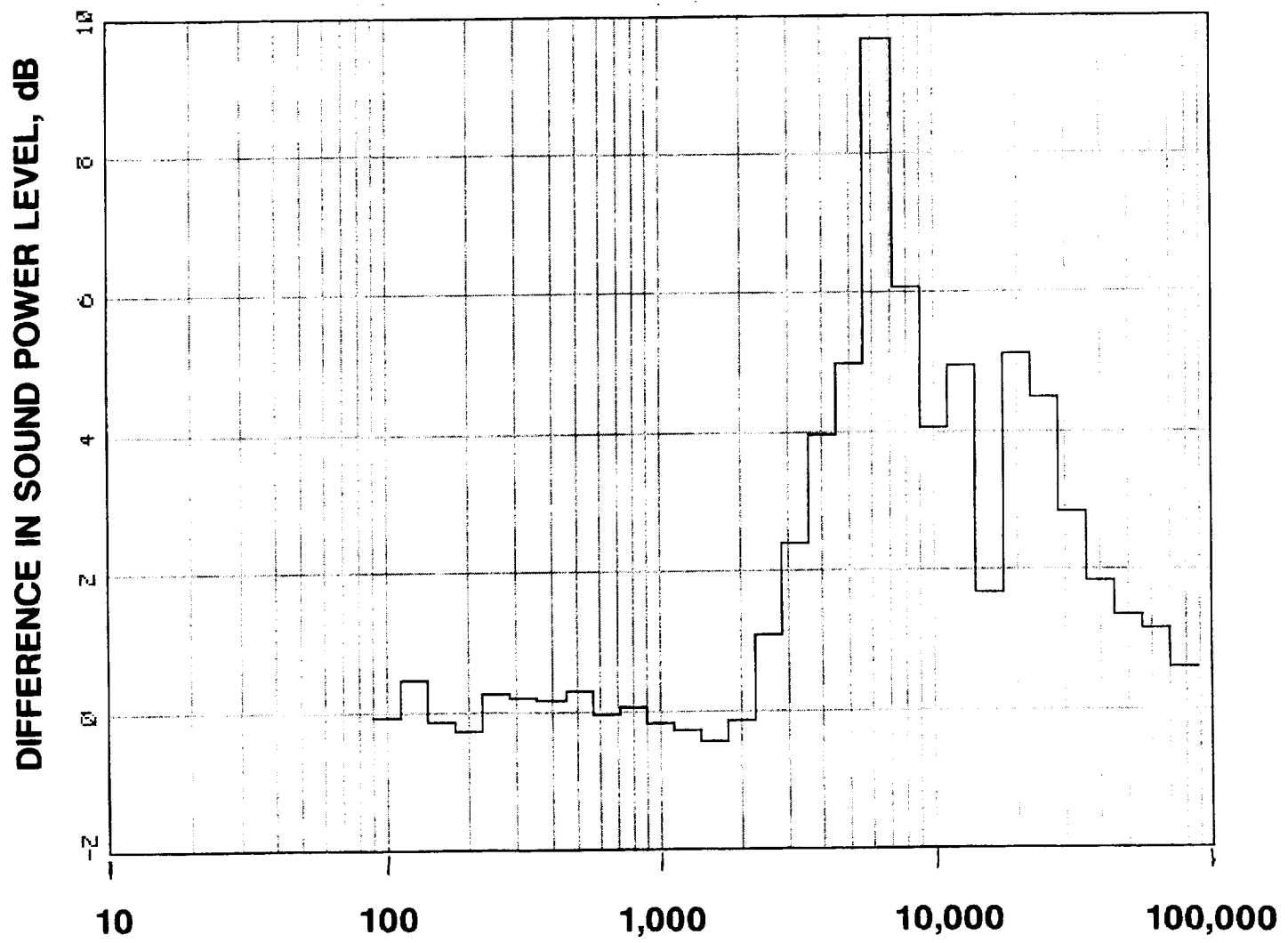


**FIGURE 59 CONTINUED**

**B 7736 RPMC**

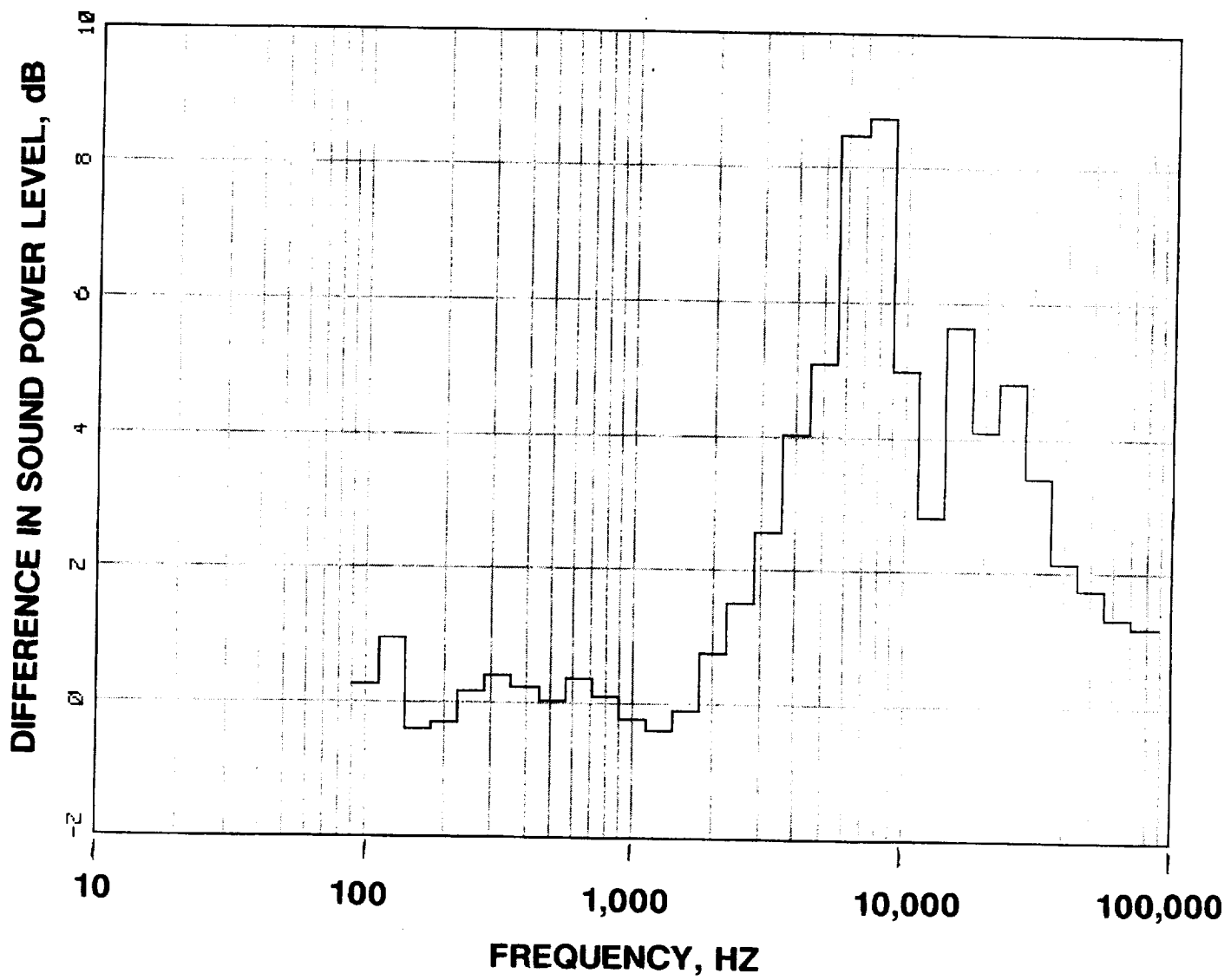


**FIGURE 59 CONTINUED**

**C 8537 RPMC**

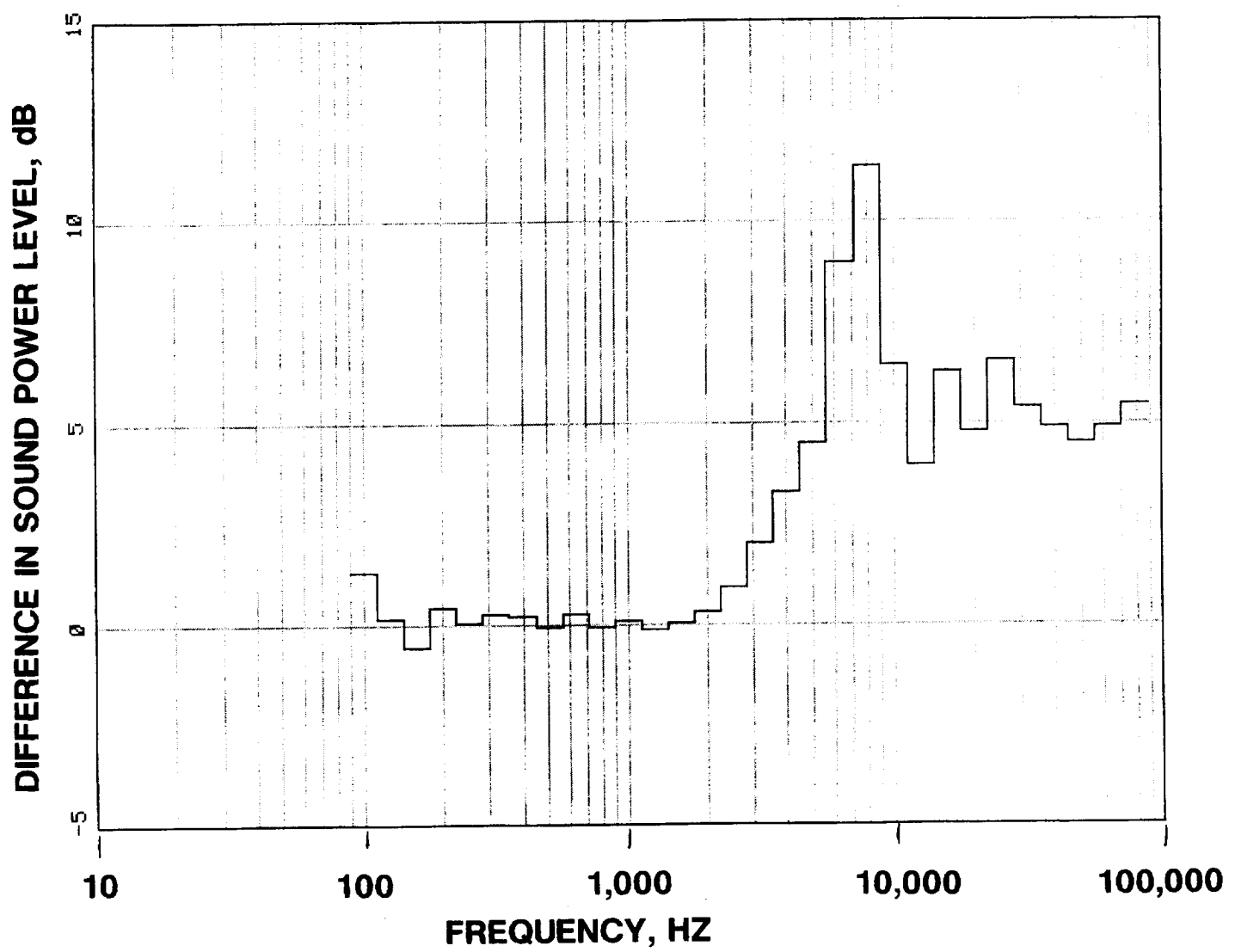


**FIGURE 59 CONTINUED**

**D 9604 RPMC**

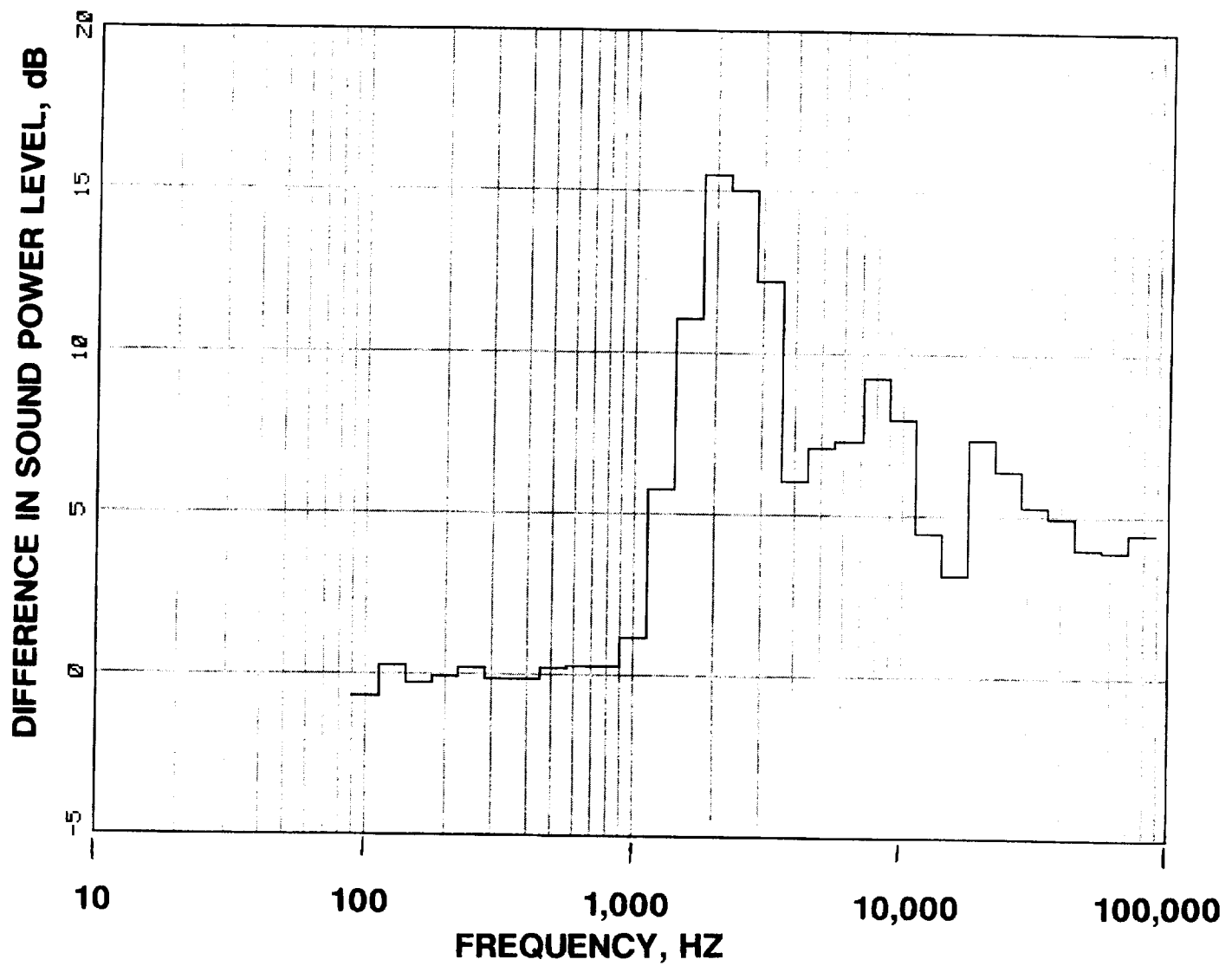


**FIGURE 59 CONTINUED**

**E 10137 RPMC**

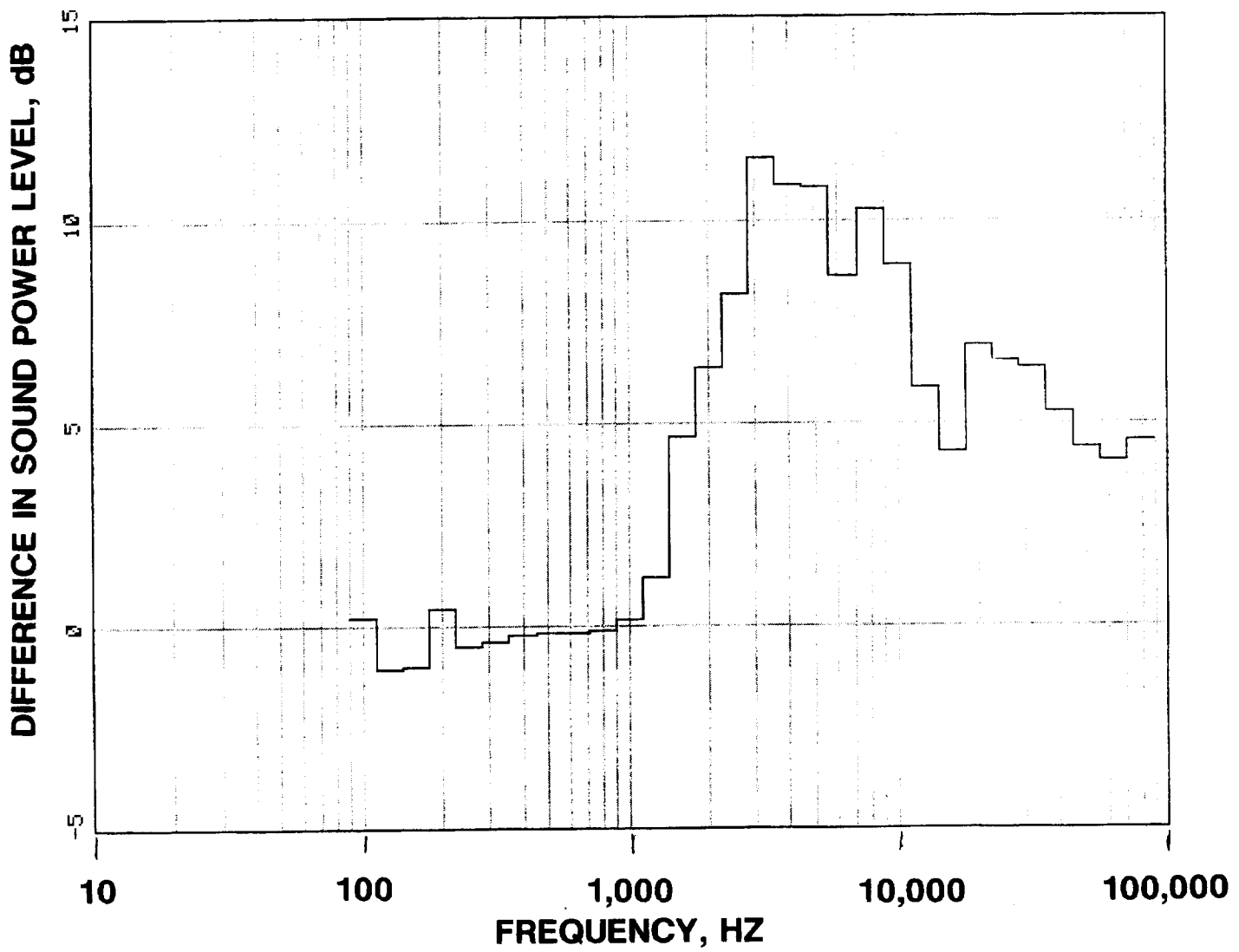


**FIGURE 59 CONCLUDED**

**F 10671 RPMC**

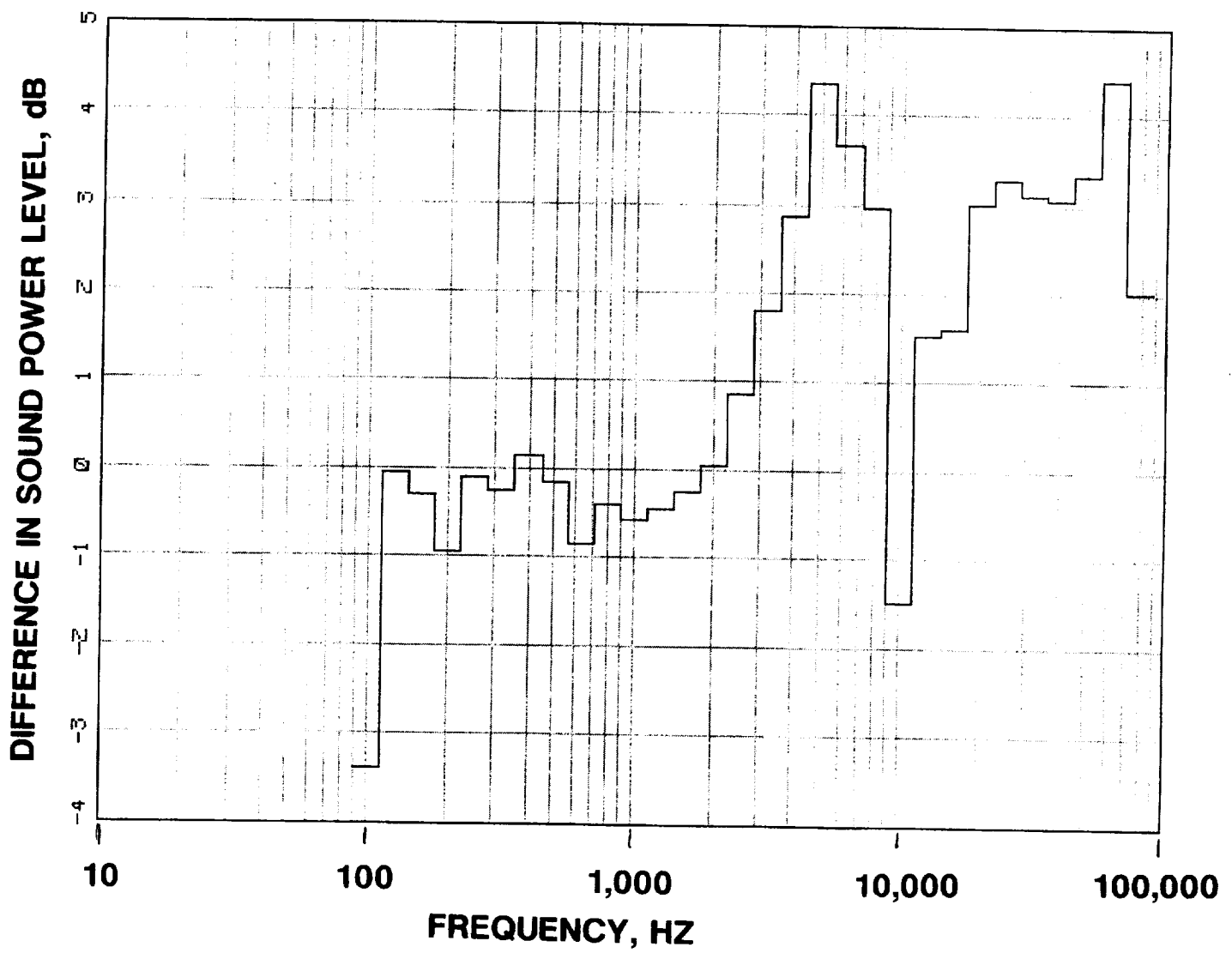


**FIGURE 60 DIFFERENCE IN FRONT SOUND POWER LEVEL ,  
HARD MINUS TREATED, FOR THE 70 VANE CONFIGURATION**

**A 6402 RPMC**

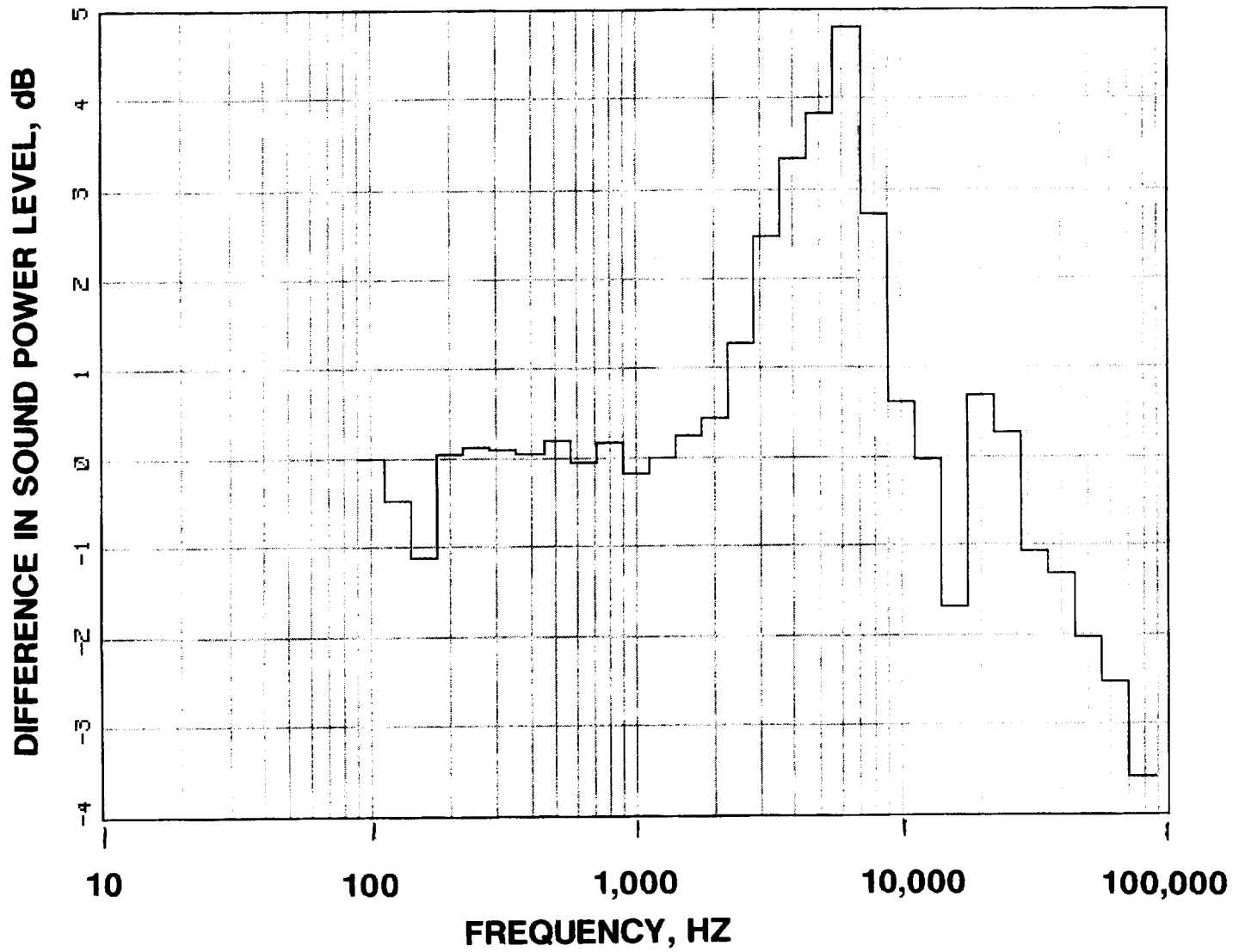


**FIGURE 60 CONTINUED**

**B 7736 RPMC**

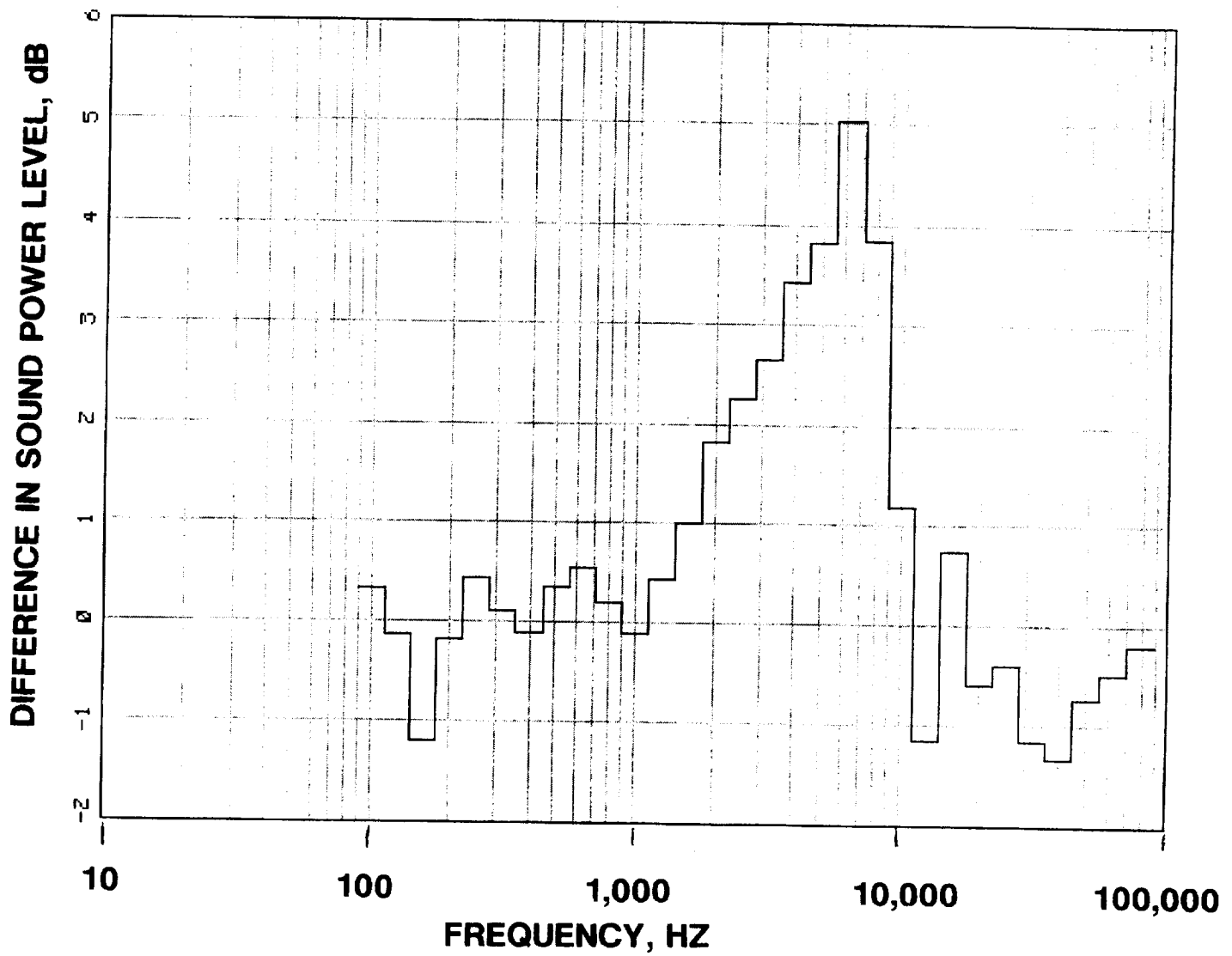


**FIGURE 60 CONTINUED**

**C 8537 RPMC**

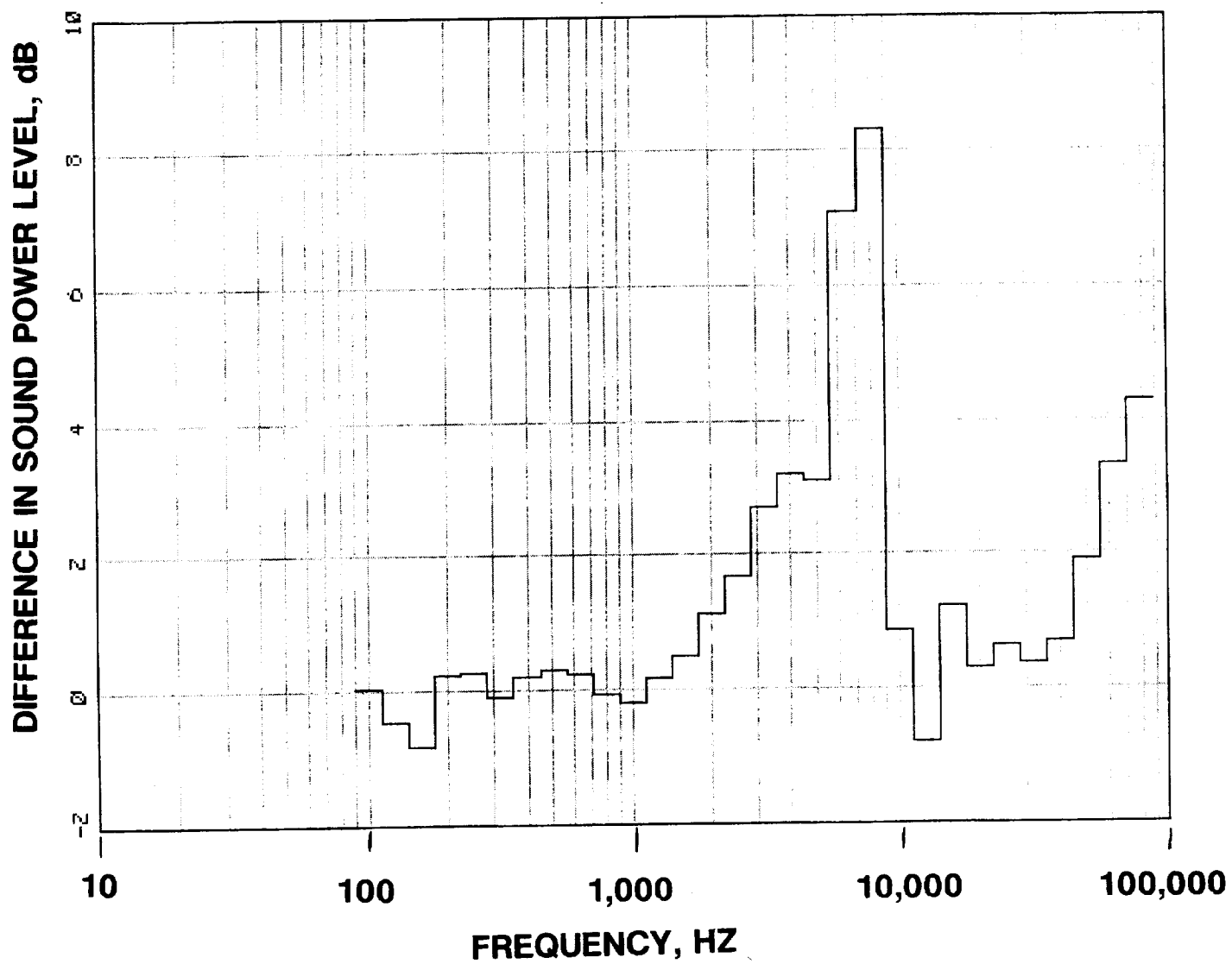


**FIGURE 60 CONTINUED**

**D 9604 RPMC**

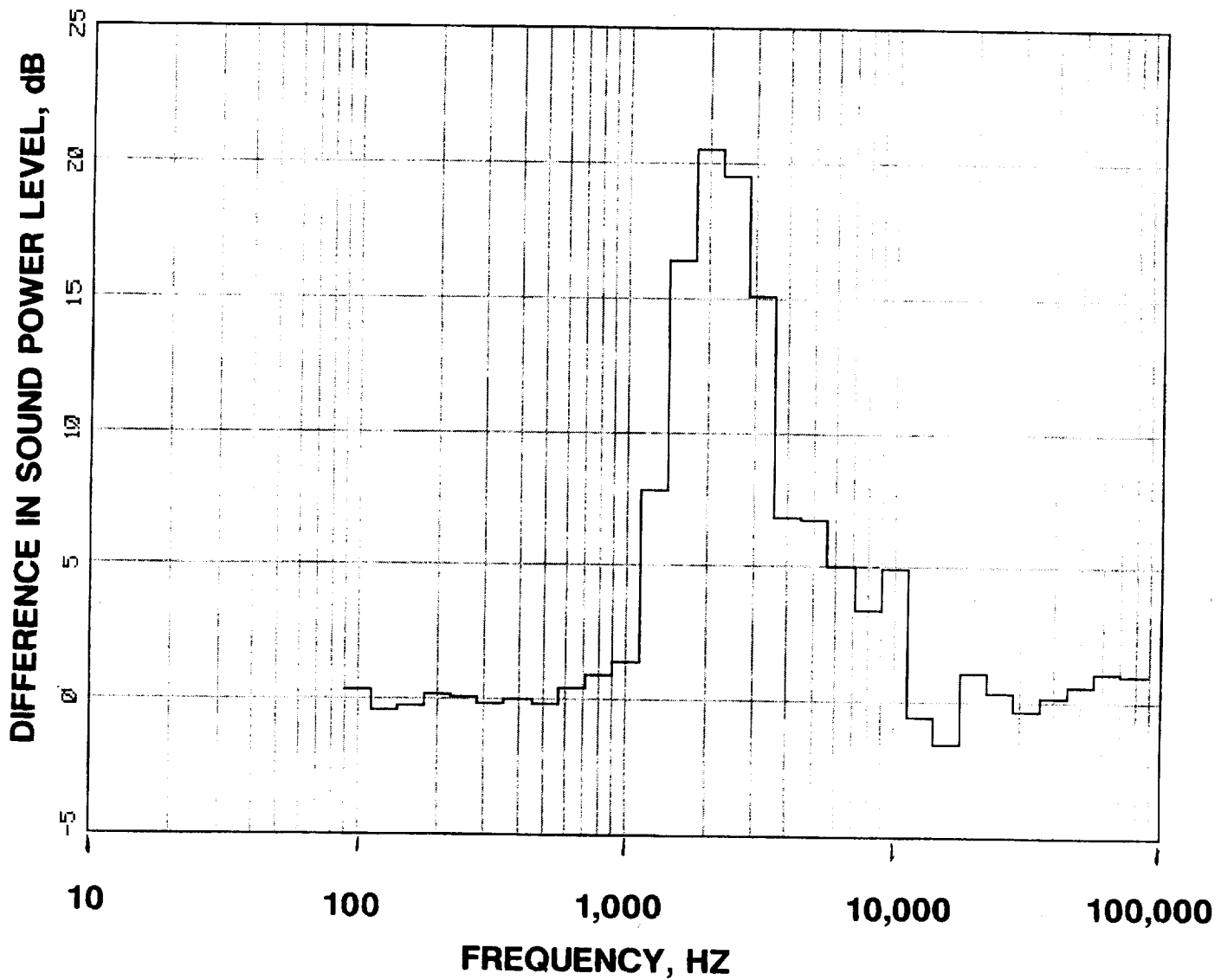


**FIGURE 60 CONTINUED**

**E 10137 RPMC**

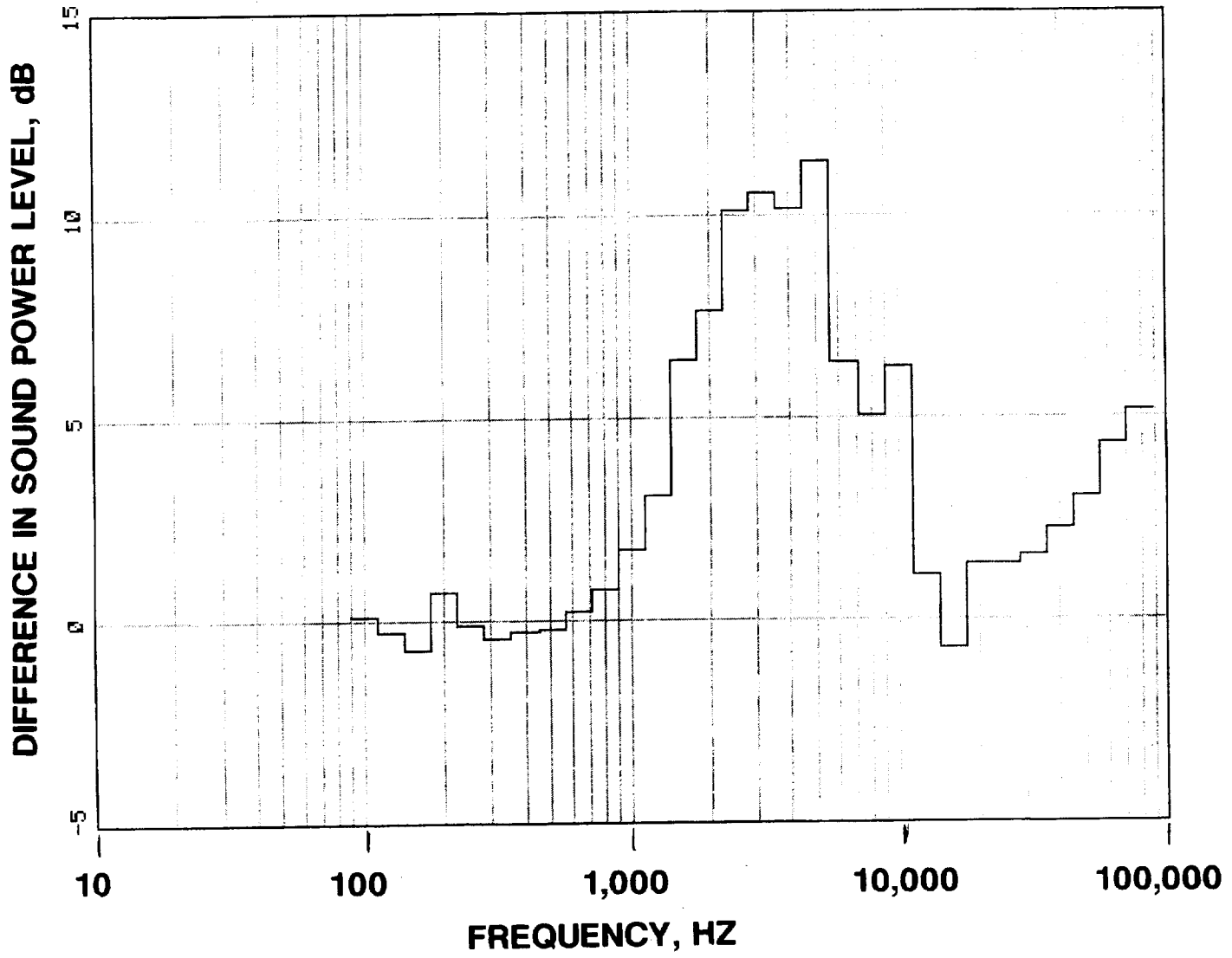


**FIGURE 60 CONCLUDED**

**F 10671 RPMC**

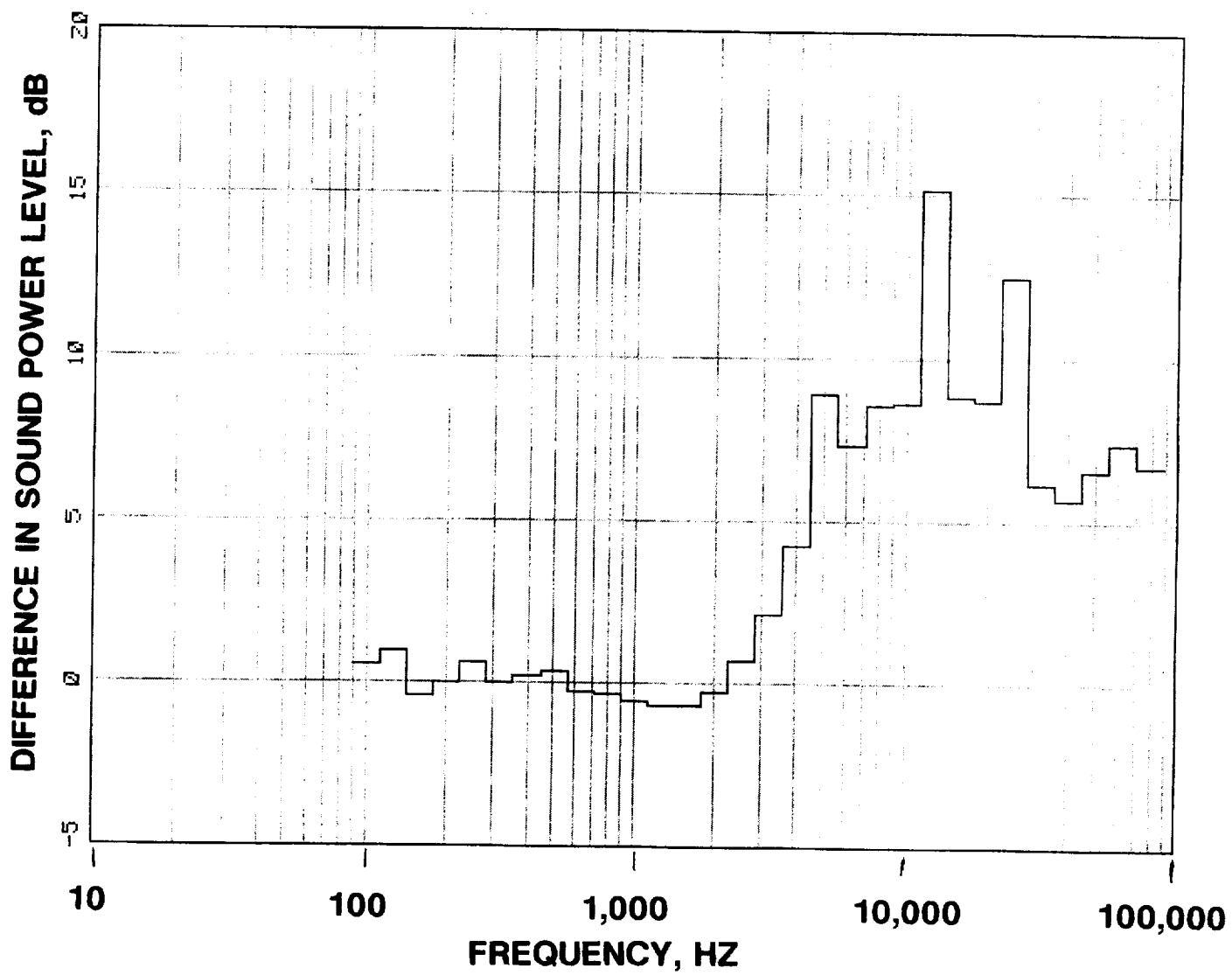


**FIGURE 61 DIFFERENCE IN AFT SOUND POWER LEVEL,**

**HARD MINUS TREATED, FOR THE 70 VANE CONFIGURATION**

**A 6402 RPMC**

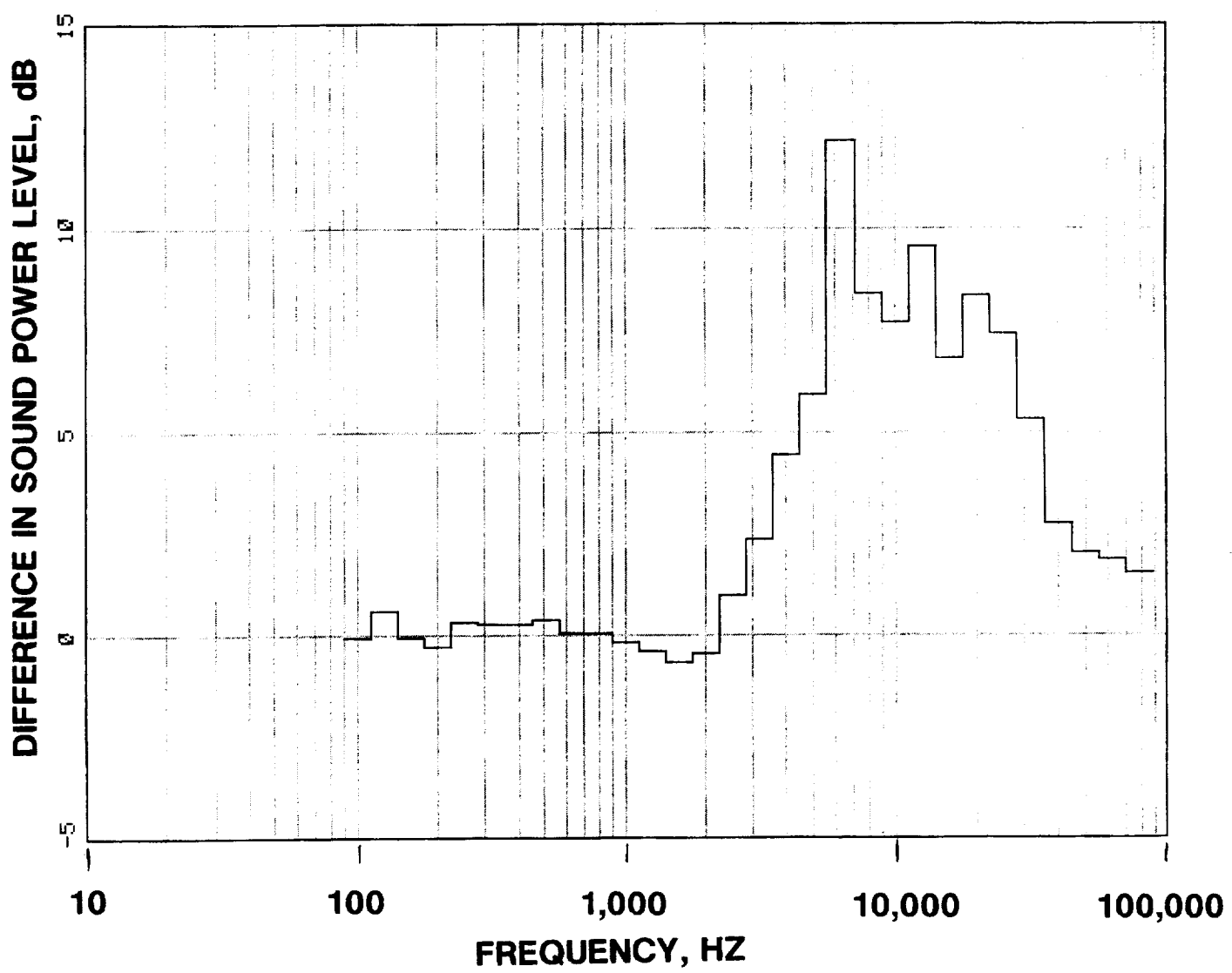


**FIGURE 61 CONTINUED**

**B 7736 RPMC**

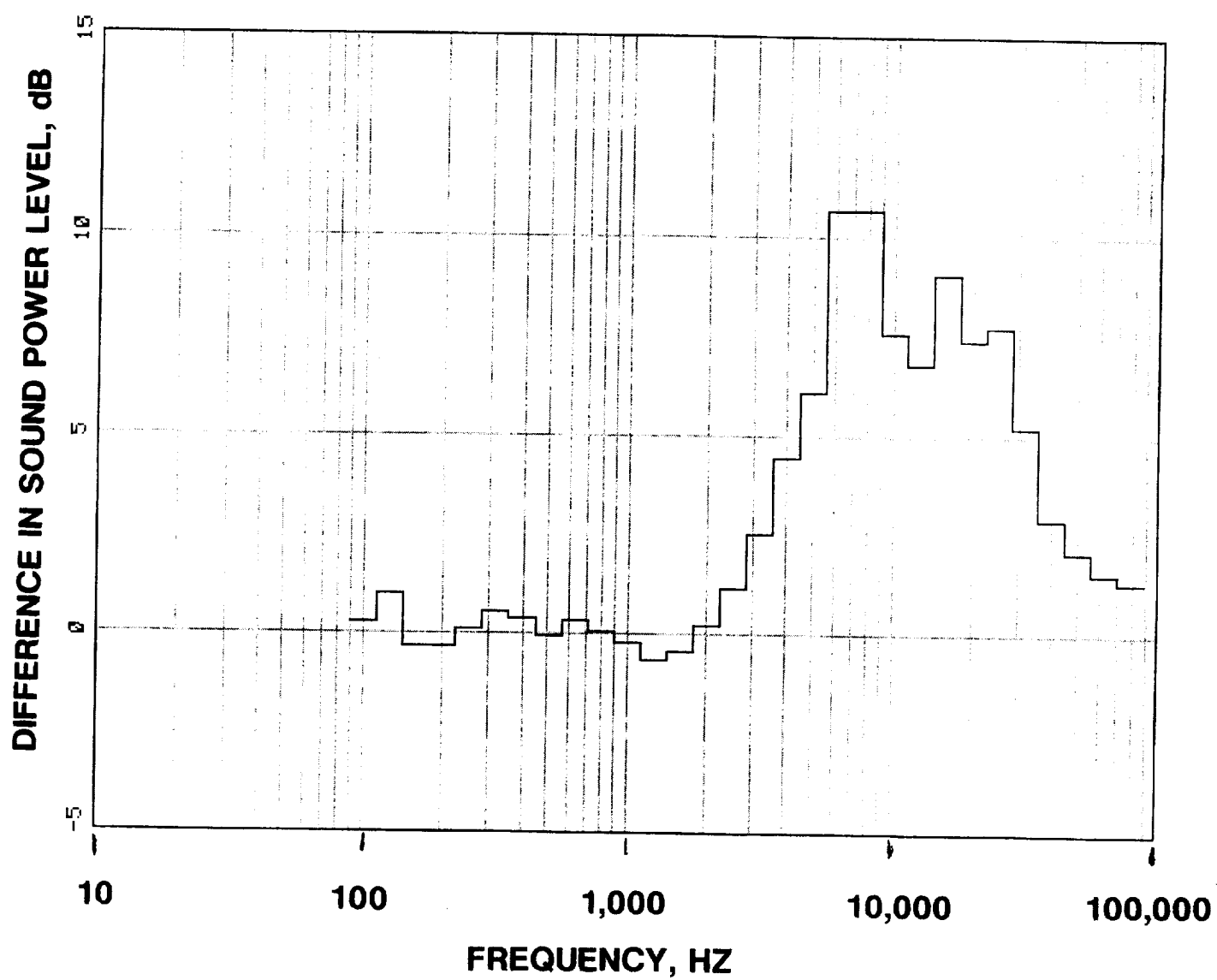


**FIGURE 61 CONTINUED**

**C 8537 RPMC**

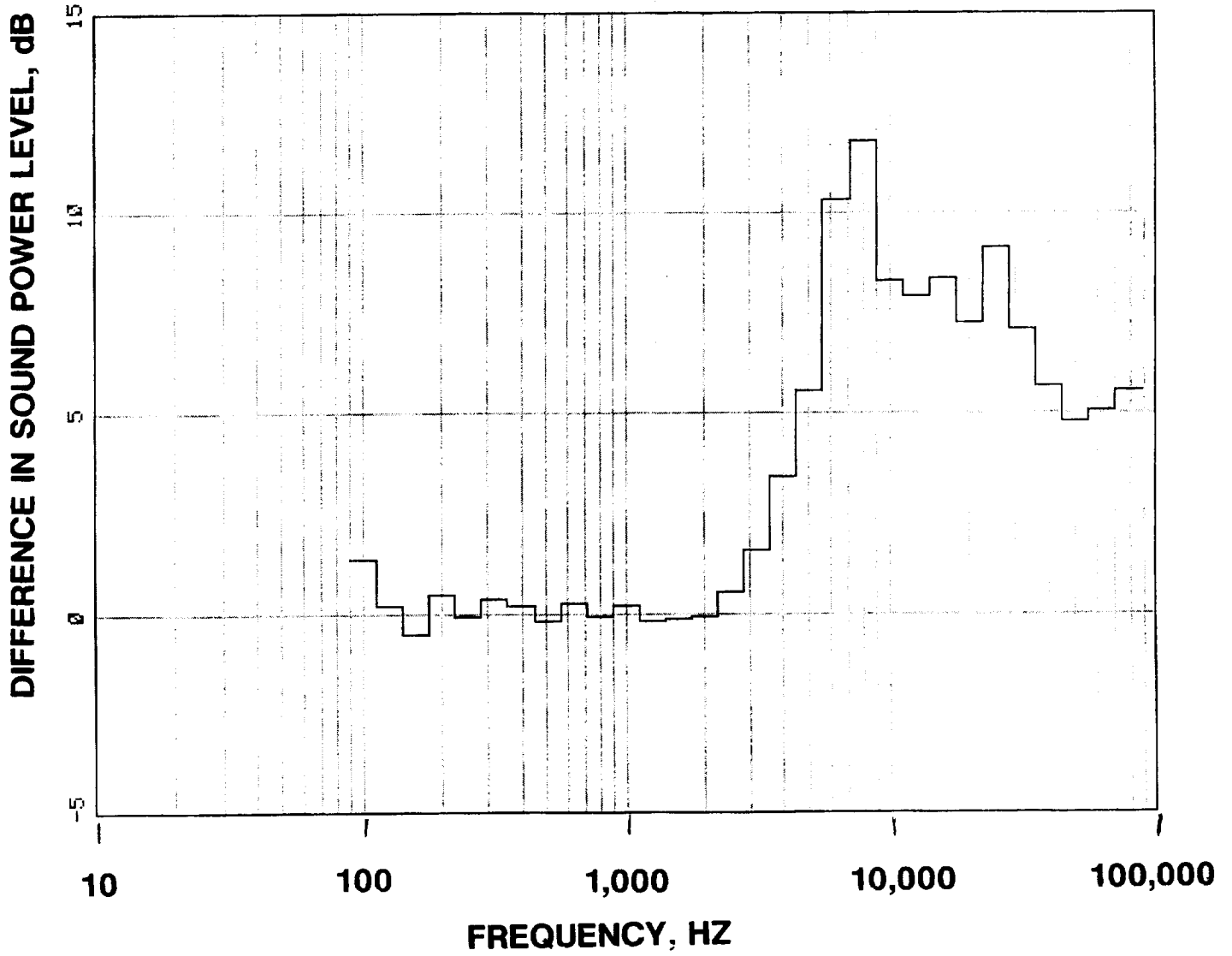


**FIGURE 61 CONTINUED**

**D 9604 RPMC**

**DIFFERENCE IN SOUND POWER LEVEL, dB**

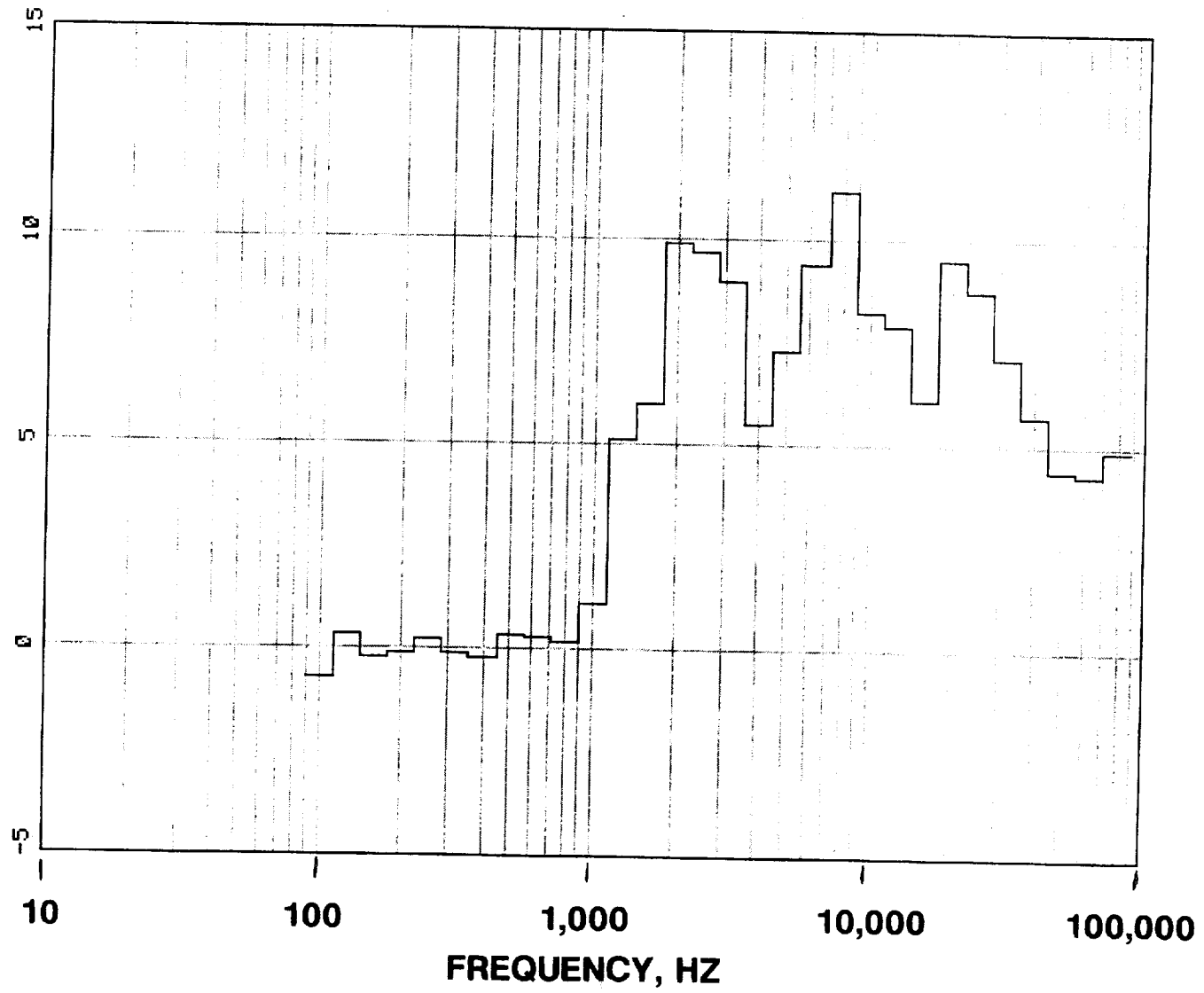


**FIGURE 61 CONTINUED**

**E 10137 RPMC**

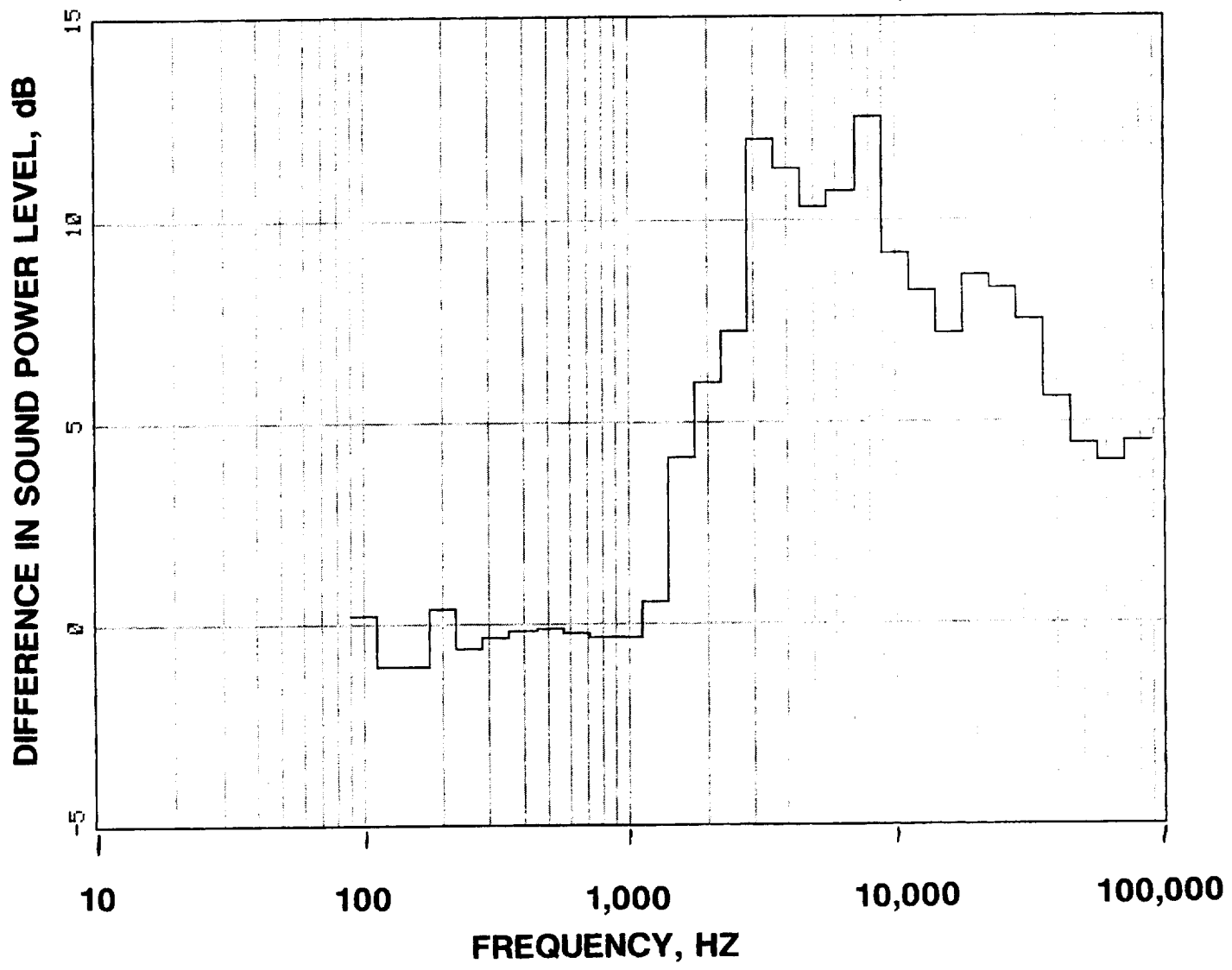


**FIGURE 61 CONCLUDED**

**F 10671 RPMC**



# Appendix A

The following pages are the output from a compressor design program that was used to design the Alternative Low Noise Fan. The program uses 11 streamlines with number 1 being at the tip and number 11 at the hub. The program uses 12 axial stations. Stations 1 to 3 are upstream of the rotor. Station 4 is the inlet to the rotor and station 5 is the rotor outlet. Station 6 is between the rotor and stator. Station 7 is the stator inlet and station 8 is the stator outlet. Stations 9 to 12 are downstream of the stator. The column headings for each station are for the most part self explanatory and the values are presented in English units.



\*\*\* INPUT DATA FOR COMPRESSOR DESIGN PROGRAM \*\*\*

PAGE NO. 1

LOW NOISE STAGE --- HIGH ASPECT RATIO---LOSS ALLOWANCE DAMPER

SCALE FACTOR IS 1.1000

THE COMPRESSOR ROTATIONAL SPEED IS 11670.9 RPM.

THE DESIRED COMPRESSOR PRESSURE RATIO IS 1.300 .

CALCULATIONS WILL BE PERFORMED ON 11 STREAMLINES .  
CALCULATIONS WILL BE MADE AT THE BLADE EDGES AND AT 8 ANNULAR STATIONS.

THE INLET FLOW RATE IS 77.803 (lb/sec).

THE MOLECULAR WEIGHT IS 28.97 .

THE COMPRESSOR HAS 2 BLADE ROWS.

THE SPECIFIC HEAT POLYNOMIAL IS IN THE FOLLOWING FORM

$$CP = .23747E+00 + .21962E-04*T + .87791E-07*T^2 + .13991E-09*T^3 + .78056E-13*T^4 + .15043E-16*T^5$$

INPUT DISTRIBUTIONS BY STREAMLINE OR STREAMTUBE

STREAMLINE No.	INLET TOTAL TEMPERATURE (Deg. R.)	INLET TOTAL PRESSURE (Psi)	INLET WHIRL VELOCITY (Ft/Sec)	STREAMTUBE NO.	STREAMTUBE FLOW FRACTION
1	518.700	14.700	.000	1	.1000
2	518.700	14.700	.000	2	.2000
3	518.700	14.700	.000	3	.3000
4	518.700	14.700	.000	4	.4000
5	518.700	14.700	.000	5	.5000
6	518.700	14.700	.000	6	.6000
7	518.700	14.700	.000	7	.7000
8	518.700	14.700	.000	8	.8000
9	518.700	14.700	.000	9	.9000
10	518.700	14.700	.000	10	1.0000
11	518.700	14.700	.000		

## INPUT DATA POINTS FOR TIP AND HUB CONTOURS.

TIP AXIAL COORDINATE (Inches)	TIP RADIUS (Inches)	HUB AXIAL COORDINATE (Inches)	HUB RADIUS (Inches)
-4.400	11.000	-4.400	4.252
-2.200	11.000	-3.300	4.526
-1.100	11.000	-2.200	4.801
-.829	10.993	-1.100	5.076
-.535	10.962	-.550	5.214
.327	10.721	.000	5.352
1.241	10.371	1.640	5.713
2.148	10.200	2.148	5.788
2.438	10.148	2.438	5.819
3.043	10.143	3.043	5.848
4.533	10.143	4.533	5.888
6.024	10.143	6.024	5.899
6.253	10.143	6.253	5.889
6.918	10.143	6.918	5.912
7.514	10.143	7.514	5.961
8.349	10.143	8.349	6.126
9.148	10.143	9.148	6.223
9.303	10.143	9.303	6.228
10.791	10.143	10.791	6.232
12.284	10.143	12.284	6.232
18.700		18.700	6.232

THE INPUT PROFILE LOSS TABLES -  $\Omega(\bar{\mu})^n \cos(\beta\bar{\mu}) / (2.0 \cdot \text{SIGMA})$ 

\*\* PROFILE LOSS TABLE NO. 1 \*\*

PCT. PASS.	D-FACTOR	LOSS PARAM.								
.00	.3000	.0590	.4000	.0600	.5000	.0620	.6000	.0640	.7000	.0680
10.00	.3000	.0310	.4000	.0320	.5000	.0340	.6000	.0360	.7000	.0400
20.00	.3000	.0200	.4000	.0210	.5000	.0220	.6000	.0230	.7000	.0240
30.00	.3000	.0155	.4000	.0160	.5000	.0170	.6000	.0180	.7000	.0190
40.00	.3000	.0130	.4000	.0140	.5000	.0150	.6000	.0160	.7000	.0170
50.00	.3000	.0100	.4000	.0110	.5000	.0120	.6000	.0130	.7000	.0140
60.00	.3000	.0100	.4000	.0110	.5000	.0120	.6000	.0130	.7000	.0140
70.00	.3000	.0100	.4000	.0110	.5000	.0120	.6000	.0130	.7000	.0140
80.00	.3000	.0100	.4000	.0110	.5000	.0120	.6000	.0130	.7000	.0140
90.00	.3000	.0220	.4000	.0230	.5000	.0240	.6000	.0250	.7000	.0260
100.00	.3000	.0300	.4000	.0370	.5000	.0450	.6000	.0600	.7000	.0900

\*\* PROFILE LOSS TABLE NO. 2 \*\*

PCT. PASS.	D-FACTOR	LOSS PARAM.								
.00	.3000	.0139	.4000	.0166	.5000	.0203	.6000	.0260	.7000	.0338
10.00	.3000	.0112	.4000	.0130	.5000	.0160	.6000	.0202	.7000	.0263
20.00	.3000	.0160	.4000	.0178	.5000	.0206	.6000	.0260	.7000	.0330
30.00	.3000	.0160	.4000	.0178	.5000	.0206	.6000	.0260	.7000	.0330
40.00	.3000	.0080	.4000	.0089	.5000	.0103	.6000	.0130	.7000	.0165
50.00	.3000	.0080	.4000	.0089	.5000	.0103	.6000	.0130	.7000	.0165
60.00	.3000	.0080	.4000	.0089	.5000	.0103	.6000	.0130	.7000	.0165
70.00	.3000	.0080	.4000	.0089	.5000	.0103	.6000	.0130	.7000	.0165
80.00	.3000	.0090	.4000	.0103	.5000	.0122	.6000	.0153	.7000	.0200
90.00	.3000	.0092	.4000	.0110	.5000	.0140	.6000	.0182	.7000	.0243
100.00	.3000	.0104	.4000	.0127	.5000	.0168	.6000	.0221	.7000	.0296

\*\*\* PRINTOUT OF INPUT STATION DATA \*\*\*

\*\* INPUT SET NO. 1 IS AN ANNULAR STATION \*\*

TIP AXIAL LOCATION (Inches)	HUB AXIAL LOCATION (Inches)	TIP BLOCKAGE FACTOR	HUB BLOCKAGE FACTOR	MASS BLEED FRACTION
-4.4000	-4.4000	.0000	.0000	.0000

\*\* INPUT SET NO. 2 IS AN ANNULAR STATION \*\*

TIP AXIAL LOCATION (Inches)	HUB AXIAL LOCATION (Inches)	TIP BLOCKAGE FACTOR	HUB BLOCKAGE FACTOR	MASS BLEED FRACTION
-2.2000	-2.2000	.0000	.0000	.0000

\*\* INPUT SET NO. 3 IS AN ANNULAR STATION \*\*

TIP AXIAL LOCATION (Inches)	HUB AXIAL LOCATION (Inches)	TIP BLOCKAGE FACTOR	HUB BLOCKAGE FACTOR	MASS BLEED FRACTION
-1.1000	-1.1000	.0000	.0000	.0000

## \*\*\* PRINTOUT OF INPUT STATION DATA \*\*\*

\*\* INPUT SET NO. 4 IS ROTOR NO. 1 \*\*

\* FOR THIS BLADE ROW THE INPUT OPTIONS ARE COORD, FAB. DATA SET \*

TIP C.G. AXIAL LOCATION	HUB C.G. AXIAL LOCATION	INLET TIP BLOCKAGE	INLET HUB BLOCKAGE	INLET MASS BLEED
(Inches)	(Inches)			
.3982	.3982	.0000	.0000	.0000

LOSS SET USED	BLADE TILT ANGLE	OUTLET TIP BLOCKAGE	OUTLET HUB BLOCKAGE	OUTLET MASS BLEED
	(Degrees)			
2	.0000	.0000	.0000	.0000

TIP D FACTOR LIMIT	HUB FLOW ANGLE LIMIT	TIP SOLIDITY	NUMBER OF BLADES	CUM ENERGY ADD FRACT.
	(Degrees)			
.9000	-90.0000	1.3440	106	1.0000

\* POLYNOMIAL COEFS. FOR RADIAL PROFILES OF A BLADE AERO. PARAMETER AND BASIC BLADE ELEMENT GEOMETRY PARAMETERS \*

COEF.	ROTOR OUTLET PRESSURE	L.E. RADIUS/CHORD	T.E. RADIUS/CHORD	MAX. THICKNESS/CHORD	CHORD/TIP CHORD
CONSTANT				.0045	.0370
LINEAR	.0000	.0000	.0000	.0000	.0550
QUADRATIC	.0000	.0000	.0000	.0000	.0000
CUBIC	.0000	.0000	.0000	.0000	.0000
QUARTIC	.0000	.0000			
QUINTIC	.0000				

\* INPUT BLADE ELEMENT DEFINITION OPTIONS \*

INCIDENCE ANGLE	DEVIATION ANGLE	TURNING RATE RATIO	TRANS. PT.	CHOKE MARGIN	BLADE MATERIAL DENSITY (lb/(in) <sup>3</sup> )
TABLE (S.S.REF.)	TABLE	CIRCULAR ARC	CIRCULAR ARC	NONE	.16000

\* TABLE OF BLADE SECTION DESIGN VARIABLES INPUT \*

(VARIABLES CONTROLLED BY OTHER OPTIONS WILL APPEAR AS ZEROS IN THE TABLE.)

SUCTION SURFACE

STREAMLINE NUMBER	INCIDENCE ANGLE (DEGREES)	DEVIATION ANGLE (DEGREES)	INLET/OUTLET TURNING RATE RATIO	TRANSITION/CHORD LOCATION	(MAX - TRANSITION) LOCATION/CHORD
1	.0000	7.0000	1.0000	.5000	.0000
2	.0000	5.9000	1.0000	.5000	.0000
3	.0000	5.7000	1.0000	.5000	.0000
4	.0000	5.8000	1.0000	.5000	.0000
5	.0000	6.1000	1.0000	.5000	.0000
6	.0000	6.4000	1.0000	.5000	.0000
7	.0000	6.9000	1.0000	.5000	.0000
8	.0000	7.4000	1.0000	.5000	.0000
9	.0000	7.8000	1.0000	.5000	.0000
10	.0000	8.2000	1.0000	.5000	.0000
11	.0000	8.5000	1.0000	.5000	.0000

\*\*\* PRINTOUT OF INPUT STATION DATA \*\*\*

\*\* INPUT SET NO. 5 IS AN ANNULAR STATION \*\*

TIP AXIAL LOCATION (Inches)	HUB AXIAL LOCATION (Inches)	TIP BLOCKAGE FACTOR	HUB BLOCKAGE FACTOR	MASS BLEED FRACTION
3.6500	3.8500	.0000	.0000	.0000

NUMBER	(DEGREES)	RATE RATIO (DEGREES)	LOCATION	LOCATION/CHORD
			.0000	.0000
1	.0000	5.3000	1.0000	.5000
2	.0000	4.5000	1.0000	.5000
3	.0000	4.4000	1.0000	.5000
4	.0000	4.5000	1.0000	.5000
5	.0000	4.0000	1.0000	.5000
6	.0000	4.0000	1.0000	.5000
7	.0000	5.1000	1.0000	.5000
8	.0000	5.5000	1.0000	.5000
9	.0000	5.9000	1.0000	.5000
10	.0000	6.5000	1.0000	.5000
11	.0000	7.1000	1.0000	.5000
		7.6000	1.0000	.5000

\*\*\* PRINTOUT OF INPUT STATION DATA \*\*\*

\*\* INPUT SET NO. 6 IS A GUIDE VANE OR STATOR\*\*

\* FOR THIS BLADE ROW THE INPUT OPTIONS ARE CHORD, FAB. DATA SET \*

TIP C.G. AXIAL LOCATION	HUB C.G. AXIAL LOCATION	INLET TIP BLOCKAGE	INLET HUB BLOCKAGE	INLET MASS BLEED
(Inches)	(Inches)			
8.3050	8.3050	.0000	.0000	.0000
LOSS SET USED	BLADE TILT ANGLE	OUTLET TIP BLOCKAGE	OUTLET HUB BLOCKAGE	OUTLET MASS BLEED
	(Degrees)			
1	.0000	.0000	.0000	.0000
HUB D FACTOR LIMIT	INLET HUB MACH LIMIT	TIP SOLIDITY	NUMBER OF BLADES	
1.2000	1.5000	1.8110	14	

\* POLYNOMIAL COEFFS. FOR RADIAL PROFILES OF A BLADE AERO. PARAMETER AND BASIC BLADE ELEMENT GEOMETRY PARAMETERS \*

COEF. STATOR OUTLET V(0) L.E. RADIUS/CHORD T.E. RADIUS/CHORD MAX. THICKNESS/CHORD CHORD/TIP CHORD

INV.SQ.	.00			
INVERSE	.00			
CONSTANT	.00	.0050	.0050	.0500
LINEAR	.00	.0000	.0000	-.0100
QUADRATIC	.00	.0000	.0000	.0000
CUBIC		.0000	.0000	.0000

\* INPUT BLADE ELEMENT DEFINITION OPTIONS \*

INCIDENCE ANGLE	DEVIATION ANGLE	TURNING RATE RATIO	TRANS. PT.	CHOKE MARGIN
TABLE (S.S.REF.)	TABLE	CIRCULAR ARC	CIRCULAR ARC	NONE

\* TABLE OF BLADE SECTION DESIGN VARIABLES INPUT \*

(VARIABLES CONTROLLED BY OTHER OPTIONS WILL APPEAR AS ZEROS IN THE TABLE.)

STREAMLINES SURFACE INCIDENCE ANGLE DEVIATION ANGLE INLET/OUTLET TURNING TRANSITION/CHORD (MAX - TRANSITION)

## \*\*\* PRINTOUT OF INPUT STATION DATA \*\*\*

\*\* INPUT SET NO. 7 IS AN ANNULAR STATION \*\*

TIP AXIAL LOCATION (Inches)	HUB AXIAL LOCATION (Inches)	TIP BLOCKAGE FACTOR	HUB BLOCKAGE FACTOR	MASS BLEED FRACTION
13.2000	13.2000	.0000	.0000	.0000

\*\* INPUT SET NO. 8 IS AN ANNULAR STATION \*\*

TIP AXIAL LOCATION (Inches)	HUB AXIAL LOCATION (Inches)	TIP BLOCKAGE FACTOR	HUB BLOCKAGE FACTOR	MASS BLEED FRACTION
15.4000	15.4000	.0000	.0000	.0000

\*\* INPUT SET NO. 9 IS AN ANNULAR STATION \*\*

TIP AXIAL LOCATION (Inches)	HUB AXIAL LOCATION (Inches)	TIP BLOCKAGE FACTOR	HUB BLOCKAGE FACTOR	MASS BLEED FRACTION
17.6000	17.6000	.0000	.0000	.0000

\*\* INPUT SET NO. 10 IS AN ANNULAR STATION \*\*

TIP AXIAL LOCATION (Inches)	HUB AXIAL LOCATION (Inches)	TIP BLOCKAGE FACTOR	HUB BLOCKAGE FACTOR	MASS BLEED FRACTION
18.7000	18.7000	.0000	.0000	.0000

\*\*\* COMPUTED COMPRESSOR DESIGN PARAMETERS FOR A ROTATIONAL SPEED OF, 11670.9, RPM \*\*\*

\*\* THE CORRECTED WEIGHTFLOW PER UNIT OF CASING ANNULAR AREA AT THE INLET FACE OF THE FIRST BLADE ROW IS 40.61 Lb/sec/ft<sup>2</sup> \*\*

## \*\* MASS AVERAGED ROTOR AND STAGE AERODYNAMIC PARAMETERS \*\*

STAGE BLADE NO. TYPE	FLOW COEF.	HEAD COEF.	ID. HEAD PRESS.	TOTAL TEMP.	ADIA. RATIO	POLY. EFF.	ASPECT RATIO	FOR. AX. GAS BENDING MOMENTS		POWER (hp)
								SHAFT THRUST (Lbs)	FOR. AX. TANG. (Ft-lbs) (Ft-lbs)	
1 ROTOR	.5731	.2199	.2456	1.3315	1.0953	.8952	.8994	.626	759.63	2.064 -1.807
1 STATOR	.6566	.2098	.2456	1.3000	1.0953	.8175	.8242	.50	-340.49	1.928 10.433

## \*\* CUMULATIVE SUMS OF MASS AVERAGED ROTOR AND STAGE AERODYNAMIC PARAMETERS \*\*

STAGE BLADE NO. TYPE	WEIGHT FLOW (lb/sec)	TOTAL PRESS. (psia)	TOTAL TEMP. (Deg R.)	HEAD COEF.	IDEAL HEAD COEF.	ADIA. EFF.	POLY. EFF.	FOR. AX. POWER		FRACT ENERGY (hp)
								SHAFT THRUST (Lbs)	TORQUE (Ft-lbs)	
1 INLET	77.80	14.700	518.70							
1 ROTOR	77.80	19.572	568.11	1.3315	1.0953	.2199	.2456	.8952	.8994	759.63
1 STATOR	77.80	19.109	568.11	1.3000	1.0953	.2098	.2456	.8175	.8242	419.14

## \*\* VALUES OF PARAMETERS ON STREAMLINES AT STATION, 3, WHICH IS AN ANNULUS \*\*

STREAMLINE NO. RADIUS (In.)	AXIAL COORD. (In.)	AXIAL VEL. (Ft/sec)	NERD. VEL. (Ft/sec)	TANG. VEL. (Ft/sec)	ABS. VEL. (Ft/sec)	ABS. FLOW MACH NO.	STREAM. ANGLE (Deg)	STREAM. SLOPE (Deg)	STREAM. CURV. (1./In.)	TOTAL PRESS. (Psi)	TOTAL PRESS. (Psi)	STATIC TEMP. (deg.R.)	STATIC PRESS. (Psi)	STATIC TEMP. (deg.R.)
TIP 11.000	-1.100	459.96	460.38	.00	460.38	.4194	.00	-2.42	-.124	16.700	518.70	13.023	501.03	
1 11.000	-1.100	488.10	489.47	.00	489.47	.4470	.00	-4.28	-.126	16.700	518.70	12.815	498.73	
2 10.498	-1.100	517.26	518.74	.00	518.74	.4749	.00	-6.33	-.104	16.700	518.70	12.596	496.27	
3 9.996	-1.100	543.49	544.53	.00	544.53	.4996	.00	-3.53	-.081	16.700	518.70	12.394	493.99	
4 9.489	-1.100	565.32	565.73	.00	565.73	.5201	.00	-2.20	-.060	16.700	518.70	12.223	492.02	
5 8.972	-1.100	582.22	582.24	.00	582.24	.5362	.00	-.54	-.044	16.700	518.70	12.086	490.44	
6 8.438	-1.100	594.14	594.31	.00	594.31	.5479	.00	1.40	-.031	16.700	518.70	11.985	489.26	
7 7.878	-1.100	600.83	602.06	.00	602.06	.5555	.00	3.67	-.020	16.700	518.70	11.919	488.49	
8 7.282	-1.100	601.72	605.42	.00	605.42	.5588	.00	6.34	-.012	16.700	518.70	11.890	488.15	
9 6.635	-1.100	603.92	603.92	.00	603.92	.5573	.00	9.63	-.005	16.700	518.70	11.903	488.30	
10 5.913	-1.100	597.59	597.59	.00	597.59	.5511	.00	14.00	-.002	16.700	518.70	11.957	488.93	
11 5.076	-1.100													
HUB 5.076	-1.100													

1

INLET STREAM LINE						LAYOUT CONE					
STREAM LINE NO.	INC. PCT.	S.S. INC. ANGLE	IN.BLADE ANGLE	IN.BLADE TRAN.PT.	BLD.SET	1st SEG.	MACH NO.	SH.LOC.	COV.CHAN.	MIN.CHK.	L.E.EDGE
PASS.	(Deg)	(Deg)	(Deg)	(Deg)	(Deg)	S.S.CAM.	AT SHOCK	AS FRACT	PT.LOG.IN	CIR.CENT	R*D0/DR
1	.00	3.24	.00	62.75	62.51	55.99	55.97	9.76	1.3339	.6354	.3646
2	8.81	3.80	.00	57.94	57.91	53.15	53.14	8.57	1.2863	.5794	.4206
3	17.28	4.34	.00	54.71	54.73	50.30	50.29	8.77	1.2626	.5343	.4657
4	25.80	4.87	.00	51.89	51.90	47.42	47.42	9.35	1.2419	.4896	.5104
5	34.53	5.42	.00	49.19	49.19	44.49	44.48	10.12	1.2211	.4456	.5546
6	43.58	5.98	.00	46.48	46.48	41.37	41.37	11.09	1.2008	.4012	.5988
7	53.08	6.56	.00	43.72	43.73	37.57	37.57	12.72	1.1681	.3555	.6445
8	63.18	7.17	.00	40.83	40.86	33.23	33.24	14.79	1.1270	.3090	.6910
9	74.11	7.81	.00	37.71	37.76	28.05	28.07	17.52	1.0791	.2613	.7387
10	86.19	8.47	.00	34.21	34.29	21.58	21.62	21.18	1.0219	.2118	.7882
11	100.00	9.15	.00	30.28	30.36	13.82	13.92	25.69	.9455	.1611	.8242

\*\* VALUES OF PARAMETERS ON STREAMLINES AT STATION, 5, WHICH IS THE OUTLET OF ROTOR NUMBER, 1 \*\*

STREAMLINE NO. RADIUS (In.)	AXIAL COORD. (In.)	AXIAL VEL. (Ft/sec)	HEAD. VEL.	TANG. (Ft/sec)	ABS. VEL.	ABS. VEL.	ABS. FLOW STREAM. (Ft/sec)	MACH NO. (deg)	ANGLE (deg)	SLOPE (deg)	STREAM. CURV. (1./in.)	TOTAL PRESS. (Psia)	TOTAL TEMP. (Deg.R.)	STATIC PRESS. (Psia)	STATIC TEMP. (Deg.R.)
TIP 10.620 .576	1 10.620 .576	.486.88	521.46	293.40	598.33	.5244	29.36	-20.98	.169	19.572	.571.55	16.228	541.75		
2 10.191 .603	2 10.191 .603	518.71	533.95	295.77	610.40	.5364	28.98	-13.72	.046	19.572	.569.82	16.091	538.81		
3 9.764 .625	3 9.764 .625	533.37	540.54	313.75	625.00	.5496	30.13	-9.34	.026	19.572	.570.66	15.940	538.14		
4 9.325 .647	4 9.325 .647	540.22	543.55	330.28	636.03	.5597	31.28	-6.34	.013	19.572	.570.93	15.822	537.26		
5 8.870 .668	5 8.870 .668	550.28	551.65	334.36	645.07	.5692	31.22	-4.04	.004	19.572	.569.00	15.710	534.36		
6 8.401 .689	6 8.401 .689	561.01	561.27	338.15	655.26	.5799	31.07	-1.76	-.005	19.572	.566.88	15.583	531.13		
7 7.910 .714	7 7.910 .714	568.50	568.52	356.28	670.94	.5950	32.07	.55	-.015	19.572	.566.50	15.404	529.02		
8 7.390 .739	8 7.390 .739	575.55	576.27	378.29	689.34	.6127	33.28	2.86	-.025	19.572	.566.12	15.190	526.55		
9 6.832 .765	9 6.832 .765	583.34	585.92	408.48	714.25	.6367	34.88	5.38	-.036	19.572	.566.04	14.898	523.56		
10 6.224 .791	10 6.224 .791	591.97	598.18	450.78	749.01	.6702	37.00	8.26	-.049	19.572	.566.29	14.482	519.57		
11 5.547 .812	11 5.547 .812	611.89	625.67	503.52	803.11	.7236	38.83	12.04	-.097	19.572	.566.08	13.810	512.36		
HUB 5.547 .812															

STREAMLINE NO. R/RTIP	REL. FLOW (deg)	REL. ANGLE	REL. TANG. VEL. (Ft/sec)	REL. VEL. (Ft/sec)	REL. MACH NUMBER	WHEEL SPEED (Ft/sec)	FLOW COEF.	HEAD COEF.	IDEAL HEAD ADJAB. EFF.	DIFFUSION FACTOR	LOSS COEF.	SHOCK LOSS COEF.	SHOCK LOSS COEF.	DEGREE REACTION
TIP 1.0000	1 1.0000	56.51	788.20	945.08	.8282	1081.60	.4430	.2199	.2628	.8369	.3058	.0958	.0285	.7006
2 .9596	2 .9596	54.27	742.19	914.30	.8034	1037.95	.4720	.2199	.2542	.8652	.3217	.0778	.0209	.7919
3 .9195	3 .9195	51.55	680.73	869.24	.7643	994.48	.4853	.2199	.2583	.8513	.3490	.0889	.0177	.8245
4 .8781	4 .8781	48.73	619.45	824.11	.7252	949.73	.4916	.2199	.2597	.8468	.3739	.0945	.0152	.8645
5 .8353	5 .8353	45.89	569.06	792.56	.6993	903.42	.5007	.2199	.2501	.8793	.3821	.0746	.0128	.8552
6 .7910	6 .7910	42.67	517.43	763.39	.6756	855.58	.5105	.2199	.2395	.9181	.3868	.0508	.0106	.8552
7 .7448	7 .7448	38.32	449.33	724.65	.6426	805.61	.5173	.2199	.2376	.9254	.4026	.0481	.0073	.8367
8 .6959	8 .6959	33.01	376.36	687.19	.6108	752.65	.5237	.2199	.2357	.9328	.4160	.0453	.0038	.8035
9 .6434	9 .6434	26.13	287.40	652.61	.5817	695.87	.5308	.2199	.2354	.9344	.4255	.0471	.0012	.7469
10 .5861	10 .5861	17.02	183.14	625.59	.5598	633.92	.5387	.2199	.2366	.9294	.4247	.0549	.0000	.6576
11 .5223	11 .5223	5.61	61.42	628.67	.5664	566.94	.5668	.2199	.2355	.9337	.3795	.0570	.0000	.4984
HUB .5223														

## \*\* VALUES OF PARAMETERS ON STREAMLINES AT STATION, 6, WHICH IS AN ANNULUS \*\*

STREAMLINE NO. RADIUS (In.)	AXIAL COORD. (In.)	AXIAL VEL. (Ft/sec)	HEED. VEL. (Ft/sec)	TANG. VEL. (Ft/sec)	ABS. VEL. (Ft/sec)	ABS. FLOW STREAM. MACH NO.	STREAM. ANGLE (Deg)	STREAM. CURV. (1./In.)	TOTAL PRESS. (Psi)	TOTAL PRESS. (Psi)	STATIC TEMP. (Deg.R.)	STATIC TEMP. (Deg.R.)
TIP 10.152	3.850											
1 10.152	3.850	742.81	742.82	306.92	803.73	.7204	22.45	-.34	.023	19.572	571.52	13.850
2 9.819	3.850	737.29	737.64	306.96	798.96	.7169	22.59	-1.77	.037	19.572	569.81	13.895
3 9.472	3.850	726.86	727.34	323.41	796.00	.7134	23.97	-2.08	.035	19.572	570.64	13.939
4 9.106	3.850	718.26	718.65	338.18	794.24	.7115	25.20	-1.88	.031	19.572	570.92	13.964
5 8.723	3.850	715.00	715.22	339.97	791.91	.7105	25.42	-1.42	.026	19.572	569.00	13.976
6 8.322	3.850	713.58	713.67	341.29	791.08	.7111	25.56	-.94	.020	19.572	566.89	13.968
7 7.900	3.850	710.66	710.68	356.67	795.16	.7154	26.65	-.43	.013	19.572	566.51	13.914
8 7.452	3.850	708.42	708.42	375.14	801.61	.7221	27.90	-.17	.006	19.572	566.13	13.829
9 6.970	3.850	707.89	707.96	400.38	813.34	.7338	29.49	.83	-.002	19.572	566.05	13.680
10 6.448	3.850	709.54	709.81	435.12	832.56	.7529	31.51	1.57	-.013	19.572	566.31	13.438
11 5.873	3.850	713.81	714.50	475.59	858.31	.7791	33.65	2.52	-.007	19.572	566.09	13.103
HUB	5.873	3.850										

STREAMLINE NO.	PRESS. PCT.	TEMP. RATIO	AERO. CHORD (in.)	ELEMENT SOLIDITY RADIUS (in.)	LOCAL BLADE FORCES			T.E.RAD. (in.)	DEV. OUT.BLADE ANGLE	OUT.BLADE ANGLE	Camber	MAX.CAMB.	T.E.EDGE PT.LOC.	CIR.CENT	MAX.CAMB. PT.LOC.	CIR.CENT	R*DO/DR	/CHORD (Deg)	/CHORD (Deg)	LAYOUT CONE (Deg)
					TANG.	(lb/in)	(lb/in)													
1	.00	1.3315	1.1019	.8399	1.3236	10.705	2.3636	-1.4751	.0045	7.00	49.51	49.47	13.03	.5013	.0783					
2	8.45	1.3315	1.0986	.8465	1.3931	10.251	2.2343	-1.5036	.0045	5.90	48.37	48.38	9.53	.5000	.0707					
3	16.86	1.3315	1.1002	.8434	1.4507	9.808	2.0506	-1.5990	.0045	5.70	45.85	45.87	8.86	.5000	.0623					
4	25.52	1.3315	1.1007	.8417	1.5177	9.356	1.8831	-1.6452	.0045	5.80	42.73	42.94	8.96	.5000	.0546					
5	34.49	1.3315	1.0970	.8407	1.5952	8.891	1.7529	-1.6138	.0045	6.10	39.79	39.79	9.40	.5000	.0507					
6	43.75	1.3315	1.0929	.8401	1.6051	8.410	1.6268	-1.5679	.0045	6.40	36.27	36.27	10.21	.5000	.0550					
7	53.42	1.3315	1.0922	.8399	1.7921	7.907	1.4497	-1.5668	.0045	6.90	31.42	31.42	12.31	.5000	.0607					
8	63.67	1.3315	1.0914	.8405	1.9235	7.372	1.3056	-1.5559	.0045	7.40	25.61	25.61	15.25	.5000	.0656					
9	74.66	1.3315	1.0913	.8426	2.0916	6.796	1.1219	-1.5454	.0045	7.80	18.33	18.34	19.42	.5000	.0753					
10	86.65	1.3315	1.0918	.8475	2.3198	6.163	.9075	-1.5328	.0045	8.20	8.82	8.86	25.43	.4984	.0873					
11	100.00	1.3315	1.0913	.8602	2.6631	5.449	.6549	-1.6084	.0045	8.50	-2.89	-2.73	33.09	.4971	.0988					

## 1 \*\* VALUES OF PARAMETERS ON STREAMLINES AT STATION, 7, WHICH IS THE INLET OF STATOR NUMBER, 1, OF STAGE NUMBER, 1\*\*

STREAMLINE NO.	AXIAL COORD. (In.)	AXIAL VEL. (Ft/sec)	VEL. (Ft/sec)	TANG. (Ft/sec)	ABS. VEL. (Ft/sec)	MACH NO.	ABS. FLOW STREAM. ANGLE (Deg)	STREAM. CURV. (1./In.)	TOTAL PRESS. (Psia)	TOTAL TEMP. (Deg.R.)	STATIC PRESS. (Psia)	STATIC TEMP. (Deg.R.)
TIP 10.147	4.247	722.84	722.84	307.08	785.36	.7023	23.02	-.07	.000	19.572	571.52	14.079
1 10.147	4.247	722.84	722.84	307.08	785.36	.7023	23.02	-.07	.000	19.572	569.81	14.045
2 9.809	4.251	724.25	724.44	307.27	786.91	.7050	22.98	-1.32	.005	19.572	569.81	14.045
3 9.458	4.264	721.41	721.68	323.87	791.02	.7085	24.17	-1.56	.007	19.572	570.64	14.002
4 9.091	4.274	719.56	719.76	338.73	795.48	.7127	25.20	-1.37	.008	19.572	570.92	13.948
5 8.709	4.274	721.75	721.85	340.53	798.14	.7166	25.26	-.96	.008	19.572	569.00	13.898
6 8.310	4.272	724.36	724.39	341.78	800.97	.7209	25.26	-.53	.008	19.572	566.89	13.844
7 7.892	4.278	724.14	724.14	357.05	807.38	.7276	26.25	-.06	.007	19.572	566.51	13.760
8 7.448	4.289	722.83	722.85	375.31	816.48	.7349	27.44	.48	.007	19.572	566.13	13.667
9 6.973	4.302	720.86	720.98	400.26	826.63	.7451	29.04	1.07	.007	19.572	566.05	13.537
10 6.456	4.323	717.82	718.14	434.59	839.40	.7598	31.18	1.70	.006	19.572	566.31	13.350
11 5.885	4.349	715.64	716.33	474.60	859.29	.7801	33.53	2.53	.008	19.572	566.09	13.091
HUB	5.885	4.349										

STREAMLINE NO. R/RTIP	FLOW COEF.	REL.FLOW ANGLE (Deg)	L.E.RAD. /CHORD	MAX.TH. /CHORD	MAX.TH. PT.LOC. /CHORD	TRAN.PT. LOCATION /CHORD	SEGMENT IN/OUT TURN RATE (DEG)	LAYOUT CONE ANG.
TIP 1.0000								
1 1.0000	.6577	45.14	.0050	.0500	.5000	.5000	1.0000	-.03
2 .9667	.6590	43.68	.0050	.0492	.5000	.5000	1.0000	-.03
3 .9322	.6565	41.54	.0050	.0484	.5000	.5000	1.0000	.06
4 .8960	.6548	39.21	.0050	.0475	.5000	.5000	1.0000	.22
5 .8583	.6568	37.13	.0050	.0466	.5000	.5000	1.0000	.41
6 .8190	.6591	34.86	.0050	.0457	.5000	.5000	1.0000	.63
7 .7778	.6589	31.67	.0050	.0447	.5000	.5000	1.0000	.88
8 .7341	.6577	27.93	.0050	.0437	.5000	.5000	1.0000	1.18
9 .6872	.6559	23.26	.0050	.0426	.5000	.5000	1.0000	1.56
10 .6363	.6532	17.25	.0050	.0413	.5000	.5000	1.0000	1.99
11 .5800	.6512	9.88	.0050	.0400	.5000	.5000	1.0000	2.46
HUB	.5800							

INLET STREAMLINE											LAYOUT CONE										
STREAMLINE NO.	PCT. PASS.	INC. ANGLE (deg)	S.S. INC. ANGLE (deg)	IN. BLADE ANGLE (deg)	BL. ANGLE (deg)	BL. SET (deg)	1st SEG. (deg)	MACH NO. (deg)	SH.LOC.	COV.CHAN.	MIN.CHK.	MIN.CHK.	L.E.EDGE	PT.LOC. IN CIR.CENT	AS FRACT AREA	OF S.S.	MARGIN	R'DD/DR COV.CHAN.			
1	.00	4.56	.00	18.46	18.46	6.58	6.58	16.44	.7922	.1517	.8044	.0879	1.0000	.1284							
2	7.92	4.47	.00	18.51	18.80	7.16	7.16	16.11	.7895	.1504	.8135	.0840	.0000	.2440							
3	16.15	4.37	.00	19.30	20.19	7.90	7.90	16.65	.7965	.1554	.8105	.0800	1.0000	.2661							
4	24.77	4.26	.00	20.94	21.17	8.34	8.34	17.09	.8058	.1566	.8097	.0744	1.0000	.1612							
5	33.75	4.15	.00	21.10	21.23	8.21	8.23	17.17	.8094	.1511	.8142	.0681	1.0000	.1028							
6	43.09	4.04	.00	21.22	21.40	8.15	8.17	17.29	.8116	.1459	.8185	.0624	1.0000	.1756							
7	52.90	3.91	.00	22.34	22.53	8.51	8.55	17.94	.8213	.1458	.8175	.0597	1.0000	.2500							
8	63.32	3.77	.00	23.66	23.83	8.95	9.00	18.65	.8328	.1454	.8171	.0554	1.0000	.2857							
9	74.48	3.62	.00	25.41	25.55	9.50	9.58	19.67	.8490	.1455	.8155	.0547	.0000	.3433							
10	86.60	3.46	.00	27.73	27.81	10.30	10.42	20.97	.8719	.1460	.8139	.0477	.0000	.3940							
11	100.00	3.27	.00	30.26	30.23	11.22	11.40	22.28	.9010	.1441	.8158	.0389	.0000	.4219							

\*\* VALUES OF PARAMETERS ON STREAMLINES AT STATION, 8, WHICH IS THE OUTLET OF STATOR NUMBER, 1, OF STAGE NUMBER, 1\*\*

STREAMLINE NO. RADIUS (In.)	AXIAL COORD. (In.)	AXIAL VEL. (Ft/sec)	HEAD. VEL. (Ft/sec)	TANG. VEL. (Ft/sec)	ABS. VEL. (Ft/sec)	MACH NO.	ABS. FLOW ANGLE (deg)	STREAM. SLOPE (deg)	STREAM. (1./In.)	STREAM. (Psi)	TOTAL PRESS. (Deg. R.)	STATIC PRESS. (Deg. R.)
TIP 10.143	12.438	.720.62	.720.62	.00	.720.62	.6396	.00	.00	.000	.18.414	.571.26	.13.981
1 10.143	12.438	.749.22	.749.22	.00	.749.22	.6682	.00	.15	-.002	.18.871	.569.71	.13.987
2 9.805	12.433	.765.11	.765.12	.00	.765.12	.6832	.00	.25	-.003	.19.097	.570.50	.13.972
3 9.468	12.432	.772.41	.772.42	.00	.772.42	.6901	.00	.32	-.003	.19.197	.570.76	.13.960
4 9.123	12.433	.775.98	.776.00	.00	.776.00	.6948	.00	.38	-.004	.19.252	.568.96	.13.942
5 8.767	12.435	.779.04	.779.06	.00	.779.06	.6992	.00	.43	-.005	.19.306	.566.99	.13.927
6 8.400	12.435	.781.41	.781.43	.00	.781.43	.7018	.00	.48	-.006	.19.332	.566.62	.13.913
7 8.017	12.433	.783.22	.783.25	.00	.783.25	.7038	.00	.51	-.007	.19.314	.566.24	.13.875
8 7.617	12.434	.781.49	.781.52	.00	.781.52	.7022	.00	.51	-.009	.19.290	.566.17	.13.878
9 7.194	12.434	.768.34	.768.37	.00	.768.37	.6890	.00	.48	-.011	.18.961	.566.42	.13.801
10 6.738	12.433	.748.49	.748.50	.00	.748.50	.6698	.00	.37	-.018	.18.560	.566.20	.13.738
11 6.232	12.432											.519.55
MIS 6.232												

STREAMLINE NO. R/TIP	FLOW COEF.	HEAD COEF.	IDEAL HEAD PO. RATIO	STATOR PO. RATIO	STAGE AD. EFF.	DIFFUSION FACTOR	STATOR LOSS COEF.	SHOCK LOSS COEF.	ELEMENT LOSS	AERO. SOLIDITY	DEGREE CHORD	REACTION (In.)
TIP 1.0000												
1 1.0000	.6557	.1715	.2628	.9408	1.2526	.6527	.1904	.2109	.0000	.1.8110	.8.2456	-.0201
2 .9867	.6818	.1909	.2542	.9642	1.2837	.7509	.1521	.1269	.0000	.1.8733	.8.2456	-.0119
3 .9334	.6962	.2003	.2583	.9757	1.2991	.7753	.1381	.0854	.0000	.1.9415	.8.2456	-.0061
4 .8994	.7029	.2045	.2597	.9808	1.3059	.7873	.1343	.0668	.0000	.2.0174	.8.2456	-.0023
5 .8564	.7061	.2068	.2501	.9836	1.3097	.8267	.1289	.0564	.0000	.2.1027	.8.2458	.0089
6 .8281	.7089	.2090	.2395	.9864	1.3134	.8725	.1239	.0465	.0000	.2.1991	.8.2460	.0170
7 .7904	.7110	.2100	.2376	.9877	1.3151	.8839	.1271	.0413	.0000	.2.3099	.8.2465	.0315
8 .7509	.7127	.2093	.2357	.9868	1.3139	.8878	.1317	.0437	.0000	.2.4396	.8.2472	.0427
9 .7092	.7111	.2083	.2354	.9856	1.3123	.8851	.1444	.0468	.0000	.2.5947	.8.2484	.0701
10 .6643	.6992	.1946	.2366	.9688	1.2899	.8226	.1755	.0983	.0000	.2.7866	.8.2502	.0927
11 .6144	.6811	.1777	.2355	.9483	1.2626	.7545	.2173	.1563	.0000	.3.0351	.8.2525	.1329
MIS	.6144											

STREAMLINE NO.	PCT. SPAN	LOCAL BLADE FORCES		T.E. RAD.		DEV. /CHORD		OUT. BLADE ANGLE		Camber		MAX. CAMB.		T.E. EDGE	
		RADIUS (In.)	FOR. AXIAL (lbf/in)	TANG. (lbf/in)	ANGLE (deg)	ANGLE (deg)	ANGLE (deg)	PT. LOC. (deg)	CIR. CENT. (deg)	/CHORD	R <sub>DD</sub> /DR				
1	.00	10.145	.5582	15.7094	.0050	5.30	-5.30	-5.30	23.76	.5000	-.1730				
2	8.64	9.807	1.0098	15.5675	.0050	4.50	-4.50	-4.47	23.27	.5000	-.1406				
3	17.27	9.463	2.0272	15.9869	.0050	4.40	-4.40	-4.38	26.57	.5000	-.0995				
4	26.09	9.107	2.5932	16.1437	.0050	4.50	-4.50	-4.50	25.66	.5000	-.0339				
5	35.18	8.738	2.6417	15.6443	.0050	4.80	-4.80	-4.80	26.03	.5000	.0054				
6	44.58	8.355	2.6895	15.0037	.0050	5.10	-5.10	-5.10	26.50	.5000	-.0160				
7	54.35	7.955	2.8932	15.0072	.0050	5.50	-5.50	-5.52	28.05	.4987	-.0439				
8	64.60	7.532	3.0230	14.9898	.0050	5.90	-5.90	-5.93	29.76	.4982	-.0497				
9	75.41	7.083	3.1856	14.8024	.0050	6.50	-6.50	-6.56	32.11	.4975	-.0605				
10	87.06	6.597	2.8212	14.6901	.0050	7.10	-7.10	-7.22	35.03	.4966	-.0837				
11	100.00	6.059	2.5403	15.2260	.0050	7.60	-7.60	-7.81	36.04	.4954	-.1042				

## \*\* VALUES OF PARAMETERS ON STREAMLINES AT STATION, 9, WHICH IS AN ANNULUS \*\*

STREAMLINE NO. RADIUS (In.)	COORD. (In.)	AXIAL VEL. (Ft/sec)	MERID. VEL. (Ft/sec)	TANG. VEL. (Ft/sec)	ABS. VEL. (Ft/sec)	ABS. FLOW STREAM. MACH NO.	ANGLE (Deg)	SLOPE (Deg)	STREAM. CURV. (1./In.)	PRESS. (Psia)	TOTAL TEMP. (Deg.R.)	STATIC PRESS. (Psia)	STATIC TEMP. (Deg.R.)
TIP 10.143	13.200												
1 10.143	13.200	725.34	725.34	.00	725.34	.6442	.00	.00	.000	18.414	571.26	13.929	527.46
2 9.807	13.200	753.62	753.62	.00	753.62	.6725	.00	.03	.000	18.871	569.71	13.936	522.42
3 9.470	13.200	769.06	769.06	.00	769.06	.6870	.00	.06	-.001	19.097	570.50	13.925	521.25
4 9.126	13.200	775.79	775.79	.00	775.79	.6934	.00	.09	-.001	19.197	570.76	13.919	520.64
5 8.771	13.200	778.66	778.66	.00	778.66	.6975	.00	.12	-.001	19.252	568.96	13.909	518.47
6 8.406	13.200	780.87	780.87	.00	780.87	.7010	.00	.13	-.002	19.306	566.99	13.905	516.21
7 8.023	13.200	782.13	782.14	.00	782.14	.7025	.00	.14	-.002	19.332	566.62	13.905	515.68
8 7.622	13.200	782.45	782.45	.00	782.45	.7030	.00	.12	-.002	19.314	566.24	13.885	515.26
9 7.199	13.200	778.58	778.58	.00	778.58	.6993	.00	.08	-.001	19.290	566.17	13.914	515.68
10 6.742	13.200	762.16	762.16	.00	762.16	.6830	.00	.01	-.001	18.961	566.42	13.875	518.04
11 6.233	13.200	736.21	736.21	.00	736.21	.6578	.00	.01	.002	18.560	566.20	13.879	521.07
HUB 6.233	13.200												

## \*\* VALUES OF PARAMETERS ON STREAMLINES AT STATION, 10, WHICH IS AN ANNULUS \*\*

STREAMLINE NO. RADIUS (In.)	COORD. (In.)	AXIAL VEL. (Ft/sec)	MERID. VEL. (Ft/sec)	TANG. VEL. (Ft/sec)	ABS. VEL. (Ft/sec)	ABS. FLOW STREAM. MACH NO.	ANGLE (Deg)	SLOPE (Deg)	STREAM. CURV. (1./In.)	PRESS. (Psia)	TOTAL TEMP. (Deg.R.)	STATIC PRESS. (Psia)	STATIC TEMP. (Deg.R.)
TIP 10.143	15.400												
1 10.143	15.400	727.21	727.21	.00	727.21	.6460	.00	.00	.000	18.414	571.26	13.908	527.23
2 9.807	15.400	755.35	755.35	.00	755.35	.6742	.00	.00	.000	18.871	569.71	13.916	522.20
3 9.471	15.400	770.58	770.58	.00	770.58	.6895	.00	.00	.000	19.097	570.50	13.907	521.06
4 9.127	15.400	777.04	777.04	.00	777.04	.6947	.00	-.01	.000	19.197	570.76	13.904	520.48
5 8.773	15.400	779.57	779.57	.00	779.57	.6983	.00	-.01	.000	19.252	568.96	13.898	518.35
6 8.406	15.400	781.37	781.37	.00	781.37	.7014	.00	-.01	.000	19.306	566.99	13.899	516.14
7 8.025	15.400	782.18	782.18	.00	782.18	.7025	.00	-.01	.000	19.332	566.62	13.904	515.67
8 7.624	15.400	782.04	782.04	.00	782.04	.7026	.00	-.01	.000	19.314	566.24	13.890	515.31
9 7.201	15.400	777.79	777.79	.00	777.79	.6985	.00	.01	.000	19.290	566.17	13.924	515.79
10 6.744	15.400	761.21	761.21	.00	761.21	.6820	.00	.03	-.001	18.961	566.42	13.886	518.16
11 6.235	15.400	735.80	735.80	.00	735.80	.6574	.00	.02	-.001	18.560	566.20	13.884	521.12
HUB 6.235	15.400												

\*\* VALUES OF PARAMETERS ON STREAMLINES AT STATION, 11, WHICH IS AN ANNULUS \*\*

STREAMLINE NO.	RADIUS (In.)	COORD. (In.)	AXIAL VEL. (Ft/sec)	HEED. VEL. (Ft/sec)	TANG. VEL. (Ft/sec)	ABS. VEL. (Ft/sec)	ABS. FLOW STREAM. (Ft/sec)	MACH NO. (Deg)	ANGLE SLOPE (Deg)	STREAM. CURV. (1./In.)	TOTAL PRESS. (Psia)	TOTAL TEMP. (Deg.R.)	STATIC PRESS. (Psia)	STATIC TEMP. (Deg.R.)	
TIP 10.143	17.600	1	10.143	17.600	726.66	726.66	.00	726.66	.6454	.00	.000	18.414	571.26	13.914	527.30
	2	9.807	17.600	754.83	754.83	.00	754.83	.6737	.00	-.01	.000	18.871	569.71	13.922	522.27
	3	9.471	17.600	770.07	770.07	.00	770.07	.6890	.00	-.01	.000	19.097	570.50	13.913	521.12
	4	9.127	17.600	776.56	776.56	.00	776.56	.6942	.00	-.01	.000	19.197	570.76	13.910	520.54
	5	8.772	17.600	779.12	779.12	.00	779.12	.6979	.00	-.02	.000	19.252	568.96	13.904	518.41
	6	8.406	17.600	780.95	780.95	.00	780.95	.7010	.00	-.02	.000	19.306	566.99	13.904	516.20
	7	8.024	17.600	781.80	781.80	.00	781.80	.7021	.00	-.03	.000	19.332	566.62	13.909	515.72
	8	7.623	17.600	781.67	781.67	.00	781.67	.7023	.00	-.04	.000	19.314	566.24	13.894	515.36
	9	7.200	17.600	777.39	777.39	.00	777.39	.6981	.00	-.05	.000	19.290	566.17	13.929	515.84
	10	6.743	17.600	760.70	760.71	.00	760.71	.6815	.00	-.07	.000	18.961	566.42	13.892	518.23
	11	6.233	17.600	735.00	735.00	.00	735.00	.6566	.00	-.09	.000	18.560	566.20	13.893	521.22
HUB	6.233	17.600													

\*\* VALUES OF PARAMETERS ON STREAMLINES AT STATION, 12, WHICH IS AN ANNULUS \*\*

STREAMLINE NO.	RADIUS (In.)	COORD. (In.)	AXIAL VEL. (Ft/sec)	HEED. VEL. (Ft/sec)	TANG. VEL. (Ft/sec)	ABS. VEL. (Ft/sec)	ABS. FLOW STREAM. (Ft/sec)	MACH NO. (Deg)	ANGLE SLOPE (Deg)	STREAM. CURV. (1./In.)	TOTAL PRESS. (Psia)	TOTAL TEMP. (Deg.R.)	STATIC PRESS. (Psia)	STATIC TEMP. (Deg.R.)	
TIP 10.143	18.700	1	10.143	18.700	726.25	.00	726.25	.6450	.00	.00	.000	18.414	571.26	13.919	527.35
	2	9.807	18.700	754.43	754.43	.00	754.43	.6733	.00	-.01	.000	18.871	569.71	13.926	522.32
	3	9.470	18.700	769.68	769.68	.00	769.68	.6876	.00	-.01	.000	19.097	570.50	13.917	521.17
	4	9.127	18.700	776.15	776.15	.00	776.15	.6958	.00	-.02	.000	19.197	570.76	13.915	520.60
	5	8.772	18.700	778.68	778.68	.00	778.68	.6975	.00	-.03	.000	19.252	568.96	13.909	518.47
	6	8.405	18.700	780.47	780.47	.00	780.47	.7006	.00	-.03	.000	19.306	566.99	13.910	516.26
	7	8.023	18.700	781.25	781.25	.00	781.25	.7016	.00	-.04	.000	19.332	566.62	13.915	515.79
	8	7.623	18.700	781.05	781.05	.00	781.05	.7016	.00	-.05	.000	19.314	566.24	13.902	515.44
	9	7.199	18.700	776.68	776.68	.00	776.68	.6974	.00	-.07	.000	19.290	566.17	13.937	515.93
	10	6.741	18.700	759.87	759.87	.00	759.87	.6807	.00	-.08	.000	18.961	566.42	13.892	518.33
	11	6.232	18.700	734.03	734.03	.00	734.03	.6557	.00	-.11	.000	18.560	566.20	13.894	521.34
HUB	6.232	18.700													

\*\*\* COMPUTED COMPRESSOR DESIGN PARAMETERS FOR A ROTATIONAL SPEED OF, 11670.9, RPM \*\*\*

\*\* THE CORRECTED WEIGHTFLOW PER UNIT OF CASING ANNUAL AREA AT THE INLET FACE OF THE FIRST BLADE ROW IS 40.61 Lb/sec/ft<sup>2</sup> \*\*

\*\* MASS AVERAGED ROTOR AND STAGE AERODYNAMIC PARAMETERS \*\*

STAGE BLADE NO.	TYPE	FLOW COEF.	HEAD COEF.	ID. HEAD PRESS.	TOTAL TEMP.	ADIA. EFF.	POLY. EFF.	FOR AX. GAS BENDING MOMENTS			POWER (HP)
								ASPECT RATIO	SHAFT THRUST (Lbs)	FOR EACH BLADE FOR AX. TANG. (Ft-lbs) (Ft-lbs)	
1	ROTOR	.5731	.2199	.2456	1.3315	1.0953	.8952	.8994	.626	759.63	2.064
1	STATOR	.6566	.2008	.2456	1.3000	1.0953	.8175	.8242	.50	340.50	1.928

\*\* CUMULATIVE SUMS OF MASS AVERAGED ROTOR AND STAGE AERODYNAMIC PARAMETERS \*\*

STAGE BLADE NO.	TYPE	WEIGHT FLOW (Lb/sec)	TOTAL PRESS. (Psia)	TOTAL TEMP. (Deg R.)	HEAD COEF.	IDEAL HEAD COEF.	ADIA. EFF.	FOR AX. SHAFT THRUST (Lbs) (Ft-lbs)			POWER (HP)
								POLY. EFF.	FRACT ENERGY		
1	INLET	77.80	14.700	518.70							
1	ROTOR	77.80	19.572	568.11	1.3315	1.0953	.2199	.2456	.8952	.8994	759.63
1	STATOR	77.80	19.109	568.11	1.3000	1.0953	.2008	.2456	.8175	.8242	419.13



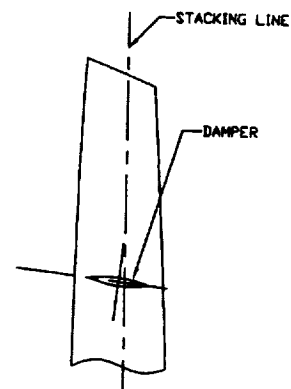
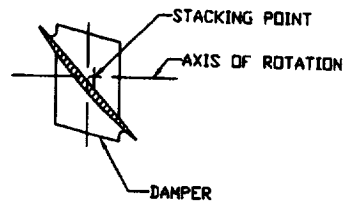
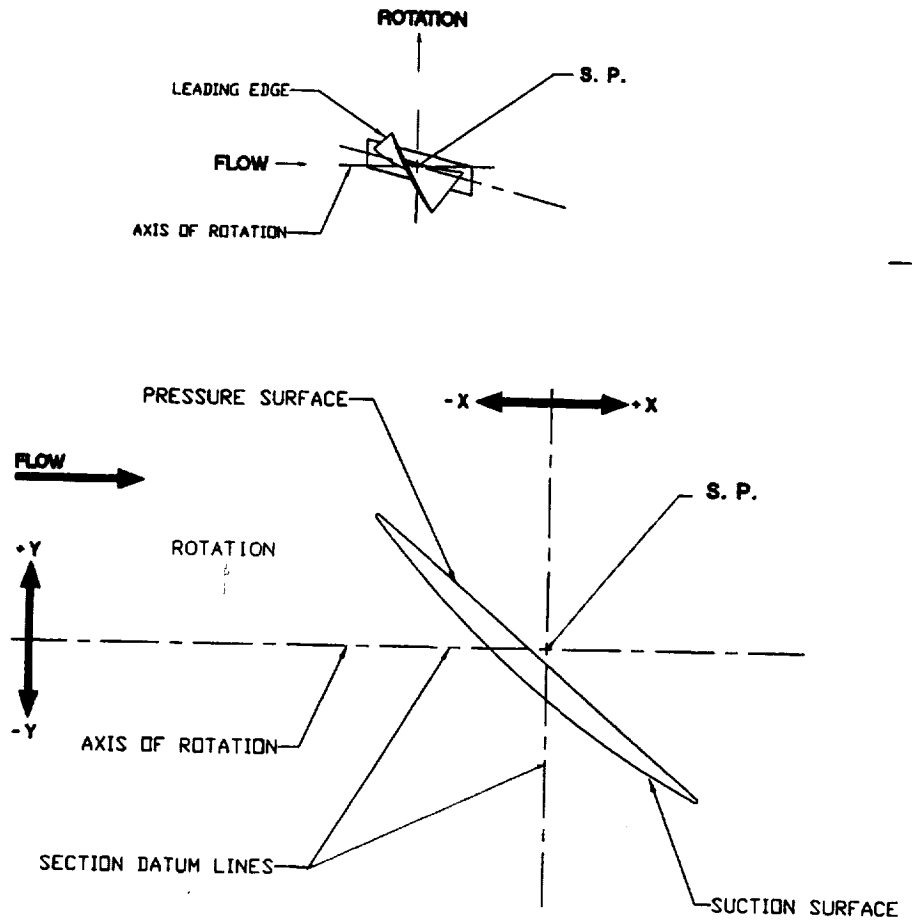
# Appendix B

## BLADE COORDINATES

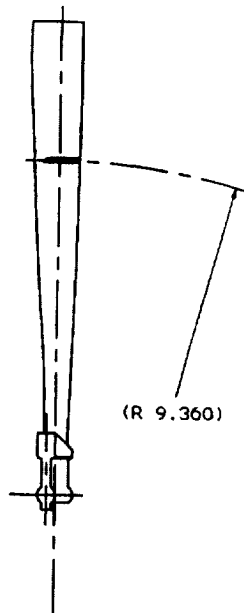
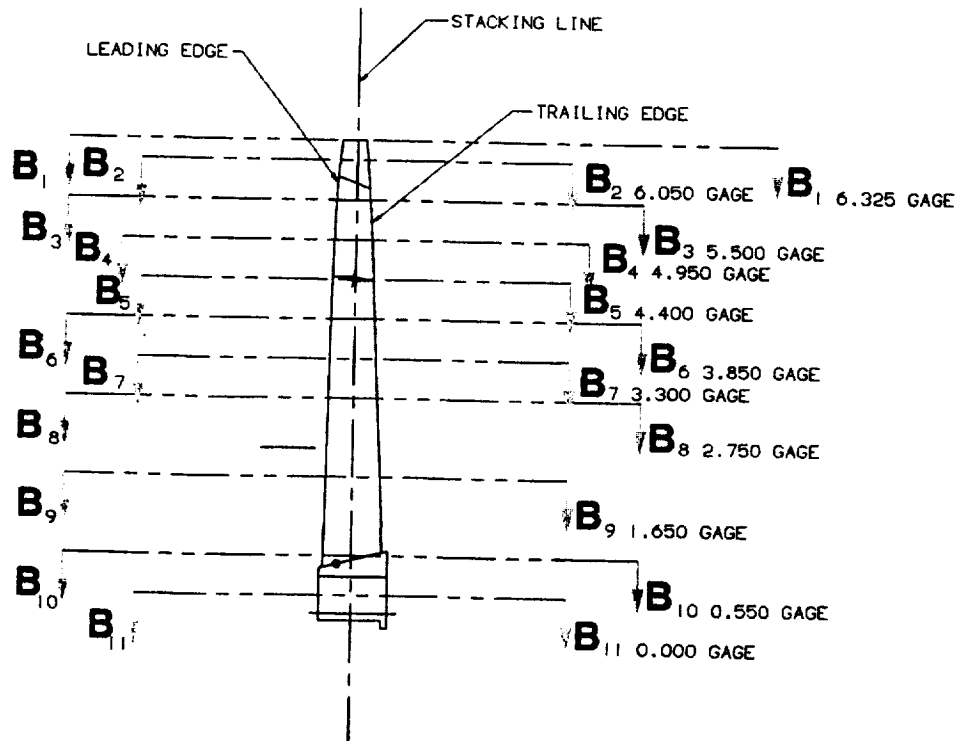


# **PART 1**

## **ROTOR BLADES**



TYPICAL AIRFOIL SECTION  
 $B_1-B_1$  THRU  $B_{11}-B_{11}$



LOW NOISE FAN ROTOR BLADE SECTION B01-B01  
 RADIUS: 11.275000 GAGE: 6.325000

SUCTION SURFACE

X	Y
*-0.246600	0.447300
*-0.229100	0.365700
-0.209100	0.285600
-0.198300	0.246200
-0.186800	0.207100
-0.174700	0.168400
-0.162000	0.130100
-0.148700	0.092100
-0.134700	0.054600
-0.120300	0.017500
-0.105200	-0.019100
-0.089600	-0.055100
-0.073500	-0.090600
-0.057000	-0.125600
-0.039800	-0.159900
-0.022300	-0.193400
-0.004300	-0.226400
0.014200	-0.258400
0.033000	-0.289700
0.052300	-0.320000
0.072000	-0.349400
0.092000	-0.377800
0.112300	-0.404900
* 0.154000	-0.455700
* 0.196900	-0.501700

PRESSURE SURFACE

X	Y
*-0.255100	0.442700
*-0.229300	0.364700
-0.202700	0.287800
-0.189100	0.249800
-0.175300	0.212100
-0.161200	0.174700
-0.146900	0.137500
-0.132400	0.100600
-0.117700	0.064000
-0.102700	0.027700
-0.087500	-0.008200
-0.072100	-0.043800
-0.056500	-0.079000
-0.040500	-0.113700
-0.024400	-0.147900
-0.007900	-0.181600
0.008900	-0.214700
0.025800	-0.247400
0.043200	-0.279300
0.060800	-0.310600
0.078800	-0.341200
0.097200	-0.370900
0.115900	-0.399900
* 0.154300	-0.455400
* 0.193900	-0.507700

LEADING EDGE

X	Y
-0.205900	0.286600
0.003400	CENTER

TRAILING EDGE

X	Y
0.114100	-0.492500
0.002900	RADIUS

LOW NOISE FAN ROTOR BLADE SECTION B02-B02  
 RADIUS: 11.000000                    GAGE: 6.050000

SUCTION SURFACE  
 X                  Y

* -0.291500	0.452200
* -0.267300	0.371500
-0.240600	0.292400
-0.226400	0.253400
-0.211600	0.214800
-0.196300	0.176500
-0.180300	0.138600
-0.163900	0.100900
-0.146900	0.063700
-0.129400	0.026800
-0.111400	-0.009600
-0.093000	-0.045700
-0.074100	-0.081300
-0.054700	-0.116400
-0.034800	-0.151100
-0.014700	-0.185200
0.006000	-0.218800
0.027000	-0.251300
0.048500	-0.284200
0.070300	-0.316000
0.092600	-0.347000
0.115100	-0.377200
0.137900	-0.406700
* 0.184600	-0.463300
* 0.232400	-0.516700

PRESSURE SURFACE  
 X                  Y

* 0.302400	0.444300
* -0.268700	0.369600
-0.234200	0.295300
-0.216700	0.258300
-0.198900	0.221300
-0.181200	0.184700
-0.163200	0.148100
-0.145100	0.111800
-0.127000	0.075600
-0.108700	0.039600
-0.090400	0.003800
-0.071800	-0.031700
-0.053100	-0.067000
-0.034200	-0.102000
-0.015300	-0.136800
0.003800	-0.171300
0.023100	-0.205400
0.042500	-0.239200
0.062100	-0.272600
0.081900	-0.305600
0.101900	-0.338200
0.122100	-0.370300
0.142500	-0.401900
* 0.184000	-0.463200
* 0.226200	-0.522100

LEADING EDGE

X	Y		X	Y
-0.237200	0.293700	CENTER	0.140100	-0.404200
	0.003500	RADIUS		0.003300

LOW NOISE FAN ROTOR BLADE SECTION B03-B03  
 RADIUS: 10.450000      GAGE: 5.500000

SUCTION SURFACE

X	Y
*-0.351600	0.445700
*-0.317600	0.368500
-0.281700	0.292500
-0.262900	0.254900
-0.243700	0.217600
-0.224000	0.180600
-0.203800	0.143800
-0.183000	0.107500
-0.161800	0.071400
-0.140200	0.035600
-0.118100	0.000200
-0.095500	-0.034800
-0.072500	-0.069500
-0.049100	-0.103800
-0.025300	-0.137900
-0.001000	-0.171500
0.023600	-0.204700
0.048700	-0.237600
0.074100	-0.269900
0.099800	-0.302000
0.126000	-0.333500
0.152400	-0.364700
0.179200	-0.395400
* 0.234000	-0.455700
* 0.290500	-0.514500

PRESSURE SURFACE

X	Y
*-0.365300	0.435600
*-0.320500	0.365900
-0.275200	0.296300
-0.252400	0.261500
-0.229600	0.226700
-0.206700	0.191900
-0.183700	0.157100
-0.160900	0.122400
-0.138000	0.087800
-0.115000	0.053200
-0.092000	0.018700
-0.069200	-0.015800
-0.046200	-0.050300
-0.023200	-0.084700
-0.000200	-0.119000
0.022900	-0.153200
0.045800	-0.187400
0.068900	-0.221500
0.092000	-0.255500
0.115100	-0.289400
0.138300	-0.323200
0.161400	-0.356900
0.184600	-0.390500
* 0.231000	-0.456900
* 0.277400	-0.522500

LEADING EDGE

X	Y
-0.278300	0.294100
0.003800	

TRAILING EDGE

X	Y
0.181700	-0.392800
0.003600	

LOW NOISE FAN ROTOR BLADE SECTION B04-B04  
 RADIUS: 9.900000      GAGE: 4.950000

SUCTION SURFACE

X	Y
*-0.384500	0.430800
*-0.345300	0.355600
-0.304200	0.282000
-0.282800	0.245800
-0.261000	0.210000
-0.238700	0.174500
-0.215700	0.139400
-0.192400	0.104700
-0.168600	0.070200
-0.144200	0.036200
-0.119400	0.002500
-0.094100	-0.030900
-0.068400	-0.063800
-0.042300	-0.096400
-0.015600	-0.128500
0.011400	-0.160400
0.038900	-0.191700
0.066900	-0.222700
0.095100	-0.253400
0.123800	-0.283500
0.152800	-0.313300
0.182200	-0.342700
0.212100	-0.371600
* 0.273300	-0.428300
* 0.336500	-0.483400

PRESSURE SURFACE

X	Y
*-0.403100	0.417800
*-0.350300	0.351900
-0.298000	0.286300
-0.271900	0.253700
-0.246000	0.221200
-0.220000	0.188500
-0.194100	0.156000
-0.168100	0.123400
-0.142300	0.090800
-0.116400	0.058100
-0.090600	0.025500
-0.064700	-0.007100
-0.038900	-0.039700
-0.013100	-0.072300
0.012600	-0.105000
0.038300	-0.137700
0.064000	-0.170300
0.089600	-0.203000
0.115200	-0.235600
0.140800	-0.268400
0.166400	-0.301100
0.191900	-0.333700
0.217500	-0.366400
* 0.268600	-0.432200
* 0.319700	-0.498300

LEADING EDGE

X	Y
-0.300900	0.283900
	CENTER
0.003800	

TRAILING EDGE

X	Y
0.214600	-0.368800
	RADIUS
0.003800	

LOW NOISE FAN ROTOR BLADE SECTION B05-B05  
 RADIUS: 9.350000 GAGE: 4.400001

SUCTION SURFACE

X	Y
*-0.408200	0.413800
*-0.365100	0.341200
-0.320000	0.270200
-0.296700	0.235300
-0.272900	0.200800
-0.248500	0.166700
-0.223600	0.133100
-0.198200	0.099800
-0.172200	0.066900
-0.145700	0.034500
-0.118700	0.002400
-0.091200	-0.029100
-0.063200	-0.060200
-0.034700	-0.090900
-0.005800	-0.121100
0.023500	-0.150800
0.053300	-0.180000
0.083600	-0.208800
0.114300	-0.237100
0.145400	-0.265000
0.176900	-0.292400
0.208800	-0.319200
0.241100	-0.345500
* 0.306900	-0.396600
* 0.374200	-0.445700

PRESSURE SURFACE

X	Y
* 0.429100	0.396900
* 0.371400	0.335900
-0.314100	0.274900
-0.285600	0.244400
-0.257200	0.213900
-0.228900	0.183400
-0.200600	0.152900
-0.172400	0.122300
-0.144200	0.091800
-0.116000	0.061000
-0.087800	0.030400
-0.059700	-0.000300
-0.031700	-0.031000
-0.003700	-0.061800
0.024300	-0.092600
0.052200	-0.123400
0.080000	-0.154200
0.107800	-0.185100
0.135600	-0.216000
0.163300	-0.247000
0.191000	-0.278000
0.218600	-0.309000
0.246200	-0.340000
* 0.301400	-0.402000
* 0.356500	-0.464000

LEADING EDGE

X	Y
-0.316800	0.272300
0.003800	CENTER

TRAILING EDGE

X	Y
0.243500	-0.342600
0.003800	RADIUS

LOW NOISE FAN ROTOR BLADE SECTION B06-B06  
 RADIUS: 8.800000      GAGE: 3.850000

SUCTION SURFACE  
 X            Y

\*-0.424700  0.402000  
 \*-0.378800  0.330600  
 -0.330800  0.261300  
 -0.306100  0.227300  
 -0.280900  0.193900  
 -0.255000  0.160800  
 -0.228600  0.128400  
 -0.201600  0.096200  
 -0.173900  0.064700  
 -0.145800  0.033600  
 -0.117200  0.003100  
 -0.088000  -0.027000  
 -0.058200  -0.056500  
 -0.028000  -0.085400  
 0.002800  -0.113900  
 0.033900  -0.141900  
 0.065700  -0.169200  
 0.097800  -0.196000  
 0.130400  -0.222200  
 0.163400  -0.247900  
 0.196900  -0.273000  
 0.230700  -0.297500  
 0.265100  -0.321400  
 \* 0.335400  -0.367400  
 \* 0.407600  -0.411000

PRESSURE SURFACE  
 X            Y

\*-0.447100  0.380900  
 \*-0.385900  0.323600  
 -0.325100  0.266200  
 -0.294900  0.237600  
 -0.264700  0.208900  
 -0.234600  0.180200  
 -0.204500  0.151400  
 -0.174400  0.122600  
 -0.144400  0.093700  
 -0.114400  0.064800  
 -0.084600  0.035900  
 -0.054800  0.006800  
 -0.024900  -0.022300  
 0.004800  -0.051300  
 0.034500  -0.080500  
 0.064100  -0.109700  
 0.093600  -0.138900  
 0.123200  -0.168300  
 0.152600  -0.197700  
 0.182000  -0.227000  
 0.211400  -0.256500  
 0.240600  -0.286000  
 0.269800  -0.315600  
 \* 0.328300  -0.374700  
 \* 0.386800  -0.433900

LEADING EDGE

X	Y	
-0.327700	0.263400	CENTER
0.003800		RADIUS

TRAILING EDGE

X	Y
0.267200	-0.318300
0.003800	

LOW NOISE FAN ROTOR BLADE SECTION B07-B07  
 RADIUS: 8.250000      GAGE: 3.300000

SUCTION SURFACE

X	Y
*-0.439000	0.387500
*-0.391300	0.318100
-0.341200	0.250700
-0.315200	0.217800
-0.288600	0.185300
-0.261200	0.153500
-0.233300	0.122100
-0.204700	0.091300
-0.175500	0.061200
-0.145800	0.031600
-0.115400	0.002600
-0.084500	-0.025800
-0.052900	-0.053500
-0.020900	-0.080600
0.011700	-0.107000
0.044800	-0.132700
0.078400	-0.157900
0.112500	-0.182400
0.147100	-0.206100
0.182100	-0.229200
0.217600	-0.251600
0.253400	-0.273300
0.289700	-0.294200
* 0.363600	-0.334100
* 0.439000	-0.371100

PRESSURE SURFACE

X	Y
*-0.464600	0.363300
*-0.400000	0.309600
-0.335800	0.256000
-0.303900	0.229200
-0.272000	0.202400
-0.240200	0.175600
-0.208500	0.148600
-0.176700	0.121700
-0.145000	0.094700
-0.113300	0.067700
-0.081700	0.040700
-0.050200	0.013600
-0.018600	-0.013600
0.012900	-0.040800
0.044300	-0.068100
0.075800	-0.095400
0.107100	-0.122800
0.138300	-0.150300
0.169700	-0.177700
0.200800	-0.205200
0.231900	-0.232800
0.263100	-0.260500
0.294100	-0.288100
* 0.355900	-0.343000
* 0.417200	-0.397500

LEADING EDGE

X	Y
-0.338200	0.253000
0.003800	

CENTER

TRAILING EDGE

X	Y
0.291700	-0.291000
0.003800	

LOW NOISE FAN ROTOR BLADE SECTION B08-B08  
 RADIUS: 7.700000      GAGE: 2.750000

SUCTION SURFACE		PRESSURE SURFACE	
X	Y	X	Y
* -0.453900	0.369300	* -0.481100	0.341400
* -0.404800	0.302100	* -0.414200	0.291900
-0.352500	0.236800	-0.347400	0.242300
-0.325200	0.204900	-0.313900	0.217600
-0.297000	0.173500	-0.280500	0.192800
-0.268200	0.142900	-0.247100	0.168000
-0.238700	0.112900	-0.213600	0.143300
-0.208400	0.083600	-0.180200	0.118500
-0.177500	0.055200	-0.146800	0.093700
-0.145900	0.027300	-0.113300	0.069000
-0.113600	0.000200	-0.079900	0.044200
-0.080700	-0.026000	-0.046500	0.019400
-0.047300	-0.051500	-0.013100	-0.005400
-0.013100	-0.076200	0.020400	-0.030100
0.021500	-0.100000	0.053800	-0.055000
0.056700	-0.123100	0.087200	-0.079800
0.092500	-0.145300	0.120700	-0.104600
0.128800	-0.166600	0.154100	-0.129400
0.165600	-0.187100	0.187500	-0.154300
0.202800	-0.206700	0.220800	-0.179100
0.240500	-0.225500	0.254300	-0.204000
0.278700	-0.243300	0.287600	-0.228900
0.317300	-0.260200	0.321000	-0.253700
* 0.395200	-0.291400	* 0.388200	-0.303500
* 0.474400	-0.318900	* 0.455700	-0.353200

LEADING EDGE		TRAILING EDGE	
X	Y	X	Y
-0.349700	0.239300	CENTER	0.318700 -0.256700
0.003800		RADIUS	0.003800

LOW NOISE FAN ROTOR BLADE SECTION B09-B09  
 RADIUS: 6.600000 GAGE: 1.650001

SUCTION SURFACE

X	Y
*-0.485300	0.330900
*-0.432000	0.263400
-0.374700	0.200200
-0.344500	0.170300
-0.313400	0.141400
-0.281400	0.1113500
-0.248400	0.086700
-0.214600	0.061000
-0.179900	0.036400
-0.144500	0.013000
-0.108300	-0.009200
-0.071300	-0.030200
-0.033800	-0.050000
0.004500	-0.068500
0.043400	-0.085800
0.082800	-0.101600
0.122800	-0.116000
0.163300	-0.129100
0.204100	-0.140800
0.245400	-0.151100
0.287000	-0.159800
0.329000	-0.167100
0.371100	-0.172900
* 0.456100	-0.179600
* 0.541900	-0.179900

PRESSURE SURFACE

X	Y
*-0.513700	0.291100
*-0.442100	0.248100
-0.370200	0.206200
-0.334000	0.185700
-0.297800	0.165500
-0.261300	0.145400
-0.224900	0.125500
-0.188400	0.105800
-0.151600	0.086300
-0.114900	0.067000
-0.077900	0.047800
-0.041000	0.028900
-0.003800	0.010100
0.033400	-0.008400
0.070700	-0.026700
0.108100	-0.044800
0.145700	-0.062800
0.183400	-0.080500
0.221000	-0.097900
0.258900	-0.115200
0.296800	-0.132200
0.334900	-0.149100
0.373100	-0.165600
* 0.449700	-0.197400
* 0.526800	-0.227600

LEADING EDGE

X	Y
-0.372000	0.202900
0.003800	CENTER
	RADIUS

TRAILING EDGE

X	Y
0.371600	-0.169100
0.003800	

LOW NOISE FAN ROTOR BLADE SECTION B10-B10  
 RADIUS: 5.500000      GAGE: 0.550000

SUCTION SURFACE

X	Y
* -0.515800	0.277000
* -0.457600	0.210900
-0.394600	0.150800
-0.361300	0.123000
-0.326800	0.096700
-0.291200	0.072000
-0.254500	0.048900
-0.216800	0.027500
-0.178300	0.007900
-0.138800	-0.010000
-0.098600	-0.025900
-0.057700	-0.040000
-0.016200	-0.052100
0.025800	-0.062200
0.068300	-0.070200
0.111200	-0.076100
0.154200	-0.079800
0.197500	-0.081300
0.240800	-0.080600
0.284100	-0.077600
0.327100	-0.072400
0.370000	-0.064800
0.412400	-0.054900
* 0.495700	-0.028200
* 0.577000	0.007700

PRESSURE SURFACE

X	Y
* -0.541300	0.226500
* -0.466600	0.190700
-0.390700	0.157300
-0.352300	0.141500
-0.313600	0.126300
-0.274700	0.111500
-0.235600	0.097300
-0.196400	0.083700
-0.156900	0.070600
-0.1117300	0.058000
-0.077500	0.046100
-0.037500	0.034700
0.002700	0.024000
0.043000	0.013800
0.083500	0.004300
0.124100	-0.004500
0.164900	-0.012700
0.205800	-0.020300
0.246800	-0.027100
0.287900	-0.033300
0.329200	-0.038700
0.370500	-0.043400
0.411900	-0.047300
* 0.495000	-0.052700
* 0.578500	-0.054900

LEADING EDGE

X	Y
-0.392000	0.153700
*	
0.003900	

CENTER

TRAILING EDGE

X	Y
0.411600	-0.051100
*	
0.003900	

LOW NOISE FAN ROTOR BLADE SECTION BII-BII  
 RADIUS: 4.950000      GAGE: 0.000000

SUCTION SURFACE  
 X            Y

* -0.526600	0.253600
* -0.466100	0.186100
-0.400400	0.126200
-0.365600	0.099100
-0.329500	0.073900
-0.292300	0.050600
-0.253900	0.029200
-0.214500	0.009800
-0.174200	-0.007500
-0.133100	-0.022500
-0.091200	-0.035300
-0.048800	-0.045800
-0.005900	-0.053900
0.037400	-0.059600
0.081000	-0.062600
0.124600	-0.063100
0.168200	-0.061000
0.211700	-0.056200
0.254800	-0.048700
0.297400	-0.038400
0.339400	-0.025500
0.380600	-0.009800
0.420900	0.008600
* 0.498800	0.053500
* 0.573100	0.109200

PRESSURE SURFACE  
 X            Y

* -0.553500	0.194800
* -0.475400	0.162500
-0.396900	0.133000
-0.357500	0.119300
-0.318000	0.106300
-0.278100	0.094100
-0.238100	0.082600
-0.197900	0.071900
-0.157500	0.061900
-0.117000	0.052700
-0.076200	0.044400
-0.035300	0.036900
0.005700	0.030300
0.046800	0.024600
0.088000	0.019800
0.129300	0.015800
0.170700	0.012800
0.212100	0.010800
0.253600	0.009800
0.295000	0.009800
0.336500	0.010800
0.377900	0.012900
0.419200	0.016100
* 0.501500	0.025800
* 0.583400	0.039900

LEADING EDGE

X	Y
-0.398100	0.129300
CENTER	
0.003900	

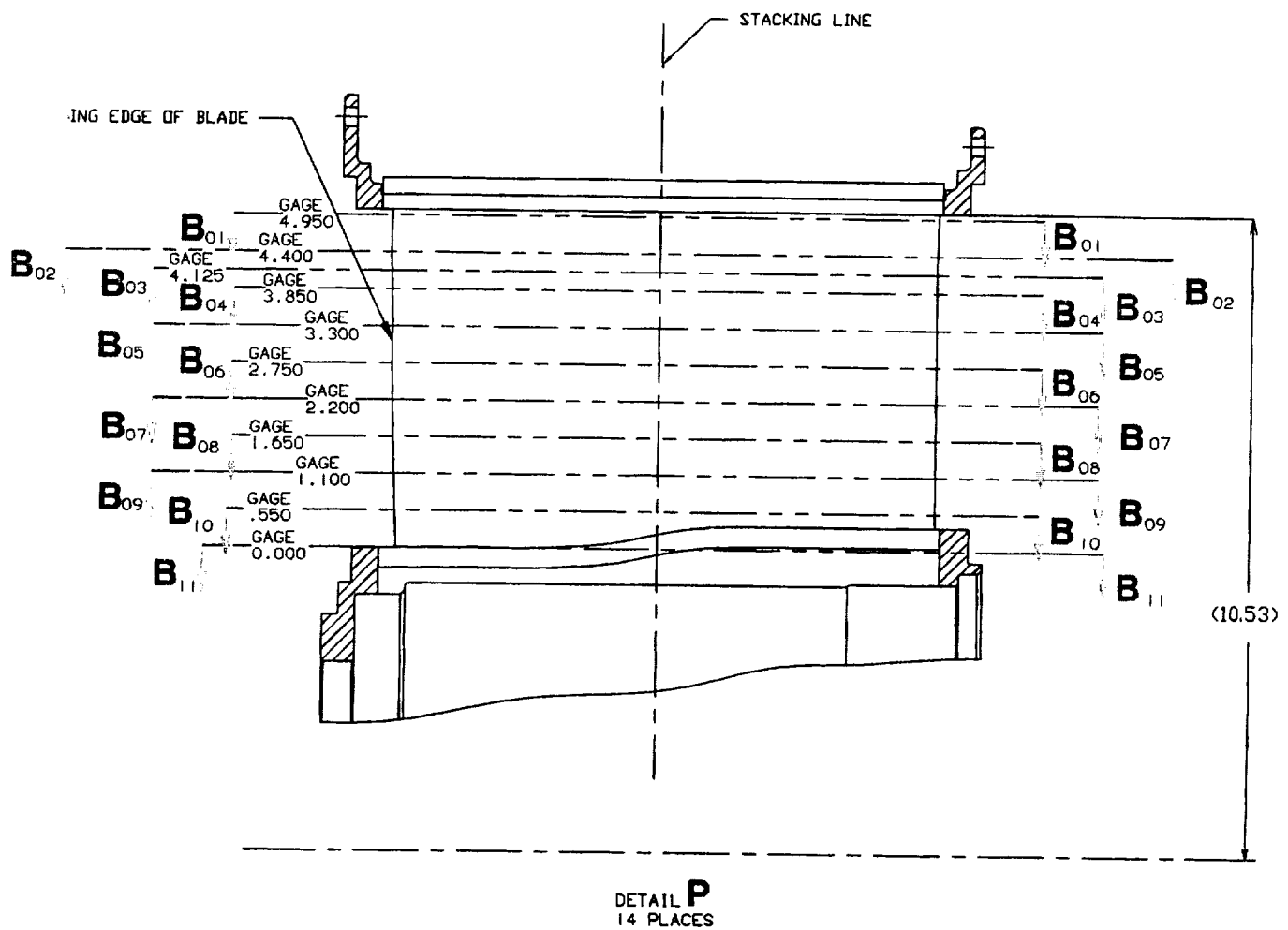
TRAILING EDGE

X	Y
0.419400	0.012200
RADIUS	
0.003900	

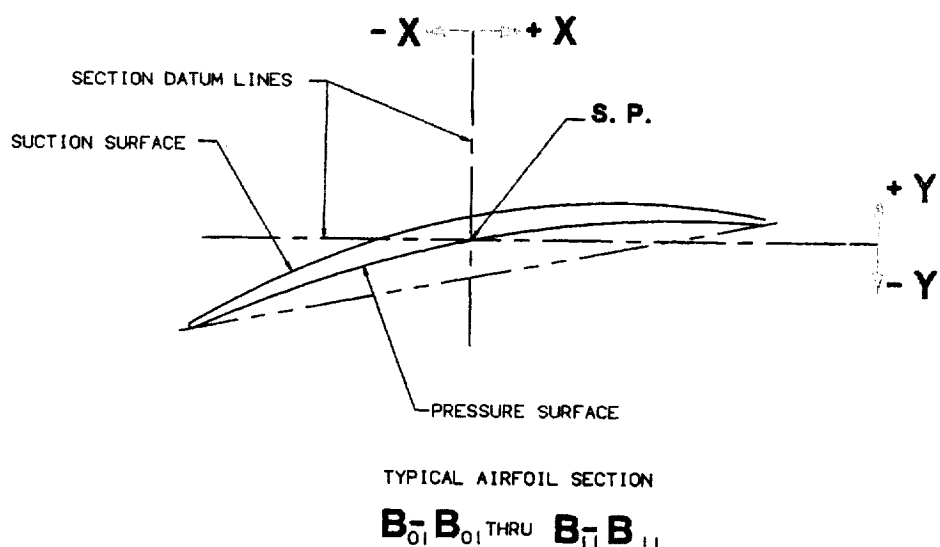


PART 2

LONG CHORD STATOR VANES



DETAIL P  
14 PLACES



ALT LOW FAN STATOR BLADE SECTION B01-B01  
 RADIUS: 10.450000 GAGE: 4.950000

SUCTION SURFACE

X	Y
*-5.489900	-1.614400
*-4.768000	-1.179800
-4.024100	-0.798800
-3.643900	-0.628400
-3.258200	-0.471400
-2.867600	-0.327400
-2.472600	-0.196200
-2.073600	-0.077700
-1.671100	0.028100
-1.265400	0.121200
-0.857000	0.201400
-0.446300	0.268700
-0.033600	0.323000
0.380700	0.364100
0.796100	0.391900
1.212200	0.406500
1.628600	0.407800
2.044800	0.395800
2.460400	0.370400
2.875100	0.331900
3.288300	0.280200
3.699800	0.215400
4.109000	0.137500
* 4.920500	-0.057600
* 5.722800	-0.305100

PRESSURE SURFACE

X	Y
*-5.557700	-1.376400
*-4.779700	-1.113200
-3.995300	-0.877200
-3.600700	-0.769400
-3.204500	-0.668400
-2.806600	-0.574100
-2.407200	-0.486300
-2.006400	-0.404900
-1.604400	-0.329800
-1.201300	-0.261100
-0.797100	-0.198600
-0.392000	-0.142400
0.014000	-0.092500
0.420700	-0.049000
0.828000	-0.011700
1.235900	0.019200
1.644300	0.043700
2.053000	0.061800
2.462000	0.073500
2.871200	0.078800
3.280500	0.077700
3.689700	0.070100
4.098800	0.056100
* 4.916700	0.008900
* 5.734200	-0.063900

LEADING EDGE

X	Y		
-4.006500	-0.836800	CENTER	4.100600
		RADIUS	0.041180
0.041930			

TRAILING EDGE

ALT LOW FAN STATOR BLADE SECTION B02-B02  
RADIUS: 9.900000 GAGE: 4.400000

SUCTION SURFACE

X	Y
*-5.526000	-1.489000
*-4.787200	-1.107400
-4.031600	-0.766600
-3.647500	-0.611500
-3.259200	-0.466600
-2.867100	-0.332200
-2.471400	-0.208400
-2.072400	-0.095500
-1.670300	0.006200
-1.265600	0.096700
-0.858500	0.175800
-0.449300	0.243400
-0.038400	0.299500
0.374000	0.343900
0.787400	0.376700
1.201600	0.397900
1.616200	0.407400
2.030900	0.405400
2.445400	0.391700
2.859300	0.366500
3.272300	0.329700
3.684100	0.281500
4.094500	0.221700
* 4.911100	0.067300
* 5.722100	-0.133500

PRESSURE SURFACE

X	Y
*-5.585300	-1.267100
*-4.797500	-1.046500
-4.005700	-0.843500
-3.608300	-0.748600
-3.209900	-0.658100
-2.810400	-0.572300
-2.409900	-0.491100
-2.008400	-0.414700
-1.606100	-0.343000
-1.202900	-0.276100
-0.799000	-0.214200
-0.394300	-0.157200
0.011000	-0.105100
0.417000	-0.058000
0.823500	-0.015900
1.230500	0.021200
1.637900	0.053200
2.045700	0.080300
2.453800	0.102300
2.862100	0.119200
3.270600	0.131200
3.679200	0.138100
4.087900	0.140000
* 4.905600	0.128800
* 5.723700	0.097600

LEADING EDGE

X	Y
-4.015600	-0.804100
0.040700	CENTER
RADIUS	

TRAILING EDGE

X	Y
4.088000	0.181100
0.041110	

ALT LOW FAN STATOR BLADE SECTION B03-B03  
RADIUS: 9.625000 GAGE: 4.125000

SUCTION SURFACE

X	Y
*-5.512300	-1.546600
*-4.776400	-1.161200
-4.024100	-0.814200
-3.641800	-0.655100
-3.255400	-0.505600
-2.864900	-0.366200
-2.470700	-0.237400
-2.073000	-0.119500
-1.672100	-0.012700
-1.268300	0.082600
-0.861900	0.166400
-0.453300	0.238600
-0.042800	0.299000
0.369300	0.347600
0.782600	0.384400
1.196700	0.409400
1.611400	0.422600
2.026300	0.424000
2.441100	0.413700
2.855400	0.391500
3.268900	0.357700
3.681200	0.312000
4.092100	0.254700
* 4.909700	0.105300
* 5.721700	-0.090500

PRESSURE SURFACE

X	Y
*-5.571600	-1.332900
*-4.786400	-1.103100
-3.997200	-0.890100
-3.601100	-0.789900
-3.204000	-0.693900
-2.805700	-0.602400
-2.406300	-0.515600
-2.005900	-0.433600
-1.604500	-0.356600
-1.202100	-0.284600
-0.798900	-0.217700
-0.394800	-0.156100
0.010100	-0.099600
0.415600	-0.048400
0.821800	-0.002600
1.228600	0.038000
1.635800	0.073300
2.043500	0.103200
2.451500	0.127800
2.859900	0.147100
3.268400	0.161000
3.677100	0.169700
4.085900	0.173000
* 4.903800	0.163400
* 5.722100	0.132200

LEADING EDGE

X	Y
-4.007700	-0.851200
	CENTER
0.040400	RADIUS

TRAILING EDGE

X	Y
4.085800	0.214100
	0.041110

ALT LOW FAN STATOR BLADE SECTION B04-B04  
RADIUS: 9.350000 GAGE: 3.850000

SUCTION SURFACE

X	Y
*-5.488200	-1.629400
*-4.760800	-1.227600
-4.015000	-0.865800
-3.635200	-0.699900
-3.250800	-0.544000
-2.862200	-0.398600
-2.469500	-0.264000
-2.073000	-0.140600
-1.673100	-0.028700
-1.270100	0.071500
-0.864400	0.159900
-0.456200	0.236300
-0.046000	0.300700
0.366000	0.353000
0.779300	0.393100
1.193600	0.421200
1.608600	0.437100
2.023800	0.440800
2.439000	0.432400
2.853800	0.411900
3.267700	0.379200
3.680600	0.334500
4.091900	0.277600
* 4.909700	0.127200
* 5.721100	-0.072000

PRESSURE SURFACE

X	Y
*-5.549000	-1.419400
*-4.770600	-1.171200
-3.986600	-0.941400
-3.592500	-0.833400
-3.197000	-0.730000
-2.800200	-0.631500
-2.402200	-0.538200
-2.002900	-0.450100
-1.602400	-0.367400
-1.200800	-0.290200
-0.798200	-0.218500
-0.394700	-0.152400
0.009800	-0.092000
0.415000	-0.037400
0.821000	0.011600
1.227700	0.054800
1.634900	0.092300
2.042600	0.124000
2.450700	0.149900
2.859200	0.170100
3.267800	0.184400
3.676700	0.193000
4.085600	0.195800
* 4.903400	0.184000
* 5.721200	0.149000

LEADING EDGE

X	Y
-3.998000	-0.902600
0.040500	CENTER
RADIUS	

TRAILING EDGE

X	Y
4.085600	0.237000
0.041140	

ALT LOW FAN STATOR BLADE SECTION B05-B05  
RADIUS: 8.800000 GAGE: 3.300000

SUCTION SURFACE

X	Y
*-5.467200	-1.699200
*-4.747300	-1.276000
-4.007000	-0.897600
-3.629200	-0.725200
-3.246300	-0.564000
-2.858700	-0.414300
-2.466800	-0.276200
-2.070900	-0.149900
-1.671400	-0.035500
-1.268700	0.066900
-0.863100	0.157100
-0.454900	0.235200
-0.044600	0.301100
0.367500	0.354600
0.781000	0.395700
1.195500	0.424400
1.610800	0.440700
2.026300	0.444500
2.441800	0.435800
2.856800	0.414600
3.271000	0.380900
3.684000	0.334800
4.095400	0.276200
* 4.913400	0.121500
* 5.725000	-0.083200

PRESSURE SURFACE

X	Y
*-5.527200	-1.497200
*-4.755800	-1.224000
-3.977200	-0.974000
-3.585200	-0.857700
-3.191400	-0.747200
-2.796000	-0.642700
-2.399000	-0.544100
-2.000500	-0.451500
-1.600700	-0.365000
-1.199500	-0.284700
-0.797200	-0.210500
-0.393800	-0.142500
0.010600	-0.080600
0.415900	-0.025000
0.822100	0.024400
1.228900	0.067500
1.636400	0.104500
2.044300	0.135100
2.452700	0.159500
2.861500	0.177600
3.270400	0.189500
3.679500	0.195000
4.088600	0.194200
* 4.906800	0.173700
* 5.725000	0.128000

LEADING EDGE

X	Y
-3.989300	-0.934700
0.041130	CENTER
	RADIUS
	0.041260

TRAILING EDGE

ALT LOW FAN STATOR BLADE SECTION B06-B06  
RADIUS: 8.250000 GAGE: 2.750000

SUCTION SURFACE

X	Y
*-5.471900	-1.682100
*-4.750200	-1.268000
-4.008900	-0.895900
-3.630900	-0.725600
-3.248000	-0.565800
-2.860500	-0.416800
-2.468700	-0.279100
-2.072800	-0.152800
-1.673300	-0.038300
-1.270500	0.064200
-0.864800	0.154500
-0.456500	0.232600
-0.046000	0.298300
0.366200	0.351600
0.780000	0.392300
1.194700	0.420400
1.610100	0.436000
2.025800	0.438900
2.441400	0.429100
2.856500	0.406700
3.270700	0.371600
3.683600	0.323700
4.094900	0.263200
* 4.912700	0.104400
* 5.724100	-0.104800

PRESSURE SURFACE

X	Y
*-5.528800	-1.493800
*-4.757300	-1.221400
-3.979000	-0.971400
-3.587300	-0.854800
-3.193900	-0.743800
-2.798800	-0.638500
-2.402100	-0.539100
-2.003800	-0.445600
-1.604200	-0.358300
-1.203100	-0.277300
-0.800800	-0.202600
-0.397400	-0.134300
0.007200	-0.072500
0.412600	-0.017200
0.819000	0.031500
1.226100	0.073700
1.633800	0.109200
2.042000	0.138000
2.450700	0.160200
2.859700	0.175600
3.268800	0.184300
3.678100	0.186200
4.087400	0.181300
* 4.906000	0.151100
* 5.724600	0.093700

LEADING EDGE

X	Y
-3.991300	-0.932600
	CENTER
0.040720	

TRAILING EDGE

X	Y
4.088200	0.222500
	RADIUS
0.041200	

ALT LOW FAN STATOR BLADE SECTION B07-B07  
RADIUS: 7.700000 GAGE: 2.200000

SUCTION SURFACE  
X Y

\*-5.446600 -1.767700  
\*-4.734600 -1.341900  
-4.001000 -0.956900  
-3.626100 -0.779700  
-3.245800 -0.612700  
-2.860700 -0.456500  
-2.470800 -0.311700  
-2.076500 -0.178500  
-1.678200 -0.057500  
-1.276300 0.051100  
-0.871100 0.147000  
-0.463000 0.230200  
-0.052500 0.300400  
0.360000 0.357500  
0.774200 0.401400  
1.189500 0.432200  
1.605600 0.449700  
2.022100 0.453800  
2.438500 0.444600  
2.854400 0.422100  
3.269300 0.386000  
3.682800 0.336600  
4.094500 0.273600  
\* 4.912500 0.106800  
\* 5.723300 -0.114400

PRESSURE SURFACE  
X Y

\*-5.506300 -1.591300  
\*-4.741600 -1.299800  
-3.969300 -1.031100  
-3.580300 -0.905300  
-3.189400 -0.785200  
-2.796400 -0.671100  
-2.401600 -0.563200  
-2.004900 -0.461800  
-1.606500 -0.367200  
-1.206500 -0.279400  
-0.804900 -0.198700  
-0.401900 -0.125200  
0.002400 -0.058900  
0.407800 0.000000  
0.814300 0.051600  
1.221600 0.095700  
1.629700 0.132300  
2.038400 0.161400  
2.447600 0.182900  
2.857100 0.196700  
3.266800 0.202900  
3.676500 0.201200  
4.086200 0.191800  
\* 4.905600 0.149900  
\* 5.725000 0.077200

LEADING EDGE

X	Y	X	Y
-3.982600	-0.992900	CENTER	4.087600 0.233000
0.040450		RADIUS	0.041190

ALT LOW FAN STATOR BLADE SECTION B08-B08  
RADIUS: 7.150000 GAGE: 1.650000

SUCTION SURFACE

X	Y
*-5.417700	-1.862200
*-4.714000	-1.424000
-3.988300	-1.025000
-3.617200	-0.840200
-3.240600	-0.665200
-2.858500	-0.500900
-2.471200	-0.347900
-2.079000	-0.206900
-1.682300	-0.078300
-1.281600	0.037400
-0.877100	0.139800
-0.469400	0.228900
-0.058900	0.304300
0.353900	0.366000
0.768600	0.413700
1.184700	0.447300
1.601700	0.466800
2.019000	0.472200
2.436400	0.463300
2.853200	0.440000
3.268900	0.402300
3.683000	0.350200
4.095200	0.283400
* 4.913900	0.105700
* 5.725000	-0.130800

PRESSURE SURFACE

X	Y
*-5.471500	-1.699400
*-4.717700	-1.387000
-3.954300	-1.097800
-3.569000	-0.961900
-3.181300	-0.831800
-2.791200	-0.707900
-2.398900	-0.590700
-2.004300	-0.480300
-1.607700	-0.377300
-1.209000	-0.281900
-0.808400	-0.194300
-0.406100	-0.114700
-0.002200	-0.043200
0.403100	0.019900
0.809700	0.074700
1.217300	0.121100
1.625900	0.158900
2.035100	0.188100
2.444900	0.208600
2.855100	0.220300
3.265400	0.223200
3.675600	0.217000
4.085700	0.201800
* 4.905600	0.144400
* 5.725100	0.051000

LEADING EDGE

X	Y
-3.968900	-1.060300
	CENTER
0.040230	

TRAILING EDGE

X	Y
4.087800	0.242900
	RADIUS
0.041190	

ALT LOW FAN STATOR BLADE SECTION B09-B09  
RADIUS: 6.600000 GAGE: 1.100000

SUCTION SURFACE

X Y

\*-5.373000 -1.978700  
\*-4.684800 -1.527400  
-3.971800 -1.112500  
-3.606000 -0.918700  
-3.234000 -0.734000  
-2.856100 -0.559600  
-2.472400 -0.396400  
-2.083200 -0.245200  
-1.688900 -0.106800  
-1.289800 0.018200  
-0.886500 0.129500  
-0.479400 0.226500  
-0.069000 0.309100  
0.344100 0.377100  
0.759400 0.430100  
1.176300 0.468200  
1.594400 0.491200  
2.013000 0.498900  
2.431600 0.491300  
2.849600 0.468300  
3.266500 0.429800  
3.681600 0.375600  
4.094400 0.305500  
\* 4.913100 0.117600  
\* 5.722600 -0.133900

PRESSURE SURFACE

X Y

\*-5.431100 -1.828800  
\*-4.688600 -1.494800  
-3.935300 -1.183200  
-3.554600 -1.035800  
-3.171200 -0.894000  
-2.785000 -0.758300  
-2.396100 -0.629600  
-2.004400 -0.508100  
-1.610100 -0.394600  
-1.213200 -0.289300  
-0.814100 -0.192700  
-0.412700 -0.105000  
-0.009400 -0.026500  
0.395700 0.042700  
0.802400 0.102400  
1.210400 0.152500  
1.619500 0.192900  
2.029500 0.223400  
2.440100 0.244000  
2.851100 0.254500  
3.262200 0.254800  
3.673200 0.244600  
4.083800 0.224000  
\* 4.903800 0.151600  
\* 5.722200 0.037600

LEADING EDGE

X Y

-3.951400 -1.146700 CENTER 4.086600 0.265100  
0.039850 RADIUS 0.041160

ALT LOW FAN STATOR BLADE SECTION B10-B10  
 RADIUS: 6.050000 GAGE: 0.550000

SUCTION SURFACE  
 X Y

\*-5.322400 -2.116400  
 \*-4.649900 -1.644700  
 -3.950600 -1.208600  
 -3.590900 -1.003900  
 -3.224500 -0.808100  
 -2.851300 -0.622300  
 -2.471600 -0.447800  
 -2.085700 -0.285700  
 -1.694000 -0.136800  
 -1.296900 -0.001900  
 -0.894900 0.118600  
 -0.488500 0.224100  
 -0.078400 0.314400  
 0.334800 0.389100  
 0.750700 0.448000  
 1.168500 0.490900  
 1.587600 0.517800  
 2.007400 0.528500  
 2.427300 0.523000  
 2.846600 0.501000  
 3.264700 0.462500  
 3.680900 0.407300  
 4.094500 0.335400  
 \* 4.913900 0.141500  
 \* 5.722900 -0.119200

PRESSURE SURFACE  
 X Y

\*-5.376800 -1.975700  
 \*-4.650800 -1.615300  
 -3.911200 -1.277300  
 -3.536300 -1.116700  
 -3.158000 -0.961700  
 -2.776300 -0.813100  
 -2.391300 -0.671700  
 -2.002900 -0.538300  
 -1.611300 -0.413400  
 -1.216600 -0.297700  
 -0.819000 -0.191500  
 -0.418700 -0.095300  
 -0.016000 -0.009300  
 0.388900 0.066200  
 0.795700 0.131200  
 1.204100 0.185500  
 1.613900 0.229000  
 2.024600 0.261400  
 2.436100 0.282700  
 2.848000 0.292800  
 3.260100 0.291400  
 3.671900 0.278600  
 4.083200 0.254000  
 \* 4.904300 0.169400  
 \* 5.723400 0.037600

LEADING EDGE

X Y

-3.928900 -1.241800 CENTER  
 0.039670 RADIUS

TRAILING EDGE

X Y

4.086500 0.295000  
 0.041140

ALT LOW FAN STATOR BLADE SECTION BII-BII  
RADIUS: 5.500000 GAGE: 0.000000

SUCTION SURFACE  
X Y

\*-5.268900 -2.237200  
\*-4.613200 -1.744200  
-3.927500 -1.287200  
-3.573400 -1.072200  
-3.211800 -0.866200  
-2.842800 -0.670600  
-2.466600 -0.486800  
-2.083500 -0.315800  
-1.694000 -0.158600  
-1.298500 -0.016000  
-0.897700 0.111600  
-0.492100 0.223600  
-0.082300 0.319700  
0.331000 0.399700  
0.747200 0.463100  
1.165600 0.510000  
1.585500 0.540200  
2.006200 0.553600  
2.427000 0.550100  
2.847300 0.529800  
3.266400 0.492400  
3.683400 0.438000  
4.097800 0.366600  
\* 4.918800 0.172800  
\* 5.729400 -0.089000

PRESSURE SURFACE  
X Y

\*-5.321900 -2.107100  
\*-4.612000 -1.718900  
-3.885700 -1.354700  
-3.516400 -1.181600  
-3.143000 -1.014500  
-2.765700 -0.854400  
-2.384200 -0.702200  
-1.998800 -0.558700  
-1.609600 -0.424600  
-1.216700 -0.300500  
-0.820400 -0.186900  
-0.421000 -0.084000  
-0.018700 0.007600  
0.386100 0.088000  
0.793100 0.157100  
1.201900 0.214500  
1.612300 0.260300  
2.023800 0.294400  
2.436100 0.316600  
2.848900 0.326900  
3.261700 0.325100  
3.674300 0.311300  
4.086300 0.285400  
\* 4.908500 0.197300  
\* 5.728300 0.060800

LEADING EDGE

X Y  
-3.904700 -1.319800  
0.039730

CENTER  
RADIUS

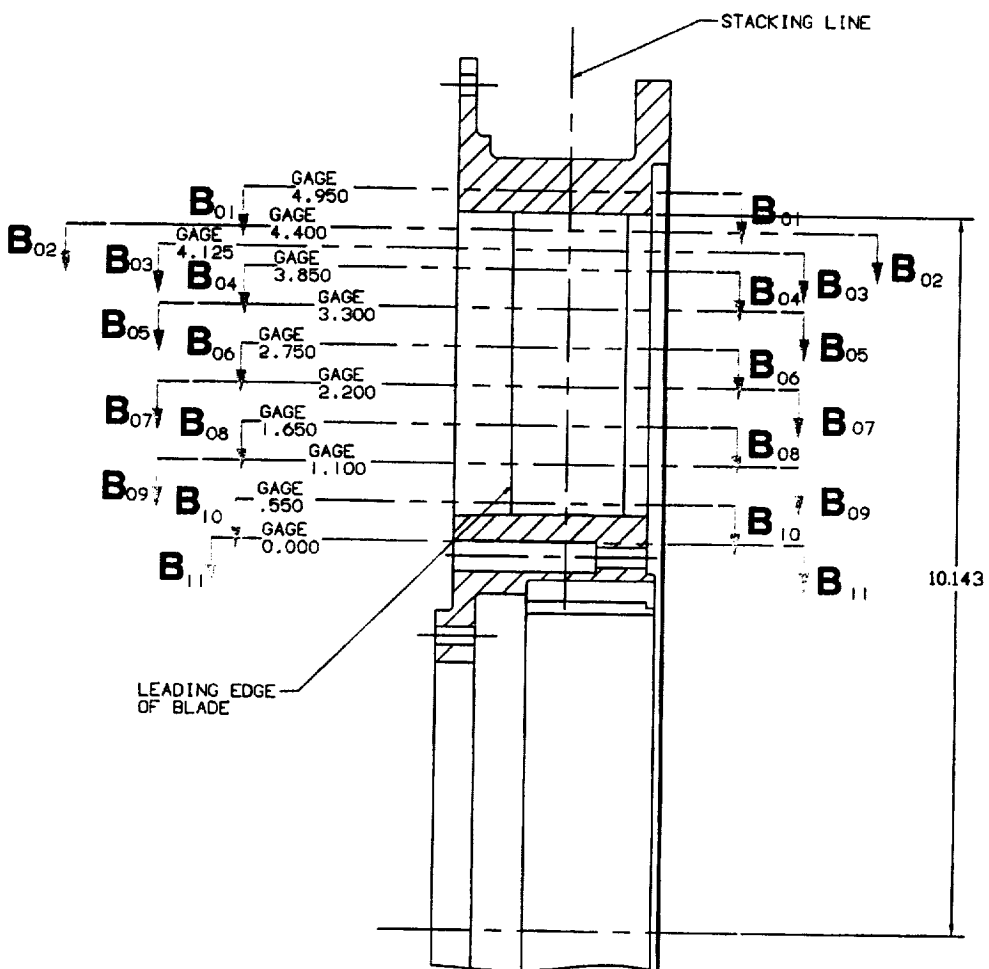
TRAILING EDGE

X Y  
4.089800 0.326300  
0.041100

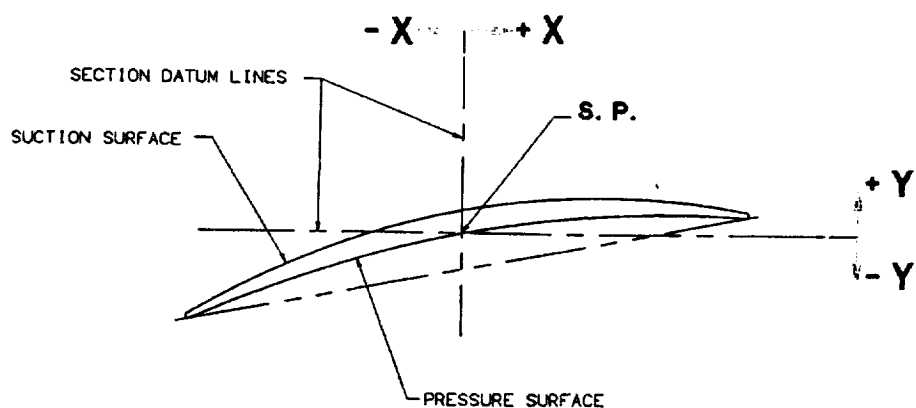


# **PART 3**

## **SHORT CHORD STATOR VANES**



DETAIL C  
70 PLACES  
EQUALLY SPACED  
(5° 8' 34")



TYPICAL AIRFOIL SECTION

B-B<sub>01</sub> THRU B-B<sub>11</sub>

ALNF SHORT STATOR  
RADIUS: 10.450000

SECTION B01-B01  
GAGE: 4.950000

SUCTION SURFACE  
X Y

\* -1.098300 -0.326800  
\* -0.953500 -0.241200  
-0.804700 -0.165200  
-0.728800 -0.130800  
-0.651900 -0.098800  
-0.574000 -0.069400  
-0.495100 -0.042400  
-0.415500 -0.018100  
-0.335100 0.003700  
-0.254000 0.023000  
-0.172400 0.039500  
-0.090300 0.053500  
-0.007800 0.064800  
0.075100 0.073400  
0.158200 0.079400  
0.241400 0.082700  
0.324700 0.083300  
0.408000 0.081200  
0.491100 0.076500  
0.574100 0.069100  
0.656800 0.059000  
0.739200 0.046300  
0.821100 0.030900  
\* 0.983400 -0.008000  
\* 1.143700 -0.057700

PRESSURE SURFACE  
X Y

\* -1.110100 -0.281600  
\* -0.955300 -0.228500  
-0.798900 -0.180600  
-0.720100 -0.158600  
-0.640900 -0.137900  
-0.561400 -0.118400  
-0.481600 -0.100200  
-0.401600 -0.083300  
-0.321300 -0.067700  
-0.240700 -0.053400  
-0.159900 -0.040400  
-0.078900 -0.028600  
0.002200 -0.018200  
0.083500 -0.009000  
0.165000 -0.001200  
0.246500 0.005400  
0.328200 0.010600  
0.409900 0.014500  
0.491700 0.017100  
0.573600 0.018500  
0.655400 0.018500  
0.737300 0.017200  
0.819100 0.014600  
\* 0.982400 0.005500  
\* 1.145300 -0.008800

LEADING EDGE

X Y  
-0.801300 -0.172700

CENTER

TRAILING EDGE

X Y  
0.819400 0.022800

0.008200

RADIUS

0.008200

ALNF SHORT STATOR  
RADIUS: 9.900000

SECTION B02-B02  
GAGE: 4.400000

SUCTION SURFACE

X Y

\*-1.102600 -0.302500  
\*-0.956200 -0.224100  
-0.805800 -0.154500  
-0.729100 -0.123000  
-0.651400 -0.093700  
-0.573100 -0.066600  
-0.493900 -0.041700  
-0.414100 -0.019000  
-0.333700 0.001400  
-0.252800 0.019500  
-0.171400 0.035300  
-0.089500 0.048900  
-0.007300 0.060100  
0.075100 0.069000  
0.157800 0.075600  
0.240600 0.079900  
0.323600 0.081800  
0.406500 0.081400  
0.489400 0.078600  
0.572200 0.073500  
0.654800 0.066100  
0.737200 0.056400  
0.819300 0.044400  
\* 0.982600 0.013500  
\* 1.144700 -0.026600

PRESSURE SURFACE

X Y

\*-1.115200 -0.257700  
\*-0.958500 -0.211900  
-0.800600 -0.170100  
-0.721200 -0.150700  
-0.641500 -0.132300  
-0.561600 -0.114800  
-0.481600 -0.098400  
-0.401300 -0.083000  
-0.320900 -0.068600  
-0.240200 -0.055100  
-0.159400 -0.042700  
-0.078500 -0.031300  
0.002600 -0.020800  
0.083800 -0.011400  
0.165100 -0.003000  
0.246500 0.004400  
0.327900 0.010800  
0.409500 0.016200  
0.491100 0.020600  
0.572800 0.024000  
0.654500 0.026300  
0.736200 0.027600  
0.817900 0.028000  
\* 0.981300 0.026100  
\* 1.144700 0.020600

LEADING EDGE

X Y

-0.802600 -0.162100 CENTER 0.817900 0.036300  
0.008300 RADIUS 0.008300

ALNF SHORT STATOR  
RADIUS: 9.625000

SECTION B03-B03  
GAGE: 4.125000

SUCTION SURFACE  
X Y

\*-1.100800 -0.315400  
\*-0.954300 -0.235000  
-0.804200 -0.163400  
-0.727800 -0.130900  
-0.650500 -0.100600  
-0.572400 -0.072600  
-0.493600 -0.046800  
-0.414000 -0.023200  
-0.333800 -0.001900  
-0.253000 0.017100  
-0.171700 0.033700  
-0.090000 0.048100  
-0.007900 0.060000  
0.074500 0.069700  
0.157200 0.077000  
0.240000 0.081900  
0.322900 0.084500  
0.405900 0.084700  
0.488900 0.082500  
0.571700 0.078000  
0.654400 0.071100  
0.736900 0.061900  
0.819000 0.050400  
\* 0.982000 0.020500  
\* 1.143400 -0.018600

PRESSURE SURFACE  
X Y

\*-1.112100 -0.271300  
\*-0.956000 -0.223100  
-0.798700 -0.178900  
-0.719600 -0.158300  
-0.640200 -0.138700  
-0.560600 -0.120200  
-0.480700 -0.102700  
-0.400600 -0.086200  
-0.320400 -0.070800  
-0.239900 -0.056500  
-0.159200 -0.043200  
-0.078400 -0.030900  
0.002600 -0.019700  
0.083700 -0.009600  
0.165000 -0.000500  
0.246300 0.007500  
0.327800 0.014400  
0.409300 0.020300  
0.490900 0.025200  
0.572600 0.029000  
0.654300 0.031700  
0.736000 0.033400  
0.817800 0.034000  
\* 0.981700 0.031900  
\* 1.146000 0.025400

LEADING EDGE

X	Y		X	Y
-0.800700	-0.170900	CENTER	0.817800	0.042200
		RADIUS	0.008200	

ALNF SHORT STATOR  
RADIUS: 9.350000

SECTION B04-B04  
GAGE: 3.850000

SUCTION SURFACE

X	Y
*-1.094400	-0.331100
*-0.950500	-0.248100
-0.802200	-0.173900
-0.726400	-0.140100
-0.649500	-0.108500
-0.571800	-0.079200
-0.493300	-0.052200
-0.414000	-0.027500
-0.334000	-0.005200
-0.253400	0.014800
-0.172200	0.032400
-0.090600	0.047600
-0.008500	0.060400
0.073900	0.070800
0.156500	0.078800
0.239400	0.084300
0.322400	0.087400
0.405400	0.088100
0.488500	0.086300
0.571400	0.082200
0.654200	0.075600
0.736800	0.066500
0.819000	0.055100
* 0.982200	0.025400
* 1.143800	-0.013500

PRESSURE SURFACE

X	Y
*-1.107300	-0.287600
*-0.952700	-0.236400
-0.796500	-0.189200
-0.717800	-0.167100
-0.638700	-0.146000
-0.559400	-0.126100
-0.479800	-0.107300
-0.400000	-0.089600
-0.319900	-0.073000
-0.239600	-0.057600
-0.159000	-0.043400
-0.078300	-0.030200
0.002600	-0.018200
0.083700	-0.007400
0.164900	0.002300
0.246200	0.010900
0.327600	0.018300
0.409200	0.024600
0.490800	0.029700
0.572500	0.033700
0.654200	0.036500
0.736000	0.038200
0.817800	0.038700
* 0.981400	0.036100
* 1.145000	0.028700

LEADING EDGE

X	Y
-0.798800	-0.181300
0.008200	CENTER

TRAILING EDGE

X	Y
0.817800	0.046900
0.008200	RADIUS

SHORT STATOR  
S: 8.800000

SECTION B05-B05  
GAGE: 3.300000

ION SURFACE

X	Y
-0.2900	-0.343500
-0.8900	-0.257800
-0.0900	-0.181300
-0.725400	-0.146500
-0.648900	-0.1114000
-0.571400	-0.083800
-0.493100	-0.056000
-0.414000	-0.030600
-0.334100	-0.007500
-0.253600	0.013100
-0.172500	0.031400
-0.090900	0.047100
-0.008800	0.060400
0.073600	0.071200
0.156300	0.079600
0.239200	0.085400
0.322300	0.088800
0.405400	0.089600
0.488500	0.087900
0.571500	0.083800
0.654400	0.077100
0.737000	0.068000
0.819300	0.056400
* 0.983000	0.025700
* 1.145500	-0.015000

PRESSURE SURFACE

X	Y
* -1.105500	-0.304000
* -0.950800	-0.247700
-0.794900	-0.196600
-0.716500	-0.173000
-0.637800	-0.150700
-0.558800	-0.129600
-0.479400	-0.109600
-0.399700	-0.090900
-0.319800	-0.073500
-0.239600	-0.057300
-0.159100	-0.042300
-0.078500	-0.028500
0.002400	-0.016000
0.083400	-0.004800
0.164700	0.005200
0.246000	0.014000
0.327500	0.021500
0.409100	0.027700
0.490800	0.032700
0.572500	0.036400
0.654300	0.038800
0.736100	0.040000
0.817900	0.040000
* 0.981500	0.036400
* 1.145100	0.028000

LEADING EDGE

X	Y
-0.797300	-0.188700
0.008200	

CENTER

RADIUS

TRAILING EDGE

X	Y
0.817900	0.048300
	0.008300

ALNF SHORT STATOR  
RADIUS: 8.250000

SUCTION SURFACE

X	Y
* -1.090600	-0.342700
* -0.948200	-0.257700
-0.801000	-0.181500
-0.725600	-0.146700
-0.649000	-0.114100
-0.571600	-0.083900
-0.493200	-0.056000
-0.414100	-0.030600
-0.334200	-0.007500
-0.253600	0.013100
-0.172500	0.031200
-0.090800	0.046900
-0.008700	0.060000
0.073800	0.070700
0.156500	0.078900
0.239500	0.084500
0.322600	0.087600
0.405700	0.088200
0.488800	0.086200
0.571900	0.081700
0.654700	0.074700
0.737300	0.065200
0.819600	0.053200
* 0.983300	0.021700
* 1.145800	-0.019800

LEADING EDGE

X	Y
-0.797400	-0.188900
	CENTER
0.008200	RADIUS

SECTION B06  
GAGE: 2.7500

PRESSURE SURFACE

X	Y
* -1.105200	-0.304800
* -0.950700	-0.248400
-0.795000	-0.196800
-0.716700	-0.172800
-0.638100	-0.150000
-0.559100	-0.128500
-0.479800	-0.108300
-0.400200	-0.089400
-0.320200	-0.071800
-0.240000	-0.055400
-0.159600	-0.040400
-0.078900	-0.026700
0.002100	-0.014300
0.083200	-0.003200
0.164400	0.006500
0.245900	0.015000
0.327400	0.022100
0.409100	0.027800
0.490800	0.032300
0.572600	0.035400
0.654400	0.037200
0.736300	0.037700
0.818100	0.036800
* 0.981400	0.030800
* 1.144300	0.019200

TRAILING EDGE

X	Y
0.818200	0.045100
0.008300	

ALNF SHORT STATOR  
RADIUS: 7.700000

SECTION B07-B07  
GAGE: 2.200000

SUCTION SURFACE

X	Y
* -1.086900	-0.364500
* -0.945000	-0.274500
-0.798700	-0.194100
-0.723900	-0.157500
-0.648000	-0.123300
-0.571100	-0.091500
-0.493100	-0.062100
-0.414300	-0.035300
-0.334600	-0.010900
-0.254200	0.010900
-0.173200	0.030100
-0.091600	0.046700
-0.009500	0.060700
0.073100	0.072100
0.155900	0.080900
0.239000	0.087000
0.322200	0.090400
0.405500	0.091200
0.488800	0.089300
0.571900	0.084700
0.654900	0.077500
0.737600	0.067700
0.820000	0.055200
* 0.983900	0.022100
* 1.146600	-0.021800

PRESSURE SURFACE

X	Y
* -1.100100	-0.329500
* -0.946800	-0.266400
-0.792300	-0.209300
-0.714600	-0.183000
-0.636600	-0.158200
-0.558100	-0.134800
-0.479100	-0.112800
-0.399800	-0.092200
-0.320100	-0.073100
-0.240100	-0.055500
-0.159800	-0.039300
-0.079200	-0.024600
0.001700	-0.011400
0.082700	0.000400
0.164000	0.010600
0.245500	0.019400
0.327100	0.026700
0.408900	0.032500
0.490700	0.036700
0.572600	0.039500
0.654500	0.040800
0.736400	0.040500
0.818400	0.038800
* 0.982700	0.031200
* 1.147400	0.018000

LEADING EDGE

X	Y
-0.794900	-0.201500
0.008300	CENTER
0.008300	RADIUS

TRAILING EDGE

X	Y
0.818500	0.047100
0.008300	

ALNF SHORT STATOR  
RADIUS: 7.150000

SUCTION SURFACE

X	Y
*-1.078400	-0.388800
*-0.939700	-0.293900
-0.795800	-0.209000
-0.721900	-0.170300
-0.646700	-0.134100
-0.570400	-0.100300
-0.492900	-0.069200
-0.414500	-0.040700
-0.335200	-0.014800
-0.255000	0.008500
-0.174100	0.029000
-0.092500	0.046700
-0.010400	0.061800
0.072200	0.074000
0.155100	0.083400
0.238400	0.090100
0.321800	0.093900
0.405200	0.094900
0.488700	0.093100
0.572000	0.088400
0.655200	0.080900
0.738000	0.070600
0.820500	0.057500
* 0.984600	0.022900
* 1.147500	-0.022900

LEADING EDGE

X	Y
-0.791700	-0.216200
0.008300	

SECTION B08-B08  
GAGE: 1.650000

PRESSURE SURFACE

X	Y
* -1.091000	-0.355100
* -0.940900	-0.286300
-0.788800	-0.223900
-0.712000	-0.195100
-0.634700	-0.167900
-0.556700	-0.142300
-0.478300	-0.118200
-0.399400	-0.095800
-0.320100	-0.075000
-0.240300	-0.055800
-0.160200	-0.038200
-0.079700	-0.022300
0.001100	-0.008100
0.082200	0.004400
0.163500	0.015300
0.245100	0.024500
0.326800	0.032000
0.408600	0.037800
0.490600	0.041900
0.572600	0.044300
0.654600	0.044900
0.736700	0.043900
0.818700	0.041100
* 0.982400	0.030100
* 1.145700	0.011900

TRAILING EDGE

X	Y
0.819000	0.049400
0.008300	

ALNF SHORT STATOR  
RADIUS: 6.600000

SECTION B09-B09  
GAGE: 1.100000

SUCTION SURFACE  
X Y

\* -1.068300 -0.419900  
\* -0.932700 -0.318900  
-0.791500 -0.228300  
-0.718800 -0.186900  
-0.644700 -0.148100  
-0.569300 -0.111900  
-0.492600 -0.078400  
-0.414700 -0.047700  
-0.335800 -0.019700  
-0.256000 0.005400  
-0.175200 0.027600  
-0.093800 0.046900  
-0.011700 0.063200  
0.071000 0.076600  
0.154000 0.087100  
0.237400 0.094500  
0.321100 0.098900  
0.404800 0.100200  
0.488500 0.098600  
0.572100 0.093800  
0.655500 0.086100  
0.738500 0.075300  
0.821100 0.061500  
\* 0.985100 0.024900  
\* 1.147500 -0.023700

PRESSURE SURFACE  
X Y

\* -1.079800 -0.387500  
\* -0.933300 -0.311800  
-0.784000 -0.242900  
-0.708300 -0.211000  
-0.631900 -0.180800  
-0.554800 -0.152400  
-0.477100 -0.125700  
-0.398800 -0.100900  
-0.319900 -0.077800  
-0.240500 -0.056700  
-0.160600 -0.037300  
-0.080200 -0.019900  
0.000500 -0.004300  
0.081500 0.009300  
0.162900 0.021100  
0.244500 0.030900  
0.326300 0.038800  
0.408300 0.044700  
0.490400 0.048700  
0.572600 0.050800  
0.654800 0.050900  
0.737000 0.049000  
0.819100 0.045200  
\* 0.983000 0.031900  
\* 1.146500 0.011000

LEADING EDGE

X Y  
-0.787300 -0.235400 CENTER  
0.008200 RADIUS

TRAILING EDGE

X Y  
0.819600 0.053400  
0.008200

ALNF SHORT STATOR  
RADIUS: 6.050000

SECTION B10-B1C  
GAGE: 0.550000

SUCTION SURFACE  
X Y

\*-1.056400 -0.450500  
\*-0.924800 -0.343400  
-0.786800 -0.247100  
-0.715400 -0.203000  
-0.642400 -0.161600  
-0.567900 -0.123000  
-0.491900 -0.087300  
-0.414700 -0.054400  
-0.336300 -0.024500  
-0.256700 0.002400  
-0.176200 0.026200  
-0.094900 0.047000  
-0.012800 0.064700  
0.069900 0.079200  
0.153100 0.090500  
0.236700 0.098700  
0.320500 0.103700  
0.404400 0.105400  
0.488400 0.104000  
0.572200 0.099300  
0.655800 0.091400  
0.739000 0.080400  
0.821700 0.066100  
\* 0.985600 0.027600  
\* 1.147500 -0.024100

PRESSURE SURFACE  
X Y

\*-1.068700 -0.419400  
\*-0.925300 -0.336800  
-0.778700 -0.261400  
-0.704200 -0.226400  
-0.628900 -0.193200  
-0.552700 -0.162100  
-0.475700 -0.132900  
-0.397900 -0.105700  
-0.319500 -0.080600  
-0.240500 -0.057500  
-0.160800 -0.036500  
-0.080700 -0.017500  
-0.000100 -0.000700  
0.081000 0.014000  
0.162300 0.026600  
0.244000 0.037100  
0.326000 0.045400  
0.408100 0.051500  
0.490400 0.055500  
0.572700 0.057300  
0.655100 0.057000  
0.737400 0.054500  
0.819600 0.049800  
\* 0.983700 0.033800  
\* 1.147400 0.009000

LEADING EDGE

X Y  
-0.782300 -0.254000

TRAILING EDGE

X Y  
0.820200 0.058000

0.008200

RADIUS

0.008200

ALNF SHORT STATOR  
RADIUS: 5.500000

SECTION B11-B11  
GAGE: 0.000000

SUCTION SURFACE  
X Y

\* -1.050500 -0.468400  
\* -0.920300 -0.356700  
-0.783700 -0.256600  
-0.713000 -0.210900  
-0.640700 -0.168100  
-0.566700 -0.128200  
-0.491100 -0.091200  
-0.414200 -0.057300  
-0.336000 -0.026500  
-0.256600 0.001300  
-0.176200 0.025800  
-0.094900 0.047200  
-0.012800 0.065400  
0.069900 0.080300  
0.153100 0.091900  
0.236800 0.100300  
0.320700 0.105400  
0.404800 0.107200  
0.488800 0.105800  
0.572800 0.101100  
0.656500 0.093100  
0.739800 0.081900  
0.822600 0.067600  
\* 0.986700 0.029700  
\* 1.148800 -0.020600

PRESSURE SURFACE  
X Y

\* -1.060100 -0.438200  
\* -0.919700 -0.350400  
-0.775300 -0.270600  
-0.701600 -0.233700  
-0.626900 -0.198800  
-0.551200 -0.166100  
-0.474700 -0.135400  
-0.397300 -0.107000  
-0.319100 -0.080800  
-0.240300 -0.056700  
-0.160700 -0.034900  
-0.080700 -0.015300  
-0.000100 0.002100  
0.081000 0.017200  
0.162400 0.030000  
0.244200 0.040600  
0.326200 0.048900  
0.408500 0.054900  
0.490900 0.058700  
0.573300 0.060200  
0.655800 0.059500  
0.738200 0.056500  
0.820500 0.051300  
\* 0.984800 0.034300  
\* 1.148700 0.008500

LEADING EDGE

X Y  
-0.779100 -0.263400 CENTER  
0.008200 RADIUS

TRAILING EDGE

X Y  
0.821100 0.059500  
0.008200



# Appendix C

The noise data from the Alternative Low Noise Fan is presented in this appendix. The data is arranged in 5 sections corresponding to the five tested configurations: 7 vane hard, 7 vane fully treated, 7 vane partially treated, 70 vane hard and 70 vane fully treated. In each of these sections the data from the six fan speeds is presented. These are 10671, 10137, 9604, 8537, 7736, and 6402 rpmc. The data are presented at roughly 10° angular positions from 158° in the aft to 24.5° in the front. Even this mass of data is only a sampling of the data since the data is taken at roughly every 2.5°. At each of the speeds both narrow band data from 0 to 50 000 Hz and 1/3rd octave data are presented with the narrow band data being presented first. The narrow band data plots are sound pressure level in decibels plotted versus frequency in kilohertz. The title of the plot gives both the speed and the angle of the plot. The 1/3rd octave plots are sound pressure level in decibels plotted versus frequency in hertz. The frequency axis is a log scale with the lowest frequency shown being 10 Hz and the highest frequency being 100 000 Hz. Again the title of the plot gives both the speed and the angle of the plot.

Appendix C Section 1—7 Vane hard configuration

Appendix C Section 2—7 Vane fully treated configuration

Appendix C Section 3—7 Vane partially treated configuration

Appendix C Section 4—70 Vane hard configuration

Appendix C Section 5—70 Vane fully treated configuration

Appendix C is contained on the enclosed CD.

REPORT DOCUMENTATION PAGE			Form Approved OMB No. 0704-0188
<p>Public reporting burden for this collection of information is estimated to average 1 hour per response, including the time for reviewing instructions, searching existing data sources, gathering and maintaining the data needed, and completing and reviewing the collection of information. Send comments regarding this burden estimate or any other aspect of this collection of information, including suggestions for reducing this burden, to Washington Headquarters Services, Directorate for Information Operations and Reports, 1215 Jefferson Davis Highway, Suite 1204, Arlington, VA 22202-4302, and to the Office of Management and Budget, Paperwork Reduction Project (0704-0188), Washington, DC 20503.</p>			
1. AGENCY USE ONLY (Leave blank)	2. REPORT DATE	3. REPORT TYPE AND DATES COVERED	
	September 2000	Technical Memorandum	
4. TITLE AND SUBTITLE		5. FUNDING NUMBERS	
The Alternative Low Noise Fan		WU-522-81-11-00	
6. AUTHOR(S)			
James H. Dittmar, David M. Elliott, Robert J. Jeracki, Royce D. Moore, and Tony L. Parrott			
7. PERFORMING ORGANIZATION NAME(S) AND ADDRESS(ES)		8. PERFORMING ORGANIZATION REPORT NUMBER	
National Aeronautics and Space Administration John H. Glenn Research Center at Lewis Field Cleveland, Ohio 44135-3191		E-12153	
9. SPONSORING/MONITORING AGENCY NAME(S) AND ADDRESS(ES)		10. SPONSORING/MONITORING AGENCY REPORT NUMBER	
National Aeronautics and Space Administration Washington, DC 20546-0001		NASA TM—2000-209916	
11. SUPPLEMENTARY NOTES			
James H. Dittmar, David M. Elliott, Robert J. Jeracki, and Royce D. Moore, NASA Glenn Research Center, Tony L. Parrott, Langley Research Center, Hampton, Virginia 23681. Responsible person, James H. Dittmar, organization code 5940; (216) 433-3921. The noise data from the Alternative Low Noise Fan is presented in Appendix C, which is only contained on the enclosed CD.			
12a. DISTRIBUTION/AVAILABILITY STATEMENT		12b. DISTRIBUTION CODE	
Unclassified - Unlimited Subject Category: 71		Distribution: Nonstandard	
This publication is available from the NASA Center for AeroSpace Information. (301) 621-0390.			
13. ABSTRACT (Maximum 200 words)			
<p>A 106 bladed fan with a design takeoff tip speed of 1100 ft/sec was hypothesized as reducing perceived noise because of the shift of the blade passing harmonics to frequencies beyond the perceived noise rating range. A 22 in. model of this Alternative Low Noise Fan, ALNF, was tested in the NASA Glenn 9x15 Wind Tunnel. The fan was tested with a 7 vane long chord stator assembly and a 70 vane conventional stator assembly in both hard and acoustically treated configurations. In addition a partially treated 7 vane configuration was tested wherein the acoustic material between the 7 long chord stators was made inactive. The noise data from the 106 bladed fan with 7 long chord stators in a hard configuration was shown to be around 4 EPNdB quieter than a low tip speed Allison fan at takeoff and around 5 EPNdB quieter at approach. Although the tone noise behaved as hypothesized, the majority of this noise reduction was from reduced broadband noise related to the large number of rotor blades. This 106 bladed ALNF is a research fan designed to push the technology limits and as such is probably not a practical device with present materials technology. However, a low tip speed fan with around 50 blades would be a practical device and calculations indicate that it could be 2 to 3 EPNdB quieter at takeoff and 3 to 4 EPNdB quieter at approach than the Allison fan. 7 vane data compared with 70 vane data indicated that the tone noise was controlled by rotor wake—stator interaction but that the broadband noise is probably controlled by the interaction of the rotor with incoming flows. A possible multiple pure tone noise reduction technique for a fan/acoustic treatment system was identified. The data from the fully treated configuration showed significant noise reductions over a large frequency range thereby providing a real tribute to this bulk absorber treatment design. The tone noise data with the partially treated 7 vane configuration indicated that acoustic material in the source noise generation region may be more effective than similar material outside of the generation region.</p>			
14. SUBJECT TERMS		15. NUMBER OF PAGES	
Noise; Fan noise; Acoustic treatment		1339	
16. PRICE CODE		A99	
17. SECURITY CLASSIFICATION OF REPORT	18. SECURITY CLASSIFICATION OF THIS PAGE	19. SECURITY CLASSIFICATION OF ABSTRACT	20. LIMITATION OF ABSTRACT
Unclassified	Unclassified	Unclassified	